

AN ABSTRACT OF THE DISSERTATION OF

Derron Rafiq Coles for the degree of Doctor of Philosophy in Civil Engineering presented on June 5, 2007.

Title: Tidal Influence on Downstream Fining in Gravel-bed Rivers

Abstract approved:

Peter C. Klingeman

This research examines the downstream fining phenomenon as it operates in coastal gravel-bed rivers of Oregon. Downstream fining is a change in bed composition toward smaller sediment sizes in the downstream direction. Changes in stream flow discharge and channel slope affect the rate of bed-load transport, thereby altering the downstream fining regime. This research focuses on ascertaining the rate of downstream fining and the characterization of tidal influence on bed-load transport in the lower-river reaches.

For this purpose, a combination of physical and numerical analysis techniques were used. Variations of particle size distributions and specific gravity values were assessed along the main channel. Numerical analysis techniques included a MATLAB program for simulating bed-load transport as affected by tide. The numerical model developed for this investigation, TIMM (Tidally Influenced Movement Model) uses physically based excess shear stress as the underlying mechanism. Namely, an undulating water surface is applied to Shields criterion for incipient motion and bed-load transport. The **Generalized Stream Tube model for Alluvial River Simulation version 2.1 (GSTARS 2.1)**, developed by the Bureau of Reclamation, was used to validate conclusions drawn from field data analyses.

The five rivers of the Tillamook Basin were the sites of field data collection. The Tillamook Basin is located approximately 60 miles (96.6 kilometers) west of Portland, Oregon and 60 miles (96.6 kilometers) south of the Columbia River mouth at the Pacific Ocean. The basin has a total area of 570 square miles (1476 square

kilometers) including Tillamook Bay, which is the second largest estuary in Oregon. All rivers empty into the Tillamook Bay. From north to south, the rivers are the Miami, Kilchis, Wilson, Trask and Tillamook. The Kilchis River was the primary field research site and the other four rivers allowed expansion of field research for added understanding of downstream fining.

Bulk sampling of the armor and sub-armor layer of the Kilchis River was completed for five sidebars along the river, from river mile 0 to river mile 14 (0 – 22.5 km). Photo frame sampling was carried out for the armor layer of sidebars along the four additional rivers. In total, 21 sampling locations with 141 individual sampling points were used for the particle size analyses. Assessment of longitudinal variation in specific gravity of bed particles by size fraction was performed for all five rivers.

Particle size analyses showed a distinct downstream fining trend. Kilchis River surface particle sizes decreased from 216 mm at river mile 14 (22.5 km) to 10 mm at river mile 0. Miami River surface particle sizes decreased from 43 mm at river mile 9 to 29 mm at river mile 1.5 (2.4 km). Wilson River surface particle sizes decreased from 51 mm at river mile 27 to 23 mm at river mile 0. Trask River surface particle sizes decreased from 55 mm at river mile 18 to 26 mm at river mile 4 (6.4 km). Diminution coefficients (rates of size reduction) were found to be 0.55 km^{-1} for the armor layer and 0.48 km^{-1} for the sub-armor layer of the Kilchis River. The R-squared values for the armor and sub-armor coefficients are 0.92 and 0.99, respectively. Results of regression analyses performed for the photo frame sampling data were 0.02, 0.03, and 0.04 km^{-1} for the Miami, Wilson, and Trask Rivers, respectively. R-squared values of 0.19, 0.78, and 0.81, respectively. Diminution coefficients reported for all rivers were far outside the value reported for abrasion-dominated systems (0.089 km^{-1}), yet were within the range of diminution coefficients reported for selective sorting-dominated systems (0.001 to 0.05 km^{-1}). Average specific gravities for bed material were 2.78, 2.68, 2.73, 2.56, and 2.76 for the Miami, Kilchis, Wilson, Trask, and Tillamook Rivers, respectively.

Simulations of sediment transport within the tidal portion of the Kilchis River (river mile 0 to 3 or 0 to 4.8 km) using TIMM at moderate river streamflow above the threshold for transport of material showed that tidal influence causes distinct deposition zones during periods of high, low, and moderate tide levels. Depositional zones were found to propagate downstream with increases in river discharge, such that at elevated river stage the location of depositional zones associated with tide levels were undistinguishable. It can be concluded that tide has a significant influence at flows below, and moderately above the threshold for transport.

Simulations of a simplified version of the Kilchis River using GSTARS 2.1 produced comparable results to the TIMM simulations. GSTARS 2.1 was run using three scenarios, 1) a uniform bed and incoming sediment supply set at 7.9 mm, 2) a mixed bed with mean sediment diameter of 7.9 mm and coarser incoming sediment supply, and 3) a mixed bed with mean sediment diameter of 7.9 mm and finer incoming sediment supply. Each scenario had output data that show maximum deposition in the zone of tidal influence. The location of head of tide for the simplified Kilchis River was found to occur at river mile 5 instead of river mile 3 used for the head of tide in TIMM simulations.

GSTARS 2.1 simulations showed that variations in particle size distribution of incoming sediment supply influence rates of downstream fining. An incoming sediment supply that had a coarser particle size distribution than the particle size distribution of the bed resulted in an observable increase in deposition of large particle sizes in the upstream reaches; however, there was no observable increase in deposition of large particle sizes in downstream reaches. An incoming sediment supply that had a finer particle size distribution than the particle size distribution of the bed resulted in an observable increase in deposition of smaller particles in the downstream reaches, with no observable increase in deposition of smaller sizes in the upstream reaches. Therefore, simulations show evidence that sediment supply of particles coarser than the bed causes increased rates of fining in reaches near the sediment source.

Key contributions of this research are in the categories of methodology, numerical analysis, and basic understanding of the fate and transport of sediment in the zone of tidal influence. It has been shown that particle size data, collected in detail on sidebars, can be used in conjunction with specific gravity data to categorize in-stream particles based on probable origin and type. Characterization of sediment transport in the zone of tidal influence using numerical models showed the tide cycle influences the downstream fining trend in lower reaches by shifting the zone of deposition farther upstream than would the case without tidal influence, with a net effect of increasing the rate of downstream fining. Moreover, tidal influence was found to have an inverse relationship with water discharge. Finally, it was shown that numerical modeling of river reaches in the tidal zone should include consideration of tidal fluctuations in order to predict erosion and depositional areas more accurately.

© Copyright by Derron Rafiq Coles

June 5, 2007

All Rights Reserved

Tidal Influence on Downstream Fining in Gravel-bed Rivers

by
Derron Rafiq Coles

A DISSERTATION

submitted to

Oregon State University

in partial fulfillment of
the requirements for the
degree of

Doctor of Philosophy

Presented June, 5 2007
Commencement June 2008

Doctor of Philosophy dissertation of Derron Rafiq Coles presented on June 5, 2007.

APPROVED:

Major Professor, representing Civil Engineering

Head of the Department of Civil, Construction and Environmental Engineering

Dean of the Graduate School

I understand that my dissertation will become part of the permanent collection of Oregon State University libraries. My signature below authorizes the release of my dissertation to any reader upon request.

Derron Rafiq Coles, Author

ACKNOWLEDGEMENTS

I would like to thank The CCEE department and my committee members Wayne Huber, Julia Jones, Richard Cuenca, and Jim Ingle, who have assisted in my competition of this work and my growth as a researcher. I would especially like to thank my major professor, Pete Klingeman for his unwavering support and encouragement throughout this entire process. His unmatched expertise and continued guidance remains one of my most cherished gifts from Oregon State University.

I would like to thank the people who braved the marshes and cows of Tillamook, thereby making my data collection possible. Thanks go to Josh Wyrick, C.J. Poor, Beth Lambert, and Urmila Mali. I would also like to thank Bub Boquist and the Geiger family in Tillamook for allowing me access to their property and providing the relational evidence that was so valuable.

I would also like to thank my family for their undying support. This includes my extended family at the McNair Scholars Program at University of Maryland, Baltimore County. Special thanks goes to my mother, Beverly Coles, my brother, Robert Coles Jr., Cynthia Hill, and Sylvia Cooke-Martin who instilled in me the drive, determination and independence necessary to venture so far from home to pursue my life goals.

The Educational Opportunities Program at Oregon State University has been a source of funding and emotional support for my six years here at OSU. The faculty and staff at EOP have been nurturing and wonderful. Particularly, I would like to recognize Larry Griggs for his contributions to my growth as an educator. I am eternally grateful to you all.

Finally, this dissertation is dedicated to the two loves of my life, Urmila and Collin, whose love, encouragement, and humor, got me through the difficult moments. I truly love you both.

TABLE OF CONTENTS

1	Introduction.....	1
1.1	Sediment transport regime.....	1
1.1.1	General description.....	1
1.1.2	Relevance of sediment transport to watershed health.....	2
1.1.3	Connection of sediment transport to disturbance regime.....	3
1.1.4	Human influence on sediment transport regime.....	3
1.2	Downstream fining trend.....	4
1.2.1	Description of downstream fining.....	4
1.2.2	Sources of interruptions in typical spatial distribution.....	5
1.2.3	Kilchis River Study.....	6
1.3	Objectives and scope.....	7
1.3.1	Statement of hypothesis and issues addressed by this research.....	7
1.3.2	Research techniques used and expected outcomes.....	8
2	Literature Review on Downstream Fining.....	10
2.1	Overview.....	10
2.2	Characterization of downstream fining according to past investigations ...	10
2.3	Description of abrasion.....	11
2.4	Description of selective transport.....	16
2.5	Significance of disruptions in downstream fining profile.....	22
2.6	Synthesis of downstream fining knowledge for dissertation research.....	27
3	Literature Review on River Hydraulics and Sediment Transport with Tidal Influence	30
3.1	Fundamental Principles	30
3.1.1	Introduction.....	30
3.1.2	Description of fundamental principles.....	30
3.2	Extension of fundamental principles.....	36
3.2.1	Characterization of flow regime	40
3.2.2	Gradually-varied flow.....	42
3.2.3	Tidal influence on gradually varied flow.....	51
3.2.4	Effects on bed-load transport as illustrated by present-day relationships	60
4	Application of Theory.....	68
4.1	Site Selection	68
4.1.1	Relevance of field data	68
4.2	Kilchis River Watershed.....	70
4.2.1	Background on Tillamook Basin settlement and historical overview of Kilchis Watershed.....	70
4.2.2	Description of current river sediment conditions.....	72
4.2.3	Overview of the Tillamook Basin physical conditions.....	72
4.2.4	Physical and hydrologic characteristics of Kilchis River Watershed.....	76

TABLE OF CONTENTS (continued)

4.2.5	Physical and hydrologic characteristics of Kilchis River Watershed.....	77
4.2.6	Research relationship to the Kilchis River problem.....	80
4.3	Brief Description of Other Study Rivers in the Tillamook Basin.....	82
4.3.1	Characteristics of the watersheds.....	82
4.3.2	History of disturbance.....	84
5	Methodology.....	86
5.1	Overview of analyses conducted.....	86
5.2	Kilchis River downstream fining analysis.....	93
5.2.1	Particle size analysis techniques.....	93
5.2.2	Summary of Procedure with reasoning.....	94
5.3	Photo frame fining analysis.....	103
5.3.1	Particle size analysis techniques.....	103
5.4	Specific Gravity Analysis.....	113
5.4.1	Specific gravity analysis techniques.....	113
5.5	Numerical analysis of tidal influence on bed-load transport.....	115
5.5.1	Significance of numerical models.....	115
5.5.2	Description of MATLAB.....	116
5.5.3	Presentation of modeling equations.....	116
5.5.4	Summary of protocol used by numerical model.....	127
5.6	Downstream fining simulation.....	131
5.6.1	Description of HEC 6.....	131
5.6.2	Presentation of fundamental equations used by HEC 6.....	132
5.6.3	Description of GSTARS 2.1.....	134
5.6.4	Presentation of fundamental equations used by GSTARS 2.1.....	134
5.6.5	Modeling data.....	137
6	Presentation and Discussion of Results from Sampling.....	147
6.1	Particle size analysis.....	148
6.1.1	Kilchis River analysis.....	148
6.1.2	Frame Photo Sampling.....	162
6.1.3	Comparison of results to Willamette River Studies.....	179
6.1.4	Specific Gravity Determination.....	185
6.2	TIMM Simulation Results.....	192
6.2.1	Simplified version of the Kilchis River.....	192
6.2.2	Constant-discharge results and discussion.....	193
6.2.3	Varied-discharge results and discussion.....	203
6.2.4	Bed-load transport criteria comparison and TIMM sensitivity analysis.....	209
6.3	GSTARS 2.1 simulation results.....	214
7	Summary and Conclusion.....	230
8	Recommendations for Future Research.....	237

TABLE OF CONTENTS (continued)

9	Bibliography.....	238
10	Appendices.....	245
10.1	Appendix A: Kilchis River Bulk Sampling Photographic Evidence.....	246
10.2	Appendix B: Kilchis Particle size distribution by site	248
10.3	Appendix C: Willamette River particle size data.....	265
10.4	Appendix D: Hydrologic Analyses	271
10.5	Appendix E: Empirical chart reproduction.....	284
10.6	Appendix F: MATLAB Programs	288
10.6.1	TIMM constant discharge and sediment size.....	288
10.6.2	TIMM varied discharge constant sediment	294
10.7	Appendix G: GSTARS 2.1 Simulation Output Data.....	301
10.7.1	Simulation 1: uniform bed	301
10.7.2	Simulation 2: mixed bed, finer incoming sediment.....	317
10.7.3	Simulation 3: mixed bed, coarser incoming sediment.....	337

LIST OF FIGURES

Figure 2.1: Wearing processes.....	12
Figure 2.2: Typical velocity distribution with depth in a river	17
Figure 2.3: Shields diagram for incipient motion (Vanoni, 1975; Yang 1996)	18
Figure 2.4: Hjulstrom diagram for incipient motion (Hjulstrom, 1935).....	19
Figure 2.5: Similarity plot of empirical gravel transport function with indicated size ranges (Parker et al., 1982; Yang 1996)	21
Figure 3.1: Illustration of the energy equation for steady nonuniform flow	47
Figure 3.2: M1 curve representing flow into a lake or reservoir.....	52
Figure 3.3: Tide inducing centrifugal and gravitational forces	53
Figure 3.4: Tidal fluctuations at garibaldi, Oregon	54
Figure 3.6: The M1 and M2 curves that might be considered for tidal reaches.....	57
Figure 3.7: Alterations of M2 curve representing flow into an estuary with tidal influence.....	59
Figure 3.8: Sediment parameters and critical tractive force for DuBoys' bed-load equation.....	64
Figure 4.1: Sub-Watersheds of the Tillamook Basin, Oregon	69
Figure 4.2: Average Monthly Discharge for Period of Record for Kilchis River as Derived from Wilson River Gage	77
Figure 4.3: photographs of the a 2005 landslide in the kilchis watershed upstream of little south fork.....	79
Figure 4.4: Squeedunk Slough.....	81
Figure 5.1: Kilchis River with location of sampling sites.....	96
Figure 5.2: Velocity distributions for a channel near sidebars	97
Figure 5.3: Flow around a channel obstruction	98
Figure 5.4: Illustration of sampling configuration	100
Figure 5.5: 2' x 2' Delineating apparatus for sampling bed material.....	101
Figure 5.6: Procedure for data collection used in Kilchis Analysis	102
Figure 5.7: Procedure for photo frame sampling.....	105
Figure 5.8: Miami River with location of sampling sites.....	106
Figure 5.9: Wilson River with location of sampling sites.....	107
Figure 5.10: Trask River with location of sampling sites.....	108
Figure 5.11: Tillamook River with location of sampling sites.....	109
Figure 5.12: Tillamook River at river mile 3 boat ramp.....	110
Figure 5.13: Schematic of Apparatus used to determine specific gravity.....	114
Figure 5.14: Procedure for determination of specific gravity.....	115
Figure 5.15: Scatterplots for multipart function for use with sheilds diagram	120
Figure 5.15: cont'd.....	121
Figure 5.16: Scatterplots for multipart function used for the Straub bed-load relationship	122
Figure 5.16: cont'd.....	123
Figure 5.17: Reduction of observed tidal fluctuations to a step function	125
Figure 5.18: Water surface elevations for high, intermediate, and low tide	128

LIST OF FIGURES (continued)

Figure 5.19: protocol for Tidally Influenced Movement Model (TIMM)	130
Figure 5.20: Illustration of streamlines and stream tubes	135
Figure 5.21 Sketch of simplified Kilchis River for simulation	139
Figure 5.22 Line drawing of simulated simplified version of the Kilchis river with location of lateral inputs and outputs	140
Figure 5.23 representative cross section plots simplified kilchis river	141
Figure 5.24 Rating Curve for Wilson River (USGS)	147
Figure 6.1: Kilchis River Site 5 illustrating lateral input of gravel	150
Figure 6.2: Gravel bars of the Kilchis River with mean particle size (mm) for the upstream, downstream, and center-of-bar armor layer samples.....	152
Figure 6.3: Cumulative particle size distribution for Kilchis River sites.....	156
Figure 6.3: (cont'd)	157
Figure 6.4: Percent retained for downstream armor layer showing uni-modal and weak bimodal distributions	158
Figure 6.5: Regression analysis for the Kilchis River mean particle size	160
Figure 6.6: Location of samples.....	164
Figure 6.7: Miami River frame photo sampling results	165
Figure 6.8: Wilson River frame photo sampling results	167
Figure 6.9: Trask River frame photo sampling results	169
Figure 6.10: Tillamook River frame photo sampling results	171
Figure 6.11: Possible causes of shift to finer particles near center of bar	173
Figure 6.12: Miami River sediment retention structures upstream of Site 3.....	175
Figure 6.13: Regression analyses for additional rivers	178
Figure 6.14: Compilation of regression analyses for five rivers	179
Figure 6.15: mean Particle size Regression analyses for Willamette river samples	181
Figure 6.16: Development of tidally influenced zones of deposition over time for 90 days at 398 cfs	196
Figure 6.17: Development of tidally influenced zones of deposition over time	199
Figure 6.18: Shear Stress for a period of 90 days at 398 cfs	200
Figure 6.19: Velocity along channel for a period of 90 days at 398 cfs	201
Figure 6.20: Bed-load rate along channel for a period of 90 days at 398 cfs.....	202
Figure 6.21: Development of tidally influenced zones of deposition over time, for September using average daily discharge for period of record	206
Figure 6.22: Development of tidally influenced zones of deposition over time, for October using average daily discharge for period of record	207
Figure 6.23: Development of tidally influenced zones of deposition over time, for January using average daily discharge for period of record.....	208
Figure 6.24: Development of tidally influenced zones of deposition over time, for a period of 90 days using shields criterion and constant river discharge	210
Figure 6.25: Development of tidally influenced zones of deposition over time, for a period of 90 days using shields criterion and varied river discharge (cfs).....	212
Figure 6.26: Development of tidally influenced zones of deposition over time, for January using average daily discharge for period of record.....	213
Figure 6.27: Simulation 1 of GSTARS 2.1 (5 months with unifrom bed)	215

LIST OF FIGURES (continued)

Figure 6.28: Development of tidally influenced zones of deposition over time, using average monthly discharge and a mixed bed with incoming sediment of finer distribution than bed (Simulation 2)	216
Figure 6.29: Development of tidally influenced zones of deposition over time, using average monthly discharge and a mixed bed with incoming sediment of coarser distribution than bed (Simulation 3)	219
Figure 6.30: Simulation 4 of GSTARS 2.1 (5 months with uniform bed)	223
Figure 6.31: Development of tidally influenced zones of deposition over time, using average monthly discharge and a mixed bed with incoming sediment of finer distribution than bed (Simulation 5)	224
Figure 6.32: Volume of sediment retained within a reach using average monthly discharge and a mixed bed with incoming sediment of coarser distribution than bed (Simulation 6).....	227
Figure 6.32: Cont'd.....	228
Figure 6.32: Cont'd.....	229
Figure 7.1: Miami River site 1	232
Figure 10.1: Kilchis River site 1 armor and sub-armor layer (upstream end of bar sample)	246
Figure 10.2: Kilchis River site 1 armor and sub-armor layer (upstream-end-of-bar sample)	249
Figure 10.3: Kilchis River site 1 armor and sub-armor layer (center-of-bar sample)	250
Figure 10.4: Kilchis River site 1 armor and sub-armor layer (downstream-end-of-bar sample)	251
Figure 10.5: Kilchis River site 2 armor and sub-armor layer (upstream-end-of-bar sample)	252
Figure 10.6: Kilchis River site 2 armor and sub-armor layer (center-of-bar sample)	253
Figure 10.7: Kilchis River site 2 armor and sub-armor layer (downstream-end-of-bar sample)	254
Figure 10.8: Kilchis River site 3 armor and sub-armor layer (upstream-end-of-bar sample)	255
Figure 10.9: Kilchis River site 3 armor and sub-armor layer (center-of-bar sample)	256
Figure 10.10: Kilchis River site 3 armor and sub-armor layer (downstream-end-of-bar sample)	257
Figure 10.11: Kilchis River site 4 armor and sub-armor layer (upstream-end-of-bar sample)	258
Figure 10.12: Kilchis River site 4 armor and sub-armor layer (center-of-bar sample)	259
Figure 10.13: Kilchis River site 4 armor and sub-armor layer (downstream-end-of-bar sample)	260
Figure 10.14: Kilchis River site 5 armor and sub-armor layer (upstream-end-of-bar sample)	261
Figure 10.15: Kilchis River site 5 armor and sub-armor layer (center-of-bar sample)	262
Figure 10.16: Kilchis River site 5 armor and sub-armor layer (downstream-end-of-bar sample)	263

LIST OF FIGURES (continued)

Figure 10.17: Kilchis River site 5 armor and sub-armor layer (special near-bank sample)	264
Figure 10.18: Willamette river bed material data.....	265
(Random armor layer sample).....	265
Figure 10.19: Willamette river bed material data.....	266
(Exposed armor layer sample)	266
Figure 10.20: Willamette river bed material data.....	267
(Non-exposed armor layer sample).....	267
Figure 10.21: Willamette river bed material data.....	268
(Combined armor layer sample)	268
Figure 10.22: Willamette river bed material data.....	269
(Sub-armor layer sample).....	269
Figure 10.23: Willamette river bed material data.....	270
(Largest armor layer sample).....	270
Figure 10.25: Frequency distribution for log cycle class intervals for Kilchis River as derived from Wilson River gage.....	279
Figure 10.26: Flow duration curve (Log Intervals) for Kilchis River as derived from Wilson River gage.....	279
Figure 10.27: Average monthly discharge for period of record for Kilchis River as derived from Wilson River gage.....	281
Figure 10.28: Mean daily Discharge for Period of Record during the Fall Season for Kilchis River as Derived from Wilson River gage.....	281
Figure 10.29: Mean daily discharge for period of record during the winter season for Kilchis River as derived from Wilson River gage.....	282
Figure 10.30: Mean daily discharge for period of record during the spring season for Kilchis River as derived from Wilson River gage.....	282
Figure 10.31: Mean daily discharge for period of record during the spring season for Kilchis River as derived from Wilson River gage.....	283

LIST OF TABLES

Table 2.1: Summary of past investigations of downstream fining	25
Table 2.1: Summary of past investigations of downstream fining (continued)	26
Table 3.1: Common types of flow conditions	42
Table 3.2: Types of water surface profiles	44
Table 3.3: Extent of tidal influence for five Rivers of the Tillamook Basin	58
Table 4.1: Geologic History of the Tillamook Basin (Bostrom and Komar 1997)	74
Table 4.2: Characteristics of the Tillamook Basin sub-watersheds Study Areas	83
Table 5.1: Overview of Analyses used in Research	88
Table 5.2: Characteristics of systems under study	90
Table 5.3: Sampling site locations	111
Table 5.4: Sediment transport relationships incorporated in GSTARS 2.1	136
Table 5.5: Location of each cross-section for the simplified Kilchis River simulations	142
Table 5.6: Particle size distributions for the simplified Kilchis River simulations	145
Table 5.7: estimated Kilchis River Mean daily flows for the period of record for derived from Wilson River gage, using 76 years of record.....	146
Table 6.1: Results of Kilchis River gravel bar sampling.....	149
Table 6.2: Comparison of armor and sub-armor mean particle diameter.....	154
Table 6.3: Calculation of percent decrease in mean diameter downstream for Kilchis River	161
Table 6.4: Results of Photo Frame Sampling	177
Table 6.5: Diminution coefficients according to type of sample, Willamette River ..	184
Table 6.6: Results of specific gravity analyses for Kilchis River	188
Table 6.7: Kilchis Composite Statistics	190
Table 6.8: Results of specific gravity analyses for other four Tillamook Basin Rivers	191
Table 6.9: Specific gravity study of the Willamette River (Klingeman, 1981)	192
Table: 6.10 Input Parameters for TIMM	193
Table 10.1: USGS Mean monthly data for Wilson River.....	271
Table 10.2: Peak discharge values for Wilson River scaled for Kilchis River.....	273
Table 10.3: Statistical analysis for Kilchis River flood frequency analysis	275
Table 10.4: Kilchis River flood frequency values for flood frequency plot.....	276
Table 10.5: Mean daily discharge separated into size classes for Kilchis River analysis	278
Table 10.6: Mean daily discharge for Kilchis River (derived from Wilson River gage, USGS)	280

1 Introduction

1.1 Sediment transport regime

1.1.1 General description

Sediment transport is the movement of particulate matter by fluvial, aeolian, or glacial activity. Fluvial transport of inorganic material is the focus of this dissertation. The sediment transport regime of rivers and streams describes the characteristic conditions for sediment transport processes. Sediment movement can be divided into two main types of transport, suspended-load and bed-load. Suspended-load is made up of typically silt and sand-sized particles, which are carried by fluid flow above the bed of the channel. Although suspended-load may include larger clasts during periods of flood, the size of suspended-load particles is small relative to bed-load at any given period. Bed-load is the movement of particles along the river bottom. Bed-load may involve sand-sized to boulder-sized particles, depending on hydraulic characteristics. This motion includes rolling, sliding, and jumping (Yang 1996). As jumping is included among the types of bed-load motion, note that suspended-load is transport for sustained periods, versus the shorter periods that are involved in jumping motion.

Fluvial transport of organic material is also of interest to many researchers. This is due to the relevance of organic material to aquatic ecosystems and the life cycles of biota whose early life stages take place in-stream. However, inorganic particulate matter also plays an important role in the vitality or failure of fluvial ecosystems. The size, location, and magnitude of sediment, which is eroded and deposited, have serious ramifications for the types of biota that can survive, as well as the morphology of the river.

1.1.2 Relevance of sediment transport to watershed health

Since 18th-century English landscape theories, the aesthetics of a healthy watershed includes a picturesque view of pristine and tidy serpentine rivers and marshlands (Kondolf 2006). This view of a properly functioning water system may be indicative of some systems. However, the general trend over the last century has been to force historically complex, multi-threaded channels into single-thread channels. Coupled with detrimental land use, these actions have wreaked havoc on many of the world's waterway ecosystems. In the last few decades, research has improved public understanding of the form and function of rivers, including the importance of upland input processes, riparian areas, and natural river morphology. Measurements of watershed health now include holistic scientific investigation. Biologic indicators of watershed health consist of items such as sizes of in-stream fish populations and riparian tree stands. Inorganic indicators of watershed health include the geology of the watershed and its interactions with available water.

Of the currently valued indicators of watershed health, the sediment transport regime of river systems is significant in that it directly affects the form and function of a river, thereby affecting the watershed as a whole. Biological indicators are directly connected to sediment transport in that the spatial and particle size distribution of in-stream and near-stream sediment affect habitats in which flora and fauna live. For example, the spatial distribution of gravel-size sediment is of interest because it is this size range that is necessary for fish redds (spawning sites) of salmonids. Furthermore, transport of suspended-load and sand-sized bed-load into portions of the fluvial ecosystem, such as redds, could have damaging effects. Oxygen is necessary for the development of fish eggs; therefore, infilling of interstitial areas in beds of gravel is detrimental to established redds. Given that fish are not the only biota that need particular in-stream conditions to survive, understanding the impacts of human activity on the inorganic sediment transport regime is very important.

1.1.3 Connection of sediment transport to disturbance regime

The sediment transport regime is also inextricably linked to the “disturbance regime” of the watershed. Disturbance regime refers to the group of significant events that alter watershed conditions such that recovery of an ecosystem to its pre-altered form and function takes a considerable amount of time. Disturbances could be natural or human induced. For example, natural disturbance may include floods and landslides, while anthropogenic disturbance may be deforestation or landslides due to the road construction. For instance, mass earth movements such as shallow and deep-seated landslides deliver aggregate material into the river channel. The added incoming sediment must then be redistributed throughout the river system by fluvial processes. Channel adjustment to changes in incoming sediment flux depend on the existing sediment transport capacity. Another component of the history of disturbance is flood frequency. At times of high flow, such as during flood stages, sediment routing increases drastically. Therefore, by understanding and documenting the magnitude and frequency of floods in a river, one is indirectly gaining insight into the sediment transport regime of the river.

1.1.4 Human influence on sediment transport regime

Human disturbance is considered by some to be an additional component of the natural disturbance regime of a watershed. Native Americans used controlled burns to maintain fertile land and open spaces for hunting. Since then, other human influences have introduced perturbations in the dynamic equilibrium of watershed processes. Forest harvesting, road construction, and land-use changes are all activities included in the overall human impacts. Moreover, these activities have had impacts on the sediment transport regimes of rivers. For instance, denuded upland areas have been found to alter the efficiency of water routing across the watershed as well as the amount of runoff involved. Consequently, the reduced time to peak in-stream flow and the increased peak magnitude both affect the amount and frequency of sediment

transport. Un-vegetated upland areas increase the probability of landslide events, which have already been stated to affect the sediment transport regime directly. Downstream fining is one detectable response of fluvial systems to land management practices upstream.

1.2 Downstream fining trend

1.2.1 Description of downstream fining

The ability of flow to transport particles is related to hydraulic parameters such as velocity, flow depth, and channel gradient. That is, transport occurs under conditions where streamflow is able to exert a large enough force on the particles at rest on the bed to initiate movement. The maximum load (amount of particles) that a river can transport is called flow capacity. The largest particle within that load defines the flow competence (Rodrigue 2002).

Sediment sorting refers to the distribution of particle sizes in a given area of sediment. Sorting conditions can range from poorly-sorted to well-sorted. The definition of poorly-sorted versus well-sorted varies by discipline (e.g., geology versus water resources engineering). As used herein, poorly sorted is reserved for deposits that have small variations in particle sizes (i.e., they are not very sorted in size), while well-sorted deposits have a wide range of particle sizes. Patterns of sediment sorting are viewed as textural responses (changes in the feel, appearance, and structure of the bed surface, Encarta 2007) to local differences in flow competence (Powell, 1998). That is, variation in bed texture is a buffer for external factors that would otherwise cause the longitudinal profile to change. Increased profile stability then leads to stable network form and basin morphology (Surian, 2002). Therefore, downstream fining can be thought of conceptually as a textural consequence of the lateral and longitudinal flow hydraulics involved in the adjustment to sediment supply.

More specifically, downstream fining is a change in bed composition toward smaller sediment sizes in the downstream direction. The reduction in sediment size is manifested through a change in appearance and, speaking statistically, decrease in a mean sediment diameter. In particular, the mean sediment size is thought to decay exponentially in the downstream direction. Many investigators have documented the phenomenon and its exponential relationship (e.g., Pizzuto 1995, Ferguson 1996, Surian 2001). A comprehensive overview of their work is discussed in the Literature review portion of this dissertation. Looking longitudinally at entire gravel-bed rivers, the bed would seem to have increasingly larger areas of fine particles until a transition from a gravel-dominated bed to a sand-dominated bed occurs. The two generally accepted mechanisms for downstream fining are abrasion and selective sorting. In abrasion, particles are broken down into smaller clasts during transport by collisions and are reduced in size by rubbing together. Selective sorting is a process where particles are transported and deposited according to flow competence and flow capacity. In upstream river reaches, where channel gradient is high, sediment supply is limited, and the bed is composed of large particles including boulders, sediment transport is limited by flow competence. In downstream river reaches, where channel gradient is low, sediment supply is unlimited (due to tributary contributions), and particle sizes are smaller, sediment transport is limited by flow capacity.

1.2.2 Sources of interruptions in typical spatial distribution

Because downstream fining is a hydraulic response to changes in sediment supply, one can expect external factors that create adjustments in either sediment supply or stream power to interrupt the typical spatial distribution of sediment. For example, tributaries may bring additional bed-load to the main channel while adding to the streamflow required for moving bed material (it then follows that distributaries would act as sediment sinks and streamflow outlets). Lateral inputs of material from upland areas via large and small land movement events would also be expected to interrupt the equilibrated spatial distribution. Therefore, where there are interruptions in the observed downstream fining trend, one might find that changes such as watershed-

scale changes (e.g., climate), local channel-bank changes, or landslide activity had occurred upstream.

1.2.3 Kilchis River Study

Field data are necessary whether the research interest is to demonstrate that downstream fining occurs, to determine the dominating mechanisms of fining, to question the usefulness of fining information to make inferences about landslide or other disturbance activity, or to determine the roles of lake, reservoir, or tidal fluctuations on bed-load transport. To gain knowledge about the existence of downstream fining and its relation to disturbances, I selected a site in Oregon that is known for disturbances of both a hydrologic (flood) and a geologic (landslide) nature. The Tillamook Basin, in Northwestern Oregon, offers the opportunity to look at how downstream fining processes operate under land use change, river modification, flood disturbances, and frequent landslide activity.

The Tillamook Basin is also suitable due to its abundance of river systems connected to a single estuary. There are five rivers with varying watershed sizes and levels of modification. From north to south, the rivers are the Miami, Kilchis, Wilson, Trask, and Tillamook Rivers. In this dissertation, the term Tillamook Basin will be used to describe the boundary that includes all five river watersheds. The term Tillamook River watershed will be used to describe the sub-watershed of the Tillamook River, which flows into the Tillamook Bay.

The Kilchis River was the focus of the most detailed data collection for this dissertation. This river was selected as the primary site because of its level of modification, recent landslide activity, shoaling problems in its lower three river miles, and consequent morphological changes at its mouth (Kilchis Watershed Analysis 1998). Data collected on each of the five rivers include particle size and specific gravity characteristics.

1.3 Objectives and scope

1.3.1 *Statement of hypothesis and issues addressed by this research*

This research project addresses the analysis, characterization, and simulation of riverine sediment transport subject to tidal influence. In particular, the following research questions are addressed:

1. Is downstream fining a natural process for Oregon coastal streams and rivers?
2. Can downstream fining analysis be used to find areas of landslide activity or large lateral inputs of sediment?
3. Can downstream fining be significant even for highly modified channels?
4. Does tidal influence alter downstream fining processes?
5. How can sediment transport formulas be used in numerical models to create an accurate characterization of downstream fining in the tidal zones of rivers?

These research questions are addressed while testing two research hypotheses that assert the existence of the downstream fining phenomenon and divulge the impact of tidal influence on this phenomenon. Also presented are their respective null hypotheses:

Hypothesis 1: Physical characteristics of downstream fining can be detected in Oregon coastal streams regardless of the level of channel modification or sediment influx:

$$H_1 : \overline{X}_{up} > \overline{X}_{down} \quad (1.1)$$

$$H_0 : \mu_{up} = \mu_{down} \quad (1.2)$$

where \overline{X}_{up} and \overline{X}_{down} are the mean particle diameter of the upstream and downstream particle distribution of the sampled rivers, μ_{up} and μ_{down} are the mean particle diameter of the upstream and downstream particle distribution of all tested coastal rivers.

Hypothesis 2: Tidal influence has a significant effect on the sediment transport regime that includes a significant change in the downstream fining trend:

$$H_2 : \overline{X}_b \neq \overline{X}_{b-tide} \quad (1.3)$$

$$H_0 : \mu_b = \mu_{b-tide} \quad (1.4)$$

where \overline{X}_b and \overline{X}_{b-tide} are the mean bed-load transport rates with and without, respectively, consideration of tidal influence for sampled rivers, μ_b and μ_{b-tide} are the mean bed-load transport rates with and without, respectively, consideration of tidal influence for all tested coastal rivers.

1.3.2 *Research techniques used and expected outcomes*

The research hypotheses are tested by use of field data and by analytical computations. An analysis of the downstream fining trend is conducted as a means of evaluating the endurance of the downstream fining phenomenon under conditions of disturbance and river modification. In addition, a one-dimensional sediment transport numerical model is created using MATLAB (an interactive program that allows for software development involving matrix computations, MATLAB 7 user

manual 2004). It is then used with trigonometrically modified hydraulic and bed-load relationships to describe sediment transport with tidal influence. Finally, the **Generalized Stream Tube model for Alluvial River Simulation version 2.1** (GSTARS 2.1) is presented and used to validate conclusions drawn from the literature review and field data analyses.

2 Literature Review on Downstream Fining

2.1 Overview

One method for indirectly studying the sediment transport regime is through an investigation of the spatial distribution of sediment at different periods in time. Often, the location of sediment deposition is just as important as the upstream rate of sediment transport. For example, the dredging of a channel for navigation purposes is a direct consequence of sediment deposition. For the Kilchis River study where shoaling at the mouth of the river is under investigation, I exploit information known about downstream fining, a phenomenon typical of many streams and rivers. Downstream fining is a change in bed composition toward smaller sediment sizes in the downstream direction.

Changes in sediment size affect vegetation, flood characteristics, and ecological habitats (Paola et al., 1992). In this study, downstream fining is included in the characterization of the sediment transport regime prior to and throughout the zone of tidal influence. The mechanisms controlling rates of downstream fining give important clues about rates of sediment transport and origins of the transported sediment. Moreover, insight into the history of disturbance of the river can be obtained. The following section describes downstream fining and its usefulness in detail.

2.2 Characterization of downstream fining according to past investigations

Downstream fining can be thought of conceptually as a textural consequence of the lateral and longitudinal flow hydraulics involved in the adjustment to sediment supply. Patterns of sediment sorting are viewed as textural responses (changes in the feel,

appearance, and structure of the bed surface, Encarta 2007) to local differences in flow competence (Powell, 1998). That is, variation in bed texture is a buffer for external factors that would otherwise cause the longitudinal profile to change. Increased profile stability then leads to stable network form and basin morphology (Surian, 2002).

Because fining is inextricably linked to flow competence, rates of fining are a function of channel gradient. Furthermore, downstream fining has been described as a small-scale property that is very dynamic depending on sediment input, discharge changes, and energy changes, all of which are related to gradient (Surian, 2002). Spatially, length over which fining occurs can be on the order of 10^3 to 10^4 km (73 to 306 miles) according to Rice (1999). Typical river distances needed such that mean diameter (d_{50}) is halved are approximately 10 - 100 km (6.2 – 62 miles) for single thread rivers and 1 - 3 km (0.6 – 1.9 miles) for proglacial braided rivers (Ferguson et al., 1996; Shaw and Kellerhals, 1982; Dawson, 1988).

Because fining is a process that encompasses the entire network of most rivers, one can then conclude that it is important to understand the mechanisms that cause downstream fining, as they are indicators of environmental change (Hoey et al., 1999). Although the connection between downstream fining and sediment transport has been accepted since the phenomenon was first noted by Leonardo da Vinci in his “Codex Hammer” (Gomez 2001), the dominant mechanism causing downstream fining has been debated for centuries. The two generally accepted mechanisms for downstream fining are abrasion and selective sorting.

2.3 Description of abrasion

Abrasion is defined as a **wearing, grinding, or rubbing away by friction** (Meriam-Webster 2007). It is used herein as an ‘umbrella’ term for the process by which particle impacts cause a mechanical reduction in size of individual clasts. One could imagine a large particle that enters the river system and is subsequently fractured by

collisions with other large particles, as well as broken down by collisions, rubbing, and grinding with smaller particles. The amount of wearing caused by a single impact is a function of the type and force of the impact. Figure 2.1 shows the different types of impacts possible during sediment transport. For each of the five examples, the two particles before impact are shown to the left of the arrow and the two particles after impact are shown to the right of the arrow.

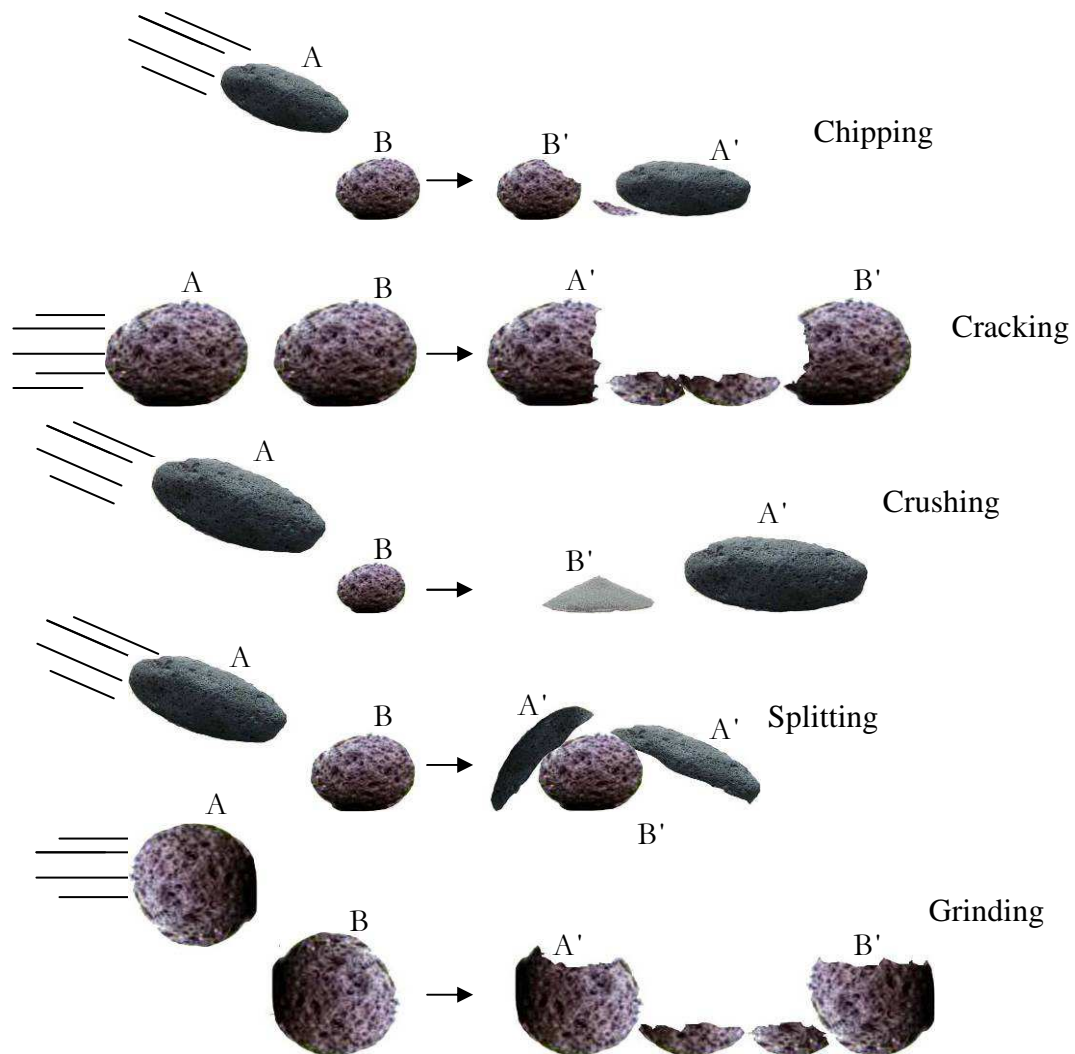


FIGURE 2.1: WEARING PROCESSES

Though many modern researchers have discounted the role that abrasion may play in downstream fining, abrasion has been noted for centuries as a potential factor. For example, in his 1697 book on hydraulics where he discusses the nature of rivers and their parts, the motion of water, confluents and estuaries, banks, and materials and application, Domenico Guglielmini (the founder of the Italian school of hydraulics) made note of abrasion as a mechanism of downstream fining. Downstream fining occurs in the downstream direction; therefore, to be a dominant mechanism, abrasion would have to operate significantly over distances on the order of a typical reach (i.e., < river mile). The rate of abrasion is a function of grain size, grain velocity, grain lithology, grain roundness, particle distribution, and extent of weathering (Kodama, 1994). That is, particles of differing geologic classification have varying potential for succumbing to abrasion (e.g., sedimentary versus igneous). Therefore, the type of rock under transport is important with regard to the ranking of mechanisms that produce downstream fining.

Quantitative research on abrasion includes Sternberg's noteworthy study of the Rhine River in Germany. In 1875, Sternberg used the Rhine data to develop his law of abrasion that described the downstream decrease in grain size as an exponential function:

$$D(L) = D_0 e^{-kL} \quad (2.1)$$

where D is particle diameter at distance L , D_0 is the initial diameter at $L = 0$ and k is a diminution coefficient (Wadell, 1932; Schoklitsch, 1933; Kuenen, 1956; Shaw and Kellerhals, 1982; Gasparini, 1999; Mikos, 1993; Sklar, 2006). The diminution coefficient describes the rate of size reduction. This coefficient depends on many physical parameters, including the lithology of the sediment. Seal et al. (1997) suggest that for selective deposition, the length of the depositional basin, rather than the rate of deposition, is the primary control on the Sternberg diminution coefficient. One could interpret this speculation to mean that abrasion will not be a major mechanism of downstream fining if the length of the depositional basin is relatively short.

The exponential model has been tested using grain size data from various natural sand-bed and gravel-bed rivers (e.g. Wentworth, 1919; Plumley, 1948; Yatsu, 1955; Pizzuto, 1995; Knighton, 1999). Research has shown that the exponential model generally works well except for two major problems that sometimes arise when applying it. First, overestimation can occur if there are not enough grain size measurements, especially in the zone where fining initiates (i.e., estimation of initial rate of fining is vital). Second, failure to consider contributions of all significant mechanisms may lead to underestimations of fining rate (Hoey et al., 1999).

Although neither of these two problems imply that the exponential model should not be used to model downstream fining, some researchers have considered alternative formulas. In their 1985 research, Brierly and Hickin developed a power law function as an alternative to the exponential model for downstream fining. This power law is shown mathematically as:

$$D(L) = aL^k \quad (2.2)$$

where D is particle diameter at distance L , and a and k are a real number and integer, respectively, that correspond to the best-fit curve.

Brierly and Hickin assert that the power law more closely modeled downstream fining for their data. They attributed this to the proximity of their study area to a significant source of sediment. Therefore, one might find a power law more appropriate in circumstances such as upland areas with high sediment influx. However, the exponential model is still used more widely (Ichim et al., 1990). A study of the accuracy of the two types of functions yielded promising results for application of either model, as they both were found to generate concave size reduction trends observed in natural rivers and streams. The exponential function was found to underestimate while the power function was found to overestimate for very large and very small size fractions of sediment (Rice, 1999). Nevertheless, the exponential model was found to be more accurate for trends toward grain size reduction.

Although the exponential model was generally accepted as a good predictor of fining trends, laboratory experiments using tumbling machines and flumes were conducted over the years to verify and replicate downstream fining rates with abrasion as the sole mechanism (e.g., Krumbein, 1941; Kodama, 1992). Despite the confidence of some researchers in abrasion as a major factor in the fining process, many other researchers identify selective sorting as the essential mechanism. Numerous experimental studies revealed higher rates of particle wearing in tumblers and flumes than would be experienced over equivalent lengths of natural rivers (e.g., Adams, 1978; Mills, 1979; Deigaard, 1980; Dawson, 1988; Paola et al., 1992; Ferguson et al., 1996; Seal et al., 1997).

One study in particular showed downstream fining to occur in the complete absence of abrasion, with sorting as the controlling factor (Ferguson et al., 2003). Ferguson used numerical modeling with an idealized channel to isolate selective sorting from the process of abrasion. In his model, the bed consisted of a mixed bed of gravel and sand. The model showed downstream fining until an abrupt change from a gravel bed to a sand bed.

In a study published in 1999, Rice used a linear version of the exponential function to examine the controls on the rate of grain size decline. Rice studied sedimentary links, which Rice defined as the distance over which fining processes operate without disruption. Disruptions include any significant lateral input of sediment, such as landslides or sediment transporting tributaries. The linear version of the exponential function is written mathematically as:

$$\Psi = \Psi_o - \alpha_d L \quad (2.3)$$

where Ψ is the psi value of a percentile (referring to the percent of the bed that is finer than that particle) of the surface grain size distribution, L is the distance downstream within a link, α_d is diminution coefficient (rate of decline in grain size per unit distance), and Ψ_o is the Ψ value at $L = 0$. Rice reported selective sorting to

be the main mechanism for downstream fining. Downstream fining processes were found to operate over short lengths with sediment of relatively durable lithology. For this reason, Rice rejected abrasion as a dominant mechanism. Numerical models also verified the importance of selective sorting (Parker, 1991; Cui et al., 1996; Hoey and Ferguson, 1997; Robinson and Slingerland, 1998).

Before moving on to a discussion of selective transport, it is important to remember that even though selective transport is often found to be the main mechanism for downstream fining, Sternberg's exponential function can still be used to calculate downstream changes in sediment size. Rice found in a 1996 study that particle durability must be considered as a factor in fining because of significant differences among clasts of different composition (such as quartzite, blue limestone, and sandstones). Clasts with different geologic origin but similar values for specific gravity were found to become finer at different rates in the same river (Powell, 1998).

2.4 Description of selective transport

Selective transport is the preferential entrainment and downstream transport of finer particles from within a heterogeneous mixture. Full explanation of this concept requires a brief discussion of the physics behind sediment transport, beginning with flow velocity and the velocity fluctuations that produce a momentum exchange between different levels in the fluid, expressed as shear stress.

Flow velocity in a river or stream is not constant vertically, due to the roughness of the bed. In fact, because the beds of most natural rivers are rough, flow velocity is slowest at the bed and increases vertically above the bed surface. A general representation of such a distribution is shown in Figure 2.2.

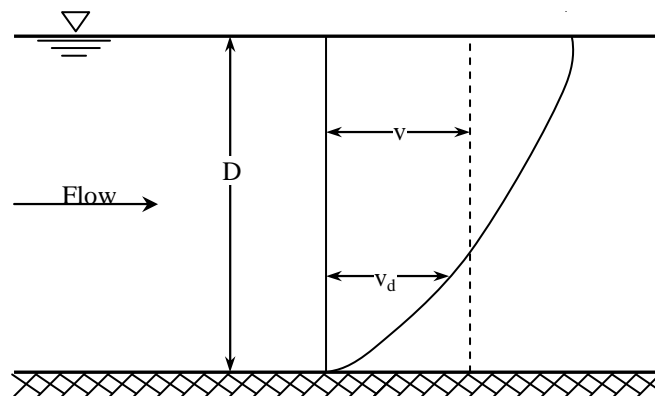


FIGURE 2.2: TYPICAL VELOCITY DISTRIBUTION WITH DEPTH IN A RIVER

The vertical changes in water velocity, related to collisions of local masses of fluid above the bed, produce shear forces parallel to the bed similar to the friction force felt when you slide your hand across a surface. The magnitudes of shear stresses that develop at the solid boundary of a channel are used as the most common way to measure flow competence. To calculate shear stress, the laws of motion are used to derive the formula for shear stress that can be given (in two-dimensional flow) as:

$$\tau = \gamma DS \quad (2.4)$$

where τ is shear stress, γ is specific weight of water, D is water depth, and S is slope of the channel. As Equation 2.4 shows, the amount of shear stress that develops depends on the flow velocity (represented through slope) and depth of flow. Therefore, the larger is the discharge, such as during a flood, the larger will be the bed shear stress. Given a river bed with a particular particle size distribution, there exists

a discharge for which the bed shear stress reaches a critical value τ_c and causes sediment transport to begin. Moreover, considering single particles, it has been found that critical shear stress is proportional to the particle diameter.

Many formulas and diagrams make use of shear stress, or of variables with which shear stress has a functional relation, to determine whether sediment transport will ensue. Two commonly used diagrams are those of Shields (1936) and Hjulstrom (1935). Figure 2.3 shows the Shields diagram, which makes use of dimensional analysis and gives dimensionless shear stress plotted versus dimensionless boundary Reynolds number. For a given boundary Reynolds number, small dimensionless shear stresses fall below the line of relation and represent stable beds, whereas large dimensionless shear stresses fall above and represent beds that move. Thus, the line in the graph represents critical conditions for a wide range of particle sizes.

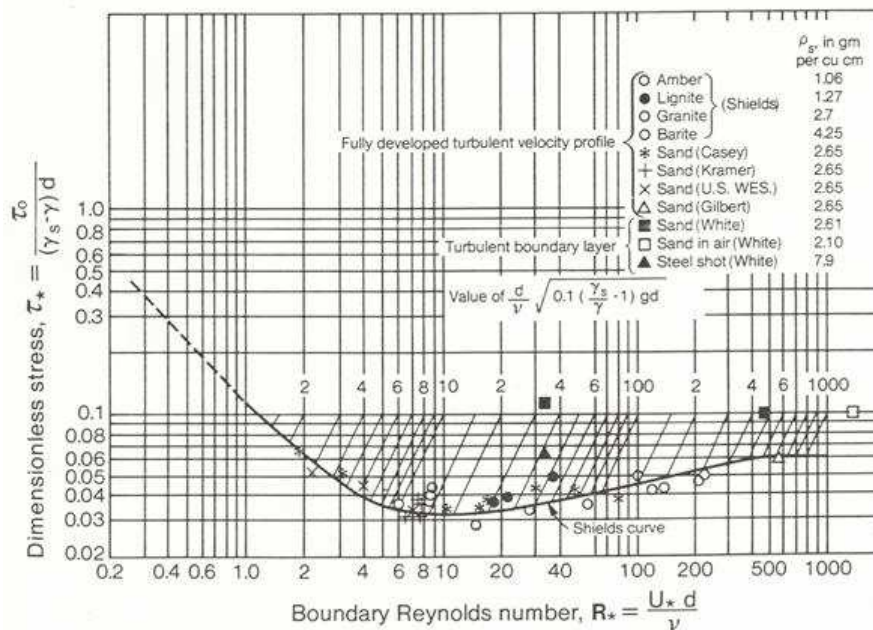


FIGURE 2.3: SHIELDS DIAGRAM FOR INCIPIENT MOTION (VANONI, 1975; YANG 1996)

Hjulstrom analyzed the average flow velocities necessary to move sediment and produced a diagram (shown in Figure 2.4) that gives the relationship between particle size and average flow velocity. The diagram has three zones and two dividing lines. One line gives the critical velocity for erosion and transport of a stable particle. The other line gives the velocity at which a moving particle will deposit on the bed and become stable.

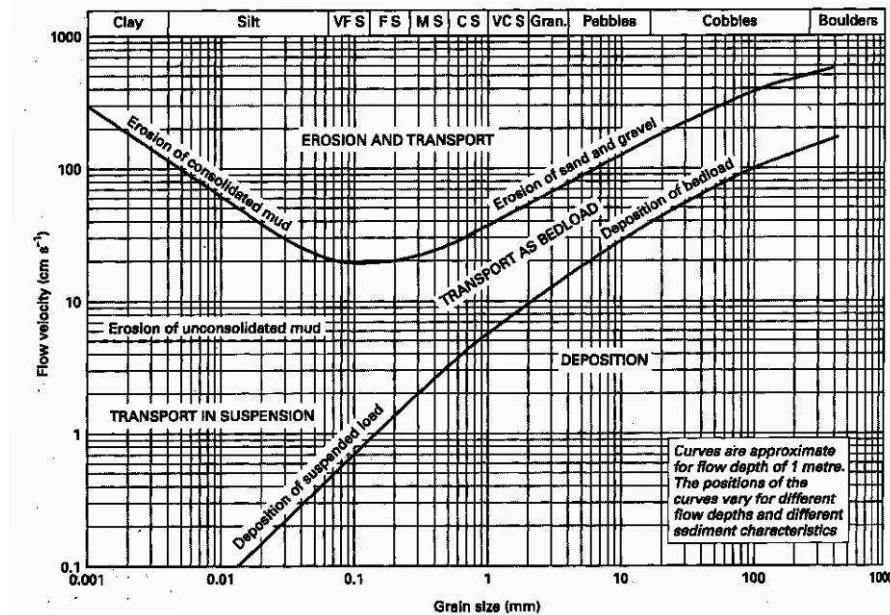


FIGURE 2.4: HJULSTROM DIAGRAM FOR INCIPIENT MOTION (HJULSTROM, 1935)

In a heterogeneous bed, the Shields diagram does not produce the fully accurate predictions of incipient bed-load transport. This is due to a hiding-exposure effect, where finer particles located in the interstitial spaces between larger particles are protected from entrainment (Andrews, 1983; Komar, 1987; Kuhnle, 1993; Wilcock, 1993).

Keeping the idea of selective entrainment in mind, there are two generally accepted types of transport that result following exceeding of critical shear stress: selective transport and equal mobility. Because exposed fine grains become suspended at lower shear stresses than coarse grains, selective transport states that there will be a preferential entrainment of finer particles at discharge levels insufficient to move the larger clasts. The subsequent deposition of the finer particles farther downstream, where channel gradient decreases and shear stresses lessen, would lead to the phenomenon of downstream fining.

On the other hand, the concept of equal mobility considers hiding effects by acknowledging the development of a pavement of coarser particles on the surface of the bed. This pavement must be mobilized prior to transport of the finer substrate material. The theory states that following destruction of the pavement, all particle sizes are equally mobilized when scaled by their concentration in the mixture. The researchers who developed this theory showed equal particle mobility on a reach scale in well-mixed gravels (Parker et al., 1982). Furthermore, Parker et al. developed an empirical gravel transport relationship between a dimensionless bed-load transport function W_i^* and dimensionless shear stress parameter ϕ_i based on field data (see Figure 2.5 Yang, 1996).

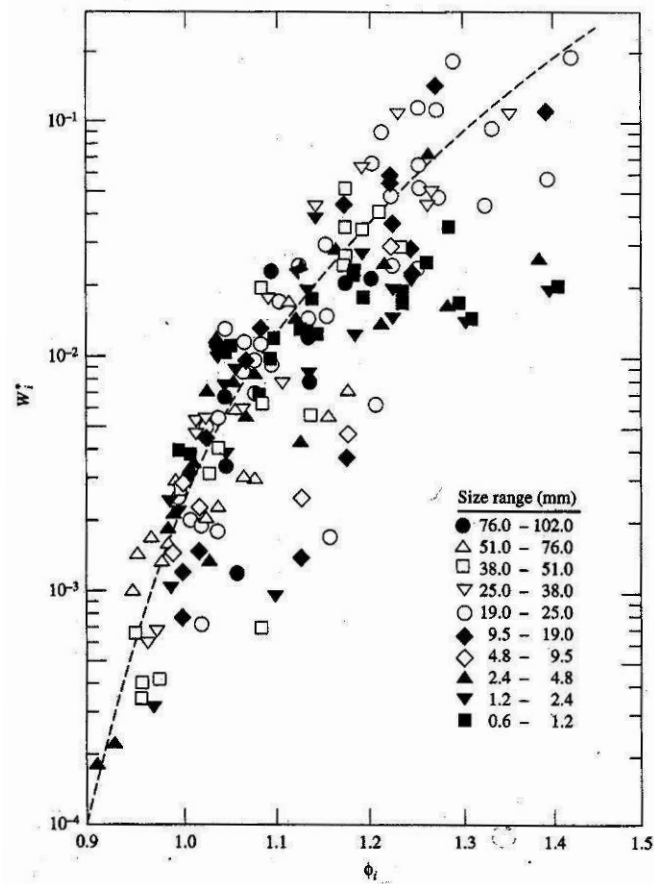


FIGURE 2.5: SIMILARITY PLOT OF EMPIRICAL GRAVEL TRANSPORT FUNCTION WITH INDICATED SIZE RANGES (PARKER ET AL., 1982; YANG 1996)

The possibilities of having selective transport and equal mobility have serious contradicting ramifications for downstream fining. If equal mobility is the transport method observed, then downstream fining should not exist as all particle sizes are mobilized simultaneously (Ferguson et al., 1996). However, researchers such as Surian (2002) have considered the problem closely and have found that both equal mobility and selective sorting may operate on the same river. Where local shear stress vastly exceeds critical shear stress, equal mobility becomes the method of sediment transport (Constantine et al., 2003). In consequence, Constantine speculated that downstream fining is the strongest in self-formed alluvial reaches where critical shear averages a threshold value 0.031, but minimal in confined reaches where critical shear exceeds that required for equal mobility to ensue at bank-full discharge. In other

words, flows producing conditions at and somewhat larger than critical shear stress may allow selective transport to dominate, whereas larger flows producing higher shear stresses may allow equal mobility to govern.

Variations in shear stress due to irregularly-shaped beds can lead to areas called “patches” where equal mobility is dominant and the particle distribution does not correspond with that of the exponential downstream fining trend (Paola and Seal, 1995; Seal and Paola, 1995). Furthermore, researchers have found that in natural rivers the downstream fining profiles can be exponential for short distances downstream, only to deviate from the predicted pattern when lateral sediment sources introduced larger clasts is to the river channel.

2.5 Significance of disruptions in downstream fining profile

The disruptions in the downstream fining trend along a river are called discontinuities. The lengths of river that lie between these discontinuities have been named sedimentary links (Rice, 1999). Sedimentary links tend to exist on a scale of 10^0 to 10^2 km (0.62 to 17.4 miles), though there is much ‘noise’ in the data used due to lateral effects, etc. (Rice, 1999). Some tributaries that contribute to the influx of sediment were also found to be the cause of a discontinuity. Potential tributary-originated disruption depends on the water discharge of the tributary, particle distribution of sediment delivered by the tributary, and rate of sediment transport into the main channel from the tributary (Ferguson et al., 1996; Ichim and Radoane, 1990; Rice, 1998; Surian, 2002). Therefore, it can be concluded that disruptions in the fining trend may be used to identify areas along the river where natural or anthropogenic disturbances occur.

This provides two different ways that an analysis of the downstream fining trend in a given river can be used to detect disturbances. Local disturbances can be uncovered by noting disruptions in the fining trend. That is, if there is significant reversal in the tendency toward smaller particle sizes downstream, an investigation of areas

immediately upstream may uncover lateral inputs originating from natural or unnatural sources. Larger-scale changes (such as changes in climate) can be revealed through analysis of rates of fining. For example, a significant change in the rate of erosion due to a shift in climate could drastically increase the rate of sediment input. This could then cause rates of downstream fining to be significantly different from rates of downstream fining observed prior to the change in climate.

Rates of downstream fining have been linked to concavity of the river profile, where higher profile concavities are associated with higher rates of downstream fining (Blissenbach, 1954; Hoey and Ferguson, 1997). Furthermore, it has been speculated that rapid fining within sedimentary links is related to rapid declines in channel gradient (Surian, 2002). Rice (1999) found that gradual reductions in channel gradient are indicative of longer sedimentary links. Even with this finding, Rice also found a significant but not strong correlation between fining rate and change of channel gradient ($r = 0.81$). This supports the theory that textural changes occur as a means to stabilize the longitudinal profile of rivers. For example, Ferguson et al. (1996) noted that rates of downstream fining are much higher than aggradation otherwise required for equilibrium.

Ferguson et al. also related downstream fining to the tendency of river hydraulics to minimize downstream variation in bed-load transport rates. Seal et al. (1997) supported the findings of Ferguson et al. (1996), noting that sediment feed rate, hence aggradation rate, had a weak effect on the fining rate during their laboratory studies. Moreover, numerical models by Hoey and Ferguson, 1997, and Robinson and Slingerland, 1998, show that the rate of downstream fining is reduced when rates of sediment supply from upstream are increased (Hoey et al., 1999).

Additional information on controls of fining rates originates from studies of alluvial fans (Hoey et al., 1999; Rice, 1999). Alluvial fans are depositional zones where rivers enter areas of abruptly flattening slopes, and where there is longitudinal fining of incoming sediment from catchments. Through comparisons of alluvial fans, Hoey et al. found that fining rates can be explained by geologic conditions (lithology, tectonic

setting), basin morphology (rate of sediment supply and grain size distribution), and physical processes (selective transport, lateral and vertical exchange of sediment). Correspondingly, slope reduction above a local base level control is reported to be one geomorphologic cause of downstream fining (Ferguson et al., 1996). Hoey et al. also found that rivers can have equilibrium fining rates and be near equilibrium only to have the balance interrupted by factors that create discontinuities in the downstream fining trend (such as lateral input of unconsolidated sediment from landslides).

Robinson and Slingerland (1998) suggest that the rate of land subsidence (due to compaction) and sediment supply are the most important controls over downstream fining profiles according to their comparison of alluvial fans. They state that subsidence causes enhanced deposition, especially in reaches closest to areas of significant sediment input. Furthermore, they reported degradation to be induced by base level (sea level) fall, which they assert, leads to increased rates of downstream fining. Correspondingly, they report that the aggradation initiated during base level rise leads to decreased rates of downstream fining. In their 1999 research, Seal et al. investigated fining in a laboratory study. Their results show that as progradation of alluvial deposits develop, the rate of downstream fining is controlled by the available length of the distributions, rather than rates of vertical aggradation.

Table 2.1 contains a summary of the major recent findings by investigators studying downstream fining. Information is given in chronological order. The findings can be applied to gravel-bed rivers such as the Kilchis River.

TABLE 2.1: SUMMARY OF PAST INVESTIGATIONS OF DOWNSTREAM FINING

AUTHOR	CO-AUTHOR(S)	STUDY DATE	STUDY CONDITIONS/METHODS		FINDINGS
			Laboratory	Field	
P.J. Ashworth	Rob Ferguson, Chris Paola, D.M. Powell, and K.L. Prestegard	1992		Bulk samples, pebble counts, velocity measurements	<ul style="list-style-type: none"> ▪ d_{50} was consistent both spatially and temporally. ▪ Weak size selection at entrainment ▪ Maximum bed-load d_{max} showed a weak but significant relation to shear stress showing some size selection
Chris Paola	Gary Parker, Rebecca Seal, Sanjiv Sinha, John B. Southard, and Peter R. Wilcock	1992	Steady flow and sediment influx in a 45m long flume		<ul style="list-style-type: none"> ▪ Significant fining can be produced over short distances with sufficiently poorly sorted/bimodal gravel. ▪ Bimodality and large standard deviation is important for producing size dependent variation in mobility. ▪ Variation in discharge and preexisting slope not important to produce downstream fining.
Trevor Hoey	Rob Ferguson	1994	Numerical simulation	Verification using Allt Dubhaig River, Scotland	<ul style="list-style-type: none"> ▪ Slight size selection can produce rapid fining through downstream changes in flow hydraulics. Surface grain size is a dependent variable. ▪ Hiding parameter, sediment supply, and sediment exchange processes very important. ▪ No sensitivity to reference shear stress or active layer thickness.
Tevor Hoey	Brian J. Bluck	1999	Used previous studies	Used previous studies	<ul style="list-style-type: none"> ▪ Changes in downstream fining trend can indicate disturbance but controls are interdependent. This makes identifying disturbance using fining difficult. ▪ Suggests that fining results from preferential deposition instead of selective entrainment. ▪ Suggests that fining rates are interdependent with shape and length of the channel. ▪ Fining is a byproduct of channel adjustment to sediment load.
Yoshinori Kodama		1994		Bulk samples	<ul style="list-style-type: none"> ▪ Rapid changes in lithology cannot be explained by sorting processes. Diminution coefficient 0.089 km^{-1} (0.14 mi^{-1}) ▪ Longitudinal changes in show size selection in every size class suggesting abrasion.
Yoshinori Kodama		1994		Rotating drum with three interior vanes	<ul style="list-style-type: none"> ▪ Particles of differing lithology abrade at differing rates. ▪ Abrasion depends on the presence of different sizes.
Rebecca Seal	Chris Paola	1995	Bulk Smapling, Wolman Sampling	Abrasion tests	<ul style="list-style-type: none"> ▪ Fining observed over a short length (5.45 km or 3.39 mi) ▪ Diminution coefficient 1 km^{-1} (1.6 mi^{-1}) much higher than the reported $0.001- 0.05 \text{ km}^{-1}$ ($0.001 - 0.08 \text{ mi}^{-1}$, Shaw and Kellerhals 1982). ▪ Models that use patchiness as sole mechanism of fining show comparable results to field observations. ▪ Shape of fining profile strongly influenced by depositional profile (sampling method matters).

TABLE 2.1: SUMMARY OF PAST INVESTIGATIONS OF DOWNSTREAM FINING (CONTINUED)

AUTHOR	CO-AUTHOR(S)	STUDY DATE	STUDY CONDITIONS		FINDINGS
			Laboratory	Field	
James Pizzuto		1995	Wolman Sampling	Numerical model	<ul style="list-style-type: none"> ▪ Fining strongly influenced by spatial distribution of sizes of gravel supplied at zero order basins. ▪ Lateral sources account for 80% of the decrease in sediment size. ▪ Improved models should include lateral sources ▪ Gravel transport should be time dependent making time scale and geologic history important in fining studies.
Rob Ferguson	Trevor Hoey, Simon Wathen, Alan Werrity	1996	Pebble counts and tracer pebbles		<ul style="list-style-type: none"> ▪ Showed size selection domination. ▪ Tracer pebbles disbursed in a size selective way. ▪ Numerical model results showed a comparable fining profile develop without an initial profile.
Nicole M. Gasparini	E. Tucker, Rafael L. Bras	1999		Landscape evolution model (GOLEM)	<ul style="list-style-type: none"> ▪ Fining profiles can arise from erosion in a drainage basin without the need of selective erosion in headwaters. ▪ Dynamic bed adjustment alone can cause fining. Therefore in absence of selective transport abrasion is not the only other option. ▪ Bed texture adjusts to spatial variations in shear stress and sediment supply.
Stephen Rice		1999	Wolman samples, stream survey		<ul style="list-style-type: none"> ▪ Exponential decay models most appropriate. ▪ Abrasion found to be unimportant. ▪ Rapidly declining gradients linked to rapid fining. More importantly link length and diminution rate are linked. ▪ Efficiency of longitudinal sorting is the primary determinant of within link fining rates.
Basil Gomez		2001	Wolman samples, bulk samples		<ul style="list-style-type: none"> ▪ Fining pattern continuous despite lateral inputs (104 km or 65 mi). ▪ Not affected by aggradation fining rates selective transport dominated. ▪ Lateral inputs have a similar particle distribution to bed-load. ▪ Length scale of the deposit appeared to govern fining rates (concavity)
Paul Heller		2001	Wolman samples, tree core samples,		<ul style="list-style-type: none"> ▪ Continuous introduction of new material inhibits fining trend. ▪ Tumbler study showed weathered clasts break down rapidly.
Nicole Surian		2001	Wolman samples		<ul style="list-style-type: none"> ▪ Weak fining rates due to lateral inputs, barrages, and human influence. ▪ Exponential model gives best estimate of fining pattern.
Candice Constantine	Jeffery F. Mount and Joan Florsheim	2003	Bulk samples		<ul style="list-style-type: none"> ▪ Fining is strongest where shear stress is at the threshold required for motion. ▪ Elevated shear stress leads to equal mobility and lower fining rates.

2.6 Synthesis of downstream fining knowledge for dissertation research

This dissertation centers on understanding and characterizing downstream fining as part of sediment transport in the gravel-bed rivers of Western Oregon, both upstream and within the zone of tidal influence. Investigation of downstream fining allows for a comprehensive analysis of the sediment transport regime, as well as factors that influence sediment transport. Downstream fining is useful for these purposes because changes in bed composition in the downstream direction are inextricably linked to rates of sediment input, the physics and rates of sediment transport, and disturbance regimes of rivers.

The dominant mechanisms that were reported to drive downstream fining are abrasion and sorting. The literature suggests that there are physical indicators that give clues as to the mechanism (abrasion or selective sorting) that drives the downstream fining phenomenon in any given system. Therefore, physical parameters of rivers in Oregon may be compared to those reported in the literature to gain insight about how and why downstream fining operates in gravel-bed rivers.

Factors reported to determine the significance of abrasion include lithology of particles being transported, length of depositional basins, and length between significant lateral inputs of sediment to channels. That is, durability of particles and potential for collisions (a function of length of transport), are important. Therefore, ascertaining the role of abrasion includes a study of particle lithology, coupled with a review of the lengths over which downstream fining occurs prior to disruption from lateral sources. Consequently, information is gathered on the disturbance regime (e.g., landslide activity) and the resilience of the downstream fining phenomenon (i.e., whether or not lateral sources are inadequate alter the rate of downstream fining).

According to the literature, for irregularly-shaped beds, particular hydraulic characteristics must exist for selective sorting to dominate. Shear stresses on the bed,

which depend on flow characteristics and channel geometries, must be large enough to mobilize particles. However, consideration of the magnitude and distribution of shear stresses is necessary. So-called ‘patchiness’ was linked to areas in channels where shear stresses necessary for bed movement were so great that equal mobility dominated over selective transport. This was due to bed armoring, which refers to a surface layer ‘pavement’ of large particles that protect smaller sub-surface particles from transport. Therefore, the study of in-stream forms such as sidebars, where the level of armoring is determined by the location on the bar, can provide insight into the sediment transport regime, as well regarding the existence of selective-transport-dominated downstream fining.

The rate of fining has also been used by past investigators to characterize sediment transport through downstream fining. Rates of fining have been reported to be determinants of the type of dominant mechanism causing fining. Rates of fining also have been used to verify use of Sternberg’s exponential model for sediment size decreases for systems dominated by selective sorting compared to abrasion-dominated systems. Moreover, past researchers have also linked rates of fining to concavity of channels, where steeper channel profiles lead to greater rates of downstream fining. This is an important outcome of past research because characterization of downstream fining, both upstream and through the zone of tidal influence, must involve a shift from reaches of higher to lower channel gradients. Furthermore, Rice’s findings that downstream fining operates regardless of the decreases in gradient indicative of longer sedimentary links, is vital for characterization of sediment transport in the near-sea-level environment.

Finally, results from previous numerical analyses used to simulate downstream fining lend support to the research presented herein. It has been reported that a model that can successfully simulate downstream fining would not only be useful for estimating changes in grain size along natural gravel-bed rivers but would also be useful for estimating grain size parameters for sediment routing and watershed evolution numerical models (e.g., Pizzuto 1995; Gasparini, 1999). This lends itself to showing the usefulness of characterizing sediment transport via numerical models.

3 Literature Review on River Hydraulics and Sediment Transport with Tidal Influence

3.1 Fundamental Principles

3.1.1 Introduction

Bed-load transport near the outlets of coarse-bed rivers and streams is a topic that has been generally overlooked in preference to studies of suspended sediment. This is perhaps because such outlets are viewed as bed-load deposition zones. For studies of navigation or non-point source pollution, the main interest lies in the fate of sand, silt, and/or contaminants originating from river systems. Therefore, though there are studies that consider the connection between tidal cycles and sediment transport at outlets, not much information is available regarding the effects on bed-load transport or on the corresponding empirical and theoretic bed-load transport relationships.

Literature that suggests ways to view sediment transport with tidal influence typically evoke the scenario of flow into a reservoir or lake (Chang, 1988; Julien, 1995; Klingeman, 2000). While this assumption is a widely used, and has yielded acceptable results in applications such as numerical modeling (e.g., HEC 6 and GSTARS 2.1), the need for more in-depth understanding and study of this natural scenario still exists. How this scenario can be expanded to describe clearly the mechanics of bed-load transport is discussed in this section.

3.1.2 Description of fundamental principles

The movement of sediment is dependent on flow characteristics of the surrounding fluid. The vital parameters of interest when studying sediment transport can be ascertained for any system using three physical laws that lead to relations for flow

depth and velocity. These are: the conservation of mass, the conservation of momentum, and the conservation of energy principles. Various textbooks provide detailed descriptions of these laws (e.g. Henderson, 1966; Chow 1988; Munson et al. 1990; Chanson, 1999; Strum 2001; Akan 2006). A summary has been synthesized here from these texts.

The conservation of mass principle is shown mathematically in Equation 3.1. Conservation of mass states that given a closed system (without regard to relativity effects), mass within the system is constant with respect to time:

$$\frac{dM_{sys}}{dt} = 0 \quad (3.1)$$

where M_{sys} can be rewritten using the definition of density (mass per unit volume) shown by Equation 3.2. With integration methodology, this becomes Equation 3.3:

$$\rho = \frac{M}{V} \quad (3.2)$$

$$\frac{dM}{dt} = \frac{d}{dt} \iiint \rho dx dy dz = 0 \quad (3.3)$$

where ρ , M and V are density, mass, and volume respectively, and dx , dy , dz describe the three dimensions for an incremental volume based on the Cartesian (x-y-z rectangular) coordinate system. Expanding the above relationship with respect to time, the mass flow-rate shown mathematically as Equation 3.4:

$$\frac{\Delta(\rho A \Delta x)}{\Delta t} = \rho Q_U - \rho Q_D \quad (3.4)$$

where Q_U and Q_D are the upstream and downstream discharge values, respectively, and flow occurs in the x direction.

In Cartesian coordinate form, the continuity equation is then:

$$\frac{\partial \rho}{\partial t} + \frac{\partial(\rho v_x)}{\partial x} + \frac{\partial(\rho v_y)}{\partial y} + \frac{\partial(\rho v_z)}{\partial z} = 0 \quad (3.5)$$

where v_x , v_y , and v_z , are the velocity components in the x, y, and z, directions, respectively.

For the case of incompressible fluids where density remains constant, such as water in a river channel, Equation 3.4 then becomes:

$$\frac{\partial(v_x)}{\partial x} + \frac{\partial(v_y)}{\partial y} + \frac{\partial(v_z)}{\partial z} = 0 \quad (3.6)$$

From Equation 3.6, it can be said for systems such as rivers the inflow equals the outflow. Considering a control volume of fluid where mass and energy are assumed to remain constant, this balance is generally applied by integrating Equation 3.6 across two cross-sections of known area:

$$Q = \int_{A_1} v dA = \int_{A_2} v dA \quad (3.7)$$

where Q is discharge in a channel with no flow across its side or bottom boundaries. After integration of Equation 3.7, the relationship becomes:

$$Q = v_1 A_1 = v_2 A_2 \quad (3.8)$$

where v_1 and v_2 are the velocities and A_1 and A_2 the areas of the two cross-sections.

Using Equation 3.7, the basic channel geometry (represented by cross-sectional area) and the flow-rate are now relatable. Calculations of the various variables can now be completed given some known data.

The second important physical law is the conservation of momentum. This originates from Newton's second law of motion for a system. The law states that time rate of change of linear momentum of the system must be equal to the sum of the external forces acting on the system. Given that momentum (p_m) is defined as mass multiplied by velocity and mass is equal to density multiplied by volume:

$$p_m = mv \quad (3.9)$$

$$m = \rho dV \quad (3.10)$$

Newton's second law is transformed as shown in Equation 3.11. This says that the change in momentum equals the sum of all forces applied to the control volume:

$$\sum F = \frac{d}{dt}(mv) = \frac{\partial}{\partial t} \left(\int_{cv} \rho v dV \right) + \int_{cs} v \rho v dA \quad (3.11)$$

where

$$\frac{d}{dt}(mv) = \begin{array}{l} \text{Time rate of change in linear} \\ \text{momentum in the system momentum} \end{array}$$

$$\frac{\partial}{\partial t} \left(\int_{cv} \rho v dV \right) = \begin{array}{l} \text{Time rate of change of linear} \\ \text{momentum of the contents of the} \\ \text{control volume} \end{array}$$

$$\int_{cs} \rho v dA = \begin{array}{l} \text{Net rate of flow of linear momentum} \\ \text{through the control surface} \end{array}$$

The forces acting on the control volume represented by the changes in momentum shown in Equation 3.11 are: (1) the surface forces (i.e. pressure and shear forces) acting on the control surface and (2) the volume force (i.e. gravity) applied at the center of mass of the control volume. Equation 3.11 can be re-written for an infinitesimally small volume applied to the i component of the vector equation, as shown in Equation 3.12:

$$\frac{d(\rho v_i)}{dt} = \left(\frac{\partial(\rho v_i)}{\partial t} + \sum_j v_j \frac{\partial(\rho v_i)}{\partial x_j} \right) = \rho F_{vol_i} + \sum_j \frac{\partial \sigma_{ij}}{\partial x_j} \quad (3.12)$$

where

$$\frac{\partial(\rho v_i)}{\partial t} + \sum_j v_j \frac{\partial(\rho v_i)}{\partial x_j} = \begin{array}{l} \text{The sum of the momentum} \\ \text{accumulation plus the momentum flux} \end{array}$$

$$\rho F_{vol_i} = \begin{array}{l} \text{The resultant of the volume forces} \\ \text{per unit volume (i.e. } -\nabla(gz) \text{ or} \\ \text{potential energy)} \end{array}$$

$$\sum_j \frac{\partial \sigma_{ij}}{\partial x_j} = \text{Summation of shear forces}$$

Furthermore, the stress tensor σ_{ij} can be described in terms of the linear relationship

between the magnitude of shear stress τ and the rate of deformation $\frac{\partial V}{\partial y}$. That is:

$$\sigma_{ij} = -P\delta_{ij} + \tau_{ij} \quad (3.13)$$

$$\tau_{ij} = -\frac{2\mu}{3}\epsilon\delta_{ij} + 2\mu\epsilon_{ij} \quad (3.14)$$

$$\varepsilon_{ij} = \frac{1}{2} \left(\frac{\partial v_i}{\partial x_j} + \frac{\partial v_j}{\partial x_i} \right) \quad (3.15)$$

$$\varepsilon = \text{div} \mathbf{v} = \nabla \mathbf{v} = \sum_i \frac{\partial v_i}{\partial x_i} \quad (3.16)$$

where τ_{ij} is the shear stress component of the i momentum transported by the j direction, and δ_{ij} is the identity matrix element: $\delta_{ii} = 1$ and $\delta_{ij} = 0$ (for different i and j).

However, because the stress forces on a Newtonian fluid are the pressure and viscous forces, Equation 3.12 can be re-written in Cartesian coordinates for such fluids as:

$$\left(\frac{\partial(\rho v_x)}{\partial t} + \sum_j v_j \frac{\partial(\rho v_x)}{\partial x_j} \right) = \rho F_{vol_x} - \frac{\partial P}{\partial x} + F_{visc_x} \quad (3.17a)$$

$$\left(\frac{\partial(\rho v_y)}{\partial t} + \sum_j v_j \frac{\partial(\rho v_y)}{\partial x_j} \right) = \rho F_{vol_y} - \frac{\partial P}{\partial x} + F_{visc_y} \quad (3.17b)$$

$$\left(\frac{\partial(\rho v_z)}{\partial t} + \sum_j v_j \frac{\partial(\rho v_z)}{\partial x_j} \right) = \rho F_{vol_z} - \frac{\partial P}{\partial x} + F_{visc_z} \quad (3.17c)$$

where j corresponds to the Cartesian coordinate components (i.e. $j = x, y, z$) and the vector of the viscous force is:

$$F_{visc_i} = \text{div} \tau_i = \sum_j \frac{\partial \tau_{ij}}{\partial x_j} \quad (3.18)$$

For a Newtonian fluid with incompressible flow and constant viscosity, the motion equation becomes the Navier-Stokes Equation:

$$\rho \left(\frac{\partial(v_x)}{\partial t} + \sum_j v_j \frac{\partial(v_x)}{\partial x_j} \right) = \rho F_{vol_x} - \frac{\partial P}{\partial x} + F_{visc_x} \quad (3.19a)$$

$$\rho \left(\frac{\partial(v_y)}{\partial t} + \sum_j v_j \frac{\partial(v_y)}{\partial x_j} \right) = \rho F_{vol_y} - \frac{\partial P}{\partial x} + F_{visc_y} \quad (3.19b)$$

$$\rho \left(\frac{\partial(v_z)}{\partial t} + \sum_j v_j \frac{\partial(v_z)}{\partial x_j} \right) = \rho F_{vol_z} - \frac{\partial P}{\partial x} + F_{visc_z} \quad (3.19c)$$

The energy equation shares similarities with the momentum equation but is derived from a different physical law. The first law of thermodynamics states that the net energy supplied to the system is equal to the increase in energy of the system plus the energy that is lost to the system through work. Stated mathematically the law is:

$$\frac{dE}{dt} = \frac{dQ_h}{dt} - \frac{dW_s}{dt} - \frac{dW_p}{dt} = \frac{d}{dt} \int_{CV} e \rho dV + \int_{CS} e \rho (\mathbf{V} \cdot \mathbf{n}) dA \quad (3.20)$$

where E is the total energy of the system, Q_h is the heat transfer to the fluid, W_s is the shaft work done by hydraulic machines, W_p is the work done by fluid pressure forces, and e is the sum of the internal energy, kinetic energy, and potential energy per unit mass.

3.2 Extension of fundamental principles

In application, the momentum equation is simplified by selecting a control volume with a control surface perpendicular to the direction of flow. It then follows that for a steady incompressible flow, forces acting on the control volume in the direction of flow are equivalent to the rate of change in the flow momentum. Therefore, the momentum accumulation would be zero and the momentum equation would become:

$$\sum F_s = \rho_2 A_2 v_2 v_{s2} - \rho_1 A_1 v_1 v_{s1} \quad (3.21)$$

Combined with the continuity equation for a steady and incompressible flow, Equation 3.21 would further simplify to Equation 3.22, where it is still stated that the change in momentum flux is equal to the sum of all volume and surface forces acting on the control volume:

$$\sum F_s = \rho Q (v_{s2} - v_{s1}) \quad (3.22)$$

where $\sum F_s$ is the resultant of all forces in the flow direction, subscripts 1 and 2 refer to the upstream and downstream cross-sections, respectively, and $(v_{s})_{i=1,2}$ is the velocity component in the flow direction.

In addition to Equations 3.8 and 3.22 the Bernoulli equation is a very useful, if not the most useful, relationship when analyzing fluid flow such as finding velocities and pressures at points in the flow connected by a streamline. The Bernoulli equation can be derived from the Navier-Stokes equation. To derive the Bernoulli equation a few assumptions must be made, namely:

- Flow is along a streamline
- The fluid is frictionless (i.e. $F_{\text{visc}} = 0$)
- The volume force potential (i.e. gravity) is independent of time (i.e. $\partial U / \partial t = 0$)
- Flow is steady (i.e. $\partial V / \partial t = 0$)
- Flow is incompressible (i.e. $\rho = \text{constant}$)

With these assumptions in place, the Navier-Stokes equation becomes:

$$\rho v \frac{dv}{ds} = -\rho g \frac{dz}{ds} - \frac{dP}{ds} \quad (3.23)$$

where v is the velocity along the streamline, s is the direction along the streamline, and g is acceleration of gravity. With the condition of no flow across a streamline and the velocity aligned in the s -direction, Equation 3.23 becomes:

$$\rho v dv = -\rho g dz - dP \quad (3.24)$$

or

$$\frac{dP}{ds} + g dz + d\left(\frac{v^2}{2}\right) = 0 \quad (3.25)$$

Integration of Equation 3.23 along a streamline yields the Bernoulli equation:

$$\frac{P}{\rho} + gz + \frac{v^2}{2} = \text{constant} \quad (3.26)$$

The momentum and Bernoulli equations are functional enough to be used in many open channel applications. However, there are applications such as when lateral flow direction is unknown in a spatially-varied flow scenario.

The Bernoulli equation can also be derived from the conservation of energy principle. If we look at a control volume with control surface perpendicular to the flow, the energy equation for the volume would include potential energy due to its height above the datum and kinetic energy due to its velocity. These are shown as:

$$\text{potential energy} = mgz \quad (3.27)$$

$$\text{kinetic energy} = \frac{1}{2}mv^2 \quad (3.28)$$

The fluid would also have an energy component due to the work done by the pressure, which generates a force causing the fluid to be in motion. This force is equal to the pressure multiplied by area, as pressure is force divided by area:

$$\text{force} = PA \quad (3.29)$$

Furthermore, the work done by this force is equal to the force multiplied by the length of the control volume, where the length of the control volume can be obtained mathematically using the definition of density:

$$\rho = \frac{m}{V} \quad (3.30)$$

therefore

$$V = \frac{m}{\rho} \quad (3.31)$$

and

$$\text{length of control volume} = \frac{m}{\rho A} \quad (3.32)$$

resulting in our pressure work component:

$$\text{work due to pressure} = PA \times \frac{m}{\rho A} = \frac{pm}{\rho} \quad (3.33)$$

Without consideration of changes in internal energy due to heat transfer, energy losses due to friction, or energy gains from mechanical devices, the total energy is made up of these three components. If we divide each component by weight of the fluid mass, we then obtain Equation 3.34, the total energy per unit weight (H):

$$\frac{p}{\rho g} + \frac{v^2}{2g} + z = H \quad (3.34)$$

Note the pressure component, velocity component, and potential component are named the pressure head, velocity head, and potential head, respectively, when given in the form of Equation 3.34. The total energy per unit weight is then the total head and is a constant. Compared to Equation 3.26, this is the Bernoulli equation.

However, unlike the conservation of momentum derivation, we can extend this form of the Bernoulli equation to include energy loss due to friction (h_f) as a volume of fluid moves from one section of a stream tube to another:

$$\frac{p_1}{\rho g} + \frac{v_1^2}{2g} + z_1 = \frac{p_2}{\rho g} + \frac{v_2^2}{2g} + z_2 + h_f \quad (3.35)$$

To use these principles fully and properly, it is important to be aware of the types of flow conditions to which each equation is appropriate for application. This involves knowledge of flow regimes. Furthermore, knowledge of how changes in flow regime affect the conservation principles is a major step to understanding sediment transport with tidal influence.

3.2.1 *Characterization of flow regime*

The basic idea behind the characterization of flow conditions is to describe what is happening to the characteristics of the flow (i.e., velocity, density, depth, bottom shear stress, etc.) over time and distance. The temporal part of the characterization involves two possible scenarios variation: steady and unsteady flow. When flow is steady, conditions are constant over time at any given location. When flow is unsteady, conditions change over time at any given location. The spatial part of the characterization involves two possible scenarios for spatial variation: uniform and nonuniform flow. When flow is uniform, conditions are constant over distance at any given instant in time. When flow is nonuniform, conditions change over distance at any given instant.

Combinations of these scenarios can be used to categorize a wide range of applications. Each combination or group of situations is solvable by particular

conservation equations, given the flow conditions and the assumptions involved in the formulas to be used. For example, for a steady nonuniform flow, one application may be a hydraulic jump, where flow abruptly transitions from supercritical flow to subcritical flow (e.g., downstream of a partially closed gate). This transition is accompanied by a significant amount of turbulence and loss of energy (Henderson 1966). Neglecting bottom shear stresses, the equations used to describe this case would be the modified continuity and momentum equations, shown as Equations 3.36 and 3.37, respectively:

$$v_1 y_1 B = v_2 y_2 B \quad (3.36)$$

$$\rho Q(V_{s2} - V_{s1}) = \left(\frac{1}{2} \rho g y_1^2 - \frac{1}{2} \rho g y_2^2 \right) B \quad (3.37)$$

where $y_{1,2}$ are the upstream and downstream depths and B is the width of the channel. A surge is the unsteady form of a hydraulic jump. Surge waves are caused by a sudden change in flow (e.g., such as the reduction in depth of flow caused during partial or full closure of a gate). If the cause of the surge wave is tidal in nature, it is called a bore. The same modified continuity and momentum equations can be used to describe this case. However, this situation must be analyzed in a ‘quasi-steady’ state (i.e., from the viewpoint of an observer moving in the same direction and at the same velocity as the surge).

Table 3.1 shows typical flow conditions as characterized according to whether flow conditions change with respect to time (steady versus unsteady) or with respect to distance (uniform versus nonuniform) as compiled by Klingeman (2000).

TABLE 3.1: COMMON TYPES OF FLOW CONDITIONS

SPACE TIME	UNIFORM	NONUNIFORM	
		Gradually-varied	Rapidly-varied
Steady	common- canal design	common- backwater curves	common- hydraulic jumps
Unsteady	rare	common- flood waves	common- surges and bores

3.2.2 *Gradually-varied flow*

For the case of a river entering a reservoir, many non-flood flow conditions can be considered to be represented by steady, gradually-varied, nonuniform flow. For gradually-varied flow, engineers typically compute water surface profiles using so-called ‘backwater’ calculations that incorporate shear forces as flow resistance. Knowledge of the characteristics of water surface profiles is essential for application to a wide range of gradually-varied flow situations, to allow calculating the distribution of energy along the reach of interest (i.e., the change in water depth with distance).

Depending on the actual depth (y) at any given point, the type of flow can be further categorized relative to normal depth (y_n) and critical depth (y_c). Normal depth occurs when the slopes of the water surface, channel bottom, and energy grade line are all the same (i.e., they are parallel) and the water depth remains constant. This takes place when the gravitational force acting on the water is equal to and balanced by the frictional drag; hence, there is no flow acceleration. Critical depth is defined in terms of a minimum energy condition for the given channel slope and water discharge.

Critical depth occurs when:

- Specific energy is minimized for a particular discharge
- Discharge is maximized for a particular specific energy
- Specific momentum is minimized for a particular discharge
- Discharge is maximized for a particular specific momentum, and
- Froude number is equal to unity.

Here, the Froude number can be defined as the ratio of inertial forces ($F_{inertial}$) to gravitational forces ($F_{gravitational}$):

$$F_r = \frac{F_{inertial}}{F_{gravitational}} \quad (3.38)$$

or, shown mathematically as a function of velocity and discharge for a rectangular channel, it is:

$$F_r = \frac{Q}{\sqrt{g(A^3/T)}} = \frac{v}{\sqrt{g(A/T)}} = \frac{v}{\sqrt{gy}} \quad (3.39)$$

where T is top width of the water surface. In other words, critical flow occurs when there is a balance between gravitational and inertial forces, giving a Froude number of 1. Subcritical flow occurs when the $Fr < 1$, meaning that the gravitational forces are dominant; supercritical flow occurs when inertial forces are dominant, as expected for high-velocity situations.

The possible gradually varied flow profiles are organized and labeled according to channel slope and the magnitude of actual depth relative to normal and critical depths for the same discharge (Table 3.2)

TABLE 3.2: TYPES OF WATER SURFACE PROFILES

TYPE OF SLOPE	IDENTIFIER ^a	ACTUAL DEPTH RELATIVE TO NORMAL AND CRITICAL DEPTH		
		upstream end	downstream end	Illustration of profiles
HORIZONTAL	H1	$y_c < y$	$y = y_c$	
	H2	$y < y_c$	$y = y_c$	
MILD	M1	$y_c < y = y_n$	$y_c < y_n < y$	
	M2	$y_c < y = y_n$	$y = y_c < y_n$	
	M3	$y < y_c < y_n$	$y = y_c < y_n$	
CRITICAL	C1	$y_c = y_n = y$	$y_c = y_n < y$	
	C2	$y < y_n = y_c$	$y_n = y_c = y$	

^aFollowing notation in Henderson, 1966. Note that Chow 1959, French 1985, Bedient et al., 2007 use H2, H3 instead of H1, H2 respectively, and C1, C2, C3 instead of C1, C2, respectively, and A2, A3 instead of A1, A2 respectively.

TABLE 3.2: (CONT'D)

TYPE OF SLOPE	IDENTIFIER	ACTUAL DEPTH RELATIVE TO NORMAL AND CRITICAL DEPTH		
		upstream end	downstream end	Illustration of profile
STEEP	S1	$y_n < y_c = y$	$y_n < y_c < y$	
	S2	$y_n < y_c = y$	$y_n = y < y_c$	
	S3	$y < y_n < y_c$	$y_n = y < y_c$	
ADVERSE	A1	$y < y_c$	$y = y_c$	
	A2	$y < y_c$	$y = y_c$	

Backwater calculations to determine the water surface profile begin with determination of the appropriate gradually varied flow profile. To do this, one must calculate the critical and normal depths. Critical depth can be calculated using the Froude number formula with the Froude number set equal to one. For rectangular channels, this is shown as (in U.S. customary units):

$$y_c = \sqrt[3]{\frac{Q^2}{gB^2}} = \sqrt[3]{\frac{q^2}{g}} \quad (3.40)$$

Typically, normal depth is calculated using a trial-and-error procedure that involves one of the flow resistance equations. The Manning formula is usually used. It can be shown mathematically as:

$$v = \frac{1.49}{n} R^{2/3} S_f^{1/2} \quad (3.41a)$$

$$Q = \frac{1.49}{n} AR^{2/3} S_f^{1/2} \quad (3.41b)$$

where velocity (v) units are given in ft/s, discharge (Q), is given in ft³/s, 1.49 is a conversion factor between U.S. customary units and metric units, R is hydraulic radius (area divided by wetted perimeter) in feet, and S_f is the energy slope, which is dimensionless. The energy slope can be shown pictorially in a sketch of the energy equation such as Figure 3.1.

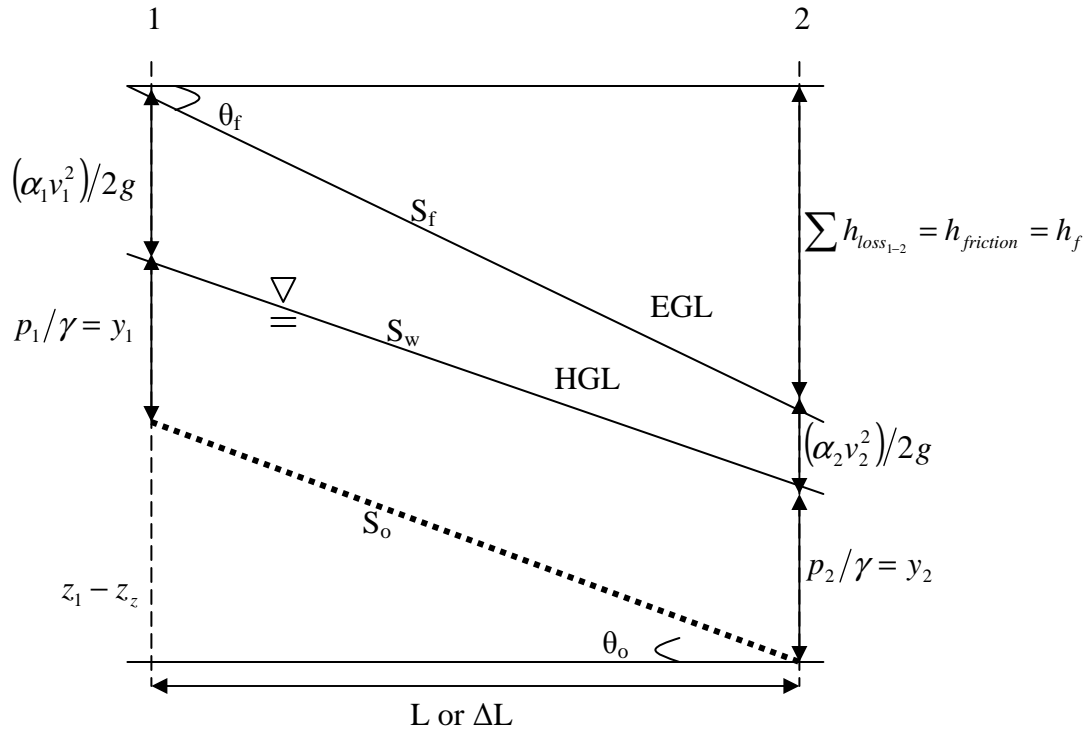


FIGURE 3.1: ILLUSTRATION OF THE ENERGY EQUATION FOR STEADY NONUNIFORM FLOW

At normal depth, the flow is steady and uniform, such that the energy slope is parallel to and numerically equal to the water slope and bottom slope (i.e., $S_f = S_w = S_o$).

For computational purposes, Equation 3.41b is rewritten in a form that has the numerically known terms the right side:

$$AR^{2/3} = \frac{nQ}{1.49S_f^{1/2}} \quad (3.42)$$

then for rectangular channels, the left side can become:

$$By_n \left(\frac{By_n}{B + 2y_n} \right)^{2/3} = \frac{nQ}{1.49S_f^{1/2}} \quad (3.43)$$

Then, y_n is found by substituting known quantities (e.g., n , Q , S_f values) and a trial-and-error testing of various values for normal depth is used until equality of the two sides is achieved.

All backwater computations begin with the flow depth at a control point and proceed in the downstream direction in which the control operates (French, 1985). If flow is found to be subcritical and subject to downstream control (disturbance propagates upstream as well as downstream), the backwater method can then be used to develop the water surface profile starting at the downstream end. Equation 3.44 shows the energy equation to use for determining incremental distances:

$$\Delta L = \frac{(y_1 + \alpha_1 v_1^2 / 2g) - (y_2 + \alpha_2 v_2^2 / 2g)}{S_{f-avg} - S_o} = \frac{E_1 - E_2}{S_{f-avg} - S_o} \quad (3.44)$$

where

$$S_{f-avg} = \left[\frac{nv_{avg}}{1.49R_{avg}^{2/3}} \right]^2 \quad (3.45)$$

$$v_{avg} = \frac{v_1 + v_2}{2} \quad (3.46)$$

$$R_{avg} = \frac{R_1 + R_2}{2} \quad (3.47)$$

and α_1 and α_2 are the energy coefficients (to compensate for the nonuniform velocity distribution) at sections 1 and 2, respectively.

Equation 3.44 has many methods for solution (French, 1985). Two common methods are: (1) the direct step method and (2) the standard step method (Chow,

1959). Other authors refer to these two methods as the step method and standard step method (e.g., Henderson 1966, French 1985, and Chanson 1999). The direct step method is used for prismatic channels (those with constant cross-sectional shape and distance). The standard step method is used for channels of irregular shape where cross-sectional properties have been determined at pre-selected locations.

In the step method, the downstream conditions are used as a starting point and a reasonable incremental upstream depth is chosen between critical and normal depth. The corresponding conditions for that upstream depth are calculated and entered into Equation 3.44, resulting in determination of the corresponding incremental distance upstream. The newly determined upstream conditions are then used as the new “downstream” conditions in the next iteration. The iterations are continued until the entire profile is completed.

In the standard step method, depths at specific known distances upstream are calculated. To perform this computation, Equation 3.44 is solved for change in distance by first noting that the derivative of the specific energy equation for rectangular sections, shown in Equation 3.48, is equal to one minus the square of the Froude number (see Equation 3.49). Subsequently, substitution of Equation 3.49 into Equation 3.44 allows for a revised Equation 3.44 with change in depth a function of incremental distances (see Equation 3.50):

$$E = y + \frac{q^2}{2gy^2} \quad (3.48)$$

$$\frac{dE}{dy} = 1 - Fr^2 \quad (3.49)$$

$$\Delta d = \frac{S_o - S_f}{1 - Fr^2} \Delta s \quad (3.50)$$

Both step methods are valid for subcritical and supercritical flows, where depths differ from normal depth. Near normal depth, the incremental distances become very large for small increments of depth change (e.g., in Equation 3.44). The standard step method breaks down at critical flow as a Froude number of unity causes the denominator of Equation 3.50 to become zero (i.e., undefined).

Either method may be used to compute the water surface profile for the reach of interest. Once this has been computed and the depths are known throughout the reach, then relationships for incipient motion and sediment transport can be used to make predictions about transport rates. Consequently, the locations of potential bed degradation and aggradation processes would be ascertainable.

There are important similarities and differences in descriptions of nonuniform flow offered by the more popular authors of open channel hydraulics texts (e.g., Henderson, Chow, and Chanson). In their chapters on gradually varied flow, Henderson (1966), Chow (1959), and Chanson (1999) each described nonuniform flow and backwater calculations using variations of the energy and resistance equations outlined above. However, each author presents information in such a way that insight into the subject is gained.

Henderson characterized uniform flow as a ‘control’ because water surface profiles of interest typically move toward uniform depth asymptotically. At uniform depth, flow characteristics can be calculated as can be done at a conventional control such as a weir. Furthermore, he generally described the possible profiles and critical flow situations that can occur in natural and man-made channels in a manner similar to those already shown in Table 3.2.

Henderson’s analysis does not directly describe the scenario of tidal influence on gradually varied flow profiles. One could think of the rise and fall of the tide as a downstream control, yet Henderson did not mention such a dynamic control in his text. There was mention of the challenge engineers face when considering natural controls, a comment indirectly applicable to my work. Henderson made note that

unlike weirs or spillways, natural controls are describable; however, the interplay between the control and the profile is not fully understood and characterized. He wrote that large magnitudes of water discharge have the potential to “drown out” the influence of the control. Henderson’s useful observation and its implications are investigated further in the next section of this dissertation, following a theoretical description of tidal influence as a downstream control.

Chow indirectly addressed tide as a downstream control through a more applicable summary of gradually varied flow. Chow covered the profile types in more detail by providing additional examples not offered by Henderson. Of particular interest to my work, were the descriptions of the potential variations on the M2 curve. According to Chow, there are three different M2 curves possible. Two of the three do not involve the downstream end terminating with a vertical slope at critical depth. Chow’s finding is expanded upon as a part of the following theoretical description of tidal influence as a downstream control.

3.2.3 Tidal influence on gradually varied flow

The development of a formal description of sediment transport with tidal influence continues here with consideration of a scenario where the flow is identified by two different gradually varied flow profiles over the course of a day. For this particular scenario, it is necessary to develop the relevant relationships that describe the mechanisms of transport.

Flow entering a lake or reservoir from a river typically has an M1 backwater curve in the lower reaches of the river and adjacent portion of the reservoir, where the depth of flow increases downstream as shown in Figure 3.2 (Julien, 1995). This could also be considered an idealized analogy to the water surface profile of a river under tidal influence (such as flow entering an estuary), if the fluctuating tidal elevations could be represented by some single mean tidal height.

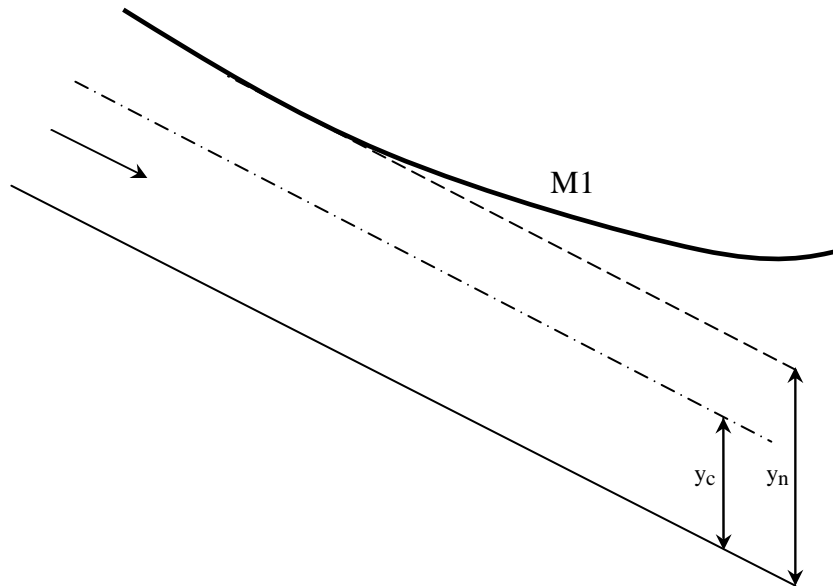


FIGURE 3.2: M1 CURVE REPRESENTING FLOW INTO A LAKE OR RESERVOIR

Furthermore, the mean tidal height would have to be greater than the normal depth of the river if it is to cause the M1 backwater curve.

A more realistic consideration of the tidal processes requires understanding how and why the tidal levels change. The following is a brief summary of the subject of tides compiled from texts on coastal engineering (Kiyoshi 1978, Reeve et al. 2004, Sorenson 2006). Tide fluctuations are caused by forces acting on the earth's surface. These forces include the centrifugal force of the earth caused by its rotation about its center of gravity, the gravitational force of the moon, and the gravitational force of the sun. Figure 3.3 shows the configuration of the centrifugal force of the earth and the gravitational force of the moon (lengths of the arrows indicate magnitudes of the forces). Also shown in Figure 3.3 is the increase in oceanic depth that results from these forces. Each oceanic increase is due to an imbalance of the gravitational and centrifugal force. On the side of the earth opposite the moon, the magnitude of the lunar-derived gravitational force is insufficient to cancel the larger tide inducing centrifugal force of the earth. On the side of the earth facing the moon, the

magnitude of the centrifugal force of the earth is insufficient to counteract the tide inducing force caused by the gravitational force of the moon.

Rotation of the earth through areas of increased oceanic depth causes two high tides and two low tides each day for most shorelines on earth (i.e., semidiurnal tide cycle). However, due to the inclination of the moon the location of the maximum oceanic height is typically above and below the equator of the earth. This means that some places have a single high and low tide each day (i.e., diurnal tide cycle) as they only pass through a single area of increased depth.

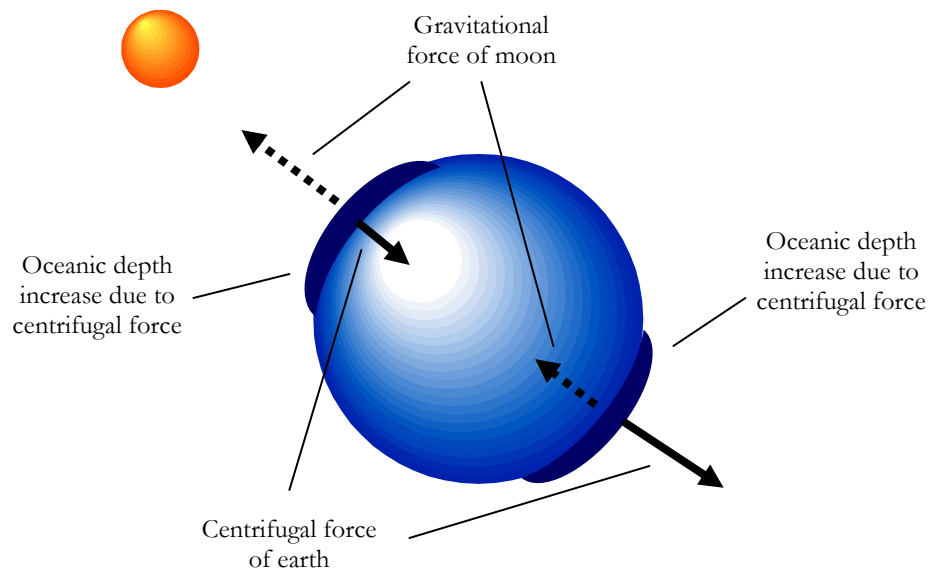


FIGURE 3.3: TIDE INDUCING CENTRIFUGAL AND GRAVITATIONAL FORCES

Solar-derived gravitational forces also play a role in the tidal phenomenon. However, due to its distance from the earth relative to the moon, the sun has a much smaller influence on tide ($\approx 46\%$). During the new moon and full moon, the sun and moon are collinear, where the summation of the gravitational forces of the sun and moon

cause large tidal ranges (highs to lows) called spring tides. During the first and last quarter of the moon, when the moon is perpendicular to the sun, the smallest tidal ranges, so-called neap tides, result.

Tides along the Oregon Coast have two high tides and two low tides during each 24.8-hour cycle, identified as the higher high tide, lower high tide, higher low tide, and lower low tide (NOAA tide tables for the Oregon Coast). As an example of typical tidal fluctuations of water surface elevation, a graph of the predicted and observed tidal fluctuations for Garibaldi, near the mouth of the Tillamook Bay, over a period of 31 days is shown in Figure 3.4.

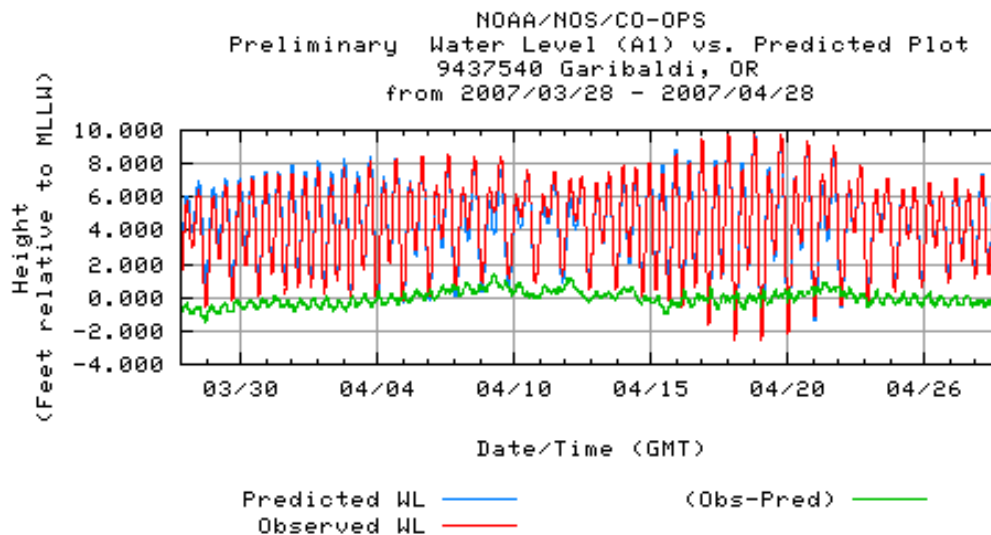


FIGURE 3.4: TIDAL FLUCTUATIONS AT GARIBALDI, OREGON (source: NOAA 2007)

Figure 3.5 shows tidal fluctuations over a given day according to type of tide cycle: semidiurnal, mixed, and diurnal.

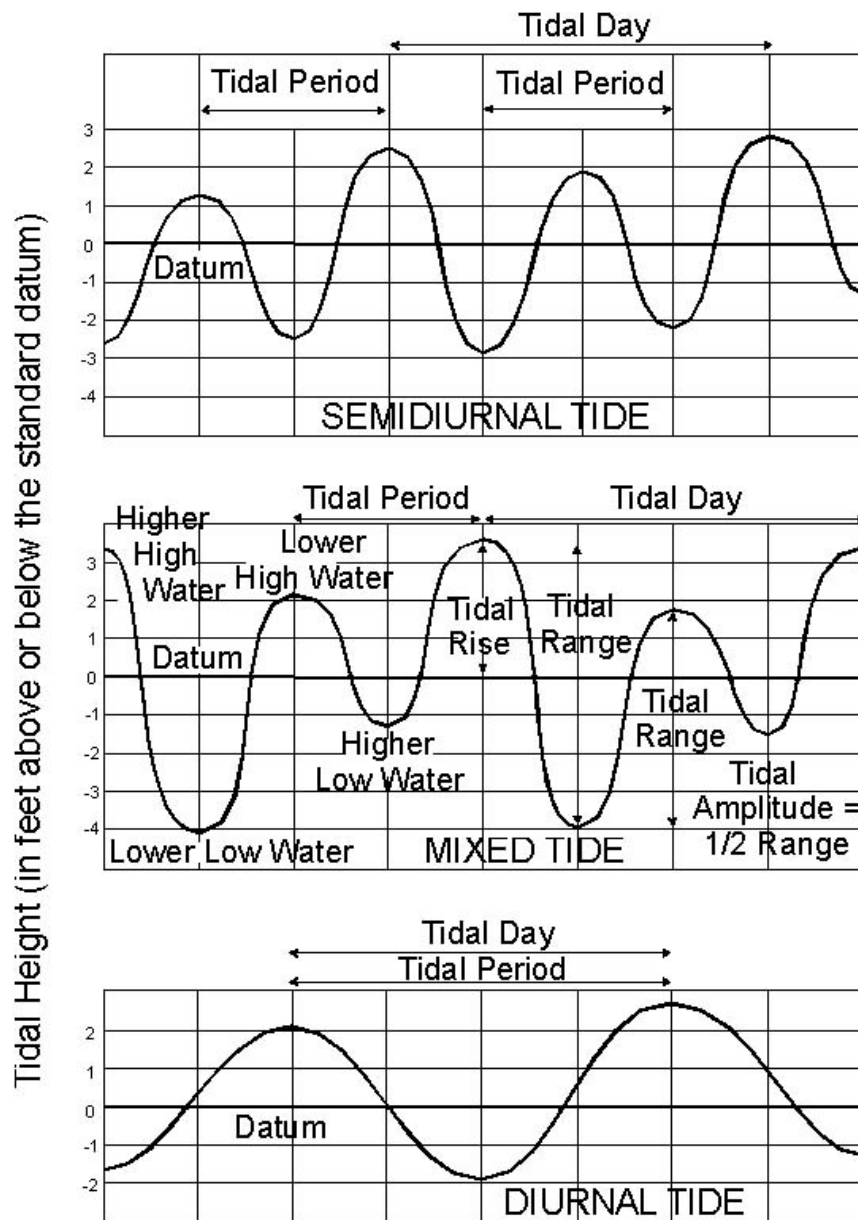


FIGURE 3.5: DISTRIBUTION OF TIDAL PHASES (source: NOAA 2007)

The diurnal tide fluctuations depicted in Figure 3.4, lead to a twice-daily water depth increase in estuaries, and a rise of water levels in rivers that flow into zones of tidal influence. Correspondingly, there will be a twice-daily decrease in depth of water in these areas. Therefore, the water surface profile of rivers impacted by tide would be time variant. The range in water surface elevation fluctuations of the downstream end of rivers depends on factors such as the level of tidal influence, tidal conditions (e.g., spring tide versus neap tide), and river flow conditions (e.g., magnitude of water discharge).

In the case where tidal influence is large and parameters such as water discharge, which would typically diminish tidal effects, are insufficient, atypical conditions might occur. For example, during summer months when streamflow is at its lowest, tidal fluctuations could cause flow reversals. That is, the forces exerted by the rise in tide can cause flow in channels to halt and propagate upstream. In their 1969 study, Clark and Snyder documented this phenomenon on the Lower Columbia River. They report that during periods of low river stage, flow reversal in the Lower Columbia River extends up to 40 kilometers (25 miles) upstream. Their velocity measurements and tracer dye study showed a rise in water level followed by a decrease in downstream flow and subsequent flow reversal. Klingeman reported extensive observations of flow reversal at the mouth of the Willamette River, 100 miles (161 kilometers) upstream of the Columbia River mouth (Klingeman et al., 1982). Such a large tidal influence is less likely in rivers that do not empty directly into the ocean. However, studies of rivers such as the Columbia show that flow reversal is possible.

In general, the shape of the water surface profile due to tidal fluctuations can be represented by a time-dependent M1 curve that may shift toward a time-dependent M2 curve (shown in Figure 3.6). During periods at or near high tides, elevated water surfaces might behave like the M1 curve, while during periods at or near low tides, shallow depths might induce an M2 curve. The amount of tidal change in the downstream end affects upstream depths, as the river must adjust back to 'normal' depth over some distance. Therefore, the effects of tidal periodicity are not local to

the tail-water end of the system. Tidal influence has been observed to create changes in flow depth farther upstream. Table 3.3 shows the head of tide (extent of tidal influence) for each of the five Rivers of the Tillamook Basin as reported by the Oregon Department of State Lands (2007).

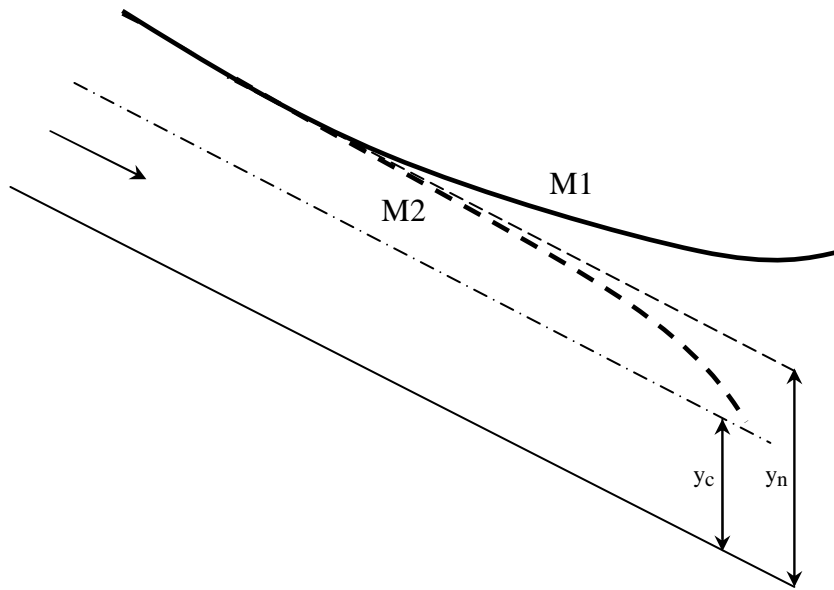


FIGURE 3.6: THE M1 AND M2 CURVES THAT MIGHT BE CONSIDERED FOR TIDAL REACHES

TABLE 3.3: EXTENT OF TIDAL INFLUENCE FOR FIVE RIVERS OF THE TILLAMOOK BASIN (Oregon Department of State Lands 2007)

RIVER	LOCATION OF HEAD OF TIDE (River mile)	LOCATION OF HEAD OF TIDE (km)
Miami	0.8	1.3
Kilchis	2.0	3.2
Wilson	3.1	5.0
Trask	4.3	6.9
Tillamook	6.0	9.7

Returning to Chow's summary of possible profiles, the M2 curve may be altered to a picture more like Figure 3.7, where the downstream end is still below normal depth, but is not necessarily below critical depth. The modified M2 curve is a reasonable assumption given that critical flow typically occurs when the channel abruptly becomes steep, such as at a waterfall, weir, or spillway. At mouths of rivers entering estuaries or oceans, the mean water elevation is sea level. Therefore, it would be unlikely to observe a sudden freefall or abrupt steepening of the channel. However, if the depth of an estuary is much greater than that of the river entering the bay, exit flow from the river may approach critical flow during low tide. In this case, the range of tidal fluctuations and geometry of the estuary, and geometry of the channel at its mouth would be factors determining the proper profile configuration.

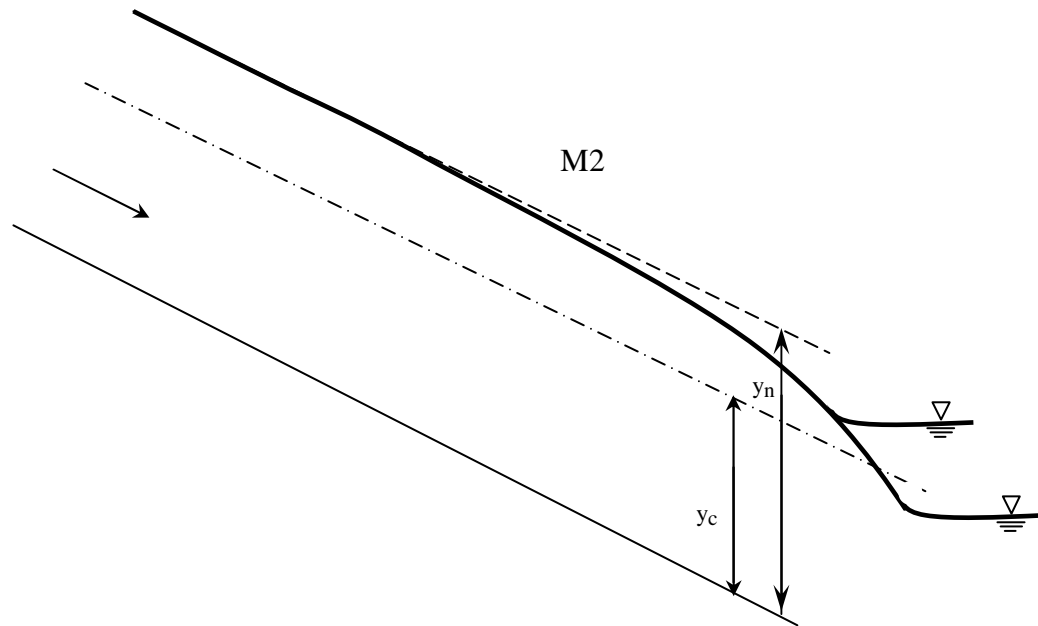


FIGURE 3.7: ALTERATIONS OF M2 CURVE REPRESENTING FLOW INTO AN ESTUARY WITH TIDAL INFLUENCE

However, despite the choice of configuration, this continual change in water surface profile over time in turn affects bed-load transport because changes in depth alter velocities, shear stresses, and stream power. Due to changes in these variables, any approach taken to characterize the river in this zone of tidal fluctuation must include provisions for changes in bed-load transport.

Henderson asserted that there is an interplay between natural controls on flow hydraulic characteristics and fundamental hydraulic parameters such as discharge. If this assertion is correct, the extent to which tidal fluctuations alter sediment transport processes in the zone of tidal influence may be dependent on the magnitude of discharge. During periods of large river discharge, tidal fluctuations might be drowned out or reflected as small changes in the large transport rate. However, during periods of smaller discharge the minor alterations of transport rate may be more significant in relation to the total transport rate.

There is an ongoing debate about the role of catastrophic events versus non-extreme events in overall transport of material. If bank-full flow conditions transport the largest net amount of material, as some investigators claim, tidal fluctuations may be a vital consideration when predicting sediment transport in the zone of tidal influence. Furthermore, during low flow conditions any bed-load (should it be possible) will consist of fine material. In downstream reaches of tidal rivers, the tide could play a significant role in shifting fine sediment upstream through flow reversal. Developed bed-load transport relationships will be used as a first step to investigating these ideas.

3.2.4 Effects on bed-load transport as illustrated by present-day relationships

Virtually all bed-load transport formulae include criteria for incipient motion. Furthermore, there are several methods to determine the flow conditions necessary to cause bed-load transport. Two widely accepted and applied approaches to determine if sediment transport will occur are shear stress and velocity approaches. Both methods involve calculation of threshold values necessary for bed-load transport. The title of each method gives the threshold parameter considered, namely velocity and shear stress.

The velocity approach described by Hjulstrom and ASCE studies is summarized in the downstream fining section of this chapter. It is a good conceptual way to describe incipient motion and bed-load transport. The method determines the velocity necessary to create large enough forces on the channel bottom to cause the transport of material of a particular size.

The shear stress approach involves comparison of existing bottom shear stresses to a shear stress threshold necessary to move particles of a certain size. The threshold is named critical shear stress. A typical evaluation method is the Shields approach described in the downstream fining chapter. Use of a critical shear stress criterion could be a first step in showing the relative importance of tidal influence on the mechanics of bed-load transport.

Stating that tidal influence is important implies that changes in flow conditions at the downstream end of a channel may cause modification of water surface profiles upstream sufficiently to alter the transport capacity of streamflow. This assumption is plausible as long as flow is not supercritical (where disturbances cannot travel upstream), such that backwater calculations can be computed. Among the approaches that can be used to investigate transport capacity, incipient motion, and the subsequent bed-load transport, there are options such as probabilistic, stochastic, discharge, bed form, energy slope, and regression approaches to quantifying rate of bed-load transport (Yang, 1996). Of the potential methods, I use two that involve calculation of threshold values for shear stress and velocity. Critical shear stress and critical velocity approaches were chosen because of the ease in making direct correlations to the physical parameters such as channel geometry and depth of flow, that are altered by tidal influence.

Shields analyses of incipient motion and bed-load transport are examples of the critical shear stress approach for estimating bed-load transport. In 1936, Shields created an equation that related rate of bed-load transport to shear stress, critical shear stress, mean particle size, and channel slope. This is shown by Equation 3.51:

$$\frac{q_b \gamma_s}{q \mathcal{S}} = 10 \frac{\tau - \tau_c}{(\gamma_s - \gamma) d} \quad (3.51)$$

here, q_b is bed-load transport per unit channel width, q is water discharge per unit channel width, d is sediment particle diameter, \mathcal{S} is bed slope, γ is specific weight of water, γ_s is specific weight of sediment, and τ is shear stress. In the context of my research, changes in channel water depth caused by tidewater fluctuations are manifest through variations in shear stress and velocity. The result is variations in the rate and location of bed-load transport over time. Consequences for channel bed elevations due to the variations in bed-load transport are investigated using numerical analysis, as outlined in section 5.5 of this dissertation.

The methods for calculation of bed-load transport developed by DuBoys are representative of both the critical shear stress and critical velocity approaches to bed-load transport. Written here as Equation 3.52, the DuBoys formula based on critical shear stress shows the rate of bed-load transport to be a function of depth, critical depth for incipient motion, mean particle size, channel slope, and critical shear stress (called critical tractive force):

$$q_b = \frac{0.173}{d_{50}^{0.75}} \tau(\tau - \tau_c) \quad (3.52)$$

where d_{50} is the mean particle diameter. DuBoys created a coefficient, K , which is related to characteristics of sediment particles. K is shown with its associated units in Equation 3.53:

$$K = \frac{0.173}{d_{50}^{0.75}} = \frac{ft^6}{lb^2 - s} \quad (3.53)$$

Equation 3.54 can be shown in a form that includes K :

$$q_b = K\tau(\tau - \tau_c) \quad (3.54)$$

The critical velocity approach to rate of bed-load transport estimation was developed by first, rewriting Equation 3.54 as:

$$q_b = K(\gamma S D)(\gamma S D - \gamma S D_c) = K(\gamma S)^2 (D)(D - D_c) \quad (3.55)$$

here, D and D_c are the normal and critical water depths at incipient motion, respectively. Then, DuBoys used Chezy's resistance equation for velocity to create the critical velocity equation shown mathematically as:

$$q_b = \frac{K}{C^4} \gamma^2 v^2 (v^2 - v_c^2) \quad (3.56)$$

where, C is Chezy's roughness coefficient, v is average velocity, and v_c is critical velocity.

K can be obtained graphically, by using computed critical shear stress and mean particle diameter, along with the critical tractive force graph shown in Figure 3.7 (Straub 1935; Yang 1996). Figure 3.8 is a graphical representation of the relationship between critical shear stress and mean particle diameter. K is used in both the critical shear stress and critical velocity approaches to estimating bed-load transport (Equation 3.54 and Equation 3.56). Therefore, Figure 3.8 is a graphical representation of the relationship between the critical shear stress and critical velocity methods for estimation of bed-load transport rates.

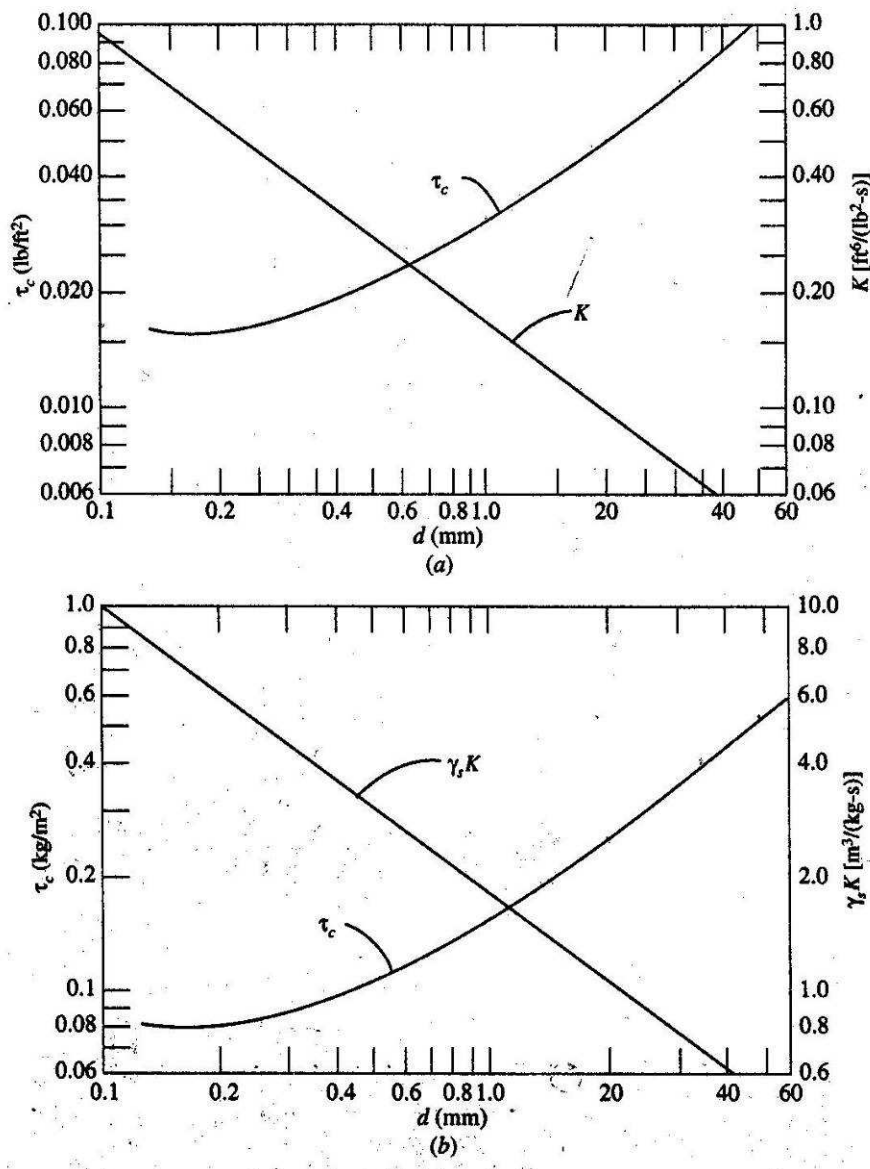


FIGURE 3.8: SEDIMENT PARAMETERS AND CRITICAL TRACTIVE FORCE FOR DUBOYS' BED-LOAD EQUATION

From Equation 3.55 it can be concluded that changes in water depth directly affect rates of bed-load transport. Equation 3.52 is used in the MATLAB numerical analysis to explore the relationship between tide and rates of bed-load transport along the zone of tidal influence. Considering the M1 curve to depict periods of high tide, one would expect increases in depths in the downstream direction to cause decreases in shear stresses along the bed, due to decreases in velocity. The reduction in shear

stresses is expected to reduce the ability of the streamflow to transport bed-load. At low tide, depths in the estuary are expected to be at their minimums; therefore, water surface profiles of the channel would be an M2 curve with depth below normal depth. In this case, one would expect to see either a reduced impact on stream power or an increase in the ability to move particles.

The above assertions must be considered in the context of flow conditions, which vary over time. During times of large streamflow and large rates of bed-load transport, the tidal influence may be insignificant. For instance, during winter months in Oregon the changes in bed-load transport rates due to tide might be insignificant when compared to the large overall fluvial-induced bed-load rates during this period. During seasons of low discharge (such as the summer months in Oregon), the effects of tidal fluctuations may be very significant on the small rates of bed-load transport at such times (Note: during periods of low discharge in gravel-bed streams, bed-load transport rates are usually zero.).

With the above in mind, any bed-load transport during low-flow periods should consist of particles much smaller than particles transported during periods of high flow. That is, bed-load may consist of silt-to-sand size particles during the summer months and coarse sand plus gravel during winter months. Furthermore, if tidal fluctuations do have enough of an impact to cause bed motion during periods of low-flow, the extent of bed-load transport initiated by tide should be analyzed carefully. If this bed-load transport is significant, the movement of small particles in the upstream direction due to flow reversals could change the texture of the bed through the introduction of fine material. Textural changes would have further implications for the bed-load transport of larger particles during periods of high flow (e.g., due to infilling of interstitial spaces and burial of larger particles by smaller particles).

Differences in the rate of downstream fining in the zone of tidal influence versus the rate of downstream fining in riverine reaches may be another key component to understanding the extent of influence of tidal fluctuations. If significant changes in the rate of downstream fining occur in the tidal zone, one could conclude that tidal

fluctuations have a significant influence on sediment transport and downstream fining. Furthermore, the analysis of bed-load transport must be considered at temporal scales of hours to months, to ascertain short and longer-range impacts of tides. For example, the overall volume of sediment transported could balance out if the effects during low tide are equal to effects during high tide. Subsequent chapters of this dissertation address the influence of tidal fluctuations on rates of bed-load transport at different temporal and spatial scales through physical and numerical studies of downstream fining and sediment transport.

4 Application of Theory

4.1 Site Selection

4.1.1 *Relevance of field data*

Field data are necessary whether the research interest is to demonstrate that downstream fining occurs, to determine the dominating mechanisms of fining, to question the usefulness of fining information to make inferences about landslide or other disturbance activity, or to determine the roles of lake, reservoir, or tidal fluctuations on bed-load transport. To gain knowledge about the existence of downstream fining and its relation to watershed disturbances, I selected a site in the Tillamook Basin of Northwestern Oregon that is known for having disturbances of both hydrologic (flood) and geologic (landslide) types. This site offers the opportunity to look at how downstream fining processes operate under land use change, river modification, flood disturbances, and frequent landslide activity.

The Tillamook Basin is also well suited to this study of downstream fining due to its abundance of river systems that each connects to a single estuary, Tillamook Bay. There are five rivers with varying watershed sizes and levels of modification. From north to south, the rivers are the Miami, Kilchis, Wilson, Trask, and Tillamook Rivers. The Kilchis River was the focus of the most detailed data collection. This river was selected as the primary site because of its level of modification, recent landslide activity, lower-river shoaling problems, and consequent morphological changes at its mouth. Figure 4.1 shows the Tillamook Basin separated into the five sub-watersheds. The types of data collected on each of the five rivers include particle size and specific gravity. The methods of data collection for the Kilchis River differed from the sampling methods of the other four rivers. The differences in methodology are outlined in Chapter 5 of this dissertation.

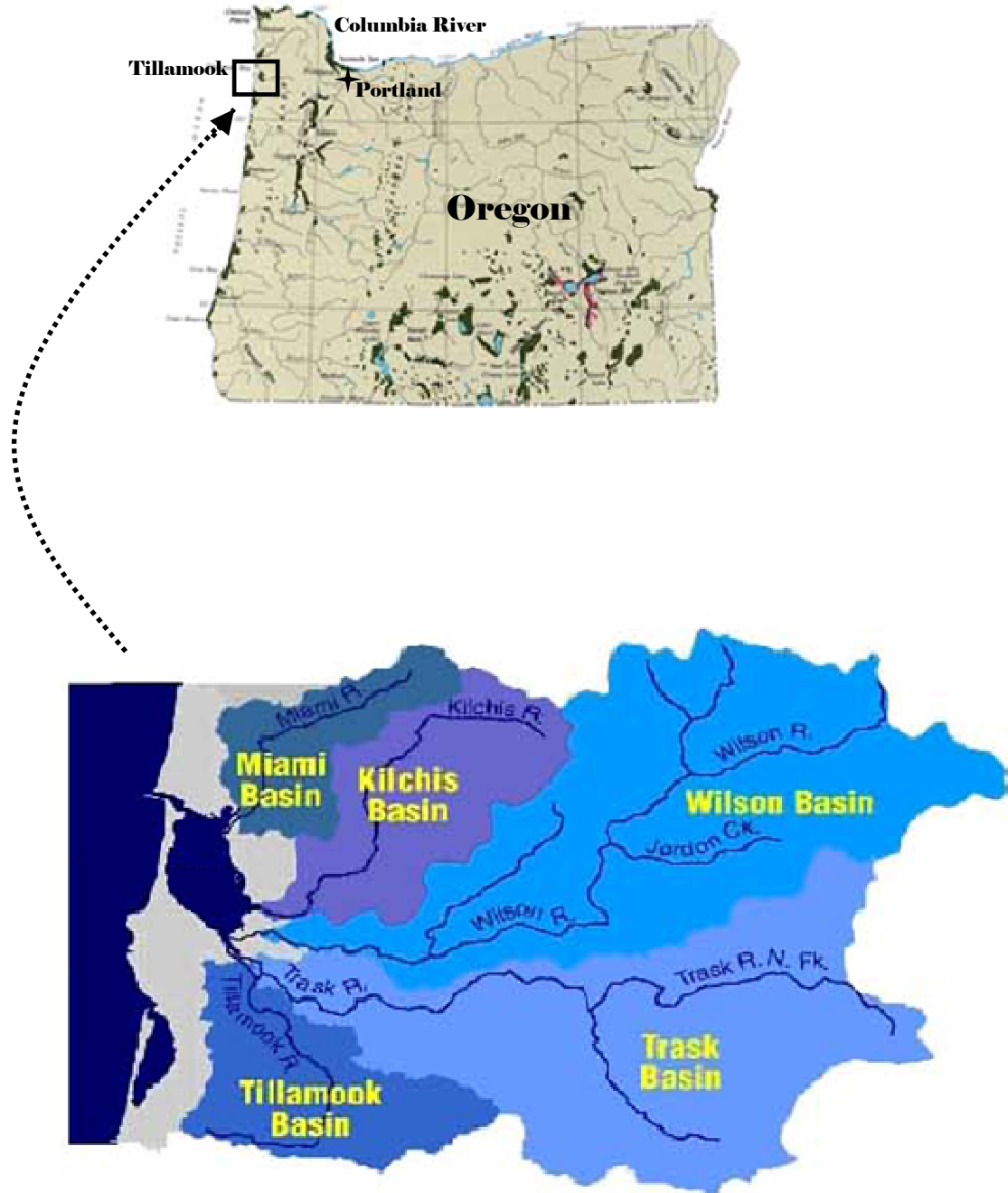


FIGURE 4.1: SUB-WATERSHEDS OF THE TILLAMOOK BASIN, OREGON
(source: USGS and Tillamook Bay Watershed Council, 2007)

4.2 Kilchis River Watershed

4.2.1 Background on Tillamook Basin settlement and historical overview of Kilchis Watershed

Much of Tillamook County depends on forestry, agriculture, and a dairy farming industry to maintain its economic stability. To date, approximately 86% of the lowland areas in Tillamook Basin have been converted to agricultural use or urban development (Kilchis Watershed Project 1998). The estuarine environment is typically used for commercial and sport fisheries and shellfish production, as well as for recreation. Furthermore, forest harvest from upland areas has been a source of revenue and employment. The combination of these land use activities (urbanization, agriculture, and forest harvesting) within the Kilchis River watershed has altered the flow regime, the disturbance regime, and the form and hydraulic function of the river and its floodplain.

Prior to European settlement, the area was inhabited by Native Americans whose anthropogenic influence on the basin was limited to periodic forest burning to create clearings for wildlife use and harvesting. The area has historically been an appealing place for human settlement due to its temperate environment, high amount of rainfall, extensive waterways, and prolific estuary. Unfortunately, the history of disturbances in the area has led to an alteration of the natural processes and depletion of the natural resources in the basin.

Removal of logjams (tree trunks and large woody debris) beginning in the 1800's has aided in creating a river disconnected from its floodplain with an elevated amount of aggregate material to transport (Styllas 2001). Prior to the early removal of large logjams, they served as sediment traps and as mechanisms to encourage flooding of the surrounding floodplain. During floods, the floodplain became part of the active channel. At these times, it was a source of refuge for fish populations, as the

velocities in sloughs were much lower in the main channel. Furthermore, as streamflow expanded across the floodplain, the bed-load was left in the channel and much of the transported smaller sediment from upstream settled out on the land. The floodplain thus served as an important sink for excess sediment originating from landslides farther upstream.

During past periods of forest road construction to support forest harvest operations, additional landslides originated from side slopes of roads. In addition, increased overland flow occurred due to increases in the extent of impervious surfaces. In-stream sediment routing mechanisms allowed increased rates of shoaling in the lower reaches of the river channel. Residents living in the area speculate that shoaling in this area will continue (Boquist, personal communication 2004). In past years, dredging and sediment removal from in the lower reaches were used to mitigate shoaling (Styllus 2006). However, state regulation has been implemented to control dredging, gravel mining, riprap placement and channel alteration (Tillamook County Stream Corridor Management Plan 2000).

Reductions in populations of important biota, such as salmon, and frequent and costly floods, have prompted government officials and residents to take measures to rehabilitate and restore a more natural form and function of the landscape and waterways. The Tillamook Bay Estuary Project, involving scientists, governmental officials, and community members, has spearheaded ecological studies of the current state of the basin. The efforts have resulted in a detailed characterization of the basin that includes hydrologic, biotic, and geologic databases. Many of the basin characteristics reported here are based on or verified by the collection of research papers developed for the Tillamook Bay Estuary Project. Assessments of the Kilchis River watershed are ongoing, while the issue of shoaling in the main channel remains a concern for the residents of the agricultural lowland areas (Geiger, personal communication 2006).

4.2.2 Description of current river sediment conditions

Due to the extent of shoaling, the hydraulic conditions of the downstream sections have been greatly changed, leading to morphologic changes of the lower reaches. Squeedunk Slough, is a diked distributary of the Kilchis River. During low-flow season and periods of low tide, residents have observed redirection of flow to Squeedunk Slough, causing it to become a major conveyance for discharge (Boquist, personal communication 2004). The increased flow in this under-used portion of the river system has been observed to cause accelerated bank erosion in areas where flow velocities and associated shear stresses are concentrated. Landowners are apprehensive about this development, as a change in river direction could mean a loss of farmland (Geiger, personal communication 2006). Repair of the Geiger levee on the banks of Squeedunk Slough has been listed as a necessary project to undertake in a recent Army Corps feasibility study (U.S. Army Corps of Engineers, 2004). In this situation, the management question was how to protect farmland while allowing the river to cope with the variety of human influences in the watershed.

4.2.3 Overview of the Tillamook Basin physical conditions

The Tillamook Basin is located approximately 60 miles (96.6 kilometers) west of Portland, Oregon and 60 miles south of the Columbia River mouth at the Pacific Ocean (Figure 4.1). The basin has a total area of 570 mi² (1476 km²) and has five main rivers (Miami, Kilchis, Wilson, Trask, and Tillamook Rivers) that route alluvium to the Tillamook Bay. Tillamook Bay is a shallow estuary 23 mi² (59.6 km²) in area, 6.2 miles (10 kilometers) long, 2.1 miles (3.4 kilometers) wide, with an average depth of 6.6 feet (2 meters). The Basin has a history of disturbance that is in part natural and in part human induced (Kilchis watershed analysis, 1998).

The geology of Tillamook Basin has been discussed in detail by reports on sediment accumulation in the Tillamook Bay (Bostrom and Komar 1997, Pearson 2002). Walker and MacLeod produced geologic mapping in 1991. Bostrom and Komar compiled data from the geologic mapping and separated it into information for each

of the five rivers (Miami, Kilchis, Wilson, Trask and Tillamook). Sediment in the five sub-watersheds was found to derive from volcanic and marine sediment formations. An important conclusion of Bostrom and Komar's description of the geology of the five sub-watersheds is the incapability to detect significant differences between the geologic compositions of the particles found in each watershed using currently available data sets.

A summary of the specific geologic makeup of the river sediments as reported by Bostrom and Komar is shown in Table 4.1. Tillamook volcanic rock occurs in each of the five watersheds. Moreover, the study showed a dominant composition of Augite and Diopside originating from each watershed. Contributions to Tillamook Bay of Augite and Diopside non-opaque heavy minerals were 97, 98, 95, 92, and 95% for the Miami, Kilchis, Wilson, Trask and Tillamook River watersheds, respectively. The foregoing information shows that bed-load sediment sources are similar for all five rivers. Hence, one would also expect similarities in some of the characteristics of downstream fining.

TABLE 4.1: GEOLOGIC HISTORY OF THE TILLAMOOK BASIN (BOSTROM AND KOMAR 1997)

WATERSHED	IDENTIFIER	TYPE	DESCRIPTION
Miami Wilson Trask	Ti	Oligocene mafic intrusions	Sheets, sills, and dykes of massive granophyric ferrogabbro, pegmatic gabbro, ferrogranophyte, and granophyre. Date: 30Ma (Ma = million years)
Miami Trask	Tss	Upper/middle Eocene Tuffaceous siltstone and shale	Marine tuffaceous mudstone and siltstone with local deposits of fine to coarse grained sandstone. Locally carbonaceous, and Micaceous. Consists of the Nestucca fm and Keasey fm.
Miami Kilchis Wilson Trask Tillamook	Ttv	Upper/middle Eocene, Tillamook volcanics	Subaerial basaltic flows and breccia, and submarine basaltic breccia, pillow lavas, lapilli and augite rich tuff. Interbedded basaltic sandstone, siltstone and conglomerate. Some andesite and dacite. Date 40-46 Ma
Trask	Tmst	Middle Miocene/upper Eocene marine sedimentary and tuffaceous rocks.	Tuffaceous and arkosic sandstone, locally fossiliferous, tuffaceous siltstone, tuff, glauconitic sandstone, minor conglomerate layers and several thin coal beds. Contains the Scappoose fm.
Tillamook	Tms	Lower/middle Miocene marine sedimentary rocks	Fine to coarse grained marine siltstone and sandstone that commonly contains tuff beds. Contains the Astoria fm, Gnat creek fm.
Kilchis Wilson Trask	Ttvm	Maritime facies	Basaltic clastic rocks and pillow lavas

TABLE 4.1: (CONT'D)

WATERSHED	IDENTIFIER	TYPE	DESCRIPTION
Wilson Trask	Ty	Upper/middle Eocene, Yamhill formation	Massive and thin bedded marine siltstone and thin interbedded arkosic and basaltic sandstone. Locally interbedded basaltic lava flows and lapilli tuff.
Wilson Trask	Tsr	Middle/lower Eocene to Paleocene, Siletz River Volcanics	Aphanitic to porphyritic, vesicular pillow flow, tuff breccias, massive lava flows and sills of tholeiitic and alkalic basalt. Upper sequence has numerous interbeds of basaltic siltstone, sandstone, tuff and conglomerate. Most are marine and have been interpreted as seafloor crust and/or seamounts. Date: 50-62 Ma

4.2.4 *Physical and hydrologic characteristics of Kilchis River Watershed*

The highest point in the Kilchis River watershed has an elevation of 3,294 feet (1,004 meters). The lowest point is at sea level. The watershed has a total area of 87 mi² (225 km²), with approximately 92% of that area being forestland. Agriculture makes up about 5.8%, while urban development comprises 0.3% of the total area. The river flows through the northern portion of the City of Tillamook prior to entering Tillamook Bay. Five major tributaries of the Kilchis River deliver sediment to the main stem: the North Fork, South Fork, Little South Fork, Clear Creek, and Sam Downs Creek (U.S. Army Corps of Engineers 2002). Mean annual precipitation on the watershed is 136 inches (3,454 mm).

There is no gaging station on the Kilchis River. However, hydrologic streamflow conditions may be estimated from prior OSU coursework in the Civil Engineering Department circa 1996-98. With the drainage area of 65 mi² (168 km²) and a prior estimate for North Coast Basin annual discharge per unit area of 4.98 cfs/mi² (0.14 cms/mi²), the annual discharge at the Kilchis River mouth is expected to be approximately 324 cfs (9 cms).

While creating a website for hydrology research in the Northwest, Coles and Bogavelli compiled a flood frequency analysis for the Kilchis River (2003; updated 2005). Detailed results of that study are presented in an appendix of this dissertation and are found on the CWEST website (<http://water.oregonstate.edu/streamflow/index.htm>).

The flow pattern of the Kilchis River for a typical water year follows the general trend for areas west of the Cascade Mountains, that is, low flows during summer months and peak flows during winter months (Coles, 2005). Figure 4.2 shows average monthly discharge for the period of record of the USGS Wilson River gage, based on correlation to Kilchis River based on drainage areas. It has been reported that though the highest flows occur during the months of December and January, tidal influence

and storm surge lengthen the flood period to November through February. Storm surges (also called meteorological tides) are associated with atypical rises in sea level and freshwater flooding due to low atmospheric pressure fronts and strong winds pushing on the surface of the ocean and bays (Horikawa 1978).

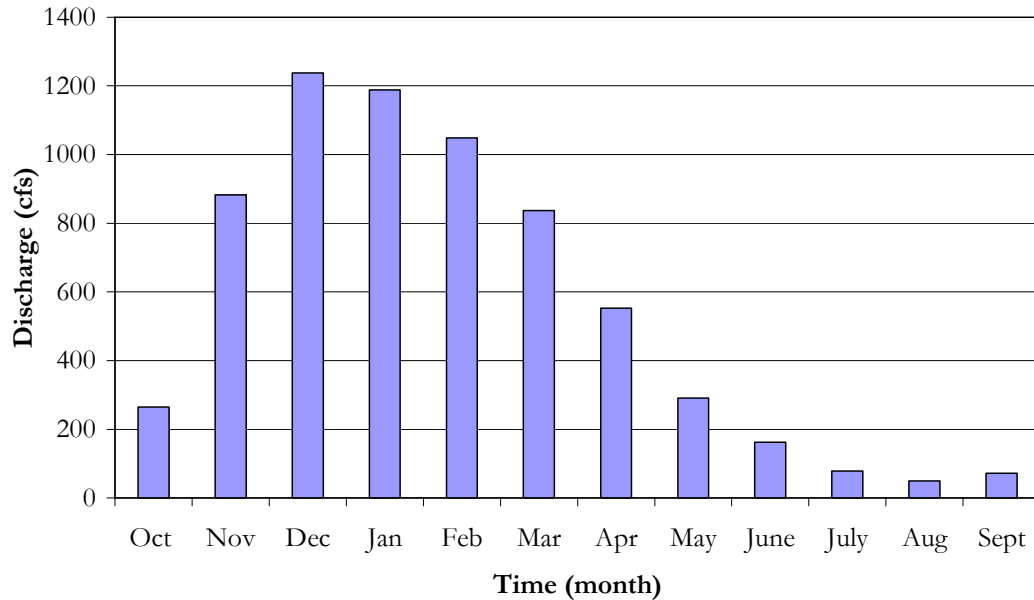


FIGURE 4.2: AVERAGE MONTHLY DISCHARGE FOR PERIOD OF RECORD FOR KILCHIS RIVER AS DERIVED FROM WILSON RIVER GAGE

4.2.5 *Physical and hydrologic characteristics of Kilchis River Watershed*

Flood disturbances can be attributed to both human and natural causes. Heavy rainfall in the upland areas, tides, storm surges, and rain-on-snow events are all natural causes of flooding in the Kilchis River. Constructed levees and dikes contribute to the frequency of flooding by decreasing the storage capacity of the channel and by disconnecting the river from the floodplain. Furthermore, in-stream logjams that once served as mechanisms for connecting the river with sloughs have

been removed, leading to decreased deposition areas for sediment and vegetative detritus.

Because about 80% of the lowlands have been converted to residential and agricultural uses, the Kilchis flood regime has changed over time. Lowland areas protected by dikes no longer are sites for inundated wetlands, sediment storage, and zones of channel reworking. Flood damage in lowland areas has become costly. For example, the 1996 floods in the Tillamook Basin caused approximately 53 million dollars in damages (Tillamook County Flood Hazard Mitigation Plan, 1996).

Also contributing to hydraulic problems in the Kilchis River watershed is the fire disturbance regime. Catastrophic fires occurred from 1918 through 1951, burning some areas up to four times. In particular, there were the Cedar Butte Fire in 1918 and the Tillamook Burns in 1933, 1939, 1945, and 1951. The destruction of approximately 200,000 acres (809 km²) has contributed to decreased time to peak flow during storm runoff and increased incidence of landslides. Like flooding, landslide activity can be attributed to both natural and anthropogenic causes. In addition to increased landslide activity following forest fires, the construction of roads for logging operations lead to road washouts, which have historically initiated shallow landslides. Older forest roads are reported to be less likely to cause landslides. Presently, newer roads are constructed on ridge tops using improved construction methods. An Oregon Department of Forestry (ODF) program was developed to upgrade existing roads, construct new roads, and decommission abandoned roads to combat this human impact (Kilchis Watershed Analysis, 1998).

Landslide disturbances are a significant part of the sediment problems in the Kilchis River. Landslides deliver large amounts of sediment to the channel. Figure 4.3 shows a landslide that was initiated upstream of the South Fork of the Kilchis River in 2005. Without floodplain connectivity and large in-channel logjams, the sediment introduced by landslides would be routed through the narrow upper portions of the river network (tributaries, tributary junctions, and main channel) to the lowland dike-confined channel. This can be disastrous for aquatic habitat and biotic species that

are dependent on areas free of fine sediment (e.g., salmonids in spawning areas). Furthermore, the increased introduction of sediment exacerbates flooding as sediment shoaling in the lower reaches causes decreased water storage capacity and greater vulnerability of adjacent floodplain land to high tides and storm surges.



FIGURE 4.3: PHOTOGRAPHS OF THE A 2005 LANDSLIDE IN THE KILCHIS WATERSHED UPSTREAM OF LITTLE SOUTH FORK

4.2.6 *Research relationship to the Kilchis River problem*

Therein lies the link between basic research on downstream fining and a consequent practical river problem. Pea-size gravel is accumulating in the lower reaches of the Kilchis River. This has caused morphological changes in the area, such as shoaling, and shifted the zone of tidal influence farther upstream. Such changes are unwanted from landowner perspective. The exact origin of this sediment is not yet known, other than coming from up river. Downstream fining of channel sediment is apparently involved. Historically, the Kilchis River was able to adjust laterally in response to incoming sediment. However, with the river now confined in its present configuration and with the regulation of former mitigation methods such as dredging and bar scalping, alternative methods of channel adjustment have developed. Squeedunk Slough, previously a small distributary channel, is now often the main route for water, periodically, during low-flow seasons. Furthermore, Squeedunk Slough is a distributary for sediment that exits the system at its downstream end. Figure 4.4 shows some features of Squeedunk Slough. Because the slough is smaller than the Kilchis main stem, Squeedunk Slough is currently undergoing severe channel enlargement through private agricultural land.

To the extent that my research requires accurate field data to demonstrate tidal effects on downstream fining, the research is also relevant to real problems in the river selected for the main field data collection. It is my purpose to characterize sediment transport in the zone of tidal influence, determine the general origin of the sediment shoaling at the mouth, and identify the role of tidal fluctuations in the context of downstream fining. Because of the apparent complexity of the lower reach of the Kilchis River, additional field data from other lower-river systems are required to help clarify the basic tidal-fining relationship.



(a)



(b)



(c)



(d)

FIGURE 4.4: SQUEEDUNK SLOUGH

(a) Downstream of confluence with Kilchis, (b) typical particle distribution in this area (c) and (d) Squeedunk as it winds through Geiger Farm toward Tillamook Bay

4.3 Brief Description of Other Study Rivers in the Tillamook Basin

4.3.1 *Characteristics of the watersheds*

The Tillamook Bay National Estuary Project (TBNEP) has funded watershed assessments for each sub-watershed in the Tillamook Basin (with the exception of the Tillamook River). This provides characteristics for the five main rivers in the basin: Miami, Kilchis, Wilson, Trask, and Tillamook. The following is a summary of the pertinent characteristics found in the TBNEP documents (Follansbee 1998, Kai et al. 2001, Sullivan et al. 2001).

The terrain of each watershed in Tillamook Basin is similar in that they all have upland areas that are steep with confined channels leading to lowland areas that historically had meandering unconfined channels. With the exception of the Tillamook River (Pearson 2002), average slope for rivers in each watershed is <1% in the lowland areas and is >16% in the upland areas. As previously stated, the geology of the watersheds is similar as well. Upland areas have primarily volcanic derived igneous rock, while lowland areas are covered in layers of marine derived sedimentary rock. In general, lowland areas in Tillamook Basin have been diked and contain tide gates on major flow conveyances.

The differences among the watersheds include watershed size, total length of river, maximum elevation, number of significant tributaries, and floodplain area. Table 4.2 shows these differences. Mean annual precipitation has a common range from approximately 90 inches (2,286 millimeters) in lowland areas to 200 inches (5,080 millimeters) in area of higher elevation. Streamflow data are available through the USGS for the Wilson and Trask Rivers only. Mean annual temperature for the Tillamook Basin is 50.4°F (10.2°C).

TABLE 4.2: CHARACTERISTICS OF THE TILLAMOOK BASIN SUB-WATERSHEDS STUDY AREAS (PEARSON 2002)

WATERSHED	WATERSHED AREA		FLOODPLAIN AREA		TOTAL RIVER LENGTH		MAXIMUM ELEVATION		NUMBER OF TRIBUTARIES	ANNUAL FLUVIAL SEDIMENT DELIVERY	
	mi ²	km ²	mi ²	km ²	mi	km	ft	m		TONS	TONS/mi ²
Miami	36	93	0.2 ^a	0.5	14	22.5	1,700	518	4 ^a	3,155	88
Kilchis	87	225	1.0 ^a	2.6	21	33.8	3,294 ^a	1,004	5 ^a	5,760	66
Wilson	193	500	7.7 ^a	19.9	44	70.8	2,200	671	10 ^a	15,130	78
Trask	176	456	5.6 ^a	14.5	31	49.9	3,442	1,049	5 ^a	34,279	195
Tillamook	61	158	2.7 ^a	7.0	17	27.4	400	122	7 ^a	8,169	134

Sources: ^a TBNEP 1998

4.3.2 *History of disturbance*

The disturbance regimes listed for the Kilchis River apply to the Tillamook Basin as a whole. Differences in most cases are only in extent and frequency. Sediment supply in each watershed is contributed primarily due to landslide activity (Follansbee 1998, Kai et al. 2001, Sullivan et al. 2001, Pearson 2002).

The Miami River is the smallest and reportedly, the least engineered of all Tillamook Basin Rivers (Pearson 2002). Very confined (58% of segments) in its upper reaches, the Miami is not very sensitive to disturbance. Further, small stream enhancement projects and bridge construction are the major in-stream modifications. The Miami is the site of extensive forest management, with 60% State-owned and 33% private industrial landownership. Though gravel extraction was conducted in the past, it was phased out by October 1, 1997. Natural and road-initiated landslides are a major part of the Miami Rivers disturbance regime. Sediment transport in the river is said to be supply-limited, with a history of low sediment supply that has become moderate due to the heightened disturbance activities caused by forest management and road construction.

The Wilson and Trask rivers have very similar characteristics. The Wilson River watershed has upland areas of mostly State forestland and lowland areas of mostly agricultural land. Landslide activity is the dominant mechanism of sediment supply for both rivers. Furthermore, both rivers have a disturbance regime that includes extensive fires, forest harvest, and road construction. Table 4.1 shows the mean annual fluvial sediment contributions from each sub-watershed of the Tillamook Basin. The values include sediment derived from forest and agricultural land. Together, the Wilson and Trask Rivers contribute 74% of the annual fluvial sediment delivered to the Tillamook Bay (Pearson 2002) and represent 67% of the total drainage area for the Tillamook Basin.

The Wilson and Trask rivers have differences in their level of river modifications. Barney Reservoir is located on the Trask River, between Tillamook and Hillsboro. The reservoir has a storage capacity of 20 million gallons (75.7 million liters) of water, which is released into the Tualatin River to supply water for the cities of the Tualatin Valley Water District (Hillsboro, Beaverton, Forest Grove and Tigard, TVWD Joint Water Commission 2007). Both the Wilson and Trask Rivers have hardened banks. The Trask River also has a history of stream cleaning (removal of tree trunks and large woody debris) for fish passage, beaver eradication, dredging, and gravel mining.

The disturbance regime of the Tillamook River is drastically different from the other four rivers. The Tillamook River has much lower channel slopes along its entire length. Bank caving, rather than landslides, is the dominant form of disturbance. This type of disturbance delivers a high volume of fine material and woody debris to the channel according to Pearson (2002). Furthermore, Pearson reported minimal gravel bar development in the Tillamook River. Floods are a major part of the disturbance regime in the Tillamook Basin. In particular, the Tillamook River is the major contributor to lowland flooding despite its lowland levees.

5 Methodology

5.1 Overview of analyses conducted

For description of the analyses conducted during this research, it is useful to remember the research questions stated in Chapter 1. These are as follows:

1. Is downstream fining a natural process for Oregon coastal streams and rivers?
2. Can downstream fining analysis be used to find areas of landslide activity or large lateral inputs of sediment?
3. Can downstream fining be significant even for highly modified channels?
4. Does tidal influence alter downstream fining processes?
5. How can sediment transport formulas be used in numerical models to create an accurate characterization of downstream fining in the tidal zones of rivers?

Chapter 1 also sets out the research hypotheses. These are:

Hypothesis 1: Physical characteristics of downstream fining can be detected in Oregon coastal streams regardless of the level of channel modification or sediment influx.

Hypothesis 2: Tidal influence has a significant effect on the sediment transport regime that includes a significant change in the downstream fining trend.

Three main types of analyses were used to address research questions and test the research hypotheses: 1) particle size analysis, 2) specific gravity analysis, and 3) numerical analysis. Table 5.1 shows the specific types of analyses involved in the three categories.

TABLE 5.1: OVERVIEW OF ANALYSES USED IN RESEARCH

CATEGORY OF ANALYSIS	NAME OF ANALYSIS	DESCRIPTION	OBJECTIVE
Particle Size	Bulk sampling	Surface and subsurface sampling of bars along the Kilchis River	<ul style="list-style-type: none"> ▪ Study grain size and its relation to channel geometry and hydraulic characteristics ▪ Determine spatial relationship between armor and sub-armor layer
	Photo frame sampling	Systematic sampling of bars along the other four Tillamook	<ul style="list-style-type: none"> ▪ Study grain size and its relation to channel geometry and hydraulic characteristics
Specific gravity	Submerged weight measurement	Measurement of specific gravity of particles according to particle size for all rivers	<ul style="list-style-type: none"> ▪ Compare particles of each watershed ▪ Investigate dominant mechanism for downstream fining
Numerical	MATLAB	Evaluation of tidal influence on sediment transport using bed-load functions and temporally-varied water surface profiles by developing a new model	<ul style="list-style-type: none"> ▪ Complete simplified description of sediment transport with tidal influence ▪ Investigate significance of tidal influence
	GSTARS 2.1	Evaluation of tidal influence on sediment transport through established numerical model	<ul style="list-style-type: none"> ▪ Validate simplified description of sediment transport with tidal influence ▪ Investigate significance of tidal influence using a more complex and widely used model.

The particle size and numerical analyses involve a study of the relationship between grain size distribution and geometric and hydraulic characteristics. Because the Kilchis River is a typical gravel-bed river on the Oregon Coast, it may be concluded that existence of downstream fining in the Kilchis River would be a good indication that the phenomenon is also typical for other gravel bed rivers in Oregon.

Furthermore, due to the level of modification and history of disturbance of the Kilchis River, it could also be deduced that downstream fining processes operate regardless of the level of modification or incidence of disturbance.

Bulk sampling on the Kilchis River was initially to be the only in-situ particle size analysis. However, there is large variation in hydrologic, hydraulic, and sediment inflow of systems in Oregon. Because these differences may or may not lead to drastically different transport regimes, a more robust statistical study was conducted to be certain that the Kilchis River is representative of other north-coast rivers in Oregon. Specifically, particle size analyses of four additional rivers (Miami, Wilson, Trask, and Tillamook) were conducted. Sampling completed for the Kilchis River included surface and subsurface samples. For the additional rivers, sampling consisted of only surface samples.

The characteristics of the additional rivers were presented in section 4.3. Along the study length of each additional river, the mean sediment diameter size for particle distributions on the surface of sidebars was determined using photo frame sampling (described in Table 5.1 and section 5.3). Subsequently, the exponential relationship between mean particle size and distance from river mile 0 was investigated using regression analyses. Downstream fining coefficients (diminution coefficients) were recorded from the exponent of each regression analysis-derived exponential function. Subsequently, the recorded diminution coefficients were compared to the diminution coefficients reported by researchers cited in the downstream fining literature review chapter of this dissertation. Comparisons of the diminution coefficients for the Tillamook Basin rivers to diminution coefficients for the Willamette River were also completed.

The Rivers of the Tillamook Basin have differing topographic and hydrologic characteristics. However, because they are all coastal river systems, a non-coastal river was also investigated. The Willamette River has been researched in detail over the past years. Results from particle size analyses the Willamette River were used to further illustrate the existence of the downstream fining phenomenon in Oregon gravel-bed rivers. The Willamette River has a much larger watershed and empties into the Columbia River, instead of an estuary. Table 5.2 shows other differences in the characteristics of the Willamette River compared to the five Tillamook Basin rivers (Percy et al. 1974).

TABLE 5.2: CHARACTERISTICS OF SYSTEMS UNDER STUDY

SYSTEM	LENGTH		DRAINAGE AREA		AVERAGE ANNUAL DISCHARGE	
	mi	km	mi ²	km ²	cfs	cms
Miami River	14	22.5	36	93		
Kilchis River	13.8	22.2	87	225		
Wilson River	44	70.8	193	500	1,205	34
Trask River	31	49.9	176	456	959	27
Tillamook River	17	27.4	61	158		
Willamette River	187 ^a	301	11,100 ^a	28,749	33,000 ^b	934

Sources: ^aWest Multnomah Soil Conservation District, ^bUSGS

The photo frame analysis was developed after bulk sampling on the Kilchis River began. Consequently, the Kilchis River photographic evidence does not include photographs of every surface sampled. The other four rivers were photographed prior to extraction of particles for measurement. The snapshot approach of these

analyses was evaluated to determine their appropriateness to study the existence of downstream fining and to identify local disruptions in the downstream fining trend. Whether this information is also useful in locating recent disturbances such as landslides or helpful in the characterization of sediment transport in the zone of tidal influence was also ascertained.

The probability of abrasion being the dominant mechanism for downstream fining in a river system depends on the mineralogical composition of the bed-load under transport. Kodama (1994) noted the significance of abrasion by linking the disappearance of andesite particles in the downstream direction. He asserted that abrasion must operate because selective sorting of a particular grain size is unlikely. The sediment in areas of higher elevation in the Tillamook Basin originates from volcanic formations. The sediment in areas of lower elevation in the Tillamook Basin originates from marine sedimentary deposits. A study of the longitudinal variation in specific gravity (which is linked to type of rock) may give insight into the significance of abrasion as a mechanism for downstream fining in gravel-bed rivers.

Specific gravity is also a useful tool for determining the influence of lateral and tributary inputs into the system. That is, if there is an abrupt longitudinal shift in the average specific gravity of the bed-load one can deduce that an outside influence has contributed material of a significantly different geology. Although results of the geologic analyses presented in chapter 4 suggest that such a use of specific gravity analysis may not be as essential as the particle size analyses, specific gravity analyses were conducted for verification purposes.

Comparison of the various rivers under study is another use of the specific gravity information. The literature provided general and specific data about the origin of sediment, but did not list specific gravities of the particles under study. Firsthand knowledge of the particular differences in composition of the sediment in the watersheds could be vital to fully describing results of the particle size analyses. Furthermore, results of the specific gravity analyses were used as part of input data for numerical models.

Numerical models are used to study temporal changes in bed-load transport and size distribution caused by changes in hydraulic parameters. The computing power of MATLAB (an interactive program that allows for software development involving matrix computations, MATLAB 7 user manual 2004) is used to describe the mechanics of sediment transport with tidal influence using simple, generally accepted hydraulic calculations. The analysis involves computation of bed elevation degradation and aggradation using a typical bed-load transport formula, coupled with a tide-simulating relationship and dimensionless coefficients. The final analysis uses the computing power of GSTARS 2.1 (Generalized Stream Tube model for Alluvial River Simulation version 2.1) to simulate downstream fining in an idealized gravel-bed river. GSTARS2.1 is a movable-channel-boundary, semi-two-dimensional, numerical model developed by the U.S. Bureau of Reclamation for the simulation of sediment transport and bed evolution. The model uses backwater calculations and bed-load functions to perform simulations.

The remainder of this chapter is devoted to a detailed description of each analysis. The descriptions include procedures, relevant equations, and equipment used to complete the analyses. Analyses are presented in the same order as they were chronologically performed. Physically based studies were conducted prior to numerical analyses, so that in-situ data from the particle size and composition analyses could be incorporated into the subsequent numerical analyses. The particular order of analysis was as follows:

1. Particle size analysis of Kilchis River bed materials
2. Particle size analysis of bed material for the four additional Tillamook Basin rivers
3. Specific gravity analysis of the samples taken from the five Tillamook Basin rivers
4. Numerical characterization of sediment transport with tidal influence using MATLAB

5. Simulation of downstream fining in an idealized gravel-bed river using GSTARS 2.1

5.2 Kilchis River downstream fining analysis

5.2.1 *Particle size analysis techniques*

The most basic analysis conducted of downstream fining was the determination of the particle size distribution for several sites along approximately 14 river miles of the Kilchis River. The purpose of this analysis was to determine the change in mean particle diameter (d_{50}) along the river, beginning upstream of the confluence of the North and South Fork. Side bars (bars that run parallel to the bank) in accessible areas were chosen as study sites. Study sites were chosen upstream of the confluences of significant tributaries. This was done to avoid including potential local disruptions in the downstream fining trend into the data collected.

Locations of study sites are shown in Figure 5.1. Sampling locations were chosen such that particle sizes on the bar were comparable to particles on the bed of the channel. High water marks and age of vegetation was used as indicators of return period for bar inundating flow. According to indicators, each bar with the exception of Site 3 is expected to be inundated annually. In one instance, the bar selected was severely disturbed by human traffic. For this site, on-site sampling locations were modified to account for the condition of the bar. Appendix A shows photographic evidence for each site. In part, the results of this analysis may be used to determine the cause for sediment shoaling at the mouth of the Kilchis River (river mile 0 to river mile 2, approximately).

Downstream fining is the expected natural process affecting any changes of particle size distribution, as this occurs in many gravel bed rivers (See literature review). Any observed interruptions of downstream fining trends may indicate lateral introductions

of sediment particles of various sizes. These lateral inputs may come from tributary contributions, landslides, or eroding and failing banks.

A regression analysis was used to examine the relationship between mean particle diameter and longitudinal distance along the channel. The regression analysis was performed using the expected exponential relationship represented by Equation 2.1. The Sternberg relationship has been used successfully (see literature review) in various studies of downstream fining. The power relationship (Equation 2.2) developed by Brierly and Kickin (1985) was reported to be appropriate for study areas near major sources of sediment. Rice (1999) used linear regression (Equation 2.3) to fit data for rivers where disruptions in the downstream fining trend are frequent. In the event that the data appear to fit better either the power or linear model, I have used the models where appropriate.

The research hypothesis implies that there is a significant relationship between d_{50} and distance from the river mouth. The associated null hypothesis states that there is no relationship between these variables. The average particle diameters of samples from five sidebars from river mile 14 to river mile 0 were tested against the distance downstream. A description of sampling procedures is given in a following section of this chapter.

5.2.2 Summary of Procedure with reasoning

Sampling locations were selected based on achieving the best representation of typical variations in particle size on gravel bars. Gravel bars form when upstream channel obstructions or other factors that affect the planform, or slope and cause converging turbulent flow at the centerline of the channel (Wyrick 2005). Reduced velocities due to redirection of the thalweg (line of maximum channel velocity, Wyrick 2005) toward the opposite bank cause deposition of coarse particles (see Figure 5.2).

The nature of flow around gravel bars and the resulting variations in particle size can also be investigated through descriptions of flow around submerged objects and channel contractions. For example, Henderson (1966) stated that the velocity distribution at a contraction has higher magnitudes of velocity near the contraction than velocities some distance away from the contraction. The flow accelerations in this area toward the opposite bank due to the contraction maintain the bar and its coarse particle distribution at the upstream end.

At higher river stage, velocities at the upstream end of the bar would increase and smaller particle sizes would be transported downstream (Wyrick 2005). However, the redirection of flow toward the outside bank would still cause coarse particles to deposit.

At section 2 in Figure 5.2, the armor layer may be as coarse if not coarser than that of section 1, depending on bar height, degree of inundation, and frequency of inundation by flow. When submerged, the velocities and associated shear stresses that exist at section 1 during periods of lower river stage would shift toward section 2. Furthermore, the velocities and associated shear stresses would be greater, as discharges would be larger than discharges at lower river stages. If submersion of the bar occurs quite frequently, the armor layer at section 2 might contain larger particles than those of the armor layer at section 1.

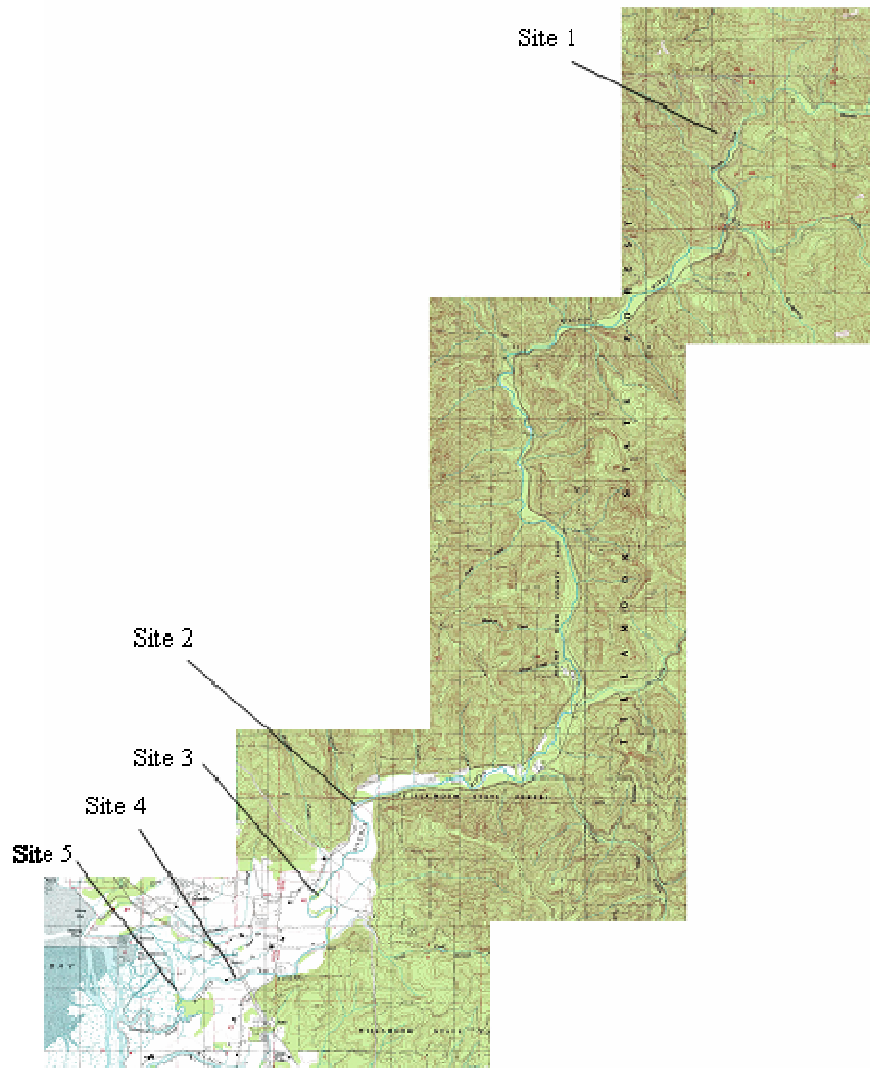


FIGURE 5.1: KILCHIS RIVER WITH LOCATION OF SAMPLING SITES

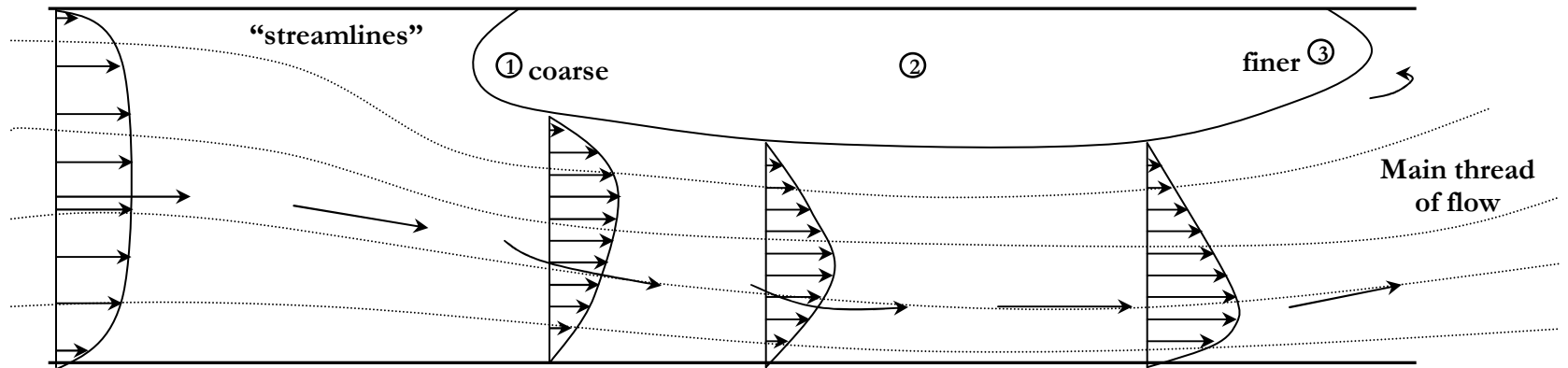


FIGURE 5.2: VELOCITY DISTRIBUTIONS FOR A CHANNEL NEAR SIDEBARS

In their study of variations in turbulence caused by channel obstructions, Tritico and Hotchkiss (2005) also showed increased magnitudes of velocity near submerged bodies. The accelerated flow and wake zone of low energy and recirculating flow is shown in a simplification of a visual presented in their results (see Figure 5.3). Section 3 in Figure 5.2 can be thought of as a wake zone area. Therefore, the size distribution of surface particles in these areas would be finer than the particles of sections 1 and 2.

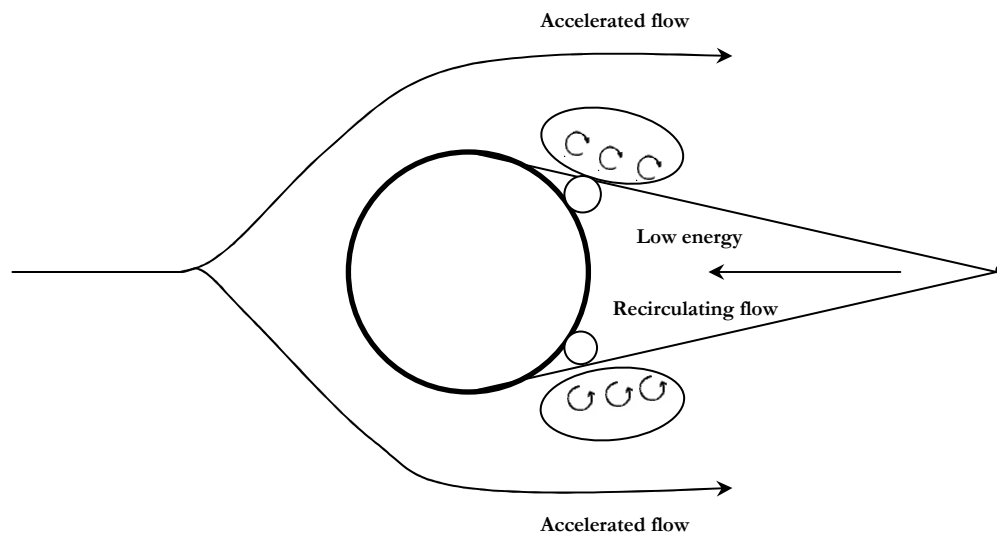


FIGURE 5.3: FLOW AROUND A CHANNEL OBSTRUCTION (modified from Tritico and Hotchkiss 2005)

Due to expected variation in particle size along each bar, sediment samples were collected at the center of side channel bars at each study site in the Kilchis River, as well as at the upstream and downstream ends. Upstream and downstream sampling locations were chosen 1 ft (0.3 m) inland from the water surface (see the left half of Figure 5.4). In one instance, at site three, where the bar appeared to be disturbed by human traffic such as ATV activities or camping, the sediment sample was taken in the channel parallel to the on-bar location that would have otherwise been selected.

In addition, at site 1 indirect field measurement was used for all particles larger than 3 inches (76.2 mm) in diameter, as I had to carry the sediment samples up a very steep incline after walking approximately a ¼ mile (0.4 km) downstream. Specific gravity calculations, described in detail later in this section, were used to estimate the weights of those particles left in the field. Their weights could then be included with the weights of the other particles brought to the lab. This allowed complete particle size analysis. The specific gravity calculation included an assumption that particles were spherical in shape (for particle diameter and volume estimations).

All sediment samples were collected from within a fixed area of four square feet. A metal frame was used to delineate this area, with outside dimensions of 2-feet-by-2-feet (0.6-square meter-by-0.6-square meter, shown in Figure 5.5). The armor and sub-armor layers, each down to the depth of the largest armor layer particle present in the sampling area, were separately collected, labeled, and taken back to the lab for oven-dry sieve analysis.

Samples were dried overnight in an oven set at 104 °F (40 °C). The temperature of the oven was hot enough to remove moisture without eradicating any organic material present in the samples. After drying, sediment samples were passed through and collected on sieves of varying opening sizes from 152.4 to 0.075 mm (6 in to 0.0029 in). According to Lane et al (1947), this size range covers large cobbles to very fine sand. Note: cobbles are in the size range of 64 mm to 250 mm (2.52 in to 9.8 in), gravel is in the size range of 2 mm to 64 mm (0.08 in to 2.52 in), and sand is in the size range of 0.064 mm to 2 mm (0.0025 in to 0.08 in), according to the AGU classification given in Vanoni, 1975.

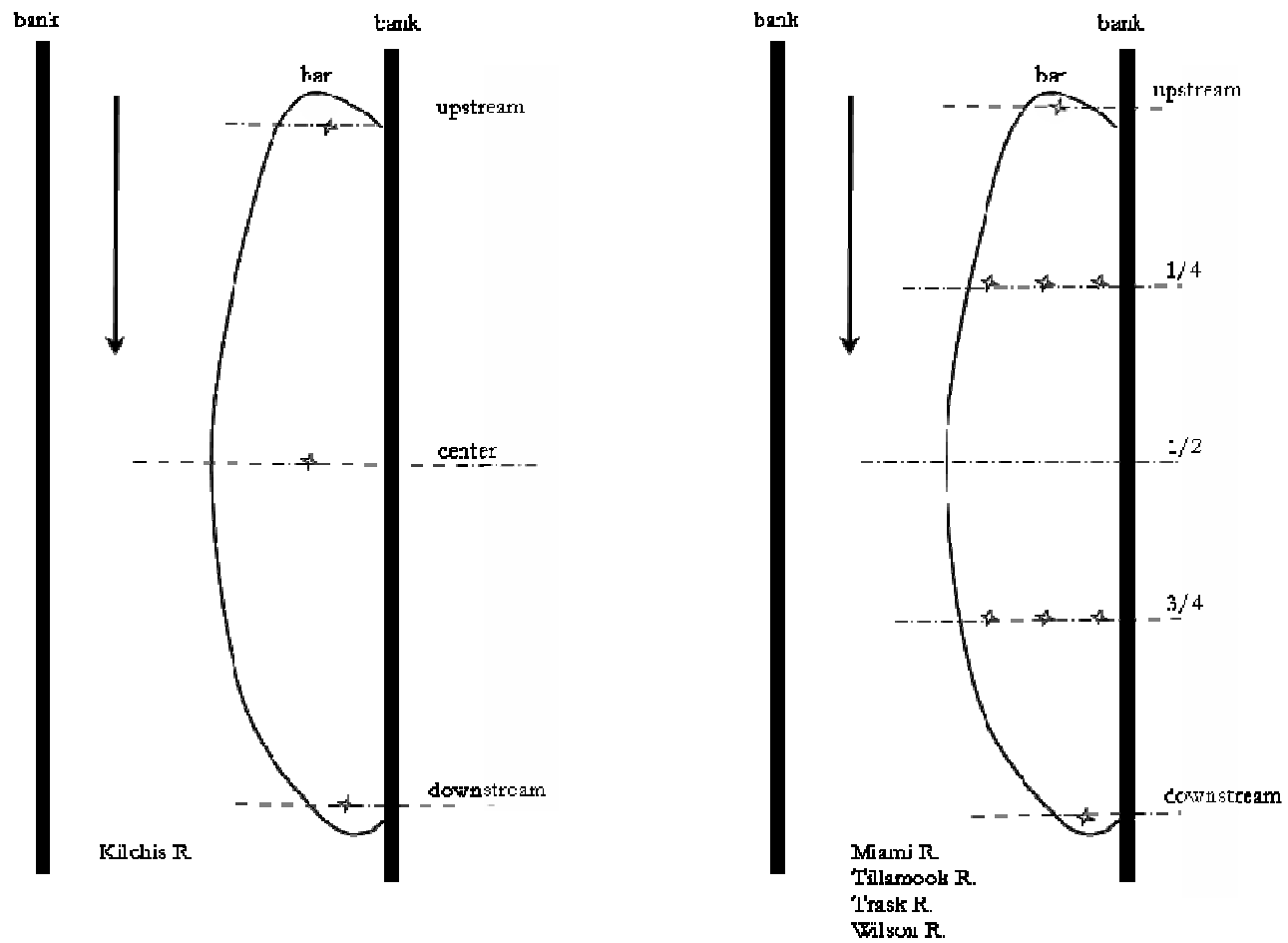


FIGURE 5.4: ILLUSTRATION OF SAMPLING CONFIGURATION
 *Stars represent sampling locations

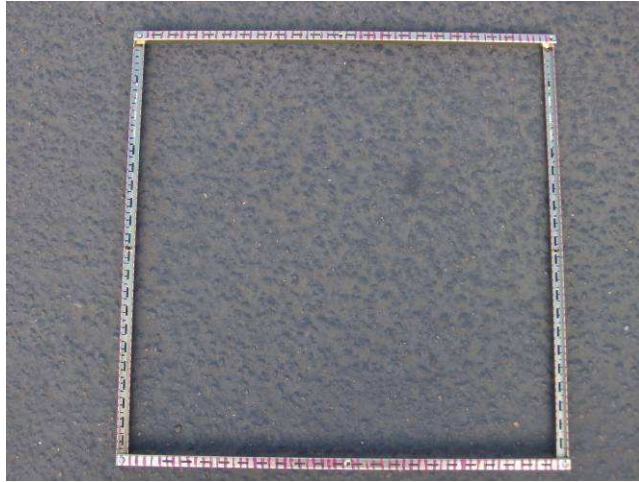


FIGURE 5.5: 2' x 2' DELINEATING APPARATUS FOR SAMPLING BED MATERIAL

The sieves were placed in Rotap machines that shake the sieves with several degrees of freedom. Each stack of sieves were shaken for eight-minute intervals to allow time for particles to pass through larger sieves and settle on the appropriate size sieve which had a grid size smaller than that of the particle mean diameter. Subsequently, the sieves were removed and the sediment particles that had been trapped on each sieve were weighed. When the number of particles on a particular sieve was easily countable, these numbers were also recorded. Finally, a cumulative frequency distribution was created for each sediment sample and the mean particle diameter (d_{50}) for each sample was identified from the data and recorded for later comparison. Results of sieve analysis are outlined in the Results chapter of this dissertation.

Also included in the Results chapter is photographic evidence of the particle size distribution of the surfaces sampled. Photos were taken prior to sampling the sediment, to show undisturbed conditions. The same 2-foot-by-2-foot (0.6-meter-by-0.6-meter) delineator used to determine the sampling area was used for scale in the

photographs. While a study of these photographs was not used directly in the particle size analysis, the photos serve as evidence of results and provide a quick visual verification of the downstream fining analysis results. In-stream underwater photographs of surface particles were also taken to use in conjunction with on-bar evidence of particle size distributions. The procedure for data collection at each side bar is summarized in Figure 5.6.

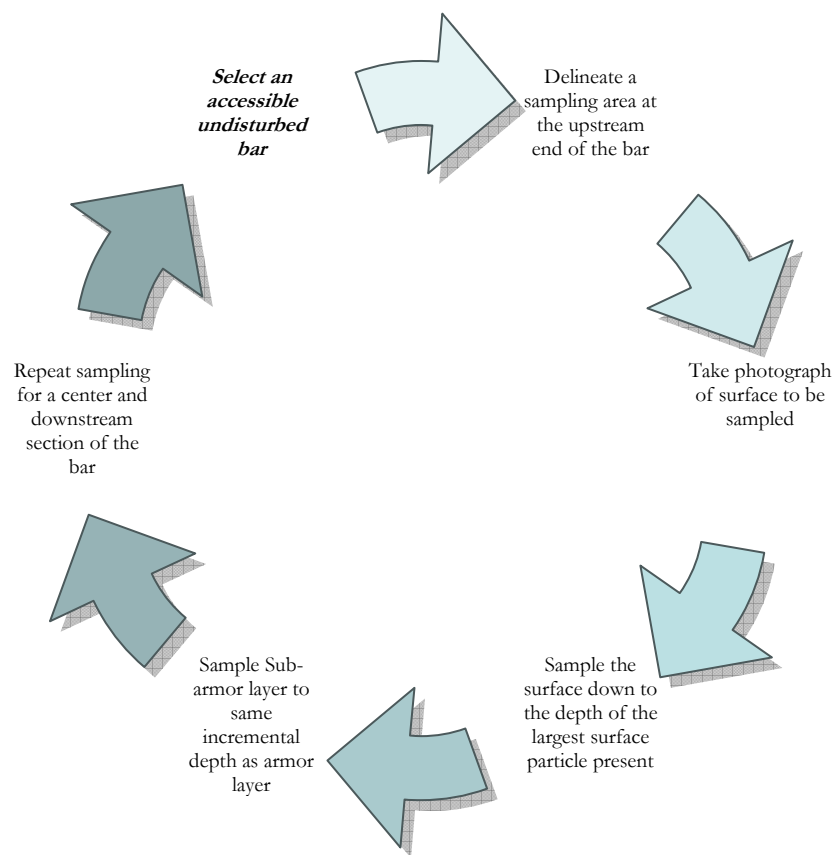


FIGURE 5.6: PROCEDURE FOR DATA COLLECTION USED IN KILCHIS ANALYSIS

5.3 Photo frame fining analysis

5.3.1 *Particle size analysis techniques*

The photo frame method was used to analyze particle distributions of the remaining four Tillamook Basin rivers (Miami, Kilchis, Wilson, Trask, and Tillamook). The Wolman pebble count method (Wolman 1954), where particles are selected while walking across a bar was considered for sampling; however, a method more comparable to the bulk sampling analyses was developed instead. The procedure includes delineating a 2-foot-by-2-foot (0.6-meter-by-0.6-meter) area using the same metal frame as used in the Kilchis River analysis. Prior to sample collection, photographic evidence of each surface was taken for purposes of visual analysis. Subsequently, 50 armor layer particles from within the sampling area were randomly picked. The median diameter of each particle was measured using a metal sieve plate. In cases where surface particles were so large that 50 surface particles did not lie within the frame, the sampling area was extended to include an additional 2-foot-by-2-foot (0.6-square meter-by-0.6-square meter) area. This was the case for sites 1 on both the Wilson and Trask rivers. The sieve plate used for measurement had openings for particles from 101.6 mm to 1.59 mm (4 in to 0.0625 in). The individual particle sizes were recorded. Particles larger than 100 mm (4 in) were measured using a ruler.

Bed material data for the additional Tillamook Basin rivers were collected on the same spatial scale as for the Kilchis River analysis. That is, each study length was contingent on the location of major confluences (such as river forks). Study sites were chosen upstream of the confluences of significant tributaries. As for the Kilchis River, this was done to avoid including potential local disruptions in the downstream fining trend into the data collected. Sampling locations also matched those of the Kilchis River investigation, namely sidebars. However, eight areas were sampled per bar instead of the three at the Kilchis River bars. This allowed a more extensive

description of the bar surface without the need to transport large masses of sediment to the laboratory.

Sampling locations were chosen such that particle sizes on the bar were comparable to particles on the bed of the channel. High water marks and age of vegetation were used as indicators of return period for bar inundating flow. Comparison of bar and riverbed material was performed for each site regardless of bar height. Even where bar height and vegetation development indicated an inundating flow return period of more than one-year, bed and bar material were comparable in their range of particle sizes (e.g., site 1 of Wilson River). Figure 5.4 shows a comparison of the sampling locations for the five rivers. Only surface samples were taken for examination at the rivers where photo frame methods were used.

Each bar was analyzed by means of five transects: one upstream transect 1 foot (0.3 meter) from water's edge, one downstream transect 1 foot (0.3 meter) from water's edge and one transect each at the $\frac{1}{4}$, $\frac{1}{2}$, and $\frac{3}{4}$ marks along the length of the bar. Single samples were collected at the upstream and downstream ends, and three samples each were collected at the $\frac{1}{4}$ -mark and $\frac{3}{4}$ -mark transects, giving eight sampling locations per bar (The $\frac{1}{2}$ -mark was merely used to help determine the quarter-mark transects.). For the very long bars, the $\frac{1}{2}$ -mark did not represent the variation in particle sizes; therefore, the $\frac{1}{4}$ -marks were sampled to expand coverage. The three samples at the $\frac{1}{4}$ and $\frac{3}{4}$ transects included one sample 1 foot (0.3 meter) from waters edge, one sample at the transect center point, and one sample from near the back of the bar. In the instance of a sample point occurring at a position on the bar that contains silt, photographs were taken but no sampling particle count was performed. Also, for transects less than 12 feet (3.6 meters) in width only two samples were taken. In such instances, the center sample was not collected. Figure 5.7 shows a summary of the procedure used to sample each bar. The desired sampling plan was to have five sampling sites per river. Figures 5.8 to 5.11 show the locations of sampling sites for the four additional rivers.

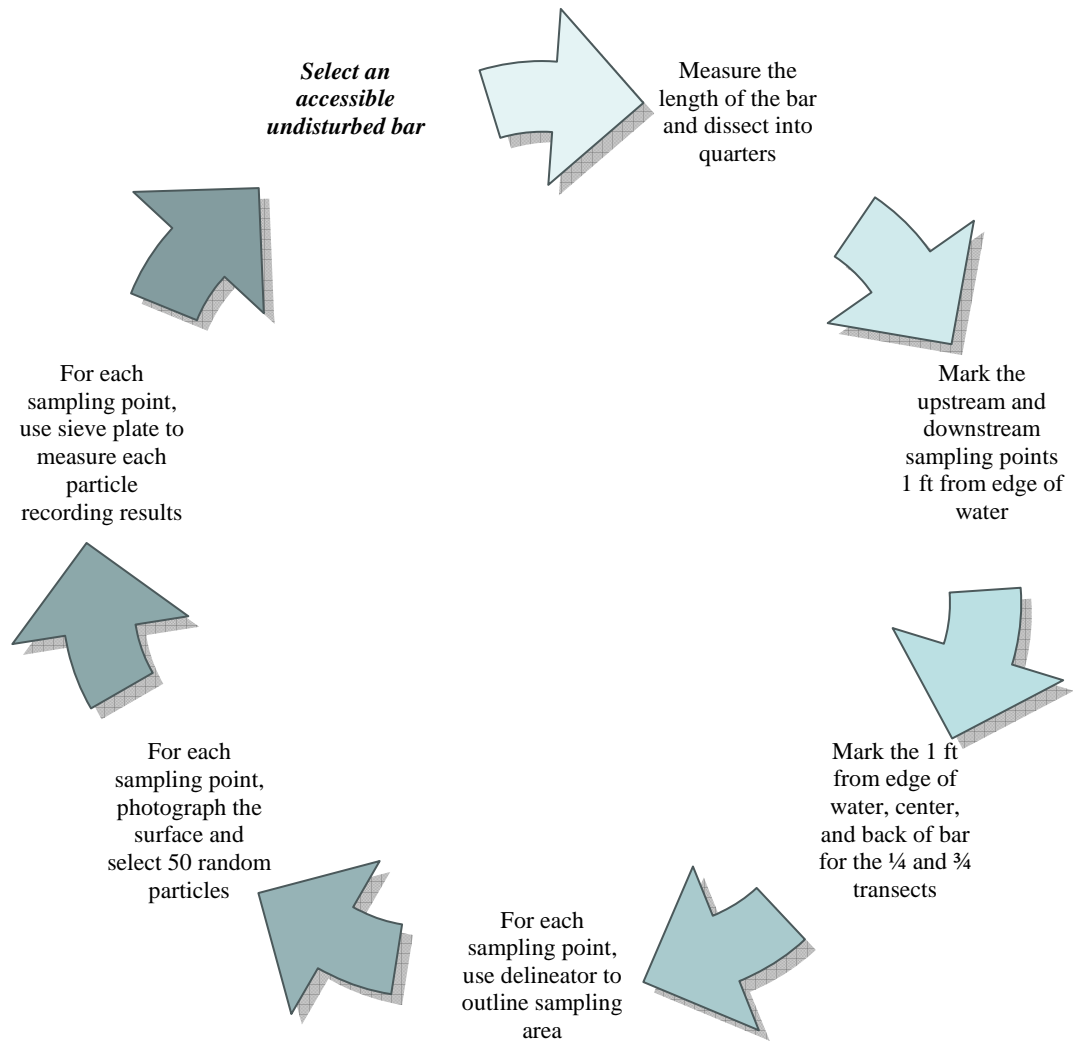


FIGURE 5.7: PROCEDURE FOR PHOTO FRAME SAMPLING

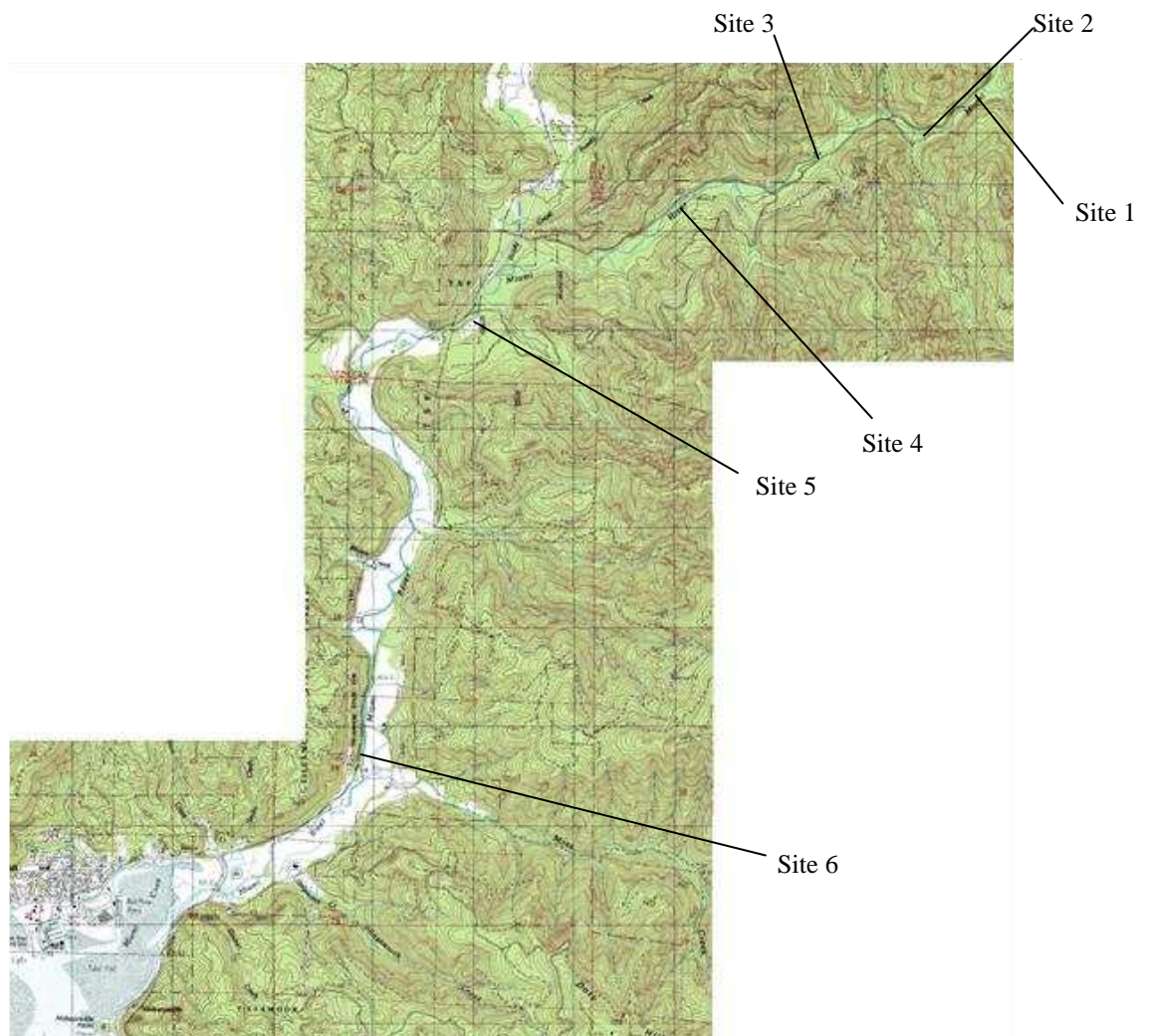


FIGURE 5.8: MIAMI RIVER WITH LOCATION OF SAMPLING SITES

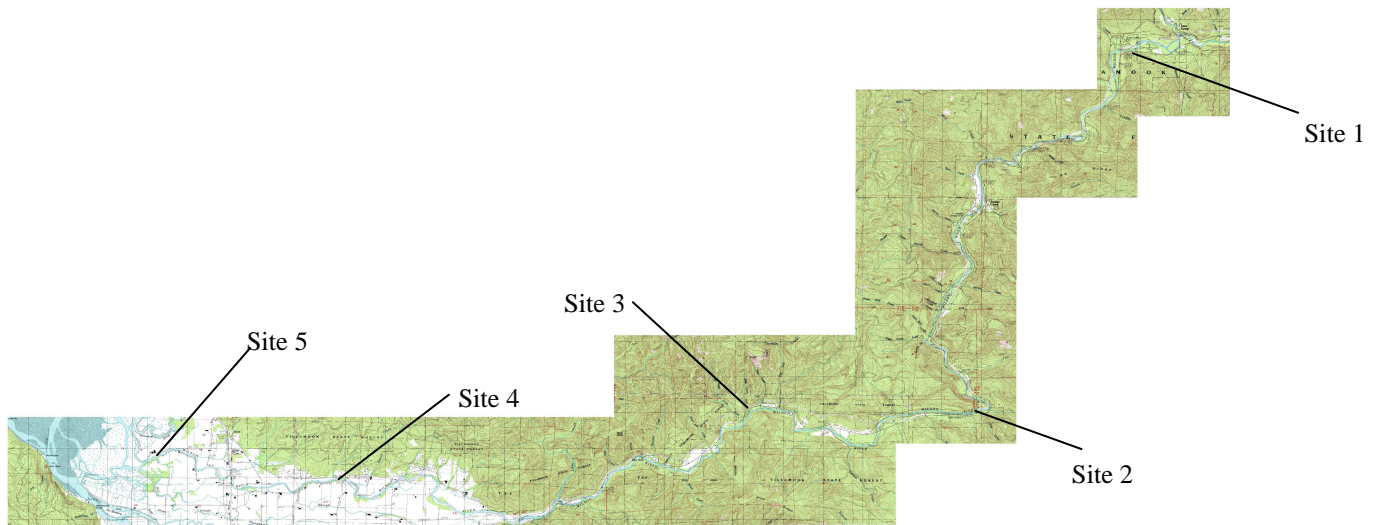


FIGURE 5.9: WILSON RIVER WITH LOCATION OF SAMPLING SITES

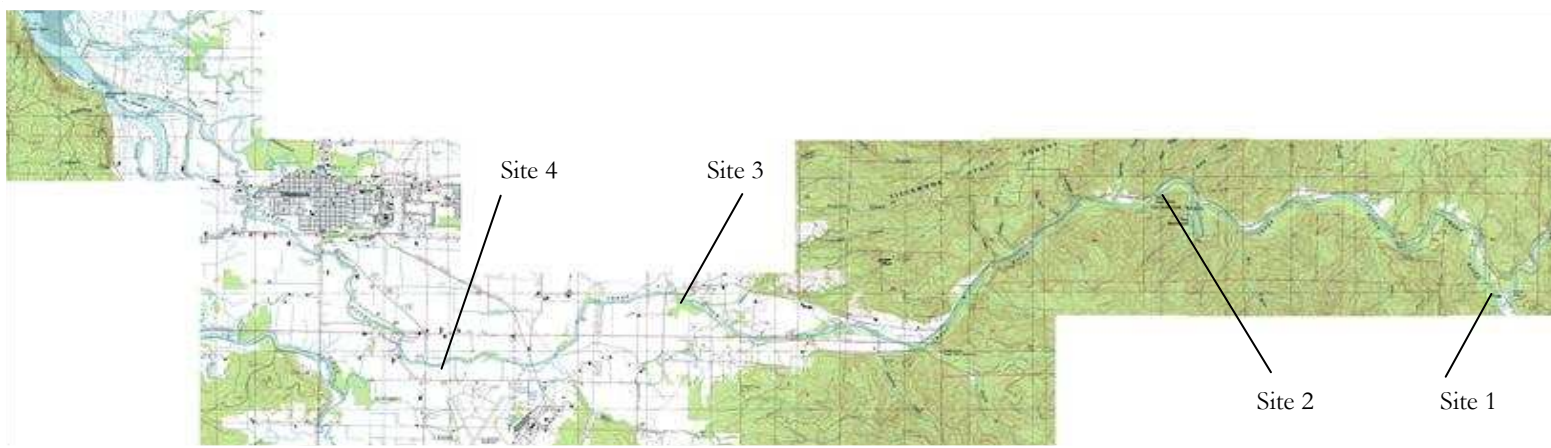


FIGURE 5.10: TRASK RIVER WITH LOCATION OF SAMPLING SITES

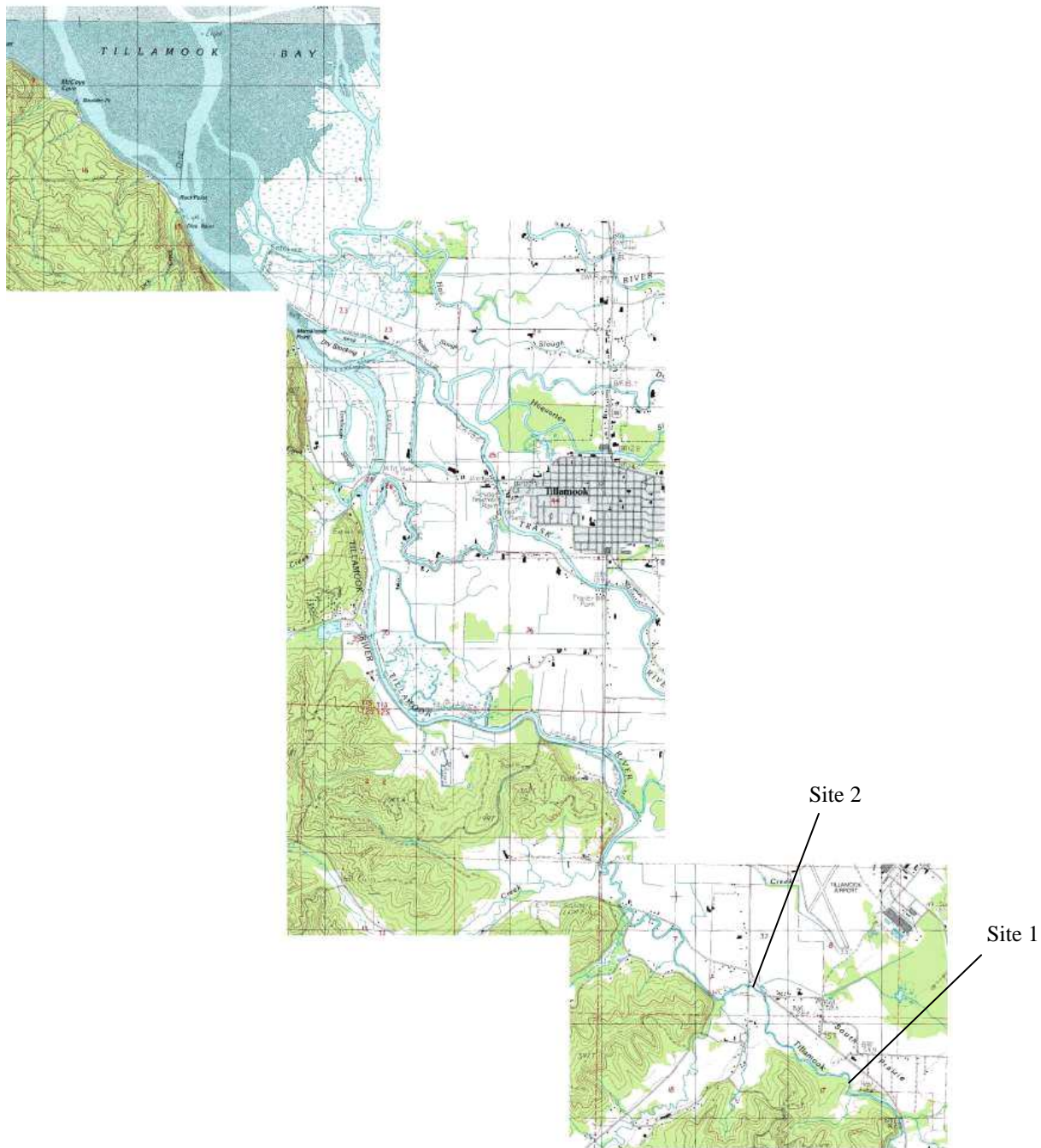


FIGURE 5.11: TILLAMOOK RIVER WITH LOCATION OF SAMPLING SITES

Unfortunately, due to accessibility constraints and abrupt transition from a gravel-bed to a silt and sand-bed, not all rivers were sampled at the five sites. Site 1 of the Miami River was not sampled, but merely photographed because of the existence of an ephemeral channel and large backwater area covered by an extensive bar of poorly sorted material. Hence, site 2 was the first regularly-shaped side bar sampled on the Miami River. The Tillamook River has two sampling locations. Due to extensive private property, access to the river was severely limited. Furthermore, the Tillamook River transitioned to a mud bottom system upstream of River mile 3 (4.8 km), as shown in Figure 5.12. The Trask River, which borders the Tillamook River in its last river mile, also transitioned to a mud bottom upstream of the last accessible site. These transitions may be indicative of a bimodal sediment distribution in these systems (Sambrook et al. 1995, Smith et al. 1997, Parker and Cui 1998, Knighton A.D. 1999). While the photo frame analysis does not allow for accurate characterization of a bimodal sediment distribution, the focus of this research is such that focusing on reduction of gravel size particles is adequate.

Table 5.3 lists the approximate locations of each sampling site for the Kilchis River analysis and for the photo frame sampling of the additional four rivers. A combined total of 21 sampling locations and 141 individual sampling points were used for the particle size analyses of the rivers of the Tillamook Basin.



FIGURE 5.12: TILLAMOOK RIVER AT RIVER MILE 3 BOAT RAMP

TABLE 5.3: SAMPLING SITE LOCATIONS

RIVER AND SITE NUMBER	SITE LOCATION	SITE LOCATION		NUMBER OF INDIVIDUAL SAMPLING POINTS
		rm	km	
Miami site 1	Confluence at Miami River road	9	14.5	0
Miami site 2	Downstream of confluence at Miami River road	8.8	14.2	8
Miami site 3	Downstream of bridge and cabled in-stream boulders	8	12.9	8
Miami site 4	Long deposit after Miami River road crosses river	6.9	11.1	8
Miami site 5	Downstream of bridge at New Miami River road	5.1	8.2	8
Miami site 6	Upstream of bend before ag land and HWY 101 junction	1.5	2.4	7
Kilchis site 1	North Fork at Zig Zag Canyon	14	22.5	3
Kilchis site 2	Upstream of public bridge and boat ramp	4	6.4	3
Kilchis site 3	Downstream of Curl bridge	3	4.8	3
Kilchis site 4	Downstream of HWY 101 bridge	1.2	1.9	3
Kilchis site 5	Downstream of confluence of Kilchis River and Squeedunk Slough	0.1	.16	3

TABLE 5.3: (CONT'D)

RIVER AND SITE NUMBER	SITE LOCATION	SITE LOCATION		NUMBER OF INDIVIDUAL SAMPLING POINTS
		rm	km	
Wilson site 1	Upstream of bridge south of Lee's Camp	28	45	8
Wilson site 2	Downstream of Fall Creek bridge	17	27.4	8
Wilson site 3	Downstream of Smith Creek road and upstream of boat ramp	12.5	20.1	8
Wilson site 4	Downstream of bridge at bend in Wilson River Loop	3.8	6.1	8
Wilson site 5	At Geiger Farm houses	0.1	0.16	7
Trask site 1	Downstream of confluence North Fork bridge and camp site	17.5	28.2	8
Trask site 2	Downstream of Peninsula at Trask River road mile 15	13	20.9	8
Trask site 3	Upstream of bridge at Trask River road	7.2	11.6	8
Trask site 4	Downstream of boat ramp and upstream of HWY 101	5.8	9.3	8
Tillamook site 1	Downstream of Tillamook rest area off HWY 101	8	12.9	8
Tillamook site 2	Upstream of bridge at Bewely Road	6.9	11.1	8

5.4 Specific Gravity Analysis

5.4.1 *Specific gravity analysis techniques*

Specific gravity analyses were performed for each Kilchis River site. Specific gravity was determined for particles according to size fraction. Particles of various size fractions may originate from different sources, so variation in specific gravity according to size fraction was investigated in addition to potential longitudinal variations.

For the Kilchis River, the armor and sub-armor layer particles were combined, as it is assumed that all material on a particular bar originated from the same source. In addition, the size fractions sampled ranged from 76.2 mm to 7.925 mm (3 in to 0.31 in). For the remaining rivers, the size fractions were determined from the field sieve plate, namely, 101.6 mm to 1.59 mm (4 in to 0.0625 in).

Particle size analyses for the other four rivers were based on size fraction alone. For each additional river, one sample (separated by size fraction) was collected from a high-elevation site and one sample was collected from a low-elevation site (separated by size fraction). The high-elevation and low-elevation samples were combined prior to analysis. The same numbers of particles were collected for each size fraction at both the upper and lower sites. For example, if five 4-inch (101.6-millimeter) particles were collected from a high-elevation site on a particular river, then five 4-inch (101.6-millimeter) particles would also be collected from a low-elevation site on that same river.

Once particles of each size fraction for each site were collected and labeled, the particles were counted and weighed in air, using a scale with a submerged wire basket attached (Figure 5.13). After the particles were weighed in air, they were placed in the submerged basket for submerged weighing. First, however, the particles were agitated to remove air bubbles and two minutes were allowed to pass prior to recording the weight registered on the scale.

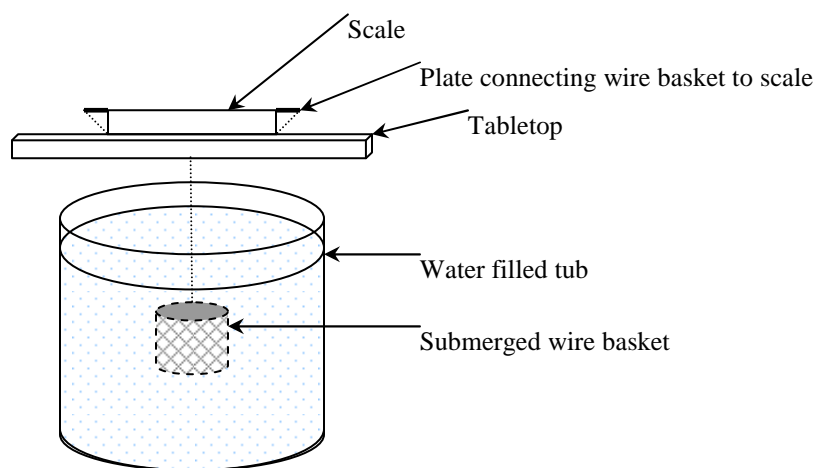


FIGURE 5.13: SCHEMATIC OF APPARATUS USED TO DETERMINE SPECIFIC GRAVITY

Once the air dry and submerged weights are known, Equation 5.1 is used to calculate the specific gravity of the size fraction.

$$SG = \frac{W}{W - W_s} \quad (5.1)$$

where W is the air dry weight in grams and W_s the submerged weight in grams. A geometric mean of the specific gravities for size fractions at each site was calculated instead of an arithmetic mean. The purpose of using the geometric mean is to account for the variation in number of particles used to determine the specific gravity of each size fraction at any given site. Figure 5.14 shows a summary of the procedure for determination of specific gravity.

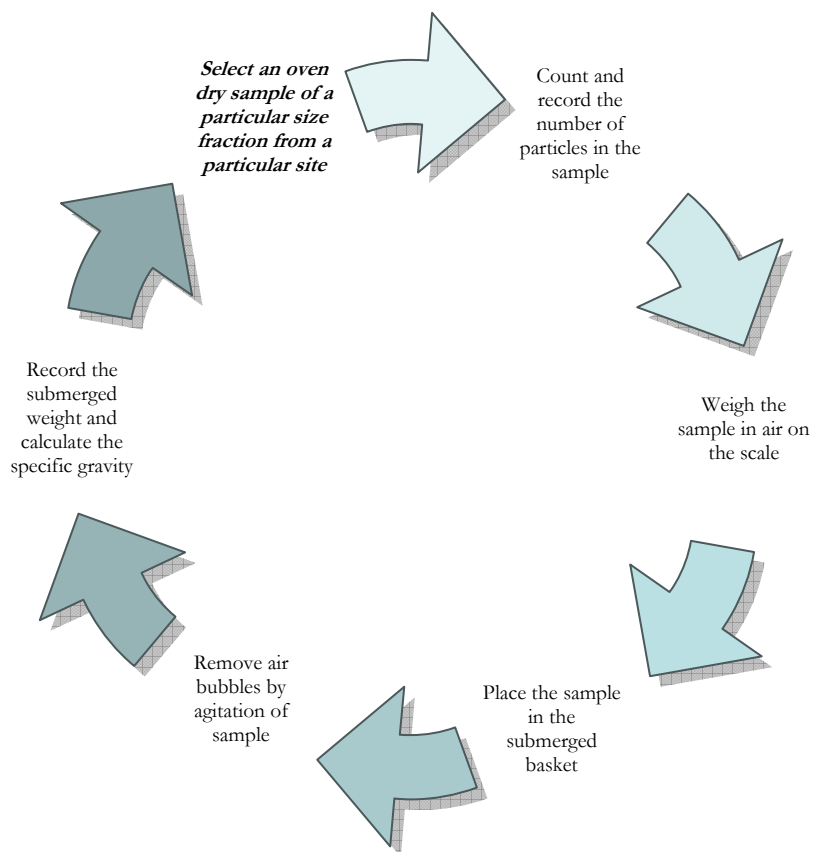


FIGURE 5.14: PROCEDURE FOR DETERMINATION OF SPECIFIC GRAVITY

5.5 Numerical analysis of tidal influence on bed-load transport

5.5.1 Significance of numerical models

A one-dimensional numerical model was developed to describe and analyze sediment transport in the zone of tidal influence. The model was constructed using the MATLAB computing package.

There are three intended uses of the numerical model:

1. To describe how the periodic nature of the tide influences river sediment transport in the zone of tidal influence
2. To create a simplified method for computing water surface profiles and bed-load rates adjusted to incorporate tidal influence
3. To investigate the probable causes for the shoaling of gravel reported by landowners to be accumulating at the mouth of the Kilchis River

5.5.2 Description of MATLAB

MATLAB and Simulink is a software package developed by MathWorks. The software is a technical computing tool. MATLAB is widely used in academia as well as in a broad range of industries that include aerospace, automotive, computer peripherals, electronics, environmental, medicine, and telecommunications. The software operates using a built-in programming language that allows high-performance numeric computing, modeling and simulation. Simulink provides interactive modeling, simulating, and analyzing for dynamic systems (Learning MATLAB 7 2004).

5.5.3 Presentation of modeling equations

Bed-load transport is typically calculated using empirical formulae. Many relationships are available, each differing primarily in the approach to transport taken by the investigator. For example, in his textbook on sediment transport Chih Ted Yang (1996) organized available bed-load transport formulae by approaches involving shear stress, energy slope, discharge, velocity, bed form, equal mobility, and probabilistic and stochastic evaluations. The numerical model developed for this investigation, TIMM (Tidally Influenced Movement Model) uses physically based excess shear stress as the underlying mechanism. Namely, an

undulating water surface is applied to calculate Shields criterion for incipient motion and bed-load transport. The model simulates reaches of the river low enough in elevation such that using bed-load functions that calculate transport capacity (maximum load that the flow can transport) are viable methods. Furthermore, the model assumes transport is not supply limited in these lower reaches due to lateral inputs of sediment including tributary contributions.

Of the many options currently available for estimation of rate of bed-load movement, the two bed-load relationships considered for use in the TIMM are the Shields relationship and the DuBoys formula. These both are relatively straight-forward to use and allow the development of the MATLAB TIMM model and its application.

The semi-empirical bed-load formula developed by Shields in 1936, was discussed in the chapter on literature review, and is shown mathematically as:

$$\frac{q_b \gamma_s}{q \gamma S} = 10 \frac{\tau - \tau_c}{(\gamma_s - \gamma) d} \quad (5.2)$$

where q_b is bed-load per unit channel width, q is water discharge per unit channel width, d is sediment particle diameter, S is slope, γ is specific weight of water, γ_s is specific weight of sediment, and τ and τ_c are the shear stress and critical shear stress.

The DuBoys formula (1879), also discussed earlier, is similar in nature (i.e., based on tractive force) but written:

$$q_b = \frac{0.173}{d_{50}^{0.75}} \tau(\tau - \tau_c) \quad (5.3)$$

where d_{50} is the sediment size at which 50% of the bed material is finer.

The average boundary shear stress in the channel is calculated using:

$$\tau = \gamma R S \quad (5.4)$$

where R is hydraulic radius for the channel at a cross section (cross sectional area divided by wetted perimeter).

Critical shear stress exerted on the channel boundary is typically found via the Shield's diagram shown earlier in Figure 2.3. In order to use the Shields diagram, shear velocity (U_*) and Boundary Reynolds number (R_e) must be calculated using in-situ data. The formulae for these parameters are:

$$U_* = (gDS)^{1/2} \quad (5.5)$$

$$R_e = \frac{U_* d}{\nu} \quad (5.6)$$

where g is gravitational acceleration, and ν is the kinematic viscosity of the water. The associated dimensionless shear stress (τ_*) can then be found as the output value on the Shields diagram. The dimensionless shear stress equation (Equation 5.7) is then solved for critical shear stress (τ_c):

$$\tau_* = \frac{\tau_c}{(\gamma_s - \gamma)d} \quad (5.7)$$

A piecewise defined function was developed to eliminate the need for manual determination of dimensionless shear stress. The function replicates the Shields diagram. Another piecewise defined function was developed to replicate the diagram constructed by Straub in 1935 that relates sediment size and critical shear stress exerted on the bed of the river (this diagram was previously shown in Figure 3.7). These piecewise defined functions make it possible to use either the Shields criterion or the critical tractive force method to investigate tidal influence on sediment transport.

The piecewise defined function for the Shields diagram is written:

$$\tau_* = \begin{cases} 0.1066x^{-1.0195} & 0.26 \leq x \leq 1 \\ 0.1061x^{-0.7173} & 1 < x \leq 5 \\ 0.0407e^{-0.0299x} & 5 < x \leq 8 \\ -5E - 07x^2 + 0.0002x + 0.0298 & 8 < x \leq 200 \\ 1E - 10x^3 - 2E - 07x^2 + 0.0001x + 0.038 & 200 < x \leq 1000 \end{cases} \quad (5.8)$$

where x is the Boundary Reynold's Number. The source of these five parts of this multipart function comes from curve fitting of five short segments of the log-log Shields diagram. Each segment was adequately short enough to result in a highly reliable trend line (R-squared >95%) that is shown in Figure 5.15.

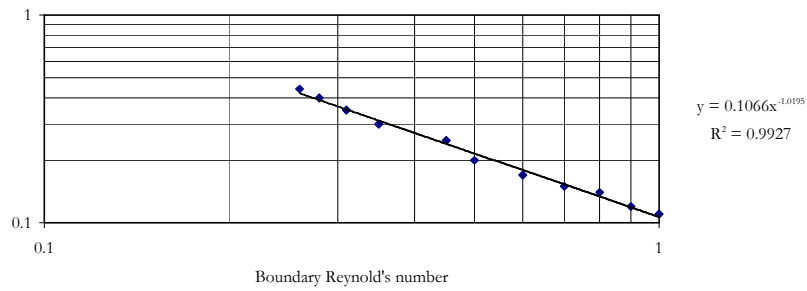
The piecewise defined function for the Straub relationship is written in metric units as:

$$\tau_c = \begin{cases} 0.0663e^{1.0124x} & 0.13 \leq x \leq 1 \\ 0.1696e^{0.0221x} & 1 < x \leq 60 \end{cases} \quad (5.9)$$

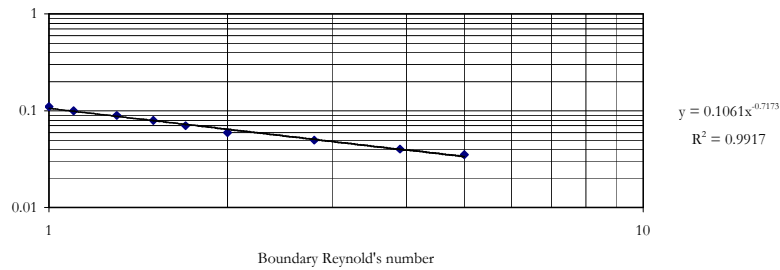
and in English units:

$$\tau_c = \begin{cases} 0.0137e^{0.875x} & 0.13 \leq x \leq 1 \\ 0.0316e^{0.0256x} & 1 < x \leq 60 \end{cases} \quad (5.10)$$

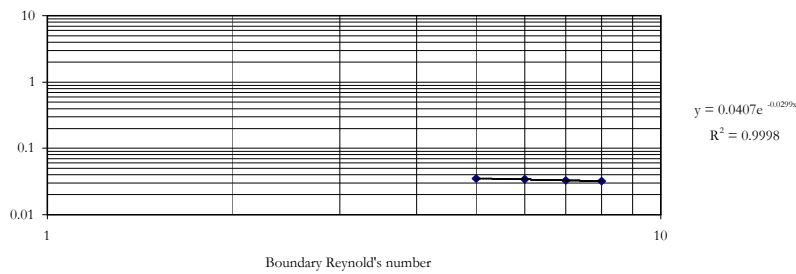
where x is the sediment diameter in millimeters. Figure 5.16 shows the scatterplots used to create the multipart functions used to describe Straub's work.



(a)

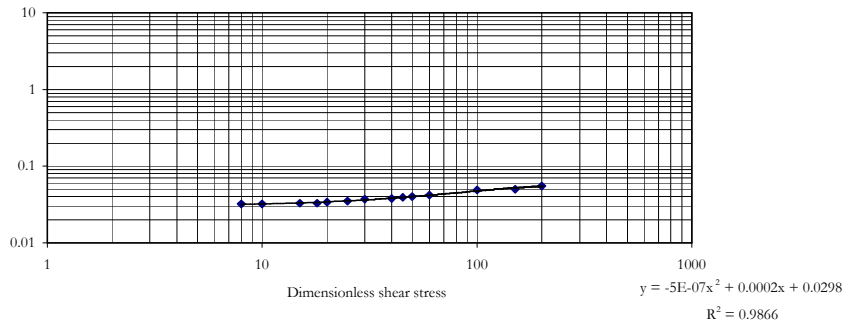


(b)

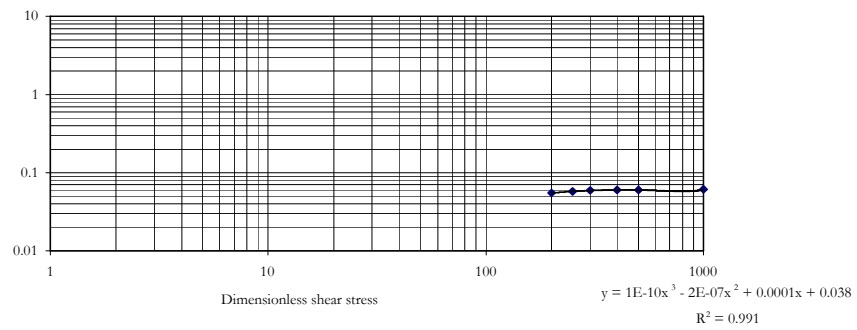


(c)

FIGURE 5.15: SCATTERPLOTS FOR MULTIPART FUNCTION FOR USE WITH SHEILDS DIAGRAM where (a) x between 0.26 and 1, (b) x between 1 and 5, (c) x between 5 and 8, (d) x between 8 and 200, (e) x between 200 and 1000



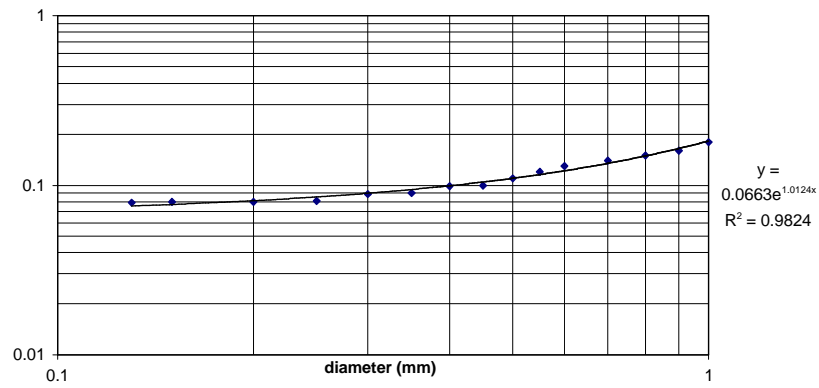
(d)



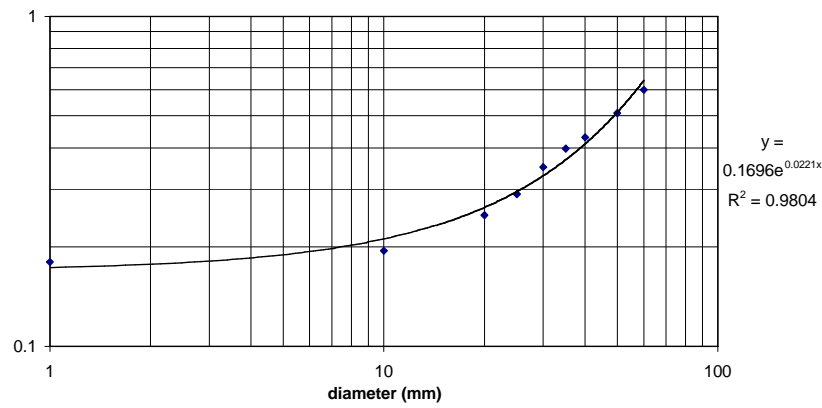
(e)

FIGURE 5.15: CONT'D

where (a) x between 0.26 and 1, (b) x between 1 and 5, (c) x between 5 and 8, (d) x between 8 and 200, (e) x between 200 and 1000



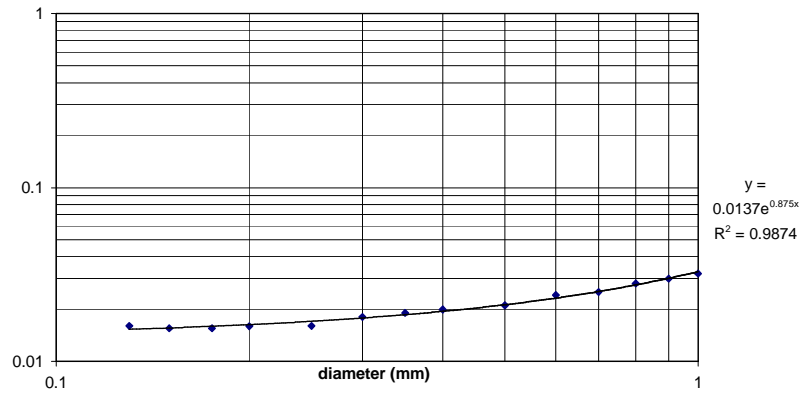
(a)



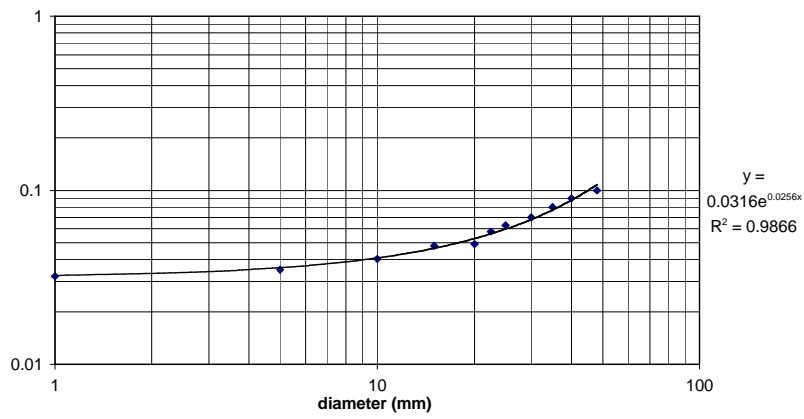
(b)

FIGURE 5.16: SCATTERPLOTS FOR MULTIPART FUNCTION USED FOR THE STRAUB BED-LOAD RELATIONSHIP

where (a) x between 0.13 and 1 mm (metric), (b) x between 1 and 60 mm (metric), (c) x between 0.13 and 1 mm (English), (d) x between 1 and 60 mm (English)



(c)



(d)

FIGURE 5.16: CONT'D

where (a) x between 0.13 and 1 mm (metric), (b) x between 1 and 60 mm (metric), (c) x between 0.13 and 1 mm (English), (d) x between 1 and 60 mm (English)

Once the critical shear stress is known, it can then be compared to the actual shear stresses along the channel bottom that are calculated using Equation 5.4. Bed-load transport can then be estimated using either Equation 5.2 or Equation 5.3.

Two methods were developed to address tidal influence on bed-load transport. First, a trigonometric function (p) was developed. It is shown mathematically as:

$$p = l_o \sin(\omega t + j) \quad (5.11)$$

where l_o , ω , and j are correction factors used to correct for the timing of highs and lows of water depth for a given tidal range. The function p is used as a factor during backwater calculations. The starting depth entered into backwater calculations at time t is determined by the value of p . Consequently, the water surface profiles in the zone of tidal influence over time are obtained for use in subsequent bed-load calculations.

When originally conceived, this first method included multiplication of p to each element of an array of numbers that represented the water surface profile. This was a major drawback because multiplication of p to each element in the array implied that tidal effects are equivalent throughout the zone of tidal influence. However, tidal influence diminishes in the upstream direction. To address this drawback, a second routine was developed. This involves taking observed tidal fluctuations and reducing them to a sinusoidal function with a maximum value equal to the average high tide channel water depth and a minimum value equal to either critical depth or some specified average low tide channel water depth. Subsequently, this sinusoidal function is reduced to a step function that repeats two average high values, two average low values, and two intermediate values for tide height. Figure 5.17 uses the NOAA tide data for Garibaldi, near the mouth of Tillamook Bay, to show this process pictorially.

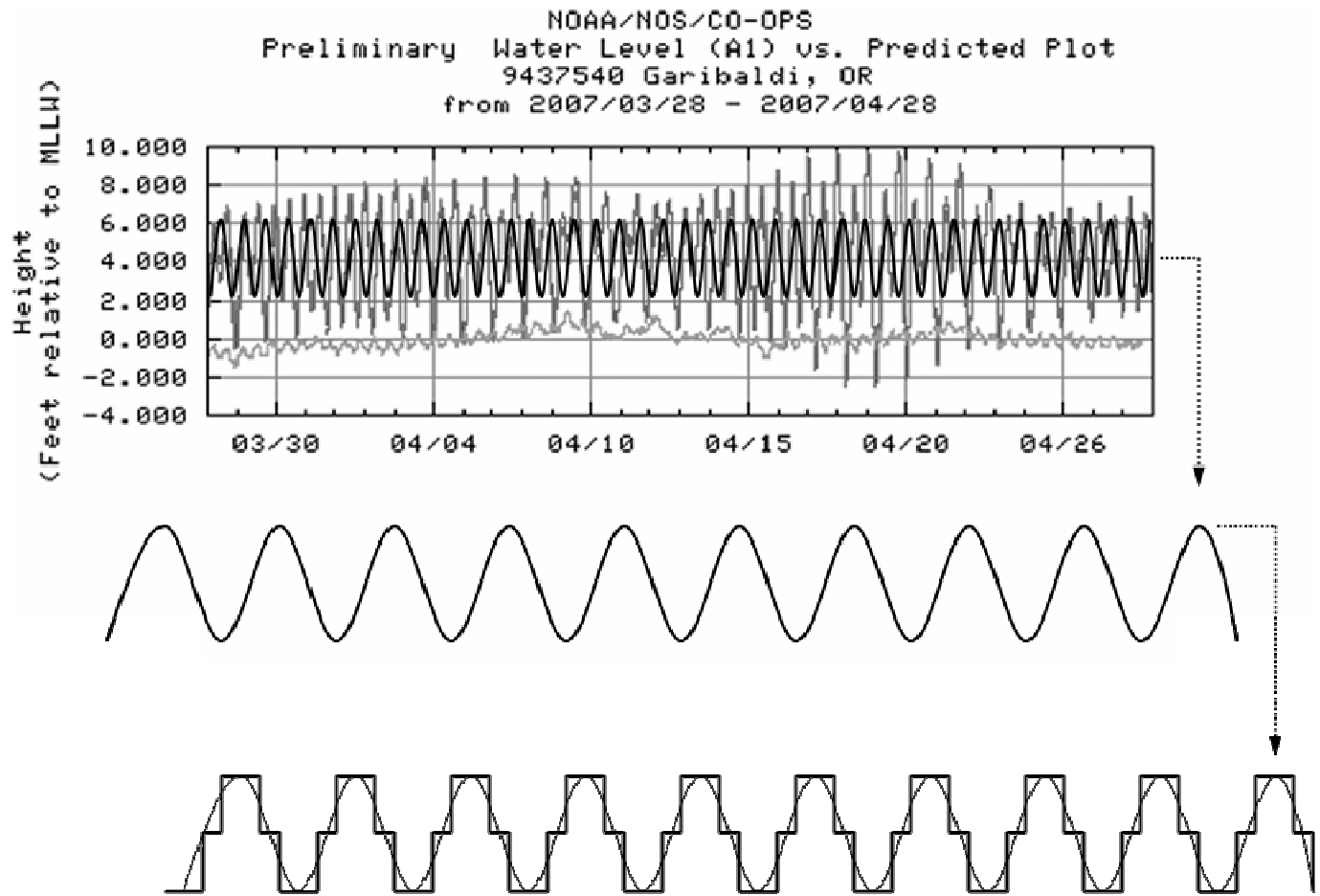


FIGURE 5.17: REDUCTION OF OBSERVED TIDAL FLUCTUATIONS TO A STEP FUNCTION

This step function partitions in-stream conditions into three scenarios: high tide, low tide, and intermediate tide. During high tide, the water surface is elevated at the downstream end to form an M1 curve. Critical depth (y_c) is calculated for comparison to downstream depth using:

$$y_c = \left(\frac{Q^2}{gB^2} \right)^{1/3} \quad (5.12)$$

and the normal depth at the upstream end is calculated using an iterative process to find the normal depth (y_n) that causes the right and left sides of Equation 5.13 to agree:

$$\frac{A^{5/3}}{P^{2/3}} = \frac{nQ}{k_n S_0^{1/2}} \quad (5.13)$$

where

$$leftside = \frac{(y_n B)^{5/3}}{(2y_n + B)^{2/3}} \quad (5.14)$$

k_n is a constant ($1.0 \text{ m}^{1/3}/\text{s} = 1.49 \text{ ft}^{1/3}/\text{s}$) and n is Manning roughness factor. Following computation of normal depth, backwater calculations are performed to adjust the water surface profile using the standard step method presented in Chapter 3 of this dissertation. As a reminder, the energy equation modified for this purpose is reproduced as Equation 5.15:

$$\Delta L = \frac{(y_1 + \alpha_1 v_1^2/2g) - (y_2 + \alpha_2 v_2^2/2g)}{S_{f-avg} - S_o} = \frac{E_1 - E_2}{S_{f-avg} - S_o} \quad (5.15)$$

The water surface profile approaches a state of normal depth in the upstream direction. The model simulates the zone of tidal influence, which can be several miles long. Once normal depth is reached, the remaining portion of the channel is set at that normal depth. The

process is then repeated beginning with a less elevated starting value for depth to represent intermediate tide. Low tide is simulated using a starting depth set at critical depth or some other specified value.

5.5.4 Summary of protocol used by numerical model

TIMM is a one-dimensional numerical model. When run, it prompts the user to enter parameters necessary to use Shields criterion for incipient motion and estimate bed-load transport. Appendix F shows the entire code for the model. Note the partitions that separate those input variables entered by the user from those parameters that are calculated by the software. Additional partitions and labels show the various calculations and iterations performed by the model. The following is a summary of these routines.

Input data include length of tidal zone, mean particle diameter of sediment, Manning roughness factor, channel width, water discharge, channel slope, and number of days for which bed-load transport is to be simulated. An array of daily discharge values equal to the number of days to be simulated is input data for the varied discharge version of the model. Finally, there are two options for the initial downstream depth:

1. Critical depth set beyond the first reach to be simulated, such that starting depth is some value reasonably above critical depth, but below normal depth
2. Average depth of the estuary

Figure 5.18 shows the configuration for the two options for downstream depth.

After necessary input data are provided, the model then cycles through a series of iterations specified by the length of simulation time for the experiment requested by the user. The program starts with a bed of known slope and infinite sediment depth. After calculation of the critical and normal depths, three arrays, each with twenty elements representing twenty locations along the channel, are created to represent the water surface profiles during high,

Each day of calculations up to the user specified number of days is broken up into the three scenarios (eight hours per setting). For successive iterations, shear stress and critical shear stress are calculated and an estimation of the bed-load movement (erosion or aggradation) is completed starting at the upstream end.

If erosion occurs, the array representing the bed has that portion of it removed and added to the next cell downstream. If actual shear stress does not surpass critical shear stress, nothing is done to that cell of the bed array during that iteration. The program continues to estimate and move material until the final number of days is reached.

At the end of each day, a record of the volume of sediment on the bed surface is saved as a frame. Output from the model is provided in the form of a movie, where the frame captured for each day is displayed consecutively. The frames are displayed on a graph one on top of the next to show the change in volume of sediment retained in each reach over time. A summary of the model protocol is shown in Figure 5.19

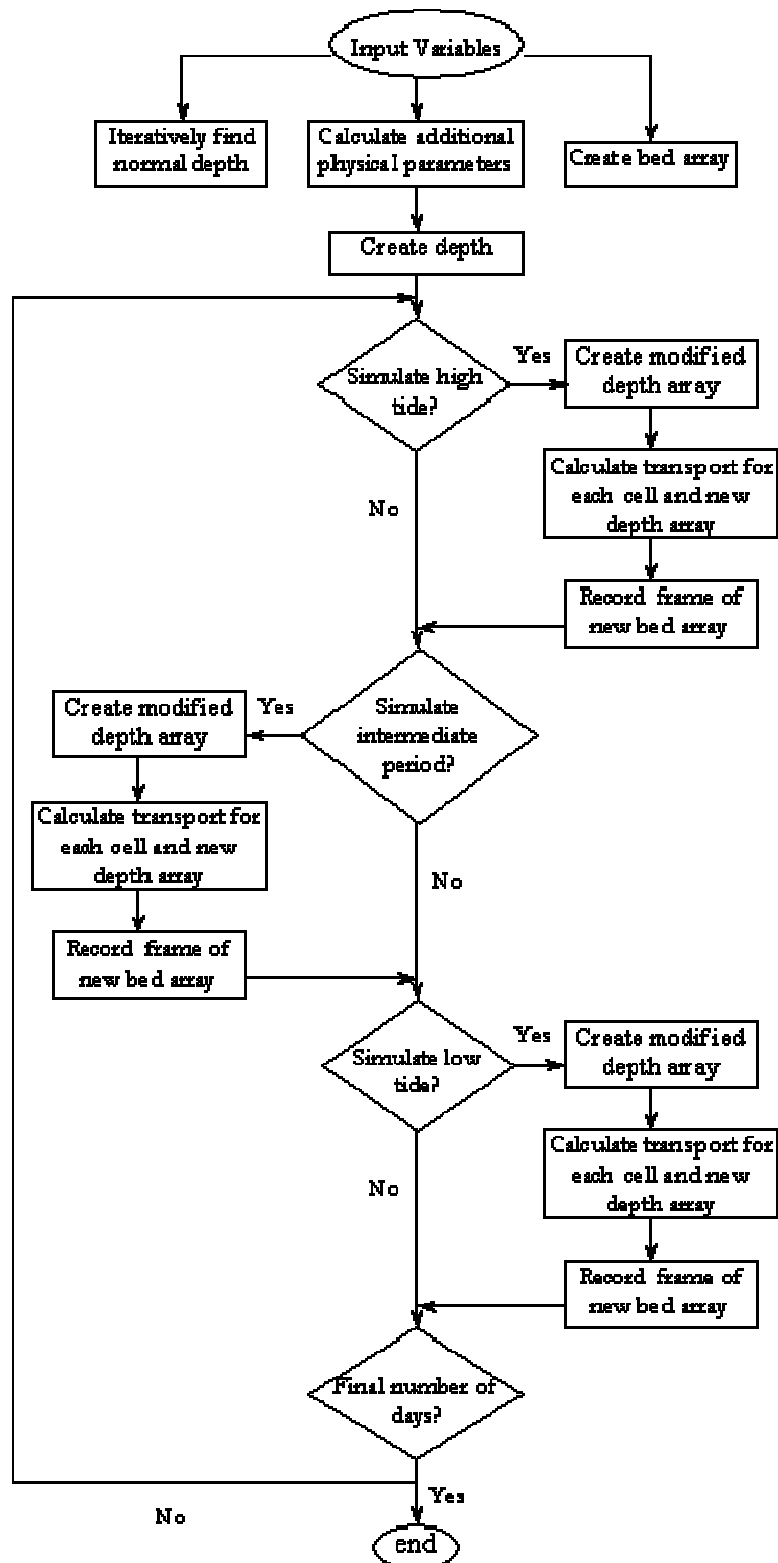


FIGURE 5.19: PROTOCOL FOR TIDALLY INFLUENCED MOVEMENT MODEL (TIMM)

5.6 Downstream fining simulation

Accurate simulation of the actual observed behavior of natural systems is essential to validate field analyses. However, a second use of robust and reliable modeling for my purposes is its relational capabilities. That is, if sediment transport is accurately modeled then changes in sediment transport and downstream fining processes resulting from tidal influence can be compared to the proposed tidal influence theory.

Two generally applied one-dimensional sediment transport models were considered for this portion of my research: HEC 6 and GSTARS 2.1.

GSTARS 2.1 was ultimately the model chosen. This was because of its improvements over HEC 6 with respect to the user interface and the simplification of information extraction. However, I feel it necessary to include a description of both models herein to show similarities between the most popular sediment transport models developed in recent decades, as well as limitations in modeling capabilities.

5.6.1 Description of HEC 6

The Hydrologic Engineering Center (HEC) of the Army Corps of Engineers developed a family of software packages that address simulation and analysis of watershed hydrology, river hydraulics, reservoir operation, stochastic stream flow generation, and flood routing. As part of this line of products, HEC 6 satisfies the modeling needs of engineers and scientists who require sediment transport analysis, including prediction of sites where scour and deposition may occur. HEC 6 is a one-dimensional numerical model that simulates erosion and deposition in a stream network. The usefulness of the program extends to river engineering projects that are concerned with volume of sediment load and impact of river engineering structures and management activities. For example, the model is capable of application to impact assessments for levees, dikes, bank stabilization, reservoir construction, and dredging activities.

5.6.2 Presentation of fundamental equations used by HEC 6

The model uses discharge data to create steady flows of variable duration. These are then used in conjunction with conservation laws, flow resistance relationships, and transport functions to accomplish simulations.

The conservation of energy relationship is used to calculate hydraulic characteristics including the water surface profile (Equation 5.16):

$$WS_2 + \frac{\alpha_2 v_2^2}{2g} = WS_1 + \frac{\alpha_1 v_1^2}{2g} + h_e \quad (5.16)$$

where WS_1 and WS_2 are water surface elevations at the upstream and downstream end of the reach, and where α_1 and α_2 are the velocity distribution coefficients for flow at the upstream and downstream ends of the reach.

The continuity equation for sediment material into and out of the reach is a form of the Exner equation shown by Equation 5.17:

$$\frac{\partial G}{\partial x} + B \cdot \frac{\partial Y_s}{\partial t} = 0 \quad (5.17)$$

where G is the average sediment discharge (ft^3/s) during each time step, x is distance along the channel, and Y_s the depth of sediment in the control volume.

Considering flow resistance, the Manning, Strickler, and Einstein equations are combined to compute the depth at which incipient motion may ensue (i.e., equilibrium depth):

$$v = \frac{1.49}{n} R^{2/3} S_f^{1/2} \quad (5.18)$$

$$n = \frac{d^{1/6}}{29.3} \quad (5.19)$$

$$\psi = \frac{\rho_s - \rho_f}{\rho_f} \cdot \frac{d}{DS_f} \quad (5.20)$$

where d is the grain diameter, ψ is transport intensity from Einstein's bed-load function related to the inverse of Shield's parameter, ρ_s is sediment density, ρ_f is density of water. When sediment transport is negligible (i.e., for $\psi = 30$) the friction slope can be found using Equation 5.21:

$$S_f = \frac{d}{18.18D} \quad (5.21)$$

Finally, equilibrium depth is then calculated using Equation 5.22:

$$D_e = \left[\frac{q}{10.21d^{1/3}} \right]^{6/7} \quad (5.22)$$

Where q is the discharge per unit width of flow and is calculated using Equation 5.23:

$$q = \frac{(1.49)(29.3)D^{5/3}}{d^{1/6}} \left[\frac{d}{18.18D} \right]^{1/2} = 10.21 \cdot D^{7/6} \cdot D^{1/3} \quad (5.23)$$

The above equations are the fundamental relations used in model simulations; however, they are not the only equations involved. Model protocol includes additional formulae for the consideration of the role of the armor layer in the vertical exchange of sediment. Moreover, the necessary parameters depend on which backwater method is used to calculate changes in bed elevation due to scour or deposition. The HEC 6 user manual provides a detailed description of all equations used by the model regardless of options for simulation.

5.6.3 Description of GSTARS 2.1

The Generalized Sediment Transport Model for Alluvial Rivers (GSTARS 2.1) was developed by the U.S. Bureau of Reclamation for simulation of hydraulic conditions and sediment transport in alluvial rivers with movable boundaries. The following explanation of the model and its capabilities is a summary of the description provided in the GSTARS 2.1 users guide (Yang and Simões 2000). GSTARS 2.1 can be run as a one-dimensional or semi-two-dimensional model for quasi-steady flow.

5.6.4 Presentation of fundamental equations used by GSTARS 2.1

In one-dimensional mode, GSTARS 2.1 uses the streamline concept, where the velocity vector of the fluid is tangential at each point and each instant in time. This is shown in the top half of Figure 5.20. However, GSTARS 2.1 has the capability to be used in semi-two-dimensional mode by incorporation of the stream tubes concept (see the lower part of Figure 5.20). Stream tubes have walls defined by streamlines; discharge of water is constant along the tube. Fluid cannot cross a stream tube wall.

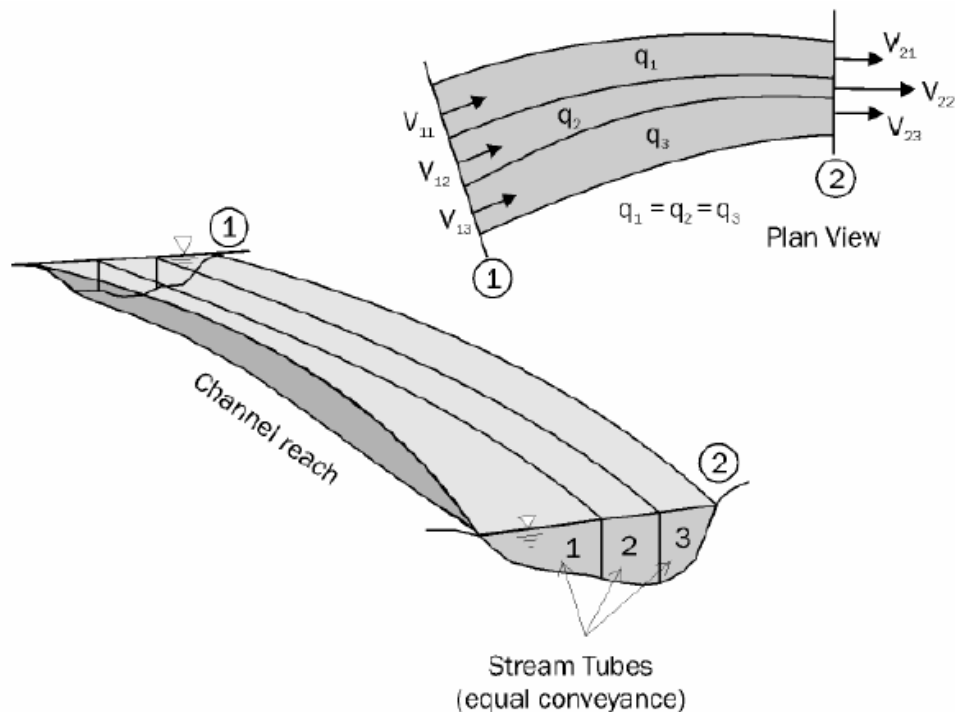


FIGURE 5.20: ILLUSTRATION OF STREAMLINES AND STREAM TUBES

(Yang and Simões 2000)

Model protocol is to compute water surface elevations using the standard step method, followed by sediment transport calculations. Equations associated with the standard step method were presented earlier in Chapter 5 of this dissertation.

Water surface profiles can be computed for sub-critical flow, super-critical flow, or any combination of the two. Sediment transport capabilities include fractional transport, bed sorting, and armoring, using any of eleven transport equations (see Table 5.4). The model also includes transport relationships for cohesive sediment fractions.

TABLE 5.4: SEDIMENT TRANSPORT RELATIONSHIPS INCORPORATED IN GSTARS 2.1

EQUATION	USED TO COMPUTE:
DuBoys (1879)	Bed-load
Meyer-Peter and Müller (1948)	
Parker (1990)	
Lauren (1958)	Bed-Material
Toffaletti (1969)	
Engelund and Hensen (1972)	
Ackers and White (1973)	
Ackers and White (HR Wallingford, 1990)	
Yang (1973) + Yang (1984)	
Yang (1979) + Yang (1984)	
Yang et al. (1996)	

GSTARS 2.1 uses the minimum energy dissipation theory to determine channel geometry adjustments due to hydraulic parameters and sediment transport. For an open system, the minimum energy dissipation theory simplifies to minimization of unit stream power, shown mathematically as:

$$QS = \text{a minimum} \quad (5.24)$$

where Q is water discharge, S is energy slope, and QS is unit stream power.

5.6.5 *Modeling data*

Model set up begins with specifying a total length for the river to be simulated, along with locations of cross-sections. Next, project parameters can be set. Project data for GSTARS 2.1 include specifying the friction loss calculation (e.g., average slope) and roughness equation (e.g., Manning), number of stream tubes, time step (i.e., seconds, hours, or days), and length of simulation (i.e., total number of time steps). For the simplified Kilchis River simulations, the average channel slope and Manning's roughness equation were used. The number of stream tubes used in computations was two. Calculations were performed hourly over a period of 3600 hours or 150 days (\approx 5 months). Simulations 1-3 were performed for 14 river miles (22.5 kilometers) without consideration of tidal influence at the downstream end. Subsequently, simulations 4-6 repeated simulations 1-3; however, only the five lower river miles were simulated to analyze tidal influence in a fashion similar to that of the TIMM analyses. For all simulations, sediment supply was assumed unlimited as would be the case for river reaches with large amounts of lateral inputs of sediment.

Additional input data required for simulation can be condensed to three main categories of data; channel geometry, sediment distribution, and discharge data. Explanations of each category are presented in this section, along with the input parameters used in simulations of the simplified Kilchis River. Raw data used in modeling efforts can be found in Appendix F of this dissertation.

Channel geometric data include cross-sectional data (elevation versus lateral distance), Manning roughness factor, and specification of channel boundaries. For the simplified Kilchis River (shown in Figure 5.21), cross sections were changed progressively downstream according to the widening of channels associated with entering runoff from tributaries. The river was separated into eight zones according to tributaries. Tributaries were used only for the delineation of zones and were not included in the transport simulations (Figure 2.22). Excluding zone 2, each zone included at least one cross-section that was representative of a cross-section found in a straight reach and one cross-section that was representative of a meander (Figure 2.23). Each reach is delineated using the cross-sections. The locations of the 21 total cross-sections relative to the eight zones are shown in Table 5.5.

Manning roughness factor was set at 0.05 for Zones 1-4. This roughness value is suggested for a channel bottom with large cobbles and boulders and seemed appropriate for areas of higher elevation (Yang 1996). Sediment transport in the lower elevation areas, Zones 5-8, was computed with Manning roughness factor set at 0.037. This roughness value is for major streams (top width > 100 feet at flood stage) that are irregular and rough (Yang 1996). Channel boundaries were set such that water could flow over the entire cross-section, but not onto the floodplain. Therefore, all sediment transport occurs within the channel.

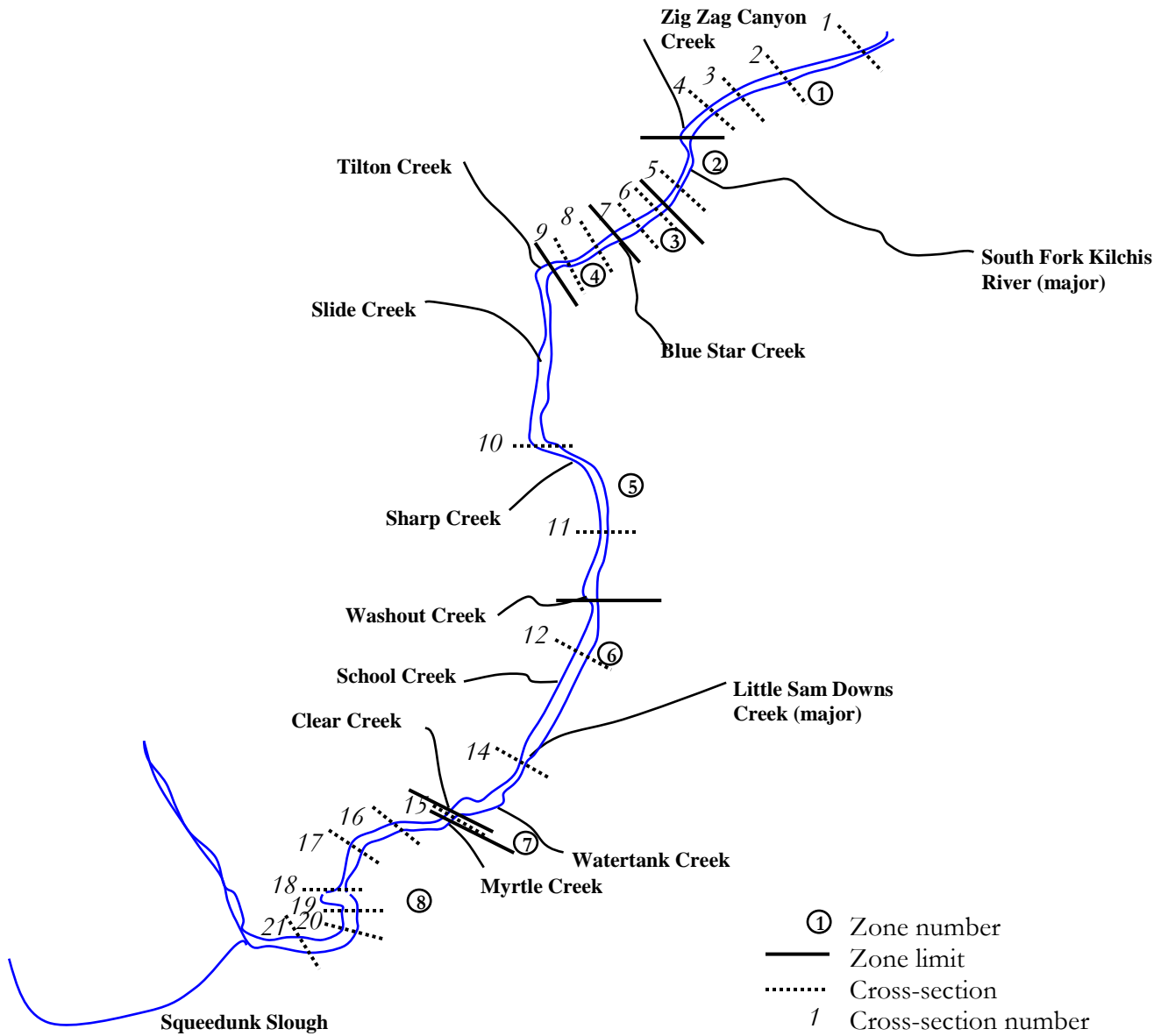


FIGURE 5.21 SKETCH OF SIMPLIFIED KILCHIS RIVER FOR SIMULATION (not to scale)

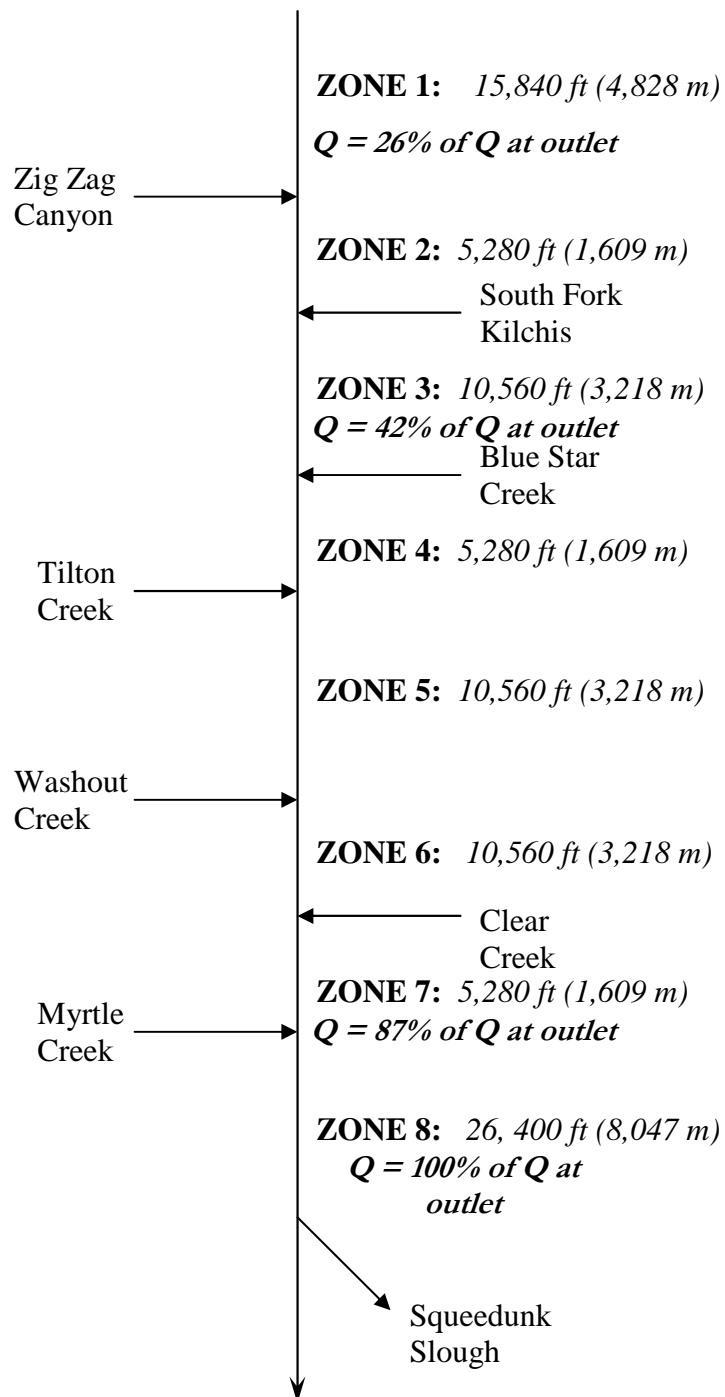


FIGURE 5.22 LINE DRAWING OF SIMULATED SIMPLIFIED VERSION OF THE KILCHIS RIVER WITH LOCATION OF LATERAL INPUTS AND OUTPUTS

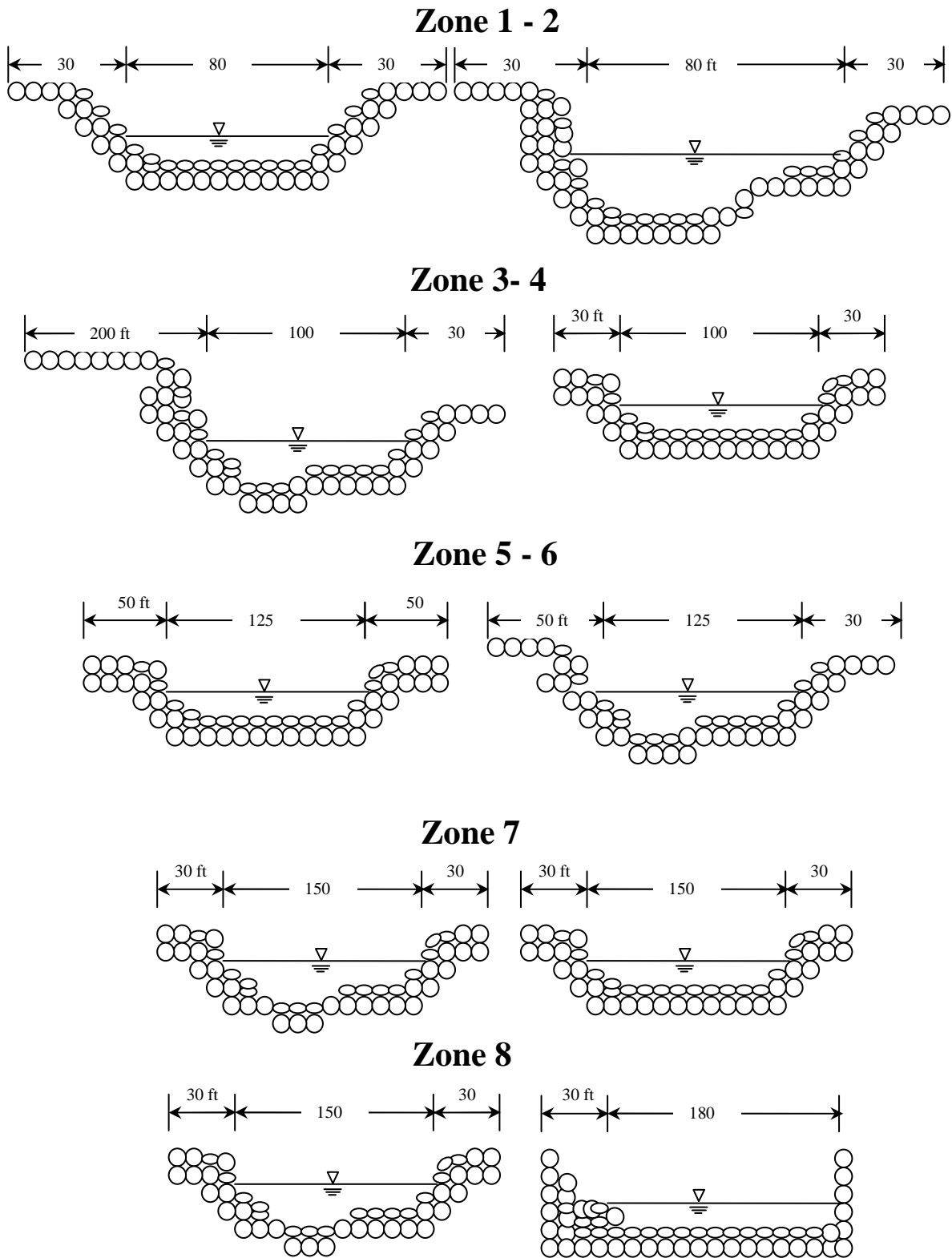


FIGURE 5.23 REPRESENTATIVE CROSS SECTION PLOTS SIMPLIFIED KILCHIS RIVER

TABLE 5.5: LOCATION OF EACH CROSS-SECTION FOR THE SIMPLIFIED KILCHIS RIVER
SIMULATIONS

Zone	Cross-section	Distance upstream	
		river mile	km
1	1	16.7	26.9
	2	15.9	25.6
	3	15.0	24.1
	4	14.2	22.9
2	5	13.4	21.6
3	6	12.5	20.1
	7	11.7	18.8
4	8	10.9	17.5
	9	10.0	16.1
5	10	9.2	14.8
	11	8.4	13.5
6	12	7.5	12.1
	13	6.7	10.8
7	14	5.8	9.3
	15	5.0	8.0
8	16	4.2	6.8
	17	3.3	5.3
	18	2.5	4.0
	19	1.7	2.7
	20	0.8	1.3
	21	0.0	0.0

Sediment distribution data requirements include information on variations of sediment sizes and the selection of a transport relationship. For the simplified Kilchis River, three types of particle distributions were used. Table 5.6 shows the particle size distributions used in each simulation. The first simulation was performed using the mean sediment size obtained from the bulk sampling analysis of the Kilchis River (7.9 mm or 0.3 inches for site 4). The bed along the entire length of the river was set at 7.9 mm (0.3 inches). For the second simulation, bed material in zones 2-8 were set as a mixed bed with a d_{50} of 7.9 mm (0.3

inches, same as d_{50} for the first simulation). Bed material in zone 1 and the incoming sediment had a particle distribution that was finer than the bed material. The third simulation was performed using a mixed-size bed that was skewed toward larger sizes in zone 1 and had the same bed composition as for simulation 2 in zones 2-8. For this third simulation, incoming sediment was set at the particle distribution of zone 1. DuBoys' transport relationship was used for all simulations.

Hydrologic data include time-variant discharge obtained from the U.S. Geological Survey Oregon database. Because the Kilchis River does not have a gauging station, discharge data from the Wilson River gage were scaled to the Kilchis River using watershed drainage area ratios. Average daily and monthly values were then calculated. Table 5.7 shows mean daily flows for the period of record. The monthly values, along with a stage discharge rating curve created from Wilson River data (see Figure 5.24), were used to create a hypothetical stage discharge table of values for the Kilchis River. For each month, the stage associated with the average monthly discharge was recorded. Although in-situ data for the Kilchis River is a more accurate way of scaling the Wilson River stage data to the Kilchis River, it is assumed that the method used is adequate for obtaining reasonable values for a hypothetical Kilchis River.

For the model runs where 14 river miles (22.5 km, zones 1-8) were simulated (simulations 1-3), the scaled mean daily discharge values were varied based on the percent of flow expected given the number of tributaries augmenting streamflows in the main channel. The ratio of drainage area above the control section to the total drainage area was used to determine the river discharge at four control sections, cross-sections 1, 6, 14, and 21. The percent of total river discharge for each control section was 26%, 42%, 87%, and 100% for cross-sections 1, 6, 14, and 21, respectively.

For runs where tidal influence was analyzed (simulations 4-6), tidal influence was treated as follows. Each day was broken into low, intermediate, and high tide segments. The average tide range for Tillamook Bay, 5.7 feet (1.7 meters) according to Komar (1997), was used to adjust river stage at the downstream control section. For the high tide periods of the day, 2.85 feet (0.87 meters) was added to water stage. During intermediate periods of the day,

1.43 feet (0.44 meters) was added to water stage. No value was added to stage for low tide periods. Backwater calculations were performed using these adjusted values, thereby simulating tidal influence.

Results of the simulations are presented and discussed in Chapter 6 of this dissertation.

TABLE 5.6: PARTICLE SIZE DISTRIBUTIONS FOR THE SIMPLIFIED KILCHIS RIVER SIMULATIONS

SIMULATION	PARTICLE SIZE FRACTIONS		ZONES	SEDIMENT DISTRIBUTION	
	MM	IN		upper limit of size range	fraction in size range
1	7.9	0.3	1-8	7.9	1
2	127 - 64 64 - 16 16 - 8 8 - 4 4 - 2 2 - 0.5 0.5 - 0.075	5 - 2.5 2.5 - 0.6 0.6 - 0.3 0.3 - 0.2 0.2 - .02 0.02 - 0.003	1	127 64 16 8 4 2 0.5-0.075	0.025 0.025 0.10 0.10 0.30 0.30 0.15
			2-8	127 64 16 8 4 2 0.5-0.075	0.05 0.05 0.10 0.40 0.20 0.13 0.07
3	127 - 64 64 - 16 16 - 8 8 - 4 4 - 2 2 - 0.5 0.5 - 0.075	5 - 2.5 2.5 - 0.6 0.6 - 0.3 0.3 - 0.2 0.2 - .02 0.02 - 0.003	1	127 64 16 8 4 2 0.5-0.075	0.15 0.30 0.30 0.10 0.10 0.03 0.02
			2-8	127 64 16 8 4 2 0.5-0.075	0.05 0.05 0.10 0.40 0.20 0.13 0.07

Particle size data from bulk sampling at site 4 was used in the above table

Simulations 1 and 4 = Uniform particle size for incoming sediment

Simulations 2 and 5 = Mixture with finer particle size for incoming sediment

Simulations 3 and 6 = Mixture with coarser particle size for incoming sediment

TABLE 5.7: ESTIMATED KILCHIS RIVER MEAN DAILY FLOWS FOR THE PERIOD OF RECORD
FOR DERIVED FROM WILSON RIVER GAGE, USING 76 YEARS OF RECORD

Day of month	Estimated mean of daily mean values for this day in ft ³ /s											
	Jan	Feb	Mar	Apr	May	Jun	Jul	Aug	Sep	Oct	Nov	Dec
1	1062	1147	845	786	394	202	110	55	53	99	514	1224
2	1129	1104	909	699	403	211	109	56	59	127	558	1474
3	1066	1041	900	650	405	187	105	56	55	126	605	1360
4	1211	981	867	668	394	180	100	55	81	140	572	1397
5	1244	902	878	690	400	174	96	53	70	145	555	1273
6	1233	1113	834	615	388	170	93	52	63	157	560	1362
7	1242	1199	827	570	359	194	91	52	60	146	577	1217
8	1161	1115	798	563	338	202	92	51	58	153	656	1051
9	1193	978	862	591	321	206	91	50	57	224	649	1156
10	1075	1032	892	590	312	190	88	49	65	232	608	1207
11	1127	987	872	580	319	181	86	48	68	238	726	1258
12	1228	1032	935	587	295	201	84	47	62	212	761	1278
13	1184	1027	900	624	293	178	83	46	61	204	776	1371
14	1375	970	854	617	295	168	81	45	62	184	870	1202
15	1379	993	851	583	284	162	79	45	66	187	884	1261
16	1312	1115	832	551	282	160	78	45	72	190	859	1258
17	1250	1176	813	561	279	156	78	44	81	187	864	1240
18	1247	1076	850	519	279	151	76	44	84	204	941	1185
19	1258	1169	842	503	274	149	74	44	93	236	956	1274
20	1261	1095	801	551	277	144	71	44	94	270	1153	1297
21	1154	1065	774	498	260	139	68	43	96	267	1056	1353
22	1145	1132	820	470	246	136	67	44	86	336	1101	1469
23	1177	1050	836	541	239	134	64	49	86	409	1112	1316
24	1275	1065	850	496	232	128	63	52	85	391	1337	1195
25	1347	957	805	450	223	130	61	58	81	416	1473	1156
26	1135	930	739	415	218	124	61	58	85	379	1316	1174
27	1087	971	745	416	212	119	60	53	82	422	1190	1320
28	1108	923	790	409	210	116	59	53	79	461	1094	1275
29	1081	1060	815	387	202	119	59	53	84	456	1059	1162
30	1003		811	388	200	114	57	53	90	500	1105	1229
31	1075		809		201		56	51		515		1109

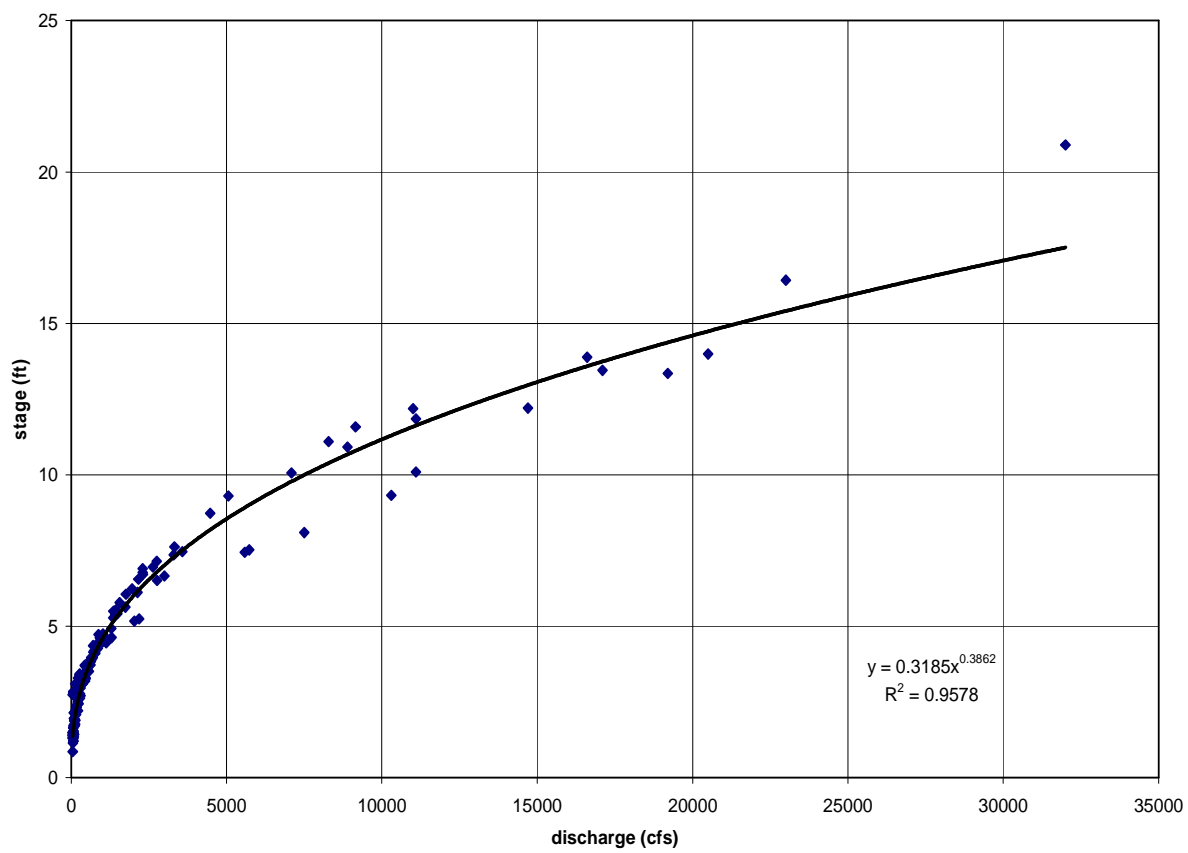


FIGURE 5.24 RATING CURVE FOR WILSON RIVER (USGS)

6 Presentation and Discussion of Results from Sampling

6.1 Particle size analysis

6.1.1 Kilchis River analysis

Results of the armor and sub-armor sampling of river sediment at five bars along the Kilchis River are presented in Table 6.1. The average mean diameter of sampled particles for each site shows a distinct decrease in the mean particle diameter in the downstream direction, for both the armor and sub-armor layer. However, important to note is the breakdown of the fining trend for the armor layer at site 5. The mean particle diameter for site 5 is 32% larger than that of site 4. This disruption in the fining trend has been investigated. It is likely that the visible bank failure at this site has introduced floodplain deposits, which have been coarser than the material in the nearby channel. Figure 6.1 shows photographic evidence of the eroding bank at site five and the difference in bed composition between those areas on the bar that are near the bank failure and those areas near the center of the bar.

TABLE 6.1: RESULTS OF KILCHIS RIVER GRAVEL BAR SAMPLING

SAMPLE LEVEL	SITE	LOCATION ON BAR	MEAN DIAMETER (mm)	MEAN DIAMETER (in)	AVERAGE D ₅₀ FOR SITE (mm)	AVERAGE D ₅₀ FOR SITE (in)
Armor	1	Upstream	281.7	11.1	215.6	8.5
		Center	334.9	13.2		
		Downstream	149.4	5.9		
	2	Upstream	63.7	2.5	53.3	2.1
		Center	65.9	2.6		
		Downstream	42.9	1.7		
	3	Upstream	57.9	2.3	38.1	1.5
		Center	35.0	1.4		
		Downstream	21.4	0.8		
	4	Upstream	7.3	0.3	7.9	0.3
		Center	11.1	0.4		
		Downstream	5.3	0.2		
	5	Upstream	12.4	0.5	10.4	0.4
		Center	18.3	0.7		
		Downstream	0.6	0.02		
Bank sample*		37.4	1.5			
Sub Armor	1	Upstream	80.7	3.2	60.2	2.4
		Center	79.1	3.1		
		Downstream	20.7	0.8		
	2	Upstream	21.7	0.9	30.7	1.2
		Center	53.6	2.1		
		Downstream	16.9	0.7		
	3	Upstream	16.2	0.6	10.3	0.4
		Center	7.2	0.3		
		Downstream	7.4	0.3		
	4	Upstream	3.3	0.1	6.2	0.2
		Center	8.6	0.3		
		Downstream	6.7	0.3		
	5	Upstream	4.1	0.2	3.8	0.2
		Center	6.8	0.3		
		Downstream	0.6	0.02		
Bank sample*		6.7	0.3			

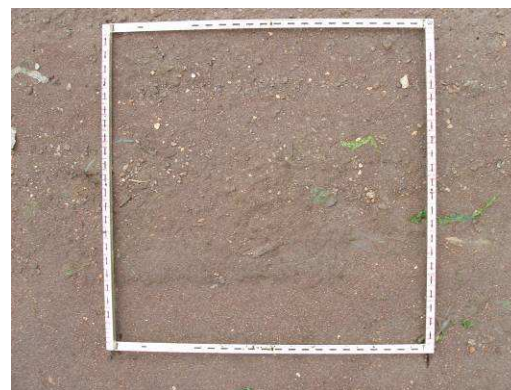
*Not used in site average



(a)



(b)



(c)

FIGURE 6.1: KILCHIS RIVER SITE 5 ILLUSTRATING LATERAL INPUT OF GRAVEL

(a) Eroding bank opposite Site 5 (b) Back of bar at Site 5 (c) Typical surface of bar at Site 5

Comparison of d_{50} values for the armor and sub-armor layers at the upstream and downstream ends of each bar produces expected results. That is, the upstream ends of the bars have larger d_{50} values than do the downstream ends. As presented in Chapter 3, the dynamics of flow past sidebars tends to create coarser bed armor at the upstream ends due to the greater shear stresses in those areas. The relative particle sizes of center-of-bar deposits depend on bar height and degree of inundation for various water stages. Therefore, variability in center-of-bar samples was also expected. Figure 6.2 shows photographic evidence of each bar alongside the associated mean particle diameter for the upstream,

center-of-bar, and downstream armor layer samples. For bars that are low in height above the adjacent bed of the channel, the d_{50} of the center-of-bar sample was found to larger than the d_{50} of the upstream end.

This general result does not apply to the sub-armor layer of site 4. For site 4, the downstream sub-armor layer is twice as coarse as the upstream sub-armor layer. This situation can be explained by sampling problems that arose at that particular site. Site 4 is the site where severe human disturbance was noted. In particular, the downstream end of the bar appeared to have been used as a boat launch. An edge-of-water, less-disturbed sample was taken to avoid the depressions left by this activity. Typical sampling procedure is to select on-bar sampling locations. The new sampling location may have also been disturbed, with mixing of the armor and sub-armor layer, leading to odd results for the sub-armor layer.

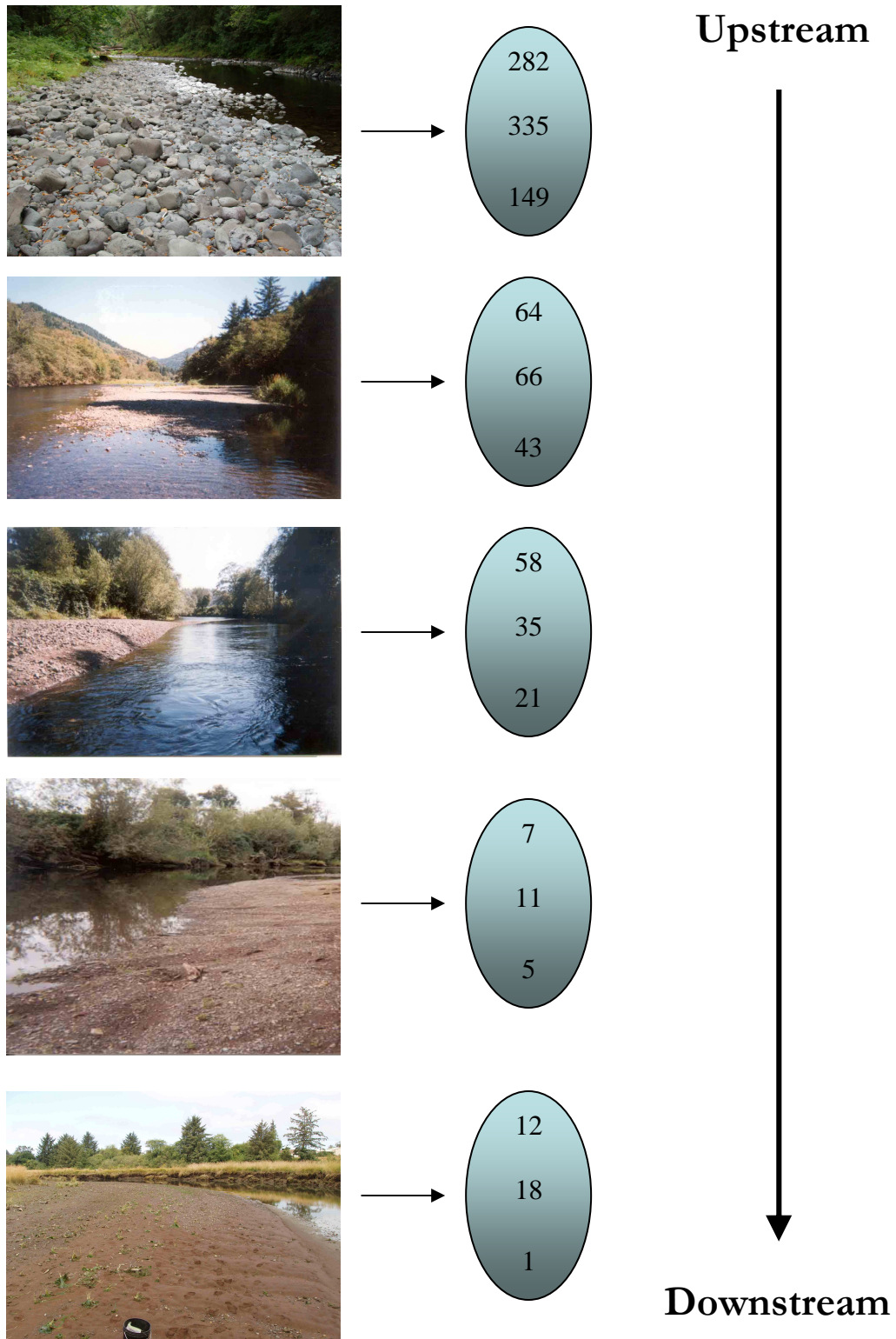


FIGURE 6.2: GRAVEL BARS OF THE KILCHIS RIVER WITH MEAN PARTICLE SIZE (MM) FOR THE UPSTREAM, DOWNSTREAM, AND CENTER-OF-BAR ARMOR LAYER SAMPLES

A modified sampling scheme was also used at Site 5, differing from the procedure noted in the methods for the Kilchis particle size analysis. At Site 5, an additional sample was taken near the eroding bank. The purpose was to have a record of the size of material being introduced from the floodplain deposits. As previously stated, this material was significantly larger than the overall sediment distribution at the site. Furthermore, it was significantly larger than the in-stream bed material. Results of this additional sample were not included in calculating the bar average, but the measured values are shown in Table 6.1 for comparison. The sediment originating from the eroding banks is of comparable size to that sampled at site 3, about three river miles (4.8 kilometers) upstream.

The disruption in the downstream fining trend due to the introduction of this bank material has important implications to my study. The extent of longitudinal sampling on the Kilchis River captured the general downstream fining trend. However, the eroding bank at site 5 was the only disruption observed stemming from natural mass wasting processes. This is vital information because it implies that local small-scale disturbances can be detected through downstream fining studies. Field reconnaissance alone may have led to the discovery of the severely eroding banks; however, longitudinal particle size distribution data may be very useful at a site where dense vegetation conceals failing banks. Moreover, downstream fining data collected by persons not interested in locating disturbances may be used prior to field reconnaissance as a first estimate of the degree of disturbance in a watershed.

The number of sampling locations in the Kilchis was five bars, yet a disruption was detected. From this arises a question regarding the level of sampling necessary to obtain the most useful results to study downstream fining. Five sites were used in this study based on objectives that include detecting any general trend and possible disruptions to that trend. If the level of sampling were increased, say, to thirty sampling sites along the same length of river, what would be the outcome? Five sites yielded a general pattern with two explainable disruptions. The one at site 4 was limited to the sub-armor layer and was human induced; the other at site 5 was limited to the armor layer and was at least partially due to natural causes. If the number of sampling sites is increased, one may find that the 'noise' from small disturbances, which cause alterations of local particle sizes, must be handled before the

general fining pattern emerges. Nonetheless, detailed spatial coverage could be of use whether the research interest is in general patterns or disruptions of patterns.

Comparisons were made of the armor and sub-armor material for each site. The average d_{50} values for the armor layers and sub-armor layers at each site were compared as ratios of armor size to sub-armor size. Results are shown in Table 6.2. As surface particles decrease in size in the downstream direction, so do the subsurface particles. One might assume that the differences in size between the armor and sub-armor layers would diminish as well. That is, in the upper steep reaches, the surface particle size distribution would be likely to include wide range of sizes from silt to boulders. In such a strong-flow, high-stress environment smaller particles hide interstitially among large particles, limiting their abundance in the armor layer. In the lower river reaches, the surface is likely to be composed of particles that are smaller overall in size. Furthermore, the bed might have less variation in the range of sizes than would be the case upstream. With smaller and less-varied sizes, one might expect that the sub-armor layer would more closely match the armor layer. If this were the case, the ratio between the armor and sub-armor layer could be expected to approach a value of 1 in the downstream direction. However, the results of this analysis do not illustrate this assumption, as the ratios shown vary randomly with no obvious pattern (see the last column in Table 6.2).

TABLE 6.2: COMPARISON OF ARMOR AND SUB-ARMOR MEAN PARTICLE DIAMETER

SITE	ARMOR LAYER D_{50}		SUB-ARMOR LAYER D_{50}		RATIO OF ARMOR D_{50} TO SUBARMOR D_{50}
	mm	in	mm	in	
1	215.6	8.5	60.2	2.4	3.58
2	53.3	2.1	30.7	1.2	1.74
3	38.1	1.5	10.3	0.4	3.70
4	7.9	0.3	6.2	0.2	1.28
5	10.4	0.4	3.8	0.15	2.71

Cumulative particle size distributions for armor and sub armor at each sample point were determined and groups of these distributions are shown in Figure 6.3. Like the less detailed Table 6.1, the d_{50} values in the cumulative particle size distribution show the expected patterns except for the anomalous site 4. The sites nearest in proximity to each other, site 2 and site 3, have distributions similar to one another. This is not surprising considering that these sites are only a river mile apart, compared to site 1 to site 2, which are approximately 10 river miles (16 kilometers) apart. This expected result is supported by the armor layer distributions for the upstream end armor layer at sites 1 and 2, which are almost identical.

The sub-armor layer does not show the same sensitivity to distance between sites. In fact, comparison of the distribution at each site shows that the armor layers of bars have progressively more variability than the sub-armor layers in the downstream direction. Note the closeness of the majority of sub-armor layer curves relative to their armor layer counterparts. The consistency of the sub-armor layer is expected and was part of the reason the outcome from the armor to sub-armor ratio analysis was unexpected.

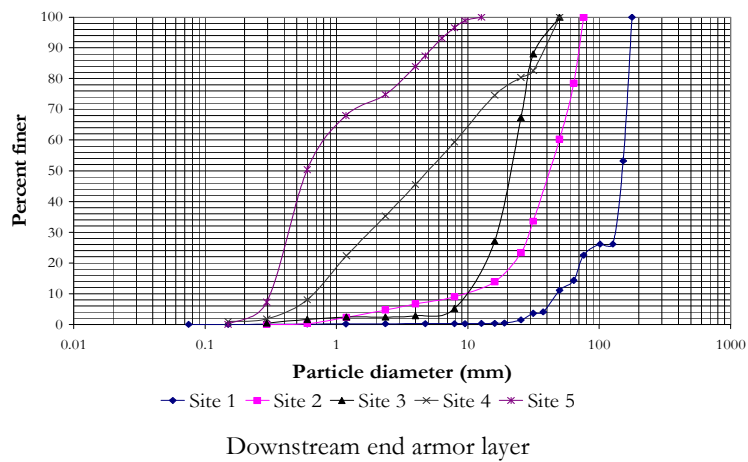
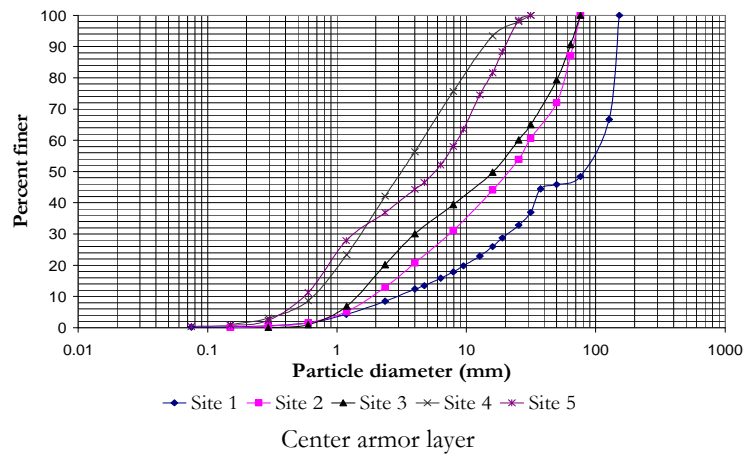
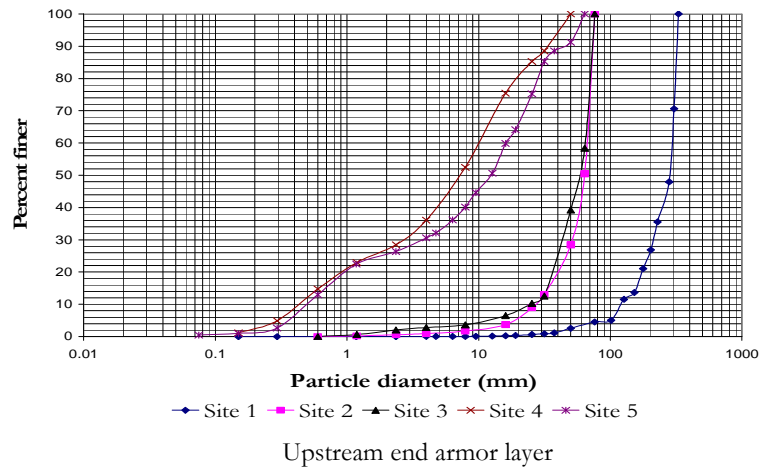


FIGURE 6.3: CUMULATIVE PARTICLE SIZE DISTRIBUTION FOR KILCHIS RIVER SITES

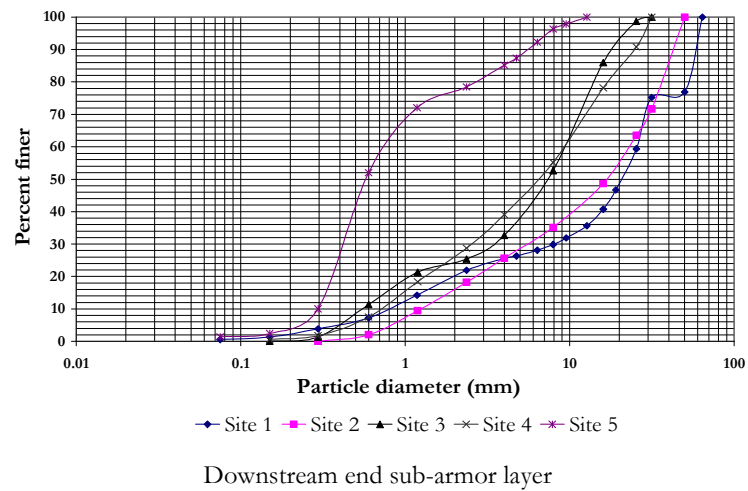
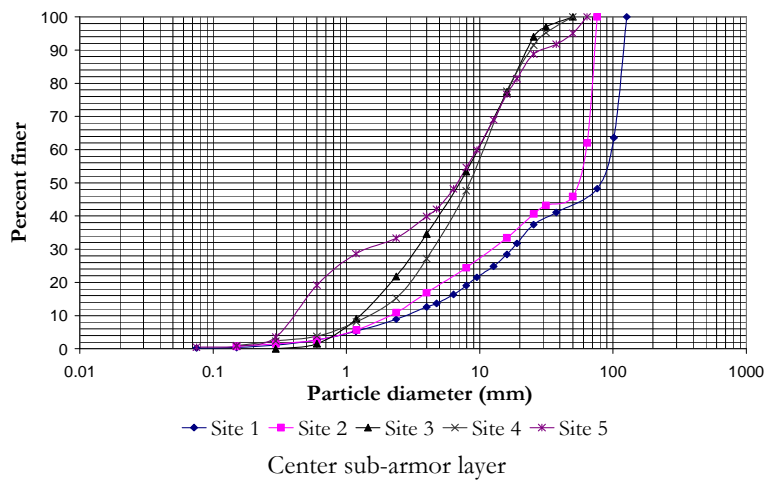
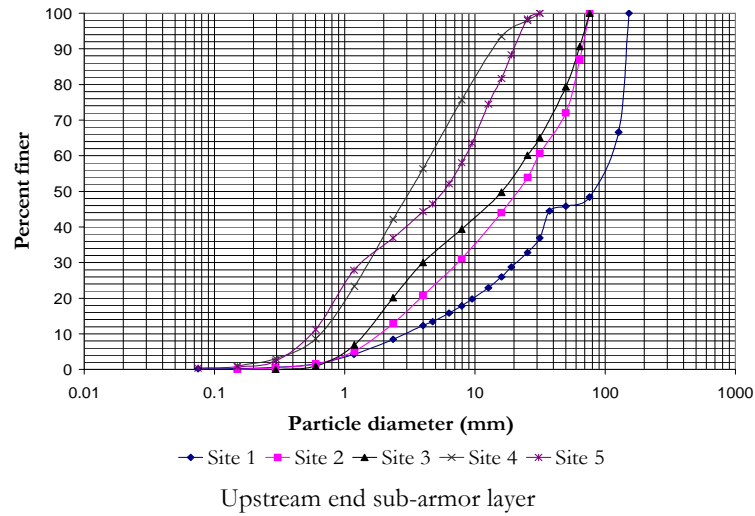


FIGURE 6.3: (CONT'D)

Also important to note is the absence of bimodal distributions and the presence of well sorted distributions at each site including site 5, which is in the estuarine environment. This is shown in Figure 6.4 where site 3 and 4 are seen as weakly bimodal with unimodal counterparts in sites upstream and downstream.

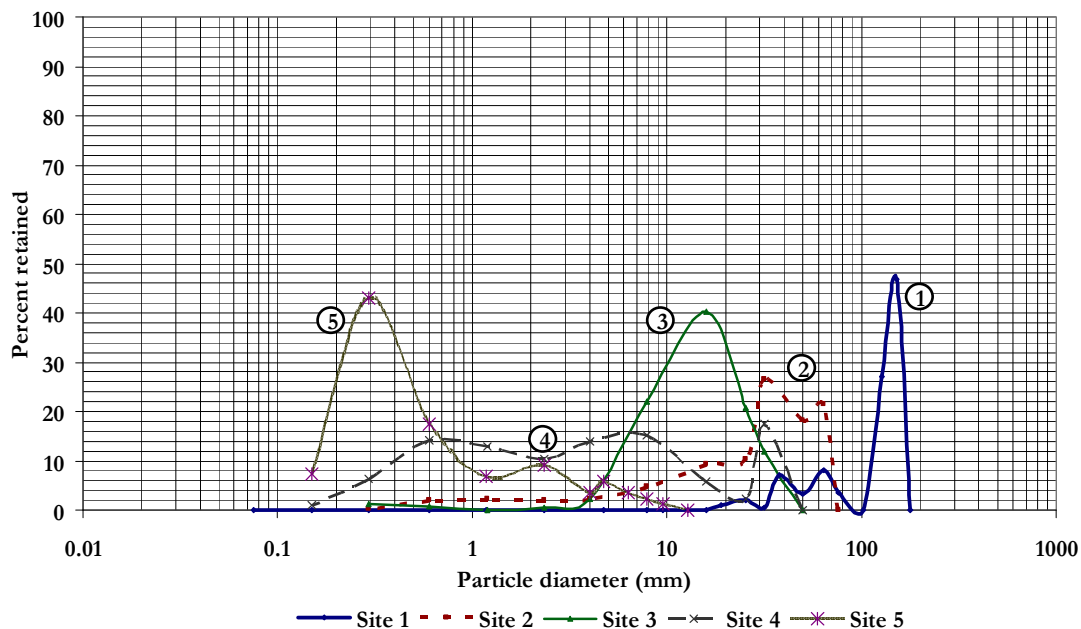


FIGURE 6.4: PERCENT RETAINED FOR DOWNSTREAM ARMOR LAYER SHOWING UNI-MODAL AND WEAK BIMODAL DISTRIBUTIONS

Figure 6.5 shows the outcome of a regression analysis performed on the site-average d_{50} plotted against the distance downstream. An exponential curve is fit to the data to determine if the Sternberg downstream fining relationship (Equation 2.1) yields the fit expected for rivers with long sedimentary links. Separate plots are given for the armor layer and sub-armor layer. Labeled in each plot is the equation for an exponential decay relationship that is indicative of a downstream fining process (see literature review for general discussion). Also given is the R-squared value for the fitted curve. Diminution coefficients for the fining process are 0.55 km^{-1} (0.89 mi^{-2}) for the armor layer and 0.48 km^{-1} (0.77 mi^{-2}) for the sub-armor layer. The R-squared values for the armor and sub-armor layers are 0.92 and 0.99, respectively. With these values for the correlation coefficient and a

level of significance set at 0.05, rejection of the null hypothesis is achieved. That is, there is a significant relationship between mean particle diameter and distance in the downstream direction.

Comparison of the downstream fining diminution coefficients obtained in this research with results reported by past investigators shows that the findings here are not comparable to reported values for fining processes based solely on abrasion. Kodama reported a diminution coefficient 0.089 km^{-1} (0.14 mi^{-2}) in his laboratory tumbling study of abrasion-dominated fining. Reported results from sorting-dominated fining studies showed great variability ranging from 0.001 to 0.05 km^{-1} (0.002 mi^{-2} to 0.08 mi^{-2} , Shaw and Kellerhals 1982) to 1 km^{-1} (1.6 mi^{-2} , Seal and Paola 1995). My results lie between the two sets of values for sorting-dominated downstream fining. Thus, while the outcome of this regression analysis is not fully validated by previous investigations, the R-squared values show that the model is quite good, with over 90% of the variability explained by the independent variable. Furthermore, the diminution coefficients obtained show a general pattern of a downstream exponential decay in mean particle size.

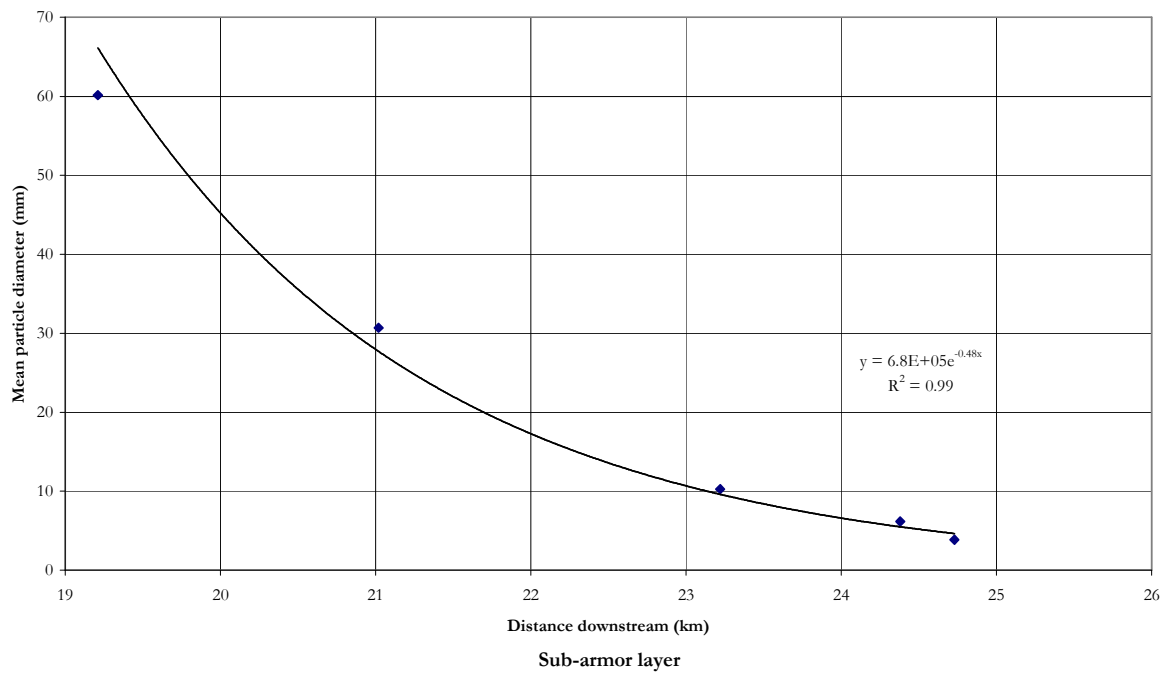
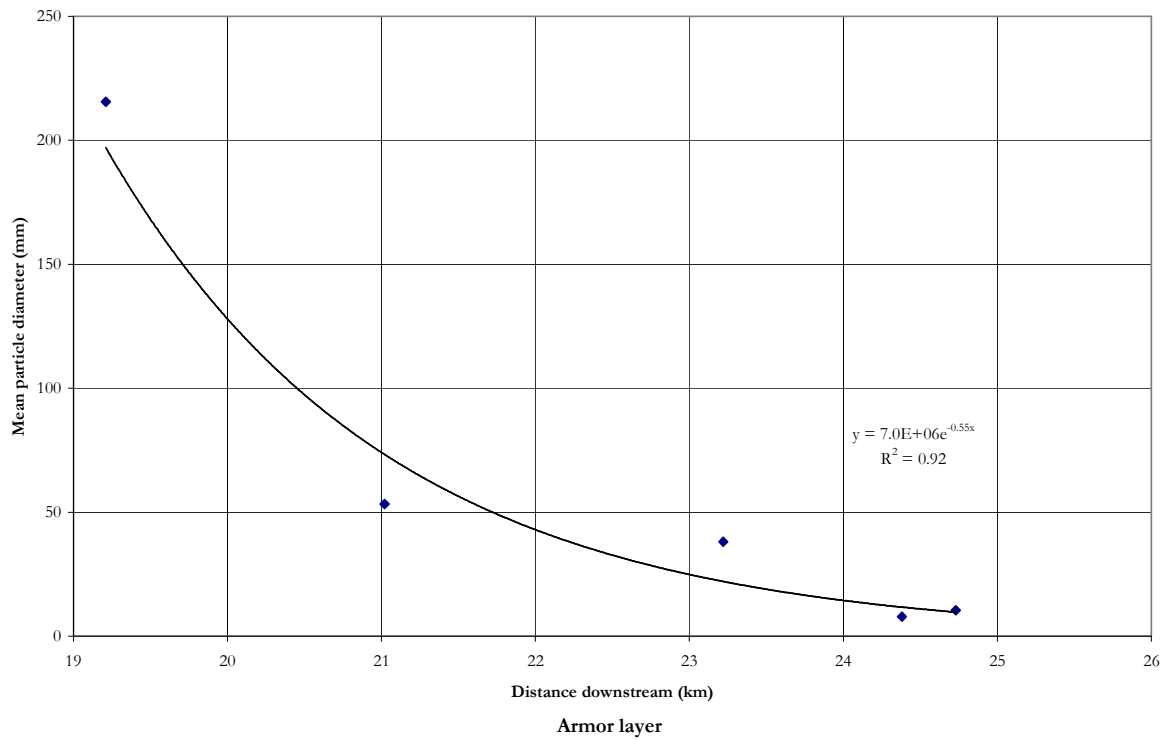


FIGURE 6.5: REGRESSION ANALYSIS FOR THE KILCHIS RIVER MEAN PARTICLE SIZE

The Kilchis River has experienced past anthropogenic modifications that include hardened banks, historic gravel mining, and dredging of lower reaches. Yet, the analysis of the longitudinal particle size variation showed a significant decrease in the mean particle diameter in the downstream direction. As shown in Table 6.3, the smallest change in diameter from one site to another was 32%.

TABLE 6.3: CALCULATION OF PERCENT DECREASE IN MEAN DIAMETER DOWNSTREAM FOR
KILCHIS RIVER

SAMPLE LEVEL	SITE	D ₅₀		DISTANCE DOWNSTREAM		CHANGE IN DIAMETER (%)
		mm	in	km	rm	
ARMOR	1	215.6	8.5	19.2	11.9	
	2	53.3	2.1	21.0	13.0	0.75
	3	38.1	1.5	23.2	14.4	0.29
	4	7.9	0.3	24.4	15.2	0.79
	5	10.4	0.4	24.7	15.3	0.32
SUB-ARMOR	1	60.2	2.4	19.2	11.9	
	2	30.7	1.2	21.0	13.0	0.49
	3	10.3	0.4	23.2	14.4	0.67
	4	6.8	0.3	24.4	15.2	0.40
	5	3.8	0.1	24.7	15.3	0.38

6.1.2 *Frame Photo Sampling*

Figure 6.6, shows the locations on each bar at which samples were selected, photographed, and extracted. Photographic evidence from the photo frame sampling is shown in Figures 6.7 to 6.10 for the Miami Wilson, Trask, and Tillamook Rivers, respectively. The letters in Figure 6.6 refer to the corresponding letters in Figures 6.7 to 6.10.

A visual comparison of the various sampling locations going downstream show results comparable to the particle size analysis performed for the Kilchis River. That is, on average there is a decrease in particle size in the downstream direction. There is also variability that depends on the system and the sampling location. The Wilson, Trask, and Tillamook Rivers appear to progress in a more expected fashion (smaller particles in the downstream direction) compared to the Miami River photographs.

There are two main ways to view the changes in particle size distribution. Most obvious is the change in the largest particle present, as can be seen in the Wilson River photographs. However, the shift in particle size distribution can also be seen by observing the prevalence of fine material through comparison of the most upstream site to the most downstream site. There is variability in the progression that is only remedied through sieve analyses such as performed for the Kilchis River. Nonetheless, comparison of the dominant size fraction shows an obvious decline in mean particle size.

Viewing the photo progression vertically instead of horizontally allows comparison of site variability. Note that for each upstream site, there is a large variation in particle sizes progressing from upstream to downstream. This method of analysis shows that the upstream bars sampled are fairly well graded. That is, there is a large variation in the particle size distribution. Progressive observations for the bars closer to river mile 0 show that the variation in sizes decreases dramatically.

Sieve analyses were not completed for the photo frame samples. However, the photo frame analysis did include measurement of 50 particles seen within the frame of each photograph.

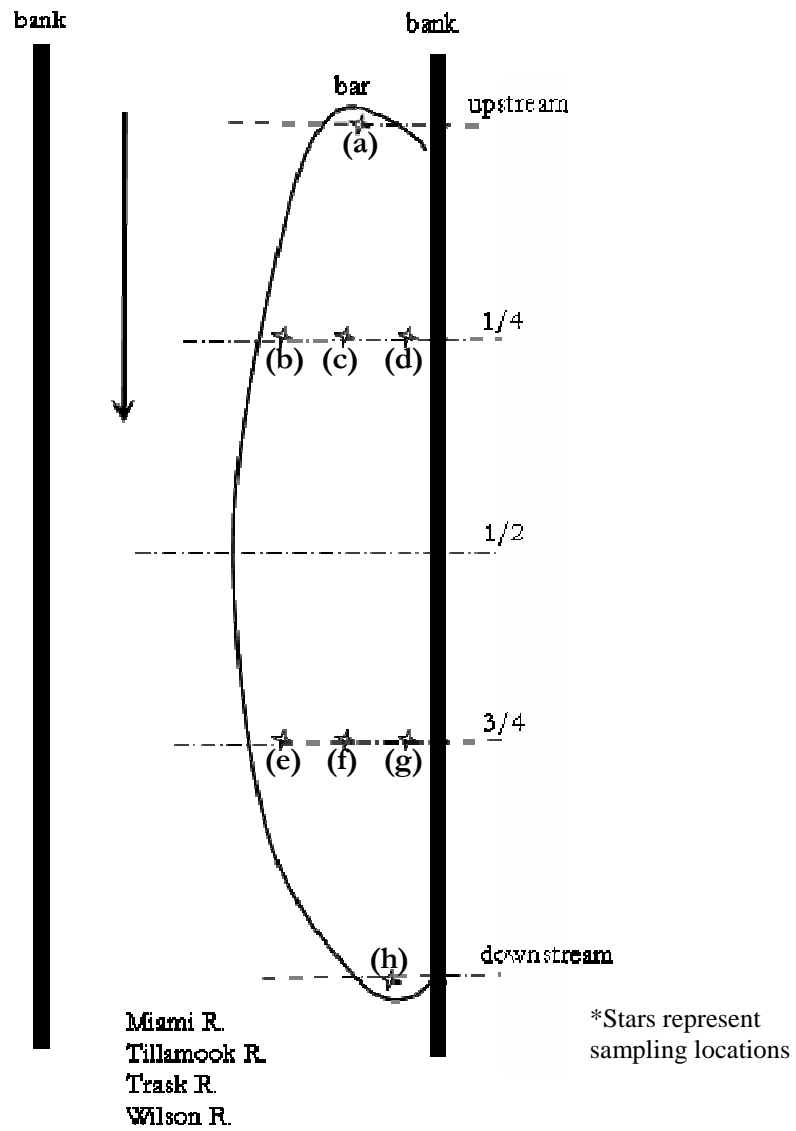


FIGURE 6.6: LOCATION OF SAMPLES

Letters correspond to the labeled composites in Figures 6.5 to 6.8



(a) upstream edge-of-water samples (progressing downstream, left to right)



(b) 1/4 transect edge-of-water samples (progressing downstream, left to right)



(c) 1/4 transect center samples (progressing downstream, left to right)



(d) 1/4 transect back-of-bar samples (progressing downstream, left to right)

FIGURE 6.7: MIAMI RIVER FRAME PHOTO SAMPLING RESULTS



(e) $\frac{3}{4}$ transect edge-of-water samples (progressing downstream, left to right)



(f) $\frac{3}{4}$ transect center samples (progressing downstream, left to right)



(g) $\frac{3}{4}$ transect back-of-bar samples (progressing downstream, left to right)



(h) downstream edge-of-water samples (progressing downstream, left to right)

FIGURE 6.7: (CONT'D)



(a) upstream edge-of-water samples (progressing downstream, left to right)



(b) 1/4 transect edge-of-water samples (progressing downstream, left to right)



(c) 1/4 transect center samples (progressing downstream, left to right)



(d) 1/4 transect back-of-bar samples (progressing downstream, left to right)

FIGURE 6.8: WILSON RIVER FRAME PHOTO SAMPLING RESULTS



(e) $\frac{3}{4}$ transect edge-of-water samples (progressing downstream, left to right)



(f) $\frac{3}{4}$ transect center samples (progressing downstream, left to right)



(g) $\frac{3}{4}$ transect back-of-bar samples (progressing downstream, left to right)



(h) downstream edge-of-water samples (progressing downstream, left to right)

FIGURE 6.8: (CONT'D)



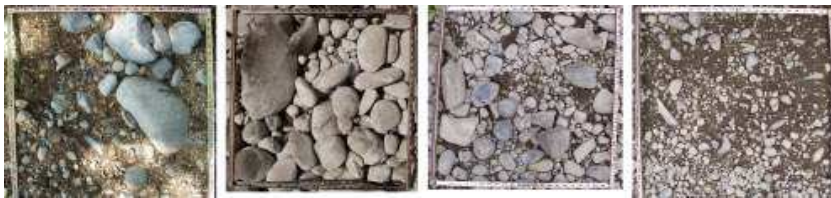
(a) upstream edge-of-water samples (progressing downstream, left to right)



(b) 1/4 transect edge-of-water samples (progressing downstream, left to right)



(c) 1/4 transect center samples (progressing downstream, left to right)



(d) 1/4 transect back-of-bar samples (progressing downstream, left to right)

FIGURE 6.9: TRASK RIVER FRAME PHOTO SAMPLING RESULTS



(e) $\frac{3}{4}$ transect edge-of-water samples (progressing downstream, left to right)



(f) $\frac{3}{4}$ transect center samples (progressing downstream, left to right)

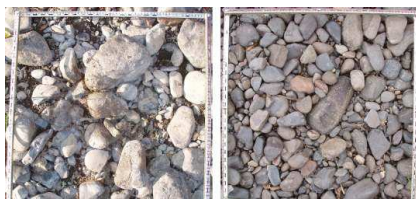


(g) $\frac{3}{4}$ transect back-of-bar samples (progressing downstream, left to right)



(h) downstream edge-of-water samples (progressing downstream, left to right)

FIGURE 6.9: (CONT'D)



(a) upstream edge-of-water samples (progressing downstream, left to right)



(b) $\frac{1}{4}$ transect edge-of-water samples (progressing downstream, left to right)



(c) $\frac{1}{4}$ transect center samples (progressing downstream, left to right)



(d) $\frac{1}{4}$ transect back-of-bar samples (progressing downstream, left to right)

FIGURE 6.10: TILLAMOOK RIVER FRAME PHOTO SAMPLING RESULTS



(e) $\frac{3}{4}$ transect edge-of-water samples (progressing downstream, left to right)



(f) $\frac{3}{4}$ transect center samples (progressing downstream, left to right)



(g) $\frac{3}{4}$ transect back-of-bar samples (progressing downstream, left to right)



(h) downstream edge-of-water samples (progressing downstream, left to right)

FIGURE 6.10: (CONT'D)

It is important to note the variability of results at the $\frac{1}{4}$ and $\frac{3}{4}$ transect sampling points. The visual downstream fining trend is typically disrupted at these locations (see Wilson River $\frac{3}{4}$ transect (f) in Figure 6.8). This may be explained by an analysis of the bar geometry. Figure 6.11 shows two typical scenarios that may explain why a sample taken near the center of the bar yields disruptions in fining.

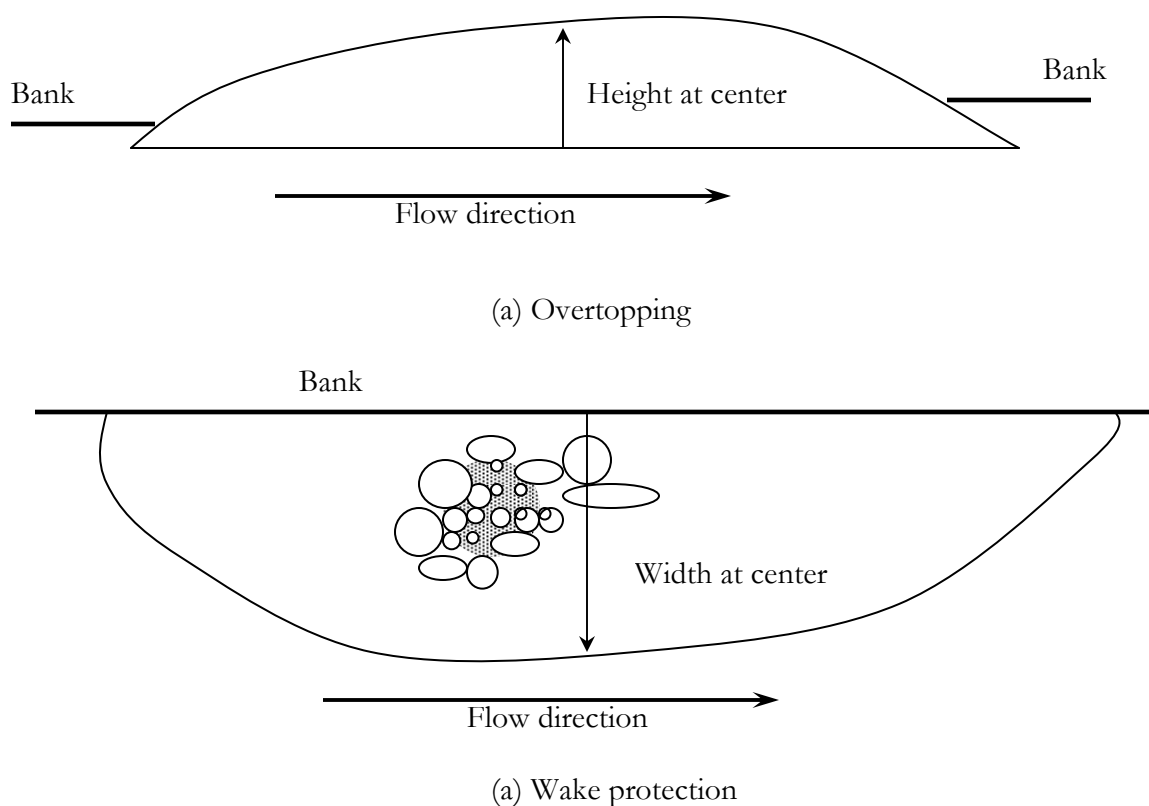


FIGURE 6.11: POSSIBLE CAUSES OF SHIFT TO FINER PARTICLES NEAR CENTER OF BAR

When bar height is great enough such that only occasional overtopping by flow occurs, the deposition of finer material may be the result. In addition, in some instances larger particles were present that probably had deposited during a major flood flow and were not subsequently transportable during bankfull or lesser flows. These larger particles create a wake zone where finer particles deposit. The photo frame sampling captured these scenarios. Furthermore, bars sampled did not include those developed near large

obstructions such as large woody debris or tree trunks. Areas directly upstream or downstream of these areas would contain particle sizes that are not representative of the overall riverbed (Lisle 1986). Woody debris located on bars sampled were rare as well; however, in the few instances where this occurred the sampling near these features was predicted to have results similar to the wake protection scenario.

Each bar was surveyed prior to sampling. Flagged pins were placed at locations specific to the sampling procedures outlined in Chapter 5. Samples were taken at those locations regardless of the on-bar conditions. The purpose of being so exact with the sampling procedure was to be as unbiased as possible in the analysis. These top-of-bar features are present on many bars; therefore, the general fining pattern is of more interest than this type of natural disruption.

The Miami River is an excellent example of how in-stream anthropogenic structures such weirs, sediment traps, drop structures, and bridge pilings can cause unnatural disruptions. It has been previously stated that the Miami River is the only system studied that did not have a clear downstream fining trend that could be identified from photographic evidence and regression analysis. There were two locations on the Miami River (over the length studied) where sediment could become trapped due to human influence. First, in-stream sediment retention structures were cabled into the river upstream of Site 3 (See Figure 6.12). Second, there was a bridge upstream of site 4 where sediment had accumulated in great amounts. Below this area of deposition, the bank was eroding on the right side of the channel and there were small gravel bars on the left side of the channel. At first inspection of field data, these structures did not appear to impede the process of downstream fining. However, given the unexpected results of the photo frame analysis, it appears that further investigation is needed into the effect in-stream structures have on bed-load transport.



FIGURE 6.12: MIAMI RIVER SEDIMENT RETENTION STRUCTURES UPSTREAM OF SITE 3

Results of statistical manipulation used for regression analyses are listed in Table 6.4. Regression analyses were completed for The Miami, Wilson, and Trask Rivers. The Tillamook River had inadequate samples to perform regression analysis. Figure 6.13 shows the regression analyses with their exponential decay models and R-squared values. Results of regression analyses for the additional systems differed from that of the Kilchis River analysis. For the additional rivers, the diminution coefficient associated with the decrease in mean particle size with distance downstream was found to be much lower. Furthermore, not all exponential relationships were found to be significant for all data sets (see Figure 6.14).

The unexpected results from the photographic compilation for the Miami River matched its equally unexpected results in the regression analysis. The diminution coefficient for the Miami River is 0.02 km^{-1} (0.03 mi^{-2}), which is comparable to the upper range of Shaw and Kellerhals (1982) 0.001 to 0.05 km^{-1} (0.002 mi^{-2} to 0.08 mi^{-2}) range. However, the R-squared value for the regression is very poor at 0.19 and does not provide confidence in the exponential model. With a level of significance set at 0.05 and degree of freedom of 3, the null hypothesis (no relationship between mean sediment size and distance in the downstream direction) could not be rejected. The Wilson and Trask regressions were comparable to the upper range of the values reported by Shaw and Kellerhals (1982). The Wilson and Trask Rivers regression analyses resulted in diminution coefficients of 0.03 km^{-1} (0.05 mi^{-2}) and 0.04 km^{-1} (0.06 mi^{-2}), respectively. Unlike the Miami River, the Wilson and Trask Rivers had improved R-squared values of 0.79 and 0.81, respectively. With a level of significance set at 0.05 and degree of freedom of 3 for both data sets, the null hypothesis (no relationship between mean sediment size and distance in the downstream direction) was rejected.

The sampling procedure for particle size distribution for the Miami, Wilson, and Trask Rivers was less robust than that conducted for the Kilchis River. Bulk sampling and sieving to determine particle sizes is much more accurate than measuring diameters of 50 surface particles. In bulk sampling of the armor and sub-armor layer, all particles within the 2-foot-by-2-foot (0.6-meter-by-0.6-meter) frame were included in the analysis. Given the less thorough 50-particle sampling and evaluation at the additional rivers, these photo frame results are considered reasonable.

TABLE 6.4: RESULTS OF PHOTO FRAME SAMPLING

RIVER	SITE #	MEAN PARTICLE DIAMETER D₅₀ (mm)	MEAN PARTICLE DIAMETER D₅₀ (in)	DISTANCE DOWNSTREAM FROM FARTHEST UPSTREAM BAR (km)*
MIAMI	2	42.5	1.7	0.9
	3	40.7	1.6	2.6
	4	55.7	2.2	6.0
	5	45.3	1.8	13.4
	6	29.3	1.2	14.7
WILSON	1	50.8	2.0	17.5
	2	48.5	1.9	24.8
	3	42.2	1.7	38.9
	4	25.9	1.0	44.9
	5	22.9	0.9	45.1
TRASK	1	55.0	2.2	8.2
	2	57.6	2.3	17.0
	3	37.0	1.5	21.4
	4	25.8	1.0	30.4

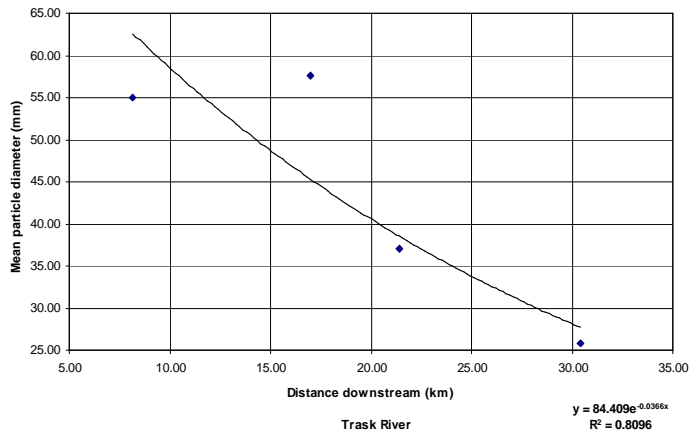
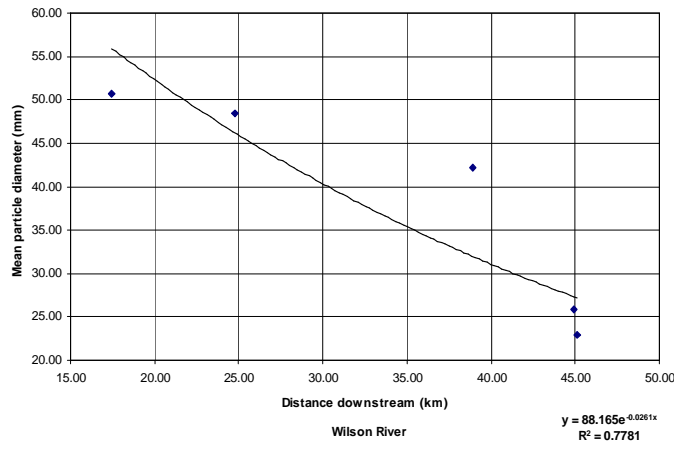
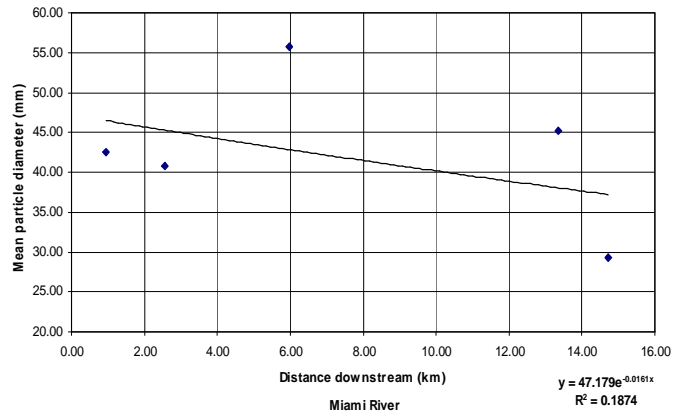


FIGURE 6.13: REGRESSION ANALYSES FOR ADDITIONAL RIVERS

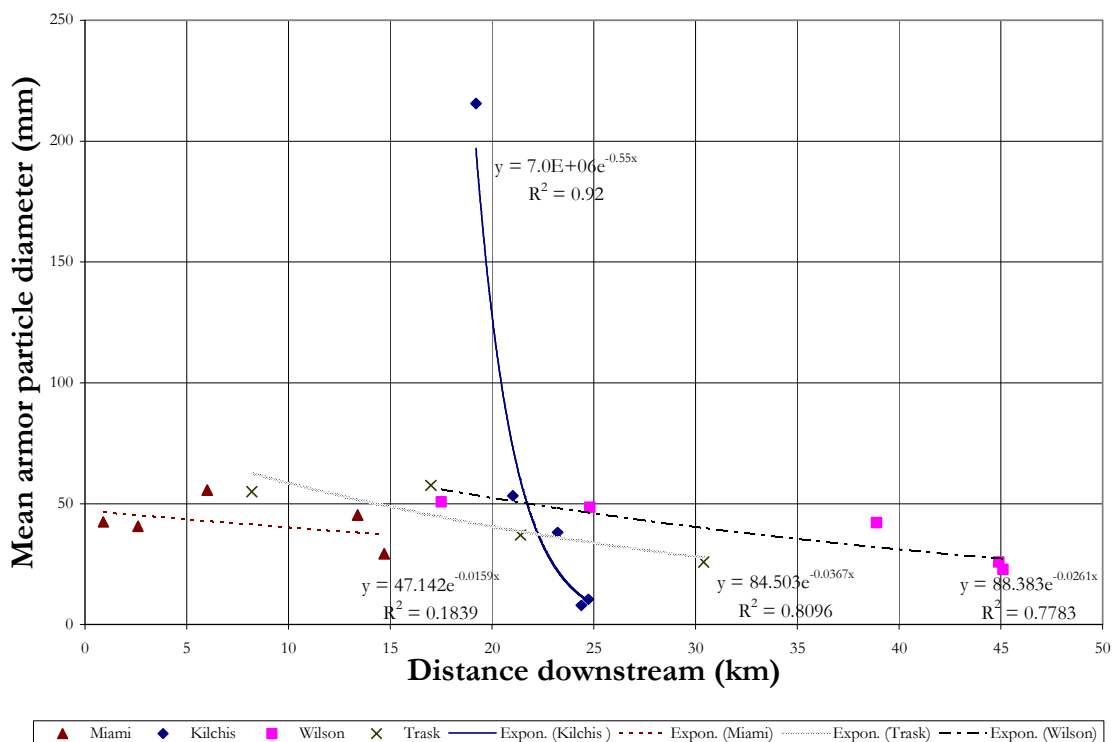


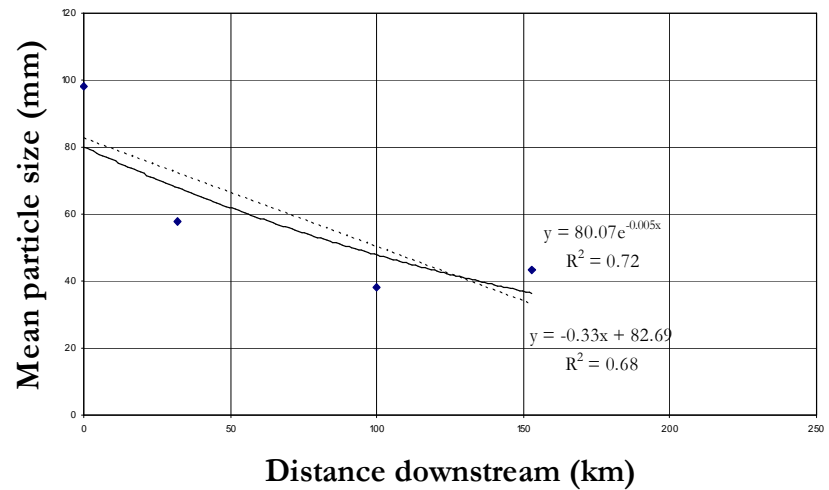
FIGURE 6.14: COMPILATION OF REGRESSION ANALYSES FOR FIVE RIVERS

6.1.3 Comparison of results to Willamette River Studies

Past particle size studies for the Willamette River were reviewed (Klingeman 1981). Comparison to the Tillamook Basin is used to validate the Tillamook Basin analyses. Results should be comparable if the rivers of the Tillamook Basin are indicative of typical gravel-bed rivers in Oregon. In the Willamette study, particle size data were collected by hand using a barrel ring and hand scoop. The types of samples collected included random armor layer, exposed armor layer, non-exposed armor layer, combined armor and sub-armor layer, sub-armor layer, and largest armor layer particle. Section 10.3 contains examples of the particle size distribution obtained for each type of sample collected on the Willamette River. Samples were collected at sites along the Willamette River from river mile 39 (62.8 km, at Wilsonville) to river mile 180 (289.7 km, at Eugene). This gives a study reach about 141 miles (227 km) in length.

The mean particle diameter data provided in the graphs were compiled from the Klingeman (1981) data for regression analyses. Figure 6.15 shows the results of this regression analyses. Particle size values were averaged in cases where several samples were taken at same sampling reach of the river. Table 6.5 shows the diminution coefficients for each type of sample along with corresponding R-squared values. The data show sediment size versus distance downstream to have a weak exponential decay relationship for each type of sample with the exception of the combined armor and sub-armor sample and the largest armor layer particle sample. The diminution coefficients corresponding to the exponential model are not comparable to the Tillamook Basin analyses. The Willamette coefficient for the combined armor and sub-armor (0.01 km^{-1} or 0.017 mi^{-2}) was the only value not an order of magnitude different from fining coefficients reported in the literature. Also, the magnitude of the R-squared values show that the sub-armor and largest armor particle functions had the most reliable fit to the data.

Random armor particles				
Sample location	Particle size (mm)	Distance (river mile)	Distance (Km)	Distance Downstream (Km)
Eugene	98.2	180	290	0
Harrisburg	57.8	160	258	32
Albany	38.3	118	190	100
Salem	43.5	85	137	153



Exposed armor particles				
Sample location	Particle size (mm)	Distance (river mile)	Distance (Km)	Distance Downstream (Km)
Eugene	74.7	180	290	0
Harrisburg	49.1	160	258	32
Albany	40.9	118	190	100
Salem	38.5	85	137	153
Wilsonville	45.2	39	63	227

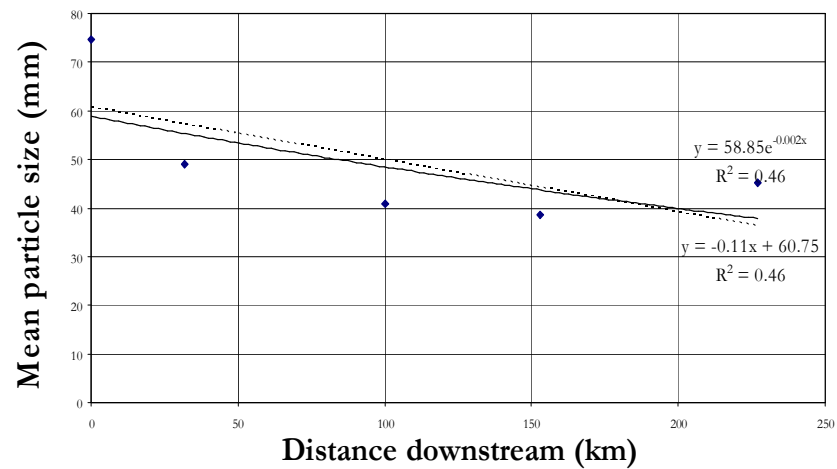
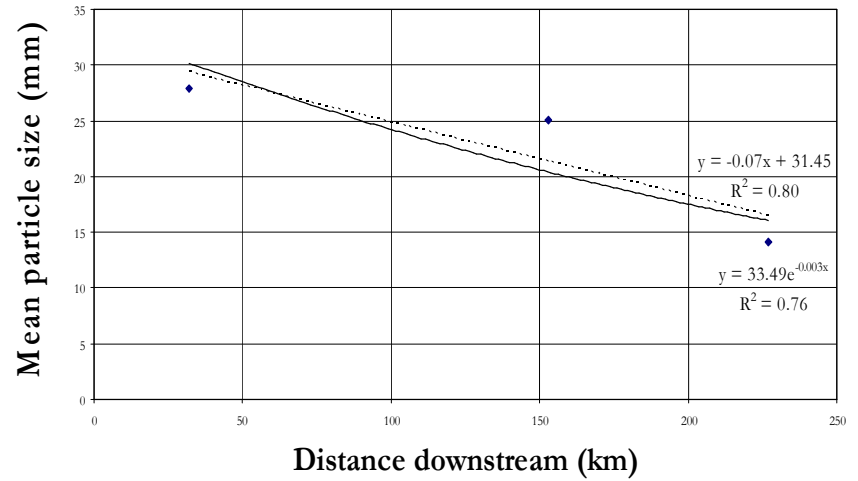


FIGURE 6.15: MEAN PARTICLE SIZE REGRESSION ANALYSES FOR WILLAMETTE RIVER SAMPLES

Non-exposed armor particles				
Sample location	Particle size (mm)	Distance (river mile)	Distance (Km)	Distance Downstream (Km)
Harrisburg	27.9	160	258	32
Salem	27	85	137	153
Salem	23.2	85	137	153
Wilsonville	14.1	39	63	227



Combined armor and sub-armor				
Sample location	Particle size (mm)	Distance (river mile)	Distance (Km)	Distance Downstream (Km)
Eugene	33.8	180	290	0
Salem	40.9	85	137	153
Wilsonville	2.03	39	63	227

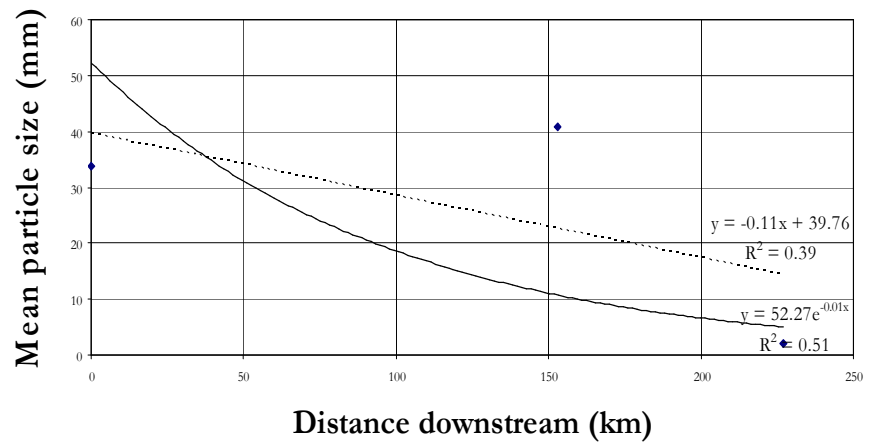
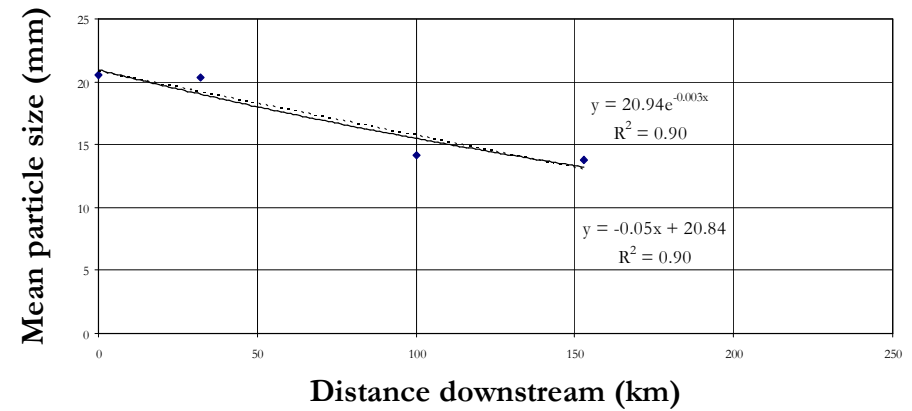


FIGURE 6.15: (CONT'D)

Sub-armor layer				
Sample location	Particle size (mm)	Distance (river mile)	Distance (Km)	Distance Downstream (Km)
Eugene	20.5	180	290	0
Harrisburg	20.3	160	258	32
Albany	14.2	118	190	100
Salem	13.8	85	137	153



Largest armor particle				
Sample location	Particle size (mm)	Distance (river mile)	Distance (Km)	Distance Downstream (Km)
Wilsonville	43.8	39	63	227
Salem	60.6	85	137	153
Albany	82.9	118	190	100
Harrisburg	195.0	160	258	32
Eugene	144.3	180	290	0

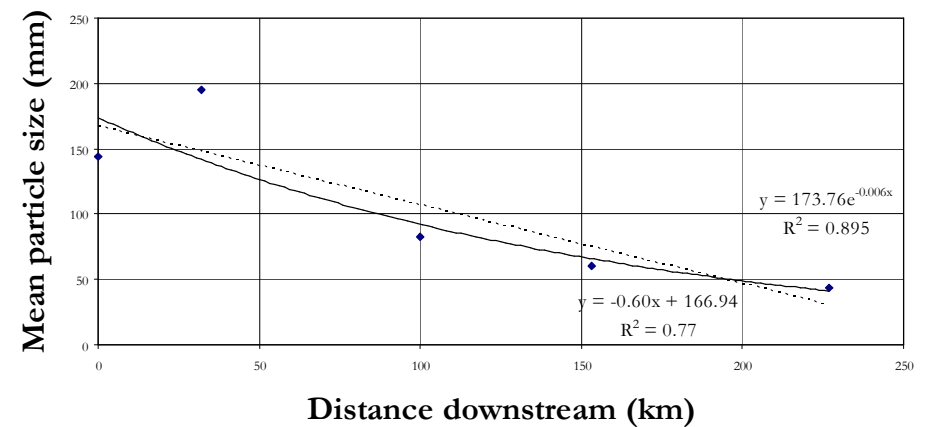


FIGURE 6.15: (CONT'D)

TABLE 6.5: DIMINUTION COEFFICIENTS ACCORDING TO TYPE OF SAMPLE, WILLAMETTE RIVER (analysis of data provided in Klingeman 1981)

TYPE OF SAMPLE	DIMINUTION COEFFICIENT (km^{-1})		R-SQUARED VALUE	
	EXPONENTIAL	LINEAR	EXPONENTIAL	LINEAR
RANDOM ARMOR	0.005	0.33	0.72	0.68
EXPOSED ARMOR	0.002	0.11	0.46	0.46
NON-EXPOSED ARMOR	0.003	0.07	0.76	0.76
COMBINED ARMOR AND SUB-ARMOR	0.010	0.01	0.51	0.39
SUB-ARMOR	0.003	0.05	0.90	0.90
LARGEST ARMOR LAYER PARTICLE	0.006	0.60	0.90	0.77

The Willamette River has many major tributaries along its length that contribute sediment to the main stem. Sediment contributions have been discussed previously as possible causes of disruptions in the downstream fining trend. With the number of tributaries along the Willamette, one might expect a large amount of ‘noise’ in data for longitudinal particle size analysis. However, the weak exponential relationships obtained from the data collected by Klingeman (1981) shows that downstream fining operates despite extensive lateral introduction of sediment.

Like the Willamette River, the rivers studied by Rice (1999) in British Columbia also have low rates of downstream fining. Rice used a linear form of the Sternberg relationship (Equation 2.3) to describe downstream fining in these rivers. Figure 6.14 includes the results of regression analyses using a linear function. Results are tabulated in Table 6.5 for comparison to the exponential function curve fitting. The linear curve fitting showed

improved results, where the non-exposed armor layer, combined armor and sub-armor layer, and sub-armor layer samples all showed diminution coefficients in the range of Shaw and Kellerhals (1982). This suggests that for systems with large amounts of lateral input or very low rates of downstream fining, the linear model may be more appropriate.

6.1.4 Specific Gravity Determination

Table 6.6 gives a compilation of the results of the specific gravity analysis made for Kilchis River bar samples. The table is divided into sub-tables for clarity, with each sub-table listing data for a single site. Each analysis was done by site and size fraction. A geometric mean of the overall specific gravity is reported in the last row of each table (geometric mean is defined as the product of n values taken to the n th root).

Sites 1 to 3 had comparable overall specific gravities. There was a large deviation in the geometric mean at Site 4. Specific gravity value returns to a more comparable value at Site 5, though, it is still 6% smaller than that of Site 3. In addition to this longitudinal variation in average specific gravity, there also exists a variation based on particle size. It appears the larger particles have higher the specific gravities. Variation in specific gravity based on particle size might imply that the larger particles present at the sites have different mineralogies than their smaller counterparts.

The discrepancy at Site 4 could be due to the introduction of large masses of bank material due to human disturbance and erosion. As previously mentioned, sediment in the upper reaches of the Kilchis River is mostly volcanic in origin. The large conglomerates of sedimentary rock and organic material show specific gravity values much less than those expected for mafic material typical of large particles in the upstream river reaches. For example, 64 mm or 2.52 inch particles at Site 1, Site 2, and Site 4 had specific gravities of 2.88, 2.85, and 1.99, respectively. The breakdown of these less-stable particles and the transport of durable particles from upstream of Site 4 is manifest through the increase in values for specific gravity toward that of quartz (2.65) as particle size decreases. In place weathering and breakdown during months of exposure to air, followed by transport

downstream during periods of bar inundation causes these particles to be highly transitory. Such introduction, breakdown, and transport of large deposits have been observed in the HJ Andrews Experimental Forest of the central Cascade Range of Oregon (Jones, Personal Communication 2007). Therefore, specific gravity analyses done longitudinally can assist in determination of landslide activity, where drastic deviations from expected values can indicate lateral introduction of material.

The significant difference in specific gravity between the 64 mm (2.52 in) particles of the upstream sites and Site 4 is not present at Site 5. This provides additional evidence of the breakdown of the larger particles from upstream. Moreover, the comparable values for specific gravity between very large particles at Site 5 versus Site 1 and 2 might indicate that bank material in this area originates from flood deposits. Therefore, specific gravity analyses done longitudinally coupled with analysis by size fraction can allow for determination of the origin of material introduced from the floodplain.

Variation of values for specific gravity based solely on particle size at a given bar is also a significant indicator of the type of material deposited. If values for specific gravity do not change at a site based on particle size, one could expect that bar material at that site dominated by fluvial deposits of durable material. If values of specific gravity increase with decreasing particle size, one might expect a situation similar to that mentioned above where introduction of less-durable material has been introduced by landslide activity or erosion. If values of specific gravity decrease with decreasing particle size then one can expect an unmodified downstream fining pattern, that is, there exists a wide range of durable clasts deposited from upstream.

The difference at Site 4 could also be a lab measurement issue. For larger particles, the sample volume necessary for the specific gravity estimation was reached with very few particles; in certain size classes, there was sometimes only one particle available on-site. For smaller particles, there was typically a wider assortment of particle types. The abundance of a variety of particles in smaller size classes may have lead to the total specific gravity for a small size class being the average of many different mineralogical compositions. Table 6.7 contains composite statistics for each Kilchis River site. The maximum standard deviation

for specific gravity by size fraction was 0.38 for the 64 mm (2.52 in) and 50 mm (1.97 in) size fractions. The overall standard deviation for each site (all size fractions) was 0.19.

As a reminder, the specific gravity of particles in the Kilchis River was found using collected bulk samples from each of five sites along approximately ten river miles. A geometric mean of specific gravities of size ranges from 76.2 to 7.925 mm (3 to 0.3 in) was calculated for each site. Finally, an average specific gravity for the river was found from these five geometric means. This value was calculated to be 2.68. For the four additional rivers emptying into Tillamook Bay, an equal number of particles in size ranges from 76.2 to 12 mm (3 to 0.5 in) were collected at each site that was sampled for photo frame analyses. The results of these analyses were 2.78, 2.73, 2.56, and 2.76 for the Miami, Wilson, Trask, and Tillamook Rivers, respectively (see Table 6.8). The overall average specific gravity for the Tillamook Basin using the geometric mean for each river is 2.70, with a standard deviation of 0.09.

The values obtained by the Tillamook Basin were compared to values from samples from the Willamette River (See Table 6.9, Klingeman 1981). The Willamette River analysis was done longitudinally. Samples were taken at sites along approximately 200 river miles (321 km, from Eugene to Mission Bar). The composite for this analysis ranged from 2.66 to 2.78 (for Salem and Eugene oven dry samples, respectively). The overall average specific gravity for the oven dry samples extracted from the Willamette River was 2.73, with a standard deviation of 0.04. This range is within the specific gravities estimated for the Tillamook Basin. This gives some confidence that the values obtained are representative for particles of similar origin in Western Oregon. More importantly, the comparison of the Willamette River results with those of Tillamook Basin gives additional confidence in the exclusion of abrasion as the major mechanism of downstream fining in rivers of Western Oregon.

TABLE 6.6: RESULTS OF SPECIFIC GRAVITY ANALYSES FOR KILCHIS RIVER

SITE 1					
Size fraction (mm)	Size fraction (in)	Number of Particles	Dry weight (g)	Submerged weight (g)	Specific Gravity
76.2	3.00	3	2389.3	1560.6	2.88
63.5	2.50	3	1719.2	1122.9	2.88
50	1.97	14	5040.6	3296.8	2.89
38.1	1.50	31	5329.3	3487.6	2.89
31.75	1.25	23	1867.2	1206	2.82
25.4	1.00	50	2449.4	1583	2.83
19.05	0.75	97	2104.3	1355	2.81
15.875	0.62	90	991.1	631	2.75
12.7	0.50	173	981.9	624.4	2.75
Geometric mean 2.83					

SITE 2					
Size fraction (mm)	Size fraction (in)	Number of Particles	Dry weight (g)	Submerged weight (g)	Specific Gravity
64	2.52	7	5833.8	3784.9	2.85
50	1.97	15	5509.5	3603.3	2.89
31.5	1.24	31	3835.1	2486	2.84
25.4	1.00	55	2500.4	1603	2.79
16	0.63	166	2699	1711.5	2.73
7.925	0.31	400	1234.8	780	2.72
Geometric mean 2.80					

TABLE 6.6: (CONT'D)

SITE 3					
Size fraction (mm)	Size fraction (in)	Number of Particles	Dry weight (g)	Submerged weight (g)	Specific Gravity
64	2.52	8	5186.6	3276.8	2.72
50	1.97	12	3748	2424.9	2.83
31.5	1.24	34	3898.1	2511.8	2.81
25.4	1.00	64	2701.1	1731.4	2.79
16	0.63	186	2881.9	1836.5	2.76
7.925	0.31	400	1408.4	894.1	2.74
Geometric mean 2.77					

SITE 4					
Size fraction (mm)	Size fraction (in)	Number of Particles	Dry weight (g)	Submerged weight (g)	Specific Gravity
64	2.52	1	372.4	185.1	1.99
50	1.97	1	168	84.3	2.01
31.5	1.24	36	3697.3	2260	2.57
25.4	1.00	126	2712.5	1674.8	2.61
16	0.63	238	3195.9	1989.6	2.65
7.925	0.31	400	1292.3	793	2.59
Geometric mean 2.38					

TABLE 6.6: (CONT'D)

SITE 5					
Size fraction (mm)	Size fraction (in)	Number of Particles	Dry weight (g)	Submerged weight (g)	Specific Gravity
63.5	2.50	1	549.4	358.3	2.87
50.8	2.00	5	1562.6	931.3	2.48
38.1	1.50	14	1928.3	1186.3	2.60
31.5	1.24	10	661.5	402.2	2.55
25.4	1.00	44	1791.8	1102	2.60
19.05	0.75	131	2456.6	1518.5	2.62
15.875	0.62	109	1036.3	637.7	2.60
12.7	0.50	336	1715.5	1049	2.57
Geometric mean 2.61					

*Average specific gravity for the Kilchis River: 2.68

TABLE 6.7: KILCHIS COMPOSITE STATISTICS

Size fraction (mm)	Size fraction (in)	Site 1	Site 2	Site 3	Site 4	Site 5	Mean for size fraction	Std Dev
64	2.52	2.88	2.85	2.72	1.99	2.87	2.61	0.38
50	1.97	2.89	2.89	2.83	2.01	2.48	2.66	0.38
31.5	1.24	2.82	2.84	2.81	2.57	2.55	2.76	0.15
25.4	1.00	2.83	2.79	2.79	2.61	2.6	2.75	0.11
16	0.63	2.75	2.73	2.76	2.65	2.6	2.72	0.07
7.925	0.31	no data	2.72	2.74	2.59	no data	2.68	0.08
Overall		2.83	2.8	2.77	2.38	2.61	2.68	0.19

TABLE 6.8: RESULTS OF SPECIFIC GRAVITY ANALYSES FOR OTHER FOUR TILLAMOOK BASIN RIVERS

Miami River

Size fraction (mm)	Size fraction (in)	Number of Particles	Dry weight	Submerged weight	Specific Gravity
76.2	3.0	4	4350.4	2891.8	2.98
64	2.5	6	4455	2858.3	2.79
50.8	2.0	12	4289.8	2719.8	2.73
38.1	1.5	18	3176.1	2011.3	2.73
25.4	1.0	57	2909.4	1857	2.76
19.05	0.75	97	1814.1	1148.8	2.73
12.7	0.5	171	1440.3	910.8	2.72
Geometric mean 2.78					

Trask River

Size fraction (mm)	Size fraction (in)	Number of Particles	Dry weight	Submerged weight	Specific Gravity
76.2	3.0	4	4894.8	2942	2.51
64	2.5	7	4777.1	2895.9	2.54
50.8	2.0	13	4705.4	2787.4	2.45
38.1	1.5	27	4184.2	2542	2.55
25.4	1.0	80	4338.7	2658	2.58
19.05	0.75	115	2304.3	1434	2.65
12.7	0.5	295	2295	1439.7	2.68
Geometric mean 2.56					

Wilson River

Size fraction (mm)	Size fraction (in)	Number of Particles	Dry weight	Submerged weight	Specific Gravity
76.2	3.0	4	4141.4	2593.5	2.68
64	2.5	7	5321.3	3425.1	2.81
50.8	2.0	9	3924	2448	2.66
38.1	1.5	25	4183.3	2662.8	2.75
25.4	1.0	87	4710.4	2976.4	2.72
19.05	0.75	143	2867.4	1831.2	2.77
12.7	0.5	274	2381.6	1501	2.70
Geometric mean 2.73					

Tillamook River

Size fraction (mm)	Size fraction (in)	Number of Particles	Dry weight	Submerged weight	Specific Gravity
76.2	3.0	2	1853.6	1157	2.66
64	2.5	4	2452	1606.4	2.90
50.8	2.0	7	2131.7	1375	2.82
38.1	1.5	8	1809.2	1155.2	2.77
25.4	1.0	37	1904.2	1219.8	2.78
19.05	0.75	88	1491.2	946	2.74
12.7	0.5	149	1349.8	849.1	2.70
Geometric mean 2.76					

TABLE 6.9: SPECIFIC GRAVITY STUDY OF THE WILLAMETTE RIVER (KLINGEMAN, 1981)

WILLAMETTE RIVER								
Location	Eugene		Albany		Salem		Mission Bar	
Date	26-Jul-81		19-Jul-79		11-Jul-1979		27-Aug-79	
Particle Size	SG Saturated surface-dry	SG Oven dried						
(inches)	-	-	-	-	-	-	-	
>4	2.73	2.79	2.71	2.72	-	-		
3-4	2.72	2.78	2.61	2.65	-	-		
2-3	2.75	2.78	2.69	2.71	2.51	2.58		
1.5-2	2.72	2.80	2.70	2.81	2.62	2.67		
1-1.5	2.71	2.80	2.68	2.75	2.61	2.68		
.75-1	2.70	2.82	2.66	2.75	2.59	2.69		
.5-.75	2.70	2.78	2.59	2.70	2.58	2.69		
Composite	2.73	2.79	2.67	2.71	2.59	2.67	2.66	2.73

6.2 TIMM Simulation Results

6.2.1 *Simplified version of the Kilchis River*

The MATLAB program, TIMM was run using a simplified version of the Kilchis River. The purpose was to characterize bed-load transport in the zone of tidal influence. The model simulates the zone from the Bay up to head of tidewater in the river. The Kilchis River was used as the basis for input data. For example, the mean particle diameter estimated from the particle size analysis presented earlier in this chapter was used as d50. Input parameters for TIMM are shown in Table 6.10.

TABLE: 6.10 INPUT PARAMETERS FOR TIMM

VARIABLE IDENTIFIER	INPUT PARAMETER	VALUE OF INPUT PARAMETERS USED FOR SIMULATIONS
d50	The 50 th percentile sediment size (mm)	7.9
mannings	Mannings roughness coefficient	0.029
rivermiles	Total number of miles under study	3
width	Average channel width (ft)	70
totaltime	Number of days to simulate	90
Q	Average discharge (cfs)	398
channelslope	Slope in (degrees)	0.0011

Appendix 10.5 shows the source code for both the constant and varied discharge versions of the TIMM. A user-defined run of the model can be achieved by copying the source code and deleting the simplified Kilchis River-specific input parameters. When run in this form, query statements prompt the user for each input parameter.

6.2.2 Constant-discharge results and discussion

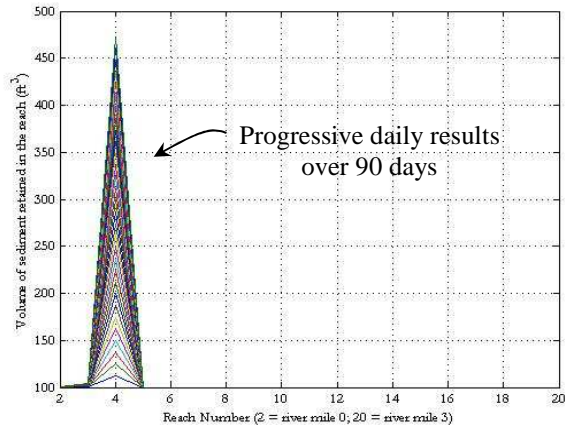
The first version of TIMM uses a constant flow rate for the duration of the run. Water surface profiles are calculated according to the procedure outlined in Chapter 5. All runs of the model use mean particle diameter and the critical tractive force method by DuBoys to estimate critical shear stresses and bed-load. The Shields criterion was used in the sensitivity

analysis to verify the results of runs using DuBoys' method. The standard step method is used in all backwater calculations. The model can be run using one of two starting depths: 1) critical depth at some point beyond the first reach, or 2) an average constant depth controlled by the estuary. I chose to set downstream depth at 6.6 feet (2 meters), which is the average depth of Tillamook Bay (Kilchis Watershed Analysis 1998).

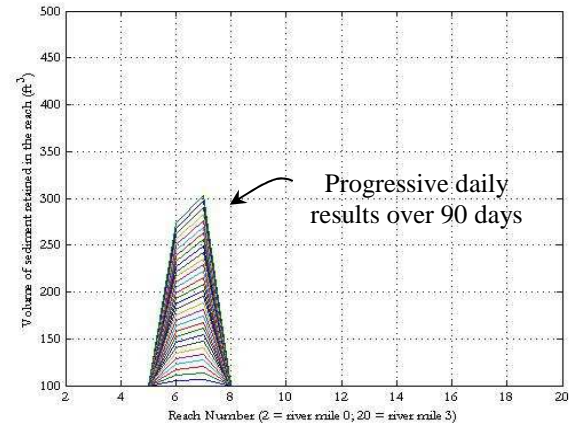
The developed model includes a user-defined optional tidal fluctuation. That is, the user may choose to simulate all tidal conditions, or choose to run the model with tidal fluctuation kept static (e.g., high tide only). I chose to begin my analysis with a constant discharge simulation for 90 days. For this simulation bed-load transport was kept separated by high tide, low tide, and intermediate tide. The results of this run are shown in Figure 6.16. Each graph shows the reach number on the x-axis (downstream direction is right to left). Reach number 2 is at river mile zero. Subsequent upstream reaches are 1/6 of a mile apart. The y-axis has both a dependent and an independent variable. Time is the independent variable. The dependent variable is the volume of sediment retained in the reach. Volume of sediment retained is the amount of material that was transported into the reach but could not be transport out of the reach. Because the model returns output data in the form of a movie, time is represented by the sequence of plots. TIMM calculates the total volume retained in a reach during a single day for the user-specified tidal conditions. The result of the first day of calculations is shown as the line closest to the x-axis on the graph. The next day's result shows as the next line above the first, and so on until all days have been simulated. Portions of the channel where net zero transport occurs (volume in = volume out) are indicated by lines near equal to the x-axis. Lines exactly equal to the x-axis are indicative of zones of zero transport (volume in = volume out = 0).

The model results show that the periodic fluctuations of water stage at the downstream end cause an adjusted water surface profile that alters bed-load transport processes. The adjusted water surface profile alters the rate of bed-load transport by decreasing velocity below the threshold at which bed-load movement can be sustained. This may occur farther upstream or downstream than would be the case without tidal influence. For the low-tide-only run, the amount of sediment into a reach matched the amount of sediment out of the reach until reach number 4. For the intermediate-tide-only run, this zone of deposition

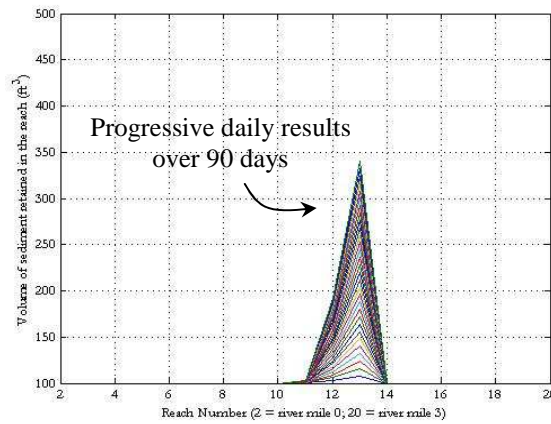
occurred between reach numbers 6 and 7. Finally, for the high-tide-only run, the zone of deposition occurred between reaches 12 and 13. Therefore, the zone of deposition exists for each tidal condition (given that incipient motion has been exceeded), but is shifted longitudinally depending on tidal levels.



(a) Low-tide



(b) Intermediate-tide



(c) High-tide

FIGURE 6.16: DEVELOPMENT OF TIDALLY INFLUENCED ZONES OF DEPOSITION OVER TIME FOR 90 DAYS AT 398 CFS

Also significant is the length of the zone of deposition. During low tide the zone of deposition was isolated to a mainly a single reach. However, transport does not come to a stop abruptly. There is large reduction in the volume of sediment, yet sediment is retained in the next reach downstream (reach number 2). The 'trail off' bed-load transport is also apparent during high tide (Figure 6.16c), yet does not occur during periods of intermediate-tide. The shape of the deposit is related to the length of deposit as well. Excluding the volume of sediment retained in the trail-off reach, the length of deposit is shortest during low tide. During low tide, the most symmetrical configuration of deposition occurs. Periods of low tide can be considered times when tide has no influence, as water levels are not elevated during these times. During low tide bed-load transport appears to continue until very close to the mouth, finally ceasing as depth becomes equal to the average depth of the estuary (average depth occurs at reach 2 for low tide condition). This can be considered an appropriate occurrence given that delta formation at the mouths of rivers is a regularly observed phenomenon. For the duration of intermediate tidal influence, where the water surface is elevated above mean estuary depth, the distance over which transport ceases is greater. This leads to a more elongated deposit. This may be due to a less abrupt shift to deeper water caused by water surface adjustment to an elevated downstream depth. Finally, the shape of the zone of deposition during high tide indicates a less abrupt transition to no bed-load transport, albeit more abrupt than that of intermediate tide.

Running TIMM with all simulated tide conditions provided more insight into the bed-load transport process as affected by tide. Figure 6.17 shows the 90-day simulation with all tidal conditions simulated throughout each day. The configurations of the deposits are the same as those of the 90-day runs with the tidal conditions kept separate. This implies that if discharge is kept constant, erosion and deposition would continue to occur in the same positions along the channel. Figures 6.18 to 6.20 show the parameters that control transport location: bed shear stresses, channel velocities, and rates of bed-load transport, respectively. For each tidal condition, the location where shear stresses on the bed begin to diminish is the location of the upstream edge of the zone of deposition (See Figures 6.17 and 6.18). Reductions in shear stresses are in accord with reduction in velocities in the downstream direction caused by changes in depth (See Figures 6.18 and 6.19). The transitions to

constant values shown in each figure (horizontal line) correspond with the water surface adjustment to normal depth. Once normal depth is reached, TIMM maintains that depth for the remainder of the simulated-channel length.

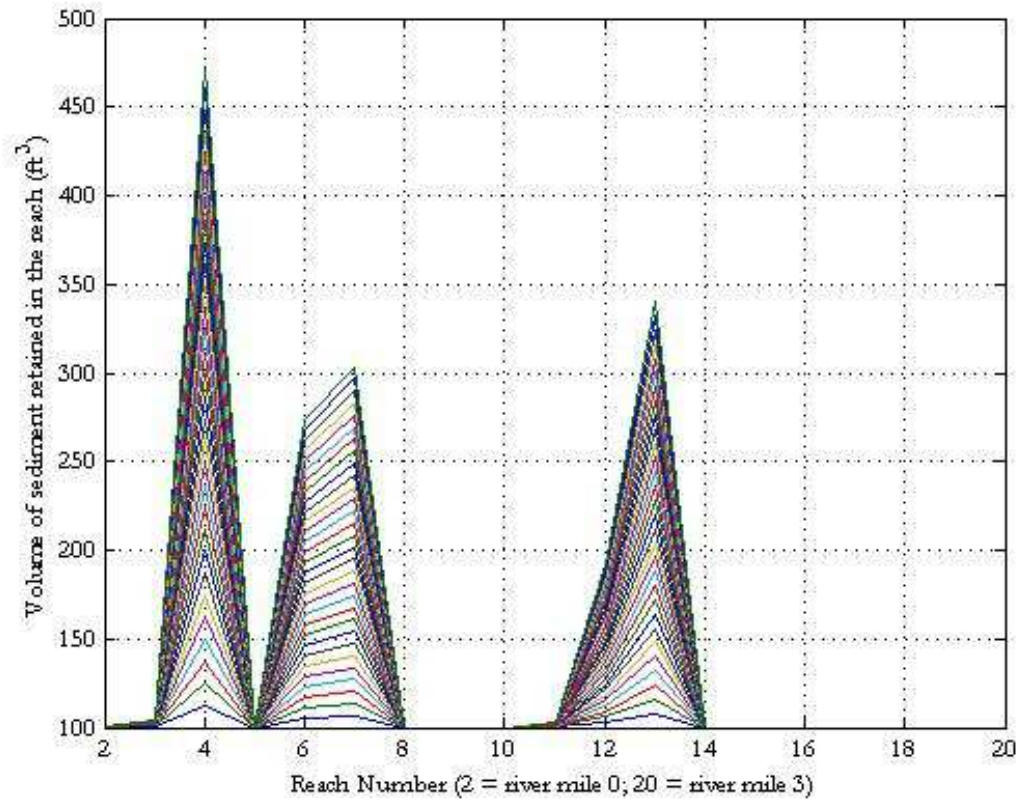
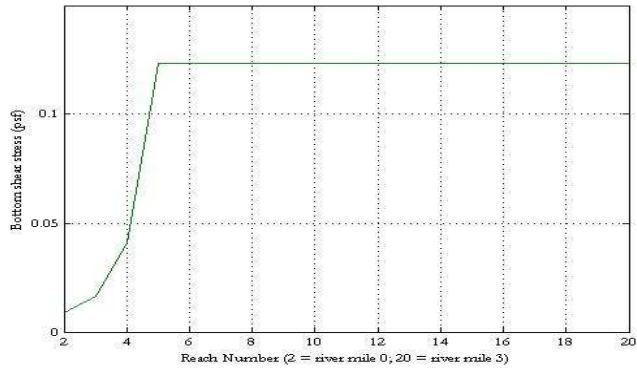
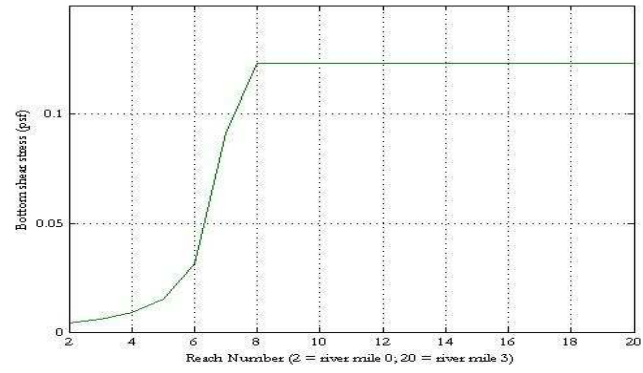


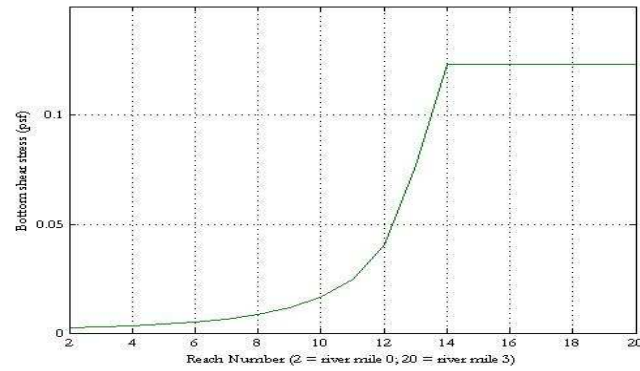
FIGURE 6.17: DEVELOPMENT OF TIDALLY INFLUENCED ZONES OF DEPOSITION OVER TIME



(a) low tide

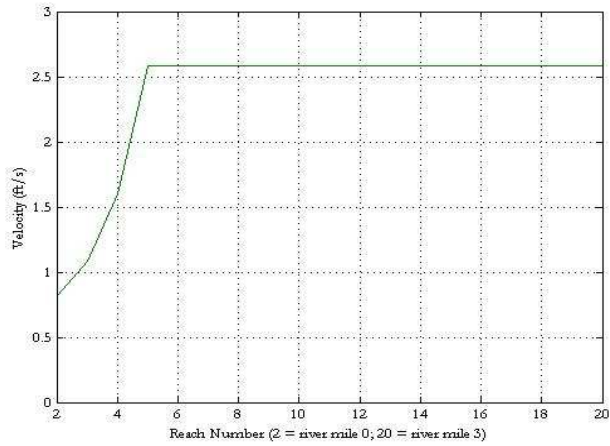


(b) Intermediate tide

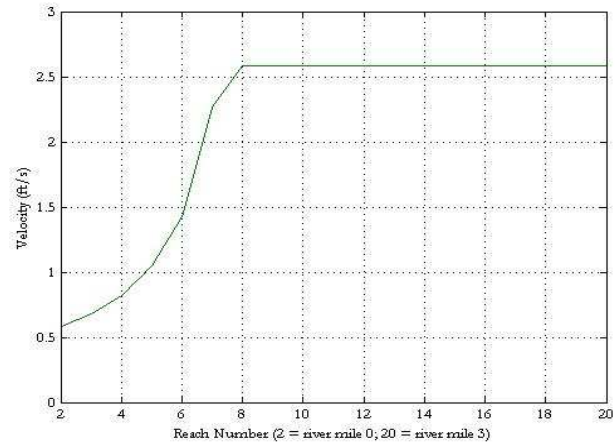


(c) high tide

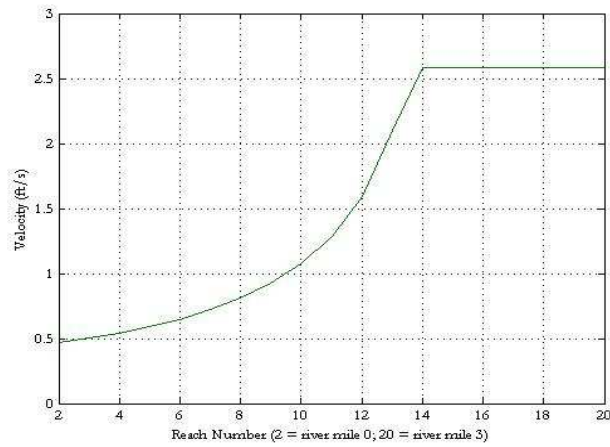
FIGURE 6.18: SHEAR STRESS FOR A PERIOD OF 90 DAYS AT 398 CFS



(a) low tide

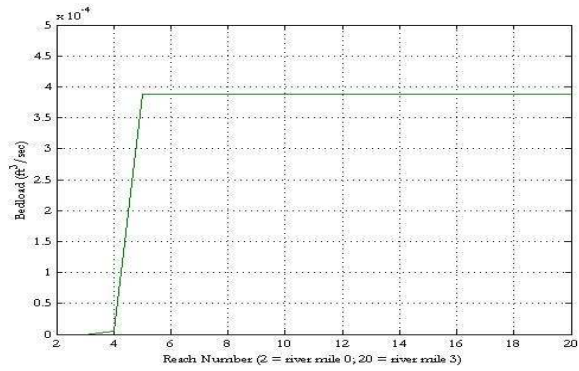


(b) intermediate tide

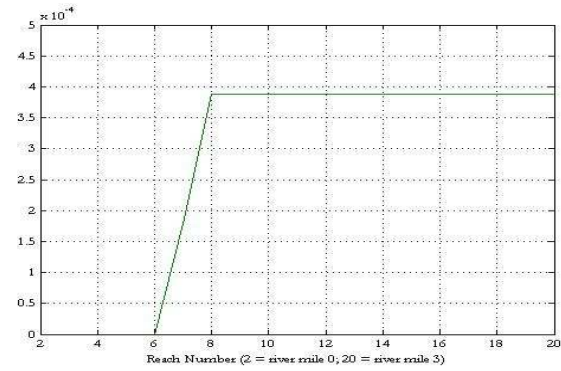


(c) high tide

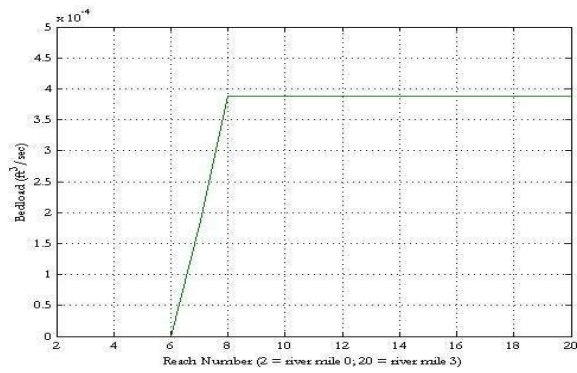
FIGURE 6.19: VELOCITY ALONG CHANNEL FOR A PERIOD OF 90 DAYS AT 398 CFS



(a) low tide



(b) intermediate tide



(c) high tide

FIGURE 6.20: BED-LOAD RATE ALONG CHANNEL FOR A PERIOD OF 90 DAYS AT 398 CFS

6.2.3 *Varied-discharge results and discussion*

Following the simulations using constant discharge, TIMM was modified to incorporate variations in daily stream discharge. The purpose was to investigate the relationship between tidal fluctuations and river discharge variations. All of the constant-discharge tidal conditions were simulated during the variable-discharge runs. The simulation time was decreased to one month instead of three so that differences in transport related to moderate changes in river discharge could be studied. Daily discharge data derived from the USGS Wilson River surface water statistics was used as the input array for these simulations (see Appendix 10.3). Simulations were executed for mean daily discharges for the period of record in September, October, and January (see Figures 6.21 to 6.23). Mean daily discharge for the period of record in August were also simulated. August flow magnitudes resulted in a zero transport scenario for the entire month.

River discharge was found to have an effect on the location and length of the deposit. For the early September (<10 days) values, the shape and length of the deposit indicates a fast transition to no transport conditions for all tidal conditions. Each deposit is isolated at one reach. However, as river discharge increases to a maximum value of 96 cfs (2.7 cms) in the middle of the month, the zone of deposition created during the intermediate tidal condition shows a lengthening. The propagation of the intermediate zone of deposition downstream indicates a significant process. As river discharge increases, there is not only an increase in the volume of sediment transported but an increase in the transport distance as well. That is, more particles are transported farther downstream than would be the case during smaller river discharges.

The simulation performed with mean daily discharge data for the period of record in October supports this assertion. The overall volume retained for the month increased and the depositional zone shifted downstream. The transport of an additional volume of sediment farther downstream occurs in conjunction with reduced velocity and shear stress caused by tides.

Tidal influence causes distinct deposition zones at moderate streamflow that is beyond the threshold for transport of bed material. However, near the end of the month when the maximum discharge for the month is reached (515 cfs or 14.6 cms), the deposition zones begin to coalesce into a single deposit. This pattern is further illustrated by the January simulation. With streamflow discharge ranging from 1,062 to 1,379 cfs (30 to 39 cms), there is no longer a clear depositional area associated with intermediate periods between low and high tide. Also, there is deposition for every reach in the tidal zone at such large values of river discharge. Moreover, maximum volume of sediment retained at reach 4 during the October simulation was only 21.4% of the maximum volume of sediment retained at reach 5 in the January simulation.

Extrapolation of this scenario to consider what might occur during flood flow, leads to the zone of deposition extending out into the estuary. That is, at elevated river stage, deposition of a large amount of sediment from the channel would occur at the mouth of the river and some distance into the estuary. The location of the overall area of deposition would vary depending on the flood frequencies and history of flows of river systems. For river systems where tidal influence is great and flows greater than bankfull flow are infrequent, the area of shoaling would be farther upstream from the mouth of the river. Alternatively, the major area of deposition would be expected to lie closer to the mouth and into the estuary, for river systems where tidal influence is minimized by a flow history that includes greater than bankfull conditions frequently throughout each water year.

With regard to the Kilchis River in particular, this would explain why there is a shoaling problem in the tidal zone but also why the channel is not filled to capacity with sediment. Juxtaposing this information about the expected location of shoaling with the specific gravity analysis results also explains the origin of the shoaled material and the large flood-related particles in the banks of the Kilchis at site 5 of the particle size distribution analysis. The large durable sediment in the area of shoaling originates from the eroding banks and the small durable material originates from the upstream river reaches.

It can be concluded that tidal influence is stronger at flow magnitudes moderately above the threshold for transport than during periods of larger river discharges. Therefore, if tidal

influence is considered a downstream control, its effect is 'drowned out' by large magnitudes of river discharge. Despite being drowned out at large river discharge, tidal influence is still significant. This, too, is shown by the Kilchis River example. If the large-magnitude events were so dominant, shoaling in the river would not be a major issue. In this scenario, the river/estuary system would interact similarly to a river flowing into a lake, where the delta formed is within the lake rather than within the river system. Therefore, it is important to include tidal effects in sediment transport analyses that extend into the zone of tidal influence. The high flow magnitude during periods of low tide would be most comparable to the interactions between rivers entering a larger river at tributary junction. The similarity of these two situations is the expected transport of the deltaic area away from the river mouth or junction. The difference between these situations is the lack of flow acceleration for the estuarine scenario. For tributary junctions, the flow associated with the larger river creates a greater flow capacity to move shoaled sediment. To determine the net effect on the over years, one would need to extend the numerical analysis to include exact the volume of bed material transported away from or to a particular location.

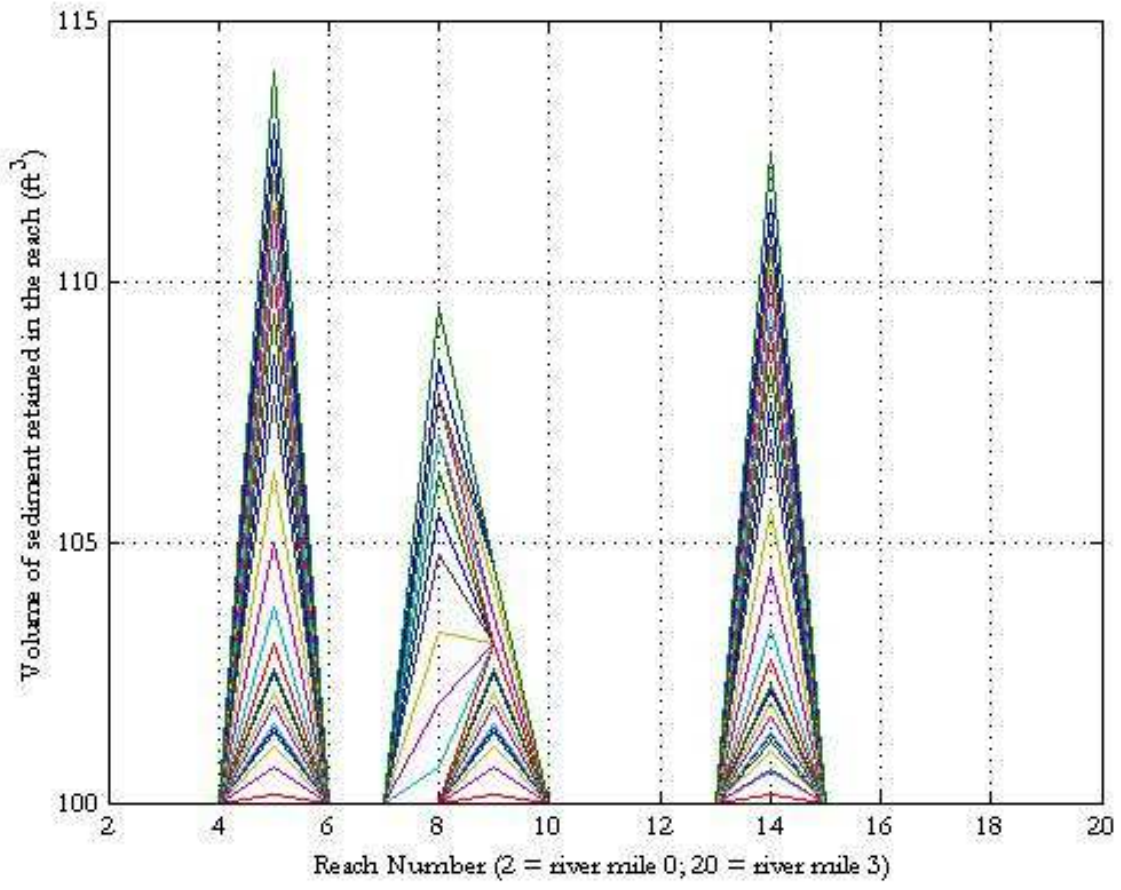


FIGURE 6.21: DEVELOPMENT OF TIDALLY INFLUENCED ZONES OF DEPOSITION OVER TIME, FOR SEPTEMBER USING AVERAGE DAILY DISCHARGE FOR PERIOD OF RECORD

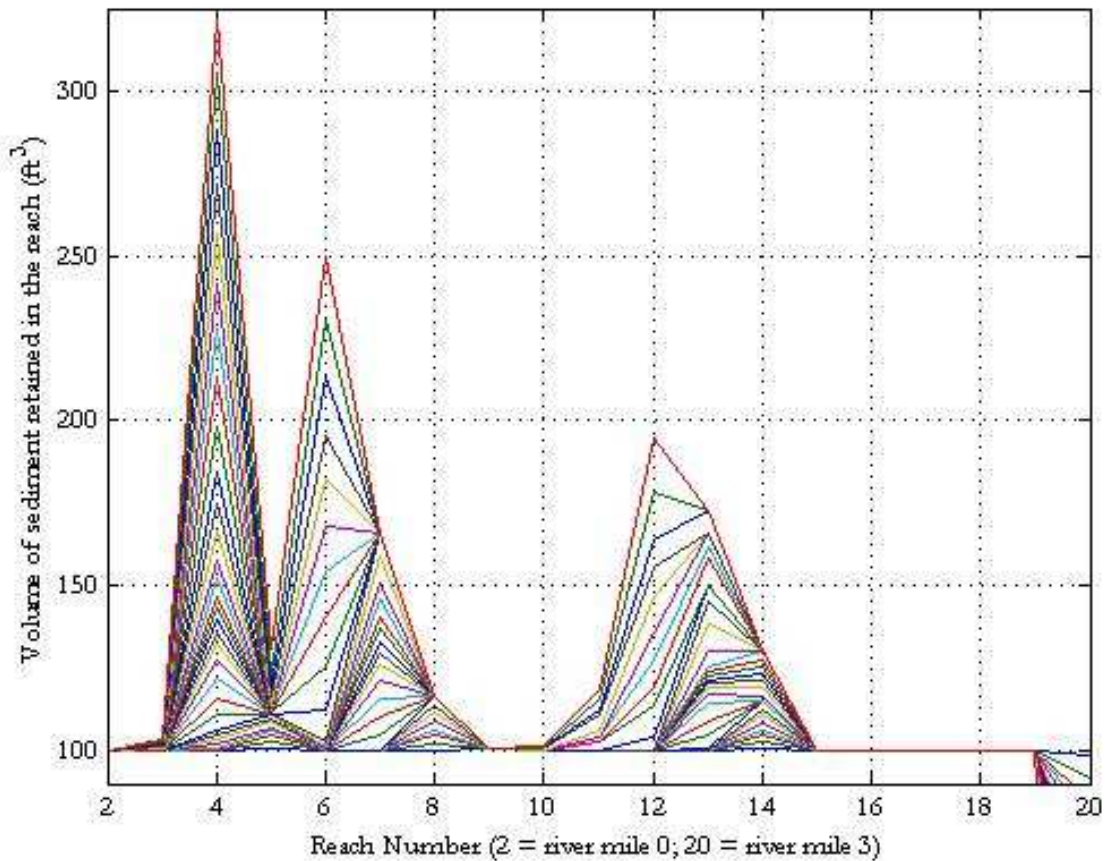


FIGURE 6.22: DEVELOPMENT OF TIDALLY INFLUENCED ZONES OF DEPOSITION OVER TIME, FOR OCTOBER USING AVERAGE DAILY DISCHARGE FOR PERIOD OF RECORD

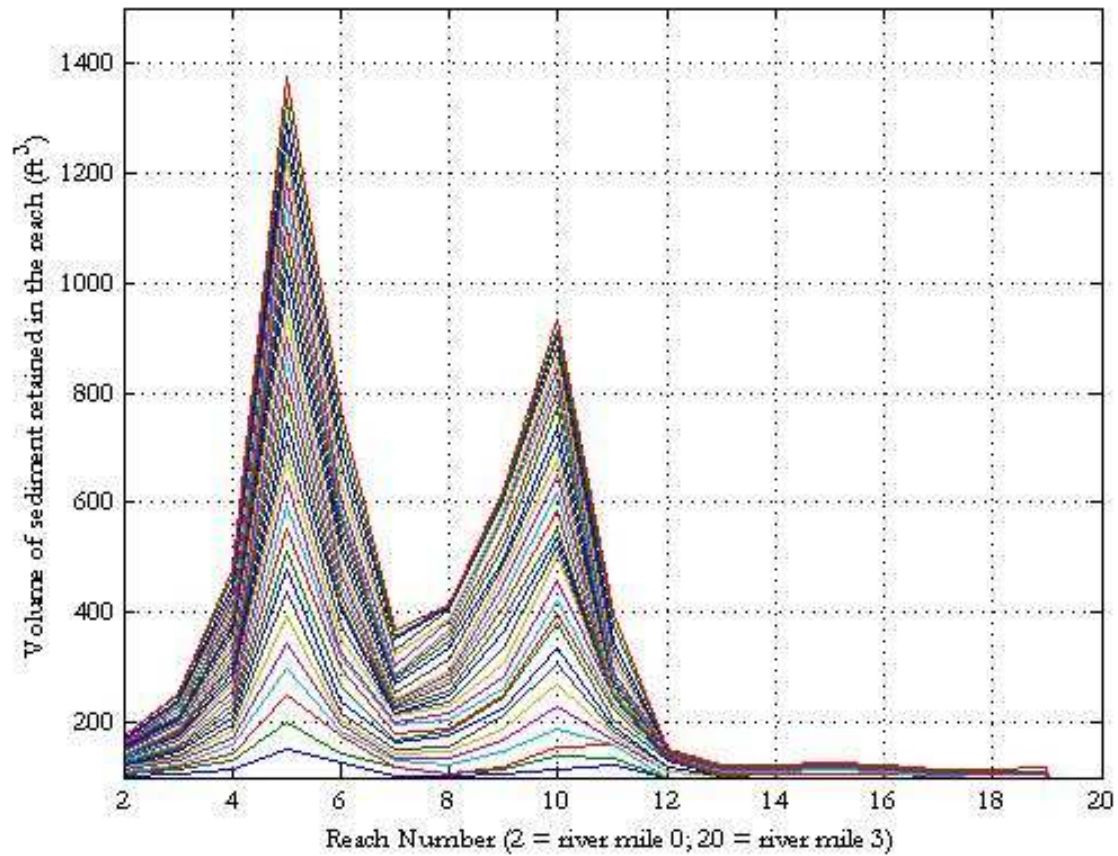


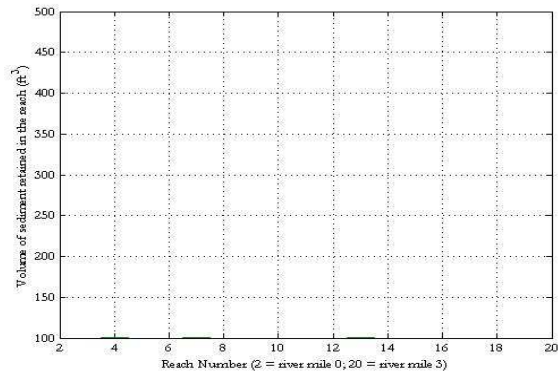
FIGURE 6.23: DEVELOPMENT OF TIDALLY INFLUENCED ZONES OF DEPOSITION OVER TIME, FOR JANUARY USING AVERAGE DAILY DISCHARGE FOR PERIOD OF RECORD

6.2.4 *Bed-load transport criteria comparison and TIMM sensitivity analysis*

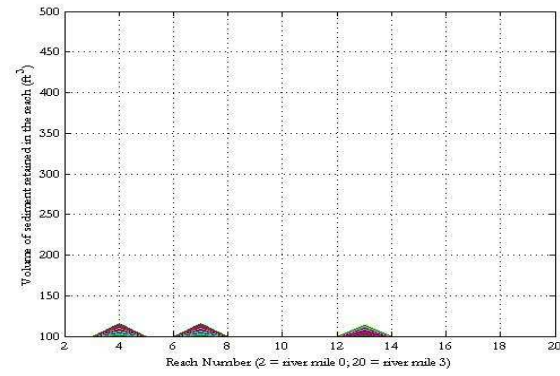
Two types of tests were performed to test the validity of the simulations performed. First, TIMM was modified to use Shields criterion and the previous DuBoys-based simulations were repeated with the new criterion. The objective is to use the critical shear stress method to find out if the relationships found using the tractive force method hold true. Second, TIMM was run for mean particle diameters from 1/8 to 32 mm (3.2 to 1.3 inches, fine sand to coarse gravel). This was done to test how the model performed for smaller and larger mean bed compositions.

Figure 6.24 shows the results of TIMM simulations using constant discharge and the Shields criterion. Differences between the DuBoys method simulations and those of the Shields criterion were related to magnitude of volume retained and length of deposit. However, the overall relationships described earlier using the DuBoys method held true for simulations using Shields criterion. Tidal fluctuations included in bed-load transport modeling using Shields criterion also caused three distinct areas of deposition. Furthermore, these areas of deposition propagate downstream with increases in discharge.

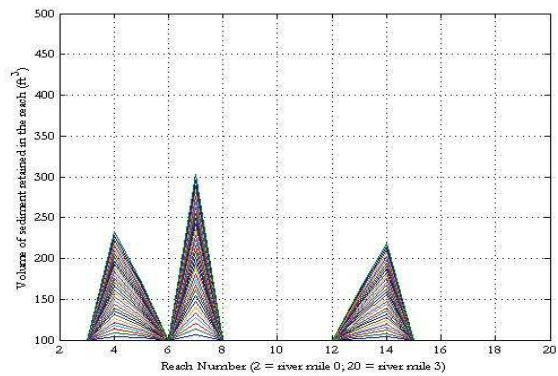
The Shields criterion gave a larger threshold value for bed-load transport than did the DuBoys method. Previously, significant transport of material occurred using mean daily discharge values for September. These values ranged from 53 to 96 cfs (1.5 to 2.7 cms). Using Shields criterion the minimum discharge for significant bed-load transport to occur was 406 cfs (11.5 cms). The higher threshold for bed-load transport led to less visually descriptive graphs for volume retained. The deposits are very symmetrical in nature. Also, the deposits are shorter in length and lack the tail that developed in the simulations involving the DuBoys method. This implies that there is a greater sensitivity to loss of transport capacity when using the Shields criterion. Finally, the reach where the most volume was retained during river discharge at a constant 500 cfs using the Shields criterion is less than that of 398 cfs (11.3 cms, using DuBoys method (see Figures 6.15 and 6.24 (d)).



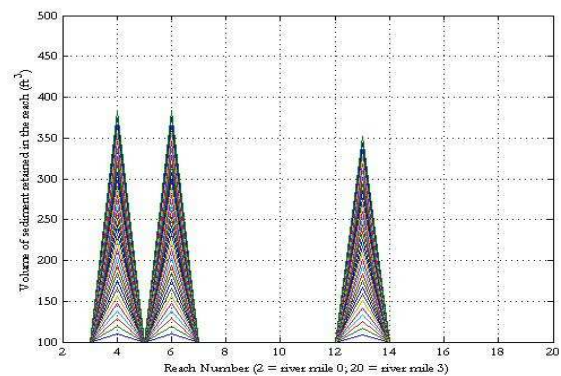
(a) constant 406 cfs



(b) constant 410 cfs



(c) constant 400 cfs

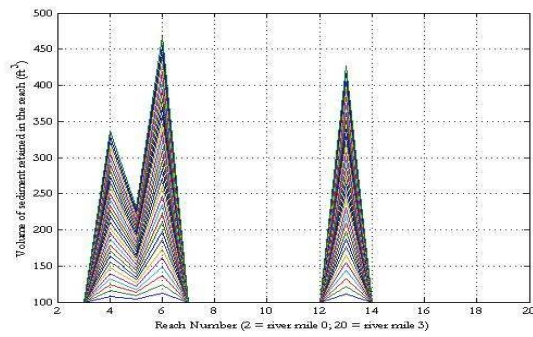


(d) constant 500 cfs

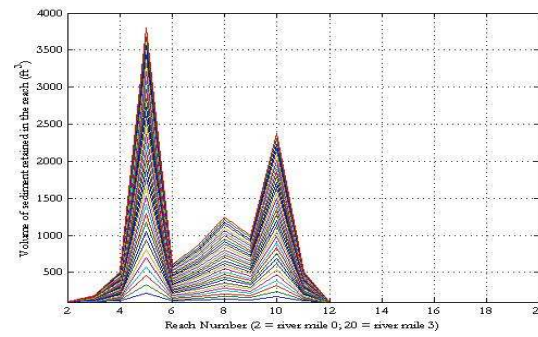
FIGURE 6.24: DEVELOPMENT OF TIDALLY INFLUENCED ZONES OF DEPOSITION OVER TIME, FOR A PERIOD OF 90 DAYS USING SHIELDS CRITERION AND CONSTANT RIVER DISCHARGE

Executions of the TIMM model using Shields criterion and variation of discharge lead to the same relationships between bed shear stress, channel velocity, rate of bed-load transport and volume retained within a reach. Figure 6.25 shows simulations using mean daily discharge values for the months of November, December, and January. November was the first month where mean daily discharge was great enough to produce results for bed-load transport and deposition. The month of bed-load initiation was September for runs using DuBoys method. Despite differences in threshold for transport, simulations using Shields criterion showed distinct areas of deposition according to tidal condition at moderate flow. As flow increased during the months of December and January, the downstream shift of the distinct deposition zones caused merging of the three zones into a single depositional zone. Moreover, just as was shown for DuBoys method, bed-load transport estimated using Shields method show that the location of the zone of deposition is not sensitive to changes in water discharge for lower tidal levels, but is sensitive to changes in water discharge for higher tidal levels. Mean daily discharge values for December values are higher than discharge values for January.

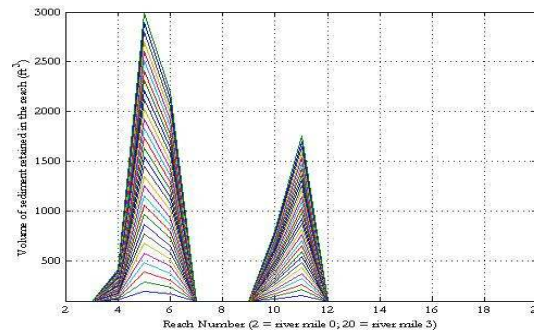
The varied-discharge version of TIMM with January mean daily discharge for the period of record was simulated multiple times using increasingly larger mean sediment size. The range in values was from 1/8 to 60 mm (3.2 to 2.4 inches). Figure 6.26 shows the results of the simulations. From the results, it can be concluded that changes in sediment size do nothing to alter the relationships described by the model. The only difference between the subplots of Figure 6.26 is the upper limit on the y-axis. That is, for smaller sediment size, more sediment can be transported and retained; however, the location of depositional areas remains constant. Therefore, my analysis using mean particle diameter of 7.9 mm (0.3 inches, from site 4 of the Kilchis River particle size analysis) is adequate for describing transport with tidal influence. A more complex method for describing and estimating bed-load transport with tidal influence could take into account a non-prismatic channel with a mixed bed of sediment. This would lead to additional provisions being necessary. For example, the changes to bed-load caused by particle hiding effects, lateral erosion, and complex bed geometry would have to be included in the analysis.



(a) using values for November

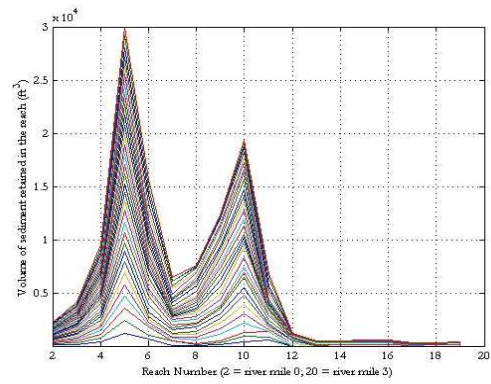


(b) Using values for December

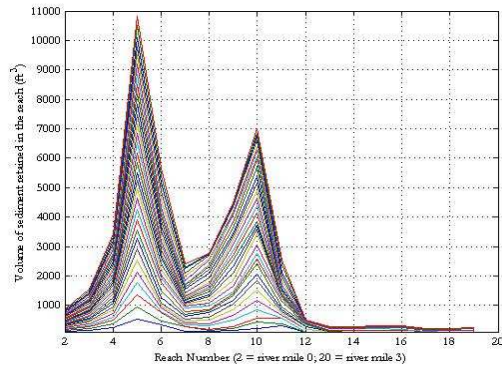


(c) Using values for January

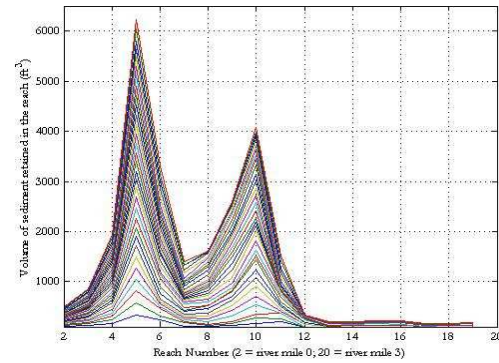
FIGURE 6.25: DEVELOPMENT OF TIDALLY INFLUENCED ZONES OF DEPOSITION OVER TIME, FOR A PERIOD OF 90 DAYS USING SHIELDS CRITERION AND VARIED RIVER DISCHARGE (CFS)



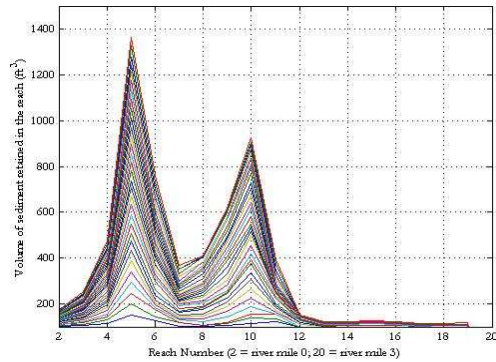
(a) 1/8 mm mean particle diameter



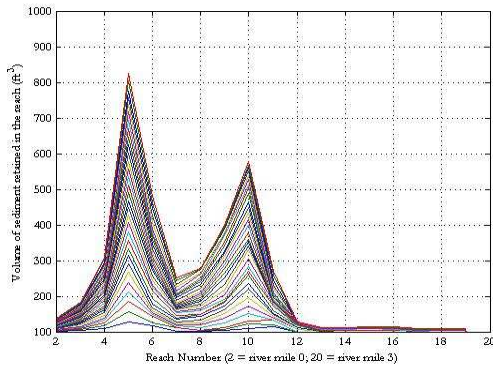
(b) 1/2 mm mean particle diameter



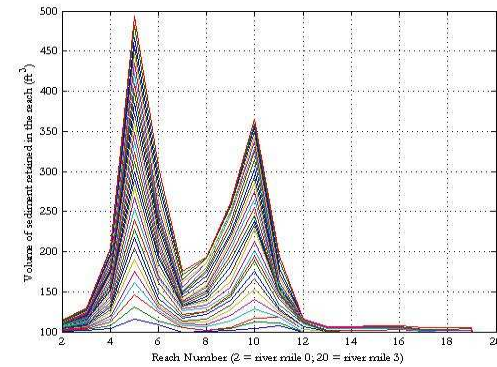
(c) 1 mm mean particle diameter



(d) 8 mm mean particle diameter



(e) 16 mm mean particle diameter



(f) 32 mm mean particle diameter

FIGURE 6.26: DEVELOPMENT OF TIDALLY INFLUENCED ZONES OF DEPOSITION OVER TIME, FOR JANUARY USING AVERAGE DAILY DISCHARGE FOR PERIOD OF RECORD

6.3 GSTARS 2.1 simulation results

Three GSTARS 2.1 simulations of the full length of the simplified Kilchis River were performed. The first simulation was run using the mean sediment size of site 4 obtained from the bulk sampling analysis of the Kilchis River (7.9 mm or 0.3 in). The bed along the entire length of the river (zones 1-8) was set at 7.9 mm and the incoming sediment from tributaries was set at 7.9 mm as well. For the second and third simulations, bed material in zones 2-8 were mixed, with a d_{50} of 7.9 mm (the same as the first simulation). For the second simulation, zone 1 and the incoming sediment had a particle distribution that was finer than the bed material. The third simulation was performed using a mixed bed that was skewed toward larger sizes in zone 1. For this third simulation, incoming sediment was set at the particle distribution of zone 1.

The results of simulation 1 are shown in Figure 6.27. Reach 21 was assumed to have a channel slope approaching horizontal. To account for this, the slope was forced to 0.0001 for that reach. Consequently, the flattening of slope over a relatively short length of channel caused increased rates of transport in this area. Although exaggerated at reach 21, the results show an area of erosion followed by an area of deposition near the mouth of the river. Without tidal influence, the area of erosion increases upstream with increasing magnitudes for streamflow. In addition, for large magnitudes of streamflow, the depositional area is shown to shift to areas within the bay. Overall, the results of the 8-zone simulations without consideration of tidal influence were inconsistent with the results from the TIMM model. This implies a need to incorporate the influence of tide in sediment transport modeling in order to obtain the most physically accurate representation of transport processes.

The results of simulations 2 and 3, where incoming sediment is finer and coarser than the mixed bed, are shown in Figures 6.28 and 6.29, respectively. The mixture of particle sizes lead to a reduction in the area of erosion at the downstream end;

however, the basic processes that operate were unaltered. There was an observable shift of the upstream zone of deposition according to type of incoming sediment (See Figures 6.28d and 2.29d). This might indicate deposition of large particles, where the coarser the incoming sediment, the sooner the deposition of larger particles occurs.

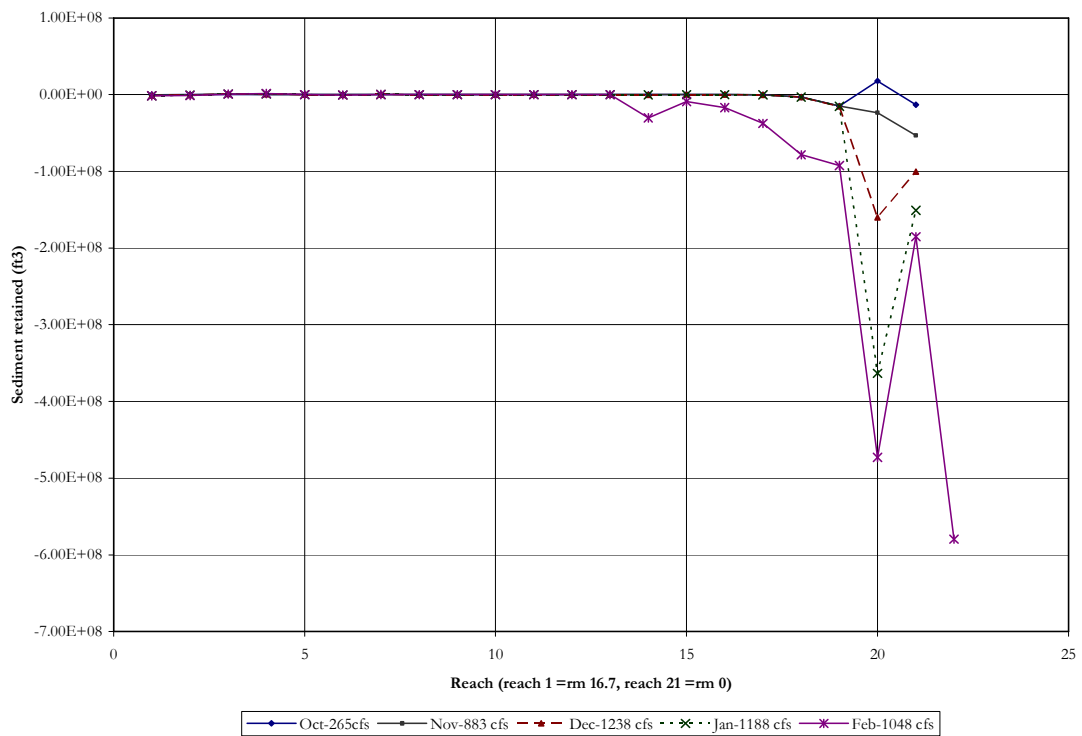
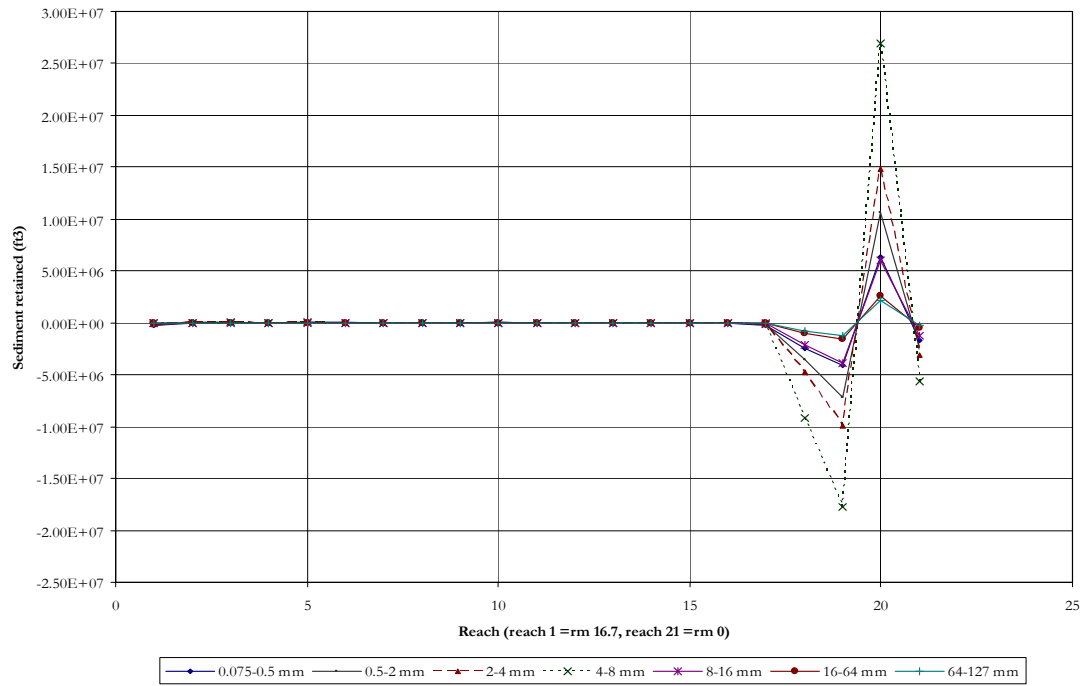
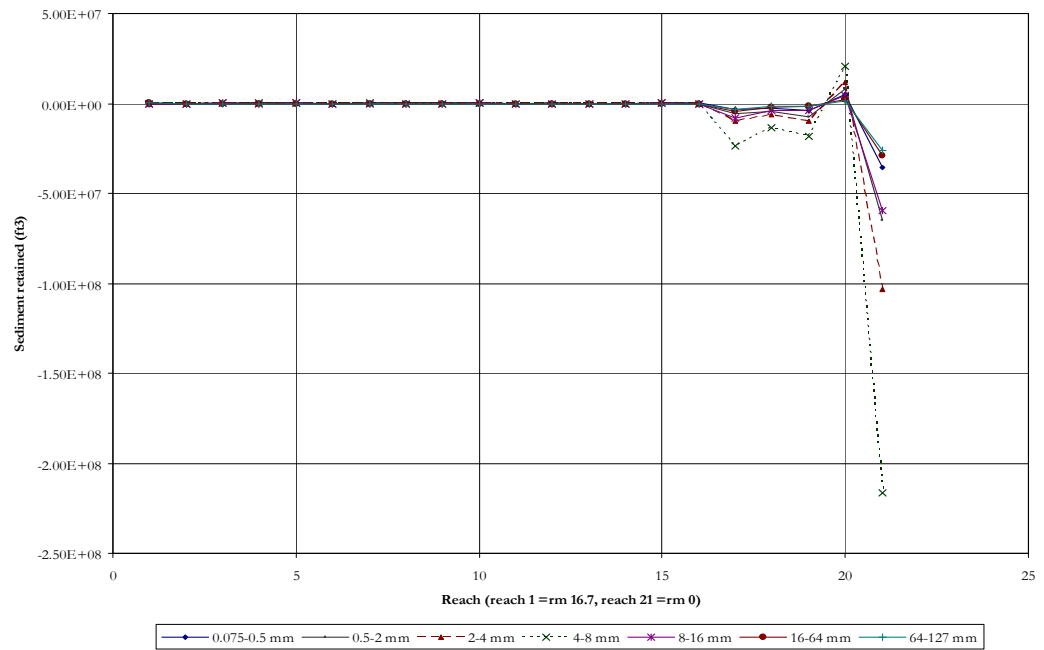


FIGURE 6.27: SIMULATION 1 OF GSTARS 2.1 (5 MONTHS WITH UNIFORM BED)

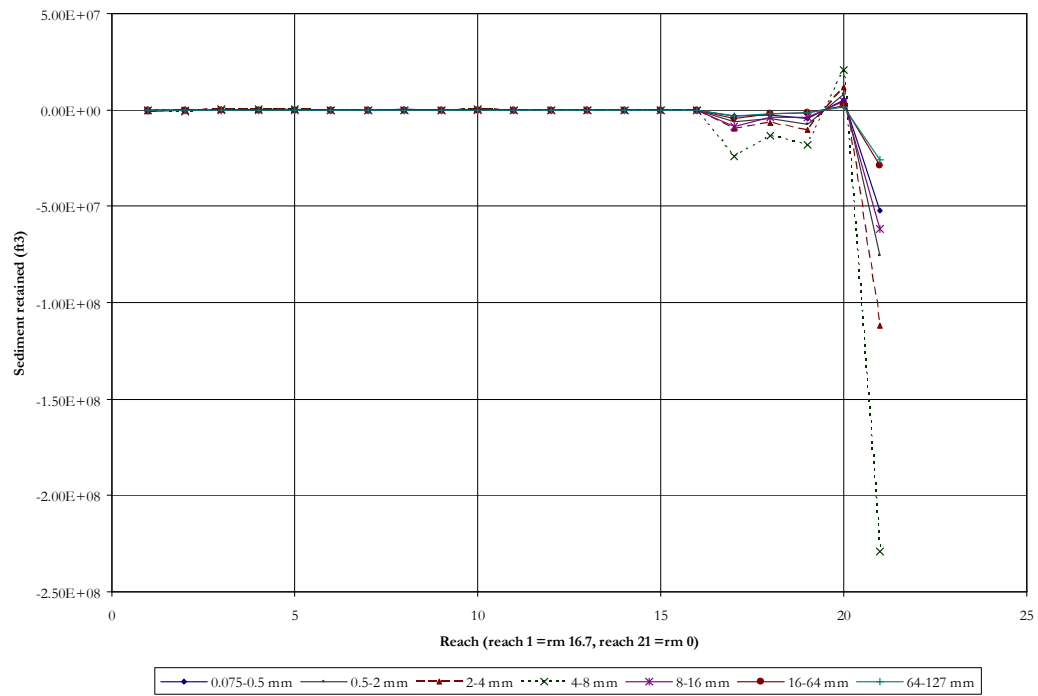


(a) Oct

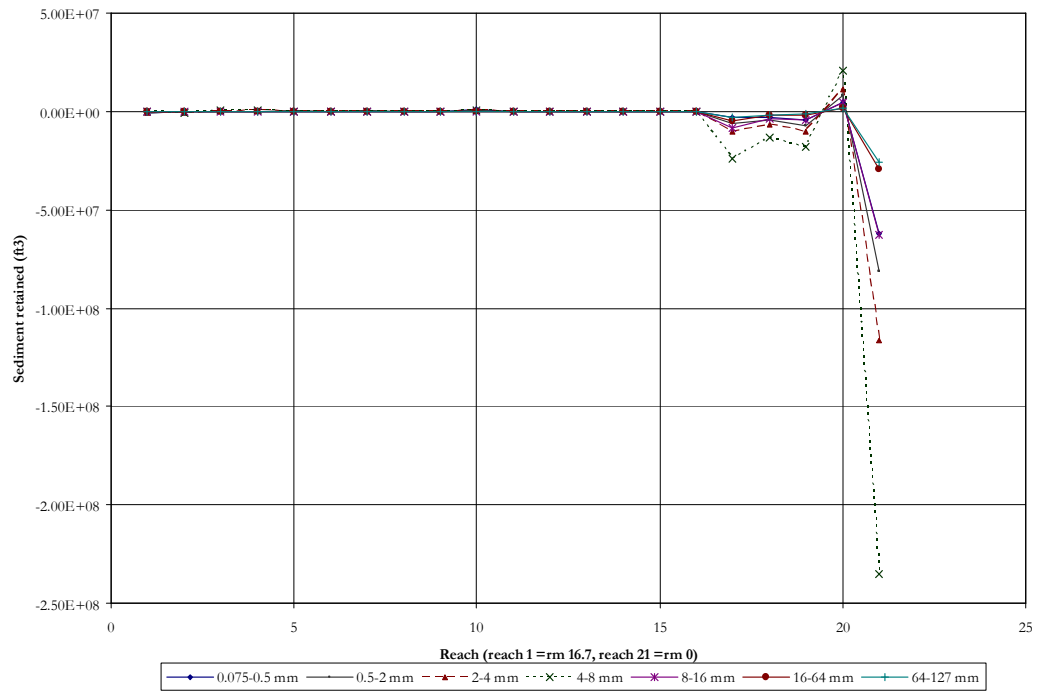


(b) Oct - Nov

FIGURE 6.28: DEVELOPMENT OF TIDALLY INFLUENCED ZONES OF DEPOSITION OVER TIME, USING AVERAGE MONTHLY DISCHARGE AND A MIXED BED WITH INCOMING SEDIMENT OF FINER DISTRIBUTION THAN BED (SIMULATION 2)

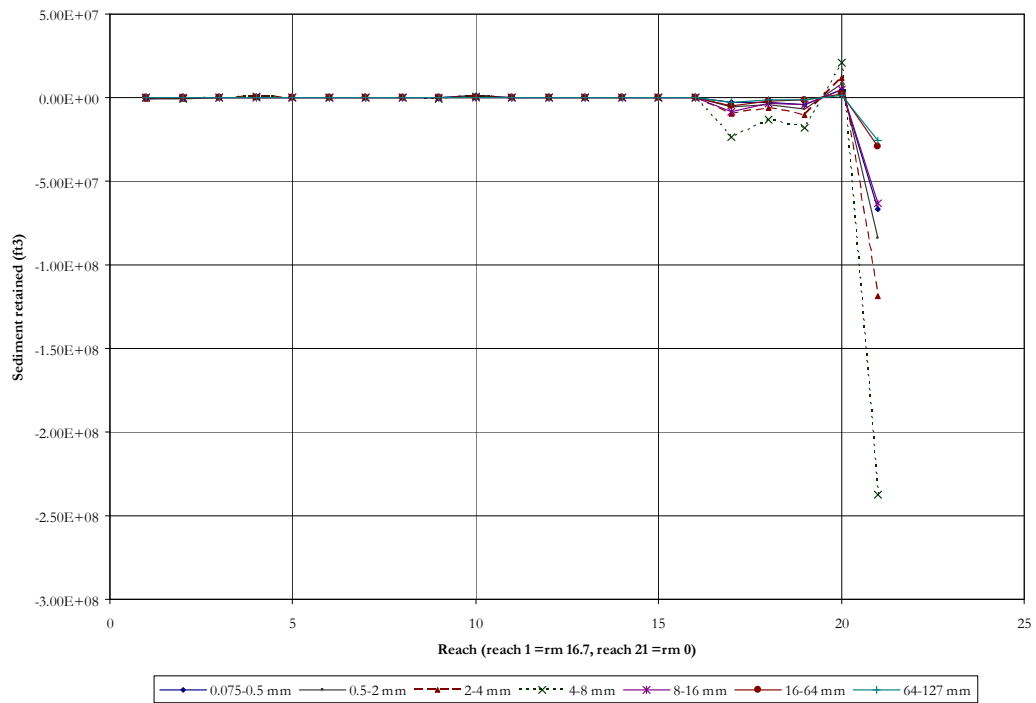


(c) Oct - Dec



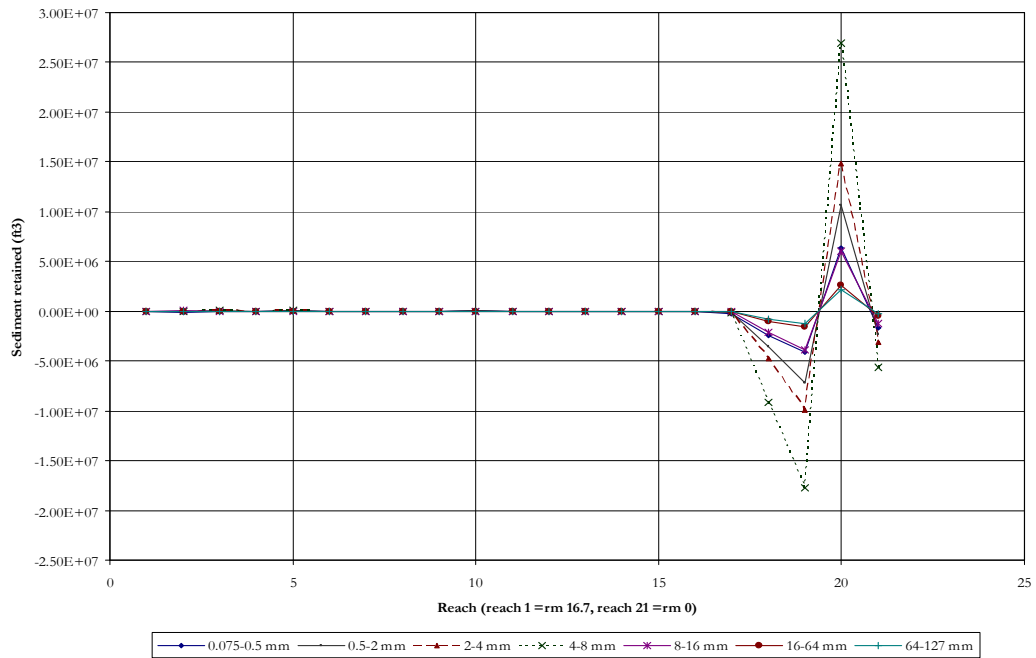
(d) Oct - Jan

FIGURE 6.28: CONT'D

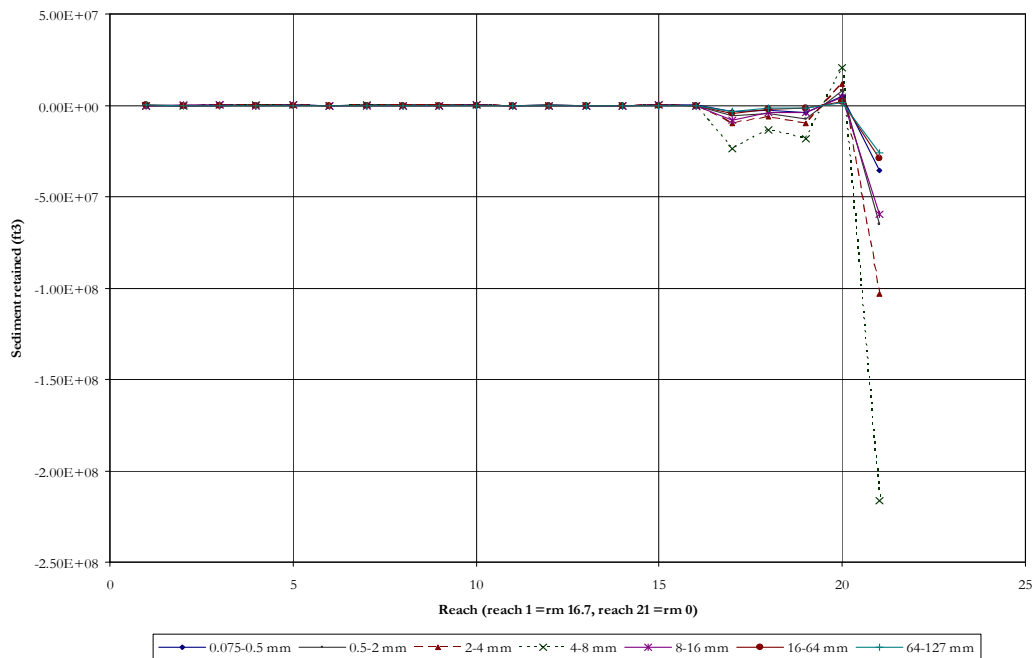


(e) Oct - Feb

FIGURE 6.28: CONT'D

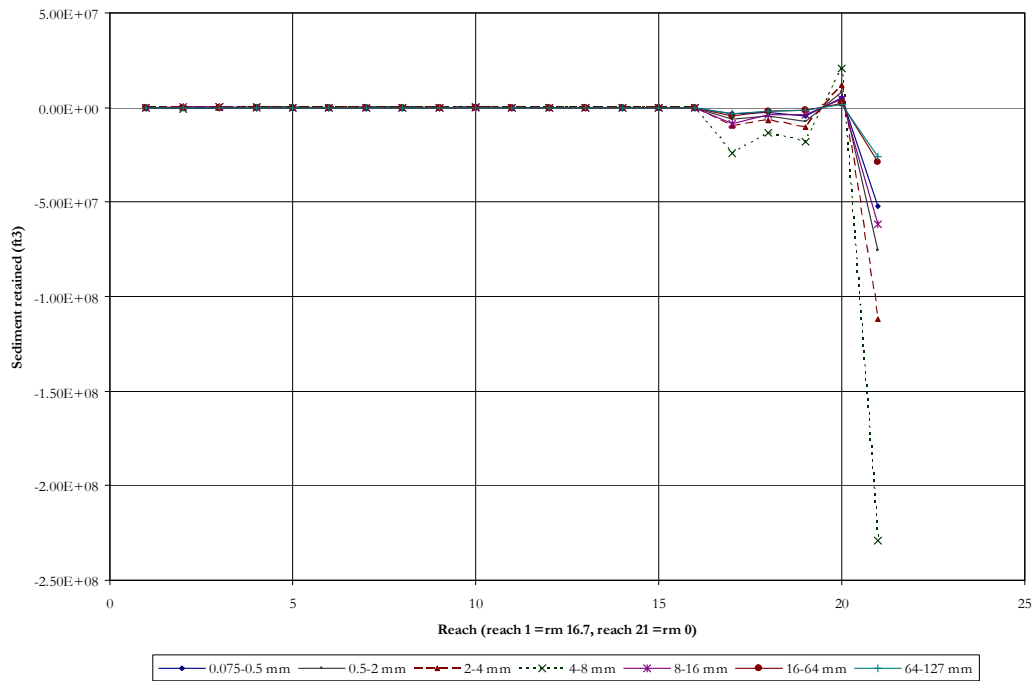


(a) Oct

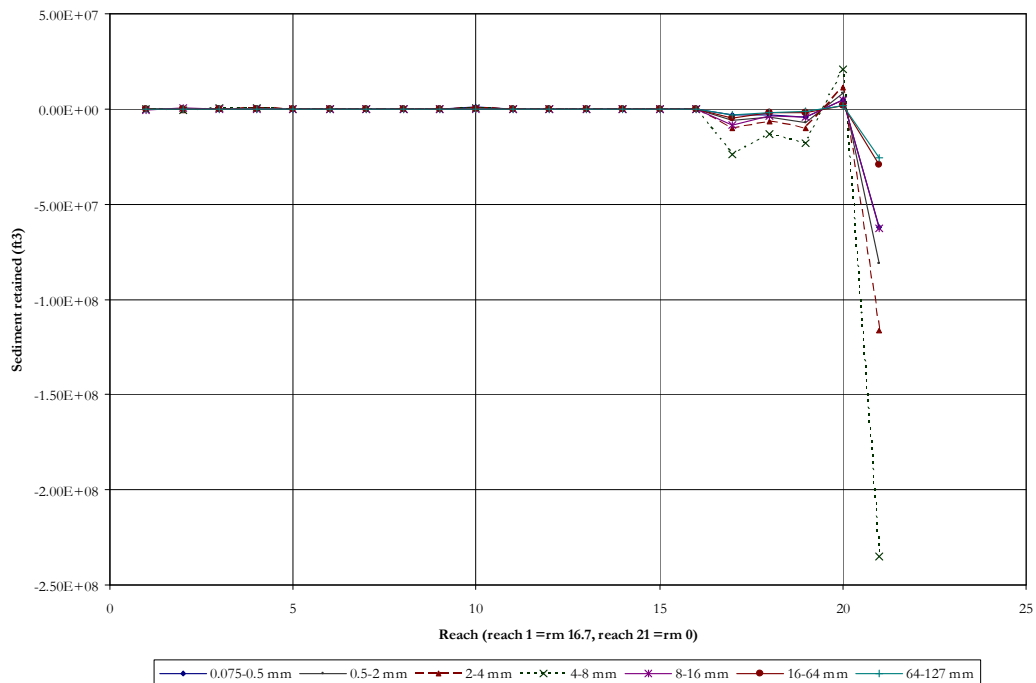


(b) Oct - Nov

FIGURE 6.29: DEVELOPMENT OF TIDALLY INFLUENCED ZONES OF DEPOSITION OVER TIME, USING AVERAGE MONTHLY DISCHARGE AND A MIXED BED WITH INCOMING SEDIMENT OF COARSER DISTRIBUTION THAN BED (SIMULATION 3)

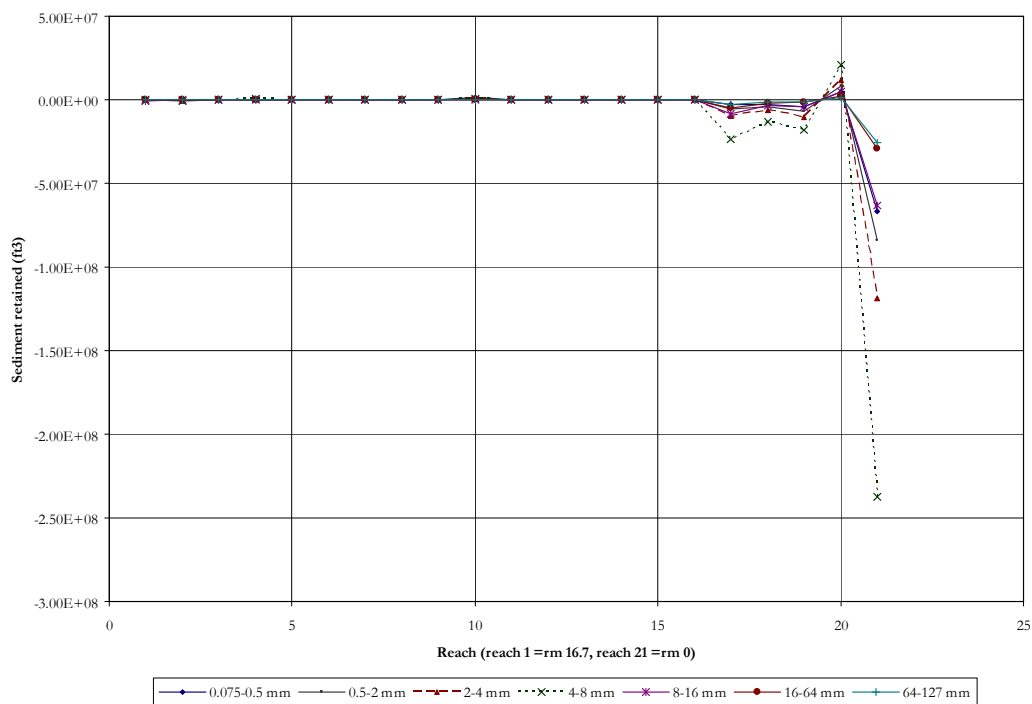


(c) Oct - Dec



(d) Oct - Jan

FIGURE 6.29: CONT'D



(e) Oct - Feb

FIGURE 6.29: CONT'D

Simulations (runs 4-6), which were performed to analyze tidal influence, showed results similar to the MATLAB simulations. A significant amount of deposition occurs within the zone of tidal influence instead of solely at the mouth of the river. Figure 6.30 shows the results of the uniform bed run (simulation 4) where tidal influence is taken into account. For the uniform bed run, tidal influence on transport appears to begin at reach number 5 (as labeled on the x-axis of the figures), which corresponds to reach number 17 of the 8-zone run. This reach is at river mile 3.3 and matches with the limit of tidal influence reported for the actual Kilchis River as well as the limit of tidal influence analyzed using the TIMM model. To get an even clearer picture of the zone of tidal influence for the simplified Kilchis River, the water surface fluctuations by hour would have to be analyzed. Although the model was run on a one-hour time step to simulate tidal fluctuations, model output was given for each month. Monthly accumulations were used because hourly output caused the model to stall prior to completion of the simulation.

GSTARS 2.1 was run twice to analyze tidal influence with a mixed bed of the same mean diameter as simulation 4 (7.9 mm or 0.3 in) and two types of incoming sediment distribution, finer (simulation 5) and coarser (simulation 6) than the mixed bed, respectively.

Results for simulations 5 and 6 were also comparable to the MATLAB simulations, where significant deposition occurs in the lower reaches (see Figures 6.31 and 6.32). Unlike the uniform bed run, the mixed bed runs show deposition to occur farther upstream than river mile 3.3 (2 km). At increased magnitudes of discharge, both simulations show accumulation of an observable amount of sediment at reach 2, particularly for sizes in the range 8 to 16 mm (0.3 to 0.6 in).

Sediment sizes much coarser than the mean (64-127 mm or 2.5-5 in) showed less accumulation despite the particle distribution of the incoming sediment. For both the finer and coarser incoming sediment distributions, as the months progressed, very large particles still did not show a noticeable increase in overall

deposition downstream. However, the run for finer incoming sediment showed erosion of particle sizes in the size range of 2-8 mm (0.08-0.3 in) starting at reach 2 and changing to deposition at reach 4. The transport of fine particles through the system might be attributed to selective transport and the subsequent deposition might be due to tidal influence on the downstream fining trend.

Transport results for sediment sizes much smaller than the mean (0.075-0.5 mm or 0.003-0.02 in) gave further insight into the mechanism of selective sorting of bed material. Deposition of very fine sediment did not take place until reach 8, the same location where accumulations became noticeable for all sediment sizes. Therefore, due to the small size of the particles once transported, these particles do not deposit until a significant change in stream power occurs. Here the change could have been caused by the decreasing slope, widening channel, or tidal influence.

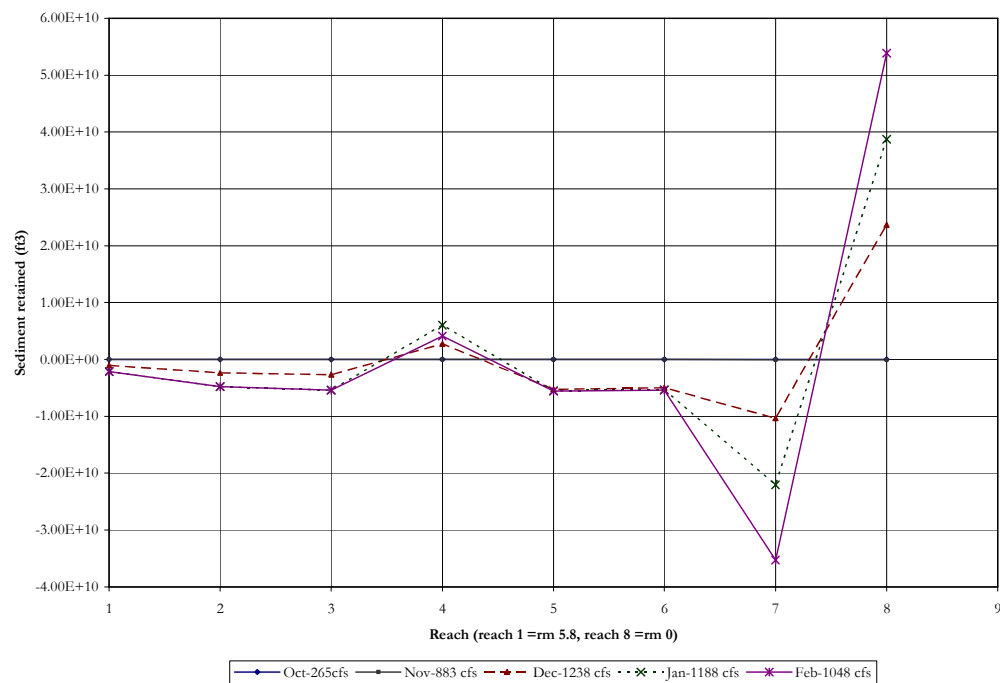
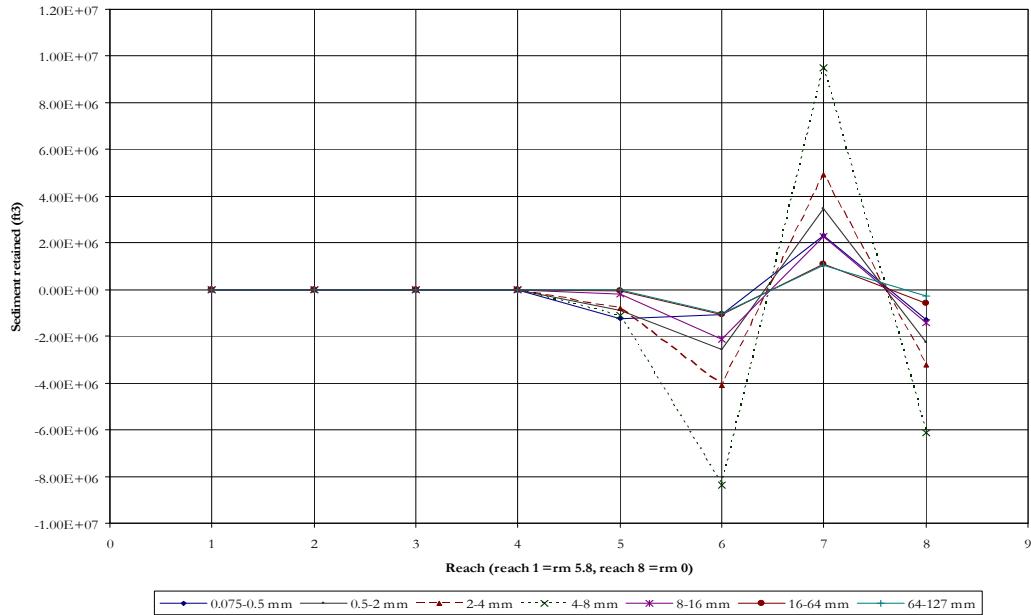
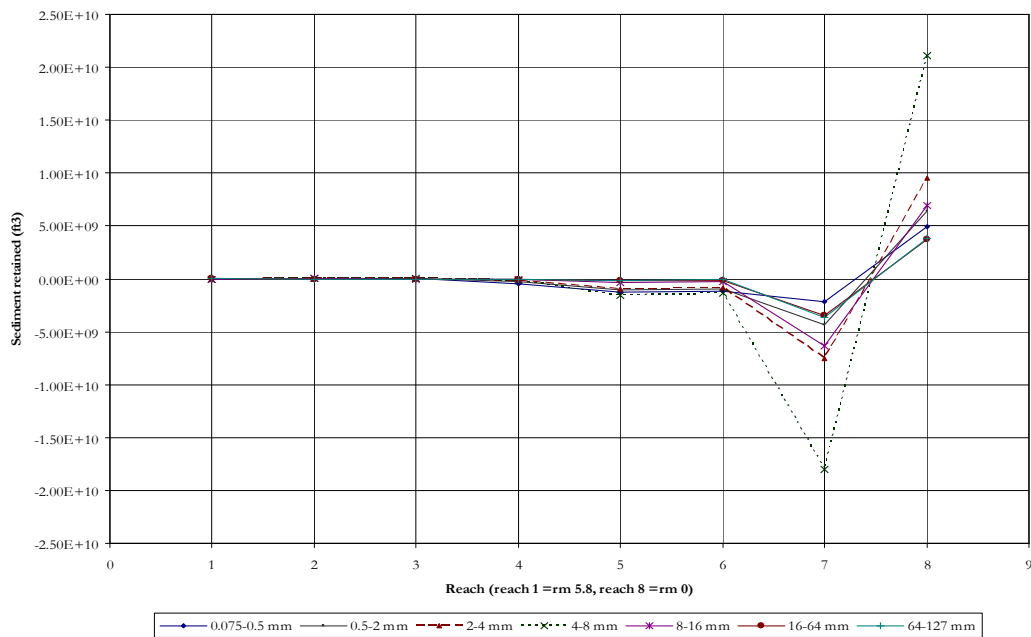


FIGURE 6.30: SIMULATION 4 OF GSTARS 2.1 (5 MONTHS WITH UNIFORM BED)

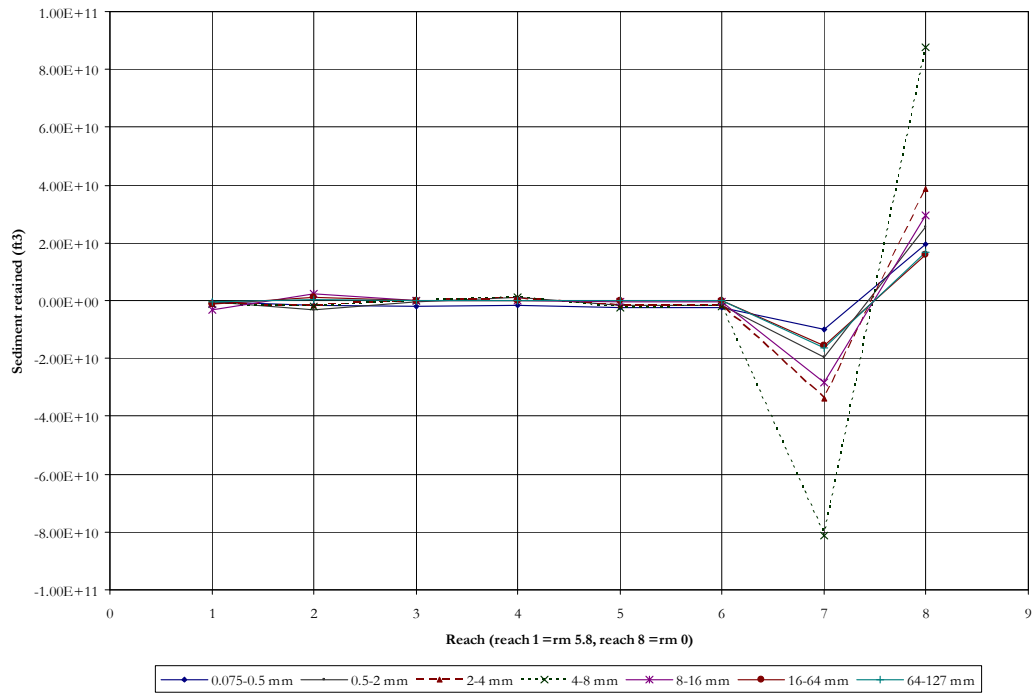


(a) Oct

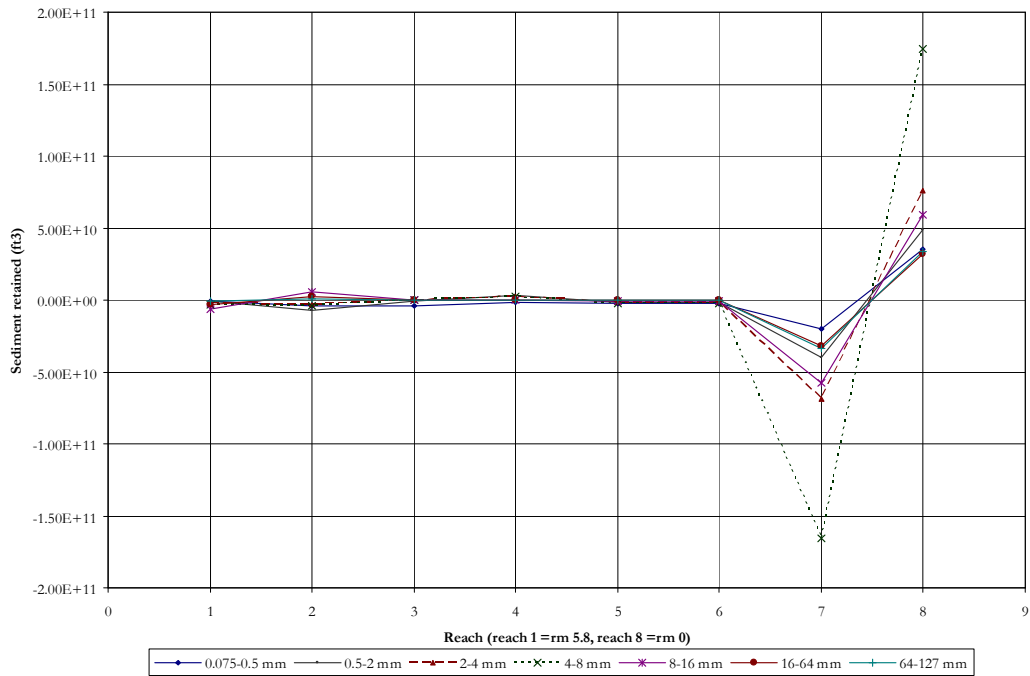


(b) Oct - Nov

FIGURE 6.31: DEVELOPMENT OF TIDALLY INFLUENCED ZONES OF DEPOSITION OVER TIME, USING AVERAGE MONTHLY DISCHARGE AND A MIXED BED WITH INCOMING SEDIMENT OF FINER DISTRIBUTION THAN BED (SIMULATION 5)

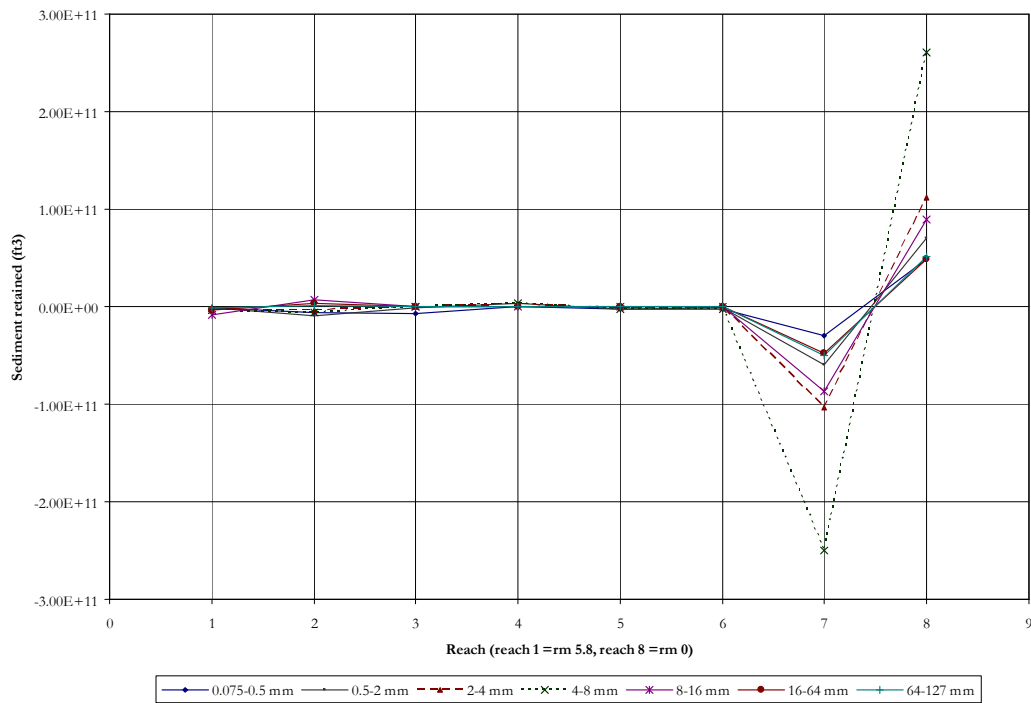


(c) Oct - Dec



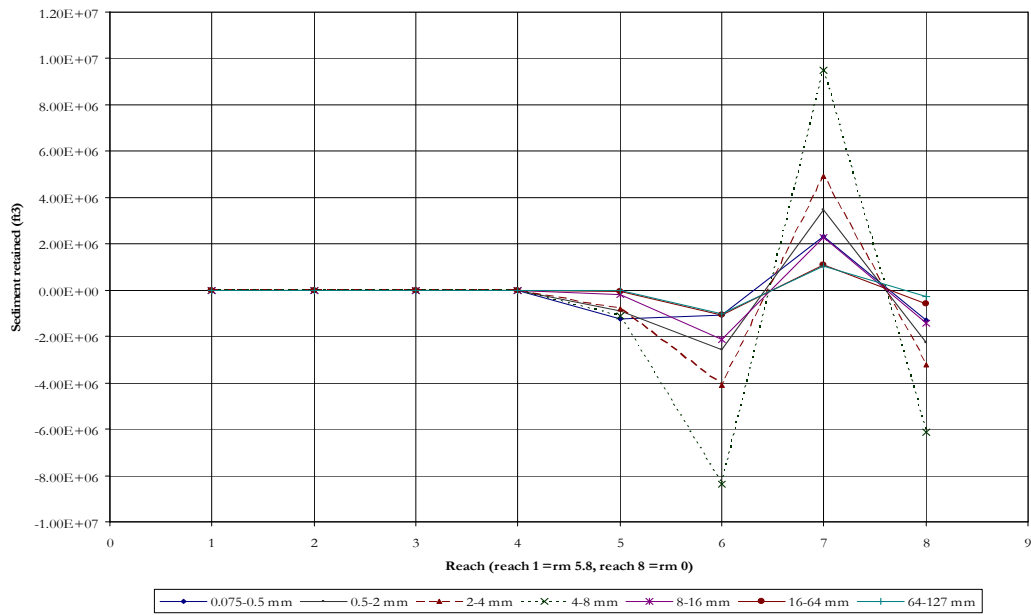
(d) Oct - Jan

FIGURE 6.31: CONT'D

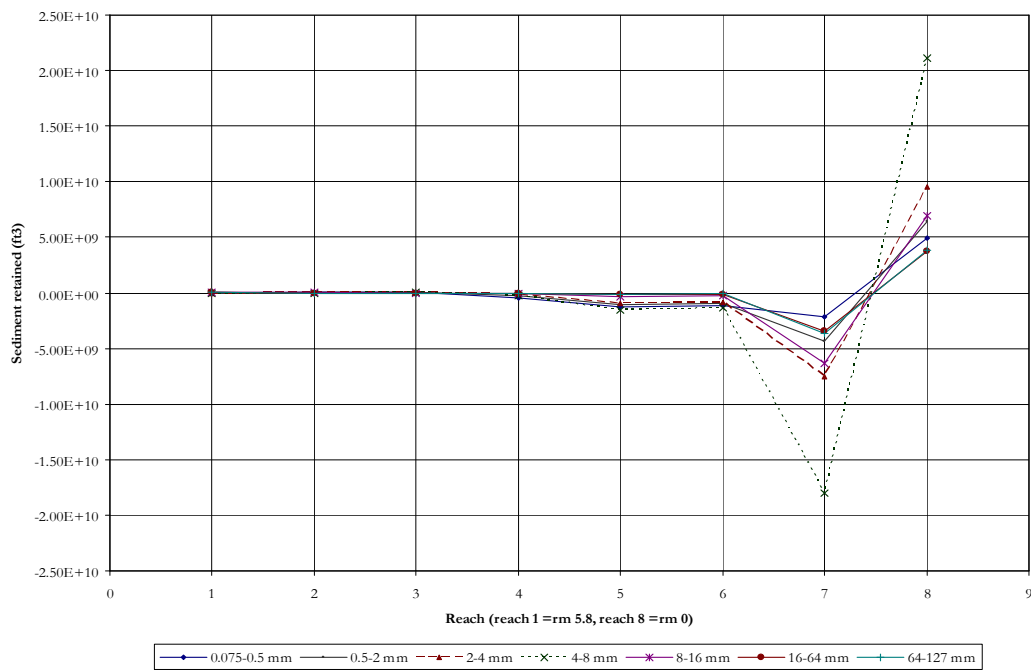


(e) Oct - Feb

FIGURE 6.31: CONT'D

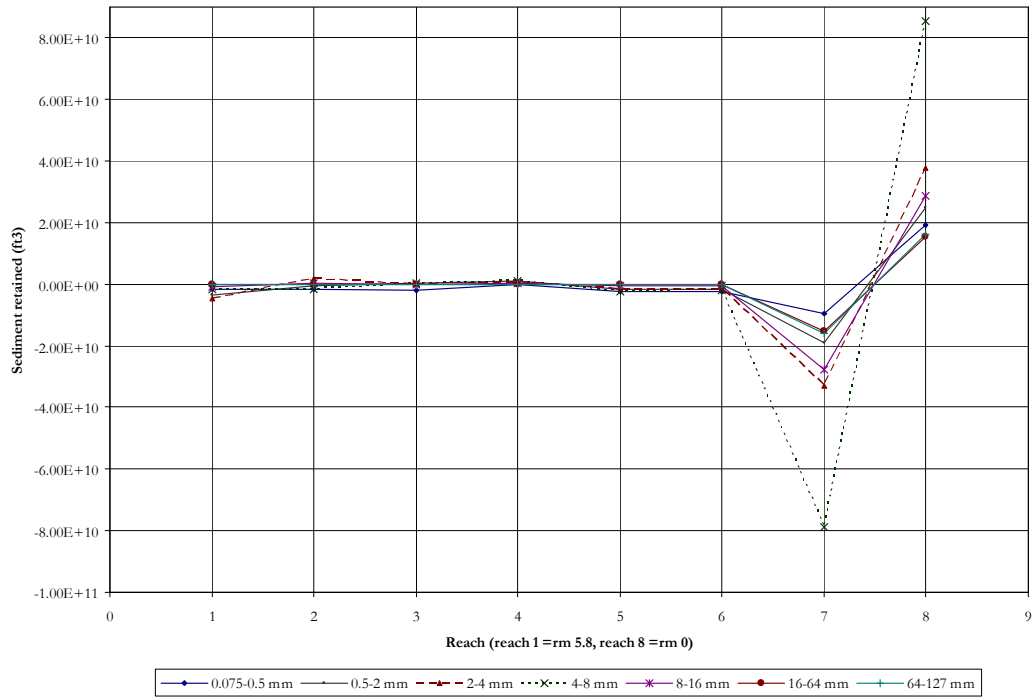


(a) Oct

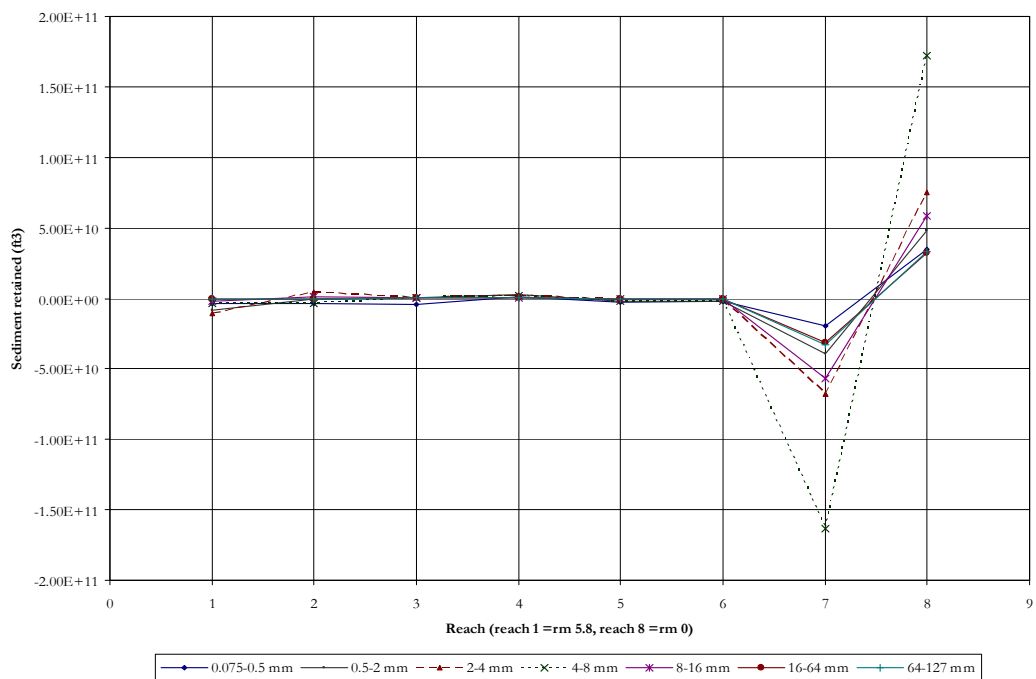


(b) Oct - Nov

FIGURE 6.32: VOLUME OF SEDIMENT RETAINED WITHIN A REACH USING AVERAGE MONTHLY DISCHARGE AND A MIXED BED WITH INCOMING SEDIMENT OF COARSER DISTRIBUTION THAN BED (SIMULATION 6)

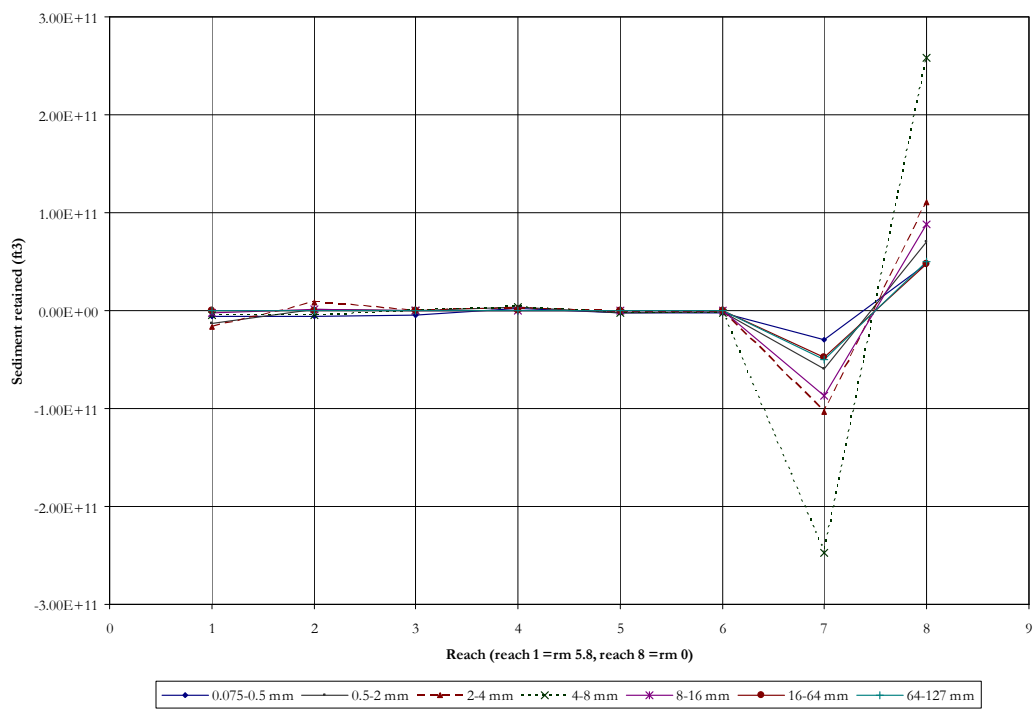


(c) Oct - Dec



(d) Oct - Jan

FIGURE 6.32: CONT'D



(e) Oct - Feb

FIGURE 6.32: CONT'D

7 Summary and Conclusion

From previous investigations, it appears that both generally accepted mechanisms explaining downstream fining - - abrasion and sorting - - operate to maintain the stability of the downstream fining phenomenon. From this research, it can be concluded that selective transport is the dominant mechanism operating in the studied gravel-bed rivers in Western Oregon. As noted in Chapter 6, diminution coefficients are not comparable to those reported by Kodama (0.089 km^{-1} or 0.14 mi^{-1}) in his laboratory tumbling study of abrasion-dominated fining. However, the Kilchis River results are within range for the coefficients estimated in sorting-dominated fining studies as reported by Shaw and Kellerhals (0.001 to 0.05 km^{-1} or $0.001 - 0.08 \text{ mi}^{-1}$, 1982) and Seal and Paola (1 km^{-1} or 1.6 mi^{-1} , 1995).

The photo frame sampling method used for the other four rivers in the Tillamook Basin (Miami, Wilson, Trask, and Tillamook Rivers) also resulted in diminution coefficients within the range reported by Shaw and Kellerhals. The results for the photo frame analysis were 0.02 , 0.03 , and 0.04 km^{-1} (0.03 , 0.05 , 0.06 mi^{-2}) for the Miami, Wilson, and Trask Rivers, respectively. Regardless of differences in the particular value of the diminution coefficients, each analysis showed a decrease in mean sediment size. Significance testing of the diminution coefficients resulted in rejection of the null hypothesis for all but the Miami River.

The Sternberg exponential relationship (1875) for decreases in mean particle size worked well, for the Tillamook Basin rivers; however, alternative versions may be appropriate given channel conditions. For example, the number of significant lateral inputs of sediment to the Willamette River caused scatter in the particle size data. Therefore, data for the analysis of the Willamette River (Klingeman 1981) had scatter such that a linear relationship was more useful than an exponential relationship. This verifies Rice's (1999) results for rivers that have short sedimentary links.

As suggested by past research, linking disruptions in the fining trend to disturbances such as landslide activity can be difficult due to the large number of possible sources of disruptions. Moreover, as a side effect of sorting incoming material, the downstream fining trend may be unimpeded regardless of human impacts, because of the large amount of available material derived from natural disturbances. For example, the available material found in the upper reaches of the Miami River are shown in Figure 7.1 and indicate the large amount of material waiting to be sorted.



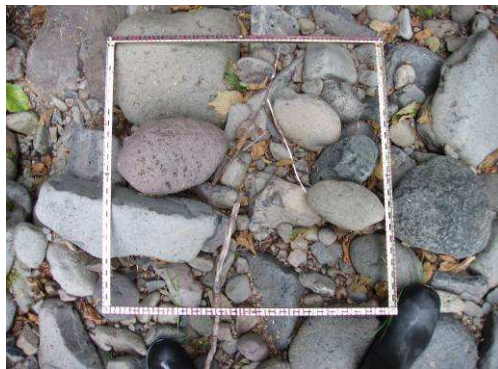
(a) Miami river site 1 bar



(b) lateral extent of site 1 bar



(c) ephemeral channel feeding site 1



(d) typical particle sizes of bar 1

FIGURE 7.1: MIAMI RIVER SITE 1

Overall, a major finding resulting from analysis of the Tillamook Basin and Willamette River sites is that downstream fining can be disrupted briefly due to human disturbance; however, the disruption is highly transitory. Farther downstream, the fining trend is repeated through the same mechanisms as long as there is a supply of material to be sorted. The distance necessary for a complete conversion back to pre-disturbance conditions is a subject for future investigation. Nevertheless, one could assume that site conditions such as sediment distribution, channel slope, streamflow, and degree of disturbance are factors to be considered.

Site 5 on the Kilchis River was an example of how downstream fining studies can show disruptions. The armor layer of Site 5 reflected materials deposited from upstream during bank-full and lower water stages as well as material introduced from local eroding banks. Verification of the above is supported by the continuation of the downstream fining trend in the sub-armor layer, which is not subjected to the surface introduction of bank material.

Sampling methods are very important when using a downstream fining study to extract information regarding the history of disturbance. Considerations include type of bar, location of bars to be sampled, on-bar locations of sampling points, and collection method. The great variability in size of material across any single bar was a factor to consider in the photo frame sampling. Furthermore, the locations of bars are vital because one can expect a larger variation in size of material if bars are located in areas where flow is presently directed. With regard to sampling techniques, bulk sampling lead to more accurate data even though fewer sampling points were chosen. The more accurate methodology, showed a much higher value for the downstream fining coefficient. It could then be concluded that rates of downstream fining are sensitive to the method used to determine the decrease in sediment size. For bulk sampling, one may want to expand the number of sampling points that I used to be sure to more accurately portray over-wash areas as well as upstream, downstream, and center-of-bar particle size variation.

For the Tillamook Basin study, the geologic history of each river watershed was similar. However, specific gravity can be a very important property in determining whether abrasion is an important mechanism in downstream fining processes. If a system has geologic characteristics that imply that abrasion may be an important factor (e.g., erosive material such as sandstone) yet the specific gravities of particles found in the channel are not comparable to the geologic history, one can conclude that a more in-depth study is necessary to describe fining in that system. For such systems, downstream fining studies should first involve a characterization of the particles present in the system. This allows the researcher to perform the downstream fining study of the highly erosive portion of the system separately from the less erosive bed material.

Variation in values for specific gravity longitudinally and by size class of material can be an indicator of origin and type of deposit. If values for specific gravity do not change at a site based on particle size, bar material at that site might be dominated by fluvial deposits of durable material from upstream. If values of specific gravity increase with decreasing particle size, one might expect introduction of less-durable material has occurred due to landslide activity or erosion. If values of specific gravity decrease with decreasing particle size then one can expect an unmodified downstream fining pattern, that is, there exists a wide range of durable clasts deposited from upstream.

Characterization of tidal influence on bed-load transport was achieved using TIMM and verified using GSTARS 2.1. During periods of bed-load movement, tidal influence can be seen as a natural form of downstream control, as the effects on the flow characteristics are measurable. Sediment transport processes are affected by the tide, leading to reduced velocities in lower reaches - - especially during periods of low flow and high tide. Separated into phases (low tide, intermediate tide, and high tide), the effects of tide are to cause a propagating depositional zone due to the reduction of velocity. The simulated river showed movement of the depositional zone throughout the day, leading to distinct peaks of volume of sediment retained

associated with each tide level. When large river discharge was modeled, the propagation of the depositional zone due to riverine forces was more pronounced such that peaks converged due to shifting downstream. Coalescence of the intermediate-tide-related peak with that of the low-tide-related peak volume of sediment retained occurred. This means, at larger river discharges, modeled tidal effects were less significant as a mechanism for reducing stream power.

GSTARS 2.1 results showed that exclusion of measures used to incorporate tidal influence into numerical modeling leads to a less accurate portrayal of transport in lower river reaches. When incorporated, tidal influence created a zone of deposition similar to that shown by TIMM. Regardless of the type of incoming sediment (coarser or finer than the bed), selective transport was shown to occur until impeded by tidal influence. Tidal influence was shown to have no effect on particles much smaller than the mean (0.075-0.5 mm or 0.003-0.2 in), such that once in transport, this material did not deposit until the reaching the bay. Without incorporation of tidal influence, deposition was shown not to occur until the mouth of the river, where expansion of flow is expected to occur.

Tidal influence may lead to flow reversals that introduce fine material in the upstream direction. Therefore, one can expect that during low-flow seasons fluvial-transport-related processes such as siltation and chemical weathering may operate. For example, at Site 5 of the Wilson River, removing surface particles for the photo frame sampling was difficult to perform because particles in the surface layer were cemented in place. From a conceptual framework and from the viewpoint of downstream fining, it can be concluded that tidal influence diminishes in the upstream direction.

Key contributions of this research are in the categories of methodology, numerical analysis, and basic understanding of the fate and transport of sediment in the zone of tidal influence. It has been shown that particle size data, collected in detail on sidebars, can be used in conjunction with specific gravity data to categorize in-stream particles based on probable origin and type. Characterization of sediment transport in the zone of tidal influence using numerical models showed the tide cycle influences

the downstream fining trend in lower reaches by shifting the zone of deposition farther upstream than would the case without tidal influence, with a net effect of increasing the rate of downstream fining. Moreover, tidal influence was found to have an inverse relationship with water discharge. Finally, it was shown that numerical modeling of river reaches in the tidal zone should include consideration of tidal fluctuations in order to predict erosion and depositional areas more accurately.

8 Recommendations for Future Research

Future research could include investigations into the following topics:

- Consider role of location of bars and sampling locations in studies of downstream fining. For instance, sample bars at different types of locations along the same reach, categorized by in-stream conditions (e.g., sidebars versus point bars or bars in directed flow versus bars near eddies).
- Study various in-stream conditions that affect armoring in the tidal zone. For example the role of aquatic vegetation and extent of siltation on the transport regime. Some studies have been done on gravel to sand transition, but in-stream sand versus silt bottom tidally influenced transport has been under analyzed.
- Study the effects of low flow in the tidal zone. Does this alter the armoring process by allowing weathering, cementing, and growth of vegetation?
- Quantify the effects of tide on the water surface elevation as a function of strength of tide (e.g., varying heights of high tide).
- Determine the range of the natural control during a typical day and the shape of the resulting profile given the level of tidal influence.
- Test numerical models against insitu data for a river reach where deposition is occurring.
- Test sensitivity of the models with regard to scale and resolution (time and space).

9 Bibliography

- Adams, J., Zimpfer, G. L., and McLane, C. F. (1978). "Basin dynamics, channel processes, and placer formation; a model study." *Economic Geology and the Bulletin of the Society of Economic Geologists*, 73(3), 416-426.
- Akan, O. A. (2006). *Open Channel Hydraulics*, McGraw-Hill, Inc, Boston.
- Andrews, E. D. (1983). "Entrainment of gravel from naturally sorted riverbed material." *Geological Society of America Bulletin*, 94(10), 1225-1231.
- Ashworth, P. J., Ferguson, R. I., Ashmore, P. E., Paola, C., Powell, D. M., and Prestegard, K. L. (1992). "Measurements in a braided river chute and lobe; 2, Sorting of bed load during entrainment, transport, and deposition." *Water Resources Research*, 28(7), 1887-1896.
- Bedient, P. B., Huber, W. C., and Vieux, B. E. (2007). *Hydrology and Floodplain Analysis*, Prentice Hall, New York.
- Blissenbach, E. (1954). "Geology of alluvial fans in semiarid regions." *Geological Society of America Bulletin*, 65(2), 175-189.
- Bogavelli, V., Coles, D. R., and Klingeman, P. C. (2004). "Streamflow Evaluation for Watershed Restoration." Oregon State University's Civil, Construction, and Environmental Engineering Department with support from the state water institutes program of the U.S. Geological Survey.
- Boquist, B. (2004). "On shoaling at the lower reaches of the Kilchis River." D. R. Coles, ed., Tillamook.
- Bostrom, G., and Komar, P. D. (1997). "Rocks of the Tillamook Bay Drainage Basin, the Coast Range of Oregon- sources of sediment accumulation in the bay." Tillamook Bay National Estuary Project.
- Brierley, G. J., and Hickin, E. J. (1985). "The downstream gradation of particle sizes in the Squamish River, British Columbia." *Earth Surface Processes and Landforms*, 10(6), 597-606.
- Chang, H. H., and Stow, D. A. (1988). "Sediment delivery in a semi-arid coastal stream." *Journal of Hydrology*, 99(3-4), 201-214.
- Chanson, H. (1999). *The Hydraulics of Open Channel Flow*, Arnold, London.
- Chow, V. T. (1959). *Open Channel Hydraulics*, McGraw-Hill, Inc, New York.
- Clark, S. M., and Snyder, G. R. (1969). "Timing and extent of flow reversal in teh

- lower Columbia River." *Limnology and Oceanography*, 14(6), 960-965.
- Constantine, C. R., Mount, J. F., and Florsheim, J. L. (2003). "The effects of longitudinal differences in gravel mobility on the downstream fining pattern in the Cosumnes River, California." *Journal of Geology*, 111(2), 233-241.
- Cui, Y., Parker, G., and Paola, C. (1996). "Numerical simulation of aggradation and downstream fining." *Journal of Hydraulic Engineering*, 34(2), 185-204.
- Dawson, M. (1988). "Sediment size variation in a braided reach of the Sunwapta River, Alberta, Canada." *Earth Surface Processes and Landforms*, 13(7), 599-618.
- Deigaard, R. (1980). "Longitudinal and transverse sorting of grain sizes in alluvial rivers." *Series Paper - Institute of Hydrodynamics and Hydraulic Engineering, Technical University of Denmark*, (26), 108.
- Document, T. C. (1996). "Hydrology and Flooding, Tillamook county flood mitigation plan: final report." Tillamook county, Nehalem.
- Document, T. C. (2000). "Stream corridor management plan for the lower Trask, Wilson, Kilchis, Miami, and Nestucca Rivers." Tillamook County, Tillamook.
- Document, T. C. (2001). "Tillamook Bay lowland floodplain integrated river management strategy and concept plan." Tillamook.
- DuBoys, M. P. (1879). "Etudes du regime et l'Action exercee par les eaux sur un lit a fond de graviers indefiniment affouilable." *Annales de Ponts et Chaussées*, 18(5), 141-195.
- Encarta. (2007). "Encarta online encyclopedia."
- Engineers, U. S. A. C. o. (1993). *HEC-6 user's manual*
- Engineers, U. S. A. C. o. (2004). "Tillamook Bay and Estuary, Oregon- General investigation on feasibility report." U.S. Army Corps of Engineers, Portland District
- Ferguson, R. I. (2003). "Emergence of abrupt gravel to sand transitions along rivers through sorting processes." *Geology Boulder*, 31(2), 159-162.
- Ferguson, R. I., Ashmore, P. E., Ashworth, P. J., Paola, C., and Prestegard, K. L. (1992). "Measurements in a braided river chute and lobe; 1, Flow pattern, sediment transport, and channel change." *Water Resources Research*, 28(7), 1877-1886.
- Ferguson, R. I., and Hoey, T. B. (2002). "Title:Find More Like ThisLong-term slowdown of river tracer pebbles; generic models and implications for interpreting short-term tracer studies." *Water Resources Research*, 38(8), 11.

- Ferguson, R. I., Hoey, T. B., Wathen, S., and Werrity, A. (1996). "Field evidence for rapid downstream fining of river gravels through selective transport." *Geology Boulder*, 24(2), 179-182.
- Ferguson, R. I., Hoey, T. B., Wathen, S., Werrity, A., Hardwick, R. I., and Sambrook Smith, G. H. (1998). "Downstream fining of river gravels; integrated field, laboratory and modeling study." *International Gravel-Bed Rivers Workshop*, 4, 85-114.
- Ferguson, R. I., and Paola, C. (1997). "Bias and precision of percentiles of bulk grain size distributions." *Earth Surface Processes and Landforms*, 22(11), 1061-1077.
- Follansbee, B., and Stark, A. (1998). "Kilchis Watershed Analysis." Tillamook Bay National Estuary Project, Tillamook.
- Gasparini, N. M., Tucker, G. E., and Bras, R. L. (1999). "Downstream fining through selective particle sorting in an equilibrium drainage network." *Geology Boulder*, 27(12), 1079-1082.
- Gomez, B., Rosser, B. J., Peacock, D. H., Hicks, D. M., and Palmer, J. A. (2001). "Downstream fining in a rapidly aggrading gravel bed river." *Water Resources Research*, 37(6), 1813-1823.
- Guglielmini, D. (1697). *Della natura dei fiumi*, A. Pisarri, Bologna.
- Hassan, M. A., Church, M., and Ashworth, P. J. (1992). "Virtual rate and mean distance of travel of individual clasts in gravel-bed channels." *Earth Surface Processes and Landforms*, 17(6), 617-627.
- Heller, P. L., McMillian, M. E., Dueker, K., and Paola, C. (2001). "Alluvial gravel transport as evidence of continental tilting and dynamic uplift of the U.S. Cordillera." *Abstracts with Programs - Geological Society of America*, 33(6), 221.
- Henderson, F. M. (1966). *Open Channel Flow*, The Macmillian Company, New York.
- Hjulstrom, F. (1935). "The morphological activity of rivers as illustrated by River Fyris." *Bulletin of the Geological Institute, Uppsala*, 25, chap. 3.
- Hoey, T. B., and Bluck, B. J. (1999). "Identifying the controls over downstream fining of river gravels." *Journal of Sedimentary Research*, 69(1), 40-50.
- Hoey, T. B., and Ferguson, R. I. (1997). "Controls of strength and rate of downstream fining above a river base level." *Water Resources Research*, 33(11), 2601-2608.
- Ichim, I. (1990). "The relationship between sediment delivery ratio and stream order; a Romanian case study." *LAHS-AISH Publication*, 189, 79-86.

- Ichim, I., and Radoane, M. (1990). "Channel sediment variability along a river; a case study of the Siret River (Romania)." *Earth Surface Processes and Landforms*, 15(3), 211-225.
- Jones, J. (2007). "On specific gravity analysis and fate of bank erosion." D. R. Coles, ed., Corvallis.
- Julien, P. Y. (1995). *Erosion and Sedimentation*, Cambridge University Press : Cambridge, United Kingdom, United Kingdom.
- Klingeman, P. C. (1981). "Willamette River bed material characteristics: Appendices." Water Resources Research Institute, Oregon State University.
- Klingeman, P. C. (2000). "CE 546 River Engineering, Lecture Notes."
- Knighton, A. D. (1999). "Downstream variation in stream power." *Geomorphology*, 29(3-4), 293-306.
- Knighton, A. D. (1999). "The gravel-sand transition in a disturbed catchment." *Geomorphology*, 27(3-4), 325-341.
- Kodama, Y. (1992). "Effect of abrasion on downstream gravel-size reduction in the Watarase River, Japan; field work and laboratory experiment." *Environmental Research Center Papers*, 15, 88.
- Komar, P. D. (1987). "Selective grain entrainment by a current from a bed of mixed sizes; a reanalysis." *Journal of Sedimentary Petrology*, 57(2), 203-211.
- Kondolf, M. G. (2006). "River restoration and meanders " *Ecology and Society*, 2(42).
- Krumbein, W. C. (1941). "The effect of abrasion on the size, shape, and roundness of rock fragments." *Journal of Geology*, 49(5), 482-520.
- Kuenen, P. H. (1956). "Rolling by current, [Part] 2 of Experimental abrasion of pebbles." *Journal of Geology*, 64(4), 336-368.
- Kuhnle, R. A. (1993). "Incipient motion of sand-gravel sediment mixtures." *Journal of Hydraulic Engineering*, 119(12), 1400-1415.
- Kuhnle, R. A. (1993). "Equal mobility on Goodwin Creek." *Eos, Transactions, American Geophysical Union*, 74(16), 158.
- Lands, O. D. o. S. (2007). "Public ownership of submerged and submersible land : Tidally-influenced waterways." Oregon Department of State Lands.
- Lisle, T. E. (1986). "Stabilization of a gravel channel by large streamside obstructions and bedrock bends, Jacoby Creek, northwestern California." *Geological Society of*

America Bulletin, 999-1011.

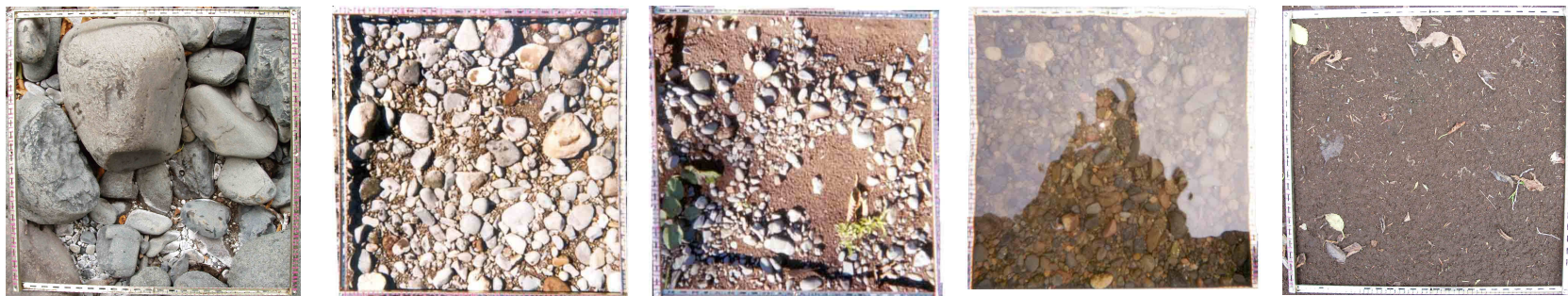
- Mathworks. (2004). *Learning MATLAB 7 (user manual)*.
- Mikos, M., and Jaeggi, M. N. R. (1993). "Abrasion experiments with gravel sediment mixtures in a tumbling barrel and their mathematical description." *Eos, Transactions, American Geophysical Union*, 74(16), 158.
- Mills, H. H. (1979). "Downstream rounding of pebbles; a quantitative review." *Journal of Sedimentary Petrology*, 49(1), 295-302.
- Munson, B. R., Young, D. F., and Okiishi, T. H. (2005). *Fundamentals of Fluid Mechanics*, Wiley, New York.
- NOAA. (2007). "Preliminary water level (A1) vs. Predicted plot 9437540 Garibaldi, OR." National Oceanic and Atmospheric Administration.
- NOAA, E. o. (2007). "Distribution of tidal phases." restfig6.gif, ed., National Oceanic and Atmospheric Administration.
- Paola, C., Hellert, P. L., and Angevine, C. L. (1992). "The large-scale dynamics of grain-size variation in alluvial basins; 1, Theory." *Basin Research*, 4(2), 73-90.
- Paola, C., Parker, G., Seal, R., Sinha, S. K., Southward, J. B., and Wilcock, P. R. (1992). "Downstream fining by selective deposition in a laboratory flume." *Science*, 258(5089), 1757-1760.
- Paola, C., and Seal, R. (1995). "Grain size patchiness as a cause of selective deposition and downstream fining." *Water Resources Research*, 31(5), 1395-1407.
- Parker, G. (1991). "Selective sorting and abrasion of river gravel; I, Theory." *Journal of Hydraulic Engineering*, 117(2), 131-149.
- Parker, G. (1991). "Selective sorting and abrasion of river gravel; II, Applications." *Journal of Hydraulic Engineering*, 117(2), 150-171.
- Parker, G., Dhamotharan, S., and Stefan, H. (1982). "Model experiments on mobile, paved gravel bed streams." *Water Resources Research*, 18(5), 1395-1408.
- Parker, G., and Klingeman, P. C. (1982). "On why gravel bed streams are paved." *Water Resources Research*, 18(5), 1409-1423.
- Pearson, M. L. (2002). "Fluvial geomorphic analysis of Tillamook Bar rivers." Portland district, U.S. Army Corps of Engineers and Tillamook County, Tillamook.
- Percy, K. L., Sutterlin, C., Bella, D. A., and Klingeman, P. C. (1974). "Descriptions

- and information sources for Oregon estuaries." Oregon State university.
- Pizzuto, J. E. (1995). "A laboratory and field study of cobble abrasion." *Water Resources Research*, 31(3), 753-759.
- Plumley, W. j. (1948). "Black Hills terrace gravels; a study in sediment transport." *Journal of Geology*, 56(6), 526-577.
- Powell, M. (1998). "Patterns and processes of sediment sorting in gravel-bed rivers." *Geography*, 22(1), 1-32.
- Reeve, D., Chadwick, A., and Fleming, C. (2004). *Coastal Engineering processes, theory, design, and practice* Spon Press, New York.
- Rice, S. (1998). "Which tributaries disrupt downstream fining along gravel-bed rivers?" *Geomorphology*, 22(1), 39-56.
- Rice, S. (1999). "The nature and controls on downstream fining within sedimentary links." *Journal of Sedimentary Research*, 69(1), 32-39.
- Rice, S., and Church, M. (1998). "Grain size along two gravel-bed rivers; statistical variation, spatial pattern and sedimentary links." *Earth Surface Processes and Landforms*, 23(4), 345-363.
- Robinson, R. A. J., and Slingerland, R. L. (1998). "Grain-size trends, basin subsidence and sediment supply in the Campanian Castlegate Sandstone and equivalent conglomerates of central Utah." *Basin Research*, 10(1), 109-127.
- Schoklitsch, A. (1933). "Abrasion of pebbles in stream courses; with special reference to the Gail River, Carinthia, Austria." *Hydrogeology*, 142(8), 343-366.
- Seal, R., and Paola, C. (1995). "Observations of downstream fining on the North Fork Toutle River near Mount St. Helens, Washington." *Water Resources Research*, 31(5), 1409-1419.
- Seal, R., Paola, C., Parker, G., Southward, J. B., and Wilcock, P. R. (1997). "Experiments on downstream fining of gravel; I, Narrow-channel runs." *Journal of Hydraulic Engineering*, 123(10), 874-884.
- Shaw, J., and Kellerhals, R. (1982). "The composition of Recent alluvial gravels in Alberta river beds." *Bulletin - Alberta Research Council*, 41, 151.
- Shields, A. (1936). "Applications of similarity principles and turbulence research to bed-load movement." California Institute of Technology, Pasadena (translated from German).
- Sklar, L. S. e. a. (2006). "Do gravel bed river size distributions record channel network structure?" *Water Resources Research*, 42(W06D18), 22.
- Sorenson, R. M. (2006). *Basic Coastal Engineering*, Springer, New York.

- Stein, J. (1980). "The random house dictionary." Random House, New York.
- Sternberg, H. (1875). "Untersuchungen uber langen- undquerprofil geschiebefuhrender fluss." *Zeitschrift fur Bauwesen*, 25, 483-506.
- Straub, L. G. (1935). "Some observations of sorting of river sediments." *Transactions - American Geophysical Union*, Part 2, 463-467.
- Styllas, M. N. (2001). "Sediment accumulation and human impacts in Tillamook Bay, Oregon," Oregon State University, Corvallis.
- Surian, N. (2002). "Downstream variation in grain size along an Alpine river; analysis of controls and processes " *Geomorphology*, 43(1-2), 137-149.
- Tritico, H. M., and Hotchkiss, R. H. (2005). "Unobstructed and obstructed turbulent flow in gravel bed rivers." *Journal of Hydraulic Engineering*, 131(8), 635-645.
- Vanoni, V. A., ed. (1975). "Sedimentation engineering, ASCE Task Committee for the Preparation of the manual on sedimentation of the Sedimentation Committee of the Hydraulics Division (Reprinted 1977)."
- W., S. T. (2001). *Open Cabnnel Hydraulics*, McGraw-Hill, New york.
- Wadell, H. A. (1932). "Sedimentation and Sedimentology." *Science*, 75, 20.
- Wentworth, C. K. (1919). "A laboratory and field study of cobble abrasion." *Journal of Geology*, 27(7), 507-521.
- Wilcock, P. R., and McArdell, B. W. (1993). "Observations of plane-bed transport rates and downstream fining." *Eos, Transactions, American Geophysical Union*, 74(16), 158.
- Wolman, M.G., (1954). "A method of sampling coarse river-bed material" *Transactions of the American Geophysical Union*, 35, p. 951-956.
- Wyrick, J. R. (2005). "On the formation of fluvial islands," Oregon State University, Corvallis.
- Yang, C., Ted. (1996). *Sediment Transport Theory and Practice*, New York.
- Yang, C., Ted, and Simoes, F. J. M. (2000). *GSTARs 2.1 user manual*, Bureau of Reclamation.
- Yatsu, E. (1955). "On the longitudinal profile of the graded river." *Transactions - American Geophysical Union*, 36(4), 655-663.

10 APPENDICES

10.1 Appendix A: Kilchis River Bulk Sampling Photographic Evidence



(a) upstream bulk samples for each site (progressing downstream, left to right)



(b) center bulk samples for each site (progressing downstream, left to right)

FIGURE 10.1: KILCHIS RIVER SITE 1 ARMOR AND SUB-ARMOR LAYER (UPSTREAM END OF BAR SAMPLE)



(c) downstream bulk samples for each site (progressing downstream, left to right)



(d) site five special bulk sample of armor layer near failing floodplain deposit

FIGURE 10.1: CONT'D

10.2 Appendix B: Kilchis Particle size distribution by site

The data that follow are the raw data used in the construction of composite plots for the upstream, downstream, center armor and sub-armor layer of the sampled Kilchis River bars. The data are separated using the convention shown on the first data sheet.

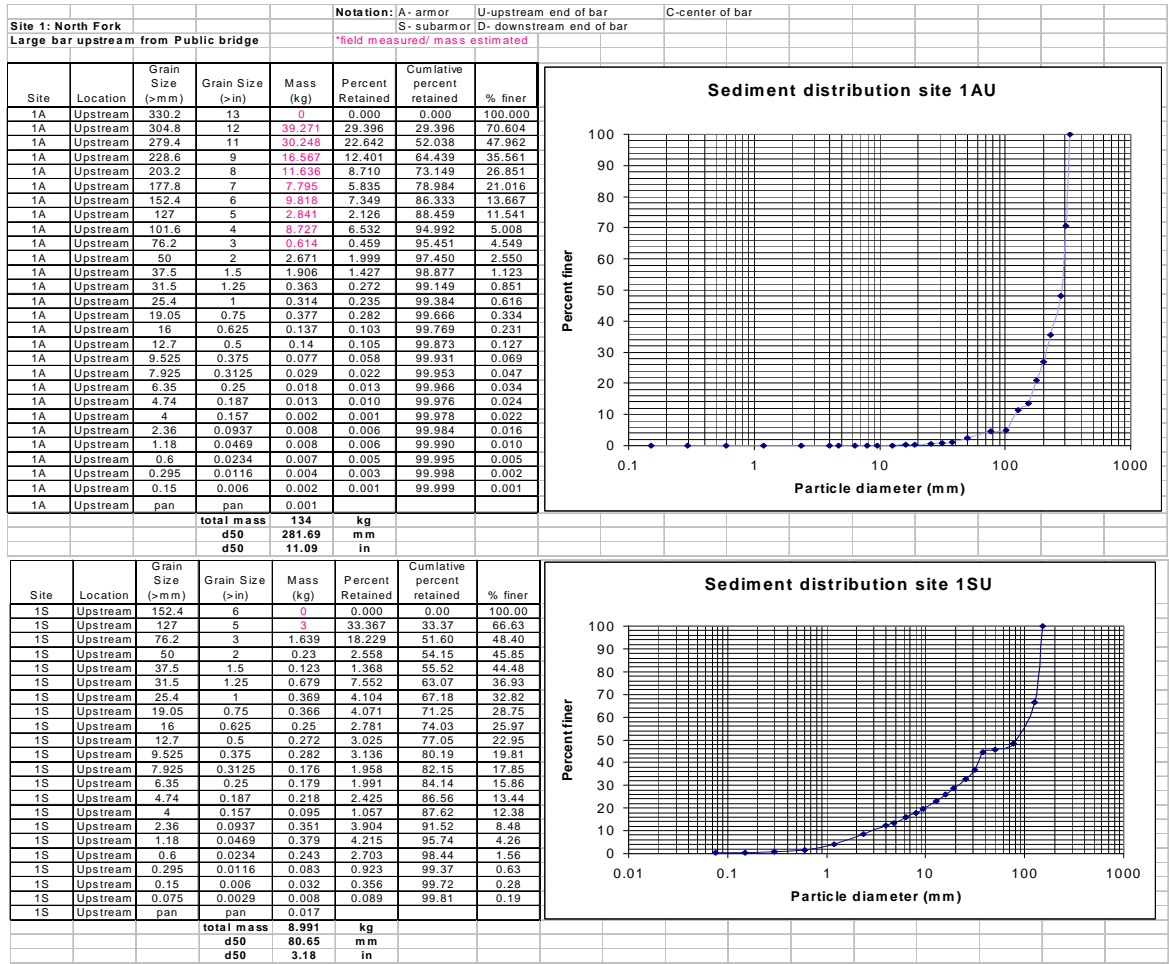
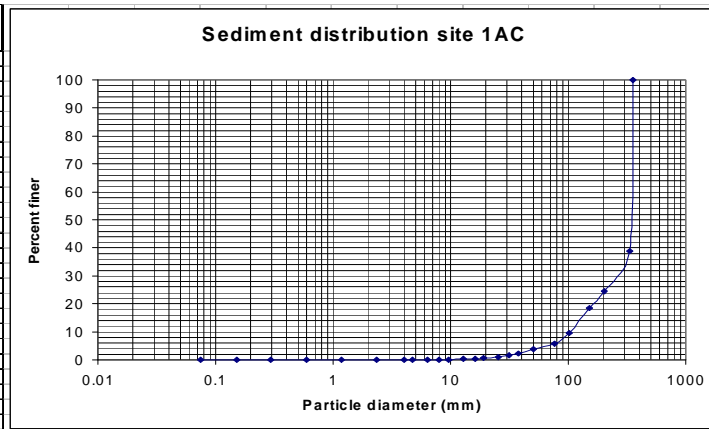


FIGURE 10.2: KILCHIS RIVER SITE 1 ARMOR AND SUB-ARMOR LAYER (UPSTREAM-END-OF-BAR SAMPLE)

Site	Location	Grain Size (>mm)	Grain Size (>in)	Mass (kg)	Percent Retained	Cumulative percent retained	% finer
1A	Center	355.6	14	0	0.000	0.00	100.00
1A	Center	330.2	13	49.929	61.296	61.30	38.70
1A	Center	203.2	8	11.636	14.285	75.58	24.42
1A	Center	152.4	6	4.909	6.026	81.61	18.39
1A	Center	101.6	4	7.272	8.928	90.53	9.47
1A	Center	76.2	3	3.068	3.766	94.30	5.70
1A	Center	50	2	1.457	1.789	96.09	3.91
1A	Center	37.5	1.5	1.258	1.544	97.63	2.37
1A	Center	31.5	1.25	0.675	0.829	98.46	1.54
1A	Center	25.4	1	0.538	0.660	99.12	0.88
1A	Center	19.05	0.75	0.3	0.368	99.49	0.51
1A	Center	16	0.625	0.134	0.165	99.66	0.34
1A	Center	12.7	0.5	0.116	0.142	99.80	0.20
1A	Center	9.525	0.375	0.082	0.101	99.90	0.10
1A	Center	7.925	0.3125	0.022	0.027	99.93	0.07
1A	Center	6.35	0.25	0.02	0.025	99.95	0.05
1A	Center	4.74	0.187	0.016	0.020	99.97	0.03
1A	Center	4	0.157	0.003	0.004	99.97	0.03
1A	Center	2.36	0.0937	0.006	0.007	99.98	0.02
1A	Center	1.18	0.0469	0.004	0.005	99.99	0.01
1A	Center	0.6	0.0234	0.004	0.005	99.99	0.01
1A	Center	0.295	0.0116	0.004	0.005	100.00	0.00
1A	Center	0.15	0.006	0.003	0.004	100.00	0.00
1A	Center	0.075	0.0029	0	0.000	100.00	0.00
1A	Center	pan	pan	NR			
		total mass	81.456	kg			
		d50	334.88	mm			
		d50	13.18	in			



Site	Location	Grain Size (>mm)	Grain Size (>in)	Mass (kg)	Percent Retained	Cumulative percent retained	% finer
1S	Center	127	5	0	0.000	0	100.00
1S	Center	101.6	4	2.909	36.393	36.39	63.61
1S	Center	76.2	3	1.227	15.353	51.75	48.25
1S	Center	37.5	1.5	0.576	7.206	58.95	41.05
1S	Center	25.4	1	0.292	3.653	62.61	37.39
1S	Center	19.05	0.75	0.452	5.655	68.26	31.74
1S	Center	16	0.625	0.26	3.253	71.51	28.49
1S	Center	12.7	0.5	0.289	3.616	75.13	24.87
1S	Center	9.525	0.375	0.267	3.340	78.47	21.53
1S	Center	7.925	0.3125	0.2	2.502	80.97	19.03
1S	Center	6.35	0.25	0.213	2.655	83.64	16.36
1S	Center	4.74	0.187	0.214	2.677	86.31	13.69
1S	Center	4	0.157	0.088	1.101	87.41	12.59
1S	Center	2.36	0.0937	0.293	3.666	91.08	8.92
1S	Center	1.18	0.0469	0.289	3.616	94.70	5.30
1S	Center	0.6	0.0234	0.213	2.655	97.36	2.64
1S	Center	0.295	0.0116	0.122	1.526	98.89	1.11
1S	Center	0.15	0.006	0.056	0.701	99.59	0.41
1S	Center	0.075	0.0029	0.015	0.188	99.77	0.23
1S	Center	pan	pan	0.018			
		total mass	7.993	kg			
		d50	79.09	mm			
		d50	3.11	in			

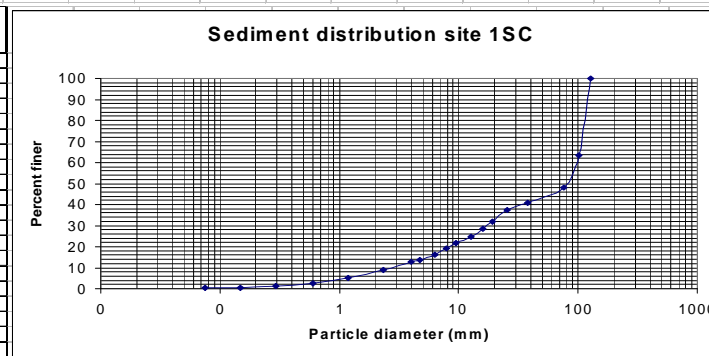


FIGURE 10.3: KILCHIS RIVER SITE 1 ARMOR AND SUB-ARMOR LAYER (CENTER-OF-BAR SAMPLE)

Site	Location	Grain Size (>mm)	Grain Size (>in)	Mass (kg)	Percent Retained	Cumulative percent retained	% finer
1A	Downstream	177.8	7	0	0.000	0.00	100.00
1A	Downstream	152.4	6	9.818	46.808	46.81	53.19
1A	Downstream	127	5	5.682	27.088	73.90	26.10
1A	Downstream	101.6	4	0.000	0.000	73.90	26.10
1A	Downstream	76.2	3	0.752	3.585	77.48	22.52
1A	Downstream	64	2.5	1.72	8.201	85.68	14.32
1A	Downstream	50	2	0.685	3.266	88.95	11.05
1A	Downstream	37.5	1.5	1.47	7.009	95.96	4.04
1A	Downstream	31.5	1.25	0.098	0.467	96.42	3.58
1A	Downstream	25.4	1	0.442	2.107	98.53	1.47
1A	Downstream	19.05	0.75	0.214	1.020	99.55	0.45
1A	Downstream	16	0.625	0.025	0.119	99.67	0.33
1A	Downstream	12.7	0.5	0.011	0.052	99.72	0.28
1A	Downstream	9.525	0.375	0.004	0.019	99.74	0.26
1A	Downstream	7.925	0.3125	0.004	0.019	99.76	0.24
1A	Downstream	4.74	0.187	0.001	0.005	99.77	0.23
1A	Downstream	2.36	0.0937	0.004	0.019	99.79	0.21
1A	Downstream	1.18	0.0469	0.01	0.048	99.83	0.17
1A	Downstream	0.6	0.0234	0.014	0.067	99.90	0.10
1A	Downstream	0.295	0.0116	0.009	0.043	99.94	0.06
1A	Downstream	0.15	0.006	0.009	0.043	99.99	0.01
1A	Downstream	0.075	0.0029	0.003	0.014	100.00	0.00
1A	Downstream	pan	pan	NR			
			total mass	20.974	kg		
			d50	149.41	mm		
			d50	5.88	in		

Site	Location	Grain Size (>mm)	Grain Size (>in)	Mass (kg)	Percent Retained	Cumulative percent retained	% finer
1S	Downstream	64	2.5	0	0	0	100.00
1S	Downstream	50	2	0.724	23.109	23.11	76.89
1S	Downstream	31.5	1.25	0.053	1.692	24.80	75.20
1S	Downstream	25.4	1	0.497	15.863	40.66	59.34
1S	Downstream	19.05	0.75	0.396	12.640	53.30	46.70
1S	Downstream	16	0.625	0.187	5.969	59.27	40.73
1S	Downstream	12.7	0.5	0.16	5.107	64.38	35.62
1S	Downstream	9.525	0.375	0.118	3.766	68.15	31.85
1S	Downstream	7.925	0.3125	0.063	2.011	70.16	29.84
1S	Downstream	6.35	0.25	0.055	1.756	71.91	28.09
1S	Downstream	4.74	0.187	0.056	1.787	73.70	26.30
1S	Downstream	4	0.157	0.024	0.766	74.47	25.53
1S	Downstream	2.36	0.0937	0.114	3.639	78.10	21.90
1S	Downstream	1.18	0.0469	0.24	7.660	85.76	14.24
1S	Downstream	0.6	0.0234	0.219	6.990	92.75	7.25
1S	Downstream	0.295	0.0116	0.106	3.383	96.14	3.86
1S	Downstream	0.15	0.006	0.08	2.553	98.69	1.31
1S	Downstream	0.075	0.0029	0.023	0.734	99.43	0.57
1S	Downstream	pan	pan	0.018			
			total mass	3.133	kg		
			d50	20.71	mm		
			d50	0.82	in		

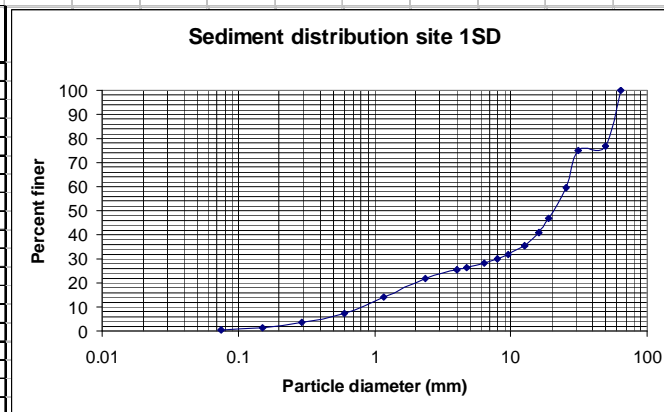
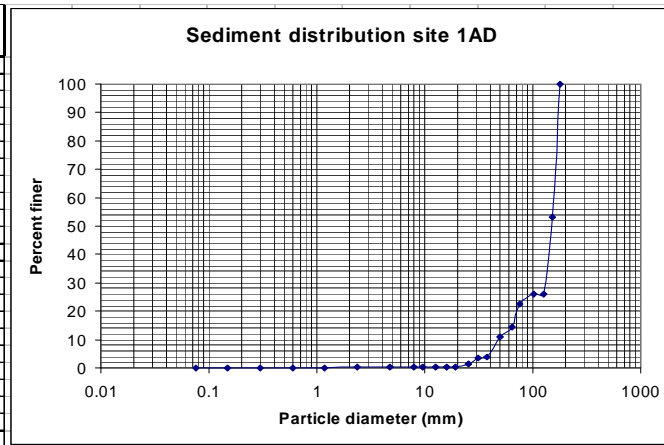
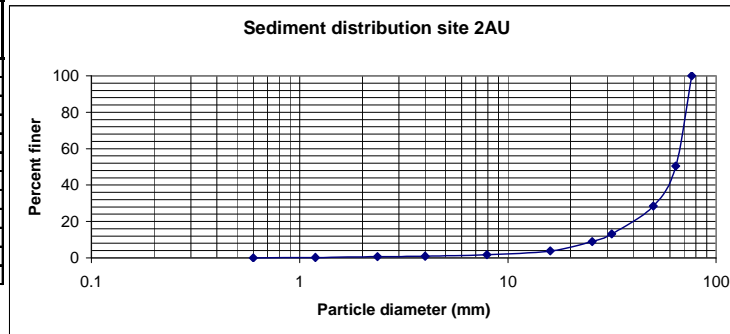


FIGURE 10.4: KILCHIS RIVER SITE 1 ARMOR AND SUB-ARMOR LAYER (DOWNSTREAM-END-OF-BAR SAMPLE)

Site 2: River mile 4
Large bar upstream from Public bridge

Site	Location	Grain Size (>mm)	Mass (kg)	Percent Retained	Cumulative percent retained	% finer
2A	Upstream	76.2	0	0.000	0.00	100.00
2A	Upstream	64	10.46	49.573	49.57	50.43
2A	Upstream	50	4.64	21.991	71.56	28.44
2A	Upstream	31.5	3.24	15.355	86.92	13.08
2A	Upstream	25.4	0.88	4.171	91.09	8.91
2A	Upstream	16	1.1	5.213	96.30	3.70
2A	Upstream	7.925	0.42	1.991	98.29	1.71
2A	Upstream	4	0.16	0.758	99.05	0.95
2A	Upstream	2.36	0.08	0.379	99.43	0.57
2A	Upstream	1.19	0.08	0.379	99.81	0.19
2A	Upstream	0.6	0.04	0.190	100.00	0.00
2A	Upstream	pan	NR			
total mass			21.10	kg		
d50			63.73	mm		
d50			2.51	in		



Site	Location	Grain Size (>mm)	Mass (kg)	Percent Retained	Cumulative percent retained	% finer
2S	Upstream	76.2	0	0.000	0.00	100.00
2S	Upstream	64	0.5	12.953	12.95	87.05
2S	Upstream	50	0.58	15.026	27.98	72.02
2S	Upstream	31.5	0.44	11.399	39.38	60.62
2S	Upstream	25.4	0.26	6.736	46.11	53.89
2S	Upstream	16	0.38	9.845	55.96	44.04
2S	Upstream	7.925	0.5	12.953	68.91	31.09
2S	Upstream	4	0.4	10.363	79.27	20.73
2S	Upstream	2.36	0.3	7.772	87.05	12.95
2S	Upstream	1.19	0.3	7.772	94.82	5.18
2S	Upstream	0.6	0.14	3.627	98.45	1.55
2S	Upstream	0.295	0.04	1.036	99.48	0.52
2S	Upstream	0.15	0.02	0.518	100.00	0.00
2S	Upstream	pan	NR			
total mass			3.86	kg		
d50			21.69	mm		
d50			0.85	in		

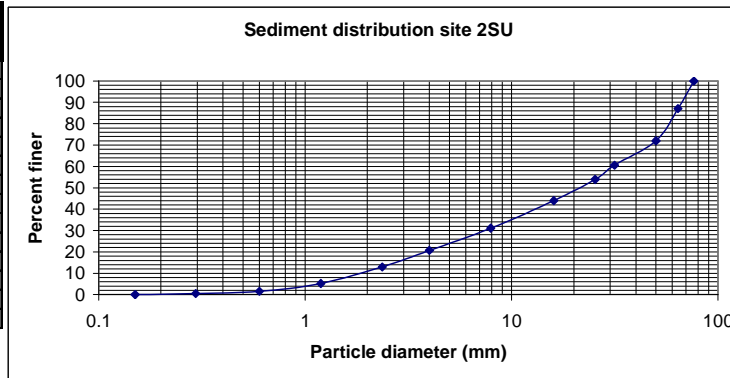
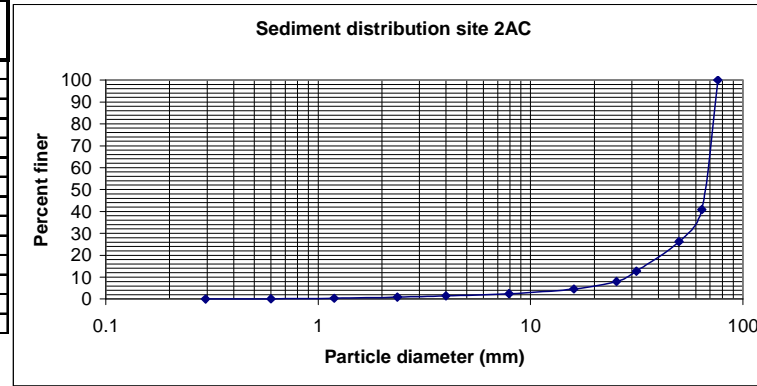


FIGURE 10.5: KILCHIS RIVER SITE 2 ARMOR AND SUB-ARMOR LAYER (UPSTREAM-END-OF-BAR SAMPLE)

Site	Location	Grain Size (>mm)	Mass (kg)	Percent Retained	Cumulative percent retained	% finer
2A	Center	76.2	0	0.000	0.00	100.00
2A	Center	64	13.62	59.115	59.11	40.89
2A	Center	50	3.38	14.670	73.78	26.22
2A	Center	31.5	3.1	13.455	87.24	12.76
2A	Center	25.4	1.1	4.774	92.01	7.99
2A	Center	16	0.78	3.385	95.40	4.60
2A	Center	7.925	0.5	2.170	97.57	2.43
2A	Center	4	0.22	0.955	98.52	1.48
2A	Center	2.36	0.14	0.608	99.13	0.87
2A	Center	1.19	0.12	0.521	99.65	0.35
2A	Center	0.6	0.06	0.260	99.91	0.09
2A	Center	0.295	0.02	0.087	100.00	0.00
2A	Center	0.15	NR			
2A	Center	pan	NR			
total mass			23.04	kg		
d50			5.68	mm		
d50			0.22	in		



Site	Location	Grain Size (>mm)	Mass (kg)	Percent Retained	Cumulative percent retained	% finer
2S	Center	76.2	0	0.000	0.00	100.00
2S	Center	64	2.02	37.970	37.97	62.03
2S	Center	50	0.86	16.165	54.14	45.86
2S	Center	31.5	0.14	2.632	56.77	43.23
2S	Center	25.4	0.14	2.632	59.40	40.60
2S	Center	16	0.38	7.143	66.54	33.46
2S	Center	7.925	0.48	9.023	75.56	24.44
2S	Center	4	0.4	7.519	83.08	16.92
2S	Center	2.36	0.32	6.015	89.10	10.90
2S	Center	1.19	0.28	5.263	94.36	5.64
2S	Center	0.6	0.16	3.008	97.37	2.63
2S	Center	0.295	0.06	1.128	98.50	1.50
2S	Center	0.15	0.04	0.752	99.25	0.75
2S	Center	pan	0.04	0.752	100.00	0.00
total mass			5.32	kg		
d50			53.58	mm		
d50			2.11	in		

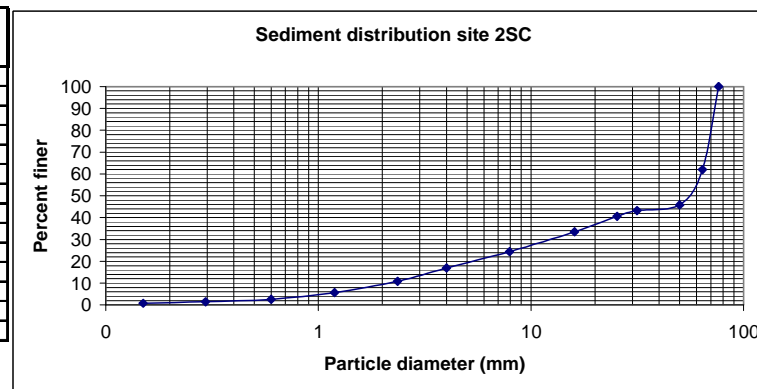
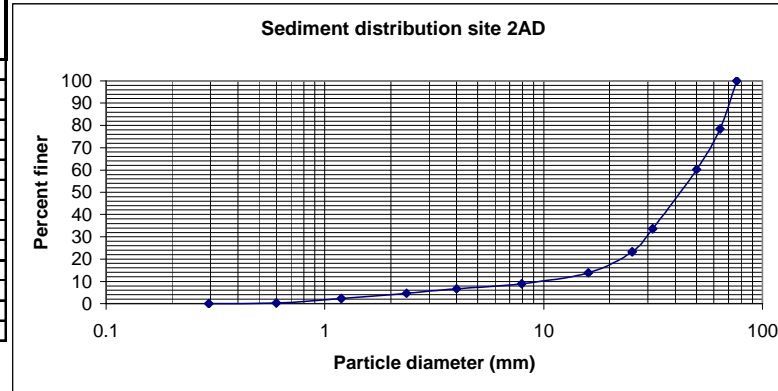


FIGURE 10.6: KILCHIS RIVER SITE 2 ARMOR AND SUB-ARMOR LAYER (CENTER-OF-BAR SAMPLE)

Site	Location	Grain Size (>mm)	Mass (kg)	Percent Retained	Cumulative percent retained	% finer
2A	Down	76.2	0	0.000	0.00	100.00
2A	Down	64	1.68	21.538	21.54	78.46
2A	Down	50	1.42	18.205	39.74	60.26
2A	Down	31.5	2.08	26.667	66.41	33.59
2A	Down	25.4	0.8	10.256	76.67	23.33
2A	Down	16	0.74	9.487	86.15	13.85
2A	Down	7.925	0.38	4.872	91.03	8.97
2A	Down	4	0.18	2.308	93.33	6.67
2A	Down	2.36	0.16	2.051	95.38	4.62
2A	Down	1.19	0.18	2.308	97.69	2.31
2A	Down	0.6	0.16	2.051	99.74	0.26
2A	Down	0.295	0.02	0.256	100.00	0.00
2A	Down	0.15	NR			
2A	Down	pan	NR			

total mass 7.80 kg
d50 42.88 mm
d50 1.69 in



Site	Location	Grain Size (>mm)	Mass (kg)	Percent Retained	Cumulative percent retained	% finer
2S	Down	50	0	0.000	0.00	100.00
2S	Down	31.5	0.84	28.378	28.38	71.62
2S	Down	25.4	0.24	8.108	36.49	63.51
2S	Down	16	0.44	14.865	51.35	48.65
2S	Down	7.925	0.4	13.514	64.86	35.14
2S	Down	4	0.28	9.459	74.32	25.68
2S	Down	2.36	0.22	7.432	81.76	18.24
2S	Down	1.19	0.26	8.784	90.54	9.46
2S	Down	0.6	0.22	7.432	97.97	2.03
2S	Down	0.295	0.06	2.027	100.00	0.00
2S	Down	0.15	NR			
2S	Down	pan	NR			

total mass 2.96 kg
d50 16.85 mm
d50 0.66 in

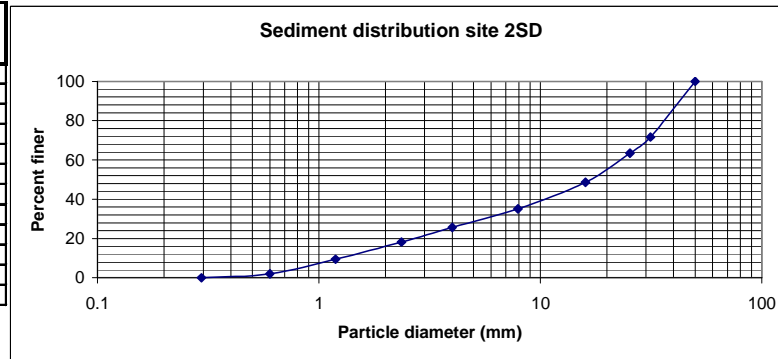
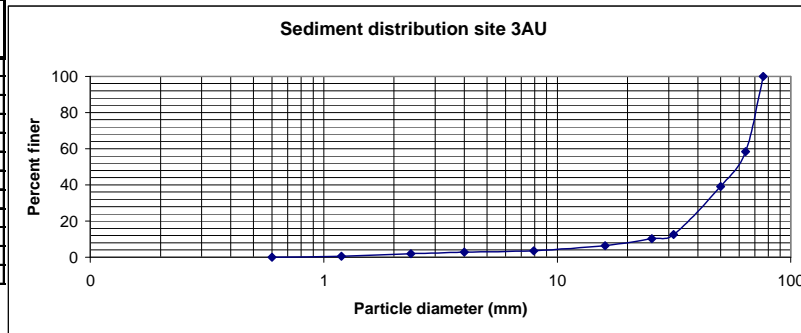


FIGURE 10.7: KILCHIS RIVER SITE 2 ARMOR AND SUB-ARMOR LAYER (DOWNSTREAM-END-OF-BAR SAMPLE)

Site 3: River mile 3
Large bar downstream from Curl bridge

Site	Location	Grain Size (>mm)	Mass (kg)	Percent Retained	Cumulative percent retained	% finer
3A	Upstream	76.2	0	0.000	0.00	100.00
3A	Upstream	64	4.12	41.616	41.62	58.38
3A	Upstream	50	1.9	19.192	60.81	39.19
3A	Upstream	31.5	2.64	26.667	87.47	12.53
3A	Upstream	25.4	0.22	2.222	89.70	10.30
3A	Upstream	16	0.38	3.838	93.54	6.46
3A	Upstream	7.925	0.28	2.828	96.36	3.64
3A	Upstream	4	0.08	0.808	97.17	2.83
3A	Upstream	2.36	0.08	0.808	97.98	2.02
3A	Upstream	1.19	0.14	1.414	99.39	0.61
3A	Upstream	0.6	0.06	0.606	100.00	0.00
3A	Upstream	pan	NR			
total mass			9.9	kg		
d50			57.88	mm		
d50			2.28	in		



Site	Location	Grain Size (>mm)	Mass (kg)	Percent Retained	Cumulative percent retained	% finer
3S	Upstream	76.2	0	0.000	0.00	100.00
3S	Upstream	64	0.38	9.360	9.36	90.64
3S	Upstream	50	0.46	11.330	20.69	79.31
3S	Upstream	31.5	0.58	14.286	34.98	65.02
3S	Upstream	25.4	0.2	4.926	39.90	60.10
3S	Upstream	16	0.42	10.345	50.25	49.75
3S	Upstream	7.925	0.42	10.345	60.59	39.41
3S	Upstream	4	0.38	9.360	69.95	30.05
3S	Upstream	2.36	0.4	9.852	79.80	20.20
3S	Upstream	1.19	0.54	13.300	93.10	6.90
3S	Upstream	0.6	0.24	5.911	99.01	0.99
3S	Upstream	0.295	0.04	0.985	100.00	0.00
3S	Upstream	0.15	NR			
3S	Upstream	pan	NR			
total mass			4.06	kg		
d50			16.22	mm		
d50			0.64	in		

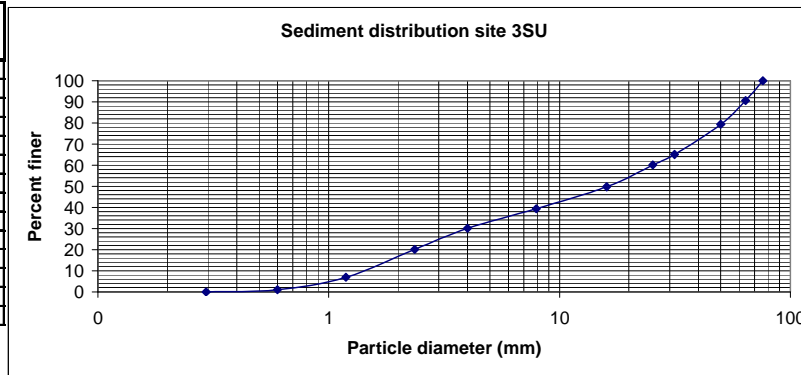
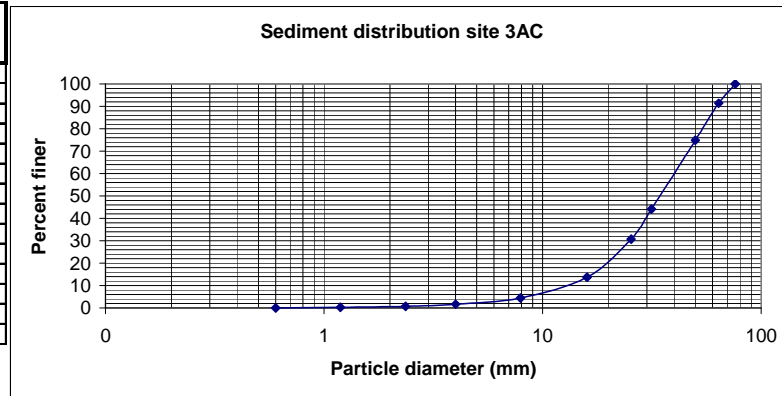


FIGURE 10.8: KILCHIS RIVER SITE 3 ARMOR AND SUB-ARMOR LAYER (UPSTREAM-END-OF-BAR SAMPLE)

Site	Location	Grain Size (>mm)	Mass (kg)	Percent Retained	Cumulative percent retained	% finer
3A	Center	76.2	0	0.000	0.00	100.00
3A	Center	64	0.74	8.605	8.60	91.40
3A	Center	50	1.42	16.512	25.12	74.88
3A	Center	31.5	2.64	30.698	55.81	44.19
3A	Center	25.4	1.16	13.488	69.30	30.70
3A	Center	16	1.46	16.977	86.28	13.72
3A	Center	7.925	0.8	9.302	95.58	4.42
3A	Center	4	0.24	2.791	98.37	1.63
3A	Center	2.36	0.08	0.930	99.30	0.70
3A	Center	1.19	0.04	0.465	99.77	0.23
3A	Center	0.6	0.02	0.233	100.00	0.00
3A	Center	0.295	NR			
3A	Center	0.15	NR			
3A	Center	pan	NR			

total mass 8.6 kg
d50 35.00 mm
d50 1.38 in



Site	Location	Grain Size (>mm)	Mass (kg)	Percent Retained	Cumulative percent retained	% finer
3S	Center	50	0	0.000	0.00	100.00
3S	Center	31.5	0.08	3.008	3.01	96.99
3S	Center	25.4	0.08	3.008	6.02	93.98
3S	Center	16	0.44	16.541	22.56	77.44
3S	Center	7.925	0.64	24.060	46.62	53.38
3S	Center	4	0.5	18.797	65.41	34.59
3S	Center	2.36	0.34	12.782	78.20	21.80
3S	Center	1.19	0.34	12.782	90.98	9.02
3S	Center	0.6	0.2	7.519	98.50	1.50
3S	Center	0.295	0.04	1.504	100.00	0.00
3S	Center	0.15	NR			
3S	Center	pan	NR			

total mass 2.66 kg
d50 7.22 mm
d50 0.28 in

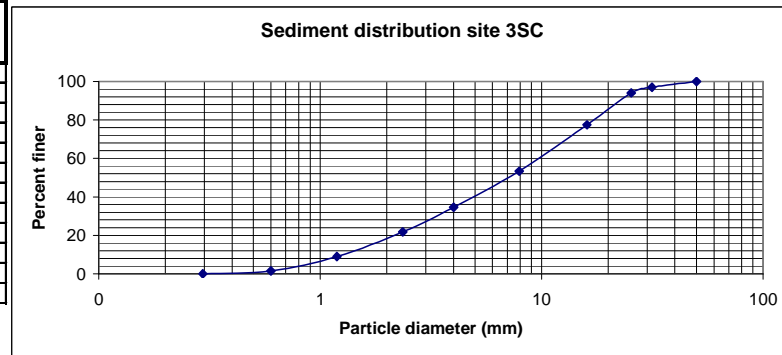
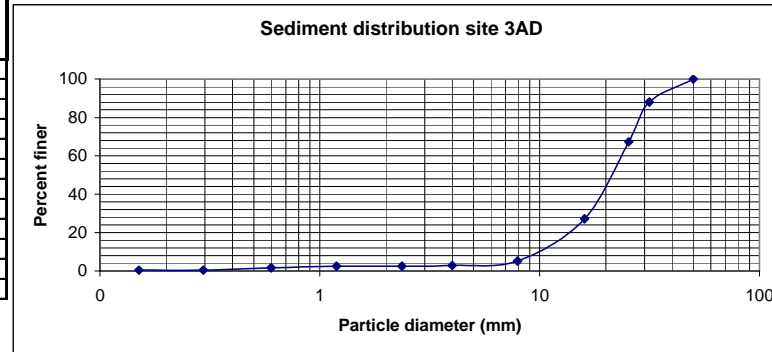


FIGURE 10.9: KILCHIS RIVER SITE 3 ARMOR AND SUB-ARMOR LAYER (CENTER-OF-BAR SAMPLE)

Site	Location	Grain Size (>mm)	Mass (kg)	Percent Retained	Cumulative percent retained	% finer
3A	Down	50	0	0.000	0.00	100.00
3A	Down	31.5	0.6	11.952	11.95	88.05
3A	Down	25.4	1.04	20.717	32.67	67.33
3A	Down	16	2.02	40.239	72.91	27.09
3A	Down	7.925	1.1	21.912	94.82	5.18
3A	Down	4	0.12	2.390	97.21	2.79
3A	Down	2.36	0.02	0.398	97.61	2.39
3A	Down	1.19	0	0.000	97.61	2.39
3A	Down	0.6	0.04	0.797	98.41	1.59
3A	Down	0.295	0.06	1.195	99.60	0.40
3A	Down	0.15	0	0.000	99.60	0.40
3A	Down	pan	0.02	0.398	100.00	0.00
total mass			5.02	kg		
d50			21.35	mm		
d50			0.84	in		



Site	Location	Grain Size (>mm)	Mass (kg)	Percent Retained	Cumulative percent retained	% finer
3S	Down	31.5	0	0.000	0.00	100.00
3S	Down	25.4	0.04	1.333	1.33	98.67
3S	Down	16	0.38	12.667	14.00	86.00
3S	Down	7.925	1	33.333	47.33	52.67
3S	Down	4	0.6	20.000	67.33	32.67
3S	Down	2.36	0.22	7.333	74.67	25.33
3S	Down	1.19	0.12	4.000	78.67	21.33
3S	Down	0.6	0.3	10.000	88.67	11.33
3S	Down	0.295	0.3	10.000	98.67	1.33
3S	Down	0.15	0.04	1.333	100.00	0.00
3S	Down	pan	NR			
total mass			3	kg		
d50			7.40	mm		
d50			0.29	in		

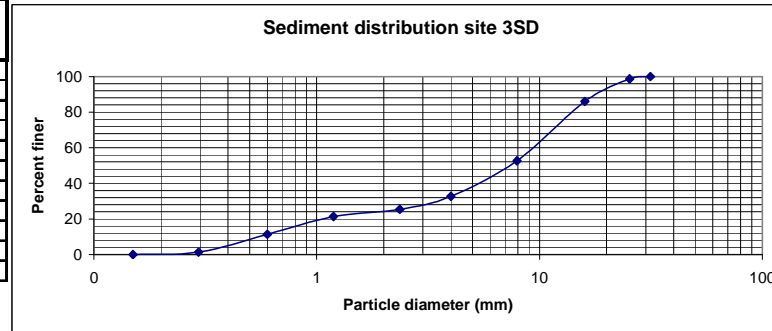
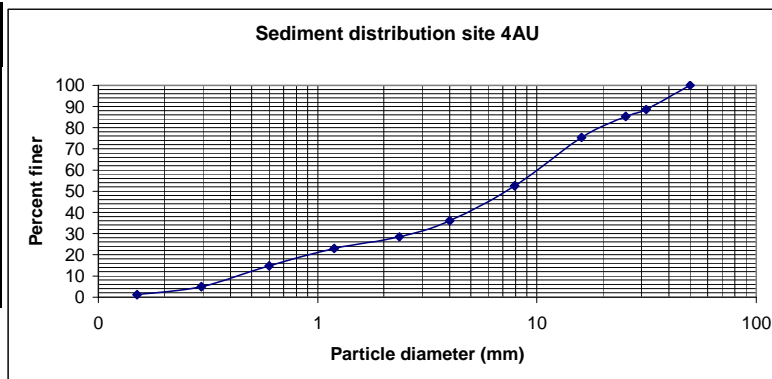


FIGURE 10.10: KILCHIS RIVER SITE 3 ARMOR AND SUB-ARMOR LAYER (DOWNSTREAM-END-OF-BAR SAMPLE)

Site 4: River mile 1
Large bar downstream of Highway 101 bridge

Site	Location	Grain Size (>mm)	Mass (kg)	Percent Retained	Cumulative percent retained	% finer
4A	Upstream	50	0	0.000	0.00	100.00
4A	Upstream	31.5	0.42	11.475	11.48	88.52
4A	Upstream	25.4	0.12	3.279	14.75	85.25
4A	Upstream	16	0.36	9.836	24.59	75.41
4A	Upstream	7.925	0.84	22.951	47.54	52.46
4A	Upstream	4	0.6	16.393	63.93	36.07
4A	Upstream	2.36	0.28	7.650	71.58	28.42
4A	Upstream	1.19	0.2	5.464	77.05	22.95
4A	Upstream	0.6	0.3	8.197	85.25	14.75
4A	Upstream	0.295	0.36	9.836	95.08	4.92
4A	Upstream	0.15	0.14	3.825	98.91	1.09
4A	Upstream	pan	0.04	1.093	100.00	0.00
total mass			3.66	kg		
d50			7.34	mm		
d50			0.29	in		
d65			12.34	mm		



Site	Location	Grain Size (>mm)	Mass (kg)	Percent Retained	Cumulative percent retained	% finer
4S	Upstream	31.5	0	0.000	0.00	100.00
4S	Upstream	25.4	0.08	2.030	2.03	97.97
4S	Upstream	16	0.18	4.569	6.60	93.40
4S	Upstream	7.925	0.7	17.766	24.37	75.63
4S	Upstream	4	0.76	19.289	43.65	56.35
4S	Upstream	2.36	0.56	14.213	57.87	42.13
4S	Upstream	1.19	0.74	18.782	76.65	23.35
4S	Upstream	0.6	0.58	14.721	91.37	8.63
4S	Upstream	0.295	0.22	5.584	96.95	3.05
4S	Upstream	0.15	0.08	2.030	98.98	1.02
4S	Upstream	pan	0.04	1.015	100.00	0.00
total mass			3.94	kg		
d50			3.27	mm		
d50			0.13	in		
d65			5.76	mm		

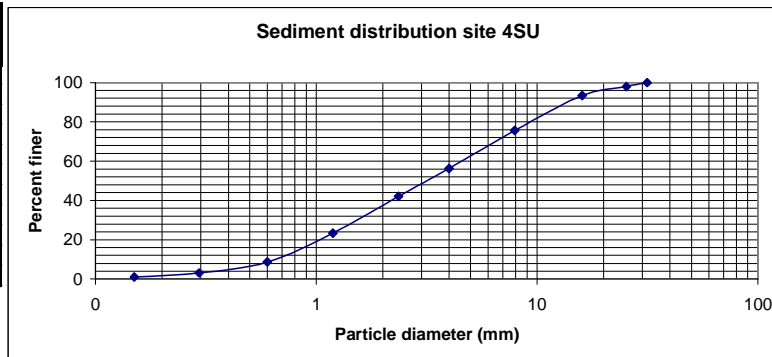


FIGURE 10.11: KILCHIS RIVER SITE 4 ARMOR AND SUB-ARMOR LAYER (UPSTREAM-END-OF-BAR SAMPLE)

Site	Location	Grain Size (>mm)	Mass (kg)	Percent Retained	Cumulative percent retained	% finer
4A	Center	76.2	0	0.000	0.00	100.00
4A	Center	64	0.36	6.818	6.82	93.18
4A	Center	50	0.1	1.894	8.71	91.29
4A	Center	31.5	0.3	5.682	14.39	85.61
4A	Center	25.4	0.96	18.182	32.58	67.42
4A	Center	16	1.76	33.333	65.91	34.09
4A	Center	7.925	1.22	23.106	89.02	10.98
4A	Center	4	0.26	4.924	93.94	6.06
4A	Center	2.36	0.1	1.894	95.83	4.17
4A	Center	1.19	0.08	1.515	97.35	2.65
4A	Center	0.6	0.1	1.894	99.24	0.76
4A	Center	0.295	0.04	0.758	100.00	0.00
4A	Center	0.15	NR			
4A	Center	pan	NR			

total mass 5.28 kg
d50 11.09 mm
d50 0.44 in
d65 24.72 mm

Site	Location	Grain Size (>mm)	Mass (kg)	Percent Retained	Cumulative percent retained	% finer
4S	Center	50	0	0.000	0.00	100.00
4S	Center	31.5	0.2	4.762	4.76	95.24
4S	Center	25.4	0.16	3.810	8.57	91.43
4S	Center	16	0.58	13.810	22.38	77.62
4S	Center	7.925	1.26	30.000	52.38	47.62
4S	Center	4	0.86	20.476	72.86	27.14
4S	Center	2.36	0.5	11.905	84.76	15.24
4S	Center	1.19	0.3	7.143	91.90	8.10
4S	Center	0.6	0.18	4.286	96.19	3.81
4S	Center	0.295	0.06	1.429	97.62	2.38
4S	Center	0.15	0.06	1.429	99.05	0.95
4S	Center	pan	0.04	0.952	100.00	0.00

total mass 4.2 kg
d50 8.57 mm
d50 0.34 in
d65 12.60 mm

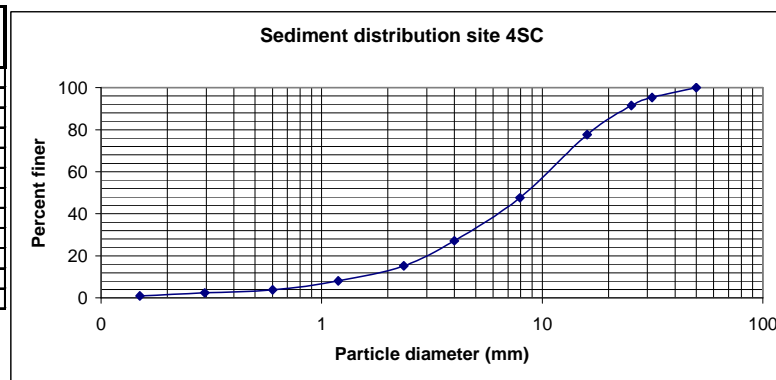
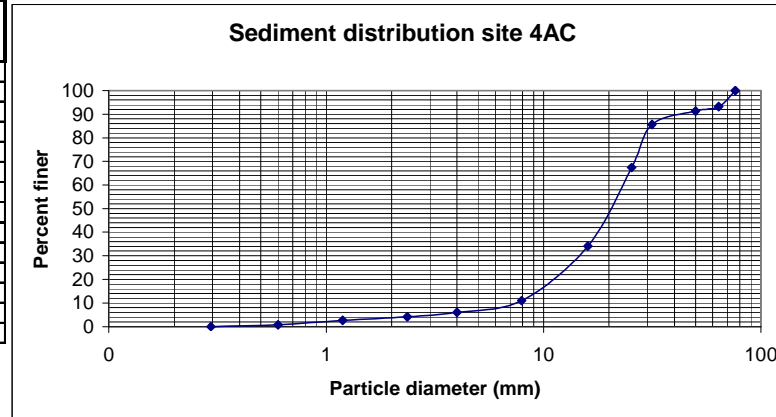
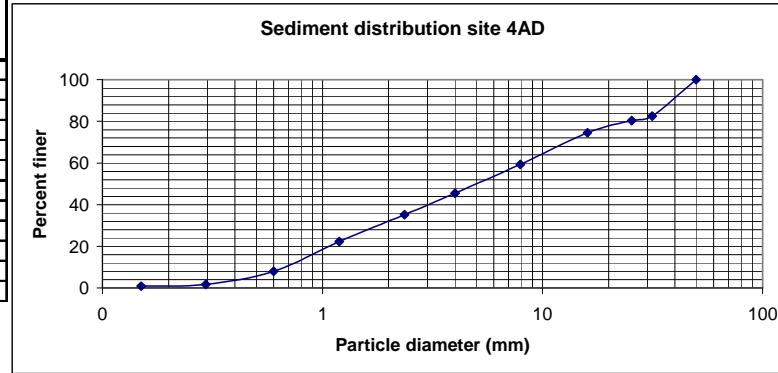


FIGURE 10.12: KILCHIS RIVER SITE 4 ARMOR AND SUB-ARMOR LAYER (CENTER-OF-BAR SAMPLE)

Site	Location	Grain Size (>mm)	Mass (kg)	Percent Retained	Cumulative percent retained	% finer
4A	Down	50	0	0.000	0.00	100.00
4A	Down	31.5	0.78	17.411	17.41	82.59
4A	Down	25.4	0.1	2.232	19.64	80.36
4A	Down	16	0.26	5.804	25.45	74.55
4A	Down	7.925	0.68	15.179	40.63	59.38
4A	Down	4	0.62	13.839	54.46	45.54
4A	Down	2.36	0.46	10.268	64.73	35.27
4A	Down	1.19	0.58	12.946	77.68	22.32
4A	Down	0.6	0.64	14.286	91.96	8.04
4A	Down	0.295	0.28	6.250	98.21	1.79
4A	Down	0.15	0.04	0.893	99.11	0.89
4A	Down	pan	0.04	0.893	100.00	0.00
total mass			4.48	kg		
d50			5.27	mm		
d50			0.21	in		
d65			10.92	mm		



Site	Location	Grain Size (>mm)	Mass (kg)	Percent Retained	Cumulative percent retained	% finer
4S	Down	31.5	0	0.000	0.00	100.00
4S	Down	25.4	0.32	9.195	9.20	90.80
4S	Down	16	0.44	12.644	21.84	78.16
4S	Down	7.925	0.8	22.989	44.83	55.17
4S	Down	4	0.56	16.092	60.92	39.08
4S	Down	2.36	0.36	10.345	71.26	28.74
4S	Down	1.19	0.36	10.345	81.61	18.39
4S	Down	0.6	0.38	10.920	92.53	7.47
4S	Down	0.295	0.2	5.747	98.28	1.72
4S	Down	0.15	0.04	1.149	99.43	0.57
4S	Down	pan	0.02	0.575	100.00	0.00
total mass			3.48	kg		
d50			6.66	mm		
d50			0.26	in		
d65			11.38	mm		

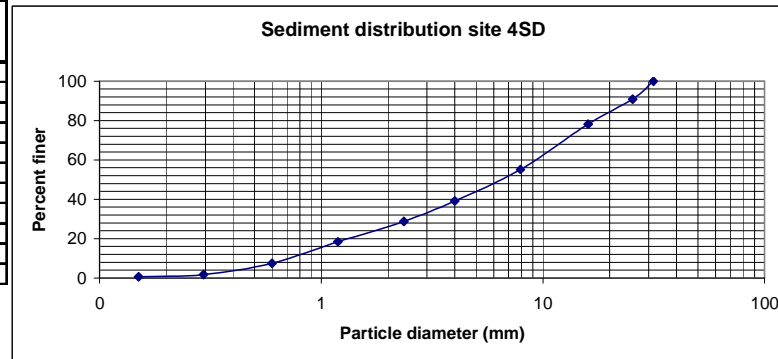
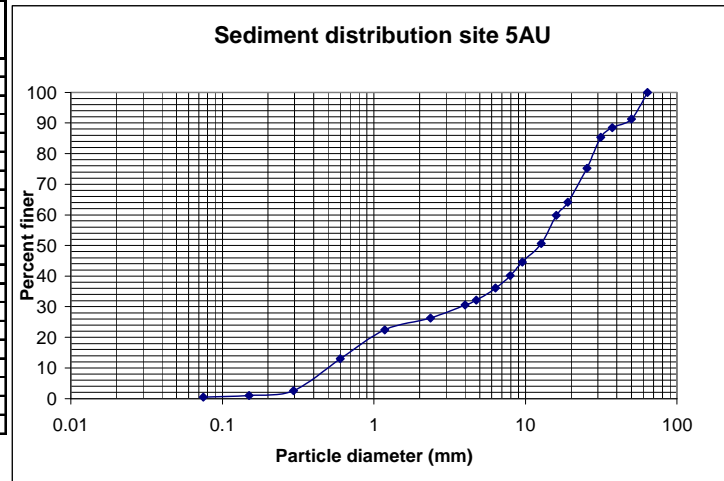


FIGURE 10.13: KILCHIS RIVER SITE 4 ARMOR AND SUB-ARMOR LAYER (DOWNSTREAM-END-OF-BAR SAMPLE)

Site 5: River mile 0.25
Large bar upstream from mouth

Site	Location	Grain Size (>mm)	Grain Size (>in)	Mass (kg)	Percent Retained	Cumulative percent retained	% finer
5A	Upstream	64	2.5	0	0.000	0.00	100.00
5A	Upstream	50	2	0.489	8.742	8.74	91.26
5A	Upstream	37.5	1.5	0.153	2.735	11.48	88.52
5A	Upstream	31.5	1.25	0.181	3.236	14.71	85.29
5A	Upstream	25.4	1	0.563	10.064	24.78	75.22
5A	Upstream	19.05	0.75	0.624	11.155	35.93	64.07
5A	Upstream	16	0.625	0.238	4.255	40.19	59.81
5A	Upstream	12.7	0.5	0.514	9.188	49.37	50.63
5A	Upstream	9.525	0.375	0.336	6.006	55.38	44.62
5A	Upstream	7.925	0.3125	0.252	4.505	59.89	40.11
5A	Upstream	6.35	0.25	0.224	4.004	63.89	36.11
5A	Upstream	4.74	0.187	0.224	4.004	67.89	32.11
5A	Upstream	4	0.157	0.086	1.537	69.43	30.57
5A	Upstream	2.36	0.0937	0.237	4.237	73.67	26.33
5A	Upstream	1.18	0.0469	0.218	3.897	77.57	22.43
5A	Upstream	0.6	0.0234	0.53	9.474	87.04	12.96
5A	Upstream	0.295	0.0116	0.577	10.315	97.35	2.65
5A	Upstream	0.15	0.006	0.093	1.662	99.02	0.98
5A	Upstream	0.075	0.0029	0.028	0.501	99.52	0.48
5A	Upstream	pan	pan	0.027			
				total mass	5.594	kg	
				d50	12.37	mm	
				d50	0.49	in	



Site	Location	Grain Size (>mm)	Grain Size (>in)	Mass (kg)	Percent Retained	Cumulative percent retained	% finer
5S	Upstream	31.5	1.25	0	0.000	0.00	100.00
5S	Upstream	25.4	1	0.046	1.589	1.59	98.41
5S	Upstream	19.05	0.75	0.292	10.086	11.68	88.32
5S	Upstream	16	0.625	0.194	6.701	18.38	81.62
5S	Upstream	12.7	0.5	0.206	7.116	25.49	74.51
5S	Upstream	9.525	0.375	0.318	10.984	36.48	63.52
5S	Upstream	7.925	0.3125	0.159	5.492	41.97	58.03
5S	Upstream	6.35	0.25	0.171	5.907	47.88	52.12
5S	Upstream	4.74	0.187	0.164	5.665	53.54	46.46
5S	Upstream	4	0.157	0.063	2.176	55.72	44.28
5S	Upstream	2.36	0.0937	0.214	7.392	63.11	36.89
5S	Upstream	1.18	0.0469	0.261	9.016	72.12	27.88
5S	Upstream	0.6	0.0234	0.481	16.615	88.74	11.26
5S	Upstream	0.295	0.0116	0.258	8.912	97.65	2.35
5S	Upstream	0.15	0.006	0.046	1.589	99.24	0.76
5S	Upstream	0.075	0.0029	0.01	0.345	99.59	0.41
5S	Upstream	pan	pan	0.012			
				total mass	2.895	kg	
				d50	4.14	mm	
				d50	0.16	in	

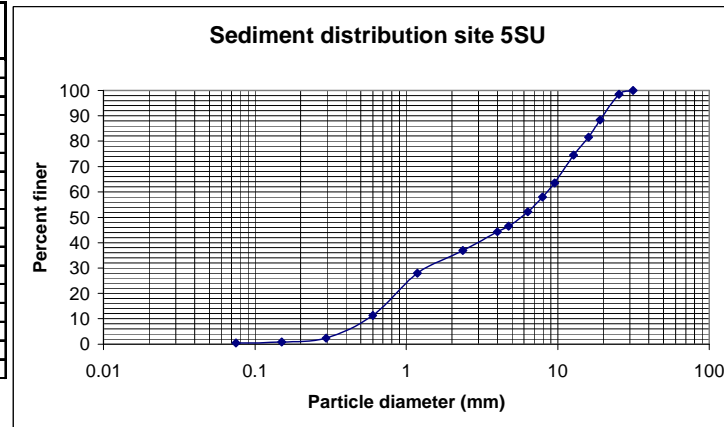
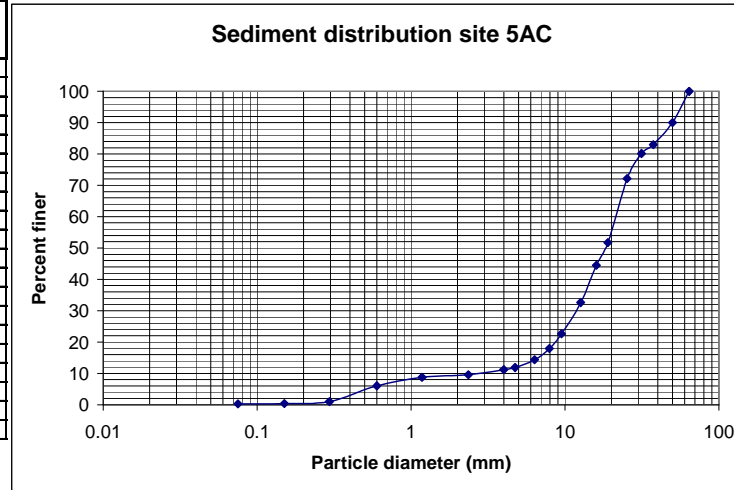


FIGURE 10.14: KILCHIS RIVER SITE 5 ARMOR AND SUB-ARMOR LAYER (UPSTREAM-END-OF-BAR SAMPLE)

Site	Location	Grain Size (>mm)	Grain Size (>in)	Mass (Kg)	Percent Retained	Cumulative percent retained	% finer
5A	Center	64	2.5	0	0.000	0.00	100.00
5A	Center	50	2	0.312	9.949	9.95	90.05
5A	Center	37.5	1.5	0.222	7.079	17.03	82.97
5A	Center	31.5	1.25	0.088	2.806	19.83	80.17
5A	Center	25.4	1	0.251	8.004	27.84	72.16
5A	Center	19.05	0.75	0.641	20.440	48.28	51.72
5A	Center	16	0.625	0.226	7.207	55.48	44.52
5A	Center	12.7	0.5	0.375	11.958	67.44	32.56
5A	Center	9.525	0.375	0.312	9.949	77.39	22.61
5A	Center	7.925	0.3125	0.147	4.688	82.08	17.92
5A	Center	6.35	0.25	0.112	3.571	85.65	14.35
5A	Center	4.74	0.187	0.077	2.455	88.11	11.89
5A	Center	4	0.157	0.023	0.733	88.84	11.16
5A	Center	2.36	0.0937	0.05	1.594	90.43	9.57
5A	Center	1.18	0.0469	0.026	0.829	91.26	8.74
5A	Center	0.6	0.0234	0.086	2.742	94.01	5.99
5A	Center	0.295	0.0116	0.156	4.974	98.98	1.02
5A	Center	0.15	0.006	0.021	0.670	99.65	0.35
5A	Center	0.075	0.0029	0.003	0.096	99.74	0.26
5A	Center	pan		0.008			
				total mass	3.136 kg		
				d50	18.32 mm		
				d50	0.72 in		



Site	Location	Grain Size (>mm)	Grain Size (>in)	Mass (Kg)	Percent Retained	Cumulative percent retained	% finer
5S	Center	64	2.5	0	0.000	0.00	100.00
5S	Center	50	2	0.153	4.913	4.91	95.09
5S	Center	37.5	1.5	0.104	3.340	8.25	91.75
5S	Center	25.4	1	0.092	2.954	11.21	88.79
5S	Center	19.05	0.75	0.231	7.418	18.63	81.37
5S	Center	16	0.625	0.147	4.721	23.35	76.65
5S	Center	12.7	0.5	0.239	7.675	31.02	68.98
5S	Center	9.525	0.375	0.283	9.088	40.11	59.89
5S	Center	7.925	0.3125	0.165	5.299	45.41	54.59
5S	Center	6.35	0.25	0.201	6.455	51.86	48.14
5S	Center	4.74	0.187	0.189	6.069	57.93	42.07
5S	Center	4	0.157	0.068	2.184	60.12	39.88
5S	Center	2.36	0.0937	0.204	6.551	66.67	33.33
5S	Center	1.18	0.0469	0.145	4.656	71.32	28.68
5S	Center	0.6	0.0234	0.296	9.505	80.83	19.17
5S	Center	0.295	0.0116	0.487	15.639	96.47	3.53
5S	Center	0.15	0.006	0.085	2.730	99.20	0.80
5S	Center	0.075	0.0029	0.011	0.353	99.55	0.45
5S	Center	pan		0.014			
				total mass	3.114 kg		
				d50	6.80 mm		
				d50	0.27 in		

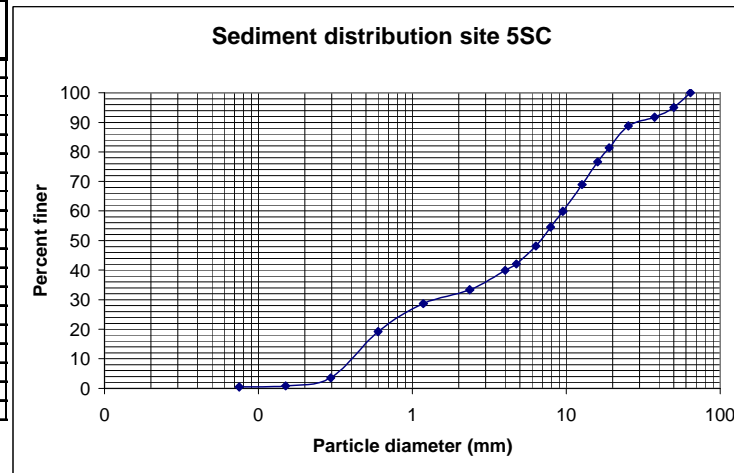
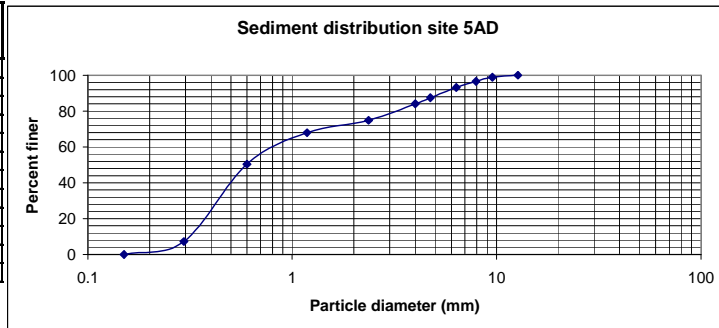


FIGURE 10.15: KILCHIS RIVER SITE 5 ARMOR AND SUB-ARMOR LAYER (CENTER-OF-BAR SAMPLE)

Site	Location	Grain Size (>mm)	Grain Size (>in)	Mass (Kg)	Percent Retained	Cumulative percent retained	% finer
5A	Downstream	12.7	0.5	0	0.000	0.00	100.00
5A	Downstream	9.525	0.375	0.003	1.145	1.15	98.85
5A	Downstream	7.925	0.3125	0.006	2.290	3.44	96.56
5A	Downstream	6.35	0.25	0.009	3.435	6.87	93.13
5A	Downstream	4.74	0.187	0.015	5.725	12.60	87.40
5A	Downstream	4	0.157	0.009	3.435	16.03	83.97
5A	Downstream	2.36	0.0937	0.024	9.160	25.19	74.81
5A	Downstream	1.18	0.0469	0.018	6.870	32.06	67.94
5A	Downstream	0.6	0.0234	0.046	17.557	49.62	50.38
5A	Downstream	0.295	0.0116	0.113	43.130	92.75	7.25
5A	Downstream	0.15	0.006	0.019	7.252	100.00	0.00
5A	Downstream	pan	pan	0			

total mass 0.262 kg
d50 0.60 mm
d50 0.02 in



Site	Location	Grain Size (>mm)	Grain Size (>in)	Mass (Kg)	Percent Retained	Cumulative percent retained	% finer
5S	Downstream	12.7	0.5	0	0.000	0.00	100.00
5S	Downstream	9.525	0.375	0.017	2.152	2.15	97.85
5S	Downstream	7.925	0.3125	0.012	1.519	3.67	96.33
5S	Downstream	6.35	0.25	0.032	4.051	7.72	92.28
5S	Downstream	4.74	0.187	0.039	4.937	12.66	87.34
5S	Downstream	4	0.157	0.017	2.152	14.81	85.19
5S	Downstream	2.36	0.0937	0.053	6.709	21.52	78.48
5S	Downstream	1.18	0.0469	0.051	6.456	27.97	72.03
5S	Downstream	0.6	0.0234	0.158	20.000	47.97	52.03
5S	Downstream	0.295	0.0116	0.332	42.025	90.00	10.00
5S	Downstream	0.15	0.006	0.06	7.595	97.59	2.41
5S	Downstream	0.075	0.0029	0.008	1.013	98.61	1.39
5S	Downstream	pan	pan	0.011			

total mass 0.79 kg
d50 0.59 mm
d50 0.02 in

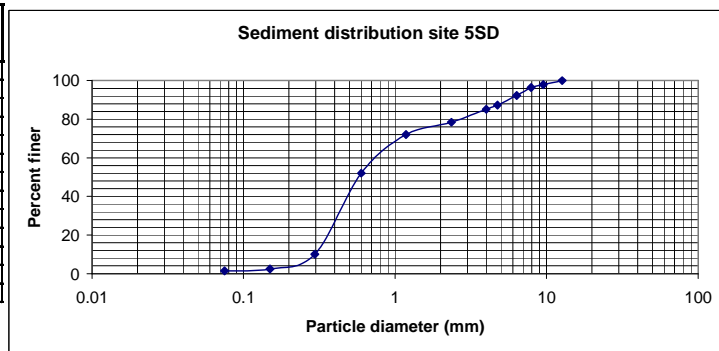
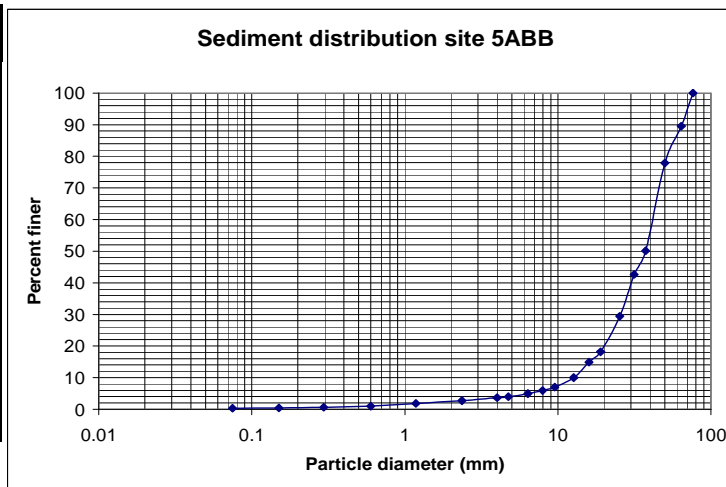


FIGURE 10.16: KILCHIS RIVER SITE 5 ARMOR AND SUB-ARMOR LAYER (DOWNSTREAM-END-OF-BAR SAMPLE)

*sample taken at the back of the bar where erosion of flood deposits was prominent

Site	Location	Grain Size (>mm)	Grain Size (>in)	Mass (kg)	Percent Retained	Cumulative percent retained	% finer
5A	BB	76.2	3	0	0.000	0.00	100.00
5A	BB	64	2.5	0.55	10.504	10.50	89.50
5A	BB	50	2	0.61	11.650	22.15	77.85
5A	BB	37.5	1.5	1.451	27.712	49.87	50.13
5A	BB	31.5	1.25	0.394	7.525	57.39	42.61
5A	BB	25.4	1	0.69	13.178	70.57	29.43
5A	BB	19.05	0.75	0.588	11.230	81.80	18.20
5A	BB	16	0.625	0.173	3.304	85.10	14.90
5A	BB	12.7	0.5	0.257	4.908	90.01	9.99
5A	BB	9.525	0.375	0.155	2.960	92.97	7.03
5A	BB	7.925	0.3125	0.055	1.050	94.02	5.98
5A	BB	6.35	0.25	0.055	1.050	95.07	4.93
5A	BB	4.74	0.187	0.05	0.955	96.03	3.97
5A	BB	4	0.157	0.016	0.306	96.33	3.67
5A	BB	2.36	0.0937	0.048	0.917	97.25	2.75
5A	BB	1.18	0.0469	0.049	0.936	98.19	1.81
5A	BB	0.6	0.0234	0.044	0.840	99.03	0.97
5A	BB	0.295	0.0116	0.019	0.363	99.39	0.61
5A	BB	0.15	0.006	0.01	0.191	99.58	0.42
5A	BB	0.075	0.0029	0.005	0.095	99.68	0.32
5A	BB	pan	pan	0.017			
				total mass	5.236	kg	
				d50	37.39	mm	
				d50	1.47	in	



Site	Location	Grain Size (>mm)	Grain Size (>in)	Mass (kg)	Percent Retained	Cumulative percent retained	% finer
5S	BB	31.5	1.25	0	0.000	0.00	100.00
5S	BB	25.4	1	0.15	10.388	10.39	89.61
5S	BB	19.05	0.75	0.082	5.679	16.07	83.93
5S	BB	16	0.625	0.055	3.809	19.88	80.12
5S	BB	12.7	0.5	0.129	8.934	28.81	71.19
5S	BB	9.525	0.375	0.145	10.042	38.85	61.15
5S	BB	7.925	0.3125	0.08	5.540	44.39	55.61
5S	BB	6.35	0.25	0.1	6.925	51.32	48.68
5S	BB	4.74	0.187	0.102	7.064	58.38	41.62
5S	BB	4	0.157	0.045	3.116	61.50	38.50
5S	BB	2.36	0.0937	0.133	9.211	70.71	29.29
5S	BB	1.18	0.0469	0.139	9.626	80.33	19.67
5S	BB	0.6	0.0234	0.135	9.349	89.68	10.32
5S	BB	0.295	0.0116	0.086	5.956	95.64	4.36
5S	BB	0.15	0.006	0.037	2.562	98.20	1.80
5S	BB	0.075	0.0029	0.009	0.623	98.82	1.18
5S	BB	pan	pan	0.017			
				total mass	1.444	kg	
				d50	6.65	mm	
				d50	0.26	in	

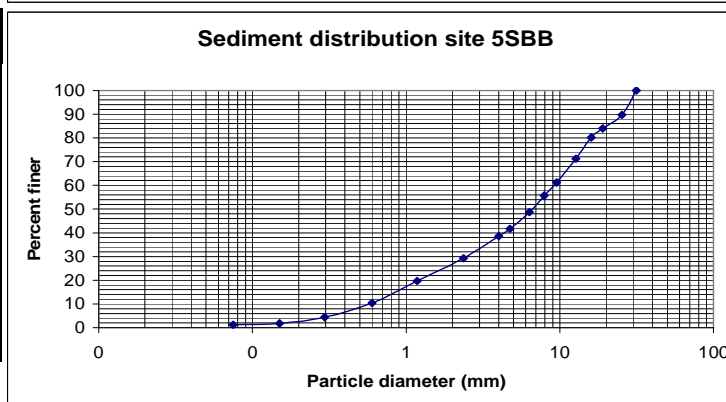


FIGURE 10.17: KILCHIS RIVER SITE 5 ARMOR AND SUB-ARMOR LAYER (SPECIAL NEAR-BANK SAMPLE)

10.3 Appendix C: Willamette River particle size data

10.3.1 Willamette River Bed Material Characteristics (Klingeman 1981)

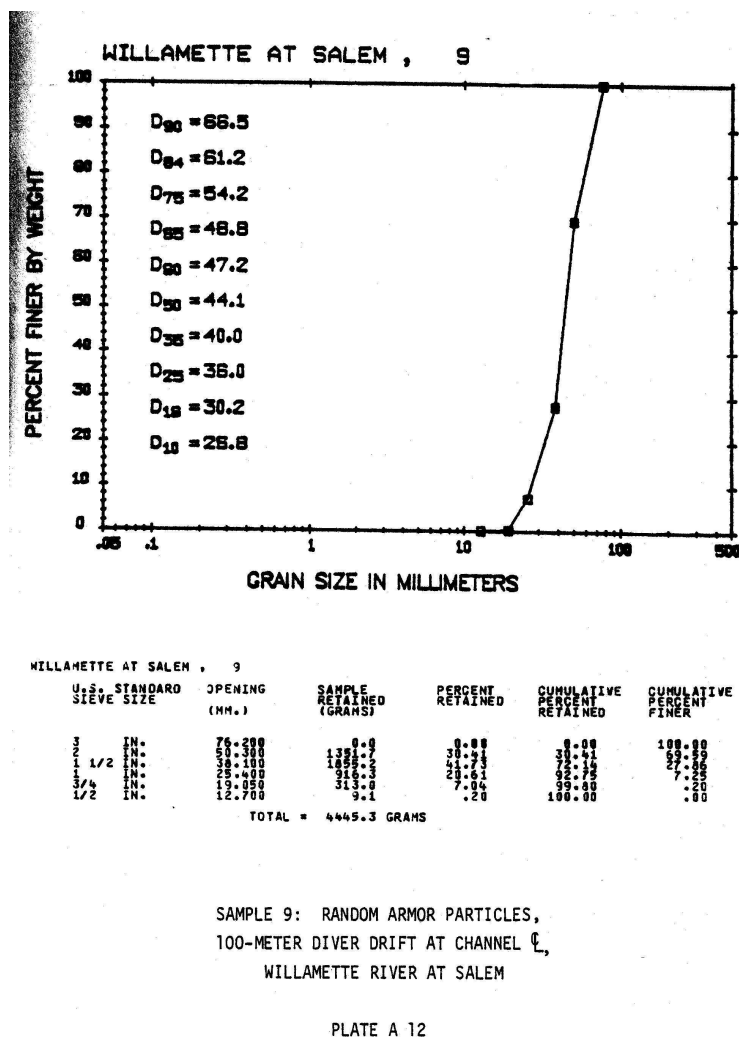
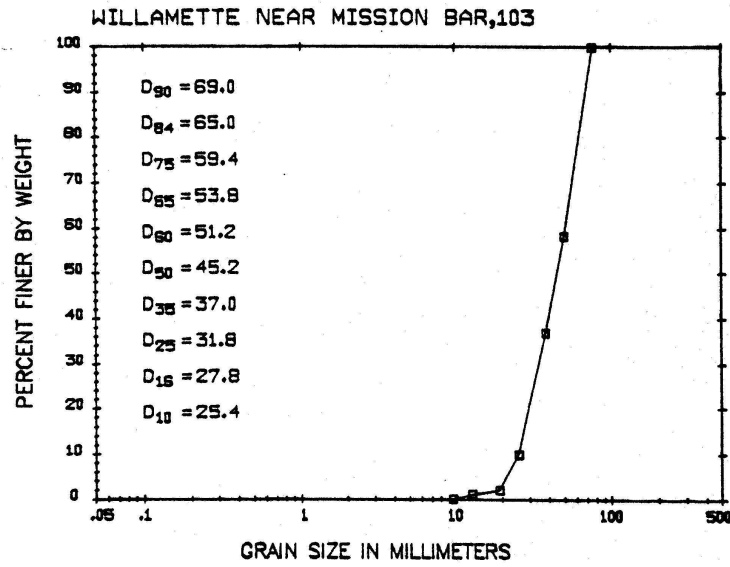


FIGURE 10.18: WILLAMETTE RIVER BED MATERIAL DATA (RANDOM ARMOR LAYER SAMPLE)



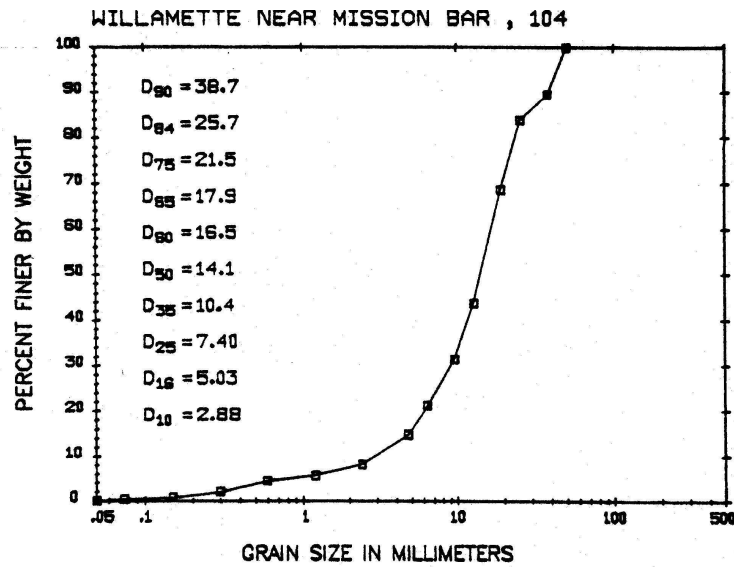
WILLAMETTE NEAR MISSION BAR, 103

U.S. STANDARD SIEVE SIZE	OPENING (MM.)	SAMPLE RETAINED (GRAMS)	PERCENT RETAINED	CUMULATIVE PERCENT RETAINED	CUMULATIVE PERCENT FINER
76	3.00	0.00	0.00	0.00	100.00
100	1.50	2839.0	41.25	41.25	58.75
150	1.00	1431.0	20.89	62.14	37.86
200	0.75	1837.1	27.00	89.14	10.86
250	0.60	539.8	7.80	96.94	3.06
300	0.50	338.6	4.90	101.84	0.16
375	0.425	72.6	1.07	102.91	0.09
		TOTAL = 6884.8 GRAMS			

SAMPLE 103: EXPOSED ARMOR PARTICLES,
 SAMPLER IN SHALLOW WATER NEAR RIGHT-SIDE BAR,
 WILLAMETTE RIVER NEAR MISSION BAR

PLATE A 4

FIGURE 10.19: WILLAMETTE RIVER BED MATERIAL DATA
 (EXPOSED ARMOR LAYER SAMPLE)



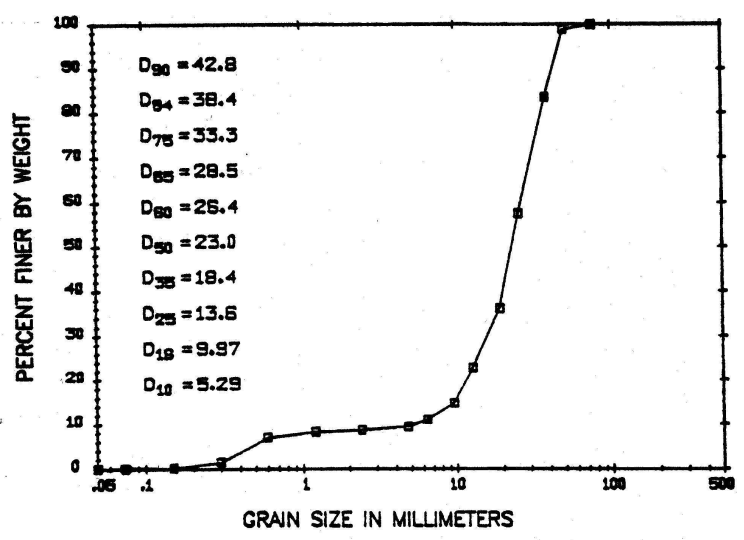
WILLAMETTE NEAR MISSION BAR , 104

U.S. STANDARD SIEVE SIZE	OPENING (MM.)	SAMPLE RETAINED (GRAMS)	PERCENT RETAINED	CUMULATIVE PERCENT RETAINED	CUMULATIVE PERCENT FINER
2	1/2	0.00	0.00	0.00	100.00
1	1/4	0.00	0.00	0.00	100.00
3/4	19.0	0.00	0.00	0.00	100.00
1/2	12.5	0.00	0.00	0.00	100.00
3/8	9.5	0.00	0.00	0.00	100.00
1/4	6.3	0.00	0.00	0.00	100.00
6	2.0	0.00	0.00	0.00	100.00
4	1.18	0.00	0.00	0.00	100.00
3	0.85	0.00	0.00	0.00	100.00
2	0.60	0.00	0.00	0.00	100.00
1	0.425	0.00	0.00	0.00	100.00
1/2	0.25	0.00	0.00	0.00	100.00
3/8	0.15	0.00	0.00	0.00	100.00
2	0.075	0.00	0.00	0.00	100.00
4	0.0475	0.00	0.00	0.00	100.00
10	0.02	0.00	0.00	0.00	100.00
20	0.0075	0.00	0.00	0.00	100.00
40	0.00425	0.00	0.00	0.00	100.00
80	0.002	0.00	0.00	0.00	100.00
150	0.001	0.00	0.00	0.00	100.00
300	0.0005	0.00	0.00	0.00	100.00
600	0.00025	0.00	0.00	0.00	100.00
1000	0.000125	0.00	0.00	0.00	100.00
TOTAL		3257.9	100.00	100.00	0.00

SAMPLE 104; NON-EXPOSED ARMOR PARTICLES,
SAMPLER IN SHALLOW WATER NEAR RIGHT-SIDE BAR,
WILLAMETTE RIVER NEAR MISSION BAR

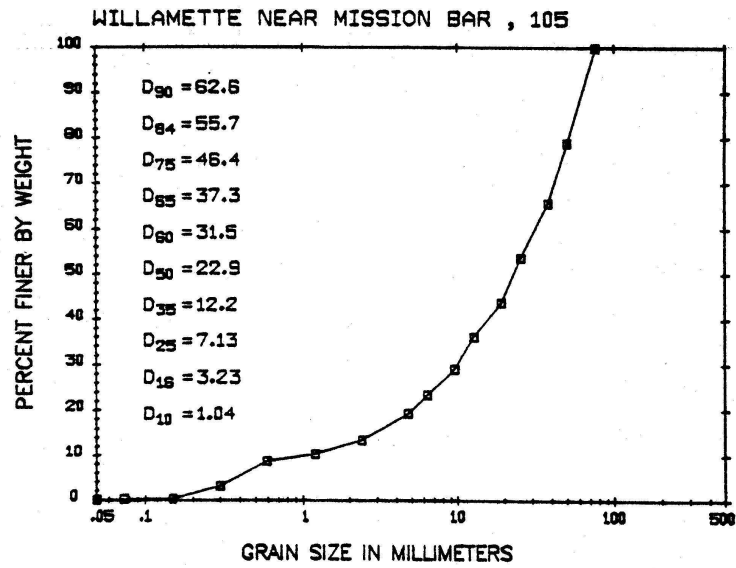
PLATE A 5

FIGURE 10.20: WILLAMETTE RIVER BED MATERIAL DATA
(NON-EXPOSED ARMOR LAYER SAMPLE)



WILLAMETTE AT SALEM , 5

U.S. STANDARD SIEVE SIZE	OPENING (MM.)	SAMPLE RETAINED (GRAMS)	PERCENT RETAINED	CUMULATIVE PERCENT RETAINED	CUMULATIVE PERCENT FINER
3/8 IN.	75	0.0	0.00	0.00	100.00
1/2 IN.	125	217.7	1.20	1.20	98.80
3/4 IN.	190	2787.0	15.22	16.42	83.58
1 IN.	250	4744.7	26.10	42.51	57.49
1 1/4 IN.	375	3869.2	21.28	63.80	36.20
1 1/2 IN.	425	2444.9	13.65	77.45	22.55
2 IN.	500	1461.9	8.14	85.59	14.41
2 1/2 IN.	625	682.6	3.84	89.43	11.07
3 IN.	750	306.1	1.68	91.11	8.89
3 1/2 IN.	900	148.2	.77	91.88	8.12
4 IN.	1000	51.2	.28	92.16	7.84
4 1/2 IN.	1125	234.1	1.29	93.45	6.55
5 IN.	1250	181.8	.97	94.42	5.58
5 1/2 IN.	1375	237.7	1.31	95.73	4.27
6 IN.	1500	18.0	.10	95.83	4.17
6 1/2 IN.	1625	3.6	.02	95.85	4.15
7 IN.	1750			95.85	4.15
7 1/2 IN.	1875			95.85	4.15
8 IN.	2000			95.85	4.15
8 1/2 IN.	2125			95.85	4.15
9 IN.	2250			95.85	4.15
9 1/2 IN.	2375			95.85	4.15
10 IN.	2500			95.85	4.15
10 1/2 IN.	2625			95.85	4.15
11 IN.	2750			95.85	4.15
11 1/2 IN.	2875			95.85	4.15
12 IN.	3000			95.85	4.15
12 1/2 IN.	3125			95.85	4.15
13 IN.	3250			95.85	4.15
13 1/2 IN.	3375			95.85	4.15
14 IN.	3500			95.85	4.15
14 1/2 IN.	3625			95.85	4.15
15 IN.	3750			95.85	4.15
15 1/2 IN.	3875			95.85	4.15
16 IN.	4000			95.85	4.15
16 1/2 IN.	4125			95.85	4.15
17 IN.	4250			95.85	4.15
17 1/2 IN.	4375			95.85	4.15
18 IN.	4500			95.85	4.15
18 1/2 IN.	4625			95.85	4.15
19 IN.	4750			95.85	4.15
19 1/2 IN.	4875			95.85	4.15
20 IN.	5000			95.85	4.15
20 1/2 IN.	5125			95.85	4.15
21 IN.	5250			95.85	4.15
21 1/2 IN.	5375			95.85	4.15
22 IN.	5500			95.85	4.15
22 1/2 IN.	5625			95.85	4.15
23 IN.	5750			95.85	4.15
23 1/2 IN.	5875			95.85	4.15
24 IN.	6000			95.85	4.15
24 1/2 IN.	6125			95.85	4.15
25 IN.	6250			95.85	4.15
25 1/2 IN.	6375			95.85	4.15
26 IN.	6500			95.85	4.15
26 1/2 IN.	6625			95.85	4.15
27 IN.	6750			95.85	4.15
27 1/2 IN.	6875			95.85	4.15
28 IN.	7000			95.85	4.15
28 1/2 IN.	7125			95.85	4.15
29 IN.	7250			95.85	4.15
29 1/2 IN.	7375			95.85	4.15
30 IN.	7500			95.85	4.15
30 1/2 IN.	7625			95.85	4.15
31 IN.	7750			95.85	4.15
31 1/2 IN.	7875			95.85	4.15
32 IN.	8000			95.85	4.15
32 1/2 IN.	8125			95.85	4.15
33 IN.	8250			95.85	4.15
33 1/2 IN.	8375			95.85	4.15
34 IN.	8500			95.85	4.15
34 1/2 IN.	8625			95.85	4.15
35 IN.	8750			95.85	4.15
35 1/2 IN.	8875			95.85	4.15
36 IN.	9000			95.85	4.15
36 1/2 IN.	9125			95.85	4.15
37 IN.	9250			95.85	4.15
37 1/2 IN.	9375			95.85	4.15
38 IN.	9500			95.85	4.15
38 1/2 IN.	9625			95.85	4.15
39 IN.	9750			95.85	4.15
39 1/2 IN.	9875			95.85	4.15
40 IN.	10000			95.85	4.15
40 1/2 IN.	10125			95.85	4.15
41 IN.	10250			95.85	4.15
41 1/2 IN.	10375			95.85	4.15
42 IN.	10500			95.85	4.15
42 1/2 IN.	10625			95.85	4.15
43 IN.	10750			95.85	4.15
43 1/2 IN.	10875			95.85	4.15
44 IN.	11000			95.85	4.15
44 1/2 IN.	11125			95.85	4.15
45 IN.	11250			95.85	4.15
45 1/2 IN.	11375			95.85	4.15
46 IN.	11500			95.85	4.15
46 1/2 IN.	11625			95.85	4.15
47 IN.	11750			95.85	4.15
47 1/2 IN.	11875			95.85	4.15
48 IN.	12000			95.85	4.15
48 1/2 IN.	12125			95.85	4.15
49 IN.	12250			95.85	4.15
49 1/2 IN.	12375			95.85	4.15
50 IN.	12500			95.85	4.15
50 1/2 IN.	12625			95.85	4.15
51 IN.	12750			95.85	4.15
51 1/2 IN.	12875			95.85	4.15
52 IN.	13000			95.85	4.15
52 1/2 IN.	13125			95.85	4.15
53 IN.	13250			95.85	4.15
53 1/2 IN.	13375			95.85	4.15
54 IN.	13500			95.85	4.15
54 1/2 IN.	13625			95.85	4.15
55 IN.	13750			95.85	4.15
55 1/2 IN.	13875			95.85	4.15
56 IN.	14000			95.85	4.15
56 1/2 IN.	14125			95.85	4.15
57 IN.	14250			95.85	4.15
57 1/2 IN.	14375			95.85	4.15
58 IN.	14500			95.85	4.15
58 1/2 IN.	14625			95.85	4.15
59 IN.	14750			95.85	4.15
59 1/2 IN.	14875			95.85	4.15
60 IN.	15000			95.85	4.15
60 1/2 IN.	15125			95.85	4.15
61 IN.	15250			95.85	4.15
61 1/2 IN.	15375			95.85	4.15
62 IN.	15500			95.85	4.15
62 1/2 IN.	15625			95.85	4.15
63 IN.	15750			95.85	4.15
63 1/2 IN.	15875			95.85	4.15
64 IN.	16000			95.85	4.15
64 1/2 IN.	16125			95.85	4.15
65 IN.	16250			95.85	4.15
65 1/2 IN.	16375			95.85	4.15
66 IN.	16500			95.85	4.15
66 1/2 IN.	16625			95.85	4.15
67 IN.	16750			95.85	4.15
67 1/2 IN.	16875			95.85	4.15
68 IN.	17000			95.85	4.15
68 1/2 IN.	17125			95.85	4.15
69 IN.	17250			95.85	4.15
69 1/2 IN.	17375			95.85	4.15
70 IN.	17500			95.85	4.15
70 1/2 IN.	17625			95.85	4.15
71 IN.	17750			95.85	4.15
71 1/2 IN.	17875			95.85	4.15
72 IN.	18000			95.85	4.15
72 1/2 IN.	18125			95.85	4.15
73 IN.	18250			95.85	4.15
73 1/2 IN.	18375			95.85	4.15
74 IN.	18500			95.85	4.15
74 1/2 IN.	18625			95.85	4.15
75 IN.	18750			95.85	4.15
75 1/2 IN.	18875			95.85	4.15
76 IN.	19000			95.85	4.15
76 1/2 IN.	19125			95.85	4.15
77 IN.	19250			95.85	4.15
77 1/2 IN.	19375			95.85	4.15
78 IN.	19500			95.85	4.15
78 1/2 IN.	19625			95.85	4.15
79 IN.	19750			95.85	4.15
79 1/2 IN.	19875			95.85	4.15
80 IN.	20000			95.85	4.15
80 1/2 IN.	20125			95.85	4.15
81 IN.	20250			95.85	4.15
81 1/2 IN.	20375			95.85	4.15
82 IN.	20500			95.85	4.15
82 1/2 IN.	20625			95.85	4.15
83 IN.	20750			95.85	4.15
83 1/2 IN.	20875			95.85	4.15
84 IN.	21000			95.85	4.15
84 1/2 IN.	21125			95.85	4.15
85 IN.	21250			95.85	4.15
85 1/2 IN.	21375			95.85	4.15
86 IN.	21500			95.85	4.15
86 1/2 IN.	21625			95.85	4.15
87 IN.	21750			95.85	4.15
87 1/2 IN.	21875			95.85	4.15
88 IN.	22000			95.85	4.15
88 1/2 IN.	22125			95.85	4.15
89 IN.	22250			95.85	4.15
89 1/2 IN.	22375			95.85	4.15
90 IN.	22500			95.85	4.15
90 1/2 IN.	22625			95.85	4.15
91 IN.	22750			95.85	4.15
91 1/2 IN.	22875			95.85	4.15
92 IN.	23000			95.85	4.15
92 1/2 IN.	23125			95.85	4.15
93 IN.	23250			95.85	4.15
93 1/2 IN.	23375			95.85	4.15
94 IN.	23500			95.85	4.15
94 1/2 IN.	23625			95.85	4.15
95 IN.	23750			95.85	4.15
95 1/2 IN.	23875			95.85	4.15
96 IN.	24000			95.85	4.15
96 1/2 IN.	24125			95.85	4.15
97 IN.	24250				



WILLAMETTE NEAR MISSION BAR , 105

U.S. STANDARD SIEVE SIZE	OPENING (MM.)	SAMPLE RETAINED (GRAMS)	PERCENT RETAINED	CUMULATIVE PERCENT RETAINED	CUMULATIVE PERCENT FINER
3	IN.	76.200	0.0	0.00	100.00
2	IN.	59.300	0.0	0.00	78.85
1 1/2	IN.	38.100	2076.7	13.28	65.56
1	IN.	25.400	226.5	12.86	53.70
3/4	IN.	19.050	1860.8	9.96	43.74
1/2	IN.	12.700	1430.0	7.66	36.08
3/8	IN.	9.525	1334.3	7.03	29.05
1/4	IN.	6.350	1027.2	5.47	23.58
6		5.750	774.0	4.22	19.36
8		4.750	1774.0	3.86	15.50
16		2.360	571.3	3.08	11.42
30		.990	311.1	2.00	9.42
50		.297	1044.9	1.00	8.42
100		.149	522.1	2.01	7.41
200		.074	21.9	.12	7.29
< 200		.058	21.9	.12	7.17

TOTAL = 10766.7 GRAMS

SAMPLE 105: SUBARMOR LAYER,
SAMPLER IN SHALLOW WATER NEAR RIGHT-SIDE BAR,
WILLAMETTE RIVER NEAR MISSION BAR

PLATE A 6

FIGURE 10.22: WILLAMETTE RIVER BED MATERIAL DATA
(SUB-ARMOR LAYER SAMPLE)

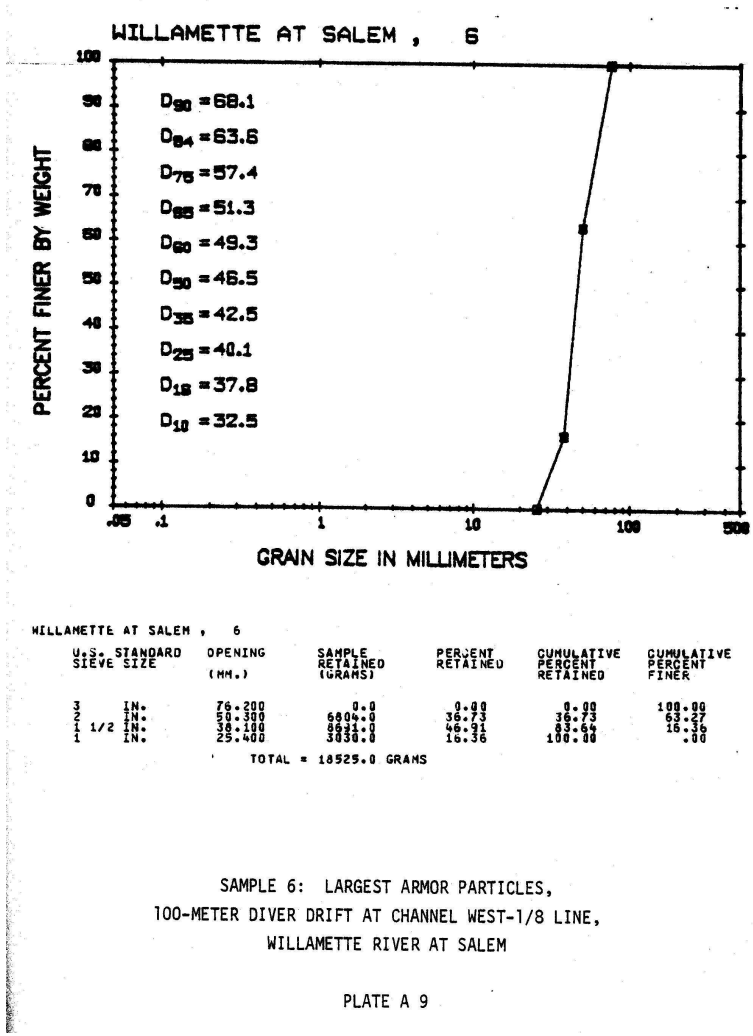


FIGURE 10.23: WILLAMETTE RIVER BED MATERIAL DATA
(LARGEST ARMOR LAYER SAMPLE)

10.4 Appendix D: Hydrologic Analyses

10.4.1 Wilson River mean monthly discharge data used in Kilchis River analysis (USGS)

TABLE 10.1: USGS MEAN MONTHLY DATA FOR WILSON RIVER

Date	Oct	Nov	Dec	Jan	Feb	Mar	Apr	May	Jun	July	Aug	Sept
1914	1100	1500	1135									
1915				2612	1956	1232	1044	612	355	222	127	99
1916												136
1931	804	2244	2235								98	121
1932	197	2973	3411	2753	2213	3323	1823	428	187	122	99	76
1933	1192	1149	7988	2920	2016	2892	1265	1391	876	208	118	397
1934	2087	3975	3091	3721	718	1764	914	744	191	131	98	124
1935	216	794	1446	3068	1549	2039	1131	438	196	171	106	132
1936	88	87	2133	4527	2044	1668	633	932	470	266	142	120
1937	430	3621	4000	940	2658	2101	2550	876	637	304	169	120
1938	222	1453	1744	2145	1588	2269	1445	439	183	111	78	75
1939	271	422	3056	2041	2659	1540	426	202	253	156	89	74
1940	346	1105	1429	1527	3301	1858	926	873	181	108	79	77
1941	781	1443	3119	2064	751	595	489	704	285	146	120	765
1942	213	3280	3178	1015	1778	943	563	617	577	278	141	95
1943	487	784	1666	1647	2921	1407	1758	476	389	183	121	89
1944	167	1149	852	1540	1380	1072	1165	402	359	133	86	101
1945	206	3086	3105	2246	2535	2497	1399	896	268	127	91	432
1946	615	2750	3709	3006	2736	1990	1115	352	264	298	120	97
1947	2230	2278	1651	1933	2233	1211	938	273	457	222	123	230
1948	581	2216	3487	2437	2596	1603	1539	1386	312	153	109	169
1949	455	2332	2497	694	4268	1718	715	920	186	124	91	91
1950	1285	2610	3096	3055	3506	3294	1790	660	238	126	107	93
1951	1942	1807	2717	3498	2944	1664	852	445	200	104	69	111
1952	58	146	1718	1699	2453	1515	939	446	213	127	83	67
1953	599	1950	3686	5776	2314	1495	872	916	405	191	155	141
1954	613	1922	1908	3413	3540	1215	1489	269	469	266	139	159
1955	1588	3935	4368	1781	1834	1930	2069	821	287	202	117	122
1956	705	1033	2398	3476	1130	3637	1238	317	268	126	104	88
1957	198	932	3740	818	2394	2170	1059	429	317	177	133	81
1958	233	2974	2270	3036	2884	909	1943	400	201	102	68	69
1959	1476	1675	1593	3429	1587	1452	1456	859	510	245	106	780
1960	467	3583	1414	1359	2795	1727	1751	1138	359	136	120	91
1961	591	1550	2878	2379	4619	3159	827	689	199	106	68	87
1962	930	2962	1758	1419	1171	1688	1301	902	267	126	124	154
1963	649	2749	1443	952	2269	1059	1724	788	205	139	129	119
1964	244	1850	4576	4595	1329	1926	764	503	299	175	211	119
1965	131	1300	1380	3395	1979	597	587	520	218	108	81	64

1966	392	1135	3706	3924	1550	2663	845	316	175	115	64	64
1967	1237	1129	2231	3331	1463	1679	923	383	167	79	44	40
1968	826	2515	3133	2028	3646	1882	846	464	738	160	240	350
1969	648	1058	2196	2203	1833	1660	1300	570	337	200	103	238
1970	519	1822	3788	3876	1916	1005	947	538	191	101	58	98
1971	706	2262	2841	4389	2019	3073	1520	640	391	272	135	294
1972	111	945	3335	4854	3058	3105	1630	518	203	122	73	205
1973	449	3780	3752	2318	642	1162	671	385	318	197	87	220
1974	68	1147	2638	3930	2591	2599	1765	677	453	254	113	76
1975	993	2284	4143	3847	2498	1881	849	798	211	125	127	119
1976	97	271	378	3151	2021	2076	1190	496	296	177	110	79
1977	672	3129	4693	344	674	2135	640	557	490	130	127	455
1978	185	796	1482	1839	1585	840	1016	952	370	162	116	474
1979	388	715	2535	677	2692	1633	759	728	200	142	76	130
1980	90	1518	3762	2524	1685	1307	1104	323	212	122	68	72
1981	1040	1668	3448	753	2756	725	1512	535	810	250	111	125
1982	623	1345	3209	2822	3765	1707	1552	415	164	103	73	88
1983	117	3066	1617	2777	2521	2215	1061	496	363	514	175	176
1984	527	2785	1630	1738	1695	1465	1109	1287	552	217	114	127
1985	676	1312	1030	665	986	1070	1094	409	634	145	99	142
1986	242	2086	1148	1956	2582	1275	634	625	197	118	62	101
1987	44	170	2342	1794	2002	2532	570	384	290	137	83	58
1988	120	2509	1353	1957	1180	1563	1233	784	498	189	94	83
1989	158	834	2334	2748	1432	2251	1102	262	162	138	88	59
1990	404	2289	1446	3790	3353	1548	678	475	604	162	91	77
1991	70	1123	1848	2144	2036	1385	2622	547	331	165	90	64
1992	139	1329	1809	2115	1565	406	1055	389	131	77	50	86
1993	71	95	1681	1589	634	1601	1885	874	454	199	113	70
1994	595	2328	4603	2131	2130	1723	910	281	404	148	82	74
1995	527	4266	3690	2265	2611	1596	896	440	214	113	81	89
1996	828	1978	4750	3176	5037	1041	2605	922	318	149	92	120
1997	2249	2305	1837	2997	1784	3071	1195	588	372	200	106	520
1998	343	3012	4799	3562	1973	1673	587	460	255	132	77	71
1999	143	3210	3721	3533	5165	1996	956	985	312	146	88	62
2000	192	326	1039	1940	1923	1389	611	975	864	195	102	92
2001	168	2512	4003	674	837	756	709	799	278	139	126	78
2002	55	409	1800	3400	2164	1996	1550	373	238	156	78	58
2003	422	1321	2113	2854	1952	3347	1241	535	181	104	77	73
2004				2674	1689	1058	730	417	568	159	241	535
2005										312	1725	2335
2006	5374	1941	1328	858	3041	278	118	70	67			

10.4.2 Kilchis River flood frequency analysis using Wilson River derived data

TABLE 10.2: PEAK DISCHARGE VALUES FOR WILSON RIVER SCALED FOR KILCHIS RIVER

Source	Gage	Date	Year	Peak Q (Wilson)	Peak Q (Kilchis)		YEAR	MAX
USGS	14301500	1/14/1915	1915	7500	3540		1915	3540
USGS	14301500	1/18/1932	1932	16700	7883		1932	7883
USGS	14301500	12/19/1932	1932	12900	6089		1933	14161
USGS	14301500	12/21/1933	1933	30000	14161		1935	6750
USGS	14301500	1/22/1935	1935	14300	6750		1936	9205
USGS	14301500	1/12/1936	1936	19500	9205		1937	10007
USGS	14301500	12/22/1936	1936	16600	7836		1939	8025
USGS	14301500	12/27/1937	1937	21200	10007		1941	8827
USGS	14301500	2/14/1939	1939	15800	7458		1942	8402
USGS	14301500	12/15/1939	1939	17000	8025		1943	5617
USGS	14301500	1/18/1941	1941	11900	5617		1945	10763
USGS	14301500	12/19/1941	1941	18700	8827		1946	8544
USGS	14301500	11/23/1942	1942	17800	8402		1948	6373
USGS	14301500	12/2/1943	1943	11900	5617		1949	11565
USGS	14301500	2/7/1945	1945	22800	10763		1950	5145
USGS	14301500	12/28/1945	1945	17100	8072		1952	6278
USGS	14301500	12/13/1946	1946	18100	8544		1953	9583
USGS	14301500	2/22/1948	1948	13500	6373		1954	6986
USGS	14301500	2/17/1949	1949	24500	11565		1955	9960
USGS	14301500	11/27/1949	1949	20200	9535		1956	8261
USGS	14301500	12/23/1950	1950	10900	5145		1957	7742
USGS	14301500	2/4/1952	1952	13300	6278		1958	7081
USGS	14301500	1/19/1953	1953	13900	6561		1959	5429
USGS	14301500	12/9/1953	1953	20300	9583		1960	9394
USGS	14301500	11/18/1954	1954	14800	6986		1961	10243
USGS	14301500	12/21/1955	1955	21100	9960		1963	10243
USGS	14301500	12/9/1956	1956	17500	8261		1964	15153
USGS	14301500	12/19/1957	1957	16400	7742		1966	9488
USGS	14301500	11/18/1958	1958	15000	7081		1968	7506
USGS	14301500	11/22/1959	1959	11500	5429		1970	5948
USGS	14301500	11/24/1960	1960	19900	9394		1972	16994
USGS	14301500	11/22/1961	1961	21700	10243		1974	9724
USGS	14301500	2/3/1963	1963	21700	10243		1975	13878
USGS	14301500	1/25/1964	1964	25000	11801		1977	15106
USGS	14301500	12/22/1964	1964	32100	15153		1979	6278
USGS	14301500	1/5/1966	1966	17100	8072		1980	11848
USGS	14301500	12/13/1966	1966	20100	9488		1982	9063

USGS	14301500	2/4/1968	1968	15900	7506		1984	3989
USGS	14301500	12/3/1968	1968	11300	5334		1986	7317
USGS	14301500	1/18/1970	1970	12600	5948		1987	12320
USGS	14301500	12/6/1970	1970	18800	8875		1989	14634
USGS	14301500	1/20/1972	1972	36000	16994		1991	12179
USGS	14301500	12/21/1972	1972	22000	10385		1992	6137
USGS	14301500	1/15/1974	1974	20600	9724		1994	9441
USGS	14301500	1/13/1975	1975	14100	6656		1996	16522
USGS	14301500	12/4/1975	1975	29400	13878		1997	10338
USGS	14301500	3/7/1977	1977	6680	3153		1998	16663
USGS	14301500	12/13/1977	1977	32000	15106		1999	11990
USGS	14301500	3/5/1979	1979	13300	6278		2000	1770
USGS	14301500	1/12/1980	1980	16300	7694		2001	7742
USGS	14301500	12/26/1980	1980	25100	11848		2003	8402
USGS	14301500	1/24/1982	1982	19200	9063		2004	5948
USGS	14301500	12/3/1982	1982	18700	8827			
USGS	14301500	2/12/1984	1984	8450	3989			
USGS	14301500	11/2/1984	1984	7800	3682			
USGS	14301500	2/23/1986	1986	15500	7317			
USGS	14301500	2/1/1987	1987	18900	8922			
USGS	14301500	12/9/1987	1987	26100	12320			
USGS	14301500	1/10/1989	1989	10000	4720			
USGS	14301500	12/4/1989	1989	31000	14634			
USGS	14301500	4/5/1991	1991	25800	12179			
USGS	14301500	1/28/1992	1992	13000	6137			
USGS	14301500	11/21/1992	1992	11600	5476			
USGS	14301500	2/24/1994	1994	8180	3861			
USGS	14301500	11/30/1994	1994	20000	9441			
USGS	14301500	2/8/1996	1996	35000	16522			
USGS	14301500	12/29/1996	1996	15400	7270			
USGS	14301500	10/30/1997	1997	21900	10338			
USGS	14301500	12/27/1998	1998	35300	16663			
USGS	14301500	11/25/1999	1999	25400	11990			
USGS	14301500	12/23/2000	2000	3750	1770			
USGS	14301500	12/16/2001	2001	16400	7742			
USGS	14301500	1/31/2003	2003	17800	8402			
USGS	14301500	1/29/2004	2004	12600	5948			

TABLE 10.3: STATISTICAL ANALYSIS FOR KILCHIS RIVER FLOOD FREQUENCY

ANALYSIS

RANK	YEAR	MAX	LOG Q	$(\log Q - \text{avg}(\log Q))^2$	$(\log Q - \text{avg}(\log Q))^3$	Tr	Exceed
1	1915	16994	4.230	0.0877	0.0260	20.00	0.050
2	1932	16663	4.222	0.0827	0.0238	10.00	0.100
3	1933	16522	4.218	0.0806	0.0229	6.67	0.150
4	1935	15153	4.180	0.0607	0.0149	5.00	0.200
5	1936	15106	4.179	0.0600	0.0147	4.00	0.250
6	1937	14634	4.165	0.0534	0.0124	3.33	0.300
7	1939	14161	4.151	0.0471	0.0102	2.86	0.350
8	1941	13878	4.142	0.0433	0.0090	2.50	0.400
9	1942	12320	4.091	0.0245	0.0038	2.22	0.450
10	1943	12179	4.086	0.0229	0.0035	2.00	0.500
11	1945	11990	4.079	0.0209	0.0030	1.82	0.550
12	1946	11848	4.074	0.0195	0.0027	1.67	0.600
13	1948	11565	4.063	0.0166	0.0021	1.54	0.650
14	1949	10763	4.032	0.0096	0.0009	1.43	0.700
15	1950	10338	4.014	0.0064	0.0005	1.33	0.750
16	1952	10243	4.010	0.0058	0.0004	1.25	0.800
17	1953	10243	4.010	0.0058	0.0004	1.18	0.850
18	1954	10007	4.000	0.0044	0.0003	1.11	0.900
19	1955	9960	3.998	0.0041	0.0003	1.05	0.950
20	1956	9724	3.988	0.0029	0.0002	1.00	1.000
21	1957	9583	3.981	0.0022	0.0001	0.95	1.050
22	1958	9488	3.977	0.0018	0.0001	0.91	1.100
23	1959	9441	3.975	0.0017	0.0001	0.87	1.150
24	1960	9394	3.973	0.0015	0.0001	0.83	1.200
25	1961	9205	3.964	0.0009	0.0000	0.80	1.250
26	1963	9063	3.957	0.0005	0.0000	0.77	1.300
27	1964	8827	3.946	0.0001	0.0000	0.74	1.350
28	1966	8544	3.932	0.0000	0.0000	0.71	1.400
29	1968	8402	3.924	0.0001	0.0000	0.69	1.450
30	1970	8402	3.924	0.0001	0.0000	0.67	1.500
31	1972	8261	3.917	0.0003	0.0000	0.65	1.550
32	1974	8025	3.904	0.0009	0.0000	0.63	1.600
33	1975	7883	3.897	0.0014	-0.0001	0.61	1.650
34	1977	7742	3.889	0.0021	-0.0001	0.59	1.700
35	1979	7742	3.889	0.0021	-0.0001	0.57	1.750
36	1980	7506	3.875	0.0035	-0.0002	0.56	1.800
37	1982	7317	3.864	0.0049	-0.0003	0.54	1.850
38	1984	7081	3.850	0.0071	-0.0006	0.53	1.900
39	1986	6986	3.844	0.0081	-0.0007	0.51	1.950
40	1987	6750	3.829	0.0110	-0.0012	0.50	2.000
41	1989	6373	3.804	0.0169	-0.0022	0.49	2.050
42	1991	6278	3.798	0.0186	-0.0025	0.48	2.100
43	1992	6278	3.798	0.0186	-0.0025	0.47	2.150

44	1994	6137	3.788	0.0214	-0.0031	0.45	2.200
45	1996	5948	3.774	0.0255	-0.0041	0.44	2.250
46	1997	5948	3.774	0.0255	-0.0041	0.43	2.300
47	1998	5617	3.750	0.0341	-0.0063	0.43	2.350
48	1999	5429	3.735	0.0398	-0.0079	0.42	2.400
49	2000	5145	3.711	0.0496	-0.0111	0.41	2.450
50	2001	3989	3.601	0.1111	-0.0370	0.40	2.500
51	2003	3540	3.549	0.1483	-0.0571	0.39	2.550
52	2004	1770	3.248	0.4708	-0.3231	0.38	2.600
	avg	9277	3.934	1.6894	-0.3119		
	var	0.0331					
	std dev	0.182					
	skew cof	-1.0552					

TABLE 10.4: KILCHIS RIVER FLOOD FREQUENCY VALUES FOR FLOOD FREQUENCY PLOT

Return period	Freq factor (K)	logQ	Q (cfs) Kilchis
2	0.18	3.967	9267
5	0.848	4.089	12261
10	1.107	4.136	13667
25	1.324	4.175	14968
50	1.435	4.195	15680
100	1.518	4.210	16235
200	1.581	4.222	16670

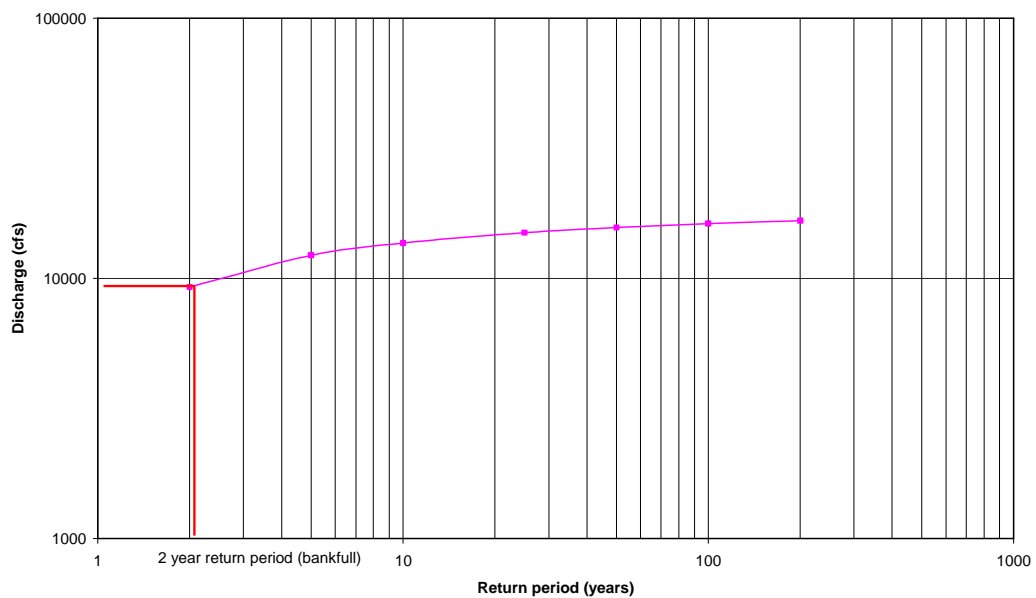


FIGURE 10.24: FLOOD FREQUENCY ANALYSIS FOR THE KILCHIS RIVER AS DERIVED FROM THE WILSON RIVER GAGE

10.4.3 Flow duration analysis for the Kilchis River derived from scaled Wilson river data

TABLE 10.5: MEAN DAILY DISCHARGE SEPARATED INTO SIZE CLASSES FOR KILCHIS
RIVER ANALYSIS

Class Boundaries	Class Boundaries	# of occurrences in each class	Cumulative # of days	Percent of time flow is exceeded (%)	Exceedence Frequency (%) (100-% Not Exceeded)
15	0-14	0	0	0.00	100.00
20	15-19	49	49	0.18	99.82
30	20-29	752	801	2.95	97.05
40	30-39	1665	2466	9.09	90.91
50	40-49	1669	4135	15.25	84.75
70	50-69	2192	6327	23.33	76.67
100	70-99	1822	8149	30.05	69.95
150	100-149	2083	10232	37.73	62.27
200	150-199	1562	11794	43.49	56.51
300	200-299	2548	14342	52.88	47.12
400	300-399	2135	16477	60.76	39.24
500	400-499	1718	18195	67.09	32.91
700	500-699	2521	20716	76.39	23.61
1000	700-999	2160	22876	84.35	15.65
1500	1000-1499	1874	24750	91.26	8.74
2000	1500-1999	916	25666	94.64	5.36
3000	2000-2999	850	26516	97.77	2.23
4000	3000-3999	294	26810	98.86	1.14
5000	4000-4999	147	26957	99.40	0.60
7000	5000-6999	126	27083	99.86	0.14
10000	7000-9999	28	27111	99.97	0.03
15000	10000-14999	9	27120	100.00	0.00

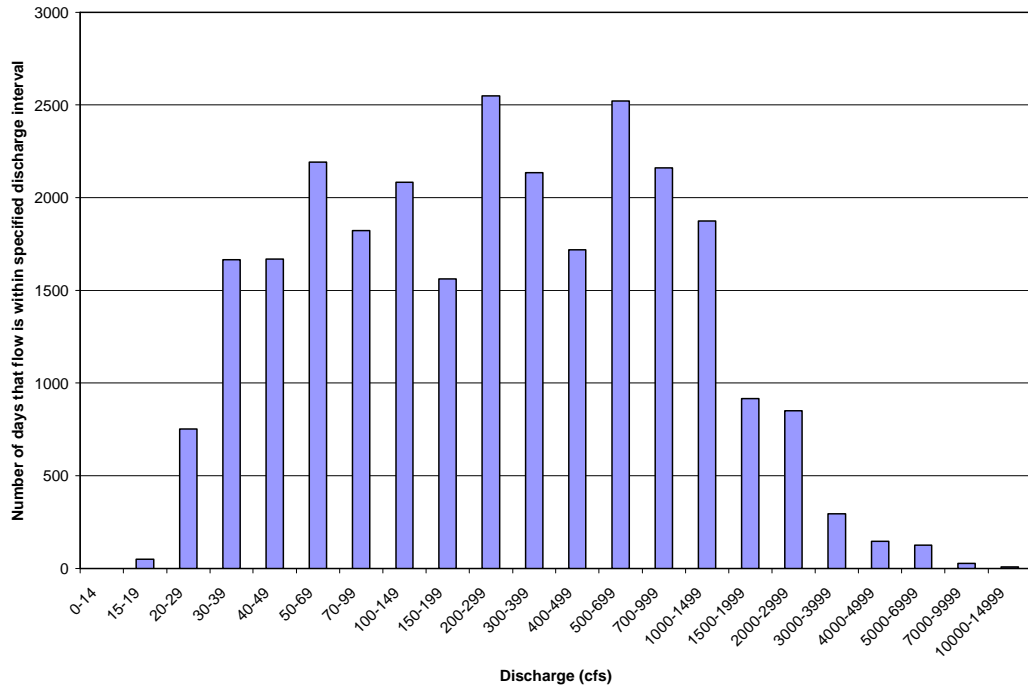


FIGURE 10.25: FREQUENCY DISTRIBUTION FOR LOG CYCLE CLASS INTERVALS FOR KILCHIS RIVER AS DERIVED FROM WILSON RIVER GAGE

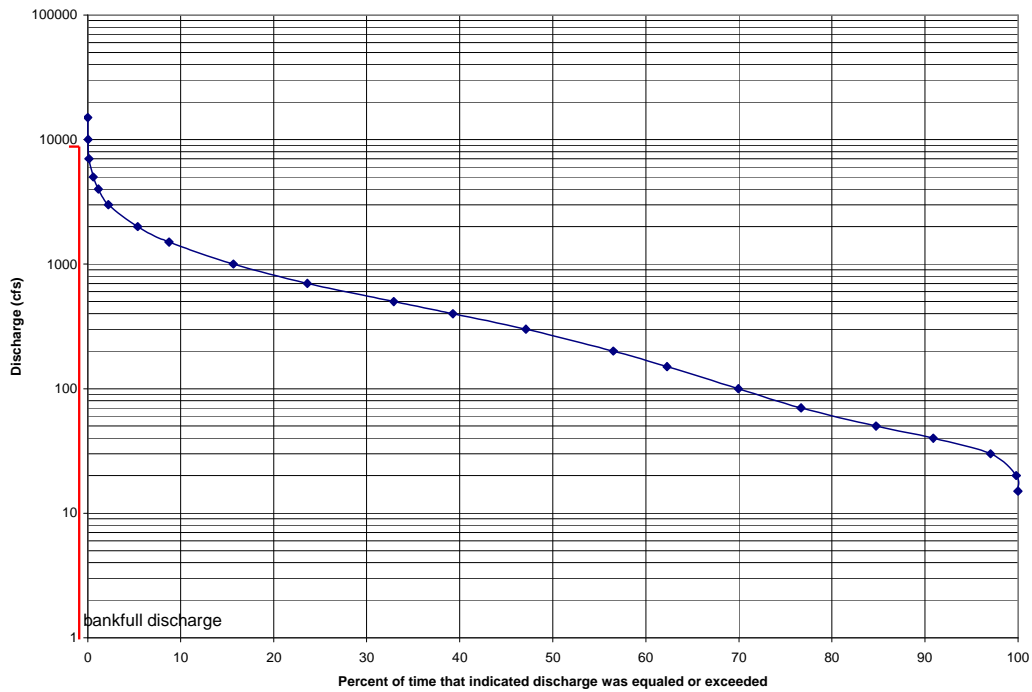


FIGURE 10.26: FLOW DURATION CURVE (LOG INTERVALS) FOR KILCHIS RIVER AS DERIVED FROM WILSON RIVER GAGE

TABLE 10.6: MEAN DAILY DISCHARGE FOR KILCHIS RIVER (DERIVED FROM WILSON RIVER GAGE, USGS)

Day of month	Mean of daily mean values for this day for 76 years of record ¹ , in ft ³ /s											
	Jan	Feb	Mar	Apr	May	Jun	Jul	Aug	Sep	Oct	Nov	Dec
1	1062	1147	845	786	394	202	110	55	53	99	514	1224
2	1129	1104	909	699	403	211	109	56	59	127	558	1474
3	1066	1041	900	650	405	187	105	56	55	126	605	1360
4	1211	981	867	668	394	180	100	55	81	140	572	1397
5	1244	902	878	690	400	174	96	53	70	145	555	1273
6	1233	1113	834	615	388	170	93	52	63	157	560	1362
7	1242	1199	827	570	359	194	91	52	60	146	577	1217
8	1161	1115	798	563	338	202	92	51	58	153	656	1051
9	1193	978	862	591	321	206	91	50	57	224	649	1156
10	1075	1032	892	590	312	190	88	49	65	232	608	1207
11	1127	987	872	580	319	181	86	48	68	238	726	1258
12	1228	1032	935	587	295	201	84	47	62	212	761	1278
13	1184	1027	900	624	293	178	83	46	61	204	776	1371
14	1375	970	854	617	295	168	81	45	62	184	870	1202
15	1379	993	851	583	284	162	79	45	66	187	884	1261
16	1312	1115	832	551	282	160	78	45	72	190	859	1258
17	1250	1176	813	561	279	156	78	44	81	187	864	1240
18	1247	1076	850	519	279	151	76	44	84	204	941	1185
19	1258	1169	842	503	274	149	74	44	93	236	956	1274
20	1261	1095	801	551	277	144	71	44	94	270	1153	1297
21	1154	1065	774	498	260	139	68	43	96	267	1056	1353
22	1145	1132	820	470	246	136	67	44	86	336	1101	1469
23	1177	1050	836	541	239	134	64	49	86	409	1112	1316
24	1275	1065	850	496	232	128	63	52	85	391	1337	1195
25	1347	957	805	450	223	130	61	58	81	416	1473	1156
26	1135	930	739	415	218	124	61	58	85	379	1316	1174
27	1087	971	745	416	212	119	60	53	82	422	1190	1320
28	1108	923	790	409	210	116	59	53	79	461	1094	1275
29	1081	1060	815	387	202	119	59	53	84	456	1059	1162
30	1003		811	388	200	114	57	53	90	500	1105	1229
31	1075		809		201		56	51		515		1109

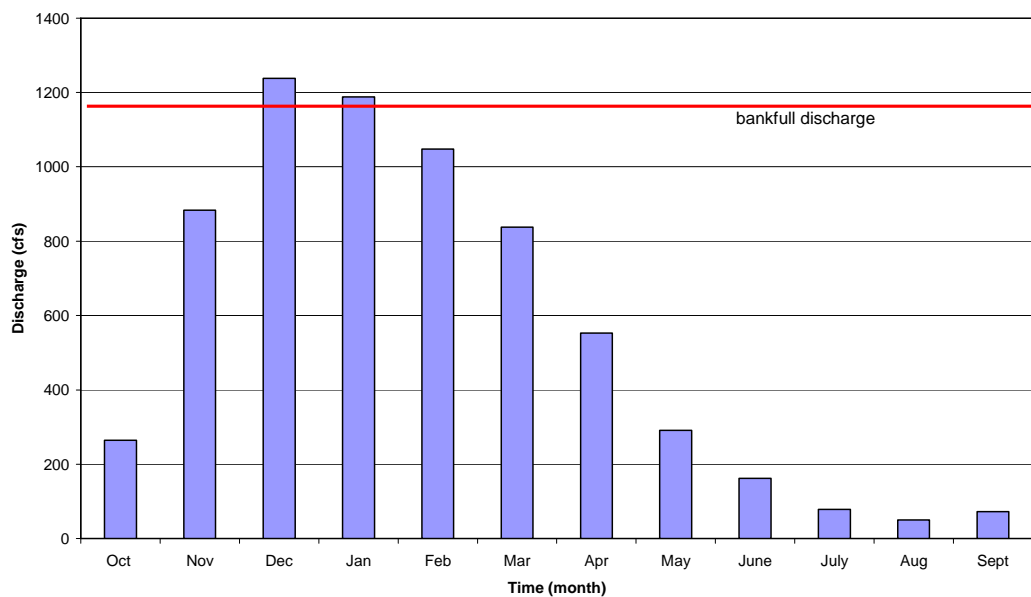


FIGURE 10.27: AVERAGE MONTHLY DISCHARGE FOR PERIOD OF RECORD FOR KILCHIS RIVER AS DERIVED FROM WILSON RIVER GAGE

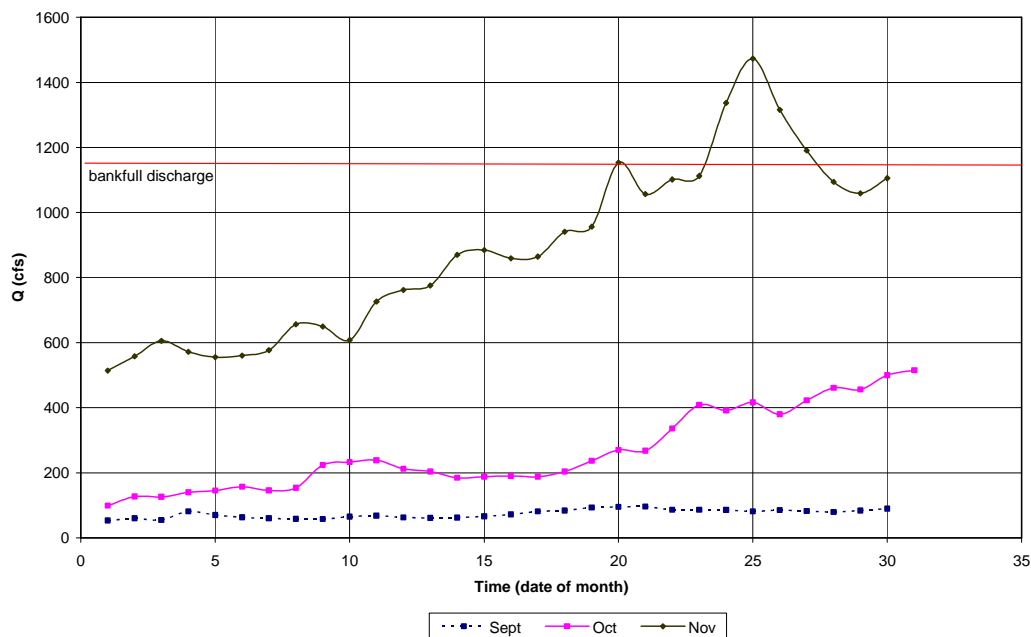


FIGURE 10.28: MEAN DAILY DISCHARGE FOR PERIOD OF RECORD DURING THE FALL SEASON FOR KILCHIS RIVER AS DERIVED FROM WILSON RIVER GAGE

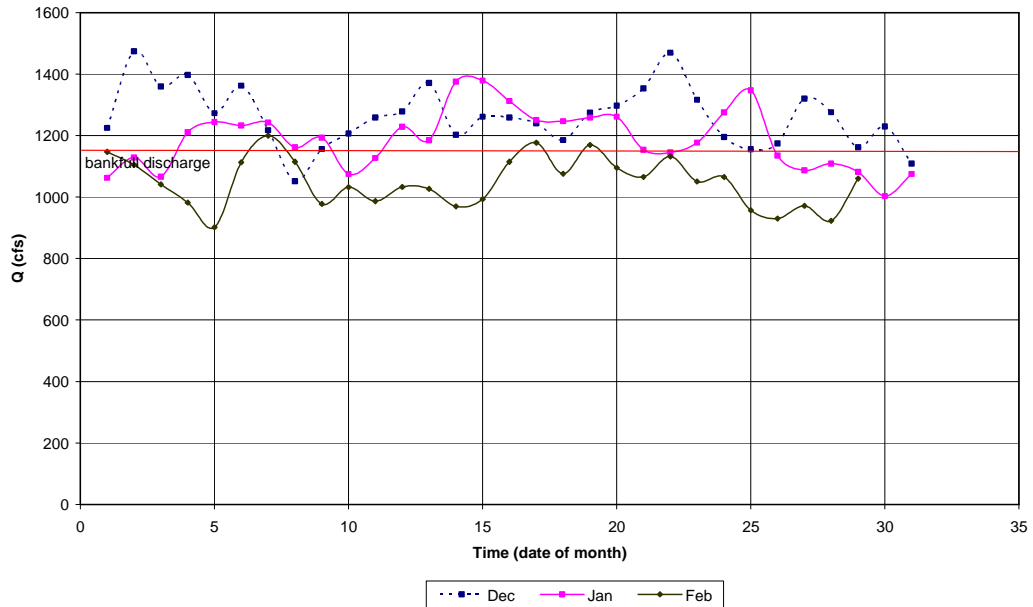


FIGURE 10.29: MEAN DAILY DISCHARGE FOR PERIOD OF RECORD DURING THE WINTER SEASON FOR KILCHIS RIVER AS DERIVED FROM WILSON RIVER GAGE

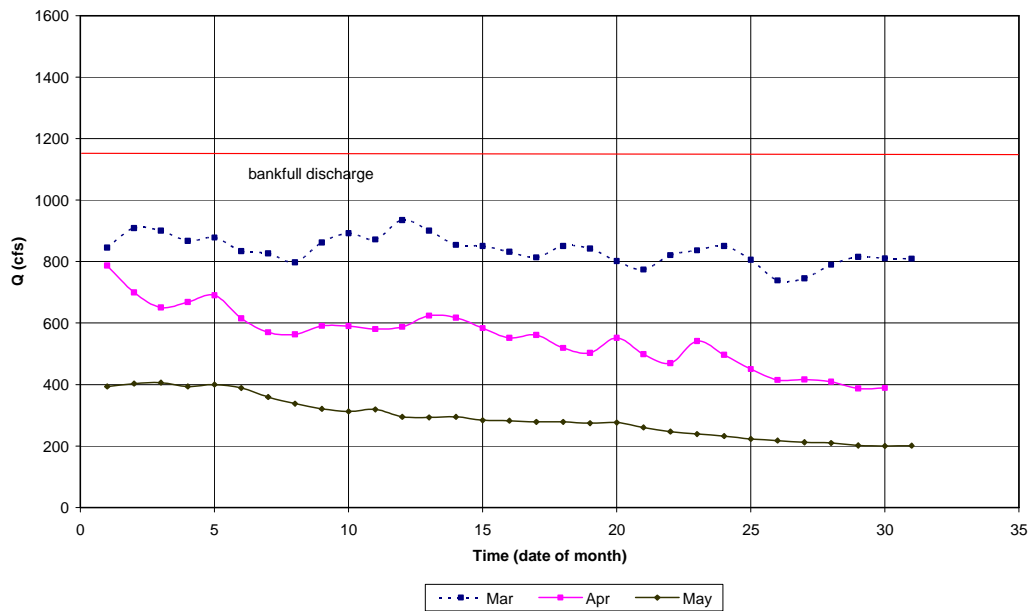


FIGURE 10.30: MEAN DAILY DISCHARGE FOR PERIOD OF RECORD DURING THE SPRING SEASON FOR KILCHIS RIVER AS DERIVED FROM WILSON RIVER GAGE

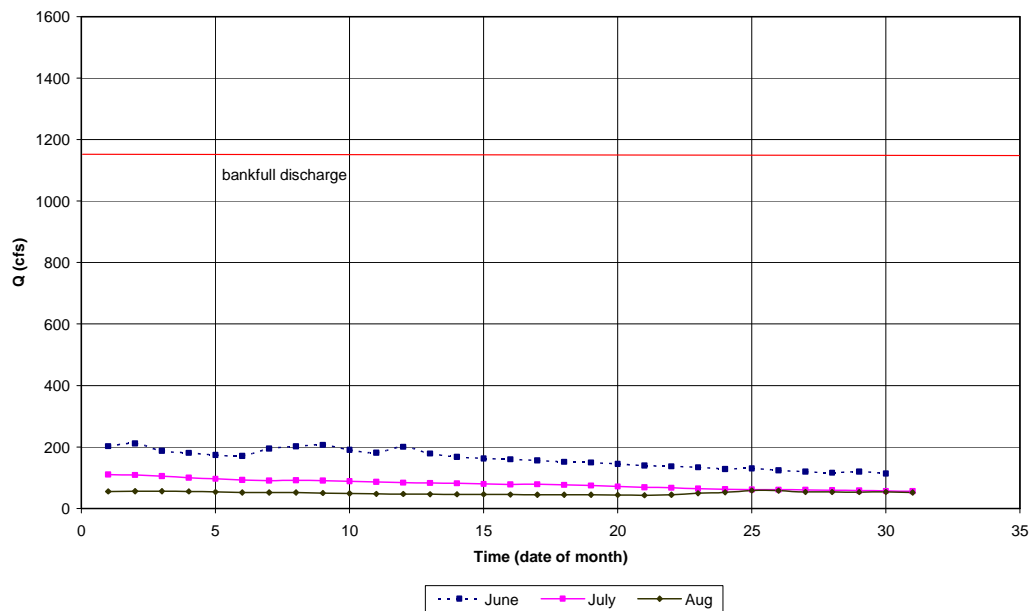
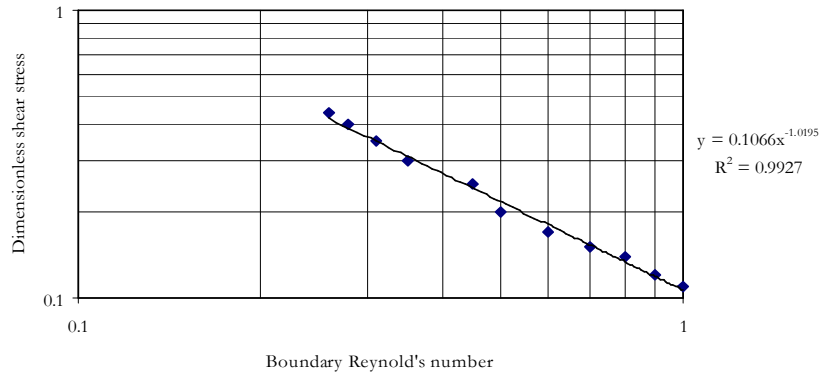


FIGURE 10.31: MEAN DAILY DISCHARGE FOR PERIOD OF RECORD DURING THE SPRING SEASON FOR KILCHIS RIVER AS DERIVED FROM WILSON RIVER GAGE

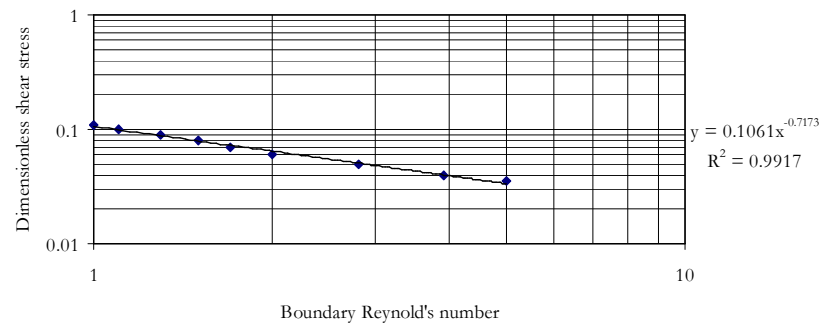
10.5 Appendix E: Empirical chart reproduction

10.5.1 *Reproduction of Shields' diagram*

Boundary Reynold's number (0.26 to 1.0)	
x	y
0.26	0.44
0.28	0.4
0.31	0.35
0.35	0.3
0.45	0.25
0.5	0.2
0.6	0.17
0.7	0.15
0.8	0.14
0.9	0.12
1	0.11



Boundary Reynold's number (1.0 to 5.0)	
x	y
1	0.11
1.1	0.1
1.3	0.09
1.5	0.08
1.7	0.07
2	0.06
2.8	0.05
3.9	0.04
5	0.035



Boundary Reynold's number (5.0 to 8.0)	
x	y
5	0.035
6	0.034
7	0.033
8	0.032

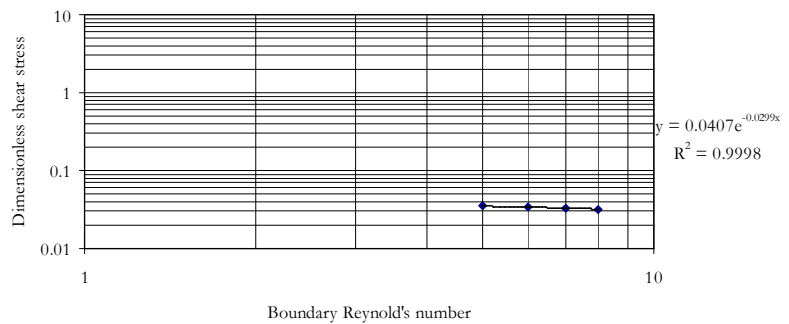
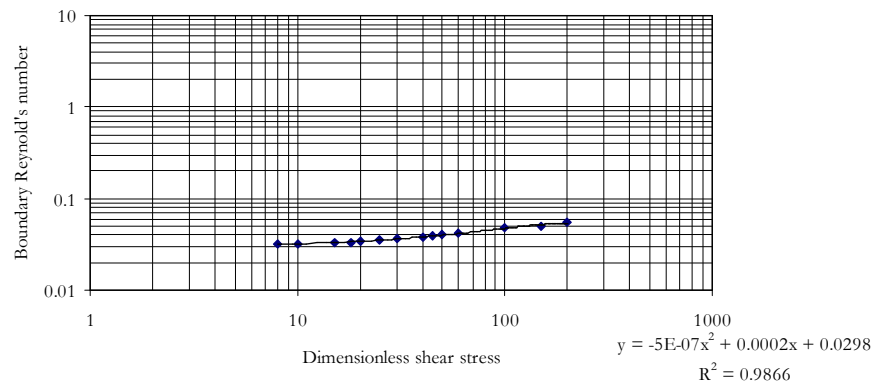


FIGURE 10.32: DATA AND CORRESPONDING SCATTER PLOTS FOR PIECEWISE DEFINED SHIELD'S DIAGRAM

Boundary Reynold's number (8.0 to 200.0)	
x	y
8	0.032
10	0.032
15	0.033
18	0.033
20	0.034
25	0.035
30	0.037
40	0.038
45	0.039
50	0.04
60	0.042
100	0.049
150	0.05
200	0.055



Boundary Reynold's number (200.0 to 1000.0)	
x	y
200	0.055
250	0.057
300	0.059
400	0.0598
500	0.06
1000	0.0608

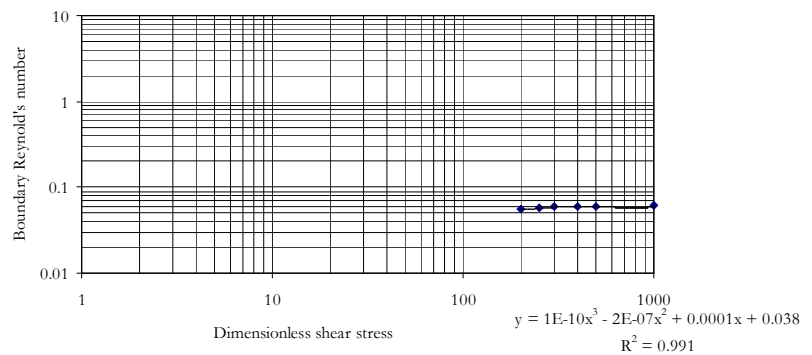
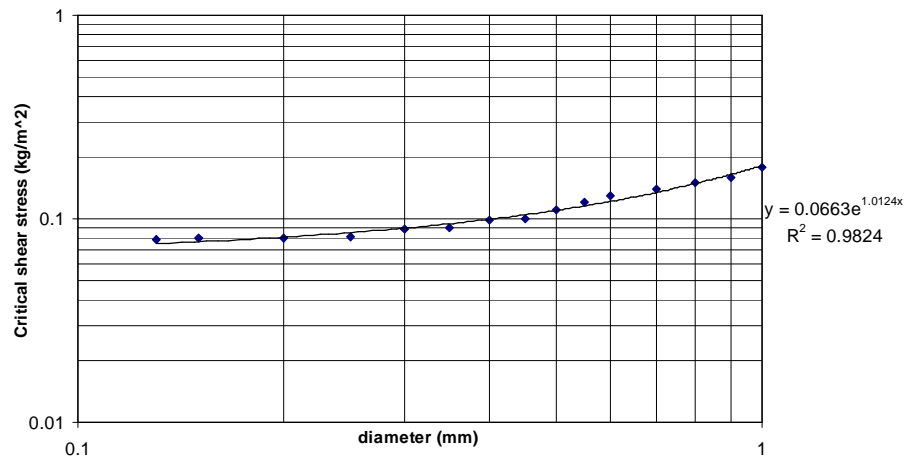


FIGURE 10.33: DATA AND CORRESPONDING SCATTER PLOTS FOR PIECEWISE DEFINED SHIELD'S DIAGRAM (CONT'D)

10.5.2 Reproduction of Straub's critical tractive force diagram for DuBoys's Bed-load formula

.13 to 1 mm diameter	
0.13	0.079
0.15	0.08
0.2	0.08
0.25	0.081
0.3	0.089
0.35	0.09
0.4	0.099
0.45	0.1
0.5	0.11
0.55	0.12
0.6	0.13
0.7	0.14
0.8	0.15
0.9	0.16
1	0.18



1 to 60 mm diameter	
1	0.18
10	0.195
20	0.25
25	0.29
30	0.35
35	0.398
40	0.43
50	0.51
60	0.6

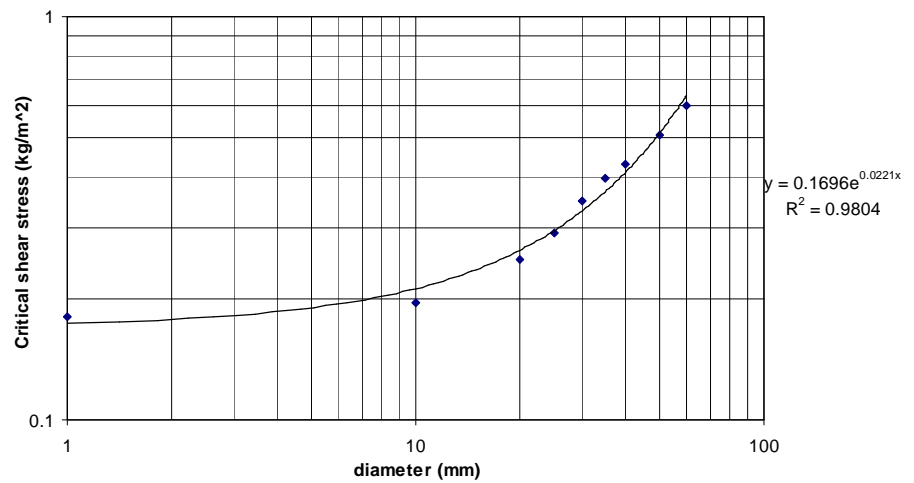
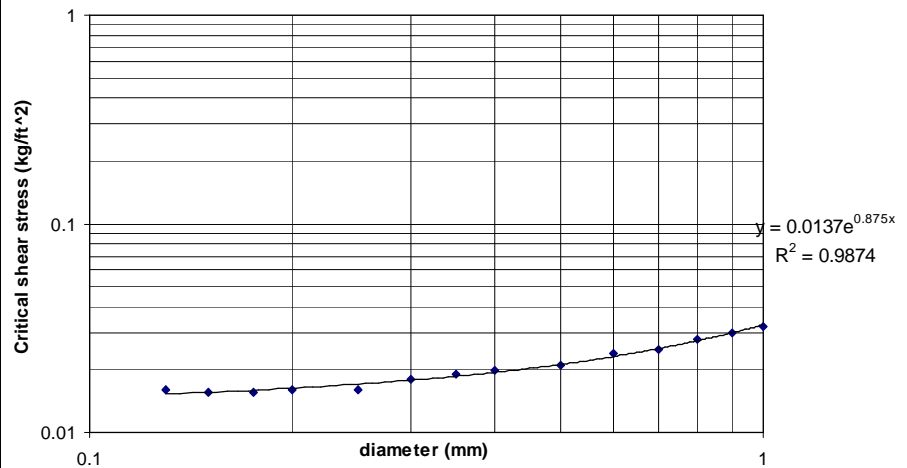


FIGURE 10.34: DATA AND CORRESPONDING SCATTER PLOTS FOR PIECEWISE-DEFINED CRITICAL TRACTIVE FORCE DIAGRAM

.13 to 1 mm diameter	
0.13	0.016
0.15	0.0155
0.175	0.0155
0.2	0.0159
0.25	0.016
0.3	0.018
0.35	0.019
0.4	0.0199
0.5	0.021
0.6	0.024
0.7	0.025
0.8	0.028
0.9	0.0298
1	0.032



1 to 48 mm diameter	
1	0.032
5	0.035
10	0.0403
15	0.048
20	0.049
22.5	0.058
25	0.063
30	0.07
35	0.08
40	0.09
48	0.1

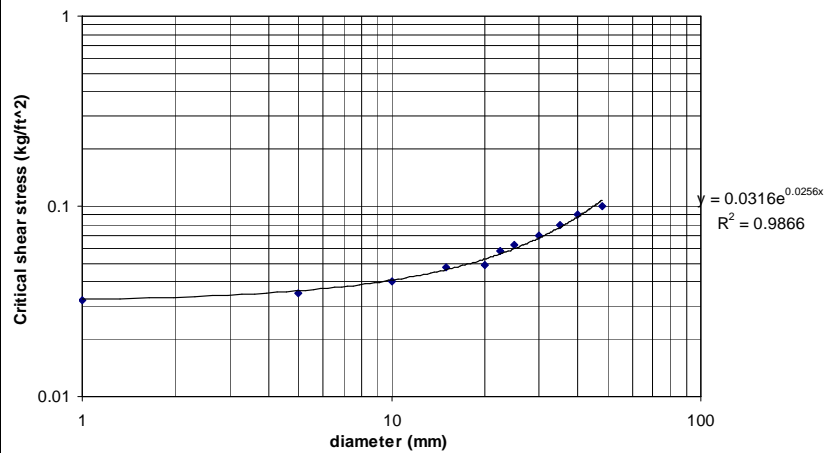


FIGURE 10.35: DATA AND CORRESPONDING SCATTER PLOTS FOR PIECE-WISE DEFINED CRITICAL TRACTIVE FORCE DIAGRAM (CONT'D)

10.6 Appendix F: MATLAB Programs

10.6.1 TIMM constant discharge and sediment size

```

%=====
% PROGRAM: TIMM
%
% A program to simulate erosion and aggradation of a streambed with
% tidal influence. Discharge and sediment size are a constant values
%
% 6/06 Derron Rafiq Coles
%=====

%%%%%%%%%%%%%%%%%%%%%%%%%%%%%%%%%%%%%%%%%%%%%%%%%%%%%%%%%%%%%%%%%%%%%%%%
%Constant parameters
%%%%%%%%%%%%%%%%%%%%%%%%%%%%%%%%%%%%%%%%%%%%%%%%%%%%%%%%%%%%%%%%%%%%%%%%

waterdensity      = 62.33;      %density of water [lbs/ft^3]
gravity           = 32.2;       %acceleration of gravity [ft/s^2]
specificgravity   = 2.68;      %specific gravity
kinematicvisc    = 1.09e-5;    %kinematic viscosity [ft^2/s]
dynamicvisc      = kinematicvisc*waterdensity;
                    %dynamic viscosity [lbs-s/ft^2]
kn                = 1.49;      %for Mannings formula [ft^3/s]
specificweight    = 62.3;      %specific weight of water [lbs/ft^3]

%%%%%%%%%%%%%%%%%%%%%%%%%%%%%%%%%%%%%%%%%%%%%%%%%%%%%%%%%%%%%%%%%%%%%%%%
%Input parameters
%%%%%%%%%%%%%%%%%%%%%%%%%%%%%%%%%%%%%%%%%%%%%%%%%%%%%%%%%%%%%%%%%%%%%%%%

d90               = 127; %input('what is the 90 percentile sediment
size?')
d50               = 7.9; %input('what is the 50 percentile sediment
size?')
mannings          = 0.029; %input('what is the mannings n value?')
rivermiles        = 3; %input('how many river miles are you
studying?')
width             = 70; %input('what is the channel width in feet?')
totaltime         = 30; %input('How long in days?')
Q                 = 398; %input('what is the discharge in cfs?')
channelslope      = 0.0011; %input('what is the channel slope in
degrees?')

%%%%%%%%%%%%%%%%%%%%%%%%%%%%%%%%%%%%%%%%%%%%%%%%%%%%%%%%%%%%%%%%%%%%%%%%
%Parameters calculated from input parameters
%%%%%%%%%%%%%%%%%%%%%%%%%%%%%%%%%%%%%%%%%%%%%%%%%%%%%%%%%%%%%%%%%%%%%%%%

totallength       = rivermiles*1609; %converts total river miles to
meters
q                 = Q/width; %discharge per unit width for bed-load
                    %calculation
sed_density       = specificgravity*waterdensity; %calculates the
density of sediment
reacharray        = 0:totallength/20:totallength;
                    %reacharray is an array of 20
                    %equally-sized reaches

```

```

%%%%%%%%%%%%%%%%%%%%%%%%%%%%%%%%%%%%%%%%%%%%%%%%%%%%%%%%%%%%%%%%%%%%%%%%
% Calculation of normal depth
%%%%%%%%%%%%%%%%%%%%%%%%%%%%%%%%%%%%%%%%%%%%%%%%%%%%%%%%%%%%%%%%%%%%%%%%

criticaldepth      = (Q^2/(gravity*width^2))^(1/3);
normaldepth       = criticaldepth;

leftside          =
((normaldepth*width)^(5/3))/((2*normaldepth+width)^(2/3));
rightside         = (mannings*Q)/(1.49*(channelslope^(.5)));

while leftside < rightside +.1
    normaldepth    = normaldepth+0.1;
    leftside       =
((normaldepth*width)^(5/3))/((2*normaldepth+width)^(2/3));
end

%%%%%%%%%%%%%%%%%%%%%%%%%%%%%%%%%%%%%%%%%%%%%%%%%%%%%%%%%%%%%%%%%%%%%%%%
% calculation of water depth array for high tide
%%%%%%%%%%%%%%%%%%%%%%%%%%%%%%%%%%%%%%%%%%%%%%%%%%%%%%%%%%%%%%%%%%%%%%%%

initialdepth      = 12.30; %average depth of Tillamook Bay + mean tidal
range
index             = 2;
distance(1)       = 0;
watersurface(1)   = initialdepth;
depthchange       = 0.05; %change in depth

initialdist       = 0;
initialarea       = initialdepth*width;
initialwetterdp   = 2*initialdepth + width;
initialvelocity   = Q/initialarea;
initialradius     = initialarea/(initialwetterdp);
initialEnergy     = initialdepth + (initialvelocity^2/(2*gravity));
initialfriction   =
(mannings^2/kn^2)*(initialvelocity^2/initialradius^(4/3));
newdepth          = initialdepth-depthchange;

while newdepth >= normaldepth

    newarea        = newdepth*width;
    newwetterdp    = 2*newdepth + width;
    newvelocity    = Q/newarea;
    newradius      = newarea/(newwetterdp);
    newEnergy      = newdepth + (newvelocity^2/(2*gravity));
    newfriction    =
(mannings^2/kn^2)*(newvelocity^2/newradius^(4/3));

    energychange   = initialEnergy - newEnergy;
    meanfriction   = 0.5*(initialfriction + newfriction);
    distancechange = energychange/(channelslope - meanfriction);

    watersurface(index) = newdepth;
    distanceup          = initialdist + distancechange;
    distance(index)    = distanceup;

    newdepth          = newdepth - depthchange;
    initialEnergy     = newEnergy;
    initialfriction   = newfriction;
    initialdist       = distanceup;
    index             = index + 1;
    j                 = 2;
    xhigh             = 0;
end

high_fit           = polyfit(distance,watersurface,3);
high_tide_array(1) = 12.30; %Depth array to be used for periods
of high tidal influence

while j <= 20
    high_depth      = high_fit(1)*xhigh + high_fit(2)*xhigh +
high_fit(3)*xhigh + high_fit(4);
end

```

```

if high_depth > normaldepth
    high_tide_array(j) = high_depth;
else
    high_tide_array(j) = normaldepth;
end

j      = j + 1;
xhigh  = xhigh + 880;
end

%%%%%%%%%%%%%%%%%%%%%%%%%%%%%%%%%%%%%%%%%%%%%%%%%%%%%%%%%%%%%%%%%%%%%%%%
% calculation of water depth array for intermediate tide
%%%%%%%%%%%%%%%%%%%%%%%%%%%%%%%%%%%%%%%%%%%%%%%%%%%%%%%%%%%%%%%%%%%%%%%%

initialdepth      = 9.45; %average depth of Tillamook Bay + 0.5*mean
tidal range
index             = 2;
distance(1)       = 0;
watersurface(1)  = initialdepth;
depthchange       = 0.05; %change in depth

initialdist       = 0;
initialarea       = initialdepth*width;
initialwetterdp   = 2*initialdepth + width;
initialvelocity   = Q/initialarea;
initialradius     = initialarea/(initialwetterdp);
initialEnergy     = initialdepth + (initialvelocity^2/(2*gravity));
initialfriction   =
(mannings^2/kn^2)*(initialvelocity^2/initialradius^(4/3));
newdepth          = initialdepth-depthchange;

while newdepth >= normaldepth

    newarea        = newdepth*width;
    newwetterdp    = 2*newdepth + width;
    newvelocity    = Q/newarea;
    newradius      = newarea/(newwetterdp);
    newEnergy      = newdepth + (newvelocity^2/(2*gravity));
    newfriction    =
(mannings^2/kn^2)*(newvelocity^2/newradius^(4/3));

    energychange   = initialEnergy - newEnergy;
    meanfriction   = 0.5*(initialfriction + newfriction);
    distancechange = energychange/(channelslope - meanfriction);

    watersurface(index) = newdepth;
    distanceup          = initialdist + distancechange;
    distance(index)    = distanceup;

    newdepth          = newdepth - depthchange;
    initialEnergy     = newEnergy;
    initialfriction   = newfriction;
    initialdist       = distanceup;
    index             = index + 1;
    j                 = 2;
    xinter            = 0;
end

inter_fit          = polyfit(distance,watersurface,3);
inter_tide_array(1) = 9.45; %Depth array to be used for periods
of intermediate tidal influence

while j <= 20

    inter_depth      = inter_fit(1)*xinter + inter_fit(2)*xinter +
inter_fit(3)*xinter + inter_fit(4);

    if inter_depth > normaldepth

        inter_tide_array(j) = inter_depth;

    else

```

```

        inter_tide_array(j) = normaldepth;
    end

    j      = j + 1;
    xinter = xinter + 880;
end

%%%%%%%%%%%%%%%%%%%%%%%%%%%%%%%%%%%%%%%%%%%%%%%%%%%%%%%%%%%%%%%%%%%%%%%%
% calculation of water depth array for low tide
%%%%%%%%%%%%%%%%%%%%%%%%%%%%%%%%%%%%%%%%%%%%%%%%%%%%%%%%%%%%%%%%%%%%%%%%

initialdepth = 6.6; %average depth of Tillamook Bay
index        = 2;
distance(1)  = 0;
watersurface(1) = initialdepth;
depthchange  = 0.05; %change in depth

initialdist  = 0;
initialarea  = initialdepth*width;
initialwetterp = 2*initialdepth + width;
initialvelocity = Q/initialarea;
initialradius = initialarea/(initialwetterp);
initialEnergy = initialdepth + (initialvelocity^2/(2*gravity));
initialfriction =
(mannings^2/kn^2)*(initialvelocity^2/initialradius^(4/3));
newdepth     = initialdepth-depthchange;

while newdepth >= normaldepth

    newarea      = newdepth*width;
    newwetterp   = 2*newdepth + width;
    newvelocity  = Q/newarea;
    newradius    = newarea/(newwetterp);
    newEnergy    = newdepth + (newvelocity^2/(2*gravity));
    newfriction  =
(mannings^2/kn^2)*(newvelocity^2/newradius^(4/3));

    energychange = initialEnergy - newEnergy;
    meanfriction = 0.5*(initialfriction + newfriction);
    distancechange = energychange/(channelslope - meanfriction);

    watersurface(index) = newdepth;
    distanceup          = initialdist + distancechange;
    distance(index)     = distanceup;

    newdepth          = newdepth - depthchange;
    initialEnergy     = newEnergy;
    initialfriction   = newfriction;
    initialdist       = distanceup;
    index             = index + 1;
    j                 = 2;
    xlow              = 0;
end

low_fit          = polyfit(distance,watersurface,3);
low_tide_array(1) = 6.6; %Depth array to be used for periods
of low tidal influence

while j <= 20

    low_depth = low_fit(1)*xlow + low_fit(2)*xlow +
low_fit(3)*xlow + low_fit(4);

    if low_depth > normaldepth
        low_tide_array(j) = low_depth;
    else
        low_tide_array(j) = normaldepth;
    end

    j      = j + 1;
    xlow   = xlow + 880;
end

```

end

```

%%%%%%%%%%%%%%%%%%%%%%%%%%%%%%%%%%%%%%%%%%%%%%%%%%%%%%%%%%%%%%%%%%%%%%%%
%Sediment transport calculation: This portion of the model uses
%the water surface elevations to calculate bed-load movement. Three
%routines are used to simulate high, intermediate, and low tide
%%%%%%%%%%%%%%%%%%%%%%%%%%%%%%%%%%%%%%%%%%%%%%%%%%%%%%%%%%%%%%%%%%%%%%%%

bed          = ones(1,20); %beginning with a matrix of ones
bed          = bed*100; %infinite depth of sediment available for
transport

% calculation refinements if set to 1 then the program computes the
% transport for that scenario, otherwise it iterates without consideration
% of the scenario (e.g., low_tide_calc = 1 means low tide transport will be
% calculated.

low_tide_calc    = 1;
high_tide_calc   = 1;
inter_tide_calc  = 1;

% create figure used by plot

fig1 = figure(1);
set(fig1, 'Color', [0.8706 0.9216 0.9804]);
set(fig1, 'Name', 'Sediment transport with tidal influence');
set(fig1, 'NextPlot','replacechildren')

% configure the axes

axes1 = axes('Parent', fig1);
set(axes1, 'FontName', 'Garamond');
set(axes1, 'XGrid', 'on');
set(axes1, 'YGrid', 'on');

% limit ranges on the graph

xlim(axes1,[2 20]);
ylim(axes1,[100 500]);

% label graph

xlabel(axes1,'Reach Number (2 = river mile 0; 20 = river mile 3)');
ylabel(axes1,'Volume of sediment retained in the reach (ft^3)');
box(axes1,'on');
hold(axes1, 'all');

% create movie structure to hold graph

winsize = get(fig1, 'Position');
winsize(1:2) = [0 0];
numframes = totaltime;
CUMULATIVE = moviein(numframes, fig1, winsize);

% number of hours per tidal condition
hours = 8;

for td=1:totaltime

%%%%%%%%%%%%%%%%%%%%%%%%%%%%%%%%%%%%%%%%%%%%%%%%%%%%%%%%%%%%%%%%%%%%%%%%
%Routine #1: Sediment transport during high tide
%%%%%%%%%%%%%%%%%%%%%%%%%%%%%%%%%%%%%%%%%%%%%%%%%%%%%%%%%%%%%%%%%%%%%%%%

% for t = number of hours
if (high_tide_calc == 1)
    for t=1:hours
        i          = 20;

        while i >= 2
            d          = high_tide_array(i);
            inst_velocity = Q/(width*d);
            hydraulicradius = (width*d)/(2*d+width);
            energyslope =
            ((inst_velocity*mannings)/(1.49*hydraulicradius^(2/3)))^2;
            shearstress =
            specificweight*energyslope*hydraulicradius;
            critshearstress = 0.031*exp(0.0256*d50);

            if critshearstress <= shearstress

```

```

                                % erosion rate calculation
                                qb      = (0.173/d50^0.75)*shearstress*(shearstress-
critshearstress);
                                % calculation of total volume moved during 1 hour
                                volume  = qb * 3600;
                                % removal of sediment from upstream reach
                                bed(i)  = bed(i) - volume;
                                bed(i-1) = bed(i-1) + volume; %addition of sediment to
next reach downstream
                                else
                                end
                                i = i - 1;
                                end
                                end
                                end

%%%%%%%%%%%%%%%%%%%%%%%%%%%%%%%%%%%%%%%%%%%%%%%%%%%%%%%%%%%%%%%%%%%%%%%%%%
%Routine #2: Sediment transport during intermediate period
%%%%%%%%%%%%%%%%%%%%%%%%%%%%%%%%%%%%%%%%%%%%%%%%%%%%%%%%%%%%%%%%%%%%%%%%%%

if (inter_tide_calc == 1)
    for t=0:hours
        i      = 20;

        while i>=2
            d      = inter_tide_array(i);
            inst_velocity = Q/(width*d);
            hydraulicradius = (width*d)/(2*d+width);
            energyslope =
((inst_velocity*mannings)/(1.49*hydraulicradius^(2/3)))^2;
            shearstress =
specificweight*energyslope*hydraulicradius;
            critshearstress = 0.031*exp(0.0256*d50);

            if critshearstress <= shearstress
                qb      = (0.173/d50^0.75)*shearstress*(shearstress-
critshearstress); %erosion rate calculation
                volume  = qb*3600; %calculation of total volume moved
during 1 hour
                bed(i)  = bed(i) - volume; %removal of sediment from
upstream reach
                bed(i-1)= bed(i-1) + volume; %addition of sediment to
next reach downstream
                i      = i-1;
            else
                i      = i-1;
            end
        end
    end
end

%%%%%%%%%%%%%%%%%%%%%%%%%%%%%%%%%%%%%%%%%%%%%%%%%%%%%%%%%%%%%%%%%%%%%%%%%%
%Routine #3: Sediment transport during low tide
%%%%%%%%%%%%%%%%%%%%%%%%%%%%%%%%%%%%%%%%%%%%%%%%%%%%%%%%%%%%%%%%%%%%%%%%%%

if (low_tide_calc == 1)
    for t=0:hours
        i      = 20;

        while i>=2
            d      = low_tide_array(i);
            inst_velocity = Q/(width*d);
            hydraulicradius = (width*d)/(2*d+width);
            energyslope =
((inst_velocity*mannings)/(1.49*hydraulicradius^(2/3)))^2;
            shearstress =
specificweight*energyslope*hydraulicradius;
            critshearstress = 0.031*exp(0.0256*d50);

            if critshearstress <= shearstress
                qb      = (0.173/d50^0.75)*shearstress*(shearstress-
critshearstress); %erosion rate calculation
                volume  = qb*3600; %calculation of total volume moved
during 1 hour
                bed(i)  = bed(i) - volume; %removal of sediment from
upstream reach
                bed(i-1)= bed(i-1) + volume; %addition of sediment to
next reach downstream
                i      = i-1;
            end
        end
    end
end

```

```

        else
            i = i-1;
        end
    end
end
end
end

plot(axes1, bed);
CUMULATIVE(:,td) = getframe(fig1, winsize);

end % for number of days

repeat = 1;
frames_per_second = 500;

movie(fig1,CUMULATIVE,repeat,frames_per_second,winsize)

```

10.6.2 TIMM varied discharge constant sediment

```

%=====
% PROGRAM: TIMM
%
% A program to simulate erosion and aggradation of a streambed with
% tidal influence. Varied discharge and constant sediment size
%
% 6/06 Derron Rafiq Coles
%=====

%%%%%%%%%%%%%%%%%%%%%%%%%%%%%%%%%%%%%%%%%%%%%%%%%%%%%%%%%%%%%%%%%%%%%%%%
%%Constant parameters
%%%%%%%%%%%%%%%%%%%%%%%%%%%%%%%%%%%%%%%%%%%%%%%%%%%%%%%%%%%%%%%%%%%%%%%%

waterdensity = 62.33; %density of water [lbs/ft^3]
gravity = 32.2; %acceleration of gravity [ft/s^2]
specificgravity = 2.68; %specific gravity
kinematicvisc = 1.09e-5; %kinematic viscosity [ft^2/s]
dynamicvisc = kinematicvisc*waterdensity;
%dynamic viscosity [lbs-s/ft^2]
kn = 1.49; %for Mannings formula [ft^1.3/s]
specificweight = 62.3; %specific weight of water [lbs/ft^3]
bed = ones(1,20); %beginning with a matrix of ones
bed = bed*100; %infinite depth of sediment available for
transport

%%%%%%%%%%%%%%%%%%%%%%%%%%%%%%%%%%%%%%%%%%%%%%%%%%%%%%%%%%%%%%%%%%%%%%%%
%%Input parameters
%%%%%%%%%%%%%%%%%%%%%%%%%%%%%%%%%%%%%%%%%%%%%%%%%%%%%%%%%%%%%%%%%%%%%%%%

d90 = 127; %input('what is the 90 percentile sediment
size?')
d50 = 7.9; %input('what is the 50 percentile sediment
size?')
mannings = 0.029; %input('what is the mannings n value?')
rivermiles = 3; %input('how many river miles are you
studying?')
width = 70; %input('what is the channel width in feet?')
totaltime = 30; %input('How long in days? must have the same
number of discharge entries')
discharge_array = input('An array of mean daily discharge values for
the total number of days');
channelslope = 0.0011; %input('what is the channel slope in
degrees?')
input_discharge = 1;

% create figure used by plot

fig1 = figure(1);
set(fig1, 'Color', [0.8706 0.9216 0.9804]);
set(fig1, 'Name', 'Sediment transport with tidal influence');
set(fig1, 'NextPlot','replacechildren')

% configure the axes

```

```

axes1 = axes('Parent', fig1);
set(axes1, 'FontName', 'Garamond');
set(axes1, 'XGrid', 'on');
set(axes1, 'YGrid', 'on');

% limit ranges on the graph

xlim(axes1,[2 20]);
ylim(axes1,[100 115]);

% label graph

xlabel(axes1,'Reach Number (2 = river mile 0; 20 = river mile 3)');
ylabel(axes1,'Volume of sediment retained in the reach (ft^3)');
box(axes1,'on');
hold(axes1, 'all');

% create movie structure to hold graph

winsize = get(fig1, 'Position');
winsize(1:2) = [0 0];
numframes = totaltime;
CUMULATIVE = moviein(numframes, fig1, winsize);

while input_discharge <= totaltime

    Q            = discharge_array(input_discharge);

    %%%%%%%%%%%%%%%%%%%%%%%%%%%%%%%%%%%%%%%%%%%%%%%%%%%%%%%%%%%%%%%%%%%%%%%%%
    %Parameters calculated from input parameters
    %%%%%%%%%%%%%%%%%%%%%%%%%%%%%%%%%%%%%%%%%%%%%%%%%%%%%%%%%%%%%%%%%%%%%%%%%

    toalllength      = rivermiles*1609;    %converts total river miles
    to meters
    q                = Q/width;           %discharge per unit width for bed-
    load
    %calculation
    sed_density      = specificgravity*waterdensity; %calculates the
    density of sediment

    reacharray      = 0:totallength/20:totallength;
    %reacharray is an array of 20
    %equally-sized reaches

    %%%%%%%%%%%%%%%%%%%%%%%%%%%%%%%%%%%%%%%%%%%%%%%%%%%%%%%%%%%%%%%%%%%%%%%%%
    % Calculation of normal depth
    %%%%%%%%%%%%%%%%%%%%%%%%%%%%%%%%%%%%%%%%%%%%%%%%%%%%%%%%%%%%%%%%%%%%%%%%%

    criticaldepth    = (Q^2/(gravity*width^2))^(1/3);
    normaldepth      = criticaldepth;

    leftside         =
    ((normaldepth*width)^(5/3))/((2*normaldepth+width)^(2/3));
    rightside        = (mannings*Q)/(1.49*(channelslope^(.5)));

    while leftside < rightside +.1
        normaldepth  = normaldepth+0.1;
        leftside     =
    ((normaldepth*width)^(5/3))/((2*normaldepth+width)^(2/3));
    end

    %%%%%%%%%%%%%%%%%%%%%%%%%%%%%%%%%%%%%%%%%%%%%%%%%%%%%%%%%%%%%%%%%%%%%%%%%
    % calculation of water depth array for high tide
    %%%%%%%%%%%%%%%%%%%%%%%%%%%%%%%%%%%%%%%%%%%%%%%%%%%%%%%%%%%%%%%%%%%%%%%%%

    initialdepth     = 12.30; %average depth of Tillamook Bay + mean
    tidal range
    index             = 2;
    distance(1)       = 0;
    watersurface(1)   = initialdepth;
    depthchange       = 0.05; %change in depth

    initialdist       = 0;

```

```

initialarea      = initialdepth*width;
initialwettedp  = 2*initialdepth + width;
initialvelocity = Q/initialarea;
initialradius   = initialarea/(initialwettedp);
initialEnergy   = initialdepth + (initialvelocity^2/(2*gravity));
initialfriction = (mannings^2/kn^2)*(initialvelocity^2/initialradius^(4/3));
newdepth        = initialdepth-depthchange;

while newdepth >= normaldepth

    newarea      = newdepth*width;
    newwettedp  = 2*newdepth + width;
    newvelocity = Q/newarea;
    newradius   = newarea/(newwettedp);
    newEnergy   = newdepth + (newvelocity^2/(2*gravity));
    newfriction = (mannings^2/kn^2)*(newvelocity^2/newradius^(4/3));

    energychange = initialEnergy - newEnergy;
    meanfriction = 0.5*(initialfriction + newfriction);
    distancechange = energychange/(channelslope -
meanfriction);

    watersurface(index) = newdepth;
    distanceup          = initialdist + distancechange;
    distance(index)     = distanceup;

    newdepth           = newdepth - depthchange;
    initialEnergy      = newEnergy;
    initialfriction    = newfriction;
    initialdist        = distanceup;
    index              = index + 1;
    j                  = 2;
    xhigh              = 0;
end

high_fit              = polyfit(distance,watersurface,3);
high_tide_array(1)   = 12.30; %Depth array to be used for
periods of high tidal influence

while j <= 20

    high_depth         = high_fit(1)*xhigh + high_fit(2)*xhigh +
high_fit(3)*xhigh + high_fit(4);

    if high_depth > normaldepth
        high_tide_array(j) = high_depth;
    else
        high_tide_array(j) = normaldepth;
    end

    j                  = j + 1;
    xhigh              = xhigh + 880;
end

%%%%%%%%%%%%%%%%%%%%%%%%%%%%%%%%%%%%%%%%%%%%%%%%%%%%%%%%%%%%%%%%%%%%%%%%
% calculation of water depth array for intermediate tide
%%%%%%%%%%%%%%%%%%%%%%%%%%%%%%%%%%%%%%%%%%%%%%%%%%%%%%%%%%%%%%%%%%%%%%%%

initialdepth        = 9.45; %average depth of Tillamook Bay + 0.5*mean
tidal range         = 2;
index               = 0;
distance(1)         = 0;
watersurface(1)    = initialdepth;
depthchange         = 0.05; %change in depth

initialdist         = 0;
initialarea         = initialdepth*width;
initialwettedp      = 2*initialdepth + width;
initialvelocity     = Q/initialarea;
initialradius       = initialarea/(initialwettedp);
initialEnergy       = initialdepth + (initialvelocity^2/(2*gravity));

```

```

initialfriction =
(mannings^2/kn^2)*(initialvelocity^2/initialradius^(4/3));
newdepth = initialdepth-depthchange;

while newdepth >= normaldepth

    newarea = newdepth*width;
    newwettedp = 2*newdepth + width;
    newvelocity = Q/newarea;
    newradius = newarea/(newwettedp);
    newEnergy = newdepth + (newvelocity^2/(2*gravity));
    newfriction =
(mannings^2/kn^2)*(newvelocity^2/newradius^(4/3));

    energychange = initialEnergy - newEnergy;
    meanfriction = 0.5*(initialfriction + newfriction);
    distancechange = energychange/(channelslope -
meanfriction);

    watersurface(index) = newdepth;
    distanceup = initialdist + distancechange;
    distance(index) = distanceup;

    newdepth = newdepth - depthchange;
    initialEnergy = newEnergy;
    initialfriction = newfriction;
    initialdist = distanceup;
    index = index + 1;
    j = 2;
    xinter = 0;
end

inter_fit = polyfit(distance,watersurface,3);
inter_tide_array(1) = 9.45; %Depth array to be used for
periods of intermediate tidal influence

while j <= 20

    inter_depth = inter_fit(1)*xinter +
inter_fit(2)*xinter + inter_fit(3)*xinter + inter_fit(4);

    if inter_depth > normaldepth

        inter_tide_array(j) = inter_depth;

    else

        inter_tide_array(j) = normaldepth;

    end

    j = j + 1;
    xinter = xinter + 880;

end

%%%%%%%%%%%%%%%%%%%%%%%%%%%%%%%%%%%%%%%%%%%%%%%%%%%%%%%%%%%%%%%%%%%%%%%%
% calculation of water depth array for low tide
%%%%%%%%%%%%%%%%%%%%%%%%%%%%%%%%%%%%%%%%%%%%%%%%%%%%%%%%%%%%%%%%%%%%%%%%

initialdepth = 6.6; %average depth of Tillamook Bay
index = 2;
distance(1) = 0;
watersurface(1) = initialdepth;
depthchange = 0.05; %change in depth

initialdist = 0;
initialarea = initialdepth*width;
initialwettedp = 2*initialdepth + width;
initialvelocity = Q/initialarea;
initialradius = initialarea/(initialwettedp);
initialEnergy = initialdepth + (initialvelocity^2/(2*gravity));
initialfriction =
(mannings^2/kn^2)*(initialvelocity^2/initialradius^(4/3));
newdepth = initialdepth-depthchange;

```

```

while newdepth >= normaldepth

    newarea          = newdepth*width;
    newwettedp      = 2*newdepth + width;
    newvelocity     = Q/newarea;
    newradius       = newarea/(newwettedp);
    newEnergy       = newdepth + (newvelocity^2/(2*gravity));
    newfriction     = (mannings^2/kn^2)*(newvelocity^2/newradius^(4/3));

    energychange    = initialEnergy - newEnergy;
    meanfriction    = 0.5*(initialfriction + newfriction);
    distancechange  = energychange/(channelslope -
meanfriction);

    watersurface(index) = newdepth;
    distanceup         = initialdist + distancechange;
    distance(index)   = distanceup;

    newdepth          = newdepth - depthchange;
    initialEnergy     = newEnergy;
    initialfriction   = newfriction;
    initialdist       = distanceup;
    index             = index + 1;
    j                 = 2;
    xlow              = 0;
end

low_fit              = polyfit(distance,watersurface,3);
low_tide_array(1)   = 6.6; %Depth array to be used for
periods of low tidal influence

while j <= 20

    low_depth        = low_fit(1)*xlow + low_fit(2)*xlow +
low_fit(3)*xlow + low_fit(4);

    if low_depth > normaldepth

        low_tide_array(j) = low_depth;

    else

        low_tide_array(j) = normaldepth;

    end

    j                = j + 1;
    xlow             = xlow + 880;
end

%%%%%%%%%%%%%%%%%%%%%%%%%%%%%%%%%%%%%%%%%%%%%%%%%%%%%%%%%%%%%%%%%%%%%%%%%%
%Sediment transport calculation: This portion of the model uses
%the water surface elevations to calculate bed-load movement. Three
%routines are used to simulate high, intermediate, and low tide
%%%%%%%%%%%%%%%%%%%%%%%%%%%%%%%%%%%%%%%%%%%%%%%%%%%%%%%%%%%%%%%%%%%%%%%%%%

% calculation refinements if set to 1 then the program computes the
% transport for that scenario, otherwise it iterates without
consideration
% of the scenario (e.g., low_tide_calc = 1 means low tide transport will
be
% calculated.

low_tide_calc       = 0;
high_tide_calc      = 0;
inter_tide_calc     = 1;

% number of hours per tidal condition
hours = 8;

```

```

%%%%%%%%%%%%%%%%%%%%%%%%%%%%%%%%%%%%%%%%%%%%%%%%%%%%%%%%%%%%%%%%%%%%%%%%
%Routine #1: Sediment transport during high tide
%%%%%%%%%%%%%%%%%%%%%%%%%%%%%%%%%%%%%%%%%%%%%%%%%%%%%%%%%%%%%%%%%%%%%%%%

if (high_tide_calc == 1)
    for t=1:hours
        i = 20;

        while i >= 2
            d = high_tide_array(i);
            inst_velocity = Q/(width*d);
            hydraulicradius = (width*d)/(2*d+width);
            energyslope =
            ((inst_velocity*mannings)/(1.49*hydraulicradius^(2/3)))^2;
            shearstress =
            specificweight*energyslope*hydraulicradius;
            critshearstress = 0.031*exp(0.0256*d50);

            if critshearstress <= shearstress

                % erosion rate calculation
                qb = (0.173/d50^0.75)*shearstress*(shearstress-
                critshearstress);
                % calculation of total volume moved during 1 hour
                volume = qb * 3600;
                % removal of sediment from upstream reach
                bed(i) = bed(i) - volume;
                bed(i-1) = bed(i-1) + volume; %addition of sediment to
            next reach downstream
            else
                end
                i = i - 1;
            end
        end
    end

%%%%%%%%%%%%%%%%%%%%%%%%%%%%%%%%%%%%%%%%%%%%%%%%%%%%%%%%%%%%%%%%%%%%%%%%
%Routine #2: Sediment transport during intermediate period
%%%%%%%%%%%%%%%%%%%%%%%%%%%%%%%%%%%%%%%%%%%%%%%%%%%%%%%%%%%%%%%%%%%%%%%%

if (inter_tide_calc == 1)
    for t=0:hours
        i = 20;

        while i>=2
            d = inter_tide_array(i);
            inst_velocity = Q/(width*d);
            hydraulicradius = (width*d)/(2*d+width);
            energyslope =
            ((inst_velocity*mannings)/(1.49*hydraulicradius^(2/3)))^2;
            shearstress =
            specificweight*energyslope*hydraulicradius;
            critshearstress = 0.031*exp(0.0256*d50);

            if critshearstress <= shearstress
                qb = (0.173/d50^0.75)*shearstress*(shearstress-
                critshearstress); %erosion rate calculation
                volume = qb*3600; %calculation of total volume moved
                during 1 hour
                bed(i) = bed(i) - volume; %removal of sediment from
                upstream reach
                bed(i-1)= bed(i-1) + volume; %addition of sediment to
            next reach downstream
                i = i-1;
            else
                i = i-1;
            end
        end
    end

%%%%%%%%%%%%%%%%%%%%%%%%%%%%%%%%%%%%%%%%%%%%%%%%%%%%%%%%%%%%%%%%%%%%%%%%
%Routine #3: Sediment transport during low tide
%%%%%%%%%%%%%%%%%%%%%%%%%%%%%%%%%%%%%%%%%%%%%%%%%%%%%%%%%%%%%%%%%%%%%%%%

if (low_tide_calc == 1)
    for t=0:hours
        i = 20;

```

```

        while i>=2
            d = low_tide_array(i);
            inst_velocity = Q/(width*d);
            hydraulicradius = (width*d)/(2*d+width);
            energyslope =
            ((inst_velocity*mannings)/(1.49*hydraulicradius^(2/3)))^2;
            shearstress =
            specificweight*energyslope*hydraulicradius;
            critshearstress = 0.031*exp(0.0256*d50);

            if critshearstress <= shearstress
                qb = (0.173/d50^0.75)*shearstress*(shearstress-
                critshearstress); %erosion rate calculation
                volume = qb*3600; %calculation of total volume moved
                during 1 hour
                bed(i) = bed(i) - volume; %removal of sediment from
                upstream reach
                bed(i-1)= bed(i-1) + volume; %addition of sediment to
                next reach downstream
                i = i-1;
            else
                i = i-1;
            end
        end
    end
end
plot(axes1, bed);

CUMULATIVE(:,input_discharge) = getframe(fig1, winsize);

input_discharge = input_discharge + 1;
end
repeat = 1;
frames_per_second = 500;
movie(fig1,CUMULATIVE,repeat,frames_per_second,winsize)

```

10.7 Appendix G: GSTARS 2.1 Simulation Output Data

10.7.1 Simulation 1: uniform bed

***** SUMMARY OF INPUT PARAMETERS *****

Number of cross sections:..... 21
 Number of stream tubes:..... 2
 Number of time steps:..... 3600
 Number of sediment time steps (NITRQS):..... 24
 Duration of time step (days):..... 4.1667E-02
 Formula selected for conveyance calculations:..... manning
 Formula selected for friction slope:..... average
 Formula for sediment transport: Garde (1965)
 NALT for active layer thickness:..... 14
 Transport parameter CFACTOR:..... 1.00
 Printout control is 3; print interval:..... 720
 Number of time steps to generate x-sec plots:..... 3600
 Number of time steps for thalweg plots:..... 720
 No minimization requested.

Sect. #	Location (ft)	ISWITCH	ITYP (ft)	Thalweg Coef.	Bed slope	Loss	NDIVI	NPOINTS
1	8.8247E+04	0	0	1.1145E+03	2.0456E-03	0.00	1	15
2	8.3835E+04	0	0	1.1055E+03	2.0456E-03	0.00	1	15
3	7.9422E+04	0	0	1.0969E+03	1.9545E-03	0.00	1	15
4	7.5010E+04	0	0	1.0884E+03	1.9096E-03	0.00	1	18
5	7.0598E+04	0	0	1.0792E+03	2.0909E-03	0.00	1	19
6	6.6185E+04	0	0	1.0726E+03	1.5012E-03	0.00	1	19
7	6.1773E+04	0	0	1.0659E+03	1.5016E-03	0.00	1	24
8	5.7361E+04	0	0	1.0593E+03	1.5016E-03	0.00	1	24
9	5.2948E+04	0	0	1.0523E+03	1.5919E-03	0.00	1	35
10	4.8536E+04	0	0	1.0003E+03	1.1792E-02	0.00	1	35
11	4.4124E+04	0	0	1.0460E+03	-1.0375E-02	0.00	1	24
12	3.9711E+04	0	0	1.0412E+03	1.0934E-03	0.00	1	24
13	3.5299E+04	0	0	1.0372E+03	9.1228E-04	0.00	1	35
14	3.0886E+04	0	0	1.0332E+03	9.1208E-04	0.00	1	26
15	2.6474E+04	0	0	1.0284E+03	1.0936E-03	0.00	1	24
16	2.2062E+04	0	0	1.0251E+03	7.3096E-04	0.00	1	24
17	1.7649E+04	0	0	1.0211E+03	9.1208E-04	0.00	1	23
18	1.3237E+04	0	0	1.7775E+01	2.2741E-01	0.00	1	24
19	8.8247E+03	0	0	1.5550E+01	5.0427E-04	0.00	1	22
20	4.4124E+03	0	0	1.0130E+03	-2.2607E-01	0.00	1	25
21	0.0000E+00	1	1	1.0123E+03	1.6431E-04	0.00	1	25

Coefficients used in Exner equation and in
 computing hydraulic properties for sediment capacity

C1WP C2WP C3WP C1WPU C2WPU

0.250 0.500 0.250 0.750 0.250
 C1Q C2Q C3Q C1QD C2QD C1QU C2QU
 0.000 1.000 0.000 0.000 1.000 1.000 0.000

Number of particle size classes: 1

Class #	Geometric Dry specific			
	DRL (mm)	DRU (mm)	mean (mm)	weight (lb/ft ³)
1	7.9000E+00	7.9000E+00	7.9000E+00	9.9260E+01

Percentage of bed material for each size fraction and for each cross section

Section # 1 Bed material size fraction for each group

1	100.0
2	100.0
3	100.0
4	100.0
5	100.0
6	100.0
7	100.0
8	100.0
9	100.0
10	100.0
11	100.0
12	100.0
13	100.0
14	100.0
15	100.0
16	100.0
17	100.0
18	100.0
19	100.0
20	100.0
21	100.0

 TIME STEP NO. 720 AFTER 3.0000E+01 DAYS; DISCHARGE IS 2.6500E+02 CFS

 * RESULTS OF BACKWATER COMPUTATIONS *
 * DISCHARGE = 2.6500E+02 C.F.S. *

STA. STATION WATER SURFACE FLOW AREA FLOW VELCTY ENERGY GRADE
 FROUDE

(ft) ELEVATION(ft) (ft²) (ft/s) LINE ELEV(ft) NUMBER

```

*****
1 8.8247E+04 1.11582E+03 1.30477E+02 2.03101E+00 1.11589E+03 2.60143E-01
2 8.3835E+04 1.10736E+03 1.33028E+02 1.99207E+00 1.10742E+03 2.54531E-01
3 7.9422E+04 1.09917E+03 9.26683E+01 2.85966E+00 1.09930E+03 4.04170E-01
4 7.5010E+04 1.08988E+03 7.86188E+01 3.37069E+00 1.09006E+03 4.66276E-01
5 7.0598E+04 1.08064E+03 1.15623E+02 2.29194E+00 1.08073E+03 3.81384E-01
6 6.6185E+04 1.07386E+03 1.30470E+02 2.03112E+00 1.07393E+03 3.18642E-01
7 6.1773E+04 1.06742E+03 1.25669E+02 2.10871E+00 1.06749E+03 3.09901E-01
8 5.7361E+04 1.06103E+03 1.38867E+02 1.90831E+00 1.06109E+03 2.68125E-01
9 5.2948E+04 1.05452E+03 1.00440E+02 2.63838E+00 1.05463E+03 3.31901E-01
10 4.8536E+04 1.05084E+03 1.02758E+04 2.57887E-02 1.05084E+03 8.93750E-04
11 4.4124E+04 1.04764E+03 1.32562E+02 1.99906E+00 1.04771E+03 2.86791E-01
12 3.9711E+04 1.04335E+03 1.79001E+02 1.48044E+00 1.04338E+03 1.85501E-01
13 3.5299E+04 1.04071E+03 1.30007E+02 2.03834E+00 1.04078E+03 2.17781E-01
14 3.0886E+04 1.03931E+03 6.00213E+02 4.41510E-01 1.03931E+03 3.88016E-02
15 2.6474E+04 1.03927E+03 1.33082E+03 1.99126E-01 1.03927E+03 1.18700E-02
16 2.2062E+04 1.03927E+03 1.81441E+03 1.46053E-01 1.03927E+03 7.82722E-03
17 1.7649E+04 1.03927E+03 3.19777E+03 8.28703E-02 1.03927E+03 3.98460E-03
18 1.3237E+04 1.03927E+03 4.27068E+03 6.20510E-02 1.03927E+03 2.61183E-03
19 8.8247E+03 1.03926E+03 3.43641E+03 7.71154E-02 1.03926E+03 3.50932E-03
20 4.4124E+03 1.03926E+03 4.72860E+03 5.60420E-02 1.03926E+03 2.17575E-03
21 0.0000E+00 9.74134E+02 2.99076E+01 8.86061E+00 9.75462E+02 5.87883E-01

```

```

*****
*   SEDIMENT ROUTING RESULTS FOR TIME STEP   720   *
*****

```

```

-----
INCOMING SEDIMENT DISTRIBUTION PER SIZE FRACTION
SIZE FRACTION    PERCENT    QSED (TON/DAY)
      1          100.00    1.5800E+01
TOTAL                    1.5800E+01
-----

```

```

*****
*   STREAM TUBE NO.   1   *
*****
STA DISTANCE    TOTAL LOAD    CHANGE DIRECTION
(TONS)          (FT**3)    (FT)
*****
1 8.8247E+04 1.9189E-01 2.3199E+00 0.000 VERTICAL
2 8.3835E+04 1.6637E-01 2.0114E+00 0.000 VERTICAL
3 7.9422E+04 4.4893E-02 5.4274E-01 0.000 VERTICAL
4 7.5010E+04 1.5557E-01 1.8808E+00 0.000 VERTICAL
5 7.0598E+04 0.0000E+00 0.0000E+00 0.000 VERTICAL
6 6.6185E+04 0.0000E+00 0.0000E+00 0.000 VERTICAL
7 6.1773E+04 9.0181E-03 1.0903E-01 0.000 VERTICAL
8 5.7361E+04 0.0000E+00 0.0000E+00 0.000 VERTICAL
9 5.2948E+04 9.6404E-02 1.1655E+00 0.000 VERTICAL
10 4.8536E+04 0.0000E+00 0.0000E+00 0.000 VERTICAL
11 4.4124E+04 0.0000E+00 0.0000E+00 0.000 VERTICAL
12 3.9711E+04 0.0000E+00 0.0000E+00 0.000 VERTICAL
13 3.5299E+04 0.0000E+00 0.0000E+00 0.000 VERTICAL
14 3.0886E+04 0.0000E+00 0.0000E+00 0.000 VERTICAL
15 2.6474E+04 0.0000E+00 0.0000E+00 0.000 VERTICAL

```


13	0.0000E+00	0.0000E+00	0.0000E+00
14	0.0000E+00	0.0000E+00	0.0000E+00
15	0.0000E+00	0.0000E+00	0.0000E+00
16	0.0000E+00	0.0000E+00	0.0000E+00
17	-4.2991E+02	-8.6624E+03	-8.6624E+03
18	-5.7449E+04	-1.1575E+06	-1.1575E+06
19	-9.5927E+04	-1.9328E+06	-1.9328E+06
20	1.5337E+05	3.0904E+06	3.0904E+06
21	-6.8890E+05	-1.3881E+07	-1.3881E+07
SUM	-6.8886E+05	-1.3880E+07	-1.3880E+07

ACCUMULATED SEDIMENT DISTRIBUTION THAT EXITED THE REACH (TONS)

SIZE FR	TOTAL	TUBE #1	TUBE #2	TUBE #
1	6.8933E+05	3.3674E+05	3.5259E+05	
TOTAL	6.8933E+05	3.3674E+05	3.5259E+05	

TIME STEP NO. 1440 AFTER 6.0000E+01 DAYS; DISCHARGE IS 8.8300E+02 CFS

* RESULTS OF BACKWATER COMPUTATIONS *

* DISCHARGE = 8.8300E+02 C.F.S. *

STA. STATION WATER SURFACE FLOW AREA FLOW VELCTY ENERGY GRADE
FROUDE

#	(ft)	ELEVATION(ft)	(ft ²)	(ft/s)	LINE ELEV(ft)	NUMBER
1	8.8247E+04	1.11529E+03	3.30022E+02	2.67558E+00	1.11541E+03	2.23985E-01
2	8.3835E+04	1.10962E+03	3.12752E+02	2.82332E+00	1.10975E+03	2.53559E-01
3	7.9422E+04	1.10106E+03	1.87208E+02	4.71667E+00	1.10142E+03	5.07818E-01
4	7.5010E+04	1.09140E+03	1.79648E+02	4.91515E+00	1.09180E+03	4.86675E-01
5	7.0598E+04	1.08292E+03	2.40837E+02	3.66638E+00	1.08313E+03	4.30762E-01
6	6.6185E+04	1.07539E+03	2.53752E+02	3.47977E+00	1.07558E+03	3.97724E-01
7	6.1773E+04	1.06888E+03	2.82377E+02	3.12703E+00	1.06904E+03	3.20063E-01
8	5.7361E+04	1.06320E+03	2.99523E+02	2.94802E+00	1.06334E+03	2.97929E-01
9	5.2948E+04	1.05606E+03	2.10058E+02	4.20360E+00	1.05636E+03	3.95627E-01
10	4.8536E+04	1.05193E+03	1.04851E+04	8.42148E-02	1.05193E+03	2.87865E-03
11	4.4124E+04	1.04958E+03	3.14827E+02	2.80471E+00	1.04971E+03	2.75329E-01
12	3.9711E+04	1.04692E+03	5.07638E+02	1.73943E+00	1.04697E+03	1.40845E-01
13	3.5299E+04	1.04274E+03	2.85080E+02	3.09737E+00	1.04294E+03	3.73510E-01
14	3.0886E+04	1.03686E+03	3.06218E+02	2.88357E+00	1.03700E+03	2.87619E-01
15	2.6474E+04	1.03421E+03	6.38987E+02	1.38188E+00	1.03424E+03	1.09006E-01
16	2.2062E+04	1.03385E+03	1.02670E+03	8.60039E-01	1.03387E+03	5.63107E-02
17	1.7649E+04	1.03378E+03	2.04641E+03	4.31487E-01	1.03378E+03	2.38821E-02
18	1.3237E+04	1.03373E+03	3.05360E+03	2.89167E-01	1.03373E+03	1.44583E-02
19	8.8247E+03	1.01709E+03	4.60194E+02	1.91876E+00	1.01717E+03	1.87175E-01
20	4.4124E+03	9.20776E+02	8.88551E+01	9.93753E+00	9.22313E+02	4.29379E-01
21	0.0000E+00	7.22287E+02	6.39925E+01	1.37985E+01	7.25357E+02	9.88847E-01

 * SEDIMENT ROUTING RESULTS FOR TIME STEP 1440 *

 INCOMING SEDIMENT DISTRIBUTION PER SIZE FRACTION
 SIZE FRACTION PERCENT QSED (TON/DAY)
 1 100.00 1.5800E+01
 TOTAL 1.5800E+01

 * STREAM TUBE NO. 1 *

 STA DISTANCE TOTAL LOAD CHANGE DIRECTION
 (TONS) (FT**3) (FT)

 1 8.8247E+04 5.0877E-01 6.1509E+00 0.000 VERTICAL
 2 8.3835E+04 8.0679E-01 9.7537E+00 0.000 VERTICAL
 3 7.9422E+04 9.4535E-01 1.1429E+01 0.000 VERTICAL
 4 7.5010E+04 8.3812E-01 1.0132E+01 0.000 VERTICAL
 5 7.0598E+04 4.3609E-01 5.2721E+00 0.000 VERTICAL
 6 6.6185E+04 2.8445E-01 3.4389E+00 0.000 VERTICAL
 7 6.1773E+04 3.8711E-01 4.6800E+00 0.000 VERTICAL
 8 5.7361E+04 2.5435E-01 3.0750E+00 0.000 VERTICAL
 9 5.2948E+04 1.0367E+00 1.2533E+01 0.000 VERTICAL
 10 4.8536E+04 0.0000E+00 0.0000E+00 0.000 VERTICAL
 11 4.4124E+04 1.5374E-01 1.8586E+00 0.000 VERTICAL
 12 3.9711E+04 0.0000E+00 0.0000E+00 0.000 VERTICAL
 13 3.5299E+04 7.5090E-01 9.0781E+00 0.000 VERTICAL
 14 3.0886E+04 1.9291E-01 2.3322E+00 0.000 VERTICAL
 15 2.6474E+04 0.0000E+00 0.0000E+00 0.000 VERTICAL
 16 2.2062E+04 0.0000E+00 0.0000E+00 0.000 VERTICAL
 17 1.7649E+04 0.0000E+00 0.0000E+00 0.000 VERTICAL
 18 1.3237E+04 0.0000E+00 0.0000E+00 0.000 VERTICAL
 19 8.8247E+03 7.0028E+01 8.4661E+02 -0.006 VERTICAL
 20 4.4124E+03 1.0444E+02 1.2626E+03 -0.006 VERTICAL
 21 0.0000E+00 1.4884E+02 1.7994E+03 -0.012 VERTICAL

 * STREAM TUBE NO. 2 *

 STA DISTANCE TOTAL LOAD CHANGE DIRECTION
 (TONS) (FT**3) (FT)

 1 8.8247E+04 5.0877E-01 6.1509E+00 0.000 VERTICAL
 2 8.3835E+04 8.0679E-01 9.7537E+00 0.000 VERTICAL
 3 7.9422E+04 9.4535E-01 1.1429E+01 0.000 VERTICAL
 4 7.5010E+04 8.3812E-01 1.0132E+01 0.000 VERTICAL
 5 7.0598E+04 4.3611E-01 5.2724E+00 0.000 VERTICAL
 6 6.6185E+04 2.8409E-01 3.4345E+00 0.000 VERTICAL
 7 6.1773E+04 3.8709E-01 4.6798E+00 0.000 VERTICAL
 8 5.7361E+04 2.5298E-01 3.0584E+00 0.000 VERTICAL
 9 5.2948E+04 1.0654E+00 1.2880E+01 0.000 VERTICAL
 10 4.8536E+04 0.0000E+00 0.0000E+00 0.000 VERTICAL

11	4.4124E+04	1.5684E-01	1.8962E+00	0.000	VERTICAL
12	3.9711E+04	0.0000E+00	0.0000E+00	0.000	VERTICAL
13	3.5299E+04	2.9691E-01	3.5896E+00	0.000	VERTICAL
14	3.0886E+04	2.1922E-01	2.6503E+00	0.000	VERTICAL
15	2.6474E+04	0.0000E+00	0.0000E+00	0.000	VERTICAL
16	2.2062E+04	0.0000E+00	0.0000E+00	0.000	VERTICAL
17	1.7649E+04	0.0000E+00	0.0000E+00	0.000	VERTICAL
18	1.3237E+04	0.0000E+00	0.0000E+00	0.000	VERTICAL
19	8.8247E+03	0.0000E+00	0.0000E+00	0.000	VERTICAL
20	4.4124E+03	1.0760E+02	1.3008E+03	-0.002	VERTICAL
21	0.0000E+00	1.4909E+02	1.8024E+03	-0.012	VERTICAL

 *** ACCUMMULATED DEPOSITION FOR WHOLE STREAM ***

 STA ACCU.DEPS. ACCU DEPS. ACCU. DEPS. FOR DIFFRNT SIZE GROUPS (FT^3)
 NO. (TONS) (FT^3) 1

1	-3.4696E+04	-6.9909E+05	-6.9909E+05
2	-6.6547E+03	-1.3409E+05	-1.3409E+05
3	1.3318E+04	2.6834E+05	2.6834E+05
4	-1.3162E+04	-2.6521E+05	-2.6521E+05
5	2.8437E+04	5.7298E+05	5.7298E+05
6	7.8966E+03	1.5911E+05	1.5911E+05
7	-7.2926E+03	-1.4694E+05	-1.4694E+05
8	8.6873E+03	1.7504E+05	1.7504E+05
9	-1.9572E+04	-3.9437E+05	-3.9437E+05
10	2.3987E+04	4.8332E+05	4.8332E+05
11	-2.8985E+03	-5.8402E+04	-5.8402E+04
12	2.8985E+03	5.8402E+04	5.8402E+04
13	-7.4111E+03	-1.4933E+05	-1.4933E+05
14	3.9062E+03	7.8707E+04	7.8707E+04
15	3.4837E+03	7.0193E+04	7.0193E+04
16	-3.6332E+02	-7.3205E+03	-7.3205E+03
17	-4.5372E+01	-9.1421E+02	-9.1421E+02
18	-5.7449E+04	-1.1575E+06	-1.1575E+06
19	-1.6903E+05	-3.4058E+06	-3.4058E+06
20	-2.2715E+06	-4.5769E+07	-4.5769E+07
21	-2.8171E+06	-5.6762E+07	-5.6762E+07
SUM	-5.3146E+06	-1.0708E+08	-1.0708E+08

 ACCUMULATED SEDIMENT DISTRIBUTION THAT EXITED THE REACH (TONS)
 SIZE FR TOTAL TUBE #1 TUBE #2 TUBE #
 1 5.3155E+06 2.6102E+06 2.7054E+06
 TOTAL 5.3155E+06 2.6102E+06 2.7054E+06

 TIME STEP NO. 2160 AFTER 9.0000E+01 DAYS; DISCHARGE IS 1.2380E+03 CFS


```

*****
*   RESULTS OF BACKWATER COMPUTATIONS   *
*   DISCHARGE = 1.2380E+03 C.F.S.     *
*****

```

STA. STATION WATER SURFACE FLOW AREA FLOW VELCTY ENERGY GRADE
FROUDE

```

# (ft)  ELEVATION(ft)  (ft^2)  (ft/s)  LINE ELEV(ft)  NUMBER
*****
1  8.8247E+04  6.85577E+02  2.04677E+01  6.04854E+01  7.43986E+02  1.86036E+01
2  8.3835E+04  6.85567E+02  3.04555E+01  4.06494E+01  7.11404E+02  1.02433E+01
3  7.9422E+04  6.85467E+02  2.56221E+01  4.83176E+01  7.22087E+02  1.22488E+01
4  7.5010E+04  6.85367E+02  2.04153E+01  6.06408E+01  7.43032E+02  1.53472E+01
5  7.0598E+04  6.85357E+02  5.02793E+01  2.46225E+01  6.94803E+02  6.16547E+00
6  6.6185E+04  6.85257E+02  5.01499E+01  2.46860E+01  6.94750E+02  6.18470E+00
7  6.1773E+04  6.85157E+02  4.04574E+01  3.06001E+01  6.99773E+02  7.69022E+00
8  5.7361E+04  6.85057E+02  3.91653E+01  3.16096E+01  7.00678E+02  8.09450E+00
9  5.2948E+04  6.84957E+02  6.97556E+00  1.77477E+02  1.22410E+03  5.26055E+01
10 4.8536E+04  6.84947E+02  2.05000E+01  6.03903E+01  7.42194E+02  1.53158E+01
11 4.4124E+04  6.84937E+02  3.80859E+01  3.25055E+01  7.01487E+02  8.43397E+00
12 3.9711E+04  6.84927E+02  3.94319E+01  3.13959E+01  7.00326E+02  8.00068E+00
13 3.5299E+04  6.84827E+02  8.19645E+00  1.51041E+02  1.10010E+03  5.61000E+01
14 3.0886E+04  6.84817E+02  2.40312E+01  5.15163E+01  7.35466E+02  1.85112E+01
15 2.6474E+04  6.84807E+02  4.96538E+01  2.49327E+01  6.94506E+02  6.31285E+00
16 2.2062E+04  6.84797E+02  5.04976E+01  2.45160E+01  6.94171E+02  6.15361E+00
17 1.7649E+04  6.84787E+02  6.54466E+01  1.89162E+01  6.90363E+02  4.74224E+00
18 1.3237E+04  6.84687E+02  1.75871E+01  7.03927E+01  2.68949E+06  7.55779E+01
19 8.8247E+03  6.84587E+02  1.70879E+01  7.24487E+01  2.76898E+06  7.72472E+01
20 4.4124E+03  6.84487E+02  1.73281E-02  7.14447E+04  7.94000E+07  2.52031E+04
21 0.0000E+00  0.00000E+00  8.04031E+01  1.53974E+01  3.83922E+00  9.99821E-01

```

```

*****
*   SEDIMENT ROUTING RESULTS FOR TIME STEP 2160   *
*****

```

```

-----
INCOMING SEDIMENT DISTRIBUTION PER SIZE FRACTION
SIZE FRACTION    PERCENT    QSED (TON/DAY)
1                100.00    1.5800E+01
TOTAL                1.5800E+01
-----

```

```

*****
*   STREAM TUBE NO. 1   *
*****
STA DISTANCE    TOTAL LOAD    CHANGE DIRECTION
(TONS)          (FT**3)      (FT)
*****
1  8.8247E+04  1.2155E+03  1.4695E+04  -0.363  VERTICAL
2  8.3835E+04  3.5772E+03  4.3247E+04  -0.363  VERTICAL
3  7.9422E+04  5.6575E+03  6.8397E+04  -0.363  VERTICAL
4  7.5010E+04  8.0230E+03  9.6995E+04  -0.363  VERTICAL
5  7.0598E+04  5.2343E+03  6.3280E+04  0.294  VERTICAL
6  6.6185E+04  5.2923E+03  6.3982E+04  -0.005  VERTICAL

```



```

4 -7.2223E+07 -1.4552E+09 -1.4552E+09
5 8.5153E+07 1.7158E+09 1.7158E+09
6 -1.6616E+06 -3.3479E+07 -3.3479E+07
7 -1.0552E+08 -2.1261E+09 -2.1261E+09
8 -8.0303E+07 -1.6180E+09 -1.6180E+09
9 -4.8756E+07 -9.8238E+08 -9.8238E+08
10 -5.5941E+07 -1.1272E+09 -1.1272E+09
11 -8.7512E+07 -1.7633E+09 -1.7633E+09
12 -8.4190E+07 -1.6963E+09 -1.6963E+09
13 -6.8549E+07 -1.3812E+09 -1.3812E+09
14 -8.9853E+07 -1.8105E+09 -1.8105E+09
15 3.8441E+08 7.7455E+09 7.7455E+09
16 3.0309E+07 6.1069E+08 6.1069E+08
17 1.9975E+08 4.0248E+09 4.0248E+09
18 -2.6100E+08 -5.2590E+09 -5.2590E+09
19 -2.4687E+08 -4.9742E+09 -4.9742E+09
20 -5.1322E+08 -1.0341E+10 -1.0341E+10
21 1.1748E+09 2.3672E+10 2.3672E+10
SUM -1.3879E+07 -2.7964E+08 -2.7964E+08

```

```

-----
ACCUMULATED SEDIMENT DISTRIBUTION THAT EXITED THE REACH (TONS)
SIZE FR TOTAL TUBE #1 TUBE #2 TUBE #
1 1.3880E+07 6.8914E+06 6.9887E+06
TOTAL 1.3880E+07 6.8914E+06 6.9887E+06
-----

```

```

*****
*****
TIME STEP NO. 2880 AFTER 1.2000E+02 DAYS; DISCHARGE IS 1.1880E+03 CFS
*****
*****

```

```

*****
* RESULTS OF BACKWATER COMPUTATIONS *
* DISCHARGE = 1.1880E+03 C.F.S. *
*****

```

```

STA. STATION WATER SURFACE FLOW AREA FLOW VELCTY ENERGY GRADE
FROUDE

```

```

# (ft) ELEVATION(ft) (ft^2) (ft/s) LINE ELEV(ft) NUMBER
*****
1 8.8247E+04 6.53334E+02 2.04665E+01 5.80460E+01 7.07125E+02 1.78524E+01
2 8.3835E+04 6.53324E+02 3.04555E+01 3.90077E+01 6.77115E+02 9.82963E+00
3 7.9422E+04 6.53224E+02 2.56221E+01 4.63662E+01 6.86945E+02 1.17541E+01
4 7.5010E+04 6.53124E+02 2.04152E+01 5.81921E+01 7.06225E+02 1.47274E+01
5 7.0598E+04 6.53114E+02 5.02800E+01 2.36277E+01 6.61811E+02 5.91651E+00
6 6.6185E+04 6.53014E+02 5.01493E+01 2.36892E+01 6.61755E+02 5.93507E+00
7 6.1773E+04 6.52914E+02 4.04563E+01 2.93651E+01 6.66373E+02 7.37975E+00
8 5.7361E+04 6.52814E+02 3.89519E+01 3.04991E+01 6.67361E+02 7.83314E+00
9 5.2948E+04 6.52714E+02 6.73417E+00 1.76414E+02 1.18154E+03 5.15756E+01
10 4.8536E+04 6.52704E+02 2.05000E+01 5.79513E+01 7.05420E+02 1.46972E+01
11 4.4124E+04 6.52694E+02 3.77984E+01 3.14299E+01 6.68180E+02 8.18872E+00
12 3.9711E+04 6.52684E+02 3.93180E+01 3.02151E+01 6.66947E+02 7.71123E+00
13 3.5299E+04 6.52584E+02 8.04513E+00 1.47667E+02 1.04516E+03 5.50387E+01
14 3.0886E+04 6.52574E+02 2.37808E+01 4.99563E+01 7.00290E+02 1.80600E+01

```

15	2.6474E+04	6.52564E+02	4.96538E+01	2.39257E+01	6.61494E+02	6.05789E+00
16	2.2062E+04	6.52554E+02	5.04976E+01	2.35259E+01	6.61186E+02	5.90508E+00
17	1.7649E+04	6.52544E+02	6.54466E+01	1.81522E+01	6.57677E+02	4.55071E+00
18	1.3237E+04	6.52444E+02	1.77748E+01	6.68361E+01	2.44939E+06	7.19238E+01
19	8.8247E+03	6.52344E+02	1.75856E+01	6.75552E+01	2.47606E+06	7.25105E+01
20	4.4124E+03	6.52244E+02	1.41195E-02	8.41387E+04	1.10057E+08	2.96724E+04
21	0.0000E+00	0.00000E+00	7.80004E+01	1.52307E+01	3.73994E+00	9.99384E-01

 * SEDIMENT ROUTING RESULTS FOR TIME STEP 2880 *

 INCOMING SEDIMENT DISTRIBUTION PER SIZE FRACTION
 SIZE FRACTION PERCENT QSED (TON/DAY)
 1 100.00 1.5800E+01
 TOTAL 1.5800E+01

 * STREAM TUBE NO. 1 *

STA	DISTANCE (TONS)	TOTAL LOAD (FT**3)	CHANGE (FT)	DIRECTION
1	8.8247E+04	1.2154E+03	1.4694E+04	-0.363 VERTICAL
2	8.3835E+04	3.5771E+03	4.3246E+04	-0.363 VERTICAL
3	7.9422E+04	5.6573E+03	6.8395E+04	-0.363 VERTICAL
4	7.5010E+04	8.0229E+03	9.6994E+04	-0.363 VERTICAL
5	7.0598E+04	4.4356E+03	5.3625E+04	0.378 VERTICAL
6	6.6185E+04	4.4852E+03	5.4224E+04	-0.005 VERTICAL
7	6.1773E+04	7.8966E+03	9.5467E+04	-0.363 VERTICAL
8	5.7361E+04	1.0469E+04	1.2656E+05	-0.363 VERTICAL
9	5.2948E+04	1.2073E+04	1.4596E+05	-0.363 VERTICAL
10	4.8536E+04	1.4003E+04	1.6928E+05	-0.363 VERTICAL
11	4.4124E+04	1.7042E+04	2.0603E+05	-0.363 VERTICAL
12	3.9711E+04	1.9774E+04	2.3906E+05	-0.363 VERTICAL
13	3.5299E+04	2.2134E+04	2.6760E+05	-0.363 VERTICAL
14	3.0886E+04	2.5696E+04	3.1066E+05	-0.363 VERTICAL
15	2.6474E+04	1.1091E+04	1.3409E+05	1.259 VERTICAL
16	2.2062E+04	1.0200E+04	1.2332E+05	0.075 VERTICAL
17	1.7649E+04	4.6517E+03	5.6238E+04	0.090 VERTICAL
18	1.3237E+04	4.7500E+03	5.7425E+04	-0.001 VERTICAL
19	8.8247E+03	5.0059E+03	6.0519E+04	-0.002 VERTICAL
20	4.4124E+03	2.3969E+04	2.8977E+05	-0.363 VERTICAL
21	0.0000E+00	2.3601E+02	2.8533E+03	11.304 VERTICAL

 * STREAM TUBE NO. 2 *

STA	DISTANCE (TONS)	TOTAL LOAD (FT**3)	CHANGE (FT)	DIRECTION
1	8.8247E+04	1.2154E+03	1.4694E+04	-0.363 VERTICAL

2	8.3835E+04	3.5771E+03	4.3246E+04	-0.363	VERTICAL
3	7.9422E+04	5.6573E+03	6.8395E+04	-0.363	VERTICAL
4	7.5010E+04	8.0225E+03	9.6989E+04	-0.363	VERTICAL
5	7.0598E+04	4.4360E+03	5.3629E+04	0.378	VERTICAL
6	6.6185E+04	4.4799E+03	5.4160E+04	-0.004	VERTICAL
7	6.1773E+04	7.9809E+03	9.6486E+04	-0.363	VERTICAL
8	5.7361E+04	1.0651E+04	1.2877E+05	-0.363	VERTICAL
9	5.2948E+04	1.2201E+04	1.4751E+05	-0.363	VERTICAL
10	4.8536E+04	1.3919E+04	1.6828E+05	-0.363	VERTICAL
11	4.4124E+04	1.6612E+04	2.0083E+05	-0.363	VERTICAL
12	3.9711E+04	1.9394E+04	2.3447E+05	-0.363	VERTICAL
13	3.5299E+04	2.1523E+04	2.6020E+05	-0.363	VERTICAL
14	3.0886E+04	2.3847E+04	2.8830E+05	-0.363	VERTICAL
15	2.6474E+04	1.0993E+04	1.3290E+05	1.332	VERTICAL
16	2.2062E+04	1.0200E+04	1.2332E+05	0.066	VERTICAL
17	1.7649E+04	4.6540E+03	5.6265E+04	0.090	VERTICAL
18	1.3237E+04	4.7500E+03	5.7425E+04	-0.001	VERTICAL
19	8.8247E+03	5.0059E+03	6.0519E+04	-0.002	VERTICAL
20	4.4124E+03	2.3968E+04	2.8977E+05	-0.363	VERTICAL
21	0.0000E+00	2.3503E+02	2.8414E+03	11.255	VERTICAL

 *** ACCUMMULATED DEPOSITION FOR WHOLE STREAM ***

 STA ACCU.DEPS. ACCU DEPS. ACCU. DEPS. FOR DIFFRNT SIZE GROUPS (FT^3)
 NO. (TONS) (FT^3) 1

1	-7.4775E+07	-1.5066E+09	-1.5066E+09
2	-1.4522E+08	-2.9261E+09	-2.9261E+09
3	-1.2790E+08	-2.5770E+09	-2.5770E+09
4	-1.4546E+08	-2.9308E+09	-2.9308E+09
5	1.9620E+08	3.9533E+09	3.9533E+09
6	-3.1079E+06	-6.2621E+07	-6.2621E+07
7	-2.1252E+08	-4.2822E+09	-4.2822E+09
8	-1.6146E+08	-3.2532E+09	-3.2532E+09
9	-9.7584E+07	-1.9662E+09	-1.9662E+09
10	-1.1240E+08	-2.2648E+09	-2.2648E+09
11	-1.7625E+08	-3.5512E+09	-3.5512E+09
12	-1.6956E+08	-3.4165E+09	-3.4165E+09
13	-1.3804E+08	-2.7813E+09	-2.7813E+09
14	-1.8096E+08	-3.6463E+09	-3.6463E+09
15	8.0948E+08	1.6310E+10	1.6310E+10
16	5.6368E+07	1.1358E+09	1.1358E+09
17	3.7150E+08	7.4854E+09	7.4854E+09
18	-2.7439E+08	-5.5287E+09	-5.5287E+09
19	-2.6507E+08	-5.3409E+09	-5.3409E+09
20	-1.0940E+09	-2.2043E+10	-2.2043E+10
21	1.9231E+09	3.8749E+10	3.8749E+10
SUM	-2.2014E+07	-4.4356E+08	-4.4356E+08

 ACCUMULATED SEDIMENT DISTRIBUTION THAT EXITED THE REACH (TONS)
 SIZE FR TOTAL TUBE #1 TUBE #2 TUBE #
 1 2.2016E+07 1.0967E+07 1.1048E+07

TOTAL 2.2016E+07 1.0967E+07 1.1048E+07

 TIME STEP NO. 3600 AFTER 1.5000E+02 DAYS; DISCHARGE IS 1.0480E+03 CFS

 * RESULTS OF BACKWATER COMPUTATIONS *
 * DISCHARGE = 1.0480E+03 C.F.S. *

STA. STATION WATER SURFACE FLOW AREA FLOW VELCTY ENERGY GRADE
 FROUDE

#	(ft)	ELEVATION(ft)	(ft^2)	(ft/s)	LINE ELEV(ft)	NUMBER
1	8.8247E+04	1.11397E+03	3.97560E+02	2.63608E+00	1.11408E+03	2.01021E-01
2	8.3835E+04	1.10908E+03	3.55010E+02	2.95203E+00	1.10922E+03	2.47891E-01
3	7.9422E+04	1.10112E+03	2.13453E+02	4.90974E+00	1.10151E+03	4.98285E-01
4	7.5010E+04	1.09220E+03	2.07946E+02	5.03977E+00	1.09263E+03	4.76541E-01
5	7.0598E+04	1.08388E+03	2.64469E+02	3.96266E+00	1.08413E+03	4.46966E-01
6	6.6185E+04	1.07588E+03	2.75378E+02	3.80567E+00	1.07611E+03	4.19012E-01
7	6.1773E+04	1.06937E+03	3.24009E+02	3.23448E+00	1.06954E+03	3.12658E-01
8	5.7361E+04	1.06316E+03	3.07866E+02	3.40407E+00	1.06335E+03	3.38993E-01
9	5.2948E+04	1.05571E+03	2.41621E+02	4.33738E+00	1.05603E+03	3.85278E-01
10	4.8536E+04	1.05200E+03	1.01691E+04	1.03057E-01	1.05200E+03	3.57521E-03
11	4.4124E+04	1.04978E+03	3.58309E+02	2.92485E+00	1.04992E+03	2.71125E-01
12	3.9711E+04	1.04655E+03	4.28907E+02	2.44342E+00	1.04665E+03	2.12440E-01
13	3.5299E+04	1.04258E+03	3.45671E+02	3.03179E+00	1.04277E+03	3.35206E-01
14	3.0886E+04	1.03727E+03	3.32487E+02	3.15200E+00	1.03743E+03	3.07793E-01
15	2.6474E+04	1.03264E+03	3.89944E+02	2.68757E+00	1.03275E+03	2.62957E-01
16	2.2062E+04	1.02955E+03	4.68468E+02	2.23708E+00	1.02963E+03	2.01078E-01
17	1.7649E+04	6.51928E+02	6.54466E+01	1.60130E+01	6.55923E+02	4.01443E+00
18	1.3237E+04	6.51828E+02	1.78099E+01	5.88437E+01	1.90245E+06	6.33529E+01
19	8.8247E+03	6.51728E+02	1.77552E+01	5.90250E+01	1.90838E+06	6.35012E+01
20	4.4124E+03	6.51628E+02	1.41195E-02	7.42234E+04	8.56462E+07	2.61756E+04
21	0.0000E+00	0.00000E+00	7.15957E+01	1.46378E+01	3.44408E+00	9.99408E-01

 * SEDIMENT ROUTING RESULTS FOR TIME STEP 3600 *

INCOMING SEDIMENT DISTRIBUTION PER SIZE FRACTION		
SIZE FRACTION	PERCENT	QSED (TON/DAY)
1	100.00	1.5800E+01
TOTAL		1.5800E+01

 * STREAM TUBE NO. 1 *

 STA ACCU.DEPS. ACCU DEPS. ACCU. DEPS. FOR DIFFRNT SIZE GROUPS (FT^3)
 NO. (TONS) (FT^3) 1

1	-7.4791E+07	-1.5070E+09	-1.5070E+09
2	-1.4524E+08	-2.9265E+09	-2.9265E+09
3	-1.2790E+08	-2.5771E+09	-2.5771E+09
4	-1.4545E+08	-2.9307E+09	-2.9307E+09
5	1.9622E+08	3.9536E+09	3.9536E+09
6	-3.1030E+06	-6.2522E+07	-6.2522E+07
7	-2.1252E+08	-4.2821E+09	-4.2821E+09
8	-1.6146E+08	-3.2533E+09	-3.2533E+09
9	-9.7606E+07	-1.9667E+09	-1.9667E+09
10	-1.1236E+08	-2.2640E+09	-2.2640E+09
11	-1.7625E+08	-3.5514E+09	-3.5514E+09
12	-1.6955E+08	-3.4163E+09	-3.4163E+09
13	-1.3805E+08	-2.7816E+09	-2.7816E+09
14	-1.8096E+08	-3.6463E+09	-3.6463E+09
15	8.0949E+08	1.6310E+10	1.6310E+10
16	5.6372E+07	1.1358E+09	1.1358E+09
17	2.7438E+08	5.5284E+09	5.5284E+09
18	-2.7520E+08	-5.5451E+09	-5.5451E+09
19	-2.6809E+08	-5.4018E+09	-5.4018E+09
20	-1.7507E+09	-3.5276E+10	-3.5276E+10
21	2.6741E+09	5.3880E+10	5.3880E+10
SUM	-2.8770E+07	-5.7969E+08	-5.7969E+08

 ACCUMULATED SEDIMENT DISTRIBUTION THAT EXITED THE REACH (TONS)
 SIZE FR TOTAL TUBE #1 TUBE #2 TUBE #
 1 2.8772E+07 1.4353E+07 1.4419E+07
 TOTAL 2.8772E+07 1.4353E+07 1.4419E+07

This page intentionally left blank

10.7.2 Simulation 2: mixed bed, finer incoming sediment

***** SUMMARY OF INPUT PARAMETERS *****

Number of cross sections:..... 21
 Number of stream tubes:..... 2
 Number of time steps:..... 3600
 Number of sediment time steps (NITRQS):..... 24
 Duration of time step (days):..... 4.1667E-02
 Formula selected for conveyance calculations:..... manning
 Formula selected for friction slope:..... average
 Formula for sediment transport: Garde (1965)
 NALT for active layer thickness:..... 14
 Transport parameter CFACTOR:..... 1.00
 Printout control is 3; print interval:..... 720
 Number of time steps to generate x-sec plots:..... 3600
 Number of time steps for thalweg plots:..... 720
 No minimization requested.

Sect. #	Location (ft)	ISWITCH	ITYP (ft)	Thalweg Coef.	Bed slope	Loss	NDIVI	NPOINTS
1	8.8247E+04	0	0	1.1145E+03	2.0456E-03	0.00	1	15
2	8.3835E+04	0	0	1.1055E+03	2.0456E-03	0.00	1	15
3	7.9422E+04	0	0	1.0969E+03	1.9545E-03	0.00	1	15
4	7.5010E+04	0	0	1.0884E+03	1.9096E-03	0.00	1	18
5	7.0598E+04	0	0	1.0792E+03	2.0909E-03	0.00	1	19
6	6.6185E+04	0	0	1.0726E+03	1.5012E-03	0.00	1	19
7	6.1773E+04	0	0	1.0659E+03	1.5016E-03	0.00	1	24
8	5.7361E+04	0	0	1.0593E+03	1.5016E-03	0.00	1	24
9	5.2948E+04	0	0	1.0523E+03	1.5919E-03	0.00	1	35
10	4.8536E+04	0	0	1.0003E+03	1.1792E-02	0.00	1	35
11	4.4124E+04	0	0	1.0460E+03	-1.0375E-02	0.00	1	24
12	3.9711E+04	0	0	1.0412E+03	1.0934E-03	0.00	1	24
13	3.5299E+04	0	0	1.0372E+03	9.1228E-04	0.00	1	35
14	3.0886E+04	0	0	1.0332E+03	9.1208E-04	0.00	1	26
15	2.6474E+04	0	0	1.0284E+03	1.0936E-03	0.00	1	24
16	2.2062E+04	0	0	1.0251E+03	7.3096E-04	0.00	1	24
17	1.7649E+04	0	0	1.0211E+03	9.1208E-04	0.00	1	23
18	1.3237E+04	0	0	1.7775E+01	2.2741E-01	0.00	1	24
19	8.8247E+03	0	0	1.5550E+01	5.0427E-04	0.00	1	22
20	4.4124E+03	0	0	1.0130E+03	-2.2607E-01	0.00	1	25
21	0.0000E+00	1	1	1.0123E+03	1.6431E-04	0.00	1	25

Coefficients used in Exner equation and in
 computing hydraulic properties for sediment capacity

C1WP	C2WP	C3WP	C1WPU	C2WPU	C1Q	C2Q	C3Q	C1QD	C2QD	C1QU	C2QU
0.250	0.500	0.250	0.750	0.250							
0.000	1.000	0.000	0.000	1.000	1.000	0.000					

Number of particle size classes: 7

Class #	DRL (mm)	DRU (mm)	Geometric Dry specific	
			mean (mm)	weight (lb/ft ³)
1	7.5000E-02	5.0000E-01	1.9365E-01	9.9260E+01
2	5.0000E-01	2.0000E+00	1.0000E+00	9.9260E+01
3	2.0000E+00	4.0000E+00	2.8284E+00	9.9260E+01
4	4.0000E+00	8.0000E+00	5.6569E+00	9.9260E+01
5	8.0000E+00	1.6000E+01	1.1314E+01	9.9260E+01
6	1.6000E+01	6.4000E+01	3.2000E+01	9.9260E+01
7	6.4000E+01	1.2700E+02	9.0155E+01	9.9260E+01

Percentage of bed material for each size fraction and for each cross section

Section # Bed material size fraction for each group

Section #	1	2	3	4	5	6	7
1	15.0	30.0	30.0	10.0	10.0	2.5	2.5
2	7.0	13.0	20.0	40.0	10.0	5.0	5.0
3	7.0	13.0	20.0	40.0	10.0	5.0	5.0
4	7.0	13.0	20.0	40.0	10.0	5.0	5.0
5	7.0	13.0	20.0	40.0	10.0	5.0	5.0
6	7.0	13.0	20.0	40.0	10.0	5.0	5.0
7	7.0	13.0	20.0	40.0	10.0	5.0	5.0
8	7.0	13.0	20.0	40.0	10.0	5.0	5.0
9	7.0	13.0	20.0	40.0	10.0	5.0	5.0
10	7.0	13.0	20.0	40.0	10.0	5.0	5.0
11	7.0	13.0	20.0	40.0	10.0	5.0	5.0
12	7.0	13.0	20.0	40.0	10.0	5.0	5.0
13	7.0	13.0	20.0	40.0	10.0	5.0	5.0
14	7.0	13.0	20.0	40.0	10.0	5.0	5.0
15	7.0	13.0	20.0	40.0	10.0	5.0	5.0
16	7.0	13.0	20.0	40.0	10.0	5.0	5.0
17	7.0	13.0	20.0	40.0	10.0	5.0	5.0
18	7.0	13.0	20.0	40.0	10.0	5.0	5.0
19	7.0	13.0	20.0	40.0	10.0	5.0	5.0
20	7.0	13.0	20.0	40.0	10.0	5.0	5.0
21	7.0	13.0	20.0	40.0	10.0	5.0	5.0

 TIME STEP NO. 720 AFTER 3.0000E+01 DAYS; DISCHARGE IS 2.6500E+02 CFS

 * RESULTS OF BACKWATER COMPUTATIONS *
 * DISCHARGE = 2.6500E+02 C.F.S. *

STA. STATION WATER SURFACE FLOW AREA FLOW VELCTY ENERGY GRADE
FROUDE

#	(ft)	ELEVATION(ft)	(ft^2)	(ft/s)	LINE ELEV(ft)	NUMBER
1	8.8247E+04	1.11328E+03	1.52025E+02	1.74314E+00	1.11333E+03	2.04380E-01
2	8.3835E+04	1.10728E+03	1.40847E+02	1.88147E+00	1.10734E+03	2.33993E-01
3	7.9422E+04	1.09932E+03	8.97564E+01	2.95244E+00	1.09946E+03	4.24425E-01
4	7.5010E+04	1.08973E+03	7.91980E+01	3.34604E+00	1.08991E+03	4.60400E-01
5	7.0598E+04	1.08108E+03	1.19709E+02	2.21370E+00	1.08115E+03	3.62414E-01
6	6.6185E+04	1.07400E+03	1.21549E+02	2.18020E+00	1.07408E+03	3.54070E-01
7	6.1773E+04	1.06727E+03	1.30171E+02	2.03578E+00	1.06733E+03	2.93935E-01
8	5.7361E+04	1.06120E+03	1.37670E+02	1.92489E+00	1.06126E+03	2.71967E-01
9	5.2948E+04	1.05444E+03	9.89858E+01	2.67715E+00	1.05456E+03	3.38085E-01
10	4.8536E+04	1.05060E+03	1.01077E+04	2.62177E-02	1.05060E+03	9.17187E-04
11	4.4124E+04	1.04755E+03	1.34391E+02	1.97185E+00	1.04761E+03	2.80922E-01
12	3.9711E+04	1.04396E+03	2.18612E+02	1.21220E+00	1.04399E+03	1.39405E-01
13	3.5299E+04	1.03983E+03	9.66458E+01	2.74197E+00	1.03996E+03	3.24186E-01
14	3.0886E+04	1.03549E+03	1.88258E+02	1.40765E+00	1.03553E+03	1.72629E-01
15	2.6474E+04	1.03448E+03	6.87803E+02	3.85285E-01	1.03448E+03	2.94396E-02
16	2.2062E+04	1.03445E+03	1.10692E+03	2.39403E-01	1.03445E+03	1.52562E-02
17	1.7649E+04	1.03445E+03	2.18535E+03	1.21262E-01	1.03445E+03	6.54617E-03
18	1.3237E+04	1.03445E+03	3.39239E+03	7.81159E-02	1.03445E+03	3.76474E-03
19	8.8247E+03	1.03444E+03	3.78031E+03	7.01002E-02	1.03444E+03	2.83781E-03
20	4.4124E+03	1.03444E+03	3.69780E+03	7.16643E-02	1.03444E+03	3.12371E-03
21	0.0000E+00	9.70450E+02	2.98501E+01	8.87771E+00	9.71776E+02	6.10532E-01

* SEDIMENT ROUTING RESULTS FOR TIME STEP 720 *

INCOMING SEDIMENT DISTRIBUTION PER SIZE FRACTION

SIZE FRACTION	PERCENT	QSED (TON/DAY)
1	15.00	2.3700E+00
2	30.00	4.7400E+00
3	30.00	4.7400E+00
4	10.00	1.5800E+00
5	10.00	1.5800E+00
6	2.50	3.9500E-01
7	2.50	3.9500E-01
TOTAL		1.5800E+01

* STREAM TUBE NO. 1 *

STA	DISTANCE	TOTAL LOAD	CHANGE	DIRECTION
	(TONS)	(FT**3)	(FT)	
1	8.8247E+04	4.2896E-01	5.1859E+00	0.000 VERTICAL
2	8.3835E+04	6.0223E-01	7.2807E+00	0.000 VERTICAL
3	7.9422E+04	6.5704E-01	7.9434E+00	0.000 VERTICAL
4	7.5010E+04	7.6734E-01	9.2769E+00	0.000 VERTICAL
5	7.0598E+04	5.0002E-01	6.0451E+00	0.000 VERTICAL
6	6.6185E+04	4.4730E-01	5.4077E+00	0.000 VERTICAL

4	-7.2504E+03	-1.4609E+05	-3.0888E+04	-2.2232E+04	-3.8541E+04	-5.0970E+04
5	1.3665E+04	2.7534E+05	6.8610E+04	6.8740E+04	5.8750E+04	7.5732E+04
6	4.9521E+03	9.9780E+04	5.5933E+04	2.4420E+04	1.2100E+04	7.3261E+03
7	-5.0436E+03	-1.0162E+05	-2.0536E+04	-3.2001E+04	-2.5078E+04	-2.4009E+04
8	4.3523E+03	8.7694E+04	2.5936E+04	2.6061E+04	1.9879E+04	1.5818E+04
9	-2.3181E+03	-4.6707E+04	-7.5199E+03	-6.8374E+03	-1.0064E+04	-2.1465E+04
10	1.4750E+04	2.9720E+05	1.4587E+05	7.3621E+04	4.2867E+04	3.4023E+04
11	-3.8087E+03	-7.6742E+04	-3.9702E+04	-2.1866E+04	-1.1151E+04	-4.0235E+03
12	3.3100E+03	6.6694E+04	3.2984E+04	1.9100E+04	1.0586E+04	4.0235E+03
13	-1.5173E+03	-3.0573E+04	-1.3068E+04	-7.8678E+03	-5.4531E+03	-4.1597E+03
14	1.9569E+03	3.9429E+04	1.8945E+04	1.0313E+04	5.9877E+03	4.1597E+03
15	5.9173E+01	1.1923E+03	8.4075E+02	3.2130E+02	3.0231E+01	0.0000E+00
16	0.0000E+00	0.0000E+00	0.0000E+00	0.0000E+00	0.0000E+00	0.0000E+00
17	-2.7378E+03	-5.5165E+04	-2.2780E+04	-1.2786E+04	-8.7309E+03	-9.5854E+03
18	-2.1643E+05	-4.3608E+06	-1.2621E+06	-8.9636E+05	-8.1580E+05	-1.1311E+06
19	-1.0075E+06	-2.0300E+07	-1.0654E+06	-2.5746E+06	-4.1152E+06	-8.3759E+06
20	1.2239E+06	2.4660E+07	2.3266E+06	3.4710E+06	4.9311E+06	9.5071E+06
21	-7.5210E+05	-1.5154E+07	-1.2907E+06	-2.2440E+06	-3.2335E+06	-6.1250E+06
SUM	-7.5440E+05	-1.5201E+07	-1.3130E+06	-2.2538E+06	-3.2393E+06	-6.1336E+06

 ACCUMULATED DEPOSITION FOR DIFFERENT SIZE GROUPS (CONT.)

STA	5	6	7
1	7.9835E+02	2.3877E+02	2.3877E+02
2	-1.8324E+03	0.0000E+00	0.0000E+00
3	1.9420E+03	0.0000E+00	0.0000E+00
4	-3.4591E+03	0.0000E+00	0.0000E+00
5	3.5061E+03	0.0000E+00	0.0000E+00
6	0.0000E+00	0.0000E+00	0.0000E+00
7	0.0000E+00	0.0000E+00	0.0000E+00
8	0.0000E+00	0.0000E+00	0.0000E+00
9	-8.2051E+02	0.0000E+00	0.0000E+00
10	8.2051E+02	0.0000E+00	0.0000E+00
11	0.0000E+00	0.0000E+00	0.0000E+00
12	0.0000E+00	0.0000E+00	0.0000E+00
13	-2.4394E+01	0.0000E+00	0.0000E+00
14	2.4394E+01	0.0000E+00	0.0000E+00
15	0.0000E+00	0.0000E+00	0.0000E+00
16	0.0000E+00	0.0000E+00	0.0000E+00
17	-1.1944E+03	-8.8266E+01	0.0000E+00
18	-1.8802E+05	-4.6564E+04	-2.0830E+04
19	-2.1058E+06	-1.0500E+06	-1.0133E+06
20	2.2938E+06	1.0965E+06	1.0341E+06
21	-1.4241E+06	-5.6847E+05	-2.6849E+05
SUM	-1.4243E+06	-5.6834E+05	-2.6826E+05

 ACCUMULATED SEDIMENT DISTRIBUTION THAT EXITED THE REACH (TONS)

SIZE FR	TOTAL	TUBE #1	TUBE #2	TUBE #
1	6.5233E+04	3.0678E+04	3.4556E+04	
2	1.1200E+05	5.2733E+04	5.9267E+04	
3	1.6091E+05	7.6304E+04	8.4604E+04	
4	3.0446E+05	1.4511E+05	1.5935E+05	
5	7.0736E+04	3.3924E+04	3.6812E+04	
6	2.8219E+04	1.3706E+04	1.4513E+04	

7 1.3325E+04 6.1056E+03 7.2198E+03
 TOTAL 7.5488E+05 3.5856E+05 3.9632E+05

 TIME STEP NO. 1440 AFTER 6.0000E+01 DAYS; DISCHARGE IS 8.8300E+02 CFS

 * RESULTS OF BACKWATER COMPUTATIONS *
 * DISCHARGE = 8.8300E+02 C.F.S. *

STA. STATION WATER SURFACE FLOW AREA FLOW VELCTY ENERGY GRADE
 FROUDE

#	(ft)	ELEVATION(ft)	(ft^2)	(ft/s)	LINE ELEV(ft)	NUMBER
1	8.8247E+04	1.11225E+03	3.76630E+02	2.34448E+00	1.11234E+03	1.81321E-01
2	8.3835E+04	1.10775E+03	3.17569E+02	2.78050E+00	1.10788E+03	2.40538E-01
3	7.9422E+04	1.10039E+03	1.95585E+02	4.51465E+00	1.10072E+03	4.67474E-01
4	7.5010E+04	1.09175E+03	1.83015E+02	4.82475E+00	1.09213E+03	4.77572E-01
5	7.0598E+04	1.08337E+03	2.39636E+02	3.68476E+00	1.08359E+03	4.34351E-01
6	6.6185E+04	1.07557E+03	2.49800E+02	3.53483E+00	1.07577E+03	4.07250E-01
7	6.1773E+04	1.06909E+03	2.88491E+02	3.06075E+00	1.06924E+03	3.10925E-01
8	5.7361E+04	1.06313E+03	2.85241E+02	3.09563E+00	1.06329E+03	3.19554E-01
9	5.2948E+04	1.05545E+03	2.06486E+02	4.27632E+00	1.05576E+03	3.99622E-01
10	4.8536E+04	1.05122E+03	9.80505E+03	9.00556E-02	1.05122E+03	3.19670E-03
11	4.4124E+04	1.04925E+03	3.31623E+02	2.66266E+00	1.04936E+03	2.53985E-01
12	3.9711E+04	1.04624E+03	3.87208E+02	2.28043E+00	1.04632E+03	2.07477E-01
13	3.5299E+04	1.04217E+03	3.05882E+02	2.88674E+00	1.04234E+03	3.36222E-01
14	3.0886E+04	1.03677E+03	2.98349E+02	2.95962E+00	1.03691E+03	2.98663E-01
15	2.6474E+04	1.03224E+03	3.53551E+02	2.49751E+00	1.03234E+03	2.54355E-01
16	2.2062E+04	1.02922E+03	4.20602E+02	2.09937E+00	1.02929E+03	1.97630E-01
17	1.7649E+04	8.11813E+02	6.04448E+01	1.46084E+01	8.15165E+02	3.82391E+00
18	1.3237E+04	8.11713E+02	1.33300E+01	6.62415E+01	1.81362E+06	6.65881E+01
19	8.8247E+03	8.11613E+02	1.20750E+01	7.31264E+01	2.00424E+06	7.17714E+01
20	4.4124E+03	8.11513E+02	7.37955E-02	1.19655E+04	2.32650E+06	4.31341E+03
21	0.0000E+00	0.00000E+00	6.46886E+01	1.36500E+01	3.04953E+00	9.99977E-01

 * SEDIMENT ROUTING RESULTS FOR TIME STEP 1440 *

 INCOMING SEDIMENT DISTRIBUTION PER SIZE FRACTION

SIZE FRACTION	PERCENT	QSED (TON/DAY)
1	15.00	2.3700E+00
2	30.00	4.7400E+00
3	30.00	4.7400E+00
4	10.00	1.5800E+00
5	10.00	1.5800E+00
6	2.50	3.9500E-01
7	2.50	3.9500E-01

TOTAL 1.5800E+01

* STREAM TUBE NO. 1 *

STA	DISTANCE	TOTAL LOAD	CHANGE	DIRECTION
	(TONS)	(FT**3)	(FT)	

1	8.8247E+04	6.7223E-01	8.1270E+00	0.000 VERTICAL
2	8.3835E+04	1.5550E+00	1.8799E+01	0.000 VERTICAL
3	7.9422E+04	1.8099E+00	2.1881E+01	0.000 VERTICAL
4	7.5010E+04	2.0340E+00	2.4590E+01	0.000 VERTICAL
5	7.0598E+04	2.0495E+00	2.4777E+01	0.000 VERTICAL
6	6.6185E+04	1.9544E+00	2.3627E+01	0.000 VERTICAL
7	6.1773E+04	1.9150E+00	2.3152E+01	0.000 VERTICAL
8	5.7361E+04	2.1624E+00	2.6143E+01	0.000 VERTICAL
9	5.2948E+04	3.5001E+00	4.2314E+01	0.000 VERTICAL
10	4.8536E+04	0.0000E+00	0.0000E+00	0.000 VERTICAL
11	4.4124E+04	7.4413E-01	8.9962E+00	0.000 VERTICAL
12	3.9711E+04	5.6122E-01	6.7850E+00	0.000 VERTICAL
13	3.5299E+04	1.6021E+00	1.9369E+01	0.000 VERTICAL
14	3.0886E+04	1.4784E+00	1.7873E+01	0.000 VERTICAL
15	2.6474E+04	1.1450E+00	1.3843E+01	0.000 VERTICAL
16	2.2062E+04	4.8067E-01	5.8112E+00	0.000 VERTICAL
17	1.7649E+04	5.6490E+03	6.8294E+04	-0.101 VERTICAL
18	1.3237E+04	1.6531E+04	1.9985E+05	-0.080 VERTICAL
19	8.8247E+03	2.6658E+04	3.2229E+05	-0.078 VERTICAL
20	4.4124E+03	2.8903E+05	3.4942E+06	-6.060 VERTICAL
21	0.0000E+00	3.8326E+02	4.6334E+03	142.072 VERTICAL

* STREAM TUBE NO. 2 *

STA	DISTANCE	TOTAL LOAD	CHANGE	DIRECTION
	(TONS)	(FT**3)	(FT)	

1	8.8247E+04	6.7222E-01	8.1269E+00	0.000 VERTICAL
2	8.3835E+04	1.5550E+00	1.8799E+01	0.000 VERTICAL
3	7.9422E+04	1.8099E+00	2.1881E+01	0.000 VERTICAL
4	7.5010E+04	2.0340E+00	2.4591E+01	0.000 VERTICAL
5	7.0598E+04	2.0302E+00	2.4544E+01	0.000 VERTICAL
6	6.6185E+04	1.9374E+00	2.3422E+01	0.000 VERTICAL
7	6.1773E+04	1.9145E+00	2.3146E+01	0.000 VERTICAL
8	5.7361E+04	2.1648E+00	2.6171E+01	0.000 VERTICAL
9	5.2948E+04	3.3974E+00	4.1073E+01	0.000 VERTICAL
10	4.8536E+04	0.0000E+00	0.0000E+00	0.000 VERTICAL
11	4.4124E+04	7.1374E-01	8.6288E+00	0.000 VERTICAL
12	3.9711E+04	5.3634E-01	6.4842E+00	0.000 VERTICAL
13	3.5299E+04	1.0875E+00	1.3148E+01	0.000 VERTICAL
14	3.0886E+04	1.4810E+00	1.7904E+01	0.000 VERTICAL
15	2.6474E+04	1.1076E+00	1.3391E+01	0.000 VERTICAL
16	2.2062E+04	4.7925E-01	5.7940E+00	0.000 VERTICAL
17	1.7649E+04	5.9294E+03	7.1684E+04	-0.109 VERTICAL
18	1.3237E+04	9.0409E+03	1.0930E+05	-0.023 VERTICAL

19 8.8247E+03 1.2363E+04 1.4947E+05 -0.026 VERTICAL
 20 4.4124E+03 2.7403E+05 3.3130E+06 -6.060 VERTICAL
 21 0.0000E+00 4.3172E+02 5.2193E+03 156.049 VERTICAL

 *** ACCUMMULATED DEPOSITION FOR WHOLE STREAM ***

 STA ACCU.DEPS. ACCU DEPS. ACCU. DEPS. FOR DIFFRNT SIZE GROUPS (FT^3)
 NO. (TONS) (FT^3) 1 2 3 4

1 -6.4046E+04 -1.2905E+06 -2.8126E+05 -5.1748E+05 -4.0090E+05 -7.9193E+04
 2 -3.9931E+04 -8.0458E+05 -1.3095E+05 -1.8011E+05 -1.3278E+05 -3.3681E+05
 3 1.4850E+02 2.9921E+03 -7.0998E+04 -3.7830E+04 6.1852E+04 3.9874E+04
 4 -7.2871E+03 -1.4683E+05 -9.1212E+04 -5.7197E+03 1.9082E+04 -5.7752E+04
 5 3.9966E+04 8.0527E+05 -3.2239E+04 2.8119E+05 2.3642E+05 2.8549E+05
 6 1.2935E+04 2.6062E+05 -9.0135E+03 1.5091E+05 6.7519E+04 4.8131E+04
 7 -3.7930E+03 -7.6425E+04 9.5093E+03 3.2865E+03 -3.5636E+04 -4.9784E+04
 8 1.0609E+04 2.1376E+05 5.3871E+04 5.3321E+04 4.8766E+04 5.4099E+04
 9 -3.7784E+04 -7.6131E+05 -1.4529E+05 -1.8825E+05 -1.7256E+05 -2.2552E+05
 10 9.0132E+04 1.8161E+06 7.0045E+05 4.4643E+05 3.1398E+05 3.2339E+05
 11 -2.1605E+04 -4.3532E+05 -1.8123E+05 -1.2487E+05 -7.6506E+04 -5.2712E+04
 12 1.4461E+04 2.9137E+05 9.2289E+04 8.7537E+04 6.1370E+04 5.0171E+04
 13 -2.6178E+04 -5.2746E+05 -1.5113E+05 -1.4653E+05 -1.1216E+05 -1.1188E+05
 14 3.3389E+03 6.7275E+04 -3.4697E+04 2.6077E+04 3.3993E+04 3.8513E+04
 15 1.4845E+04 2.9911E+05 1.0243E+05 8.3938E+04 5.5722E+04 5.4642E+04
 16 5.5984E+03 1.1280E+05 6.8509E+04 2.4543E+04 1.1563E+04 8.1885E+03
 17 -5.3903E+07 -1.0861E+09 -4.4142E+08 -2.3916E+08 -1.6820E+08 -1.9894E+08
 18 -2.6874E+08 -5.4148E+09 -1.2543E+09 -1.0227E+09 -9.9393E+08 -1.5653E+09
 19 -2.3709E+08 -4.7771E+09 -1.1366E+09 -9.1691E+08 -8.8644E+08 -1.3620E+09
 20 -2.2592E+09 -4.5521E+10 -2.1878E+09 -4.3309E+09 -7.5221E+09 -1.8046E+10
 21 2.8102E+09 5.6622E+10 4.9716E+09 6.4762E+09 9.5395E+09 2.1125E+10
 SUM -8.7517E+06 -1.7634E+08 -4.8715E+07 -3.3458E+07 -3.1199E+07 -4.7497E+07

 ACCUMULATED DEPOSITION FOR DIFFERENT SIZE GROUPS (CONT.)
 STA 5 6 7

1 -1.2589E+04 4.7753E+02 4.7753E+02
 2 -2.3924E+04 0.0000E+00 0.0000E+00
 3 1.0095E+04 0.0000E+00 0.0000E+00
 4 -1.1228E+04 0.0000E+00 0.0000E+00
 5 3.4417E+04 0.0000E+00 0.0000E+00
 6 3.0768E+03 0.0000E+00 0.0000E+00
 7 -3.8003E+03 0.0000E+00 0.0000E+00
 8 3.7017E+03 0.0000E+00 0.0000E+00
 9 -2.9682E+04 0.0000E+00 0.0000E+00
 10 3.1843E+04 0.0000E+00 0.0000E+00
 11 0.0000E+00 0.0000E+00 0.0000E+00
 12 0.0000E+00 0.0000E+00 0.0000E+00
 13 -5.7651E+03 0.0000E+00 0.0000E+00
 14 3.3897E+03 0.0000E+00 0.0000E+00
 15 2.3754E+03 0.0000E+00 0.0000E+00
 16 0.0000E+00 0.0000E+00 0.0000E+00
 17 -2.9266E+07 -6.4642E+06 -2.6567E+06
 18 -3.3464E+08 -1.3147E+08 -1.1239E+08

```

19 -2.7697E+08 -1.1023E+08 -8.7885E+07
20 -6.3149E+09 -3.4727E+09 -3.6459E+09
21  6.9463E+09  3.7173E+09  3.8463E+09
SUM -9.4400E+06 -3.5095E+06 -2.5213E+06
-----

```

```

-----
                ACCUMULATED SEDIMENT DISTRIBUTION THAT EXITED THE REACH (TONS)
SIZE FR  TOTAL      TUBE #1  TUBE #2  TUBE #
  1  2.4179E+06  8.7218E+05  1.5457E+06
  2  1.6608E+06  6.5749E+05  1.0033E+06
  3  1.5487E+06  6.7235E+05  8.7633E+05
  4  2.3574E+06  1.0979E+06  1.2595E+06
  5  4.6860E+05  2.3311E+05  2.3549E+05
  6  1.7420E+05  9.2059E+04  8.2140E+04
  7  1.2516E+05  6.4685E+04  6.0472E+04
TOTAL 8.7527E+06  3.6898E+06  5.0629E+06
-----

```

```

*****
*****
                TIME STEP NO. 2160 AFTER 9.0000E+01 DAYS; DISCHARGE IS 1.2380E+03 CFS
*****
*****

```

```

*****
*   RESULTS OF BACKWATER COMPUTATIONS   *
*   DISCHARGE = 1.2380E+03 C.F.S.     *
*****

```

```

STA. STATION  WATER SURFACE  FLOW AREA  FLOW VELCTY  ENERGY GRADE
FROUDE

```

```

# (ft)  ELEVATION(ft)  (ft^2)  (ft/s)  LINE ELEV(ft)  NUMBER
*****
  1  8.8247E+04  7.69687E+02  2.88383E+01  4.29290E+01  7.98434E+02  1.09983E+01
  2  8.3835E+04  7.69677E+02  3.02677E+01  4.09016E+01  7.95801E+02  1.02811E+01
  3  7.9422E+04  7.69577E+02  2.55023E+01  4.85446E+01  8.06491E+02  1.22706E+01
  4  7.5010E+04  7.69477E+02  2.03724E+01  6.07686E+01  8.27380E+02  1.53899E+01
  5  7.0598E+04  7.69467E+02  4.99267E+01  2.47964E+01  7.79049E+02  6.23689E+00
  6  6.6185E+04  7.69367E+02  4.95830E+01  2.49682E+01  7.79080E+02  6.29205E+00
  7  6.1773E+04  7.69267E+02  4.00669E+01  3.08983E+01  7.84172E+02  7.80544E+00
  8  5.7361E+04  7.69167E+02  3.95196E+01  3.13262E+01  7.84502E+02  7.98524E+00
  9  5.2948E+04  7.69067E+02  7.31155E+00  1.69321E+02  1.26441E+03  5.10665E+01
 10  4.8536E+04  7.69057E+02  2.05000E+01  6.03903E+01  8.26304E+02  1.53158E+01
 11  4.4124E+04  7.69047E+02  2.85160E+01  4.34143E+01  8.02173E+02  1.37435E+01
 12  3.9711E+04  7.69037E+02  3.61188E+01  3.42758E+01  7.87617E+02  9.18188E+00
 13  3.5299E+04  7.68937E+02  6.86007E+00  1.80465E+02  1.32429E+03  5.31388E+01
 14  3.0886E+04  7.68927E+02  1.92878E+01  6.41856E+01  8.43528E+02  2.50370E+01
 15  2.6474E+04  7.68917E+02  4.90849E+01  2.52216E+01  7.78849E+02  6.43018E+00
 16  2.2062E+04  7.68907E+02  5.03195E+01  2.46028E+01  7.78349E+02  6.18903E+00
 17  1.7649E+04  7.68897E+02  6.04448E+01  2.04815E+01  7.75486E+02  5.36127E+00
 18  1.3237E+04  7.68797E+02  1.63471E+01  7.57319E+01  2.89847E+06  7.99457E+01
 19  8.8247E+03  7.68697E+02  1.61545E+01  7.66350E+01  2.93343E+06  8.06681E+01
 20  4.4124E+03  7.68597E+02  4.00842E-02  3.08850E+04  1.50699E+07  1.09796E+04
 21  0.0000E+00  0.00000E+00  8.11547E+01  1.52548E+01  3.81759E+00  9.99860E-01

```

 * SEDIMENT ROUTING RESULTS FOR TIME STEP 2160 *

 INCOMING SEDIMENT DISTRIBUTION PER SIZE FRACTION

SIZE FRACTION	PERCENT	QSED (TON/DAY)
1	15.00	2.3700E+00
2	30.00	4.7400E+00
3	30.00	4.7400E+00
4	10.00	1.5800E+00
5	10.00	1.5800E+00
6	2.50	3.9500E-01
7	2.50	3.9500E-01
TOTAL		1.5800E+01

* STREAM TUBE NO. 1 *

STA	DISTANCE	TOTAL LOAD	CHANGE	DIRECTION
	(TONS)	(FT**3)	(FT)	

1	8.8247E+04	2.0413E+04	2.4678E+05	-6.090	VERTICAL
2	8.3835E+04	5.6655E+04	6.8494E+05	-5.598	VERTICAL
3	7.9422E+04	6.0725E+04	7.3414E+05	-0.715	VERTICAL
4	7.5010E+04	9.2517E+04	1.1185E+06	-4.907	VERTICAL
5	7.0598E+04	1.5238E+04	1.8423E+05	8.236	VERTICAL
6	6.6185E+04	1.5705E+04	1.8987E+05	-0.045	VERTICAL
7	6.1773E+04	4.3805E+04	5.2959E+05	-2.970	VERTICAL
8	5.7361E+04	5.2231E+04	6.3145E+05	-1.152	VERTICAL
9	5.2948E+04	8.0612E+04	9.7456E+05	-6.060	VERTICAL
10	4.8536E+04	1.1137E+05	1.3464E+06	-5.050	VERTICAL
11	4.4124E+04	1.4446E+05	1.7465E+06	-3.324	VERTICAL
12	3.9711E+04	8.4890E+04	1.0263E+06	6.880	VERTICAL
13	3.5299E+04	1.2615E+05	1.5251E+06	-6.060	VERTICAL
14	3.0886E+04	1.8280E+05	2.2100E+06	-5.668	VERTICAL
15	2.6474E+04	3.8882E+04	4.7007E+05	12.376	VERTICAL
16	2.2062E+04	3.4334E+04	4.1508E+05	0.369	VERTICAL
17	1.7649E+04	2.1874E+04	2.6445E+05	0.206	VERTICAL
18	1.3237E+04	2.3973E+04	2.8982E+05	-0.014	VERTICAL
19	8.8247E+03	2.5386E+04	3.0690E+05	-0.010	VERTICAL
20	4.4124E+03	3.2913E+05	3.9791E+06	-6.060	VERTICAL
21	0.0000E+00	6.4934E+02	7.8503E+03	145.731	VERTICAL

* STREAM TUBE NO. 2 *

STA	DISTANCE	TOTAL LOAD	CHANGE	DIRECTION
	(TONS)	(FT**3)	(FT)	

1	8.8247E+04	2.0440E+04	2.4711E+05	-6.090	VERTICAL
2	8.3835E+04	5.6697E+04	6.8544E+05	-5.597	VERTICAL

3	7.9422E+04	6.0737E+04	7.3429E+05	-0.710	VERTICAL
4	7.5010E+04	9.2779E+04	1.1217E+06	-4.901	VERTICAL
5	7.0598E+04	1.5178E+04	1.8349E+05	8.084	VERTICAL
6	6.6185E+04	1.5594E+04	1.8853E+05	-0.039	VERTICAL
7	6.1773E+04	4.3977E+04	5.3167E+05	-2.958	VERTICAL
8	5.7361E+04	5.1892E+04	6.2736E+05	-1.089	VERTICAL
9	5.2948E+04	7.7736E+04	9.3980E+05	-6.060	VERTICAL
10	4.8536E+04	9.8505E+04	1.1909E+06	-5.119	VERTICAL
11	4.4124E+04	1.2381E+05	1.4969E+06	-4.379	VERTICAL
12	3.9711E+04	8.5102E+04	1.0289E+06	6.720	VERTICAL
13	3.5299E+04	1.0969E+05	1.3262E+06	-6.060	VERTICAL
14	3.0886E+04	1.4279E+05	1.7263E+06	-6.060	VERTICAL
15	2.6474E+04	3.8296E+04	4.6299E+05	10.858	VERTICAL
16	2.2062E+04	3.4264E+04	4.1424E+05	0.344	VERTICAL
17	1.7649E+04	2.2954E+04	2.7750E+05	0.192	VERTICAL
18	1.3237E+04	2.3101E+04	2.7929E+05	-0.001	VERTICAL
19	8.8247E+03	2.3529E+04	2.8445E+05	-0.003	VERTICAL
20	4.4124E+03	3.2676E+05	3.9504E+06	-6.060	VERTICAL
21	0.0000E+00	7.0425E+02	8.5141E+03	159.608	VERTICAL

 *** ACCUMMULATED DEPOSITION FOR WHOLE STREAM ***

STA NO.	ACCU.DEPS. (TONS)	ACCU DEPS. (FT^3)	ACCU. DEPS. FOR DIFFRNT SIZE GROUPS (FT^3)			
			1	2	3	4
1	-5.5011E+08	-1.1084E+10	-1.1307E+09	-2.6004E+09	-3.3802E+09	-1.4647E+09
2	-9.7618E+08	-1.9669E+10	-1.0187E+09	-2.0242E+09	-3.5189E+09	-8.4452E+09
3	-1.0919E+08	-2.2002E+09	-8.9566E+08	-1.7797E+09	-2.8010E+09	-1.6163E+09
4	-8.5948E+08	-1.7318E+10	-1.0238E+09	-2.0343E+09	-3.5364E+09	-8.4874E+09
5	2.0854E+09	4.2018E+10	7.2009E+08	6.6237E+09	1.1958E+10	1.8498E+10
6	-1.1877E+07	-2.3932E+08	-9.7124E+07	-5.2463E+07	-3.7030E+07	-4.4018E+07
7	-7.6049E+08	-1.5323E+10	-1.4984E+09	-2.9776E+09	-4.4764E+09	-5.3193E+09
8	-2.2000E+08	-4.4327E+09	-1.1464E+09	-2.2782E+09	-4.1599E+08	-4.9438E+08
9	-7.3012E+08	-1.4711E+10	-7.0379E+08	-1.3984E+09	-2.4310E+09	-5.8341E+09
10	-6.9368E+08	-1.3977E+10	-7.9734E+08	-1.5854E+09	-2.7566E+09	-6.6162E+09
11	-7.8630E+08	-1.5843E+10	-1.2374E+09	-2.4587E+09	-4.2742E+09	-8.8649E+09
12	1.3233E+09	2.6663E+10	-1.1338E+09	-6.2883E+08	6.1922E+09	1.7429E+10
13	-8.8666E+08	-1.7865E+10	-8.5467E+08	-1.6982E+09	-2.9521E+09	-7.0849E+09
14	-1.2084E+09	-2.4348E+10	-1.2155E+09	-2.4152E+09	-4.1987E+09	-1.0077E+10
15	3.3447E+09	6.7392E+10	3.5439E+09	1.2707E+10	1.3386E+10	2.4572E+10
16	1.1554E+08	2.3279E+09	9.4330E+08	5.1132E+08	3.6048E+08	4.2827E+08
17	2.6613E+08	5.3623E+09	2.1706E+09	1.1768E+09	8.3035E+08	9.8798E+08
18	-4.1822E+08	-8.4268E+09	-2.2788E+09	-1.6342E+09	-1.4885E+09	-2.2451E+09
19	-3.9790E+08	-8.0173E+09	-2.1818E+09	-1.5570E+09	-1.4242E+09	-2.1303E+09
20	-1.0143E+10	-2.0437E+11	-9.8027E+09	-1.9436E+10	-3.3771E+10	-8.1034E+10
21	1.1586E+10	2.3346E+11	1.9421E+10	2.5413E+10	3.8636E+10	8.7711E+10
SUM	-3.0179E+07	-6.0807E+08	-2.1800E+08	-1.2691E+08	-9.8929E+07	-1.3060E+08

 ACCUMULATED DEPOSITION FOR DIFFERENT SIZE GROUPS (CONT.)
 STA 5 6 7

1	-1.6110E+09	-4.4303E+08	-4.5411E+08
2	-2.9557E+09	-1.3445E+09	-3.6194E+08

```

3 2.8559E+09 1.3973E+09 6.3918E+08
4 -1.6763E+09 -3.8377E+08 -1.7581E+08
5 3.1632E+09 7.2365E+08 3.3084E+08
6 -6.5316E+06 -1.4848E+06 -6.6557E+05
7 -7.8958E+08 -1.8010E+08 -8.1652E+07
8 -7.3405E+07 -1.6758E+07 -7.6153E+06
9 -2.0419E+09 -1.1230E+09 -1.1792E+09
10 -2.3158E+09 -3.9101E+08 4.8526E+08
11 1.7717E+08 5.5788E+08 2.5709E+08
12 3.6034E+09 8.2431E+08 3.7679E+08
13 -2.4797E+09 -1.3638E+09 -1.4320E+09
14 -3.5269E+09 -1.9398E+09 -9.7450E+08
15 7.1071E+09 3.5551E+09 2.5210E+09
16 6.3545E+07 1.4475E+07 6.5375E+06
17 1.4701E+08 3.3820E+07 1.5705E+07
18 -4.5839E+08 -1.7478E+08 -1.4700E+08
19 -4.2342E+08 -1.6542E+08 -1.3511E+08
20 -2.8358E+10 -1.5596E+10 -1.6375E+10
21 2.9577E+10 1.6010E+10 1.6688E+10
SUM -2.2424E+07 -6.8963E+06 -4.3141E+06

```

ACCUMULATED SEDIMENT DISTRIBUTION THAT EXITED THE REACH (TONS)

SIZE FR	TOTAL	TUBE #1	TUBE #2	TUBE #
1	1.0820E+07	4.4873E+06	6.3324E+06	
2	6.2987E+06	2.6906E+06	3.6081E+06	
3	4.9103E+06	2.1896E+06	2.7207E+06	
4	6.4819E+06	3.0235E+06	3.4584E+06	
5	1.1131E+06	5.4978E+05	5.6329E+05	
6	3.4230E+05	1.8496E+05	1.5734E+05	
7	2.1414E+05	1.2006E+05	9.4084E+04	
TOTAL	3.0180E+07	1.3246E+07	1.6934E+07	

```

*****
*****
TIME STEP NO. 2880 AFTER 1.2000E+02 DAYS; DISCHARGE IS 1.1880E+03 CFS
*****
*****

```

```

*****
* RESULTS OF BACKWATER COMPUTATIONS *
* DISCHARGE = 1.1880E+03 C.F.S. *
*****

```

STA. STATION WATER SURFACE FLOW AREA FLOW VELCTY ENERGY GRADE
FROUDE

#	(ft)	ELEVATION(ft)	(ft^2)	(ft/s)	LINE ELEV(ft)	NUMBER
1	8.8247E+04	7.69888E+02	2.88383E+01	4.11952E+01	7.96359E+02	1.05541E+01
2	8.3835E+04	7.69878E+02	3.02677E+01	3.92497E+01	7.93934E+02	9.86582E+00
3	7.9422E+04	7.69778E+02	2.55023E+01	4.65840E+01	8.03770E+02	1.17750E+01
4	7.5010E+04	7.69678E+02	2.03724E+01	5.83143E+01	8.22998E+02	1.47684E+01
5	7.0598E+04	7.69668E+02	4.99267E+01	2.37949E+01	7.78491E+02	5.98499E+00

```

6 6.6185E+04 7.69568E+02 4.95830E+01 2.39598E+01 7.78512E+02 6.03793E+00
7 6.1773E+04 7.69468E+02 4.00669E+01 2.96504E+01 7.83193E+02 7.49020E+00
8 5.7361E+04 7.69368E+02 3.95196E+01 3.00610E+01 7.83489E+02 7.66273E+00
9 5.2948E+04 7.69268E+02 7.31155E+00 1.62483E+02 1.22541E+03 4.90040E+01
10 4.8536E+04 7.69258E+02 2.05000E+01 5.79513E+01 8.21974E+02 1.46972E+01
11 4.4124E+04 7.69248E+02 2.85160E+01 4.16609E+01 7.99752E+02 1.31885E+01
12 3.9711E+04 7.69238E+02 3.61188E+01 3.28915E+01 7.86347E+02 8.81105E+00
13 3.5299E+04 7.69138E+02 6.86007E+00 1.73176E+02 1.28054E+03 5.09927E+01
14 3.0886E+04 7.69128E+02 1.92878E+01 6.15933E+01 8.37824E+02 2.40258E+01
15 2.6474E+04 7.69118E+02 4.90849E+01 2.42030E+01 7.78264E+02 6.17047E+00
16 2.2062E+04 7.69108E+02 5.03195E+01 2.36091E+01 7.77802E+02 5.93906E+00
17 1.7649E+04 7.69098E+02 6.04448E+01 1.96543E+01 7.75165E+02 5.14474E+00
18 1.3237E+04 7.68998E+02 1.64060E+01 7.24127E+01 2.65945E+06 7.65082E+01
19 8.8247E+03 7.68898E+02 1.63954E+01 7.24594E+01 2.66119E+06 7.65460E+01
20 4.4124E+03 7.68798E+02 4.00842E-02 2.96376E+04 1.38772E+07 1.05362E+04
21 0.0000E+00 0.00000E+00 7.88858E+01 1.50598E+01 3.71518E+00 9.99639E-01

```

```

*****
*   SEDIMENT ROUTING RESULTS FOR TIME STEP 2880   *
*****

```

```

-----
INCOMING SEDIMENT DISTRIBUTION PER SIZE FRACTION

```

SIZE FRACTION	PERCENT	QSED (TON/DAY)
1	15.00	2.3700E+00
2	30.00	4.7400E+00
3	30.00	4.7400E+00
4	10.00	1.5800E+00
5	10.00	1.5800E+00
6	2.50	3.9500E-01
7	2.50	3.9500E-01
TOTAL		1.5800E+01

```

*****

```

```

*   STREAM TUBE NO. 1   *

```

```

*****

```

STA	DISTANCE (TONS)	TOTAL LOAD (FT**3)	CHANGE (FT)	DIRECTION
-----	-----------------	--------------------	-------------	-----------

```

*****

```

1	8.8247E+04	2.0367E+04	2.4623E+05	-6.076 VERTICAL
2	8.3835E+04	5.5923E+04	6.7609E+05	-5.492 VERTICAL
3	7.9422E+04	5.4135E+04	6.5447E+05	0.314 VERTICAL
4	7.5010E+04	8.5301E+04	1.0313E+06	-4.810 VERTICAL
5	7.0598E+04	1.2919E+04	1.5619E+05	7.714 VERTICAL
6	6.6185E+04	1.3315E+04	1.6098E+05	-0.038 VERTICAL
7	6.1773E+04	3.8387E+04	4.6408E+05	-2.650 VERTICAL
8	5.7361E+04	4.6494E+04	5.6209E+05	-1.109 VERTICAL
9	5.2948E+04	7.4875E+04	9.0521E+05	-6.060 VERTICAL
10	4.8536E+04	1.0501E+05	1.2696E+06	-4.948 VERTICAL
11	4.4124E+04	1.3058E+05	1.5787E+06	-2.568 VERTICAL
12	3.9711E+04	7.4012E+04	8.9478E+05	6.534 VERTICAL
13	3.5299E+04	1.1527E+05	1.3936E+06	-6.060 VERTICAL
14	3.0886E+04	1.7128E+05	2.0707E+06	-5.603 VERTICAL
15	2.6474E+04	3.2967E+04	3.9856E+05	11.893 VERTICAL

13	-2.0246E+09	-4.0793E+10	-1.9514E+09	-3.8775E+09	-6.7407E+09	-1.6178E+10
14	-2.7480E+09	-5.5370E+10	-2.7754E+09	-5.5149E+09	-9.5875E+09	-2.3010E+10
15	7.4587E+09	1.5029E+11	9.0763E+09	2.7608E+10	2.9348E+10	5.4663E+10
16	2.4126E+08	4.8612E+09	1.9698E+09	1.0678E+09	7.5277E+08	8.9428E+08
17	6.1442E+08	1.2380E+10	5.0133E+09	2.7178E+09	1.9171E+09	2.2796E+09
18	-4.4464E+08	-8.9592E+09	-2.5066E+09	-1.7570E+09	-1.5714E+09	-2.3350E+09
19	-4.0654E+08	-8.1914E+09	-2.2391E+09	-1.5917E+09	-1.4529E+09	-2.1707E+09
20	-2.0685E+10	-4.1679E+11	-1.9963E+10	-3.9626E+10	-6.8870E+10	-1.6527E+11
21	2.2798E+10	4.5937E+11	3.5055E+10	4.8573E+10	7.5828E+10	1.7443E+11
SUM	-5.2196E+07	-1.0517E+09	-3.9854E+08	-2.2469E+08	-1.6763E+08	-2.1171E+08

 ACCUMULATED DEPOSITION FOR DIFFERENT SIZE GROUPS (CONT.)
 STA 5 6 7

1	-3.6787E+09	-1.0116E+09	-1.0044E+09
2	-6.7491E+09	-2.7206E+09	-6.9887E+08
3	6.8555E+09	2.9177E+09	1.3343E+09
4	-3.5005E+09	-8.0135E+08	-3.6705E+08
5	6.6053E+09	1.5110E+09	6.9061E+08
6	-1.3641E+07	-3.0987E+06	-1.3874E+06
7	-1.6487E+09	-3.7598E+08	-1.7034E+08
8	-1.5328E+08	-3.4987E+07	-1.5890E+07
9	-4.6625E+09	-2.5643E+09	-2.6926E+09
10	-5.2879E+09	-5.9718E+08	1.2438E+09
11	1.2207E+09	1.1651E+09	5.3696E+08
12	7.5245E+09	1.7212E+09	7.8652E+08
13	-5.6621E+09	-3.1142E+09	-3.2699E+09
14	-8.0535E+09	-4.4294E+09	-1.9996E+09
15	1.6014E+10	8.0686E+09	5.5085E+09
16	1.3268E+08	3.0216E+07	1.3635E+07
17	3.3883E+08	7.7644E+07	3.5663E+07
18	-4.6926E+08	-1.7525E+08	-1.4458E+08
19	-4.3104E+08	-1.6828E+08	-1.3770E+08
20	-5.7842E+10	-3.1812E+10	-3.3402E+10
21	5.9426E+10	3.2308E+10	3.3749E+10
SUM	-3.4314E+07	-9.4894E+06	-5.3355E+06

 ACCUMULATED SEDIMENT DISTRIBUTION THAT EXITED THE REACH (TONS)

SIZE FR	TOTAL	TUBE #1	TUBE #2	TUBE #
1	1.9780E+07	8.7831E+06	1.0997E+07	
2	1.1152E+07	5.0174E+06	6.1345E+06	
3	8.3201E+06	3.8240E+06	4.4961E+06	
4	1.0507E+07	4.9523E+06	5.5550E+06	
5	1.7032E+06	8.3235E+05	8.7083E+05	
6	4.7101E+05	2.4644E+05	2.2457E+05	
7	2.6485E+05	1.4407E+05	1.2077E+05	
TOTAL	5.2198E+07	2.3800E+07	2.8398E+07	

 TIME STEP NO. 3600 AFTER 1.5000E+02 DAYS; DISCHARGE IS 1.0480E+03 CFS

 * RESULTS OF BACKWATER COMPUTATIONS *
 * DISCHARGE = 1.0480E+03 C.F.S. *

STA. STATION WATER SURFACE FLOW AREA FLOW VELCTY ENERGY GRADE
 FROUDE

#	(ft)	ELEVATION(ft)	(ft ²)	(ft/s)	LINE ELEV(ft)	NUMBER
1	8.8247E+04	1.11002E+03	4.44585E+02	2.35725E+00	1.11011E+03	1.67603E-01
2	8.3835E+04	1.10617E+03	3.67592E+02	2.85099E+00	1.10631E+03	2.27277E-01
3	7.9422E+04	1.09958E+03	2.22459E+02	4.71099E+00	1.09994E+03	4.52753E-01
4	7.5010E+04	1.09294E+03	2.38144E+02	4.40070E+00	1.09327E+03	3.99317E-01
5	7.0598E+04	1.09002E+03	6.13070E+02	1.70943E+00	1.09007E+03	1.36146E-01
6	6.6185E+04	7.68859E+02	4.95830E+01	2.11363E+01	7.75819E+02	5.32639E+00
7	6.1773E+04	7.68759E+02	4.00669E+01	2.61563E+01	7.79440E+02	6.60751E+00
8	5.7361E+04	7.68659E+02	3.95196E+01	2.65185E+01	7.79648E+02	6.75972E+00
9	5.2948E+04	7.68559E+02	7.31155E+00	1.43335E+02	1.12352E+03	4.32291E+01
10	4.8536E+04	7.68549E+02	2.05000E+01	5.11220E+01	8.09573E+02	1.29652E+01
11	4.4124E+04	7.68539E+02	2.85160E+01	3.67513E+01	7.92277E+02	1.16343E+01
12	3.9711E+04	7.68529E+02	3.61188E+01	2.90154E+01	7.81843E+02	7.77271E+00
13	3.5299E+04	7.68429E+02	6.86007E+00	1.52768E+02	1.16640E+03	4.49834E+01
14	3.0886E+04	7.68419E+02	1.92878E+01	5.43348E+01	8.21878E+02	2.11944E+01
15	2.6474E+04	7.68409E+02	4.90849E+01	2.13508E+01	7.75526E+02	5.44331E+00
16	2.2062E+04	7.68399E+02	5.03195E+01	2.08269E+01	7.75165E+02	5.23917E+00
17	1.7649E+04	7.68389E+02	6.04448E+01	1.73381E+01	7.73111E+02	4.53846E+00
18	1.3237E+04	7.68289E+02	1.63728E+01	6.40087E+01	2.07398E+06	6.75904E+01
19	8.8247E+03	7.68279E+02	1.63794E+01	6.39829E+01	2.07313E+06	6.75752E+01
20	4.4124E+03	7.68179E+02	4.00842E-02	2.61450E+04	1.07994E+07	9.29457E+03
21	0.0000E+00	0.00000E+00	7.23357E+01	1.44880E+01	3.42395E+00	9.99835E-01

 * SEDIMENT ROUTING RESULTS FOR TIME STEP 3600 *

 INCOMING SEDIMENT DISTRIBUTION PER SIZE FRACTION

SIZE FRACTION	PERCENT	QSED (TON/DAY)
1	15.00	2.3700E+00
2	30.00	4.7400E+00
3	30.00	4.7400E+00
4	10.00	1.5800E+00
5	10.00	1.5800E+00
6	2.50	3.9500E-01
7	2.50	3.9500E-01
TOTAL		1.5800E+01

 * STREAM TUBE NO. 1 *

STA DISTANCE	TOTAL LOAD	CHANGE DIRECTION
(TONS)	(FT**3)	(FT)

```

*****
1  8.8247E+04  4.8224E-01  5.8301E+00  0.000 VERTICAL
2  8.3835E+04  1.2843E+00  1.5527E+01  0.000 VERTICAL
3  7.9422E+04  1.5894E+00  1.9215E+01  0.000 VERTICAL
4  7.5010E+04  1.1769E+00  1.4228E+01  0.000 VERTICAL
5  7.0598E+04  5.7070E-02  6.8995E-01  0.000 VERTICAL
6  6.6185E+04  8.0052E+03  9.6780E+04  -0.721 VERTICAL
7  6.1773E+04  2.6415E+04  3.1935E+05  -1.946 VERTICAL
8  5.7361E+04  3.0771E+04  3.7201E+05  -0.596 VERTICAL
9  5.2948E+04  5.9152E+04  7.1513E+05  -6.060 VERTICAL
10 4.8536E+04  8.5119E+04  1.0291E+06  -4.263 VERTICAL
11 4.4124E+04  9.5494E+04  1.1545E+06  -1.042 VERTICAL
12 3.9711E+04  5.0032E+04  6.0487E+05  5.251 VERTICAL
13 3.5299E+04  9.1293E+04  1.1037E+06  -6.060 VERTICAL
14 3.0886E+04  1.4286E+05  1.7271E+06  -5.159 VERTICAL
15 2.6474E+04  1.9956E+04  2.4126E+05  10.568 VERTICAL
16 2.2062E+04  1.7621E+04  2.1303E+05  0.190 VERTICAL
17 1.7649E+04  1.1223E+04  1.3569E+05  0.106 VERTICAL
18 1.3237E+04  1.2182E+04  1.4728E+05  -0.006 VERTICAL
19 8.8247E+03  1.2158E+04  1.4699E+05  0.000 VERTICAL
20 4.4124E+03  3.1773E+05  3.8412E+06  -6.060 VERTICAL
21 0.0000E+00  5.0861E+02  6.1489E+03  149.829 VERTICAL

```

```

*****
*          STREAM TUBE NO. 2          *
*****
STA DISTANCE      TOTAL LOAD      CHANGE DIRECTION
(TONS)      (FT**3)      (FT)
*****
1  8.8247E+04  4.8223E-01  5.8300E+00  0.000 VERTICAL
2  8.3835E+04  1.2843E+00  1.5527E+01  0.000 VERTICAL
3  7.9422E+04  1.5894E+00  1.9215E+01  0.000 VERTICAL
4  7.5010E+04  1.1768E+00  1.4228E+01  0.000 VERTICAL
5  7.0598E+04  5.6928E-02  6.8824E-01  0.000 VERTICAL
6  6.6185E+04  8.0012E+03  9.6732E+04  -0.712 VERTICAL
7  6.1773E+04  2.6612E+04  3.2173E+05  -1.940 VERTICAL
8  5.7361E+04  3.0547E+04  3.6930E+05  -0.542 VERTICAL
9  5.2948E+04  5.6391E+04  6.8175E+05  -6.060 VERTICAL
10 4.8536E+04  7.4439E+04  8.9994E+05  -4.448 VERTICAL
11 4.4124E+04  9.3203E+04  1.1268E+06  -3.247 VERTICAL
12 3.9711E+04  4.9334E+04  5.9643E+05  7.615 VERTICAL
13 3.5299E+04  7.3926E+04  8.9373E+05  -6.060 VERTICAL
14 3.0886E+04  1.0702E+05  1.2939E+06  -6.060 VERTICAL
15 2.6474E+04  1.9655E+04  2.3762E+05  9.079 VERTICAL
16 2.2062E+04  1.7585E+04  2.1260E+05  0.177 VERTICAL
17 1.7649E+04  1.1778E+04  1.4240E+05  0.099 VERTICAL
18 1.3237E+04  1.1774E+04  1.4235E+05  0.000 VERTICAL
19 8.8247E+03  1.1769E+04  1.4228E+05  0.000 VERTICAL
20 4.4124E+03  3.1682E+05  3.8303E+06  -6.060 VERTICAL
21 0.0000E+00  5.5514E+02  6.7114E+03  165.931 VERTICAL

```

```

*****
*** ACCUMMULATED DEPOSITION FOR WHOLE STREAM ***
*****

```

 STA ACCU.DEPS. ACCU DEPS. ACCU. DEPS. FOR DIFFRNT SIZE GROUPS (FT^3)
 NO. (TONS) (FT^3) 1 2 3 4

1	-1.2544E+09	-2.5276E+10	-2.5815E+09	-5.9372E+09	-7.7181E+09	-3.3444E+09
2	-2.2053E+09	-4.4435E+10	-2.3260E+09	-4.6220E+09	-8.0350E+09	-1.9284E+10
3	-4.6901E+07	-9.4501E+08	-2.0451E+09	-4.0639E+09	-4.5030E+09	-1.4406E+09
4	-1.9409E+09	-3.9107E+10	-2.3376E+09	-4.6450E+09	-8.0750E+09	-1.9380E+10
5	4.5923E+09	9.2531E+10	2.2977E+09	1.5479E+10	2.5663E+10	4.0285E+10
6	-3.0086E+08	-6.0620E+09	-2.4437E+09	-1.3400E+09	-9.4332E+08	-1.1175E+09
7	-2.2711E+09	-4.5761E+10	-5.3447E+09	-1.0621E+10	-1.2298E+10	-1.4612E+10
8	-6.3587E+08	-1.2812E+10	-4.0893E+09	-5.9534E+09	-1.1429E+09	-1.3582E+09
9	-2.6041E+09	-5.2471E+10	-2.5099E+09	-4.9875E+09	-8.6704E+09	-2.0809E+10
10	-2.3232E+09	-4.6811E+10	-2.8458E+09	-5.6559E+09	-9.8331E+09	-2.3600E+10
11	-2.1489E+09	-4.3298E+10	-4.4133E+09	-8.7696E+09	-1.4739E+10	-2.0440E+10
12	4.5669E+09	9.2018E+10	-4.0443E+09	4.4339E+09	2.4260E+10	5.4173E+10
13	-3.1625E+09	-6.3721E+10	-3.0481E+09	-6.0568E+09	-1.0529E+10	-2.5270E+10
14	-4.2110E+09	-8.4848E+10	-4.3352E+09	-8.6147E+09	-1.4976E+10	-3.5943E+10
15	1.1092E+10	2.2349E+11	1.6744E+10	3.8713E+10	4.2634E+10	8.1571E+10
16	3.1738E+08	6.3949E+09	2.5915E+09	1.4047E+09	9.9028E+08	1.1763E+09
17	8.2531E+08	1.6629E+10	6.7348E+09	3.6510E+09	2.5751E+09	3.0616E+09
18	-4.6054E+08	-9.2794E+09	-2.6495E+09	-1.8330E+09	-1.6210E+09	-2.3854E+09
19	-4.0626E+08	-8.1857E+09	-2.2371E+09	-1.5905E+09	-1.4520E+09	-2.1695E+09
20	-3.1238E+10	-6.2943E+11	-3.0134E+10	-5.9837E+10	-1.0401E+11	-2.4960E+11
21	3.3746E+10	6.7996E+11	4.8468E+10	7.0539E+10	1.1220E+11	2.6021E+11
SUM	-7.0577E+07	-1.4221E+09	-5.4930E+08	-3.0635E+08	-2.2499E+08	-2.7939E+08

 ACCUMULATED DEPOSITION FOR DIFFERENT SIZE GROUPS (CONT.)
 STA 5 6 7

1	-3.6787E+09	-1.0116E+09	-1.0044E+09
2	-6.7492E+09	-2.7206E+09	-6.9887E+08
3	6.8555E+09	2.9177E+09	1.3343E+09
4	-3.5005E+09	-8.0135E+08	-3.6705E+08
5	6.6053E+09	1.5110E+09	6.9061E+08
6	-1.6490E+08	-3.6836E+07	-1.5689E+07
7	-2.1685E+09	-4.9432E+08	-2.2368E+08
8	-2.0162E+08	-4.6003E+07	-2.0872E+07
9	-7.2830E+09	-4.0056E+09	-4.2059E+09
10	-7.0240E+09	-1.5299E+08	2.3008E+09
11	2.8236E+09	1.5329E+09	7.0663E+08
12	9.8983E+09	2.2637E+09	1.0339E+09
13	-8.8446E+09	-4.8645E+09	-5.1077E+09
14	-1.2580E+10	-5.8700E+09	-2.5287E+09
15	2.4448E+10	1.1425E+10	7.9505E+09
16	1.7450E+08	3.9719E+07	1.7895E+07
17	4.5493E+08	1.0414E+08	4.7699E+07
18	-4.7436E+08	-1.7452E+08	-1.4172E+08
19	-4.3083E+08	-1.6820E+08	-1.3757E+08
20	-8.7356E+10	-4.8045E+10	-5.0447E+10
21	8.9153E+10	4.8586E+10	5.0810E+10
SUM	-4.4225E+07	-1.1644E+07	-6.1736E+06

 ACCUMULATED SEDIMENT DISTRIBUTION THAT EXITED THE REACH (TONS)

SIZE FR	TOTAL	TUBE #1	TUBE #2	TUBE #
1	2.7262E+07	1.2362E+07	1.4901E+07	
2	1.5205E+07	6.9556E+06	8.2492E+06	
3	1.1167E+07	5.1852E+06	5.9817E+06	
4	1.3866E+07	6.5578E+06	7.3085E+06	
5	2.1951E+06	1.0673E+06	1.1278E+06	
6	5.7793E+05	2.9736E+05	2.8057E+05	
7	3.0646E+05	1.6370E+05	1.4276E+05	
TOTAL	7.0580E+07	3.2589E+07	3.7991E+07	

This page intentionally left blank

10.7.3 Simulation 3: mixed bed, coarser incoming sediment

***** SUMMARY OF INPUT PARAMETERS *****

Number of cross sections:..... 21
 Number of stream tubes:..... 2
 Number of time steps:..... 3600
 Number of sediment time steps (NITRQS):..... 24
 Duration of time step (days):..... 4.1667E-02
 Formula selected for conveyance calculations:..... manning
 Formula selected for friction slope:..... average
 Formula for sediment transport: Garde (1965)
 NALT for active layer thickness:..... 14
 Transport parameter CFACTOR:..... 1.00
 Printout control is 3; print interval:..... 720
 Number of time steps to generate x-sec plots:..... 3600
 Number of time steps for thalweg plots:..... 720
 No minimization requested.

Sect. #	Location (ft)	ISWITCH	ITYP (ft)	Thalweg Coef.	Bed slope	Loss	NDIVI	NPOINTS
1	8.8247E+04	0	0	1.1145E+03	2.0456E-03	0.00	1	15
2	8.3835E+04	0	0	1.1055E+03	2.0456E-03	0.00	1	15
3	7.9422E+04	0	0	1.0969E+03	1.9545E-03	0.00	1	15
4	7.5010E+04	0	0	1.0884E+03	1.9096E-03	0.00	1	18
5	7.0598E+04	0	0	1.0792E+03	2.0909E-03	0.00	1	19
6	6.6185E+04	0	0	1.0726E+03	1.5012E-03	0.00	1	19
7	6.1773E+04	0	0	1.0659E+03	1.5016E-03	0.00	1	24
8	5.7361E+04	0	0	1.0593E+03	1.5016E-03	0.00	1	24
9	5.2948E+04	0	0	1.0523E+03	1.5919E-03	0.00	1	35
10	4.8536E+04	0	0	1.0003E+03	1.1792E-02	0.00	1	35
11	4.4124E+04	0	0	1.0460E+03	-1.0375E-02	0.00	1	24
12	3.9711E+04	0	0	1.0412E+03	1.0934E-03	0.00	1	24
13	3.5299E+04	0	0	1.0372E+03	9.1228E-04	0.00	1	35
14	3.0886E+04	0	0	1.0332E+03	9.1208E-04	0.00	1	26
15	2.6474E+04	0	0	1.0284E+03	1.0936E-03	0.00	1	24
16	2.2062E+04	0	0	1.0251E+03	7.3096E-04	0.00	1	24
17	1.7649E+04	0	0	1.0211E+03	9.1208E-04	0.00	1	23
18	1.3237E+04	0	0	1.7775E+01	2.2741E-01	0.00	1	24
19	8.8247E+03	0	0	1.5550E+01	5.0427E-04	0.00	1	22
20	4.4124E+03	0	0	1.0130E+03	-2.2607E-01	0.00	1	25
21	0.0000E+00	1	1	1.0123E+03	1.6431E-04	0.00	1	25

Coefficients used in Exner equation and in
 computing hydraulic properties for sediment capacity

C1WP	C2WP	C3WP	C1WPU	C2WPU	C1Q	C2Q	C3Q	C1QD	C2QD	C1QU	C2QU
0.250	0.500	0.250	0.750	0.250							
0.000	1.000	0.000	0.000	1.000	1.000	1.000	0.000	0.000			

Number of particle size classes: 7

Class #	DRL (mm)	DRU (mm)	Geometric Dry specific	
			mean (mm)	weight (lb/ft ³)
1	7.5000E-02	5.0000E-01	1.9365E-01	9.9260E+01
2	5.0000E-01	2.0000E+00	1.0000E+00	9.9260E+01
3	2.0000E+00	4.0000E+00	2.8284E+00	9.9260E+01
4	4.0000E+00	8.0000E+00	5.6569E+00	9.9260E+01
5	8.0000E+00	1.6000E+01	1.1314E+01	9.9260E+01
6	1.6000E+01	6.4000E+01	3.2000E+01	9.9260E+01
7	6.4000E+01	1.2700E+02	9.0155E+01	9.9260E+01

Percentage of bed material for each size fraction and for each cross section

Section #	Bed material size fraction for each group						
	1	2	3	4	5	6	7
1	2.0	3.0	10.0	10.0	30.0	30.0	15.0
2	7.0	13.0	20.0	40.0	10.0	5.0	5.0
3	7.0	13.0	20.0	40.0	10.0	5.0	5.0
4	7.0	13.0	20.0	40.0	10.0	5.0	5.0
5	7.0	13.0	20.0	40.0	10.0	5.0	5.0
6	7.0	13.0	20.0	40.0	10.0	5.0	5.0
7	7.0	13.0	20.0	40.0	10.0	5.0	5.0
8	7.0	13.0	20.0	40.0	10.0	5.0	5.0
9	7.0	13.0	20.0	40.0	10.0	5.0	5.0
10	7.0	13.0	20.0	40.0	10.0	5.0	5.0
11	7.0	13.0	20.0	40.0	10.0	5.0	5.0
12	7.0	13.0	20.0	40.0	10.0	5.0	5.0
13	7.0	13.0	20.0	40.0	10.0	5.0	5.0
14	7.0	13.0	20.0	40.0	10.0	5.0	5.0
15	7.0	13.0	20.0	40.0	10.0	5.0	5.0
16	7.0	13.0	20.0	40.0	10.0	5.0	5.0
17	7.0	13.0	20.0	40.0	10.0	5.0	5.0
18	7.0	13.0	20.0	40.0	10.0	5.0	5.0
19	7.0	13.0	20.0	40.0	10.0	5.0	5.0
20	7.0	13.0	20.0	40.0	10.0	5.0	5.0
21	7.0	13.0	20.0	40.0	10.0	5.0	5.0

 TIME STEP NO. 720 AFTER 3.0000E+01 DAYS; DISCHARGE IS 2.6500E+02 CFS

 * RESULTS OF BACKWATER COMPUTATIONS *
 * DISCHARGE = 2.6500E+02 C.F.S. *

STA. STATION WATER SURFACE FLOW AREA FLOW VELCTY ENERGY GRADE
 FROUDE

```

# (ft) ELEVATION(ft) (ft^2) (ft/s) LINE ELEV(ft) NUMBER
*****
1 8.8247E+04 1.11550E+03 1.20379E+02 2.20138E+00 1.11558E+03 2.91725E-01
2 8.3835E+04 1.10660E+03 1.41626E+02 1.87113E+00 1.10666E+03 2.30432E-01
3 7.9422E+04 1.09894E+03 9.06095E+01 2.92464E+00 1.09907E+03 4.16051E-01
4 7.5010E+04 1.08957E+03 7.92362E+01 3.34443E+00 1.08975E+03 4.59079E-01
5 7.0598E+04 1.08099E+03 1.20131E+02 2.20593E+00 1.08106E+03 3.60479E-01
6 6.6185E+04 1.07397E+03 1.21744E+02 2.17670E+00 1.07405E+03 3.53212E-01
7 6.1773E+04 1.06726E+03 1.30228E+02 2.03490E+00 1.06732E+03 2.93732E-01
8 5.7361E+04 1.06119E+03 1.37653E+02 1.92513E+00 1.06125E+03 2.72008E-01
9 5.2948E+04 1.05444E+03 9.90000E+01 2.67677E+00 1.05455E+03 3.38012E-01
10 4.8536E+04 1.05060E+03 1.01073E+04 2.62186E-02 1.05060E+03 9.17222E-04
11 4.4124E+04 1.04755E+03 1.34391E+02 1.97185E+00 1.04761E+03 2.80922E-01
12 3.9711E+04 1.04396E+03 2.18612E+02 1.21220E+00 1.04399E+03 1.39405E-01
13 3.5299E+04 1.03983E+03 9.66458E+01 2.74197E+00 1.03996E+03 3.24186E-01
14 3.0886E+04 1.03549E+03 1.88258E+02 1.40765E+00 1.03553E+03 1.72629E-01
15 2.6474E+04 1.03448E+03 6.87803E+02 3.85285E-01 1.03448E+03 2.94396E-02
16 2.2062E+04 1.03445E+03 1.10692E+03 2.39403E-01 1.03445E+03 1.52562E-02
17 1.7649E+04 1.03445E+03 2.18535E+03 1.21262E-01 1.03445E+03 6.54617E-03
18 1.3237E+04 1.03445E+03 3.39239E+03 7.81159E-02 1.03445E+03 3.76474E-03
19 8.8247E+03 1.03444E+03 3.78031E+03 7.01002E-02 1.03444E+03 2.83781E-03
20 4.4124E+03 1.03444E+03 3.69780E+03 7.16643E-02 1.03444E+03 3.12371E-03
21 0.0000E+00 9.70450E+02 2.98501E+01 8.87771E+00 9.71776E+02 6.10532E-01

```

```

*****
* SEDIMENT ROUTING RESULTS FOR TIME STEP 720 *
*****

```

```

-----
INCOMING SEDIMENT DISTRIBUTION PER SIZE FRACTION
SIZE FRACTION PERCENT QSED (TON/DAY)
1 2.00 3.1600E-01
2 3.00 4.7400E-01
3 10.00 1.5800E+00
4 10.00 1.5800E+00
5 30.00 4.7400E+00
6 30.00 4.7400E+00
7 15.00 2.3700E+00
TOTAL 1.5800E+01
-----

```

```

*****
* STREAM TUBE NO. 1 *
*****
STA DISTANCE TOTAL LOAD CHANGE DIRECTION
(TONS) (FT**3) (FT)
*****
1 8.8247E+04 1.5300E-01 1.8498E+00 0.000 VERTICAL
2 8.3835E+04 3.5387E-01 4.2782E+00 0.000 VERTICAL
3 7.9422E+04 4.6489E-01 5.6204E+00 0.000 VERTICAL
4 7.5010E+04 6.3317E-01 7.6548E+00 0.000 VERTICAL
5 7.0598E+04 4.3415E-01 5.2487E+00 0.000 VERTICAL
6 6.6185E+04 4.2494E-01 5.1374E+00 0.000 VERTICAL
7 6.1773E+04 4.4317E-01 5.3577E+00 0.000 VERTICAL
8 5.7361E+04 4.0657E-01 4.9153E+00 0.000 VERTICAL

```

9	5.2948E+04	7.3623E-01	8.9007E+00	0.000	VERTICAL
10	4.8536E+04	0.0000E+00	0.0000E+00	0.000	VERTICAL
11	4.4124E+04	3.8051E-01	4.6002E+00	0.000	VERTICAL
12	3.9711E+04	4.0913E-02	4.9463E-01	0.000	VERTICAL
13	3.5299E+04	6.0647E-01	7.3319E+00	0.000	VERTICAL
14	3.0886E+04	8.1700E-02	9.8772E-01	0.000	VERTICAL
15	2.6474E+04	0.0000E+00	0.0000E+00	0.000	VERTICAL
16	2.2062E+04	0.0000E+00	0.0000E+00	0.000	VERTICAL
17	1.7649E+04	0.0000E+00	0.0000E+00	0.000	VERTICAL
18	1.3237E+04	0.0000E+00	0.0000E+00	0.000	VERTICAL
19	8.8247E+03	0.0000E+00	0.0000E+00	0.000	VERTICAL
20	4.4124E+03	0.0000E+00	0.0000E+00	0.000	VERTICAL
21	0.0000E+00	1.7892E+01	2.1631E+02	-0.002	VERTICAL

* STREAM TUBE NO. 2 *

STA	DISTANCE	TOTAL LOAD	CHANGE	DIRECTION
	(TONS)	(FT**3)	(FT)	

1	8.8247E+04	1.5300E-01	1.8497E+00	0.000	VERTICAL
2	8.3835E+04	3.5386E-01	4.2780E+00	0.000	VERTICAL
3	7.9422E+04	4.6488E-01	5.6203E+00	0.000	VERTICAL
4	7.5010E+04	6.3315E-01	7.6546E+00	0.000	VERTICAL
5	7.0598E+04	4.3408E-01	5.2479E+00	0.000	VERTICAL
6	6.6185E+04	4.2491E-01	5.1370E+00	0.000	VERTICAL
7	6.1773E+04	4.4309E-01	5.3567E+00	0.000	VERTICAL
8	5.7361E+04	4.0744E-01	4.9258E+00	0.000	VERTICAL
9	5.2948E+04	7.2517E-01	8.7670E+00	0.000	VERTICAL
10	4.8536E+04	0.0000E+00	0.0000E+00	0.000	VERTICAL
11	4.4124E+04	3.6832E-01	4.4528E+00	0.000	VERTICAL
12	3.9711E+04	4.0352E-02	4.8784E-01	0.000	VERTICAL
13	3.5299E+04	6.0614E-01	7.3280E+00	0.000	VERTICAL
14	3.0886E+04	8.1889E-02	9.9001E-01	0.000	VERTICAL
15	2.6474E+04	0.0000E+00	0.0000E+00	0.000	VERTICAL
16	2.2062E+04	0.0000E+00	0.0000E+00	0.000	VERTICAL
17	1.7649E+04	0.0000E+00	0.0000E+00	0.000	VERTICAL
18	1.3237E+04	0.0000E+00	0.0000E+00	0.000	VERTICAL
19	8.8247E+03	0.0000E+00	0.0000E+00	0.000	VERTICAL
20	4.4124E+03	0.0000E+00	0.0000E+00	0.000	VERTICAL
21	0.0000E+00	2.1291E+01	2.5740E+02	-0.003	VERTICAL

*** ACCUMMULATED DEPOSITION FOR WHOLE STREAM ***

STA NO.	ACCU.DEPS. (TONS)	ACCU DEPS. (FT^3)	ACCU. DEPS. FOR DIFFRNT SIZE GROUPS (FT^3)			
			1	2	3	4

1	-6.7312E+03	-1.3563E+05	-1.5309E+04	-2.1226E+04	-5.2380E+04	-3.0692E+04
2	-1.5889E+04	-3.2015E+05	-1.0096E+05	-1.1717E+05	-6.0020E+04	-6.3359E+04
3	5.1132E+03	1.0303E+05	-3.9974E+04	2.8418E+04	5.3993E+04	5.8813E+04
4	-9.6071E+03	-1.9358E+05	-5.7990E+04	-4.0020E+04	-4.0079E+04	-5.2040E+04
5	1.1798E+04	2.3773E+05	3.2475E+04	6.5275E+04	5.9747E+04	7.6735E+04

6	4.2534E+03	8.5701E+04	4.2177E+04	2.4216E+04	1.2124E+04	7.1848E+03
7	-5.1962E+03	-1.0470E+05	-2.3529E+04	-3.2030E+04	-2.5097E+04	-2.4043E+04
8	4.3053E+03	8.6748E+04	2.5089E+04	2.6020E+04	1.9850E+04	1.5789E+04
9	-2.3810E+03	-4.7975E+04	-8.7847E+03	-6.9519E+03	-1.0026E+04	-2.1395E+04
10	1.4808E+04	2.9838E+05	1.4700E+05	7.3761E+04	4.2843E+04	3.3960E+04
11	-3.8087E+03	-7.6742E+04	-3.9702E+04	-2.1866E+04	-1.1151E+04	-4.0235E+03
12	3.3100E+03	6.6694E+04	3.2984E+04	1.9100E+04	1.0586E+04	4.0235E+03
13	-1.5173E+03	-3.0573E+04	-1.3068E+04	-7.8678E+03	-5.4531E+03	-4.1597E+03
14	1.9569E+03	3.9429E+04	1.8945E+04	1.0313E+04	5.9877E+03	4.1597E+03
15	5.9173E+01	1.1923E+03	8.4075E+02	3.2130E+02	3.0232E+01	0.0000E+00
16	0.0000E+00	0.0000E+00	0.0000E+00	0.0000E+00	0.0000E+00	0.0000E+00
17	-2.7378E+03	-5.5165E+04	-2.2780E+04	-1.2786E+04	-8.7309E+03	-9.5854E+03
18	-2.1643E+05	-4.3608E+06	-1.2621E+06	-8.9636E+05	-8.1580E+05	-1.1311E+06
19	-1.0075E+06	-2.0300E+07	-1.0654E+06	-2.5746E+06	-4.1152E+06	-8.3759E+06
20	1.2239E+06	2.4660E+07	2.3266E+06	3.4710E+06	4.9311E+06	9.5071E+06
21	-7.5210E+05	-1.5154E+07	-1.2907E+06	-2.2440E+06	-3.2335E+06	-6.1250E+06
SUM	-7.5440E+05	-1.5201E+07	-1.3142E+06	-2.2564E+06	-3.2412E+06	-6.1336E+06

 ACCUMULATED DEPOSITION FOR DIFFERENT SIZE GROUPS (CONT.)

STA	5	6	7
-----	---	---	---

1	-2.0320E+04	2.8652E+03	1.4326E+03
2	2.1362E+04	0.0000E+00	0.0000E+00
3	1.7764E+03	0.0000E+00	0.0000E+00
4	-3.4461E+03	0.0000E+00	0.0000E+00
5	3.4931E+03	0.0000E+00	0.0000E+00
6	0.0000E+00	0.0000E+00	0.0000E+00
7	0.0000E+00	0.0000E+00	0.0000E+00
8	0.0000E+00	0.0000E+00	0.0000E+00
9	-8.1727E+02	0.0000E+00	0.0000E+00
10	8.1727E+02	0.0000E+00	0.0000E+00
11	0.0000E+00	0.0000E+00	0.0000E+00
12	0.0000E+00	0.0000E+00	0.0000E+00
13	-2.4394E+01	0.0000E+00	0.0000E+00
14	2.4394E+01	0.0000E+00	0.0000E+00
15	0.0000E+00	0.0000E+00	0.0000E+00
16	0.0000E+00	0.0000E+00	0.0000E+00
17	-1.1944E+03	-8.8266E+01	0.0000E+00
18	-1.8802E+05	-4.6564E+04	-2.0830E+04
19	-2.1058E+06	-1.0500E+06	-1.0133E+06
20	2.2938E+06	1.0965E+06	1.0341E+06
21	-1.4241E+06	-5.6847E+05	-2.6849E+05
SUM	-1.4224E+06	-5.6572E+05	-2.6706E+05

 ACCUMULATED SEDIMENT DISTRIBUTION THAT EXITED THE REACH (TONS)

SIZE FR	TOTAL	TUBE #1	TUBE #2	TUBE #
---------	-------	---------	---------	--------

1	6.5233E+04	3.0678E+04	3.4556E+04	
2	1.1200E+05	5.2733E+04	5.9267E+04	
3	1.6091E+05	7.6304E+04	8.4604E+04	
4	3.0446E+05	1.4511E+05	1.5935E+05	
5	7.0736E+04	3.3924E+04	3.6812E+04	
6	2.8219E+04	1.3706E+04	1.4513E+04	
7	1.3325E+04	6.1056E+03	7.2198E+03	
TOTAL	7.5488E+05	3.5856E+05	3.9632E+05	

 TIME STEP NO. 1440 AFTER 6.0000E+01 DAYS; DISCHARGE IS 8.8300E+02 CFS

 * RESULTS OF BACKWATER COMPUTATIONS *
 * DISCHARGE = 8.8300E+02 C.F.S. *

STA. STATION WATER SURFACE FLOW AREA FLOW VELCTY ENERGY GRADE
 FROUDE

#	(ft)	ELEVATION(ft)	(ft^2)	(ft/s)	LINE ELEV(ft)	NUMBER
1	8.8247E+04	1.11547E+03	2.61988E+02	3.37038E+00	1.11566E+03	3.13571E-01
2	8.3835E+04	1.10730E+03	3.10134E+02	2.84715E+00	1.10743E+03	2.47634E-01
3	7.9422E+04	1.09982E+03	1.95246E+02	4.52251E+00	1.10016E+03	4.62975E-01
4	7.5010E+04	1.09126E+03	1.81839E+02	4.85596E+00	1.09165E+03	4.76825E-01
5	7.0598E+04	1.08301E+03	2.41464E+02	3.65686E+00	1.08322E+03	4.29065E-01
6	6.6185E+04	1.07537E+03	2.50830E+02	3.52032E+00	1.07556E+03	4.04556E-01
7	6.1773E+04	1.06896E+03	2.89136E+02	3.05393E+00	1.06911E+03	3.09393E-01
8	5.7361E+04	1.06306E+03	2.85757E+02	3.09004E+00	1.06322E+03	3.18332E-01
9	5.2948E+04	1.05543E+03	2.06772E+02	4.27041E+00	1.05574E+03	3.98714E-01
10	4.8536E+04	1.05122E+03	9.80983E+03	9.00117E-02	1.05122E+03	3.19431E-03
11	4.4124E+04	1.04925E+03	3.31627E+02	2.66263E+00	1.04936E+03	2.53982E-01
12	3.9711E+04	1.04624E+03	3.87238E+02	2.28025E+00	1.04632E+03	2.07454E-01
13	3.5299E+04	1.04217E+03	3.05828E+02	2.88724E+00	1.04234E+03	3.36301E-01
14	3.0886E+04	1.03677E+03	2.98416E+02	2.95896E+00	1.03691E+03	2.98571E-01
15	2.6474E+04	1.03224E+03	3.53536E+02	2.49762E+00	1.03234E+03	2.54376E-01
16	2.2062E+04	1.02922E+03	4.20666E+02	2.09905E+00	1.02929E+03	1.97589E-01
17	1.7649E+04	8.11812E+02	6.04448E+01	1.46084E+01	8.15164E+02	3.82391E+00
18	1.3237E+04	8.11712E+02	1.33300E+01	6.62415E+01	1.81362E+06	6.65881E+01
19	8.8247E+03	8.11612E+02	1.20750E+01	7.31264E+01	2.00424E+06	7.17714E+01
20	4.4124E+03	8.11512E+02	7.37968E-02	1.19653E+04	2.32642E+06	4.31334E+03
21	0.0000E+00	0.00000E+00	6.46885E+01	1.36500E+01	3.04953E+00	9.99979E-01

 * SEDIMENT ROUTING RESULTS FOR TIME STEP 1440 *

 INCOMING SEDIMENT DISTRIBUTION PER SIZE FRACTION

SIZE FRACTION	PERCENT	QSED (TON/DAY)
1	2.00	3.1600E-01
2	3.00	4.7400E-01
3	10.00	1.5800E+00
4	10.00	1.5800E+00
5	30.00	4.7400E+00
6	30.00	4.7400E+00
7	15.00	2.3700E+00
TOTAL		1.5800E+01

21 0.0000E+00 4.3172E+02 5.2194E+03 156.049 VERTICAL

 *** ACCUMMULATED DEPOSITION FOR WHOLE STREAM ***

STA NO.	ACCU.DEPS. (TONS)	ACCU DEPS. (FT^3)	ACCU. DEPS. FOR DIFFRNT SIZE GROUPS (FT^3)			
			1	2	3	4
1	-2.4382E+04	-4.9127E+05	-2.2503E+04	-3.3163E+04	-1.0898E+05	-1.0322E+05
2	-4.4297E+04	-8.9254E+05	-1.4397E+05	-2.5429E+05	-2.8945E+05	-3.7088E+05
3	-7.7128E+03	-1.5541E+05	-8.3901E+04	-1.3138E+05	-3.4640E+04	5.6361E+04
4	-1.4937E+04	-3.0096E+05	-1.0660E+05	-1.2270E+05	-2.4234E+04	-3.9579E+04
5	3.1304E+04	6.3075E+05	-8.3964E+04	1.3723E+05	2.3455E+05	3.0647E+05
6	7.9333E+03	1.5985E+05	-6.0972E+04	9.9162E+04	6.8565E+04	5.0094E+04
7	-6.7651E+03	-1.3631E+05	-4.3543E+04	-5.0107E+03	-3.4486E+04	-4.9384E+04
8	9.0791E+03	1.8294E+05	2.2936E+04	5.2689E+04	4.9231E+04	5.4388E+04
9	-3.8681E+04	-7.7939E+05	-1.6401E+05	-1.8861E+05	-1.7222E+05	-2.2493E+05
10	8.9406E+04	1.8014E+06	6.8691E+05	4.4665E+05	3.1358E+05	3.2259E+05
11	-2.1606E+04	-4.3535E+05	-1.8126E+05	-1.2487E+05	-7.6503E+04	-5.2711E+04
12	1.4461E+04	2.9139E+05	9.2296E+04	8.7542E+04	6.1373E+04	5.0175E+04
13	-2.6190E+04	-5.2770E+05	-1.5121E+05	-1.4659E+05	-1.1221E+05	-1.1192E+05
14	3.3049E+03	6.6591E+04	-3.5745E+04	2.6198E+04	3.4115E+04	3.8625E+04
15	1.4873E+04	2.9968E+05	1.0322E+05	8.3878E+04	5.5639E+04	5.4567E+04
16	5.6166E+03	1.1317E+05	6.8850E+04	2.4553E+04	1.1570E+04	8.1971E+03
17	-5.3903E+07	-1.0861E+09	-4.4142E+08	-2.3916E+08	-1.6820E+08	-1.9894E+08
18	-2.6874E+08	-5.4148E+09	-1.2543E+09	-1.0227E+09	-9.9394E+08	-1.5653E+09
19	-2.3709E+08	-4.7771E+09	-1.1366E+09	-9.1691E+08	-8.8644E+08	-1.3620E+09
20	-2.2592E+09	-4.5521E+10	-2.1878E+09	-4.3309E+09	-7.5221E+09	-1.8046E+10
21	2.8102E+09	5.6622E+10	4.9716E+09	6.4762E+09	9.5395E+09	2.1125E+10
SUM	-8.7519E+06	-1.7634E+08	-4.8719E+07	-3.3465E+07	-3.1203E+07	-4.7497E+07

ACCUMULATED DEPOSITION FOR DIFFERENT SIZE GROUPS (CONT.)

STA	5	6	7
1	-2.3200E+05	5.7304E+03	2.8652E+03
2	1.6605E+05	0.0000E+00	0.0000E+00
3	3.8157E+04	0.0000E+00	0.0000E+00
4	-7.8408E+03	0.0000E+00	0.0000E+00
5	3.6453E+04	0.0000E+00	0.0000E+00
6	3.0004E+03	0.0000E+00	0.0000E+00
7	-3.8866E+03	0.0000E+00	0.0000E+00
8	3.6926E+03	0.0000E+00	0.0000E+00
9	-2.9617E+04	0.0000E+00	0.0000E+00
10	3.1721E+04	0.0000E+00	0.0000E+00
11	0.0000E+00	0.0000E+00	0.0000E+00
12	0.0000E+00	0.0000E+00	0.0000E+00
13	-5.7685E+03	0.0000E+00	0.0000E+00
14	3.3980E+03	0.0000E+00	0.0000E+00
15	2.3706E+03	0.0000E+00	0.0000E+00
16	0.0000E+00	0.0000E+00	0.0000E+00
17	-2.9266E+07	-6.4642E+06	-2.6567E+06
18	-3.3464E+08	-1.3147E+08	-1.1239E+08
19	-2.7697E+08	-1.1023E+08	-8.7885E+07
20	-6.3149E+09	-3.4727E+09	-3.6459E+09

21 6.9463E+09 3.7173E+09 3.8463E+09
 SUM -9.4360E+06 -3.5042E+06 -2.5189E+06

 ACCUMULATED SEDIMENT DISTRIBUTION THAT EXITED THE REACH (TONS)
 SIZE FR TOTAL TUBE #1 TUBE #2 TUBE #
 1 2.4179E+06 8.7218E+05 1.5457E+06
 2 1.6609E+06 6.5749E+05 1.0034E+06
 3 1.5487E+06 6.7235E+05 8.7636E+05
 4 2.3574E+06 1.0979E+06 1.2595E+06
 5 4.6859E+05 2.3311E+05 2.3548E+05
 6 1.7420E+05 9.2059E+04 8.2137E+04
 7 1.2516E+05 6.4685E+04 6.0471E+04
 TOTAL 8.7528E+06 3.6898E+06 5.0631E+06

 TIME STEP NO. 2160 AFTER 9.0000E+01 DAYS; DISCHARGE IS 1.2380E+03 CFS

 * RESULTS OF BACKWATER COMPUTATIONS *
 * DISCHARGE = 1.2380E+03 C.F.S. *

STA. STATION WATER SURFACE FLOW AREA FLOW VELCTY ENERGY GRADE
 FROUDE

#	(ft)	ELEVATION(ft)	(ft ²)	(ft/s)	LINE ELEV(ft)	NUMBER
1	8.8247E+04	7.6977E+02	3.00712E+01	4.11690E+01	7.96240E+02	1.03756E+01
2	8.3835E+04	7.69677E+02	2.99051E+01	4.13976E+01	7.96434E+02	1.04621E+01
3	7.9422E+04	7.69577E+02	2.54493E+01	4.86457E+01	8.06624E+02	1.22810E+01
4	7.5010E+04	7.69477E+02	2.03427E+01	6.08572E+01	8.27525E+02	1.53964E+01
5	7.0598E+04	7.69467E+02	4.98542E+01	2.48324E+01	7.79076E+02	6.24756E+00
6	6.6185E+04	7.69367E+02	4.98012E+01	2.48589E+01	7.78994E+02	6.24970E+00
7	6.1773E+04	7.69267E+02	4.02656E+01	3.07459E+01	7.84023E+02	7.74547E+00
8	5.7361E+04	7.69167E+02	3.94437E+01	3.13865E+01	7.84561E+02	8.00653E+00
9	5.2948E+04	7.69067E+02	7.25469E+00	1.70648E+02	1.27149E+03	5.13254E+01
10	4.8536E+04	7.69057E+02	2.05000E+01	6.03903E+01	8.26304E+02	1.53158E+01
11	4.4124E+04	7.69047E+02	2.85185E+01	4.34104E+01	8.02165E+02	1.37413E+01
12	3.9711E+04	7.69037E+02	3.61205E+01	3.42742E+01	7.87615E+02	9.18120E+00
13	3.5299E+04	7.68937E+02	6.85958E+00	1.80478E+02	1.32436E+03	5.31412E+01
14	3.0886E+04	7.68927E+02	1.91639E+01	6.46005E+01	8.44047E+02	2.52041E+01
15	2.6474E+04	7.68917E+02	4.89846E+01	2.52732E+01	7.78891E+02	6.45020E+00
16	2.2062E+04	7.68907E+02	5.02912E+01	2.46166E+01	7.78359E+02	6.19424E+00
17	1.7649E+04	7.68897E+02	6.04448E+01	2.04815E+01	7.75486E+02	5.36127E+00
18	1.3237E+04	7.68797E+02	1.63471E+01	7.57319E+01	2.89847E+06	7.99457E+01
19	8.8247E+03	7.68697E+02	1.61545E+01	7.66350E+01	2.93343E+06	8.06681E+01
20	4.4124E+03	7.68597E+02	4.00844E-02	3.08848E+04	1.50697E+07	1.09796E+04
21	0.0000E+00	0.00000E+00	8.11547E+01	1.52548E+01	3.81760E+00	9.99861E-01

 * SEDIMENT ROUTING RESULTS FOR TIME STEP 2160 *

 INCOMING SEDIMENT DISTRIBUTION PER SIZE FRACTION
 SIZE FRACTION PERCENT QSED (TON/DAY)
 1 2.00 3.1600E-01
 2 3.00 4.7400E-01
 3 10.00 1.5800E+00
 4 10.00 1.5800E+00
 5 30.00 4.7400E+00
 6 30.00 4.7400E+00
 7 15.00 2.3700E+00
 TOTAL 1.5800E+01

 * STREAM TUBE NO. 1 *

 STA DISTANCE TOTAL LOAD CHANGE DIRECTION
 (TONS) (FT**3) (FT)

 1 8.8247E+04 2.0510E+04 2.4795E+05 -6.090 VERTICAL
 2 8.3835E+04 4.7280E+04 5.7159E+05 -4.133 VERTICAL
 3 7.9422E+04 5.0410E+04 6.0944E+05 -0.551 VERTICAL
 4 7.5010E+04 8.2419E+04 9.9642E+05 -4.902 VERTICAL
 5 7.0598E+04 1.5260E+04 1.8449E+05 7.058 VERTICAL
 6 6.6185E+04 1.5364E+04 1.8575E+05 -0.010 VERTICAL
 7 6.1773E+04 4.3012E+04 5.1999E+05 -2.946 VERTICAL
 8 5.7361E+04 5.2140E+04 6.3035E+05 -1.259 VERTICAL
 9 5.2948E+04 8.0361E+04 9.7153E+05 -6.060 VERTICAL
 10 4.8536E+04 1.1109E+05 1.3430E+06 -5.053 VERTICAL
 11 4.4124E+04 1.4413E+05 1.7425E+06 -3.320 VERTICAL
 12 3.9711E+04 8.4686E+04 1.0238E+06 6.866 VERTICAL
 13 3.5299E+04 1.2596E+05 1.5228E+06 -6.060 VERTICAL
 14 3.0886E+04 1.8269E+05 2.2087E+06 -5.679 VERTICAL
 15 2.6474E+04 3.9276E+04 4.7483E+05 12.349 VERTICAL
 16 2.2062E+04 3.4428E+04 4.1623E+05 0.394 VERTICAL
 17 1.7649E+04 2.1874E+04 2.6445E+05 0.208 VERTICAL
 18 1.3237E+04 2.3973E+04 2.8982E+05 -0.014 VERTICAL
 19 8.8247E+03 2.5386E+04 3.0690E+05 -0.010 VERTICAL
 20 4.4124E+03 3.2913E+05 3.9791E+06 -6.060 VERTICAL
 21 0.0000E+00 6.4935E+02 7.8503E+03 145.731 VERTICAL

 * STREAM TUBE NO. 2 *

 STA DISTANCE TOTAL LOAD CHANGE DIRECTION
 (TONS) (FT**3) (FT)

 1 8.8247E+04 2.0515E+04 2.4802E+05 -6.090 VERTICAL
 2 8.3835E+04 4.7289E+04 5.7171E+05 -4.133 VERTICAL
 3 7.9422E+04 5.0413E+04 6.0947E+05 -0.550 VERTICAL
 4 7.5010E+04 8.2136E+04 9.9299E+05 -4.909 VERTICAL

5	7.0598E+04	1.5329E+04	1.8532E+05	7.067	VERTICAL
6	6.6185E+04	1.5292E+04	1.8487E+05	0.004	VERTICAL
7	6.1773E+04	4.3148E+04	5.2164E+05	-2.883	VERTICAL
8	5.7361E+04	5.2023E+04	6.2894E+05	-1.214	VERTICAL
9	5.2948E+04	7.7866E+04	9.4137E+05	-6.060	VERTICAL
10	4.8536E+04	9.8620E+04	1.1923E+06	-5.118	VERTICAL
11	4.4124E+04	1.2391E+05	1.4980E+06	-4.376	VERTICAL
12	3.9711E+04	8.5003E+04	1.0277E+06	6.753	VERTICAL
13	3.5299E+04	1.0958E+05	1.3248E+06	-6.060	VERTICAL
14	3.0886E+04	1.4269E+05	1.7251E+06	-6.060	VERTICAL
15	2.6474E+04	3.8644E+04	4.6719E+05	10.795	VERTICAL
16	2.2062E+04	3.4349E+04	4.1526E+05	0.366	VERTICAL
17	1.7649E+04	2.2954E+04	2.7750E+05	0.194	VERTICAL
18	1.3237E+04	2.3101E+04	2.7929E+05	-0.001	VERTICAL
19	8.8247E+03	2.3529E+04	2.8445E+05	-0.003	VERTICAL
20	4.4124E+03	3.2676E+05	3.9504E+06	-6.060	VERTICAL
21	0.0000E+00	7.0425E+02	8.5141E+03	159.608	VERTICAL

 *** ACCUMULATED DEPOSITION FOR WHOLE STREAM ***

STA NO.	ACCU.DEPS. (TONS)	ACCU DEPS. (FT^3)	ACCU. DEPS. FOR DIFFRNT SIZE GROUPS (FT^3)			
			1	2	3	4
1	-5.5238E+08	-1.1130E+10	-1.5138E+08	-2.3161E+08	-7.9519E+08	-8.7469E+08
2	-7.2098E+08	-1.4527E+10	-1.0190E+09	-2.0248E+09	-3.5200E+09	-8.4475E+09
3	-8.4215E+07	-1.6969E+09	-8.9336E+08	-1.7752E+09	-3.0859E+09	-2.2485E+09
4	-8.5811E+08	-1.7290E+10	-1.0218E+09	-2.0303E+09	-3.5294E+09	-8.4705E+09
5	1.8038E+09	3.6344E+10	-2.8207E+08	4.2368E+09	9.6452E+09	1.8517E+10
6	-8.8544E+05	-1.7841E+07	-7.3628E+06	-3.8436E+06	-2.7140E+06	-3.2656E+06
7	-7.4731E+08	-1.5058E+10	-1.4980E+09	-2.9767E+09	-4.3674E+09	-5.1898E+09
8	-2.4240E+08	-4.8841E+09	-1.1450E+09	-2.2754E+09	-6.0393E+08	-7.1775E+08
9	-7.2795E+08	-1.4667E+10	-7.0171E+08	-1.3943E+09	-2.4237E+09	-5.8167E+09
10	-6.9302E+08	-1.3964E+10	-7.9638E+08	-1.5834E+09	-2.7532E+09	-6.6081E+09
11	-7.8541E+08	-1.5825E+10	-1.2374E+09	-2.4587E+09	-4.2743E+09	-8.8504E+09
12	1.3242E+09	2.6681E+10	-1.1338E+09	-6.7576E+08	6.2356E+09	1.7453E+10
13	-8.8661E+08	-1.7864E+10	-8.5462E+08	-1.6981E+09	-2.9519E+09	-7.0845E+09
14	-1.2097E+09	-2.4375E+10	-1.2154E+09	-2.4150E+09	-4.1984E+09	-1.0076E+10
15	3.3319E+09	6.7135E+10	3.3865E+09	1.2661E+10	1.3352E+10	2.4532E+10
16	1.2310E+08	2.4804E+09	1.0051E+09	5.4481E+08	3.8410E+08	4.5632E+08
17	2.6855E+08	5.4110E+09	2.1904E+09	1.1875E+09	8.3790E+08	9.9695E+08
18	-4.1822E+08	-8.4268E+09	-2.2788E+09	-1.6342E+09	-1.4885E+09	-2.2451E+09
19	-3.9790E+08	-8.0173E+09	-2.1818E+09	-1.5570E+09	-1.4242E+09	-2.1303E+09
20	-1.0143E+10	-2.0437E+11	-9.8027E+09	-1.9436E+10	-3.3771E+10	-8.1034E+10
21	1.1586E+10	2.3346E+11	1.9421E+10	2.5413E+10	3.8636E+10	8.7711E+10
SUM	-3.0179E+07	-6.0808E+08	-2.1801E+08	-1.2691E+08	-9.8936E+07	-1.3060E+08

 ACCUMULATED DEPOSITION FOR DIFFERENT SIZE GROUPS (CONT.)
 STA 5 6 7

1	-2.8864E+09	-3.7519E+09	-2.4388E+09
2	-2.9563E+09	1.8639E+09	1.5767E+09
3	4.1252E+09	1.4963E+09	6.8454E+08
4	-1.6779E+09	-3.8414E+08	-1.7598E+08

```

5 3.1701E+09 7.2525E+08 3.3158E+08
6 -4.9043E+05 -1.1290E+05 -5.1603E+04
7 -7.7033E+08 -1.7570E+08 -7.9645E+07
8 -1.0657E+08 -2.4331E+07 -1.1057E+07
9 -2.0358E+09 -1.1197E+09 -1.1757E+09
10 -2.3129E+09 -3.9227E+08 4.8269E+08
11 1.7976E+08 5.5841E+08 2.5734E+08
12 3.6014E+09 8.2386E+08 3.7658E+08
13 -2.4795E+09 -1.3637E+09 -1.4319E+09
14 -3.5267E+09 -1.9397E+09 -1.0033E+09
15 7.1009E+09 3.5535E+09 2.5492E+09
16 6.7709E+07 1.5424E+07 6.9665E+06
17 1.4834E+08 3.4124E+07 1.5841E+07
18 -4.5839E+08 -1.7478E+08 -1.4700E+08
19 -4.2342E+08 -1.6542E+08 -1.3511E+08
20 -2.8358E+10 -1.5596E+10 -1.6375E+10
21 2.9577E+10 1.6010E+10 1.6688E+10
SUM -2.2419E+07 -6.8884E+06 -4.3105E+06

```

ACCUMULATED SEDIMENT DISTRIBUTION THAT EXITED THE REACH (TONS)

SIZE FR	TOTAL	TUBE #1	TUBE #2	TUBE #
1	1.0820E+07	4.4873E+06	6.3324E+06	
2	6.2988E+06	2.6906E+06	3.6082E+06	
3	4.9103E+06	2.1896E+06	2.7208E+06	
4	6.4819E+06	3.0235E+06	3.4584E+06	
5	1.1131E+06	5.4978E+05	5.6328E+05	
6	3.4230E+05	1.8496E+05	1.5734E+05	
7	2.1414E+05	1.2006E+05	9.4083E+04	
TOTAL	3.0180E+07	1.3246E+07	1.6934E+07	

```

*****
*****
TIME STEP NO. 2880 AFTER 1.2000E+02 DAYS; DISCHARGE IS 1.1880E+03 CFS
*****
*****

```

```

*****
* RESULTS OF BACKWATER COMPUTATIONS *
* DISCHARGE = 1.1880E+03 C.F.S. *
*****

```

STA. STATION WATER SURFACE FLOW AREA FLOW VELCTY ENERGY GRADE
FROUDE

#	(ft)	ELEVATION(ft)	(ft ²)	(ft/s)	LINE ELEV(ft)	NUMBER
1	8.8247E+04	7.69978E+02	3.00712E+01	3.95063E+01	7.94346E+02	9.95655E+00
2	8.3835E+04	7.69878E+02	2.99051E+01	3.97256E+01	7.94517E+02	1.00396E+01
3	7.9422E+04	7.69778E+02	2.54493E+01	4.66810E+01	8.03893E+02	1.17850E+01
4	7.5010E+04	7.69678E+02	2.03427E+01	5.83994E+01	8.23131E+02	1.47746E+01
5	7.0598E+04	7.69668E+02	4.98542E+01	2.38295E+01	7.78516E+02	5.99523E+00
6	6.6185E+04	7.69568E+02	4.98012E+01	2.38549E+01	7.78432E+02	5.99729E+00
7	6.1773E+04	7.69468E+02	4.02656E+01	2.95041E+01	7.83056E+02	7.43265E+00

```

8 5.7361E+04 7.69368E+02 3.94437E+01 3.01189E+01 7.83544E+02 7.68316E+00
9 5.2948E+04 7.69268E+02 7.25469E+00 1.63756E+02 1.23193E+03 4.92525E+01
10 4.8536E+04 7.69258E+02 2.05000E+01 5.79513E+01 8.21974E+02 1.46972E+01
11 4.4124E+04 7.69248E+02 2.85185E+01 4.16571E+01 7.99745E+02 1.31864E+01
12 3.9711E+04 7.69238E+02 3.61205E+01 3.28899E+01 7.86345E+02 8.81039E+00
13 3.5299E+04 7.69138E+02 6.85958E+00 1.73189E+02 1.28060E+03 5.09949E+01
14 3.0886E+04 7.69128E+02 1.91639E+01 6.19915E+01 8.38302E+02 2.41861E+01
15 2.6474E+04 7.69118E+02 4.89846E+01 2.42525E+01 7.78302E+02 6.18969E+00
16 2.2062E+04 7.69108E+02 5.02912E+01 2.36224E+01 7.77812E+02 5.94407E+00
17 1.7649E+04 7.69098E+02 6.04448E+01 1.96543E+01 7.75165E+02 5.14474E+00
18 1.3237E+04 7.68998E+02 1.64060E+01 7.24127E+01 2.65945E+06 7.65082E+01
19 8.8247E+03 7.68898E+02 1.63954E+01 7.24594E+01 2.66119E+06 7.65460E+01
20 4.4124E+03 7.68798E+02 4.00844E-02 2.96374E+04 1.38771E+07 1.05361E+04
21 0.0000E+00 0.00000E+00 7.88857E+01 1.50598E+01 3.71518E+00 9.99640E-01

```

```

*****
*   SEDIMENT ROUTING RESULTS FOR TIME STEP  2880   *
*****

```

```

-----
INCOMING SEDIMENT DISTRIBUTION PER SIZE FRACTION
SIZE FRACTION    PERCENT    QSED (TON/DAY)
  1             2.00     3.1600E-01
  2             3.00     4.7400E-01
  3            10.00     1.5800E+00
  4            10.00     1.5800E+00
  5            30.00     4.7400E+00
  6            30.00     4.7400E+00
  7            15.00     2.3700E+00
TOTAL                      1.5800E+01
-----

```

```

*****
*   STREAM TUBE NO.  1   *
*****
STA DISTANCE    TOTAL LOAD    CHANGE DIRECTION
   (TONS)      (FT**3)    (FT)
*****
  1  8.8247E+04  1.9951E+04  2.4119E+05  -5.924  VERTICAL
  2  8.3835E+04  4.6507E+04  5.6225E+05  -4.100  VERTICAL
  3  7.9422E+04  4.6524E+04  5.6246E+05  -0.003  VERTICAL
  4  7.5010E+04  7.7906E+04  9.4185E+05  -4.806  VERTICAL
  5  7.0598E+04  1.2938E+04  1.5641E+05   6.827  VERTICAL
  6  6.6185E+04  1.3026E+04  1.5748E+05  -0.008  VERTICAL
  7  6.1773E+04  3.7704E+04  4.5582E+05  -2.629  VERTICAL
  8  5.7361E+04  4.6398E+04  5.6094E+05  -1.200  VERTICAL
  9  5.2948E+04  7.4619E+04  9.0212E+05  -6.060  VERTICAL
 10  4.8536E+04  1.0473E+05  1.2661E+06  -4.951  VERTICAL
 11  4.4124E+04  1.3027E+05  1.5749E+06  -2.566  VERTICAL
 12  3.9711E+04  7.3832E+04  8.9259E+05   6.519  VERTICAL
 13  3.5299E+04  1.1510E+05  1.3916E+06  -6.060  VERTICAL
 14  3.0886E+04  1.7118E+05  2.0695E+06  -5.612  VERTICAL
 15  2.6474E+04  3.3301E+04  4.0260E+05  11.872  VERTICAL
 16  2.2062E+04  2.9191E+04  3.5291E+05   0.334  VERTICAL
 17  1.7649E+04  1.8546E+04  2.2421E+05   0.176  VERTICAL

```

18	1.3237E+04	1.9966E+04	2.4138E+05	-0.009	VERTICAL
19	8.8247E+03	2.0028E+04	2.4213E+05	0.000	VERTICAL
20	4.4124E+03	3.2595E+05	3.9406E+06	-6.060	VERTICAL
21	0.0000E+00	6.1076E+02	7.3839E+03	146.621	VERTICAL

* STREAM TUBE NO. 2 *

STA	DISTANCE	TOTAL LOAD	CHANGE	DIRECTION
	(TONS)	(FT**3)	(FT)	

1	8.8247E+04	1.9954E+04	2.4124E+05	-5.924	VERTICAL
2	8.3835E+04	4.6517E+04	5.6237E+05	-4.100	VERTICAL
3	7.9422E+04	4.6527E+04	5.6249E+05	-0.002	VERTICAL
4	7.5010E+04	7.7622E+04	9.3842E+05	-4.812	VERTICAL
5	7.0598E+04	1.2996E+04	1.5712E+05	6.837	VERTICAL
6	6.6185E+04	1.2964E+04	1.5673E+05	0.003	VERTICAL
7	6.1773E+04	3.7856E+04	4.5766E+05	-2.576	VERTICAL
8	5.7361E+04	4.6344E+04	5.6028E+05	-1.161	VERTICAL
9	5.2948E+04	7.2187E+04	8.7271E+05	-6.060	VERTICAL
10	4.8536E+04	9.2322E+04	1.1161E+06	-4.965	VERTICAL
11	4.4124E+04	1.1645E+05	1.4079E+06	-4.176	VERTICAL
12	3.9711E+04	7.4468E+04	9.0029E+05	7.288	VERTICAL
13	3.5299E+04	9.9044E+04	1.1974E+06	-6.060	VERTICAL
14	3.0886E+04	1.3216E+05	1.5977E+06	-6.060	VERTICAL
15	2.6474E+04	3.2765E+04	3.9612E+05	10.312	VERTICAL
16	2.2062E+04	2.9123E+04	3.5209E+05	0.310	VERTICAL
17	1.7649E+04	1.9461E+04	2.3527E+05	0.164	VERTICAL
18	1.3237E+04	1.9464E+04	2.3531E+05	0.000	VERTICAL
19	8.8247E+03	1.9482E+04	2.3553E+05	0.000	VERTICAL
20	4.4124E+03	3.2489E+05	3.9278E+06	-6.060	VERTICAL
21	0.0000E+00	6.6343E+02	8.0206E+03	161.489	VERTICAL

*** ACCUMMULATED DEPOSITION FOR WHOLE STREAM ***

STA NO.	ACCU.DEPS. (TONS)	ACCU DEPS. (FT^3)	ACCU. DEPS. FOR DIFFRNT SIZE GROUPS (FT^3)			
			1	2	3	4

1	-1.2419E+09	-2.5024E+10	-3.4563E+08	-5.2882E+08	-1.8156E+09	-1.9971E+09
2	-1.6389E+09	-3.3022E+10	-2.3266E+09	-4.6232E+09	-8.0371E+09	-1.9289E+10
3	-8.4688E+07	-1.7064E+09	-2.0398E+09	-4.0534E+09	-7.0464E+09	-2.8754E+09
4	-1.9377E+09	-3.9043E+10	-2.3330E+09	-4.6359E+09	-8.0591E+09	-1.9342E+10
5	4.0431E+09	8.1466E+10	1.3021E+07	1.0030E+10	2.2275E+10	4.0322E+10
6	-1.8602E+06	-3.7481E+07	-1.5318E+07	-8.1560E+06	-5.7553E+06	-6.8811E+06
7	-1.6039E+09	-3.2316E+10	-3.4205E+09	-6.7970E+09	-9.1203E+09	-1.0837E+10
8	-5.3932E+08	-1.0867E+10	-2.6147E+09	-5.1957E+09	-1.2612E+09	-1.4989E+09
9	-1.6622E+09	-3.3491E+10	-1.6021E+09	-3.1834E+09	-5.5341E+09	-1.3282E+10
10	-1.5612E+09	-3.1457E+10	-1.8194E+09	-3.6162E+09	-6.2872E+09	-1.5090E+10
11	-1.6438E+09	-3.3122E+10	-2.8254E+09	-5.6141E+09	-9.7598E+09	-1.7850E+10
12	3.0250E+09	6.0951E+10	-2.5890E+09	4.0638E+08	1.4866E+10	3.8240E+10
13	-2.0245E+09	-4.0791E+10	-1.9513E+09	-3.8773E+09	-6.7404E+09	-1.6177E+10
14	-2.7508E+09	-5.5427E+10	-2.7752E+09	-5.5145E+09	-9.5868E+09	-2.3008E+10

15	7.4318E+09	1.4975E+11	8.7465E+09	2.7510E+10	2.9278E+10	5.4578E+10
16	2.5706E+08	5.1796E+09	2.0988E+09	1.1377E+09	8.0208E+08	9.5287E+08
17	6.1947E+08	1.2482E+10	5.0545E+09	2.7402E+09	1.9328E+09	2.2984E+09
18	-4.4464E+08	-8.9591E+09	-2.5066E+09	-1.7570E+09	-1.5714E+09	-2.3350E+09
19	-4.0654E+08	-8.1914E+09	-2.2391E+09	-1.5917E+09	-1.4529E+09	-2.1707E+09
20	-2.0685E+10	-4.1679E+11	-1.9963E+10	-3.9626E+10	-6.8870E+10	-1.6527E+11
21	2.2798E+10	4.5937E+11	3.5055E+10	4.8573E+10	7.5828E+10	1.7443E+11
SUM	-5.2196E+07	-1.0517E+09	-3.9854E+08	-2.2470E+08	-1.6764E+08	-2.1171E+08

 ACCUMULATED DEPOSITION FOR DIFFERENT SIZE GROUPS (CONT.)

STA	5	6	7
1	-6.5905E+09	-8.5673E+09	-5.1790E+09
2	-6.7507E+09	4.6251E+09	3.3795E+09
3	9.7551E+09	3.1244E+09	1.4290E+09
4	-3.5039E+09	-8.0213E+08	-3.6741E+08
5	6.6198E+09	1.5143E+09	6.9215E+08
6	-1.0275E+06	-2.3574E+05	-1.0772E+05
7	-1.6085E+09	-3.6680E+08	-1.6616E+08
8	-2.2253E+08	-5.0795E+07	-2.3072E+07
9	-4.6485E+09	-2.5567E+09	-2.6845E+09
10	-5.2814E+09	-6.0046E+08	1.2377E+09
11	1.2244E+09	1.1662E+09	5.3748E+08
12	7.5204E+09	1.7202E+09	7.8608E+08
13	-5.6618E+09	-3.1140E+09	-3.2697E+09
14	-8.0530E+09	-4.4291E+09	-2.0598E+09
15	1.6001E+10	8.0653E+09	5.5673E+09
16	1.4137E+08	3.2196E+07	1.4530E+07
17	3.4160E+08	7.8277E+07	3.5949E+07
18	-4.6926E+08	-1.7525E+08	-1.4458E+08
19	-4.3104E+08	-1.6828E+08	-1.3770E+08
20	-5.7842E+10	-3.1812E+10	-3.3402E+10
21	5.9426E+10	3.2308E+10	3.3749E+10
SUM	-3.4306E+07	-9.4789E+06	-5.3307E+06

 ACCUMULATED SEDIMENT DISTRIBUTION THAT EXITED THE REACH (TONS)

SIZE FR	TOTAL	TUBE #1	TUBE #2	TUBE #
1	1.9780E+07	8.7831E+06	1.0997E+07	
2	1.1152E+07	5.0174E+06	6.1346E+06	
3	8.3202E+06	3.8240E+06	4.4962E+06	
4	1.0507E+07	4.9524E+06	5.5550E+06	
5	1.7032E+06	8.3236E+05	8.7082E+05	
6	4.7100E+05	2.4644E+05	2.2457E+05	
7	2.6485E+05	1.4407E+05	1.2077E+05	
TOTAL	5.2198E+07	2.3800E+07	2.8399E+07	

 TIME STEP NO. 3600 AFTER 1.5000E+02 DAYS; DISCHARGE IS 1.0480E+03 CFS

 * RESULTS OF BACKWATER COMPUTATIONS *
 * DISCHARGE = 1.0480E+03 C.F.S. *

STA. STATION WATER SURFACE FLOW AREA FLOW VELCTY ENERGY GRADE
 FROUDE

#	(ft)	ELEVATION(ft)	(ft ²)	(ft/s)	LINE ELEV(ft)	NUMBER
1	8.8247E+04	1.11435E+03	2.80338E+02	3.73835E+00	1.11458E+03	3.34265E-01
2	8.3835E+04	1.10593E+03	3.56824E+02	2.93702E+00	1.10608E+03	2.36802E-01
3	7.9422E+04	1.09899E+03	2.19336E+02	4.77806E+00	1.09937E+03	4.57878E-01
4	7.5010E+04	1.09208E+03	2.30856E+02	4.53962E+00	1.09243E+03	4.08253E-01
5	7.0598E+04	1.08901E+03	6.06996E+02	1.72654E+00	1.08906E+03	1.37443E-01
6	6.6185E+04	7.68859E+02	4.98012E+01	2.10437E+01	7.75757E+02	5.29054E+00
7	6.1773E+04	7.68759E+02	4.02656E+01	2.60272E+01	7.79333E+02	6.55675E+00
8	5.7361E+04	7.68659E+02	3.94437E+01	2.65695E+01	7.79691E+02	6.77774E+00
9	5.2948E+04	7.68559E+02	7.25469E+00	1.44458E+02	1.12860E+03	4.34483E+01
10	4.8536E+04	7.68549E+02	2.05000E+01	5.11220E+01	8.09572E+02	1.29652E+01
11	4.4124E+04	7.68539E+02	2.85185E+01	3.67480E+01	7.92272E+02	1.16324E+01
12	3.9711E+04	7.68529E+02	3.61205E+01	2.90140E+01	7.81842E+02	7.77213E+00
13	3.5299E+04	7.68429E+02	6.85958E+00	1.52779E+02	1.16645E+03	4.49854E+01
14	3.0886E+04	7.68419E+02	1.91639E+01	5.46861E+01	8.22250E+02	2.13359E+01
15	2.6474E+04	7.68409E+02	4.89846E+01	2.13945E+01	7.75556E+02	5.46027E+00
16	2.2062E+04	7.68399E+02	5.02912E+01	2.08386E+01	7.75172E+02	5.24359E+00
17	1.7649E+04	7.68389E+02	6.04448E+01	1.73381E+01	7.73110E+02	4.53846E+00
18	1.3237E+04	7.68289E+02	1.63728E+01	6.40087E+01	2.07398E+06	6.75904E+01
19	8.8247E+03	7.68279E+02	1.63794E+01	6.39829E+01	2.07313E+06	6.75752E+01
20	4.4124E+03	7.68179E+02	4.00844E-02	2.61448E+04	1.07993E+07	9.29451E+03
21	0.0000E+00	0.00000E+00	7.23356E+01	1.44880E+01	3.42395E+00	9.99836E-01

 * SEDIMENT ROUTING RESULTS FOR TIME STEP 3600 *

 INCOMING SEDIMENT DISTRIBUTION PER SIZE FRACTION

SIZE FRACTION	PERCENT	QSED (TON/DAY)
1	2.00	3.1600E-01
2	3.00	4.7400E-01
3	10.00	1.5800E+00
4	10.00	1.5800E+00
5	30.00	4.7400E+00
6	30.00	4.7400E+00
7	15.00	2.3700E+00
TOTAL		1.5800E+01

 * STREAM TUBE NO. 1 *

 STA DISTANCE TOTAL LOAD CHANGE DIRECTION
 (TONS) (FT**3) (FT)

 1 8.8247E+04 1.9987E-01 2.4164E+00 0.000 VERTICAL

2	8.3835E+04	8.9852E-01	1.0863E+01	0.000	VERTICAL
3	7.9422E+04	1.2325E+00	1.4901E+01	0.000	VERTICAL
4	7.5010E+04	9.5629E-01	1.1561E+01	0.000	VERTICAL
5	7.0598E+04	3.3865E-02	4.0942E-01	0.000	VERTICAL
6	6.6185E+04	7.8831E+03	9.5303E+04	-0.712	VERTICAL
7	6.1773E+04	2.6029E+04	3.1468E+05	-1.933	VERTICAL
8	5.7361E+04	3.0912E+04	3.7371E+05	-0.674	VERTICAL
9	5.2948E+04	5.9132E+04	7.1489E+05	-6.060	VERTICAL
10	4.8536E+04	8.5089E+04	1.0287E+06	-4.269	VERTICAL
11	4.4124E+04	9.5452E+04	1.1540E+06	-1.041	VERTICAL
12	3.9711E+04	4.9955E+04	6.0394E+05	5.255	VERTICAL
13	3.5299E+04	9.1227E+04	1.1029E+06	-6.060	VERTICAL
14	3.0886E+04	1.4295E+05	1.7282E+06	-5.177	VERTICAL
15	2.6474E+04	2.0159E+04	2.4371E+05	10.573	VERTICAL
16	2.2062E+04	1.7670E+04	2.1362E+05	0.202	VERTICAL
17	1.7649E+04	1.1223E+04	1.3569E+05	0.106	VERTICAL
18	1.3237E+04	1.2182E+04	1.4728E+05	-0.006	VERTICAL
19	8.8247E+03	1.2158E+04	1.4699E+05	0.000	VERTICAL
20	4.4124E+03	3.1773E+05	3.8412E+06	-6.060	VERTICAL
21	0.0000E+00	5.0862E+02	6.1490E+03	149.829	VERTICAL

* STREAM TUBE NO. 2 *

STA	DISTANCE	TOTAL LOAD	CHANGE	DIRECTION
	(TONS)	(FT**3)	(FT)	

1	8.8247E+04	1.9986E-01	2.4162E+00	0.000	VERTICAL
2	8.3835E+04	8.9852E-01	1.0863E+01	0.000	VERTICAL
3	7.9422E+04	1.2325E+00	1.4901E+01	0.000	VERTICAL
4	7.5010E+04	9.5625E-01	1.1561E+01	0.000	VERTICAL
5	7.0598E+04	3.3923E-02	4.1012E-01	0.000	VERTICAL
6	6.6185E+04	7.8458E+03	9.4853E+04	-0.700	VERTICAL
7	6.1773E+04	2.6216E+04	3.1694E+05	-1.901	VERTICAL
8	5.7361E+04	3.0696E+04	3.7110E+05	-0.613	VERTICAL
9	5.2948E+04	5.6539E+04	6.8353E+05	-6.060	VERTICAL
10	4.8536E+04	7.4568E+04	9.0150E+05	-4.446	VERTICAL
11	4.4124E+04	9.3261E+04	1.1275E+06	-3.235	VERTICAL
12	3.9711E+04	4.9296E+04	5.9598E+05	7.631	VERTICAL
13	3.5299E+04	7.3873E+04	8.9309E+05	-6.060	VERTICAL
14	3.0886E+04	1.0699E+05	1.2934E+06	-6.060	VERTICAL
15	2.6474E+04	1.9834E+04	2.3978E+05	9.042	VERTICAL
16	2.2062E+04	1.7629E+04	2.1313E+05	0.188	VERTICAL
17	1.7649E+04	1.1778E+04	1.4240E+05	0.099	VERTICAL
18	1.3237E+04	1.1774E+04	1.4235E+05	0.000	VERTICAL
19	8.8247E+03	1.1769E+04	1.4228E+05	0.000	VERTICAL
20	4.4124E+03	3.1682E+05	3.8303E+06	-6.060	VERTICAL
21	0.0000E+00	5.5514E+02	6.7115E+03	165.931	VERTICAL

*** ACCUMMULATED DEPOSITION FOR WHOLE STREAM ***

 STA ACCU.DEPS. ACCU DEPS. ACCU. DEPS. FOR DIFFRNT SIZE GROUPS (FT^3)

NO.	(TONS)	(FT ³)	1	2	3	4
1	-1.2419E+09	-2.5024E+10	-3.4564E+08	-5.2882E+08	-1.8156E+09	-1.9972E+09
2	-1.6389E+09	-3.3022E+10	-2.3266E+09	-4.6233E+09	-8.0372E+09	-1.9289E+10
3	-8.4706E+07	-1.7068E+09	-2.0398E+09	-4.0534E+09	-7.0465E+09	-2.8755E+09
4	-1.9377E+09	-3.9043E+10	-2.3330E+09	-4.6359E+09	-8.0591E+09	-1.9342E+10
5	4.0432E+09	8.1467E+10	1.3074E+07	1.0030E+10	2.2275E+10	4.0322E+10
6	-2.7336E+08	-5.5079E+09	-2.2332E+09	-1.2131E+09	-8.5384E+08	-1.0112E+09
7	-2.2349E+09	-4.5030E+10	-5.3431E+09	-1.0617E+10	-1.1998E+10	-1.4256E+10
8	-7.0112E+08	-1.4127E+10	-4.0843E+09	-6.0220E+09	-1.6592E+09	-1.9717E+09
9	-2.5964E+09	-5.2315E+10	-2.5025E+09	-4.9726E+09	-8.6445E+09	-2.0747E+10
10	-2.3213E+09	-4.6771E+10	-2.8423E+09	-5.6490E+09	-9.8211E+09	-2.3571E+10
11	-2.1459E+09	-4.3238E+10	-4.4133E+09	-8.7696E+09	-1.4730E+10	-2.0396E+10
12	4.5709E+09	9.2099E+10	-4.0443E+09	4.3785E+09	2.4362E+10	5.4214E+10
13	-3.1623E+09	-6.3718E+10	-3.0479E+09	-6.0565E+09	-1.0529E+10	-2.5269E+10
14	-4.2167E+09	-8.4963E+10	-4.3349E+09	-8.6141E+09	-1.4975E+10	-3.5941E+10
15	1.1059E+10	2.2283E+11	1.6331E+10	3.8585E+10	4.2541E+10	8.1458E+10
16	3.3817E+08	6.8138E+09	2.7612E+09	1.4967E+09	1.0551E+09	1.2534E+09
17	8.3196E+08	1.6763E+10	6.7890E+09	3.6805E+09	2.5958E+09	3.0863E+09
18	-4.6054E+08	-9.2794E+09	-2.6495E+09	-1.8330E+09	-1.6210E+09	-2.3854E+09
19	-4.0626E+08	-8.1857E+09	-2.2371E+09	-1.5905E+09	-1.4520E+09	-2.1695E+09
20	-3.1238E+10	-6.2943E+11	-3.0134E+10	-5.9837E+10	-1.0401E+11	-2.4960E+11
21	3.3746E+10	6.7996E+11	4.8468E+10	7.0539E+10	1.1220E+11	2.6021E+11
SUM	-7.0578E+07	-1.4221E+09	-5.4931E+08	-3.0636E+08	-2.2500E+08	-2.7939E+08

ACCUMULATED DEPOSITION FOR DIFFERENT SIZE GROUPS (CONT.)

STA	5	6	7
1	-6.5906E+09	-8.5673E+09	-5.1790E+09
2	-6.7507E+09	4.6251E+09	3.3795E+09
3	9.7551E+09	3.1244E+09	1.4290E+09
4	-3.5038E+09	-8.0213E+08	-3.6741E+08
5	6.6199E+09	1.5143E+09	6.9215E+08
6	-1.4916E+08	-3.3264E+07	-1.4096E+07
7	-2.1156E+09	-4.8224E+08	-2.1818E+08
8	-2.9271E+08	-6.6790E+07	-3.0307E+07
9	-7.2613E+09	-3.9937E+09	-4.1934E+09
10	-7.0194E+09	-1.5920E+08	2.2908E+09
11	2.8288E+09	1.5344E+09	7.0730E+08
12	9.8928E+09	2.2625E+09	1.0334E+09
13	-8.8441E+09	-4.8643E+09	-5.1075E+09
14	-1.2579E+10	-5.9111E+09	-2.6079E+09
15	2.4430E+10	1.1462E+10	8.0278E+09
16	1.8594E+08	4.2323E+07	1.9070E+07
17	4.5858E+08	1.0497E+08	4.8073E+07
18	-4.7436E+08	-1.7452E+08	-1.4172E+08
19	-4.3083E+08	-1.6820E+08	-1.3757E+08
20	-8.7356E+10	-4.8045E+10	-5.0447E+10
21	8.9153E+10	4.8586E+10	5.0810E+10
SUM	-4.4215E+07	-1.1630E+07	-6.1676E+06

ACCUMULATED SEDIMENT DISTRIBUTION THAT EXITED THE REACH (TONS)

SIZE FR	TOTAL	TUBE #1	TUBE #2	TUBE #
1	2.7262E+07	1.2362E+07	1.4901E+07	

2	1.5205E+07	6.9556E+06	8.2493E+06
3	1.1167E+07	5.1852E+06	5.9818E+06
4	1.3866E+07	6.5578E+06	7.3085E+06
5	2.1951E+06	1.0673E+06	1.1278E+06
6	5.7792E+05	2.9736E+05	2.8057E+05
7	3.0645E+05	1.6370E+05	1.4276E+05
TOTAL	7.0580E+07	3.2589E+07	3.7991E+07
